UNIVERSITY OF NEWCASTLE UPON TYNE
DEPARTMENT OF CIVIL ENGINEERING

THIN LAYERED SYSTEMS

FOR

THE REPAIR & PROTECTION

OF

CONCRETE STRUCTURES

By
Mohammad Reza Sohrabi
M. Sc.

July 1996

Thesis submitted to the University of Newcastle Upon Tyne
for the Degree of Doctor of Philosophy

ACKNOWLEDGEMENT

The world of science is always indebted to the people who sincerely struggle for the advance of it and paving the road for those who are interested in learning. This is an eternal effort for which gratefulness and praise are beyond the limit of any writing or speech and could never be expressed by words.

The author is most sincerely grateful to Dr. D. R. Plum, under whose supervision the work described in this thesis was carried out, for his invaluable continuous encouragement and expert guidance.

The author would like also to express his deep gratitude to professor J. Knapton, the head of the Structural group, for his unsparing expert guidance, and also for extending the facilities of the department for this research, particularly regarding the NUROLF.

Gratitude also to Dr. D. M. Lilley, for providing easier access to the LUSAS finite element software.

The author is indebted to the University of Sistan and Baluchestan, and the Ministry of Culture and Higher Education of the Islamic Republic of Iran for their financial support.

Special thanks are due to the department technicians; Mr. J. Allen, J. E. Edmonds, G. Stacy, L. Moore, F. Beadle, C. S. Hunt for their friendly assistance. The tireless assistance of Mr. W. D. Craigie during preparation of concrete specimens and keeping the experimental apparatus operational is particularly appreciated.

Appreciation is also due to the manufacturers who have provided the required materials for this work.

Last, but not least, grateful acknowledgement is due to the author's parents for their encouragement and support, and also to his wife for her encouragement, patience and moral support during the course of this work.

ABSTRACT

Thin layered systems can be considered as a solution to the repair and protection of concrete structures. This subject was studied in the current investigation. Some common uses of these systems include protection, upgrading and rehabilitation of the floor slabs, restoration of appearance of the structures, impermeability, skid resistance, wear resistance, and protection of the reinforcing steel of concrete structures against atmospheric or chemical attack. However it can be said that protection, upgrading and rehabilitation of floor slabs are the main uses for the design of modern thin layered systems. For example a thin layer of a polymer concrete with a thickness of less than 3 mm can resist a very highly concentrated load resulting from a steel wheel rolling load of 5000 N without any sign of defect.

Thin layer systems therefore include traditional screeds, externally bonded steel plates, plasters and coatings as well as the more recent hi - tech. systems.

Like any other structure, a thin layered system may break down as the result of many causes. Among other types of failures, delamination defect is the most common mode of failure and particularly relevant to a thin layered system. This phenomenon which mostly occur between the upper layer directly subjected to the load and the subsequent layer, is due to debonding or slippage at the interface of the two layers. A delamination may occur at the interface of a thin layered system even without any sign of failure in other parts of the structure. Steel wheeled trolleys and fork - lift trucks are among the most anticipated types of loading and causes of failures in the thin layered systems.

Different combinations of thin layered systems were prepared using some special flooring materials, both in small and large scales. Despite the lack of any standard test, the action of a steel wheel rolling load on the ready made and purpose made specimens of thin layered systems was well simulated using the Steel Wheel Rolling Load Rig. The NUROLF, Newcastle University Rolling Load Facility, was also used for simulating the action of a tyred vehicle wheel rolling load on the thin layered systems of large scale. Some simple ways for detecting any possible delamination at the interface of the thin layered systems were examined.

In addition to the available material characteristics tests, a relatively new simple shear box test was proposed for defining the relationship between normal stress and the corresponding shear strength for each combination of the materials at each age of the test. The results were then used as the basis for the

subsequent structural analysis. The structural analysis of the systems was carried out for both of the experiments using the finite element method and the interface technique. In spite of the simplifications made in the solution, the analytical results were consistent with the experimental results to a considerable extent.

Based on the results of this investigation, a relatively constitutive procedure was concluded for predicting the behaviour of a thin layered system under the action of a wheel rolling load with regard to the delamination defect.

CONTENTS

CHAPTER 1

INTRODUCTION

The subject of study

General description

Main objectives

Outline of contents

1-1 The subject of study

The subject that is going to be studied in this research is ' Thin layered systems for the repair and protection of concrete structures "
A thin layered system in this study is understood as a system with one or more thin layers of different physical and mechanical properties which lies on a surface of a main substrate such as a concrete slab. Each of the two other dimensions of a thin layered system may vary from a very small quantity in an isolated patch repair on an individual member of a structure, to a very large amount in a coating layer on a warehouse floor.
The importance of the study of these systems is that they have always been used in repair, protection or strengthening of concrete structures in various fields of the construction industry. Protection, upgrading and rehabilitation of floor slabs, restoration of appearance of the structures, protection of the reinforcing steel of concrete structures against atmospheric or chemical attack are some common uses of these systems. They may also offer impermeability, skid resistance, wear resistance, and water shedding properties. Some of these systems may have the capability of being installed with minimal disruption to traffic.

1-2 General description

Thin layer systems therefore include traditional screeds, externally bonded steel plates, plasters and coatings as well as the more recent hi - tech. systems.
Protection, upgrading and rehabilitation of floor slabs are the main uses for modern thin layered systems. Upgrading is largely applied to the use of layered finishes for producing level tolerances or other properties such as wear and skid resistance, and water shedding, beyond those possible in a concrete substrate. The floor slabs may be ground slabs or suspended structural slabs, although the latter types are more common. [Plum July 1990]
Like any other structure, a thin layered system may break down as the result of many causes. Some factors causing failures such as poor workmanship, improperly formulated materials or mix properties, inadequate preparation and priming of the interfaces can be avoided. Failures may occur in the constitutive materials as a result of inducing high values of stresses within the structure of the systems. These failures can also be easily predicted and avoided, as they are similar to any other structures.

In addition to the above, there is another type of failure which is particularly relevant to a thin layered system, that is the delamination defect. The delamination, which mostly occur between the upper layer directly subjected to the load and the subsequent layer, is due to debonding or slippage at the interface of the two layers. A delamination may occur at the interface of a thin layered system even without any sign of failure in other parts of the structure i.e. in the constituent materials. As any other failure, this type of failure also stem from the loading effects. Concentrated and static loads, wheel rolling loads, thermal stresses and thermal shock, impact shock, freeze thaw cycling can be enumerated as some reasons for this type of defect. Researches carried out on the behaviour of thin layered systems regarding some of these effects are mainly experimental. [Huang 1990]

With regard to the thin layered systems which will be studied in this investigation, the results of a survey carried out by Choi in 1991 [Choi 1991] showed that: [Choi 1991]

- Steel wheeled trolleys and fork - lift trucks are among the most anticipated types of loading and causes of failures
- The most common mode of failure is the interface bond failure (delamination at the interface)
- The most anticipated types of environmental conditions are internal ambient, dry condition and cleaning by washing with water

With regard to the above, the current investigation was carried out on the behaviour of thin layered systems under the action two types of loads: a steel wheel rolling load, and a pneumatic tyred vehicle wheel rolling load

1-3 Main objectives

The main objectives of this study were as follows:

- Introducing thin layered systems as a solution to the repair and protection of concrete structures along with the materials which are more commonly in use for constructing these systems
- Introducing appropriate test methods for simulating the action of rolling wheel loads on the thin layered systems made of some special flooring materials
- Examining some simple ways for detecting any possible delamination in a thin layered system.

- Carrying out appropriate tests for the determination of the material characteristics as a basis for the subsequent structural analysis.
- Introducing and carrying out proper test methods for the determination of interface bond strength as a complementary basis for the subsequent structural analysis.
- Structural analysis of the systems using the finite element method and the interface technique, based on the results of the material characteristics and interface bond strength tests.
- Comparing the results of the structural analysis and the experimental tests for different combinations of materials and at different ages and evaluating the performances of the materials and the thin layered systems under tests.
- Introducing a constitutive model which is able to explain and predict the behaviour of the thin layered systems under the action of a wheel rolling load with particular interest in the delamination defect.

1-4 Outline of contents

In order to achieve the above objectives, the present investigation can be divided into five main parts:
Chapter 2: materials in use
Chapter 3: applications and causes of failures
Chapter 4: theories of layered systems
Chapter 5: properties of materials experiments
Chapter 6 and 7: rolling load experiments

Chapter 2 deals with the different types of materials that may be most widely used for the construction of thin layered systems, in general. A summary of the specifications of the materials has been presented.

Chapter 3 deals with applications and failure causes in thin layered systems. This includes an introduction to the general uses of thin layered systems. Then it has been be tried to present some specific examples along with the views of different investigators regarding the use of thin layered systems. Also some causes of failures in a thin layered system have been reviewed.

At the beginning of chapter 4, four main groups of theoretical models, which have been developed and used for the purpose of studying a layered system,

have been discussed. These include the plate theory, layered theory, the finite element technique, and coupled theory. Examples of theories of layered systems have been presented in the subsequent section. Finally the reasons for the selection of the finite element method are presented. The proposed method for analysing a thin layered system under the action of a rolling load with particular interest in the delamination defect has been discussed and the thin interface layer has been introduced. The procedure for defining of the finite element mesh, determining the specifications of the thin interface layer, and implementing the structural analysis is illustrated.

Chapter 5 includes material characteristics and interface bond strength. In this chapter all the constitutive materials used in this investigation have been introduced. For the purpose of the subsequent structural analysis, the required types of material characteristics tests have been carried out. An idealized stress strain curve has been defined for each material. The determination of interface bond strength has been done by carrying out two types of tests; the conventional pull off test using the Elcometer or the Limpet loading equipment, and a special proposed shear - compression test using the shear box apparatus. In the proposed shear box test, the relationship between normal stress and the corresponding shear strength has been defined for each combination of the materials at each age of the test

Chapters 6 and 7 deal with the wheel rolling load experiments. Some simple ways for detecting any possible delamination at the interface of the thin layered systems are examined.

In chapter 6, the behaviour of thin layered systems under the action of a steel wheel rolling load has been studied. In the first part of this chapter the action of a steel wheel rolling load has been simulated using the Steel Wheel Rolling Load Rig. In the second part of this chapter is demonstrated a method of modelling and analysing thin layered systems in order to predict their behaviour under the prescribed loading condition using the finite element method and the interface technique. The analytical results have been then compared with the experiment.

The above procedure has been also followed in chapter 7 for studying the behaviour of the thin layered systems under the action of a pneumatic tyred vehicle wheel load. The action of a pneumatic tyred vehicle wheel load has been simulated in the first part of this chapter using the NUROLF, Newcastle

University Rolling Load Facility. The second part of the chapter presents the modelling and analysing the thin layered systems in order to predict their behaviour under the prescribed loading condition using the finite element method and the interface technique. The analytical results have been then compared with the experiment.

In addition to the above five main parts, in chapter 8 of this study, a summary of the work has been given. Then a general discussion of the results of different sections of this investigation is presented. In the subsequent section, the final conclusions of the research are drawn. Finally some recommendations have been made for the purpose of further research, based on the experiences obtained from the current investigation.

CHAPTER 2

MATERIALS USED IN THIN LAYERED SYSTEMS

Cements

Aggregates

Admixtures

Polymers

A thin layered system is normally made of concrete substrate, polymer concrete (PC) or polymer cement concrete (PCC) or any other appropriate material as the upper layer/layers of the system. [Plum July 1990]However the selection of the appropriate materials in each case depends on the desired factors to be fulfilled in each particular case, knowledge and experience of the designer.
As far as the repair of a concrete structure is concerned, preventing the cause of deterioration is more important. This is directly related to the best selection and use of the appropriate materials either at the stage of construction or repair. Similarly when we are talking about the protection of a particular structure against a potential cause of deterioration, once again the importance of having a good knowledge of the appropriate materials becomes clear.
In the following sections of this chapter, it will be tried to present a summary of the specifications of materials which may be most widely used in thin layered systems:

2-1 Cements

Concrete is a stone like material, strong in compression and relatively weak in tension. Concrete normally consists of cement, water, aggregate and some other materials like additives and admixtures. The quality of concrete depends on many factors among which are the proportions of the mix, workmanship, and the conditions of humidity and temperature in which the concrete is cured and maintained may be more important. The bonding agent of this composite material is cement which may be found in various types with different properties and performances. Therefore the type of cement used in a concrete has a vital role in the subsequent properties of the hardened structures. Portland cement has been the most widely used cement in concrete repair work. [Allen et al. 1993]
In addition to the various types of cements, available in the market, there is a variety of admixtures which can be added to Portland cement concrete, mortar or grout to impart some additional desirable properties to the mix at the time of mixing. (section 2-3)

2-1-1 Portland Cements

Portland cement is a hydraulic or water resisting cement which is usually divided into five types as follows: [Mehta, et al. 1993]

- Type I: Ordinary Portland cement:

This type of Portland cement is used when the special properties of other types are not required.

- Type II: Modified Portland cement:

This type of Portland cement is used when special properties such as moderate sulphate resistance or moderate heat of hydration is desired. In this type of cement the percentage of C_3A ($3CaO.Al_2O_2$) has been limited to a maximum of 8% and the sum of C_3S ($3Cao.SiO_2$) and C_3A must not exceed than 58%. The reason for these limitations is preventing a high heat of hydration due to the existence of C_3S and C_3A compounds in the cement.

- Type III: High strength Portland cement:

This cement is used when a high value of early strength is desired. In this type of Portland cement the C_3A content is limited to a maximum of 15% to ensure that the high strength is not mainly as the result of this compound.

- Type IV: Low heat Portland cement:

This type of cement is used when a low heat of hydration or a low rate of gain of strength is desired. Since C_3S and C_3A produce high heat of hydration, their weights are limited to maximum 35% and 7%, respectively. On the other hand since C_2S produces much lower heat of hydration, its content in the cement should be more than 40%.

- Type V: Sulphate resisting Portland cement:

This type of cement is used where the sulphate content of the water or soil in the vicinity of the concrete is high. Since in such circumstances the tricalcium aluminate, C_3A, in the Portland cement is attacked by sulphates, its content is limited to a maximum of 3% in BS4027 [Perkins 1986] or 5% in ASTM C150.

In addition to the above classification, for Portland cement types I, II and III, air - entraining Portland cement types IA, IIA, and IIIA have also been specified respectively.

Air - entraining cements are generally used for providing frost - resisting concrete, improving the workability of the concrete, reducing the water / cement ratio in concrete, reducing segregation and increasing the durability of concrete.

Portland cement may also be found in white and coloured forms. In the producing of white Portland cement , the raw materials are specially selected so that the final product becomes white. To obtain a coloured Portland cement, a

pigment is generally ground in the mix of ordinary Portland cement.
Other types of Portland cement, according to the American description, are Portland Blast-furnace (Type IS), Portland - Pozzolana (Type IP & P) and Slag cement (Type S). [Neville 1983]

2-1-2 High - alumina Cement

This cement was developed by Jules Bied, in France, as a solution to the problem of attack of gypsum bearing waters on Portland cement concrete structures. [Neville 1983] This cement has a rapid gain of strength so that it normally gains about 80% of its nominal maximum in 24 hours. This rate of gain of strength is accompanied by a rapid evolution of heat of hydration. This cement consists of mainly, about 80 per cent alumina and lime. Its colour is much darker than ordinary and rapid hardening Portland cement. [Perkins 1986] High alumina cement is susceptible to ' conversion ', a change of crystalline form, which may result in a considerable loss of strength, particularly in warm or humid conditions. Therefore current codes of practice do not allow engineers to use this product in the structural elements of a concrete structure. [Allen et al. 1993]

2-2 Aggregates

Aggregate used in concrete structures should be obtained from natural resources, complying with BS 882. Maximum size of aggregates used in repairs does not generally exceed 10 mm, and coarse aggregates may be used only in larger works. Since compacting is usually more difficult in repair work than in new structures, both for aggregates and sands, rounded particles show better performance than angular ones. Flakiness index which is covered in BS 882 is an important factor to be considered, as flaky particles decrease the workability of concrete. In order to obtain a dense concrete without segregation or bleeding, good grading of the particles is very important. The presence and the subsequent effects of organic impurities, shells, salts, chlorides and sulphates on the durability of concrete should be carefully considered. The amounts of silt or clay in sands should be limited to the allowed figures in accordance with BS 882, to prevent increasing the water demand of the mix or damaging the bond between cement and aggregate particles. Other special types of aggregates like lightweight aggregates and

specially hard metallic aggregates may also be used in some circumstances. [Perkins 1986] [Allen et al. 1993]

2-3 Admixtures

An admixture is a chemical compound which can be added to a mix of grout, mortar or concrete in order to modify or change some of the properties of an available cement, or to impart some additional desirable properties to it. There is a wide variety of admixtures for different purposes available in the market. Although the effects and properties of each product are normally described by the manufacturer, complete details of action of many of these admixtures have yet to be determined, and the user has to be sure of the performance of each material by carrying out the appropriate tests for the desired properties. The appropriate requirements for admixtures are laid down by ASTM standard C494-79 and by British standard BS 5075: Part 1: 1974. [Neville 1983]
Wherever it is possible to use an appropriate cement for a particular purpose, the alternative use of admixtures should not be considered. Admixtures should not be used with any cement other than ordinary and rapid hardening Portland cement except with the approval of the cement manufacturer. [Perkins 1986]
In the following a brief summary of more common admixtures, namely accelerators, retarders, air entraining admixtures, plasticizers, and superplasticizers will be explained.

2-3-1 Accelerators

Accelerators may be used in cold weather and when a higher rate of development of strength for concrete is required. The most well known accelerator is calcium chloride ($CaCl_2$). This compound has also some undesirable effects when used in concrete, such as a very aggressive corrosion effect on the steel reinforcement in concrete, particularly in prestressed concrete structures. It also has some effect in increasing the drying shrinkage of the mass, reducing the resistance of sulphate - resisting Portland cement to sulphate attack particularly in lean mixes, increasing the risk of an alkali - aggregate reaction for a reactive aggregate, reducing the resistance of air - entrained concrete to freezing and thawing cycles at later ages.
The calcium chloride content in cement should not be exceeded than 2 percent, unless the corresponding test results for the particular circumstances indicate

otherwise.
It should be added that the use of heated concrete or curing the concrete with heat and humidity without using any accelerator is the best way of speeding up the setting and hardening of Portland cement concrete. [Neville 1983] [Perkins 1986]

2-3-2 Retarders

Retarding admixtures may be used to extend the setting time of the cement and slow down the hardening of the paste in a grout, mortar or concrete. Some retarders may also have water reducing effect.
Retarders are usually sugars, carbohydrate derivatives, soluble zinc salts, borax. Owing to the complicated reaction between retarders and Portland cement, the prediction of the period of retardation will only be approximate, therefore great care must be taken in using the quantity of retarders in concrete. [Neville 1983] [Perkins 1986]

2-3-3 Air - entraining admixtures

Air - entraining admixtures are used to produce a large quantity of very small bubbles in the mix of mortar or concrete to increase the resistance of the structure against the effects of frost action. They also improve the workability of concrete, reduce the plastic cracking , segregation and water scouring on the surface of concrete. Resins are introduced as the best air - entraining agents. These materials may be used both in construction or repair works. [Perkins 1986]

2-3-4 Plasticizers

These admixtures may be divided into two groups regarding their action and effects on the mix.
The first group which includes lignosulphonates or lignins, and soaps or stearates act as lubricants and therefore can reduce the amount of water required in the mix to achieve a desired workability. Some of these compounds like stearates may also be referred to as waterproofing agents. It should be added that an excessive amount of these materials may result in a retarding effect or reduction in compressive strength.

The second group of plasticizers includes pulverised fuel ash, powdered hydrated lime, powdered limestone, bentonite, and Portland cement act as finely divided powders. Although these materials increase the workability of the mix, they may also result in a water demand on it. Some plasticizers have been designed so that they can impart more than one effect to the mix, e.g. plasticizers - retarders and plasticizers - accelerators. [Perkins 1986]

2-3-5 Superplasticizers

Superplasticizers may be used for increasing the workability of concrete, or for reducing the water/cement ratio of concrete of normal workability which will result in a very high strength concrete. These admixtures are sulphonated melamine formaldehyde condensates, naphthalene sulphonated formaldehyde condensates, and modified ligno - sulphonates. Among these, the first two groups are preferred, particularly sulphonated naphthalene formaldehyde which appears to be the most effective one.

Superplasticizers are able to increase the slump of concrete up to 200 mm or almost a self levelling concrete. This property is due to their dispersing action on the cement particles. However they have also some retarding effects on the mix. On the other hand superplasticizers can reduce the water demand of the mix for a given workability by 25 to 35 percent. They can also increase the 24 hour strength of concrete by 50 t0 75 percent. It should be added that these admixtures have not any adverse effects on shrinkage, creep, modulus of elasticity, resistance to freezing and thawing, and durability on exposure to sulphates.

The plasticizing action of superplasticizers may last about 30 to 90 min and after this period of time the workability returns to normal condition. [Neville 1983] [Perkins 1986]

2-4 Polymers

Over the past two decades, polymer materials have been used in repair and maintenance of structures. [Allen et al. 1993] Some of their applications include the repair of pavements and bridges, protection of structures and substructures, strengthening of large reinforced concrete beams using external bonding of steel plates, bearing plinths for beams, and crack injections in bridges. [Plum et al. 1988]

Polymer materials used in thin layered systems for the repair and protection of concrete structures may be found in two forms, polymer concrete, PC, and polymer cement concrete, PCC. [Plum 1989] [Plum 1990]

2-4-1 Polymer cement concrete, PCC

Polymer cement concrete, PCC, is produced by combining Portland cement and aggregate with a polymer modifier. PCC is normally used as a repair material. [Plum 1989]

The knowledge of adding certain polymers to cementitious mortars and renders to help solve many problems of unmodified concrete repair materials dates from the early 1950s. The polymers used in PCC for modifying the Portland cement are normally supplied in the form of milky white dispersions in water, latex. The addition of these systems to the concrete may affect the performances of the mix in the following ways: [Allen et al. 1993]

- The polymer dispersions have water - reducing effects which result in a lower water/cement ratios, and thus permit higher strength developments by the cement hydrate mix. [Concrete Society, Tech. Rep. No. 39]
- They improve the bond strength at the interface between the upper layer and the lower layer.
- They increase the tensile strength and flexural strength, and the impact resistance of the repair material.
- They reduce the permeability of the repair material to water, carbon dioxide and oils.
- They may also increase the resistance of the new layer to some chemicals. [Plum 1987] [Allen et al. 1993]

Isenberg and Vanderhoff, in their researches, have reported that the incorporating of polymer latex in a cementitious mortar will form a network of polymer strands which interpenetrate the cement matrix. This is a main factor for increasing the tensile strength of the mix after curing. On the other hand, the incorporation of a polymer latex results in a reduction of water/cement ratio, and hence shrinkage is lower. This again means that the shrinkage micro - cracks are less wide, and then the hardened mass has higher tensile and flexural strength and lower permeability. [Allen et al. 1993]

The polymers used in polymer cement concrete (PCC), include polyvinyl acetates (PVAc), styrene butadiene rubbers (SBR), polyvinylidene dichloride (PVDC), acrylics and modified acrylics.

Owing to a low possibility of releasing free chlorides, polyvinylidene dichloride latexes, PVDC, have not been recommended for repair mortars of reinforced concrete structures. Since polyvinyl acetates latexes, PVAc, may break down under wet alkaline conditions, they are not recommended under wet service conditions or for external applications.

The use of acrylics and styrene butadiene, SBR, as admixtures in concrete repair mortars is more general and if they are well formulated for compatibility with cement, their long term performance for general concrete repair will be satisfactory. [Allen et al. 1993]

Polymer cement concretes, PCCs, with styrene butadiene rubber copolymers, SBRs, have generally very good wear resistance and are widely used in industrial flooring.

Acrylics belong to a widely varying family of monomers and polymers. The range of their properties is very large so that they can be found both in hard resilient materials and very soft products and can keep their flexibility in a well below freezing condition. Their wear properties and resistance to chemicals are very good. However owing to their poor adhesion in wet conditions, an effective and appropriate priming method must be used for the best results. [Concrete Society, Tech. Rep. No. 39]

Polymer modified cementitious concrete, PCC, is mainly used when the thickness of the repair layer is more than 12 mm. However in some instances it may be covered by another protective coating in which case its thickness could be reduced to about 6 mm. [Allen et al. 1993]

2-4-2 Polymer concrete, PC

Polymer concrete, PC, is made by mixing a polymer with a filler, a special aggregate. Polymer concrete may be used as a floor screed, protective layer or repair material. Epoxy resins are the most common polymers to provide the PC in the UK. Epoxy resin materials are produced by combining modified or unmodified resins with a variety of curing agents, hardeners, amines and amidoamines. [Plum 1989]

The two other materials used in polymer concrete in the repair works are polyester and acrylic resins. The two latter ones are more appropriate where rapid strength termosettimg materials are required.

Unlike polymer cement concrete, polymer concrete may be used in layers of

thicknesses of less than 12 mm. Because of their impermeability property and good adhesion to both the steel and the concrete substrate, polymer concretes can also protect the steel reinforcement of the structure by encapsulating it. [Allen et al. 1993]

2-4-2-1 Epoxy resins

Epoxy resins became commercially available after the second world war. Epoxy resins need to be polymerised using an appropriate hardener, cross - linking agent, to obtain their adhesive properties and to form a strong three - dimensional polymer network of cross - links after curing. [Mays et al. 1992]
The curing process consists of hooking up of epoxy resin systems, in which the reactive ' hooks ' are provided by the reactive resin, and the reactive ' eyes ' are provided by the hardener. After all the right number of ' hooks ' must be mixed with the same number of ' eyes '. (figure 2-1) [Allen et al. 1993]

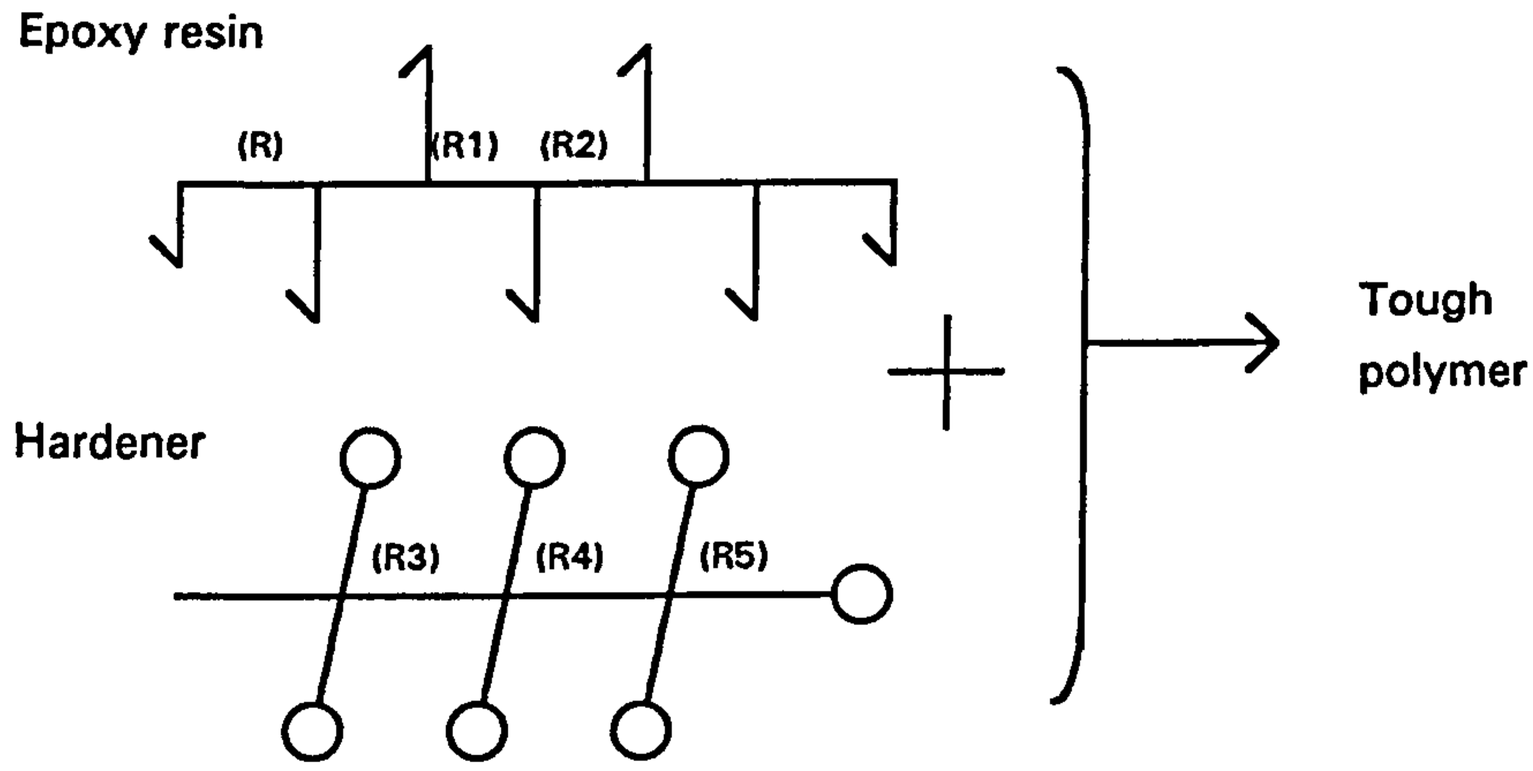

Figure 2-1: Reactive hooks and eyes in epoxy resin systems [Allen et al. 1993]

There are many types of epoxy resins and hardeners available in the market, and therefore it is the task of an experienced polymer chemist to attempt to advise on the formulating of an epoxy resin material for a particular purpose. [Perkins 1986]
The curing of epoxy resin system is based on an exothermic reaction and its rate is directly dependant on temperature. Therefore in a warm weather, the excessive exothermic heat may cause some problems. The minimum temperature for the curing of epoxy resin systems may vary between 0-5 $^{\circ}C$. In the curing of epoxy resin systems, in most conditions, the maximum heat

evolution occurs during the time that the resin is still in the fluid state, and this results in a lower thermal contraction in the repair material. The other good point is that the change in volume between the uncured epoxy resin/hardener mix and the fully - cured one is low and may be even negligible in a carefully formulated case. [Allen et al. 1993] Some other characteristics of epoxy resin systems are as follows: [Perkins 1986]

- Very good adhesive qualities to concrete and steel.
- Chemically resistant against a wide variety of acids and alkalies and other chemicals, except for acids like nitric acids due to their high oxidising characteristics, but quite weak to organic solvents.
- High coefficient of thermal expansion, about 25-30 $\times$ 10^{-6} / $^{\circ}C$ when used as a mortar.
- High compressive, tensile and flexural strength.
- Considerable loss of strength at high temperatures, at more than 80$^{\circ}C$.
- High rate of gain of strength.
- Quite low fire resistant compared with concrete.

2-4-2-2 Polyester resins

The use of unsaturated polyester resins dates from the mid - 1930s when they were initially used in formulating lacquers, especially for wood finishing and low pressure laminating resins. Now polymers may be employed in a wide range of industries. [Concrete Society, Tech. Rep. No. 39]

The main difference between polyesters and epoxy resins is that in polyester resins, the liquid resin component consists of both the ' hooks ' and the ' eyes '. However the ' hooks ' are ' blocked ', and therefore once again a hardener, catalyst, based on organic peroxide, is required to initiate the ' unlocking ' of the hooks in order to start and promote the cross - linking process throughout the resin. (figure 2-2) [Mays et al. 1992] [Allen et al. 1993]

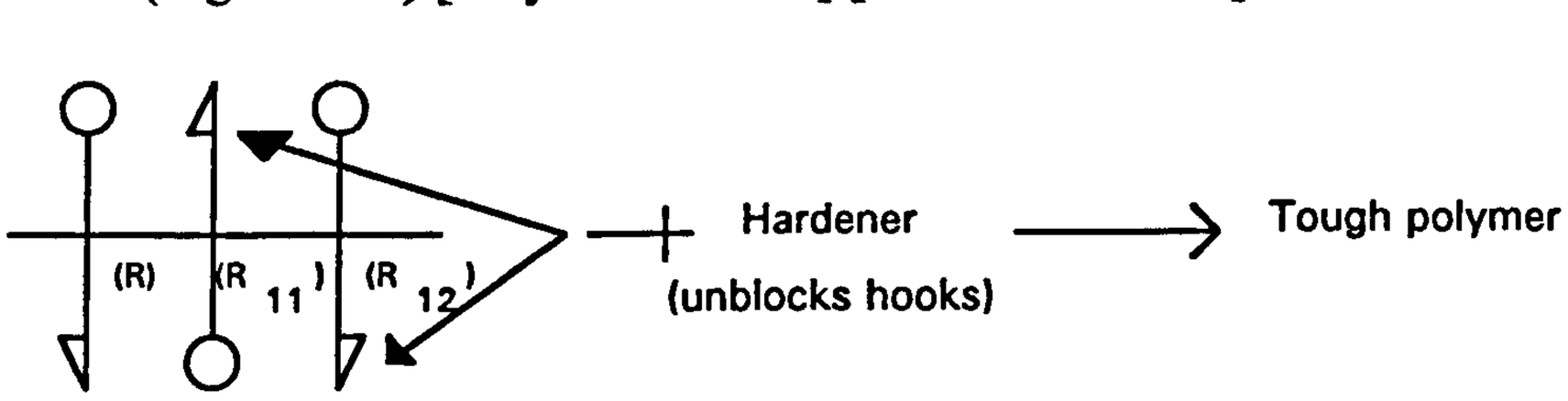

Figure 2-1: ' Hooks ' and ' eyes ' in polyester resin [Allen et al. 1993]

Unlike the epoxy resins, in the polyester resin systems the maximum heat

evolution occurs after setting the resin and this can result in a considerable thermal contraction. Consequently such a thermal contraction induces a high value of stresses at the interface with the substrate which may result in a delamination. Moreover, the curing shrinkage or the degree of volume change between the mixed, uncured polyester resin and the fully cured one is not negligible. Because of the above reasons, the use of polyester resin is to be limited to the relatively small areas/thicknesses at one time. [Allen et al. 1993]

These systems do not show a good creep resistance under sustained loads and their bonding performance under wet or damp conditions may also be poor. [Mays et al. 1992] However they may be formulated so that they can have a very rapid gain in strength. As an example, polyester resin systems have been used with aggregate/binder ratios up to 11/1 by weight for more than 20 years for airport runway repairs. [Allen et al. 1993]

Some formulations of polyester resins may also be used in sub - zero temperatures. The coefficient of thermal expansion for polyester resins may be in the range of $25 - 35 \times 10^{-6} / {}^{\circ}C$ compared with $7 - 12 \times 10^{-6} / {}^{\circ}C$ for a Portland cement mortar. [Perkins 1986]

2-4-2-3 Acrylics

The use of reactive acrylic resin systems have been widely increased in the construction industry over recent years. The most common type of these resins is methyl methacrylate monomer, MMA, which is cured by similar mechanisms to the unsaturated polyester resins. Since the viscosity of the uncured acrylic resins is very low, they can be very highly loaded by fillers and therefore they can produce mortars having less shrinkage effects than those based on unsaturated polyester resins. So the use of acrylics in heavily filled floor toppings is typical.[Concrete Society, Tech. Rep. No. 39] [Allen et al. 1993]

As an undesirable point, it should be added that the methyl - methacrylate monomers are volatile with a strong odour and they are also highly flammable with flash points below $10 {}^{\circ}C$ and therefore should be very carefully handled. [Concrete Society, Tech. Rep. No. 39] [Mays et al. 1992] [Allen et al. 1993]

2-4-3 Polymer bonding aids

The use of certain polymers for the improvement of bond strength between a

new and old concrete, either alone or mixed with cement, dates from the early 1960s in the UK and even earlier in the US.

Bond strength at the interface between the concrete and the repair or protecting material is very important, as it is likely to be subjected to high values of stresses arising from many factors. Prior to the introduction of polymer bonding - aids, the engineer had to rely on the preparation of the surface of the concrete, or to use a cement slurry. Despite giving excellent results in the laboratory, both techniques were often faced with problems in the field. [Perkins 1986]

Materials which are to be formulated as bonding aids for concrete repair must be stable in a relatively high alkaline environment and have a minimum film - forming temperature of $5^{\circ}C$. [Mays et al. 1992] It would therefor be pertinent to refer to the definition of ' Minimum Film Forming Temperature (MFFT) ' at this stage:

" When a polymer latex is applied as a thin film, the water evaporates and capillary action draws the particles together. When the ambient temperature is above what is known as the Minimum Film Forming Temperature (MFFT) of the polymer latex, the polymer particles can coalesce, because the repellent forces between the discrete particles produced by the surface - active agents are overcome. " [Concrete Society, Tech. Rep. No. 39]

Polyvinyl acetate (PVA), styrene - butadiene rubber (SBR), and acrylics are in more general use in the UK. [Perkins 1986] Other materials are styrene acrylates, polymer latex bonding aids, and epoxy resins. [Mays et al. 1992] [Allen et al. 1993] Since the PVAs are likely to be moisture susceptible, they are likely to be used in non - structural works. Acrylics and styrene acrylates show better resistance to water in this respect. It may be also said that the acrylics are less sensitive to premature film - forming in drying conditions in comparison with SBRs. For this reason, the use of polymer bonding aids has been restricted to acrylic systems by the Department of Transport in their specification on concrete bridge repair. In contrast with this, SBR cement bonding agents are much better and have generally successful performance. [Mays et al. 1992]

The use of SBR/cement slurry as a bonding aid in concrete repair works may help to lessen the effects of variation in workmanship and site conditions, particularly the effect of weathering, on the bond strength. The high pH of SBR/cement slurry, about 12.0, is also helpful with respect to its passivation effect on the rebars in concrete repairs. [Perkins 1986]

The neat or diluted latex can be used without cement in the form of relatively thin films. However, this coat has a lower tensile strength compared with systems containing ordinary Portland cement. Latices combined with cement in proper ratios produce reasonably resilient and strong bond coats. [Mays et al. 1992]

Epoxy resin bonding systems specially formulated for bonding green uncured concrete to cured concrete provide very good bond at the interface. The epoxy bonding aids may also be used as a barrier between the repair mortar and the concrete substrate. In these cases, two coats of the bonding aid are employed and for ensuring an excellent mechanical key between the two coats, each coat is dressed with clean sharp sands. [Allen et al. 1993]

CHAPTER 3

APPLICATIONS AND FAILURE CAUSES OF THIN LAYERED SYSTEMS

Applications of thin layered systems in concrete structures

Failure causes in thin layered systems

Conclusions

3-1 Applications of thin layered systems in concrete structures

3-1-1 General uses of thin layered systems

Owing to the advantages of concrete, many structures are made from this material. On the other hand no concrete structure could be built under ideal conditions. Therefore, defects in concrete structures may occur for many reasons. Poor workmanship, inappropriate materials, unsuitable concrete mix design, hostile environment, fire, impact, explosions are some reasons for defects of concrete structures. Obviously in many circumstances, the deteriorated structure can be repaired. A repair may be required in patches or in large areas. A structure may be also protected or strengthened against some predictable causes of defects.

Thin layered systems may be used in repair, protection or strengthening of concrete structures in various fields of the construction industry. Some common uses of thin layered systems are as follows:

- Protection, upgrading and rehabilitation of the floor slabs as the principal use for which modern thin layered systems are designed. [Plum July 1990]

-" Restoration of appearance of the structure. " [Plum 1987]

- Protection of the reinforcing steel of the concrete structure against atmospheric/chemical attack and bond restoration. [Plum 1987]

- Providing a wear resistance surface under the traffic anticipated. ' [Plum 1987]

- Impermeability, skid resistance, and water shedding properties: [Plum 1987]

-" Impermeability, in which reducing water, chemical penetration or carbonation is a priority. " [Plum March 1989] [Plum Sept. 1990]

- Thin layered systems may be also specified to meet a need for a quiet, hygienic wearing surface at moderate cost. [CIRIA 1985]

- A thin layered system consisting of PC materials may be installed with

minimal disruption to traffic. [Sprinkel TRR 899]

- Concrete strengthening by using externally bonded reinforcement

3-1-2 Specific examples of applications of thin layered systems

Here it is intended to present some specific examples along with the views of different investigators regarding the use of thin layered systems:

Many investigators have considered using thin layered systems for the protection and repair of concrete bridges, parking garages and other vehicle and pedestrian decks:

- According to Sprinkel [Sprinkel 1984], the installation of several thin polymer concrete overlays on portland cement concrete bridge decks has proved that such overlays of low permeability and high skid resistance can be installed successfully with a minimum of disruption to traffic and at a reasonable cost. The work can be done by a contractor or by maintenance forces. [Sprinkel 1984]

- Modern barrier coat systems with crack - bridging properties have been formulated for the protection of concrete slabs of bridges and motorway troughs against the effects of water and thawing agents with particular attention to the adhesion between barrier coat and concrete. [Bundies 1986]

- The application of thin polyester - styrene overlays is very efficient on a large scale. Since they are effective in thin layers, the dead load on the portland cement concrete overlaid bridge is reduced and also the usual need for modifications to barrier rails and sign structures is avoided. Other advantages include impermeability to water and salts, being highly abrasion resistance, rapid return of the structure to service. With regard to the above, most of the polyester - styrene concrete overlays on state roads and bridge decks placed by The California Dept. of Transpiration have been performing well. [Krauss 1988]

- Kudlapur et al. [Kudlapur et al. 1989] carried out an investigation on the performance of several materials for using as cold weather patching materials. According to their results, methyl methacrylate (MMA), and water based magnesium phosphate concrete (MPC) can be recommended when patch performance, specially durability, is of primary importance. MMA concrete may be used in the presence of moderate surface moisture, whereas MPC

concrete, particularly the water based, should be applied to dry surfaces as far as possible. If the patch is protected from water penetration, subfreezing application of water - based magnesium phosphate can be also recommended for a period of not more than about five years. [Kudlapur et al. 1989]

- Among many other buildings and civil engineering structures, roads and bridges are exposed to a greater number of damaging elements. The durability of these structures is reduced by atmospheric pollution, chemical spillage, deicing salts, frost and physical damage. The existence of durable, rapid curing, high - strength gain and low shrinkage new materials enabled the contractor to apply a waterproofing membrane on some bridges carrying the M1 motorway within four hours of completing the repair. As another example of such a work in the UK is resurfacing a major road tunnel in London by using a layer of high speed, self levelling mortar. [Anon 1990]

- The repair for several existing conventionally reinforced, cast - in - place parking garages was carried out by using complete bonded overlays. The deterioration including cracking, delamination, spalling and rust staining were mainly due to the corrosion of the embedded reinforcing steel. Oxygen, moisture, and salts can penetrate into the concrete and cause the reinforcing steel to corrode. The expansion resulted from the resultant corrosion product may cause splitting stresses and consequently cracking and spalling of the concrete. [O'Connor et al. 1990]

- Resins made from recycled polyethylene terephthalate, PET, recovered from scrap beverage bottles, can be used for producing polymer concrete, PC, at a lower cost and with adequate properties. Thin polymer concrete overlays can be applied on portland cement concrete and provide a wear and acid resistance surface with low permeability. Polymer concrete overlays are lightweight, bond strongly to the concrete substrate, and cure rapidly. [Rebeiz et al. 1991] [Rebeiz and Fowler 1991] [Rebeiz et al. 1993]

- Deterioration of traffic - bearing concrete structures owing to corrosion of steel reinforcement as a result of penetrating water and chlorides is a growing destructive problem. It has been proved that traffic bearing waterproof membrane systems can be used as an effective method of providing longer service life for both new and existing traffic decks. Among many types of these systems available in the market, built - up layers of liquid - applied materials are the most widely used. These materials can waterproof the concrete surface, and bridge minor cracks. They also incorporate special aggregates to provide a wear and skid resistance surface. [Reagan 1992]

- Sprinkel, in 1993, has shown that multiple - layer epoxy and premixed polyester styrene overlays constructed with graded silica and basalt aggregate can be used as skid resistance and protective systems against intrusion by chloride ions for 15 to 20 years. This is also an economic method for extending the service life of black steel reinforced concrete decks, specially when overlays have to be installed during off - peak traffic periods to minimize interruption to motorists. [Sprinkel 1993]

- Alberta Transportation and Utilities (AT & U) has waterproofed 66 bridge decks with thin polymer wearing surfaces since 1985 in order to reduce the rate of deterioration result from the penetration of chlorides and water, and consequently to increase the service life of the bridge decks. The temperature conditions and average freeze thaw cycles varied from $45^{\circ}C$ to $-45^{\circ}C$ and 69 to 135 cycles per year, respectively. According to this experiment the following conclusions regarding the use of the thin layered systems have been made: [Carter 1993]

1- Thin polymer wearing surfaces can provide service lives of up to 20 years providing that they are properly applied.

2- These systems can extend the service lives of existing bridges in high salt environments containing non - coated steel reinforcement even if some corrosion has began before the repair.

3- The systems are economically competitive with other repairs, particularly when overlays less than 10 mm are required.

With regard to other uses of thin layered systems such as impermeability against water, chemical penetration or carbonation, crack repair, surface repair etc., the following examples are presented:

- Fukushima et al. in 1986 carried out an investigation on the protection effects of polymeric finishes on concrete carbonation and reinforcement corrosion. It was concluded that polymeric finishes are effective enough in the retardation of concrete carbonation and the suppression of reinforcement corrosion in neutralized concrete without chloride ions under ordinary atmospheric environmental conditions. [Fukushima et al. 1986]

- A low shrinkage polyester mortar coating was used successfully on the surface of Portland cement concrete under intense heat of summer as well as temperature of several degrees below zero. The coating was highly adhesive, impermeable, waterproof as well as abrasion, impact, weathering and chemical resistant. It was also crack resistant and could resist hardened contraction

stress and thermal stress without cracking. In addition to the above advantages, its cost was three times less than a granitic floor with a construction rate 6 times faster. [Xian-Neng 1986]

- As a solution to the decontaminable flooring problems at the Susquehanna plant, Pennsylvania Power and Light, a high - strength acrylic industrial floor known as Silikal was installed on the dustless scabbled substrate surface. The resurfacing material for the floor was a self levelling system which cures in one hour. It consisted of a 4 mm pigmented base coat on a single coat of primer. Within two hours of completion, chemical could be delivered and stacked on the new floor system. [Anon 1989]

- Flexible membranes may be used for preventing the leakage through cracks in concrete water treatment tanks. This can be done by spanning the deteriorated area with a flexible sheet membrane which is properly attached to the concrete some distance from either side of the crack. [O'Connor et al. 1990]

- A thin layer of concrete repair products and protective barrier systems can be used for addressing the problems regarding hazardous materials, chemical wastes, temperature, and other environmental effects which may reduce the ability of concrete structures for maintaining positive containment. The availability of a wide range of monolithic coating and lining systems today has made it possible to protect secondary containment structures against almost all types of environments and chemical wastes. [Hazen 1991]

- Thin polymer concrete overlays provide very good abrasion - resistant surface in hydraulic structures such as dams and harbours. [Rebeiz and Fowler 1991] [Rebeiz et al. 1993]

- Thin polymer concrete coatings can be applied on horizontal, vertical, and irregular surfaces by using shotcrete equipment. The overlay can protect steel or chemical tanks, utility boxes, piles, and sewer pipes against aggressive liquids, hazardous wastes, and other corrosive actions. Owing to its low thermal conductivity and high damping characteristic, it can be also used as a good thermal and sound insulating coating. [Rebeiz and Fowler 1991]

- Concrete buildings can be damaged by fire. The extent of damage is dependent on many factors such as condition of the structure and intensity of the fire. Spalling or detachment of pieces of concrete parallel to the surface, and sloughing or the separation of concrete at some internal plane of weakness are two types of damages which may occur near the surface of the structures due to the heat generated by the fire. For these surface repairs, where the steel reinforcement is not involved, many of high performance materials like latex

modified cements may be designed to be troweled or poured into place. [Dorsch 1993]

- It is essential for a sewer reinforced concrete pipe to have excellent durability, especially chemical resistance, and high strength. Kawakami et al., in 1993, proposed and tested a precast composite sewer pipe, in which a reinforced concrete pipe was lined with polymer mortar as soon as centrifugal compaction and drainage had been completed. The results obtained by their study showed that because of the high extendibility of polymer mortar, it could protect the interior part of the structure, even if the pipe deforms and the concrete is cracked. The lined polymer offered chemical resistance to acidic and alkaline water, and also excellent abrasion and flatness which is very helpful from the viewpoint of hydraulic engineering. [Kawakami et al. 1993]

- Water is always a contributing factor in all deterioration process of concrete, except perhaps for abrasion. Chloride ions and sulphates are conveyed by water into the concrete and provide the electrolyte for corrosion. Since concrete has limited performance in preventing the passage of water, damp - proof membranes are provided for tank concrete and special precautions are taken for water - retaining structures or basements. [Cather et al. 1995]

Another type of application of thin layered systems is concrete strengthening by using externally bonded reinforcement:

Strengthening concrete members can be made by adding external reinforcement, by external post tensioning, or by a combination of these. In this regard, strengthening concrete beams by using an externally bonded steel plate is a promising method. [Hamoush et al. 1990]

The first reported application of this technique was in France in the late 1960s, where a major bridge strengthening scheme on the Autoroute due Sud was carried out. [Mays et al. 1992] A detailed historical development of this method can be found in Refs. [Mays et al. 1988] and [Mays et al. 1992].

The technique has been used to strengthen or repair bridges and buildings in many countries around the world. Epoxy - bonded steel plate technique has been used for repairing bridges damaged by accident, fire, or explosion. It has been also used for strengthening bridges with insufficient load carrying capacity owing to increased load requirements or a design or construction error. The principle of this method is very simple: steel plates are bonded to overstressed regions of reinforced concrete members using an adhesive. The steel plates are normally used in the tension zone of a beam, however, they

have been utilized in the compression and shear zones as well. The shear connection between the reinforced concrete beam and the steel plate is provided by the adhesive. The addition of plates in the tension zone increases the area of tension steel and lowers the neutral axis. The result is a reduction of live - load stresses in the existing reinforcement. In other words a tension plate can effectively increase the flexural stiffness, and therefore reduce cracking and deflection of the member. [Eberline et al. 1988]

- The results of an investigation carried out by Van Gemert et al. proved that the technique of epoxy bonded external steel reinforcement is a reliable and fast repair method, both under normal laboratory condition and atmospheric and sustained loading conditions. [Van Gemert et al 1986]
- The application of the technique of glueing flatsteel components to existing reinforced concrete structures for modifying their load bearing capacities showed promising performance under the action of fatigue loads. Negligible loss of space, " dry " application, and minor disturbance during working hours are some advantages of this method. [Holtgreve 1986]
- Bonded steel plates were used for the reduction of fatigue stresses of coupled tendons in the continuous post tensioned multispan Autobahn - bridges in the Federal Republic of Germany. The working joints of many of these bridges, where all tendons were coupled, were cracked and therefore, the fatigue stresses in the prestressing steel at the joints increased markedly. The strengthening program which was necessary to prevent premature fatigue failure proved to be efficient and economical as well. [Ranisch et al. 1986]
- The technique of strengthening of concrete structures in flexure with externally epoxy - bonded fibre - reinforced plastics (FRP) is also becoming increasingly popular. The FRP laminates are made of continuous fibres such as glass, carbon, aramid. The laminates are bonded with a polymeric matrix such as epoxy. The advantages of this method compared with bonding of steel plates or post tensioning techniques include the immunity to corrosion and efficiency of application. Strengthening of the Kattenbusch bridge in Germany by using glass - fiber - reinforced plastic (GFRP) plates, strengthening of the Ibach bridge in Switzerland by using carbon - fiber - reinforced plastic (CFRP) sheets, the retrofit of bridge columns in California by using GFRP jackets, and finally the retrofit of tall chimneys in Japan by using CFRP tapes and winding strands are some examples of applications of this technique. [Plevris et al. 1995]

3-2 Failure causes in thin layered systems

Except for the failures owing to the lack of a good workmanship, improperly formulated materials or mix proportions, in all cases, the failures stem from the loading effects. So the causes of failures and the loads are linked together.
In general the causes of failures in a thin layered system may be classified as follows: [Plum July 1990] [Plum Sep./Oct. 1991] [Plum Nov./Dec. 1991]

- Concentrated and static loads
- Moving loads
- Thermal shock and thermal stress
- Impact shock
- Reflective cracking
- vapour pressure
- Shrinkage
- Expansion due to temperature, humidity, swelling
- Freeze/Thaw cycling
- Water and moisture in the substrate
- Incompatibility of the repair or protective material with the concrete substrate

3-2-1 Concentrated and static loads

The supports of machinery, frameworks and furniture, particularly when the contact area is small, may produce a contact pressure as high as 5 MPa. [Plum Sep./Oct. 1991] Although this pressure may not be dangerous itself, the tensile stresses which tend to an interface separation in the vicinity of the load, might be critical for the system. (figure 3-1)

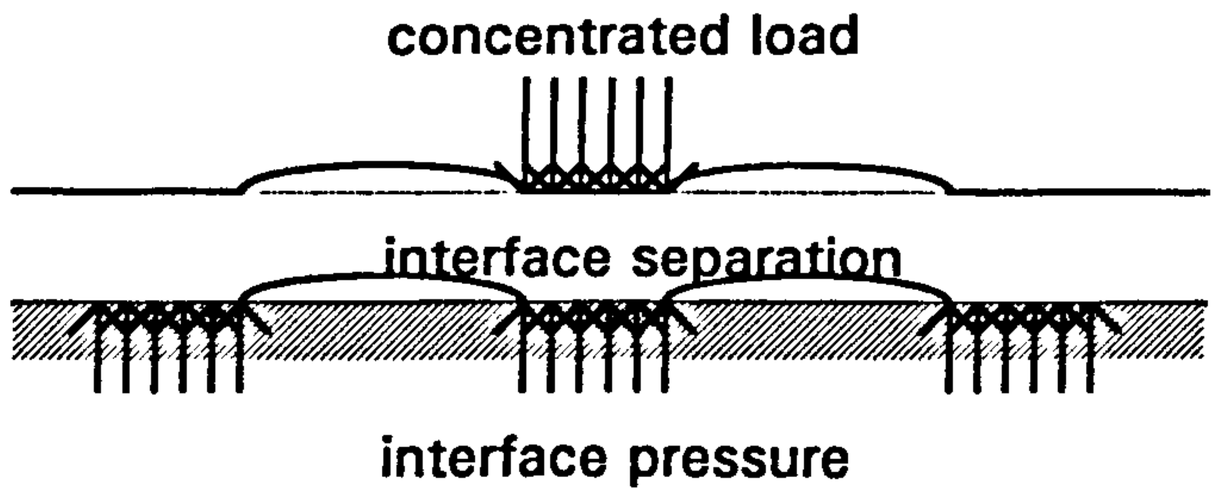

Figure 3-1: Effect of concentrated static loads [Plum Sep./Oct. 1991]

Tests have been done under the action of line load and concentrated loads, and indicate the existent of the tensile stresses at the interface. In this experiment the main failure mode was cracking and crushing of the concrete substrate by

compression. A few bond failures also occurred before the substrate cracked or crushed. [Li 1990]
The results of the an investigation carried out by the author was also consistent with the existence of tensile stresses at the interface in the vicinity of the vertical load. [Sohrabi 1993]

3-2-2 Moving loads

There are three kinds of moving loads: Rolling loads, braking or accelerating loads and cornering loads.

- Rolling loads

Rolling loads may be visualised as moving wheeled furniture on a carpeted floor (figure 3- 2). [Plum July 1990]

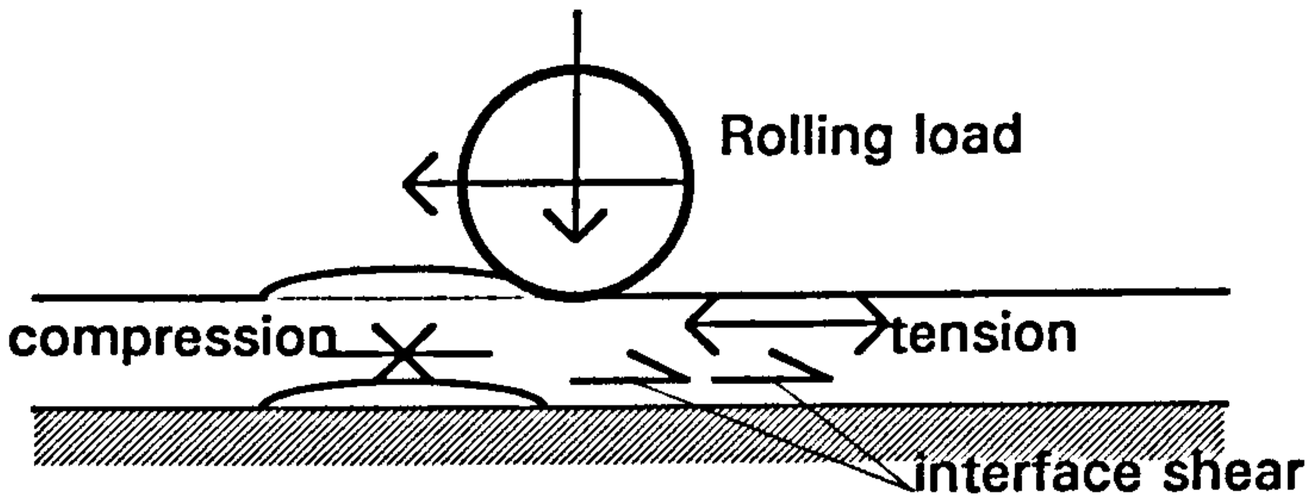

Figure 3-2: Effect of Rolling loads [Plum July 1990]

In this case the system is subjected to a combination of the vertical and horizontal forces which may produce tensile stresses like those shown in (fig 3-2). It is evident that the contact area between the tyre and the surface will affect the values of the stresses.
No theory appears to be developed to cover this situation. [Plum July 1990]
Rolling loads may be divided into two groups: solid rolling loads, and pneumatic rolling loads.
The behaviour of thin layered systems under the action of a solid (steel) wheel rolling load will be studied in chapter 6. As it will be seen in that chapter, a solid rolling load can induce high values of shear stresses at the interfaces of a thin layered system which could result in a delamination. This is consistent with the result of a questionnaire prepared by Choi [Choi 1991]. (figure 3-3)
In chapter 7, the behaviour of thin layered systems under the action of a pneumatic rolling load will be considered. As it will be seen in that chapter,

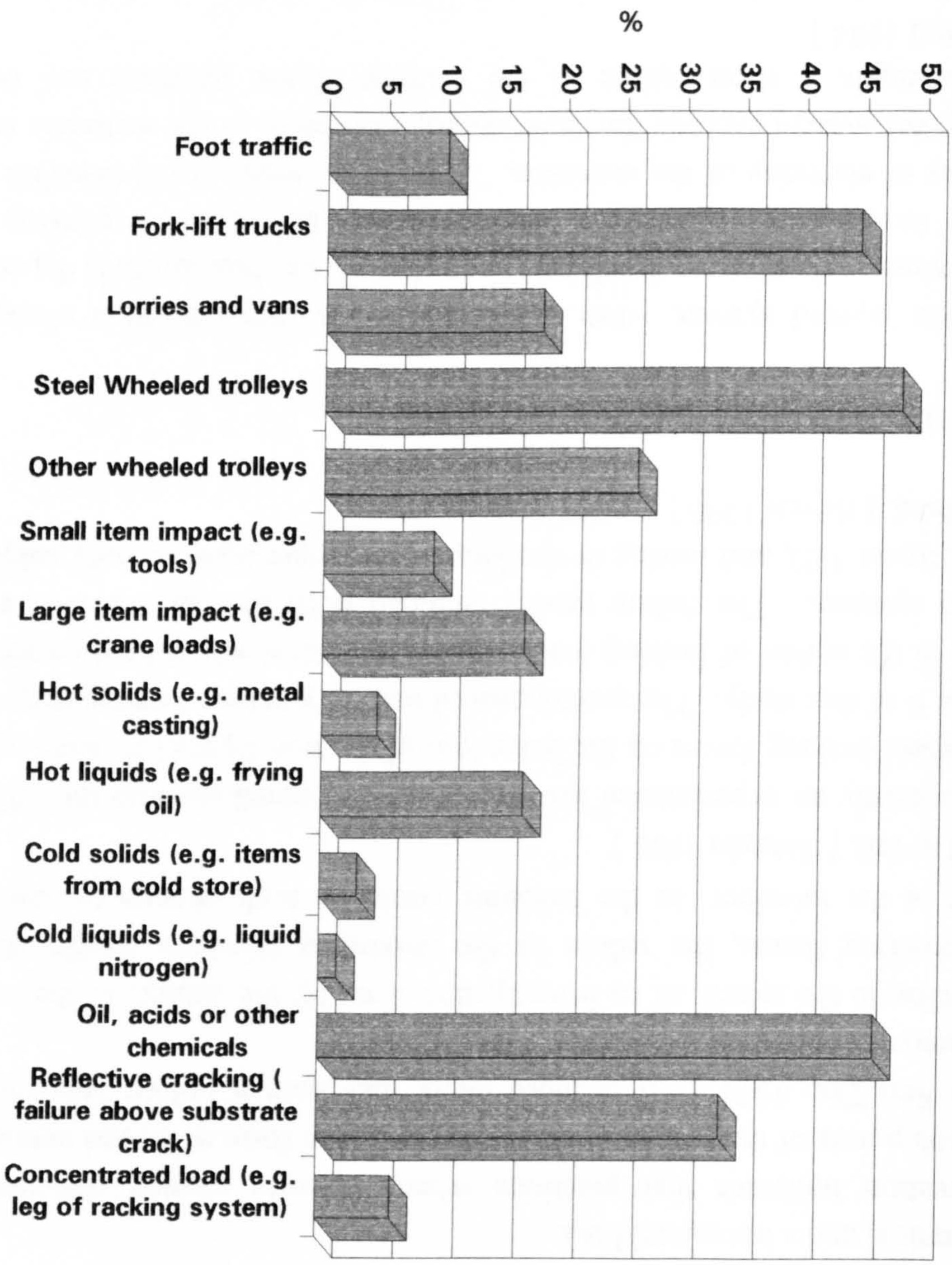

Figure 3-3: Cause of failure [Choi 1991]

no delamination is predicted under such a load. This is consistent with the results given by other investigators. [Lau et al. 1994]

- Braking and cornering loads:

In both cases, braking and cornering, the system is subjected to a combination of a vertical and a horizontal load.

Observation indicates that positions where vehicles change direction are common points of the failure of floor screeds in the form of screed debonding. [Plum Sep./Oct. 1991] It is more likely that such a failure happens in a warehouse owing to the cornering of the lift trucks.

According to the results of an investigation done by the author, in the case of the cornering forces, the values of the maximum principal tensile stresses (σ_{1max}) at the interface, in the substrate could be high enough to cause the screed to fail. [Sohrabi 1993]

More recently an experimental investigation was carried out into the effect of steel wheel braking forces on the behaviour of the thin layered systems used in chapter 6 of this study. The results proved that very severe damage may occur owing to the action of braking loads caused by a steel wheel load on the thin layered systems. The failure modes included delamination, wave or carpet effect (figure 3-2), and tearing or cracking of the upper layer directly subjected to the load. [Samin 1996]

3-2-3 Thermal shock and thermal stress

In a thin layered system, when the composite is subjected to a change in temperature, a shear stress develops. The value of the shear stress is dependent on the temperature change and the coefficient of thermal expansion and modulus of elasticity of the materials. If the shear stress at the interface of a two layered system exceeds the shear strength of either of the materials or the bond strength, a shear failure in the vicinity of the interface can occur. [Sprinkel 1984]

The effect of a sudden temperature rise or fall in a floor screed is known as thermal shock. Thermal shock may result from a hot or cold liquid or solid being spilt or placed on the screed. A temperature rise over $250^{\circ}C$ on pure polymer screeds could result in softening, removal of volatiles and charring of the binder materials. Temperature rises in the range of $100^{\circ}C$ to $200^{\circ}C$ will result in a rapid expansion, which in turn may cause the screed to buckle or to

delaminate. On the other hand, coming into contact with the surface of the screed, a very cold item can cause a rapid contraction, which might lead the screed to curl. [Plum July 1990] [Plum Sep./Oct. 1991]
The results of an experimental research showed that the direction of the curve was not predictable. (fig 3-4) [Surat 1990] According to this and another research, materials respond at different rates depending on their thermal conductivity. [Plum July 1990] So it seems that the behaviour of the materials under the condition of a thermal shock is too complex to be modelled by a theoretical approach.

Figure 3-4: Curling and debonding of the screeds due to the thermal shock
Mwape, in his research, has concluded that in most cases, the bond strength has not been affected by the thermal shock experiments. [Mwape 1990]

3-2-4 Impact shock

Impact shock is the effect of a heavy object falling on the screeds, which might result in a delamination at the interface. [Plum Sep./Oct. 1991]
Mwape [Mwape 1990] and Floros [Floros 1991] carried out two experimental works on the event of impact shock. Both of the investigators used the BRE screed tester for carrying out the impact shock. After the impact loading, the direct tensile strength of 20 mm diameter cores was measured by using the elcometer pull - off tester. [Mwape 1990] [Floros 1991]
In Mwape's tests, there was a relatively great scatter of results. However the number of failures at the substrate were more than those in the mortars. [Mwape 1990]
In the Floros' tests, most of the samples failed at the mortar and few at the concrete substrate. [Floros 1991]
The works of the above investigators were then examined, attempting an explanation, using the finite element method and the conclusions can be found in the Appendix. [Sohrabi 1994]

3-2-5 Reflective cracking

Joints or cracks in a substrate may produce erratic reflective cracks in the upper

layer. (fig 3-5) This phenomenon may occur as a result of traffic movement, thermal expansion and contraction, or temperature gradient in the vicinity of the substrate edges. [Plum Sep./Oct. 1991] [Rigo et al. 1993]

Four solutions have been suggested to this problem:

The first one is to inject the crack prior to resurfacing the substrate. In this way the situation may be improved, but it will not be guaranteed against the further tensile movements. [Plum July 1990]

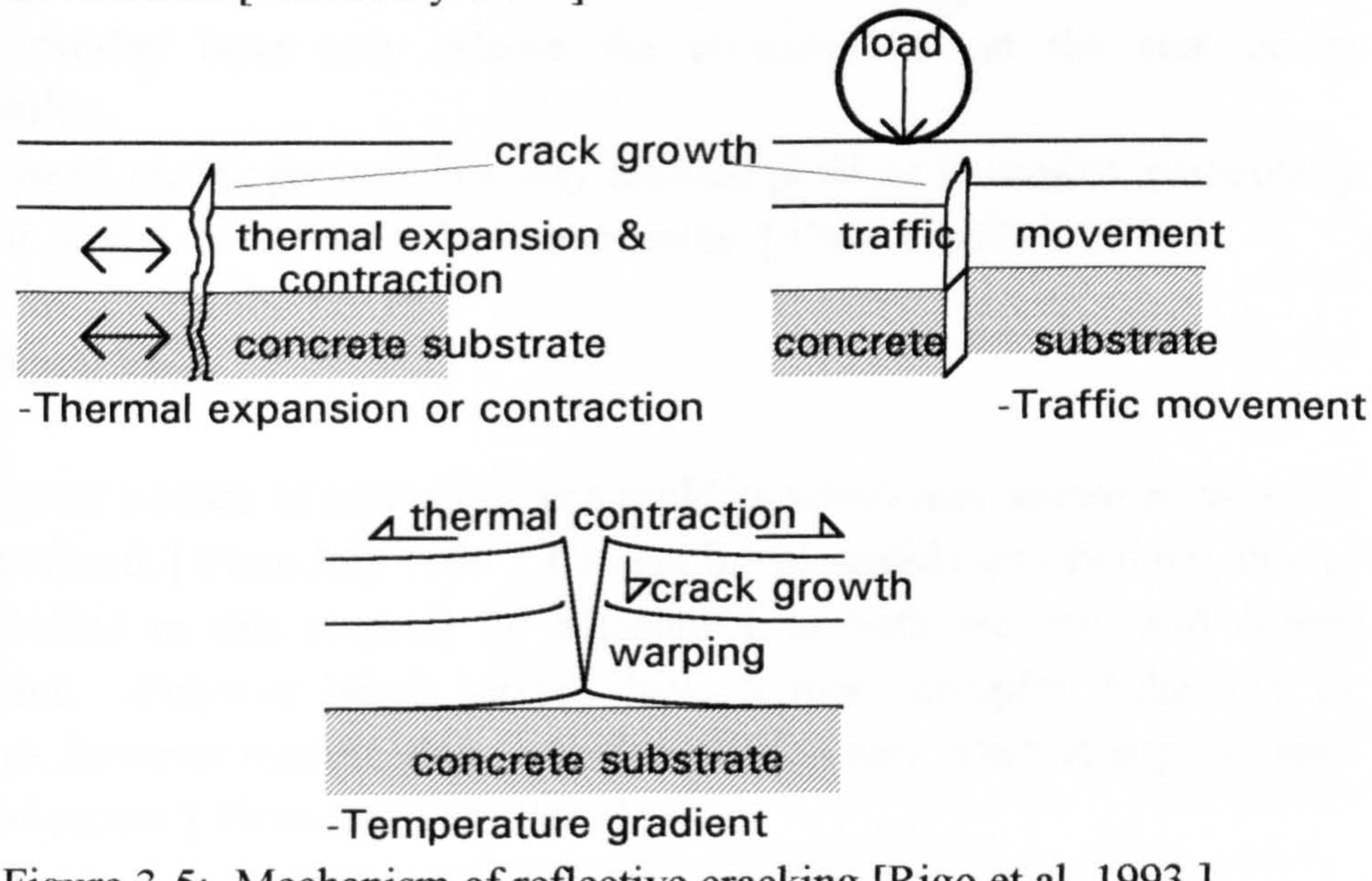

Figure 3-5: Mechanism of reflective cracking [Rigo et al. 1993]

The second one is to use a debonding strip (figure 3-6) in the vicinity of the substrate crack. However this, in turn, may act as a factor which can initiate debonding in the case of existing a high value of tensile stress at the interface. [Plum July 1990]

The third one is to allow the crack movement to continue by using crack inducers wherever possible. (figure 3-7) But the solution is not always effective. [Plum July 1990]

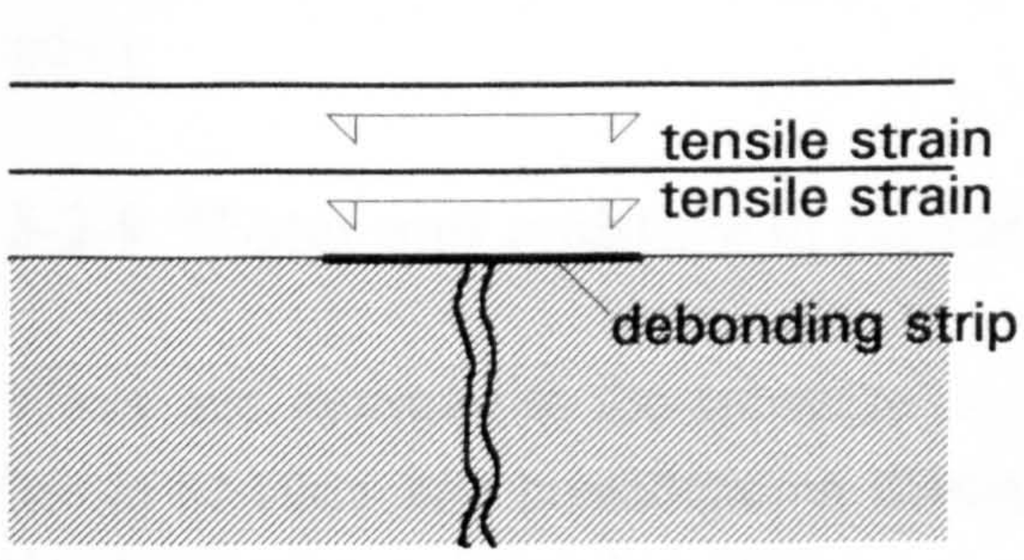

Figure 3-6: Debonding strip

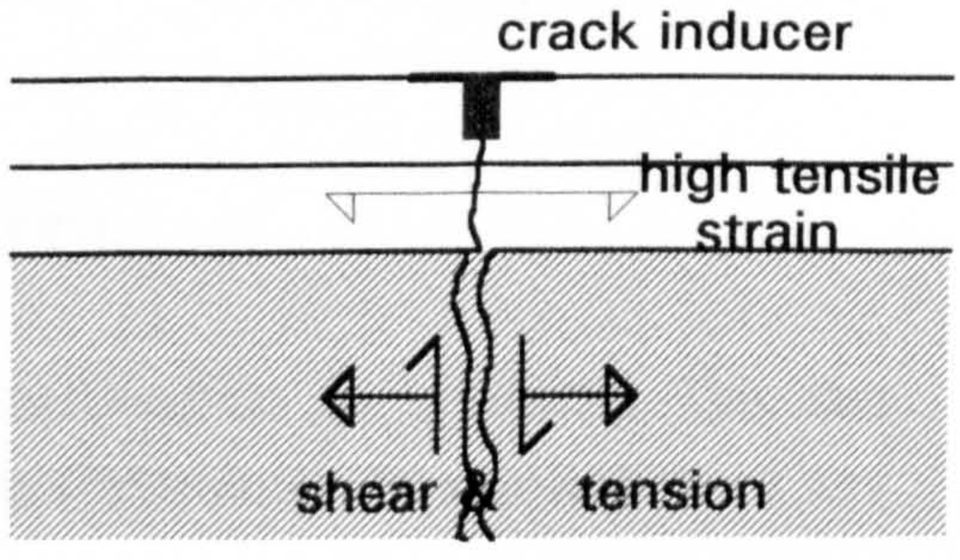

Figure 3-7: Crack inducer

Thickening the basecoat and using a light mesh of reinforcement in the vicinity of the crack may also improve the phenomenon, however this kind of treatment must be proved first. [Plum July 1990]

3-2-6 Vapour pressure

Vapour pressure beneath a thin screed can cause blistering. The use of a more porous overlay layer may release the pressure, but at the cost of its permeability.
So in general vapour pressure is a very difficult problem to combat, particularly when the screed is required to be impermeable. [Plum Sep./Oct. 1991]

3-2-7 Shrinkage

Shrinkage as a cause of separation, is a problem which may appear at the early age of a screed. [Plum July 1990] Cement based screeds are often possible to be controlled in this respect, by adjustment to both the mix and curing procedures. Polymer based screeds have a more complex behaviour in shrinkage, however modification to the formulation may result in improvement to a good extent. [Plum Sep./Oct. 1991]

3-2-8 Freeze/Thaw cycling

Freeze/Thaw cycling of the cementitious based screeds may result in failure, either by break-up the materials or by delaminating of the upper layer. [Plum July 1990]
With respect to the PC overlays, Sprinkel, in his research, concluded that the thermal cycling in a real case may be sufficient to cause delamination and eventual failure of the overlays. He noticed thermally induced cracks in the overlay, in the substrate and in the bond interface layer as well. [Sprinkel TRR 899]

3-2-9 Water and moisture in the substrate

Water and moisture in the substrate can greatly affect the adhesion. This fact has to be taken into consideration during the formulation or application of any thin barrier layer. [Bundies 1986]

In constructing a thin polymer wearing surface for preventive maintenance of bridge decks, the moisture content of the concrete substrate is a main factor for achieving proper bond strength to the deck. The existing moisture in the deck may react with the resin and consequently prevent bond strength development. [Cater 1993]

3-2-10 Incompatibility of the repair or protective material with the concrete substrate

The potential property mismatch between a repair material and its concrete substrate may cause concern. Since the repair material contracts during the curing period relative to the concrete, short term problems may arise. In a resin based mortar, the contraction is due to the cooling which occurs after the exothermic reaction, whereas a water - based cementitious material may contract during the drying shrinkage. The result of curing contraction may induce initial tensile strain in the repair or cracking at the interface. Different elastic modulus and different thermal movements between the repair and substrate concrete are other forms of incompatibilities which may create problems. [Mays et al. 1992] For example the coefficient of thermal expansion for polymer concrete is more than twice that of portland cement concrete which necessitates a careful examination of the effect of composite action between the overlay and the deck in a bridge subjected to temperature loads. [O'Connor 1993]

3-3 Conclusions

In the first part of this chapter some general uses of thin layered systems and some specific applications were presented. Considering the contents of this part of chapter 3, one can conclude that thin layered systems are in fact known as systems for the repair and protection of concrete structures in various fields. In the second part of this chapter some causes of failures in the thin layered systems were reviewed. The results of the survey carried out by Choi in 1991 [Choi 1991] showed that rolling loads are the most anticipated types of failure causes in the thin layered systems. [Choi 1991] Owing to the importance of these types of loads, studying the behaviour of thin layered systems under the action of rolling loads will be the main objective of chapters 4 to 7 of this thesis.

CHAPTER 4

THEORIES OF LAYERED SYSTEMS

Theories of layered systems in general

Examples of theories of layered systems

The proposed method for analysing a thin layered system under the action of a rolling load with particular interest in the delamination defect

Conclusions

4-1 Theories of layered systems in general

The first step for studying a layered system is the ability of determination of the stresses and displacements in the structure resulting from the loading condition. Various theoretical models have been developed and used for this purpose which may be divided into four main groups:

- Plate theory
- Layered theory
- Finite element technique
- Coupled models

These are described in this chapter.

4-1-1 Plate theory

In plate theory, a finite plate of material is assumed on a semi - infinite half space of another material. Considerable information pertaining to the state of stress can be achieved by this method, however it will not provide any information regarding the supporting media. [McCullough 1969]

Depending on the type of the plate loading characteristics, plate theories can be divided into three groups: [Timoshenko 1934] [McCullough 1969]

- Thin plate with small deflections
- Thin plates with large deflection
- Thick plates

Since the substrate in our study is concrete, the first category of the plate theories is of concern. Assumptions which are usually associated with thin plate with small deflection theories are: [McCullough 1969]

- The plate is flat and the material assumed to be homogenous, isotropic, linear - elastic, however anisotropic material may also be considered. Therefore, the second part of this assumption is related to the material properties.
- The normal strain perpendicular to the plate owing to displacement, may be neglected. This means that the vertical stress component must be always zero, and therefore, only the tangential and radial stresses are obtained.
- The straight lines normal to the middle plane of the plate remain straight during bending and normal after bending, as there is no horizontal deformation

in the middle plane of the member.

- The angle of the deflection surface is much less than 45°.
- Deflection is defined by the displacement of the middle plane of the plate.

The studies made by investigators showed that if the ratio of the thickness of the plate relative to the lateral dimensions (h/a) was less than 0.2, reasonable answers could be expected. [McCullough 1969]

Two types of supporting foundation materials have been assumed in the plate theories, dense liquid foundations or linear - elastic foundations. (figure 4-1)

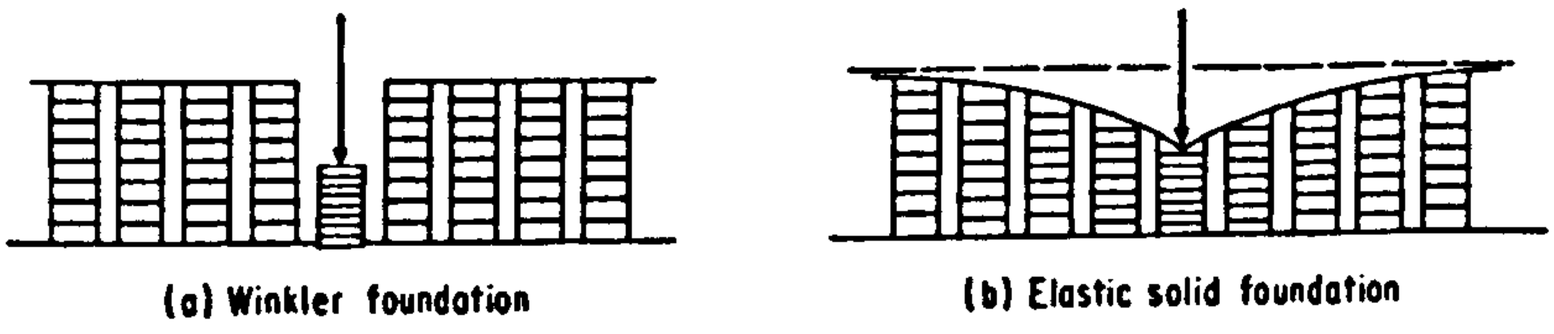

Figure 4-1: Deflection patterns for two types of foundations under a point load [Yang 1972]

In the dense liquid foundation (Winkler foundation), it is assumed that no shear stresses occur in the foundation material. (figure 4-1-a) In other words, the foundation (subgrade) is assumed to act as a set of springs supporting the upper layer. The stiffness of these springs which is called modulus of subgrade reaction (k) is determined from the results of plate - load tests performed on the subgrade. Therefore when a force is applied on the system, it is resisted by an equal and opposite force which is equal to the deflection times the modulus of subgrade reaction (k). Westergaard used this assumption for the analysis of concrete pavements in 1926 [Westergaard 1926]. He presented closed - form solutions for three conditions of load placement, namely interior, edge, and corner. [McCullough 1969] [Majidzadeh 1988]

Pickett and Ray developed influence charts for finding the stresses and deflections owing to loading [Pickett and Ray 1951]. [Huang 1993]

Using an open - form solution, Hudson developed a method which provides special capabilities for the analysis of a plate problem on a dense liquid foundation [Hudson 1965]. The solution is able to handle special problems of non - uniform supports, special loadings, and cracks. However because of the nature of the model, hand solutions are impractical and it must be employed using a computer. [McCullough 1969]

In the linear - elastic foundation, it is assumed that the plate (slab) is continuously supported by an elastic solid. (figure 4-1-b) Hogg [Hogg 1938] and Holl [Holl 1938] considered the foundation as a semi - infinite elastic solid in their analysis in 1938. The most important difference between an elastic solid subgrade and the dense liquid foundation (Winkler foundation) is that with the elastic solid, the deflection at any arbitrary point is not proportional to the stress transmitted to the foundation at that point. [Yang 1972]

As in the elastic foundation method the elastic properties of the subgrade material are used, it would be more realistic than the other method. However in order to simplify the complex mathematics of the solution, Hogg [Hogg 1938] assumed that zero shearing force at the interface of the pavement and soil existed which was not realistic. He presented solutions for curvature and normal displacement for a circular loaded area over a plate of infinite plan dimensions. Therefore no solutions for stresses were presented in this work. Pickett et al. [Pickett et al. 1951] presented solutions of boundary value problems using a plate on an elastic solid foundation which then became partially a basis for the Portland Cement Association (PCA) design method for concrete pavements. [McCullough 1969]

It is seen that in the plate theory method slab models are limited to systems consisting of two layers, and therefore, multilayered systems can not be analysed. Also slabs of finite dimensions, slabs of non - uniform thickness, non - uniform material properties or non - uniform foundation support can not be considered in this method. [Majidzadeh 1988]

4-1-2 Layered theory

In layered theory, each layer of material is represented by its modulus of elasticity, its thickness, and Poisson's ratio. (figure 4-2) The bottom layer extends both horizontally and vertically to infinity while the other layers are assumed to extend horizontally to infinity. As full continuity is normally assumed between layers, the interfaces are considered to be completely rigid so that they are capable of accepting step changes of stresses at their lines.

As the oldest theory of layered systems, the Boussinesq equations are applied for a one - layer system, which is a semi - infinite mass subjected to a point or distributed load on the surface. [Yang 1972] In this theory it is assumed that

the semi - infinite mass is an elastic homogenous half space. [Huang 1993]

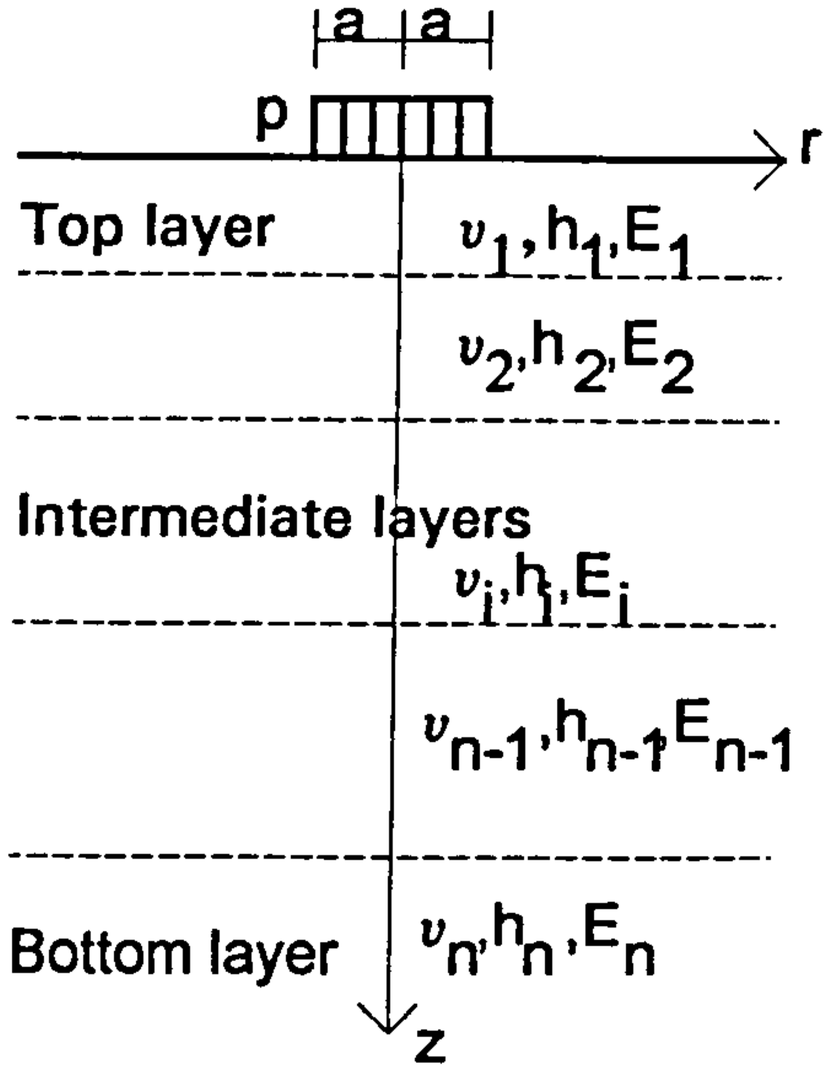

Figure 4-2: A multiple layered system

After Boussinesq other scientists attempted to analyse the stresses and displacements in a multiple layered system like that is shown in figure 4-2. In most cases the analysis was based on some assumptions as follows: [Yang 1972]

- Each layer is isotropic, homogenous and weightless.
- The system behaves like a composite structure and consequently the continuity along the interface is existent.
- Most of methods assume an elastic behaviour for the constitutive materials.

The first solution and the most practical mechanistic method for analysing a multi - layer elastic system was defined by Burmister [Burmister 1954]. [Huang 1993] Burmister presented the equations of N - layered elastic systems and solved them for a two and a three layered system. The limitation on the Burmister's work was to apply a uniform normal load which acted over a circular area. [Burmister 1954]
Burmister, in his works, added the following assumptions to those which are normally made in the elastic theory. These assumptions are applicable to the later developments made by other investigators: [McCullough 1969]

- The upper layer was assumed to be free of normal and shearing stresses

outside the loaded area.

- Stress and deflection in the bottom layer must be zero at an infinite depth.

After Burmister, Schiffman [Schiffman 1962] improved his work for more generalised asymmetric loading conditions, in which shear stresses at the surface were included. [Yang 1972]

The Burmister's solution was later extended to three - layered systems and also solved for the complete stress and strain in the pavement structures by other investigators. Hank and Scrivner also solved the problem for two different conditions between layers, full continuity and zero continuity. According to their solution, the stresses in the upper layer for the zero continuity are larger than the stresses calculated for full continuity. The difference in stress between the two conditions generally has a direct relationship with the ratio of the stiffness of the lower layer to the stiffness of the upper layer and also with the ratio of the radios of the loaded area to the surface layer thickness. [McCullough 1969]

Jones [Jones 1962] was perhaps the investigator who gave the most extensive tabulation of coefficients for layered systems. Peattie [Peattie 1962] plotted the coefficients developed by Jones. [Yang 1972]

An equivalent thickness method for evaluating a multi - layered system was also presented by Peattie, which will be mentioned in section 4-2-2 of this chapter. [Peattie 1980]

Considering the stress contours within the layered systems, like those plotted by Peattie [Peattie 1980], one may infer that the main conclusion of the general theories of layered systems is : " The use of a layer of material having a high elastic modulus reduces the stresses on any interface below that layer." [Plum 1990]

Huang, Moavenzadeh, Aston, Elliott, Luttes, Lions, Bonitzer, Newmark, Wilson, Barksdale, Hertz, Westergaard were/are known as some other investigators in the various fields of this subject. [Yang 1972]

The use of high speed, high capacity computers made it possible to analyse layered systems consisting of any number of layers and subjected to many different types of loads. The first computer program was developed by Chevron Research Company in 1963 which was capable of analysing five layered elastic systems subjected to a single load. ELSYM5 in 1972 for the analysis of layered systems subjected to multiple loads, and VESYS systems in 1976 - 1977 for the analysis of layered systems by considering viscoelastic

layer properties. In spite of the capabilities of multiple - layered systems models for the analysis of pavements with many different layers and with different material properties, they are not capable of analysing concrete pavement slabs of finite dimensions, nor various concrete pavement features such as joints, reinforcement, etc. [Majidzadeh 1988]

4-1-3 Finite element technique

In 1949, Newmark stated that " the use of the [finite - element] model offers certain advantages: there is no ambiguity concerning the boundary elements; statical checks on the results have physical meaning and can be made more adequately; variations in dimensions and physical properties can be more easily treated. " [Yang 1972]

He introduced the discrete - element method for the structural analysis of plates. He developed a model for simulating a slab by considering it as an assemblage of deformable hinges, rigid links and coil springs. [Majidzadeh 1988]

With the improved use of computer techniques, the use of the finite element method for analysing the layered systems was considered by many investigators. Hudson and Matlock [Hudson and Matlock 1966] used a finite element model for the analysis of concrete pavement slabs. In this model, the foundation was idealized as a Winkler foundation, and it also composed of rigid bars connecting elastic hinges, and torsion springs connecting adjacent parallel bars. The model was then improved and modified by other investigators. [Yang 1972] [Majidzadeh 1988]

Duncan, Monismith, et al. solved the complete state - of - stress in the pavement structure using the finite element method. In the finite element model, the anisotropic condition and also horizontal variation of material properties can be considered. The model is also able to consider non - linear problems. [McCullough 1969]

There are several types of finite - element models for the analysis of layered systems: Slab models, plane strain models, prismatic models, axisymmetric models, and three - dimensional models. A brief definition of each type of these models is given below: [Majidzadeh 1988]

In the slab models, the pavement slab, concrete, is idealized as a medium - thick plate supported by a Winkler foundation. Therefore these models are limited in their applications. Huang and Wang, Bhatia and Majidzadeh,

Tabatabaie and Barenberg are among the investigators who have developed these models for the analysis of concrete pavements. [Majidzadeh 1988]

Using a finite - element model with two dimensional thin plate bending elements, Lau et al. in 1994 calculated shear stresses in a pavement - overlay slab owing to vertical wheel loads and temperature gradient. Perfect bonding between the overlay and the pavement was assumed. In this study, a Winkler spring foundation was considered for supporting the repaired slab which was modeled as a thin plate. [Lau et al. 1994]

Khazanovich et al. in 1994 implemented a formulation proposed by Totsky into a finite element program to consider the effects of layer separation and compressibility in an unbonded concrete overlay system. The product was a finite element code called ILSL2, which was in fact an extension of the ILLI-SLAB program. A multilayered system resting on a Winkler foundation in this model is idealized as a series of alternating plate elements and springs. A special eight noded (24 degree of freedom) element was introduced in this approach. [Khazanovich et al. 1994]

In the plain strain models, the pavement system is idealized by a transverse slice of the pavement having a unit thickness. In these models variations in loads or materials along the centerline of the pavement are not considered.

The prismatic models use the idealization of the pavement system by a constant two - dimensional geometric shape regarding an infinite third dimension. Wilson, Crawford, and Pichumani have used these models for the analysis of pavement structures. The great limitation of these models is that any variation of geometrical configuration along the longitudinal axis of the pavement system can not be considered. Therefore, these models are not able to deal with any transverse discontinuities such as joints or cracks. They do not use a realistic representation for applied loads either.

In the axisymmetric models the idealization is based on representing the layered system as a multiple - layered cylindrical system which is loaded symmetrically at the centerline. Therefore, the technique assumes a nearly general three dimensional system. However it can not consider various loading conditions, or various concrete pavement features such as joints or cracks. Wilson [Wilson 1965] was the first investigator who made the formulation of an axisymmetric finite element model for the analysis of layered systems. His work was later extended by other investigators. [Majidzadeh 1988] Figure 4-3 shows the discrete circular solid ring elements used in the Barksdale's presentation. [Barksdale 1969]

Finally in the three - dimensional finite element models, which are probably the most desired models for the analysis of concrete pavements, the actual configuration of the whole system can be taken into account. However these

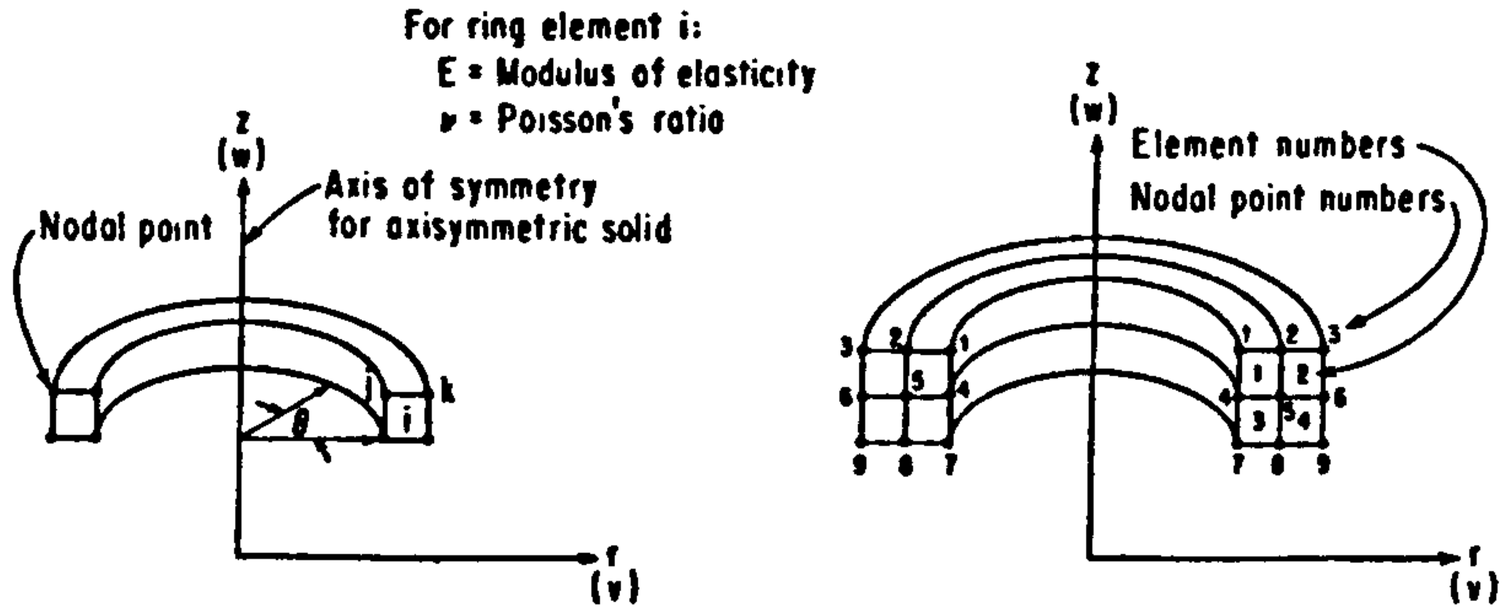

Figure 4-3: The finite element idealization of an axisymmetric solid used by Barksdale [Yang 1972]

models require a high amount of discretization and computer cost for solution of a layered systems which is not practical. [Majidzadeh 1988] As an example Wilson [Wilson 1969] developed the SAP program using three dimensional finite elements. [Majidzadeh 1988]

A three - dimensional finite element analysis was also carried out by the author in 1993 in an investigation on the distribution of vertical and principal stresses along the interface of a two layered system under the action of vertical and horizontal loads. The analysis was performed using the PAFEC finite element software. [Sohrabi 1993]

Finally Lau et al. performed a finite element analysis for evaluating the stresses due to the action of wheel braking loads. [Lau et al. 1994]

4-1-4 Coupled models

According to Ref. [Majidzadeh 1988], coupled models are obtained by coupling two or more of the following models:

- Finite - element models
- Multiple - layered systems
- Analytical models based on closed form solutions

Coupled models have been used by a number of investigators for the structural analysis of pavement systems. Saxena [Saxena 1971] formulated a coupled model by coupling the discrete - element slab model developed by Hudson and

Matlock [Hudson and Matlock 1966] with the Boussinesq's closed form solution [Boussinesq 1885]. In this model the concrete pavement slab was idealized by the discrete - element technique, while the behaviour of the subgrade was represented by the Boussinesq's equation. However this model can be only applied to single slabs with free edges. [Majidzadeh 1988]

A coupled model consisting of a finite element model and a Boussinesq's solid subgrade [Boussinesq 1885] has been formulated by Huang [Huang 1974]. [Majidzadeh 1988]

Kennedy and Prause [Kennedy and Prause 1978] developed a model, for the analysis of railroad track structures, by coupling a finite element program representing rail and tie with a multiple - layered elastic layer program representing the ballast and subgrade. Despite the usefulness of the modelling technique used in this program, it is not applicable to the analysis of concrete pavements. [Majidzadeh 1988]

Finally, Majidzadeh [Majidzadeh 1988] has coupled a finite element plate with a three - layered elastic or viscoelastic system in order to analyse multiple layered systems with various pavement features. [Majidzadeh 1988]

4-2 Examples of theories of layered systems

4-2-1 Boussinesq's Theory

In Boussinesq's theory it is assumed that the material is perfectly elastic and homogeneous.
According to this theory, the vertical stress σ_z at any depth of z due to a point load P which acts at the surface (figure 4-4) is : [Yoder 1959]

$$\sigma_z = k\frac{P}{z^2} \qquad (4\text{-}1)$$

$$k = \frac{3}{2\pi}\frac{1}{\left[1+(r/z)^2\right]^{5/2}}$$

Where: r = distance from the point load
z = depth

It is seen that the value of σ_z is dependent on the depth z and the radial distance r, but is independent of the properties of the half - space mass, beneath the load.
Integrating the equation 4-1 over a circular area with a radius of a, one can obtain the vertical stresses on a vertical plane passing through the center of the circular loaded plate: [Yoder 1959]

$$d_{\sigma_z} = \frac{3p}{2\pi z^2}\left[\frac{1}{1+(r/z)^2}\right]^{5/2} \qquad (4\text{-}2)$$

$$\sigma_z = p\left(1 - \frac{z^3}{(a^2+z^2)^{3/2}}\right) \qquad (4\text{-}3)$$

And the radial (horizontal) stress σ_r is given as follow:

$$\sigma_r = \frac{p}{2}\left[1+2\nu - \frac{2(1+\nu)z}{(a^2+z^2)^{1/2}} + \frac{z^3}{(a^2+z^2)^{3/2}}\right] \qquad (4\text{-}4)$$

Where: p = the unit load on the circular plate
z = depth
a = the radius of the plate
ν = poisson's ratio ≈ 0.5

So for a small element of soil at a depth of z below the surface, the elastic strain ε due to the load, under the center of the plate is:

$$\varepsilon=\frac{1}{E}[\sigma_z-2\nu\sigma_r] \qquad (4\text{-}5)$$

Where: E = modulus of elasticity

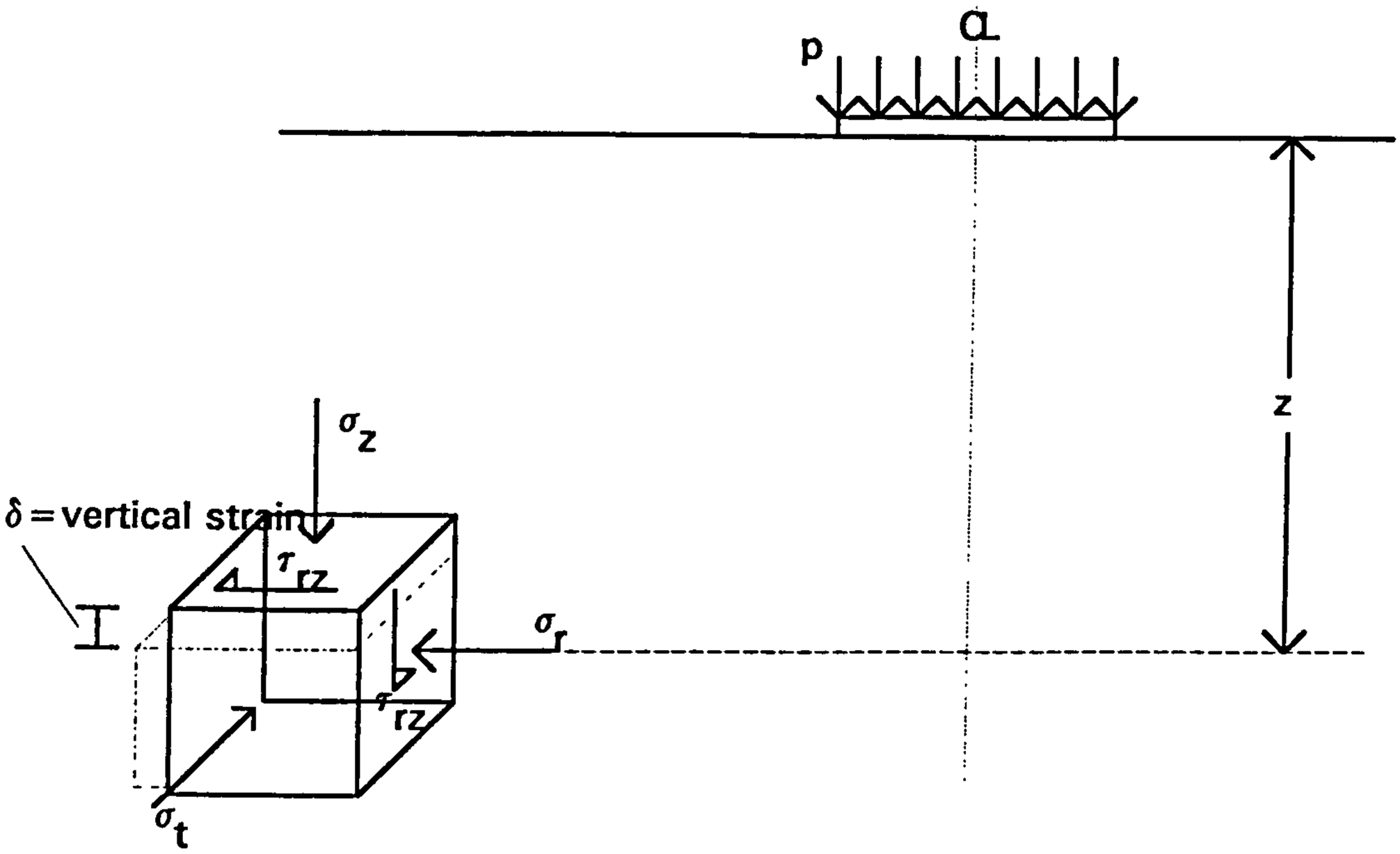

Figure 4-4: Stresses acting on an element at a depth of z [Yoder 1959]

Using equations 4-3 and 4-4 and substituting them into equation 4-5 and integrating between the two limits of z from z=z to z=∞, we have:

$$\Delta=\frac{p}{E}[(2-2\nu^2)(a^2+z^2)^{-\frac{1}{2}}-\frac{(1+\nu)z^2}{(a^2+z^2)^{\frac{1}{2}}}+(\nu+2\nu^2-1)z] \qquad (4\text{-}6)$$

And if: ν=0.5

$$\Delta=\frac{3pa^2}{2E(a^2+z^2)^{\frac{1}{2}}} \qquad (4\text{-}7)$$

$$\Delta=\frac{pa}{E}F \qquad (4\text{-}8)$$

$$F=\frac{3}{2}\frac{1}{\left[1+(z/a)^2\right]^{\frac{1}{2}}} \qquad (4\text{-}9)$$

Equation 4-8 is known as the Boussinesq settlement equation which is used for

calculating the deflection at the center of a flexible plate. [Yoder 1959]
In the case of z=0 and F=1.5, from equation 4-8, we have:

$$\Delta = 1.5\frac{pa}{E} \qquad (4\text{-}10)$$

It is seen, from equation 4-6, that the Boussinesq's theory gives only the deformations between the depth z and infinity. In other words, in this theory the elastic deformations of the subgrade only are taken into account. (figure 4-5)

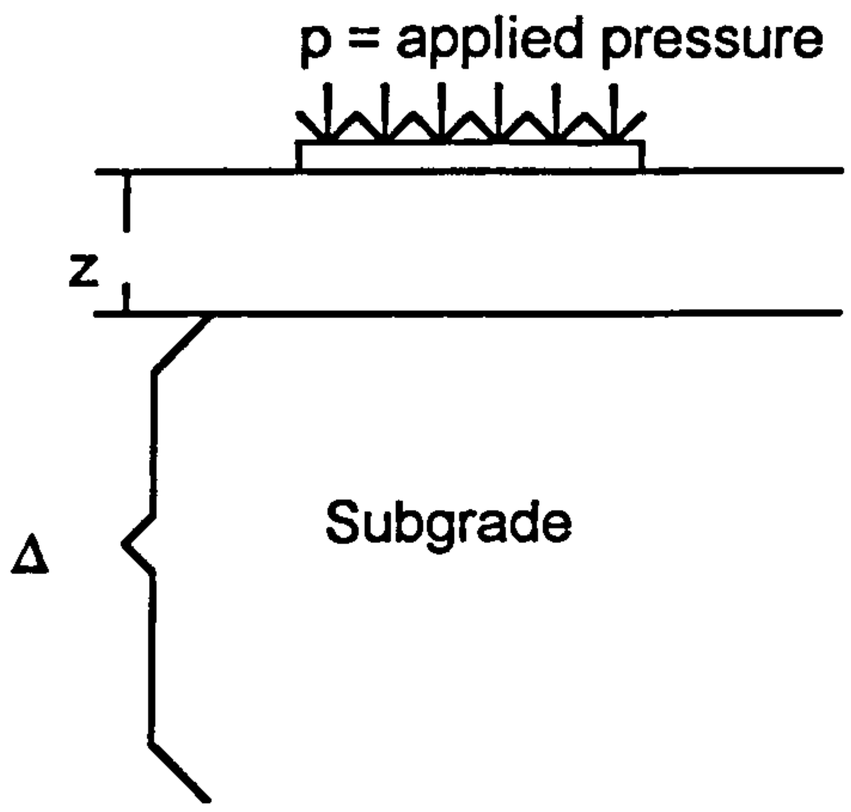

Δ = elastic deformation from z to infinity
Figure 4-5 : Diagram showing the assumptions of integration [Yoder 1959]

4-2-2 Peattie's equivalent thickness method

This method is based on the Odemark's work who formulated the principle of the theory in 1949. According to his theory, stresses, strains and deflections in a multi - layered system below a particular layer are independent of the layer changes until its flexural stiffness remains constant. [Peattie 1980]
Considering the above theory, Peattie transformed a two layered structure into its equivalent half-space by defining an equivalent thickness h_e instead of h_1. Hence he considered the same modulus of elasticity for both of the layers equal to E_2. (figure 4-6)

$$h_e = h_1 \sqrt[3]{\frac{E_1}{E_2} \times \frac{(1-\nu_2^{\,2})}{(1-\nu_1^{\,2})}} \qquad (4\text{-}11)$$

Where: h_1 = the thickness of the first layer
h_e = the equivalent thickness

E_1 & E_2 = the modulus of elasticity of layer 1& 2 respectively

ν_1 & ν_2 = Poisson's ratios

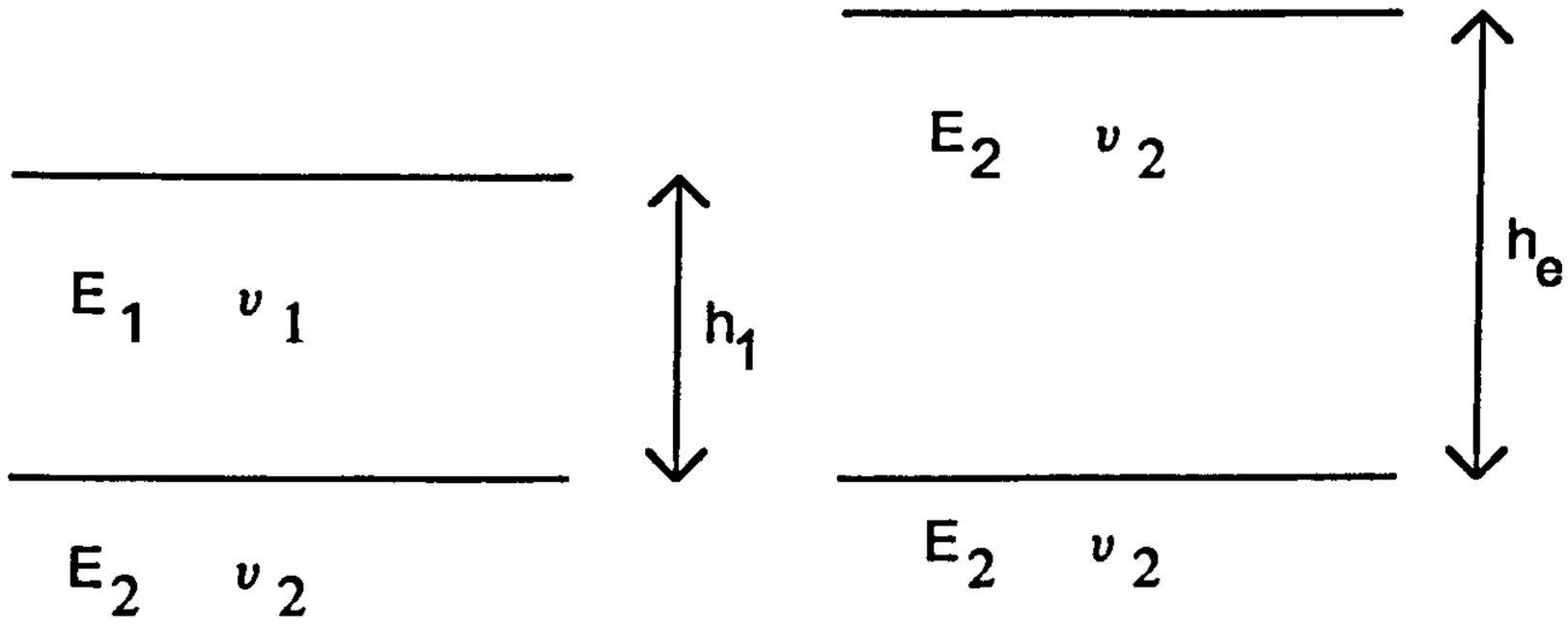

Figure 4-6 : Equivalent layered systems [Peattie 1980]

In fact he assumed that the stresses in the second layer will be identical in both of the structures. This is because of the fact that the flexural stiffness in the first layer of each structure will be the same as that for the other one.

So the values of stresses and strains in the lower layer can be calculated by using the Boussinesq's equations to an elastic half - space at a depth of at least $z = h_e$.

Obviously the values of the stresses and strains are equal for the both sides of the interface of the equal system. Hence care must be taken in computing the stresses at the interface of the real system. [Peattie 1980]

To obtain the surface deflection in this structure, the sum of the compression of the upper layer and the deflection of the lower half-space is to be calculated.

The compression of the upper layer can be calculated as follows:

$$\text{Compression of the upper layer} = (\Delta)_{z=0}^{E_1,\nu_1} - (\Delta)_{z=h_1}^{E_1,\nu_1}$$

Where: $(\Delta)_{z=0}^{E_1,\nu_1}$ = the deflection at the surface of a half - space with the values of E_1 & ν_1

$(\Delta)_{z=h_1}^{E_1,\nu_1}$ = the deflection at a depth of h_1 in a half - space with the values of E_1 & ν_1

To calculate the deflection of the lower half - space the equivalent model must be used.

It should be noted that the concept of the equivalent thickness method may be used for a multi - layered structure, in the same way done for a two layered system.

4-2-3 A closed form solution for the estimation of the shear stress due to a horizontal force

Horizontal and vertical forces are applied onto the pavement slab owing to braking or cornering of a vehicle tyre or due to the action of a snow removal equipment. The value of vertical stress due to the action of the vertical load can be calculated by using an appropriate solution like those presented in the two previous sections. The effect of the horizontal force is to be discussed here.

Lau et al. [Lau et al. 1994] have used a close form solution for the analysis of interface shear stress in overlaid concrete pavements. The solution has been made by Cerruti and Boussinesq and described by Love [Love 1927] for the displacement field in a homogeneous half space loaded by traction force acting on a point on the surface. The solution is as follows: [Lau et al. 1994]

$$u = \frac{S}{4\pi\mu}\left(\frac{\lambda+3\mu}{\lambda+\mu}\ \frac{1}{r}+\frac{x^2}{r^3}\right)-\frac{S}{2\pi(\lambda+\mu)}\ \frac{1}{r}$$

$$+\frac{S}{4\pi(\lambda+\mu)}\left[\frac{1}{z+r}\ \frac{x^2}{r(z+r)^2}\right] \qquad (4\text{-}12)$$

$$v = \frac{S}{4\pi\mu}\ \frac{xy}{r^3}\ \frac{S}{4\pi(\lambda+\mu)}\ \frac{xy}{r(z+r)^2} \qquad (4\text{-}13)$$

$$w = \frac{S}{4\pi\mu}\ \frac{xy}{r^3}+\frac{S}{4\pi(\lambda+\mu)}\ \frac{x}{r(z+r)} \qquad (4\text{-}14)$$

$$\lambda = \frac{Ev}{(1+v)(1-2v)} \qquad (4\text{-}15\text{-a})$$

$$\mu = \frac{E}{2(1+v)} \qquad (4\text{-}15\text{-b})$$

$$r = \sqrt{x^2+y^2+z^2} \qquad (4\text{-}15\text{-c})$$

Where:

E = elastic modulus of the half space

υ = Poisson's ratio

μ = shear stiffness

u, v, and w = displacement in the x, y, and z directions (The origin is at the point of the location of the load)

S = value of the horizontal load acting in the positive x direction

The shear stress, τ_{xz}, due to a point load acted on the surface has been given by:

$$\tau_{xz} = \mu \left[\frac{\partial u}{\partial z} + \frac{\partial w}{\partial x}\right] \qquad (4\text{-}16)$$

If the load is distributed over an area, the above equation must be integrated. The shear stress at a point with coordinates (x_0, y_0, z_0) due to a uniformly distributed horizontal load over a rectangular area is obtained by the following equation:

$$\tau_{xy}(x_0, y_0, z_0) = \int_{a-x_0}^{-x_0} \int_{b-y_0}^{-y_0} \mu \left[\frac{\partial u}{\partial z} + \frac{\partial w}{\partial x}\right] dydx\Big|_{z=z_0} \qquad (4\text{-}17)$$

Where:

a and b = half of the width and length of the loaded area (The origin of the coordinate system and the centroid of the load are coincident)

After performing the integration, equation 4-17 becomes: [Lau et al. 1994]

$$\tau_{xy} = \frac{S}{16\pi ab}\left\{\frac{xyz}{\mu (x^2 + z^2) r} - 2(\lambda + 2\mu)\arctan\left[\frac{xy}{zr}\right] + \frac{xyz}{\mu (x^2 + z^2) r}\right\}_{|x=a-x_0|y=b-y_0}^{|x=-a-x_0|y=-b-y_0} \qquad (4\text{-}18)$$

Earlier Bagate [Bagate 1987] used the following equation reported by Holl [Holl 1941] for estimating the in - plane shear stress at the interface resulted from a horizontal force on the surface of a concrete overlay pavement: [Bagate 1987]

$$\tau_{xy} = \frac{\text{HLOAD} \bullet y}{2\pi R^3}\left[\frac{3x^2}{R^2} + \frac{1-2\upsilon}{(R+z)^2}\left[R^2 - x^2 - \frac{2Rx^2}{R+z}\right]\right] \qquad (4\text{-}19)$$

Where: HLOAD = value of the horizontal point load acting in the positive x direction

υ = Poisson's ratio

x, y, z = distances form the origin in the x, y, and z directions

R = distance form the origin

(The origin of the coordinate system and the centroid of the load are coincident)

Obviously the above equation is valid for the geometry of the Cerruti's problem, namely a horizontal force acted at a point in the body of a semi - infinite homogeneous, isotropic, weightless, linearly elastic medium having a plane, horizontal surface. [Bagate 1987]

4-2-4 A theory of layered system in a repair application

This theory has been defined by Plum. [Plum Sept. 1990] He has divided the subject of a repair system into two main classes:

- Structural repairs
- Cosmetic repairs

4-2-4-1 Structural repairs

In this case the repair materials will be considered as a part of stress carrying system, e.g. in a column or a beam compression zone.

In a structural repair application, two factors may be related to each other, the repair function ($^{F}/_{F}$) and the area ratio (β). [Plum Sept. 1990]

Considering the effect of the degree of load relief during a repair, the author has obtained two different equations for the corresponding repair functions. Then the repair function may be plotted in terms of the area ratio (β). [Plum Sept. 1990]

As in the behaviour of the polymer materials, the creep coefficient φ_r is important, it has been taken in to account in both equations. Here are the equations: [Plum Sept. 1990]

$$F = F_c + F_r \qquad \beta = A_c / (A_c + A_r) \qquad (4\text{-}20)$$

-Full load relief during the repair:

$$F_r / F = 1 / [k_1(1/\beta - 1)(1 + \varphi_r) + 1] \qquad k_1 = \sigma_c / \varepsilon_c E_r \qquad (4\text{-}21)$$

-Imposed load relief during the repair:

$$F_r / F = 1 / [k_2(1/\beta - 1)(1 + \varphi_r) + 1] \qquad k_2 = \sigma_c / (\varepsilon_c - \varepsilon_d) E_r \qquad (4\text{-}22)$$

where:

A_c = the area of the concrete core

A_r = the area of the repair in the compression zone

F_r = the force carried by the repair

F_c = the force carried by the concrete core

σ_c = the appropriate factored stress for the concrete at failure

σ_r = stress in the repair material

E_r = elastic modulus for the repair material

Hence, it is seen that to achieve a reasonable efficiency of a repair system, φ_r should not exceed 3. So for the structural repair applications, low creep is desirable over the expected environmental range. [Plum Sept. 1990]

4-2-4-2 Cosmetic repairs

In this case the repair materials are used as isolated patch repairs or protective screeds and are not generally required to carry stress. [Plum Sept. 1990]
Expansion due to moisture and saturation, temperature or thermal shock may be a general cause of failure in floor repairs or screeds. So in this case a tolerable expansion (strain) has been defined as the repair function. This factor is related to the bond strength (P_b) and may also be related to the creep coefficient (φ_r). [Plum Sept. 1990]
Here is the equation:

Repair function $\varepsilon = k_3 P_b (1 + \varphi_r) / E_r$ (4-23)

$k_3 = L / 4rt$

Where:

P_b = bond strength (N/mm^2)

L = the length of the patch repair/screed (mm)

t = the thickness of the patch repair/screed (mm)
r = a factor by which the restraint force, provided by the interface bond, may be defined in terms of the compression force F_r due to an expansion ε of the screed.

Plotting the repair function (ε) against the bond strength (P_b), the engineer can obtain a good estimate of the behaviour of the screed under an expansion problem.

As it is seen from the above equation, for a constant value of the bond strength, the more the creep coefficient (φ_r) is increased, the more the repair function (ε) is increased. This is because of the fact that creep has a positive effect on reducing the buckling tendency of the repair screeds. [Plum July/Aug. 1991]

Related to this kind of failure, Bendeddouche [Bendeddouche 1985] has also studied the problem. He assumes that the defected areas on the concrete substrate has either a rectangular or a circular shape. He also assumes that the value of the bond strength between the screed and the substrate is very weak or non existent. The other assumption is that the tensile strength of the patch screed near the contact area is negligible. So the screed could be only restraint horizontally along its boundaries.

Considering an in-plane force system due to expansion, he models the plate as an elastic buckling problem. [Bendeddouche 1985]

It is seen that the above assumptions regarding the bond strength behaviour and imperfections are difficult to justify, so this theory has limited usefulness. [Plum Sept. 1990]

4-3 The proposed method for analysing a thin layered system under the action of a rolling load with particular interest in the delamination defect

4-3-1 The finite element method as the selected theory

Generally a thin layered system is understood as a system with one or more thin layers of different physical and mechanical properties which lies on a surface of a main substrate.

Each of the two other dimensions of a thin layered system may vary from a very small quantity in an isolated patch repair on an individual member of a structure, to a very large amount in a coating layer on a warehouse floor. Since the latter case is the main subject of this study, the substrate layer will be a concrete slab.

As will be discussed in the following and also from the previous sections of this chapter, the choice of a most appropriate model for analysing a thin layered system is the finite element method.

Although the use of plate theory has been associated for concrete pavements for a relatively long period of time, its use for the analysis of thin layered systems is eliminated for the following reason:

- In the plate theory only the state of stress in the surface layer of the layered system could be predicted, and it does not provide any information regarding the supporting media.
- Since the vertical stress in the plate theory is assumed to be zero, the complete state - of - stress can not be predicted using this theory.
- The modulus of subgrade, k, could not be measured in the laboratory, therefore elaborate field-tests are generally required.
- In the plate theory, a finite plate of material is assumed on a semi - infinite half space of another material.
- It was seen that in the plate theory method slab models were limited to systems consisting of two layers, and therefore, multilayered systems can not be analysed.
- Also slabs of finite dimensions, slabs of non - uniform thickness, non - uniform material properties or non - uniform foundation support can not be considered in this method.

In the layered theory, it might be possible to determine the complete state of stress at any point in the layered system structure. Despite the advantages, it had several deficiencies for the analysis of a thin layered system:

- In the layered theory, the bottom layer extends both horizontally and vertically to infinity while the other layers are assumed to extend horizontally to infinity. Therefore, models based on this theory are not capable of analysing layered systems of finite dimensions.
- The assumption of full continuity in the layered theory indicates that no slippage may occur at the interface between different layers. The error of this assumption is only small for large relative differences in stiffness between the layers. [McCullough 1969]
- Various support conditions such as voids under the slab, or concrete features such as joints or cracks can not be analysed.

In contrast to the above, the finite element method offers certain advantages such as feasibility of being able to take into account any variation of the material properties in horizontal direction, and also to analyse the non - linear stress - strain behaviour of the constituent materials. It can also handle layered systems of any dimensions and complex boundary conditions, any type of load at any location on the layered system, and any support condition.

With regard to the above the finite element method was selected to be used in the analysis of thin layered systems used in this investigation.

4-3-2 The finite element mesh and the constitutive materials

The most important step in the finite element analysis is creating the proper model. This model should provide the most appropriate nodal pattern which creates enough number of elements to obtain accurate results without wasting data and interpretation and processing time. Conceptual understanding of the physical system and judgement on the anticipated behaviour of the structure should be always considered as a basic requirement for a finite element modelling. [Spyrakos 1994] The finite element model should be checked against the possible errors. Ill conditioning, Locking, and Instability must be avoided by taking the appropriate measures. [Cook et al. 1989]

As it was mentioned before, the three - dimensional models are probably the most desired models for the analysis of a layered system. However these

models require a high amount of discretization and computer cost for solution of a layered systems. The problem will be particularly more serious for the analysis of a thin layered system. For this reason two dimensional plane strain finite element models have been used in this investigation. This type of idealization has been also employed by other investigators. [Lundy 1990] [Zollinger et al. 1994] Moreover in order to keep the consistency with the interface elements, and at the same time to get a more accurate results, isoparametric 8 noded elements have been used for all layers in each model of a thin layered system.

In chapter 6 the behaviour of the thin layered systems used in the Steel Wheel Rolling Load experiment will be studied. The finite element mesh and other specifications for each model will be given in that chapter. As it will be seen in section 6-3-1-1, owing to the high value of the applied contact load pressure, nonlinear behaviour will be considered for all the constitutive materials. The corresponding idealized stress - strain curves will be defined in chapter 5. To achieve the nonlinear structural analysis, the implicit ('backward Euler') elasto plastic von Mises yield surface model using the LUSAS finite element software will be employed.
The above model allows the proper definition of a tangent stiffness matrix which maintains the quadratic convergence of the Newton - Raphson iteration scheme. [LUSAS User Manual]

In chapter 7 the behaviour of the thin layered systems used in the NUROLF experiment will be studied. The finite element mesh and other specifications for each model will be given in that chapter. As it will be mentioned in section 7-3-1-1, due to the low tyre contact pressure, a linear elastic behaviour will be considered for all the constitutive materials. The corresponding values of modulus of elasticities will be given in chapter 5. Once again the LUSAS finite element software will be used for performing the analysis.

4-3-3 The thin interface layer

The main objective of this investigation is to study the behaviour of a thin layered system under the action of a rolling load with regard to the possible delamination defect at the interface between the two upper layers subjected to the load. Therefore it was necessary to employ an appropriate thin layer of

interface elements in the finite element model. Due to the appropriateness of the thin - layer interface element proposed by Desai et al. [Desai et al. 1984], it will be used as the basis for carrying out the structural analysis of the thin layered systems in this investigation. The implementation of the analysis will be then carried out using the LUSAS finite element system available in the Department of Civil Engineering of the University of Newcastle Upon Tyne.
In the section as follows, the specification of the thin interface layer will be illustrated.
Many investigators have attempted to use a thin - layer element for simulating the behaviour of interfaces. [Desai et al. 1984]
Zienkiewicz et al. [Zienkiewicz et al. 1970] proposed to use a solid element as an element interface. They considered the " weak " layers in a stratified, laminar structure (rock mass), as simply surfaces of discontinuity. (figure 4-7)
It was concluded that in such materials the constitutive relation could be described elasticity, unless in the normal direction: [Zienkiewicz et al. 1970]

$$\varepsilon'_n \rangle 0 \qquad (4\text{-}24)$$

When $\sigma'_n = 0$ $\tau'_{sn} = 0$
Which would be considered for joint opening. If the above check is satisfied, for the shear stress in the tangential direction, we have:

$$\tau'_{sn} = C + \sigma'_n \tan \Phi \qquad (4\text{-}25)$$

Where: σ'_n = normal stress to the stratification planes

τ'_{sn} = tangential stress to the stratification planes

C = cohesion

$\tan \Phi$ = coefficient of friction

If the elastic shear stress exceeds the above value, a sliding will occur in a manner of plasticity. [Zienkiewicz et al. 1970]

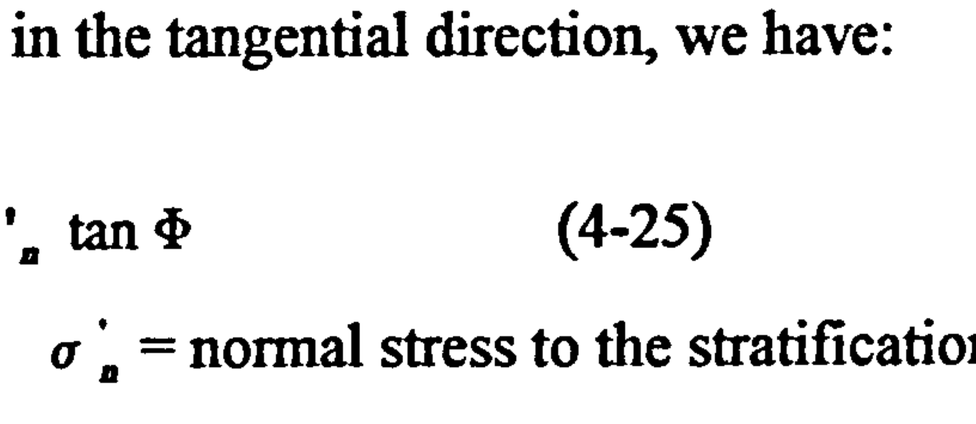

Figure 4-7: Stratified materials [Zienkiewicz et al. 1970]

In the commonly used interface elements, the formulation of the element is based on relative displacements of the solid elements which are in the vicinity of the interface element. (figure 4-8)

The stress - relative displacement relation for a two -dimensional analysis of such an element is defined as follows: [Desai et al. 1984]

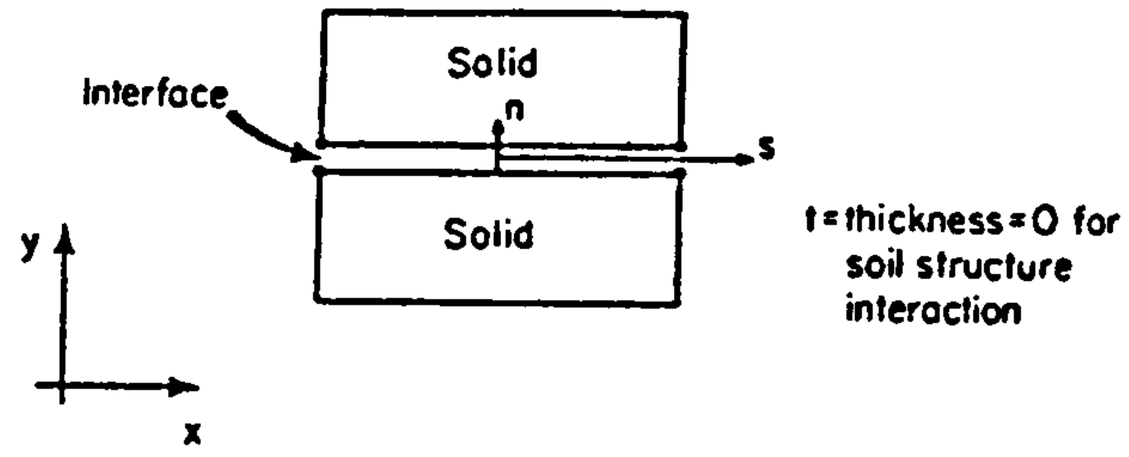

Figure 4-8: A commonly used interface element [Desai et al. 1984]

$$\begin{Bmatrix} \sigma_n \\ \tau \end{Bmatrix} = \begin{bmatrix} k_n & 0 \\ 0 & k_s \end{bmatrix} \begin{Bmatrix} v_r \\ u_r \end{Bmatrix} = [C]_i \begin{Bmatrix} v_r \\ u_r \end{Bmatrix} \qquad (4\text{-}26)$$

Where: σ_n = normal stress

τ = shear stress

k_n = normal stiffness

k_s = shear stiffness

v_r and u_r = relative normal and shear displacements, respectively

$[C]_i$ = constitutive for the interface element

In most of these models, the shear stiffness is based on a tangent modulus from laboratory direct shear tests. However for the normal stiffness, k_n, a high value, relative to other parameter, of the order of $10^8 - 10^{12}$ units is assigned, which may not be appropriate. [Desai et al. 1984]

The thin - layer proposed by Desai et al. [Desai et al. 1984], which has been used in soil - structure interaction and rock joints, is treated essentially like any other solid element. (figure 4-9) However the constitutive matrix, $[c]_i$, of the element has been expressed as: [Desai et al. 1984]

$$\{d\sigma\} = [C]_i \{d\varepsilon\} \qquad (4\text{-}26)$$

Where: $\{d\sigma\}$ = vector of increments of stresses

$\{d\varepsilon\}$ = vector of increments of strains

The constitutive matrix, $[c]_i$, is defined as follows:

$$[C]_i = \begin{bmatrix} [C_{nn}]_i & [C_{ns}]_i \\ [C_{sn}]_i & [C_{ss}]_i \end{bmatrix} \qquad (4\text{-}27)$$

Where: $[C_{nn}]$ = normal component

$[C_{ss}]$ = shear component

$[C_{ns}]$ and $[C_{sn}]$ represent coupling effects

(Since the determination of coupling components from laboratory tests is difficult, they will not be included)

As an assumption, the behaviour near the interface is considered as a finite thin zone instead of a zero thickness as found in some other formulations. (figure 4-8) [Desai et al. 1984]

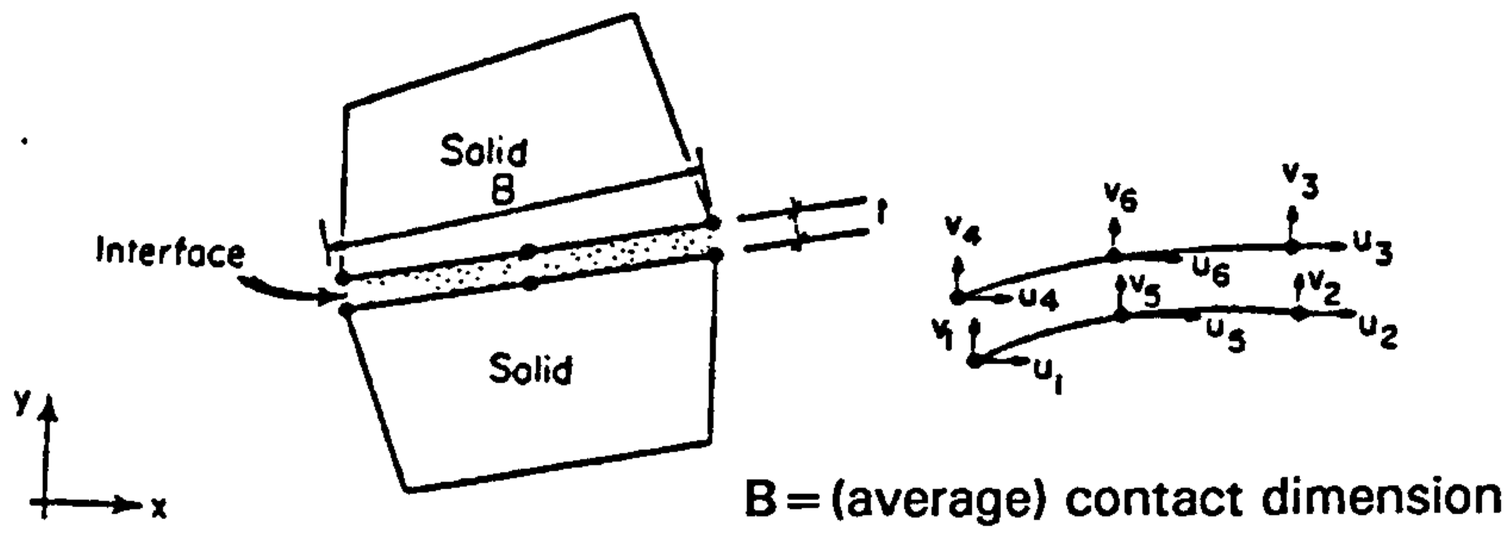

Figure 4-9: A two - dimensional thin - layer interface element
[Desai et al. 1984]

The normal properties of the interface during the deformation process must be logically dependent on the characteristics of the interface layer itself, and also the properties and stress condition of the surrounding elements. (equation 4-28)

$$\left[\bar{C}_{nn}\right]_i = \lambda_1 [C_{nn}]_i + \lambda_2 \left[C_{nn}^{\text{upper layer}}\right] + \lambda_3 \left[C_{nn}^{\text{lower layer}}\right] \qquad (4\text{-}28)$$

Where: $\left[\bar{C}_{nn}\right]$ = normal behaviour of the interface layer element

λ_1, λ_2, and λ_3 = the participating factors which vary between 0 to 1

As a simplification, it could be assumed that $\lambda_2 = \lambda_3 = 0$ and $\lambda_1 = 1$.

Appropriate values for λ_1 may be obtained by a trial and error procedure in which numerical solutions are compared with laboratory test results. It was also stated that for an interface between a geological material and concrete, satisfactory results could be obtained by assigning the interface normal component the same properties as the geological material. [Desai et al. 1984] In this investigation, an isotropic element have been used, based on the value of the shear modulus which will be discussed in the next paragraph.

The shear component, $[C_{ss}]$, has been assumed to be composed of a shear modulus, G_i, for the interface. (figure 4-10)

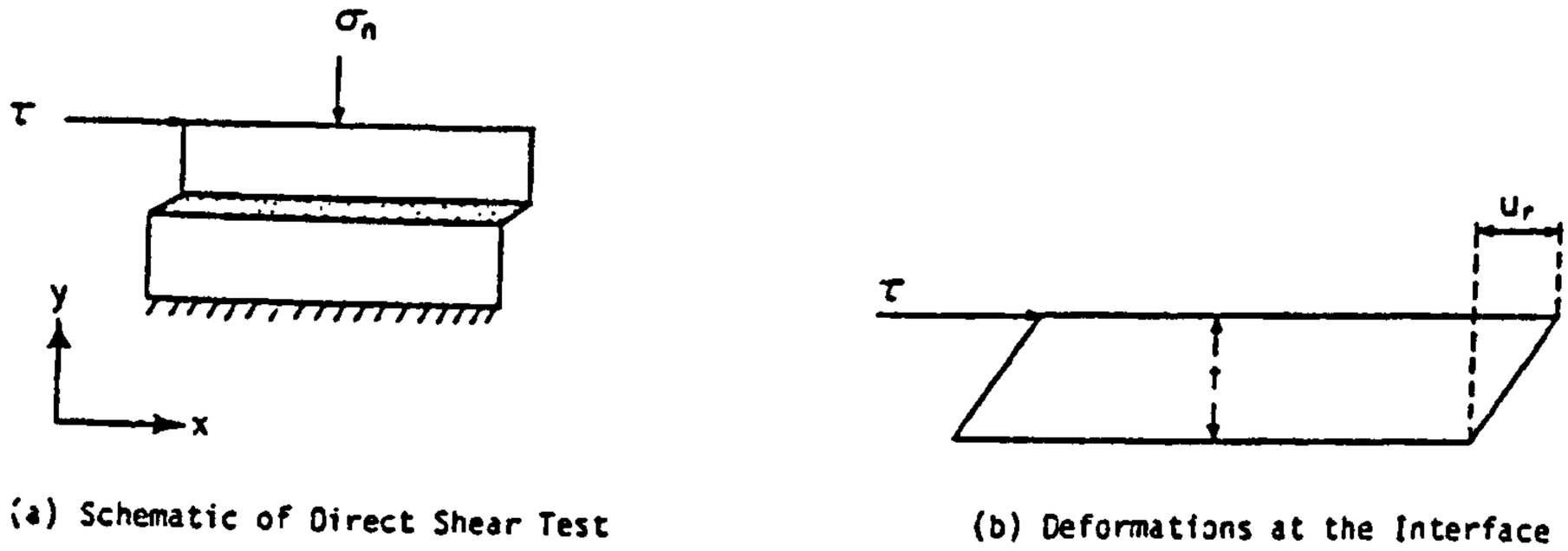

Figure 4-10: Behaviour at the interface [Desai et al. 1984]

The G_i modulus is defined as follows: [Desai et al. 1984]

$$G_{i(\sigma_n,\tau,u_r)} = \frac{\partial\,[\tau_{(\sigma_n,u_r)}]}{\partial\, u_r} \times t\Big|_{\sigma_n} \qquad (4\text{-}29)$$

Where: G is the shear modulus of the interface layer, MPa

σ_n is the normal pressure in the direct shear test

τ is the shear stress, MPa

u_r is the deformation at the interface, mm

t is the thickness of the interface layer, mm

The ratio of $\frac{\partial [\tau_{(\sigma_r, u_r)}]}{\partial u_r}$ will be defined by analysing the appropriate plane strain finite element mesh of the shear box specimens reported in chapter 5. (figures 6-9-a & 6-10-a) Since the studies carried out by Desai et al. [Desai et al. 1984] showed satisfactory correlation between the finite element analysis and the laboratory results, the above assumption would be acceptable. Moreover the interface element layer has been assumed elastic, and isotropic.

The formulation of the thin - layer interface element can be made by assuming it to be linear elastic, non - linear elastic or elastoplastic. The stiffness matrix, $[k]_i$ can be defined in the same procedure as it is done for solid elements. For a linear elastic behaviour, we have: [Desai et al. 1984]

$$[k]_i = \int_V [B]^T [C^e] [B] \, dV \qquad (4\text{-}30)$$

Where: $[B]$ = transformation matrix

V = volume

$[C^e]$ = the constitutive matrix for a linear elastic model

The equations of the element are then written as:

$$[K]_i \{q\} = \{Q\} \qquad (4\text{-}31)$$

Where: $\{q\}$ = vector of nodal displacements

$\{Q\}$ = vector of nodal forces

For two - dimensional plane strain idealization and linear elastic behaviour, the constitutive matrix, $[C^e]$, can be expressed as:

$$[C^e]_i = \begin{bmatrix} C_1 & C_2 & 0 \\ C_2 & C_1 & 0 \\ 0 & 0 & G_i \end{bmatrix} \qquad (4\text{-}32)$$

Where: $$C_1 = \frac{E(1-\upsilon)}{(1+\upsilon)(1-2\upsilon)}$$

$$C_2 = \frac{Ev}{(1+v)(1-2v)}$$

E = the elastic modulus

v = Poisson's ratio

G_i = the shear modulus defined in equation (4-29)

In order to avoid the danger of ill conditioning in the assembled elastic equation, , the elastic stiffness characteristics of the interface elements should not differ from those of adjacent, solid, elements by large amounts. As a safe rule a ratio of 1:1000 could be considered as the maximum limit. It should be added that the stiffness of the interface element is proportional to E/t, in directions corresponding to the important shear and normal deformations [Zienkiewicz et al. 1970]

With regard to the above, the thickness of the thin interface layer is a very important parameter, as it may affect the quality of the interface behaviour. If the ratio of t/B (figure 4-9) is too small, computational difficulties may arise and if it is too large, the thin - layer interface element will behave basically as a solid element. This can be done by performing parametric studies in which the predictions of the relative displacement from various thicknesses are compared

with the previous results regarding the ratio of $\frac{\partial [\tau_{(\sigma_r, u_r)}]}{\partial u_r}$. Desai et al. [Desai et al. 1984] have concluded that satisfactory simulation of interface behaviour can be obtained for t/B (B is the width of the surrounding elements) in the range of 0.01 to 0.1. Satisfactory use of much lower ratios of t/B have been also reported by other investigators. [Desai et al. 1984]

As it will be mentioned both in chapter 6 and chapter 7, the results of the current study have been also consistent with the previous findings, and therefor a ratio of t/B = 0.01 will be chosen for all the thin layered systems in those chapters.

Two failure criteria for predicting the possible delamination at the interface layer will be considered, the Mohr Coulomb criteria and the normal stress at the interface.

The above failure criteria will be implemented as follows:

In chapter 6, for the analysis of the thin layered systems used in the Steel

Wheel Rolling Load experiment, the distribution of shear stress, τ_{xy}, and normal stress, σ_y, along the interface will be drawn and compared with the corresponding values of shear strength and normal pull off bond strength. The value of shear strength will be calculated from equation (4-25). [Zienkiewicz et al.] [Desai et al. 1984]

$$Shear\ strength = C + \sigma_n \tan \Phi \qquad (4\text{-}25)$$

Where: C is the cohesion at the interface, MPa

σ_n is the normal stress

$\tan \Phi$ is the coefficient of friction

When $\tau_{xy} > C + \sigma_n \tan \Phi$, it means that a slippage may occur. Similarly if $\sigma_y > Bond\ strength$, a debonding at the interface will be predictable.

The test procedure for laboratory determination of the interface properties, namely cohesion, coefficient of friction, and tensile bond strength, along with their corresponding values for each combination of materials will be given in chapter 5.

It should be noted that after a failure occurring at each node, a new distribution of the stresses will take place within the whole volume of the structure. Therefore the results of the above analysis for each model could predict the interface nodes at which the first horizontal cracks may appear.

In chapter 7, for the analysis of the thin layered systems used in the NUROLF experiment, due to the low tyre contact pressure, a linear elastic behaviour will be considered for all the constitutive materials. This has made it possible to use a special two dimensional elasto - plastic interface model which is available in the LUSAS finite element system. The elasto - plastic interface model may be used for representing the friction - contact relationship within planes of weakness between two discrete two dimensional bodies. As it was mentioned, nonlinear behaviour is governed by an elasto - plastic constitutive law, which is formulated with a Mohr - Coulomb criteria tangential to the interface plane, and a limited tension criteria normal to the interface plane. [LUSAS User Manual]

Four modes of deformation are incorporated with this model for the thin interface layer, stick mode, slip mode, debonding mode, and rebonding mode. (figure 4-11)

The definition of the four modes of deformation had been also proposed by Desai in 1981. [Desai 1981]

The stick mode and the slip mode may occur when the normal stress is compressive. In the debonding mode, the computed normal stress can be tensile, although it is physically zero at the interface. If the normal stress in an interface which has been in the debonding or opening mode becomes compressive in subsequent loading or unloading, it may rebond or close. In a non - linear incremental analysis, any excess tensile stress is redistributed in the vicinity of the debonded zone. Details of modes of deformations computed before and after each iteration and equilibrium will be given in section 7-3-1-4 of chapter 7.[Desai et al. 1984]

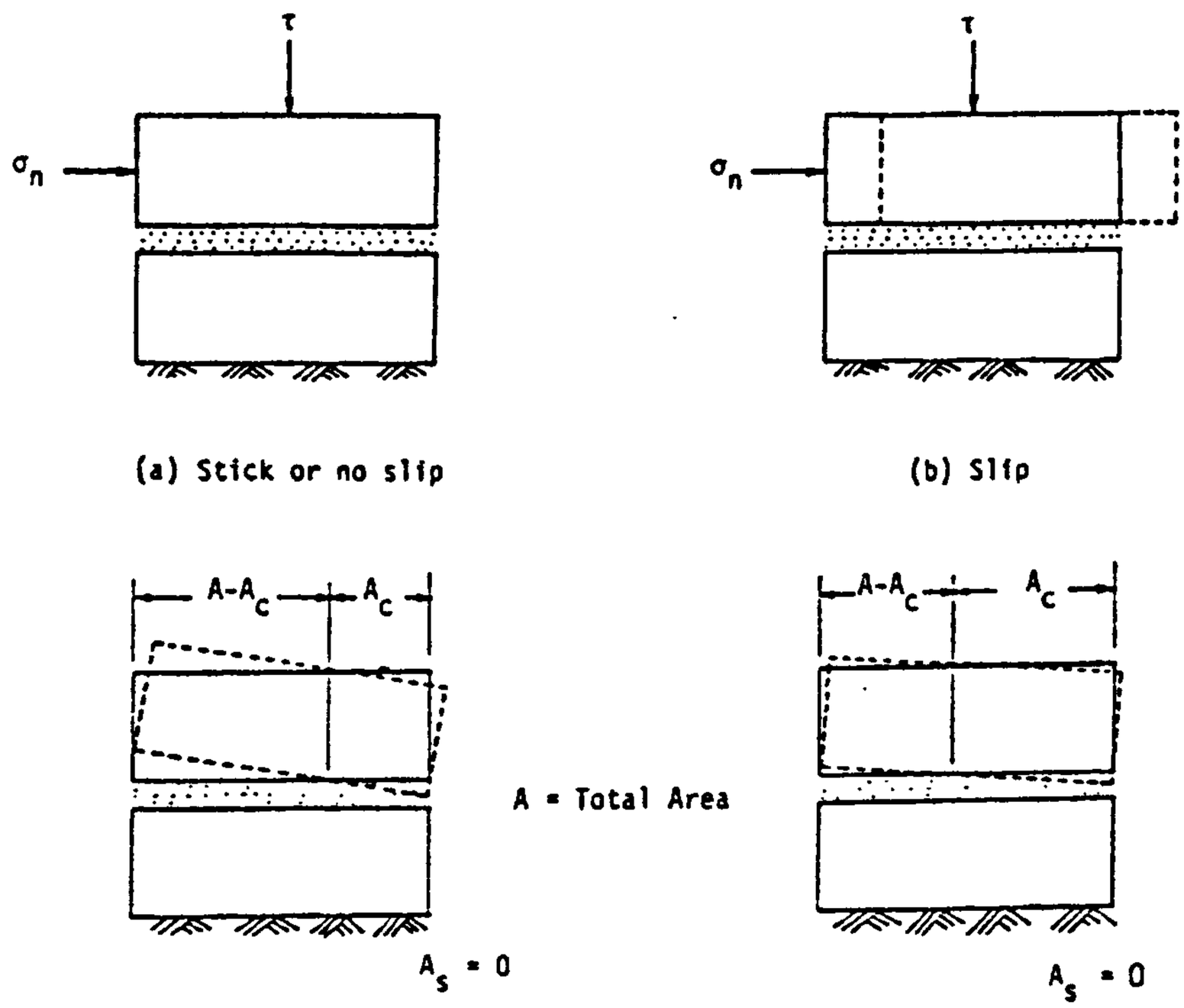

Figure 4-11: Schematic of four modes of deformation at interface
[Desai et al. 1984]

The solution for this elasto - plastic interface model will be based on an incremental - iterative procedure using Newton - Raphson iterations. The program automatically will modify the values of normal and shear stresses after each iteration and equilibrium. [LUSAS User Manual]

Once again it should be mentioned that the values of cohesion, coefficient of friction, and tensile bond strength for each combination of materials will be given in chapter 5.

As it is seen from the above expressions, in this method, when a failure occurs at any node, the redistribution of stresses and strains within the structure would be taken into account. For evaluating a thin layered system with regard to the delamination defect, it is therefor necessary to carry out the analysis on two models of the structure simultaneously, one with a friction - slip interface model and the other with a stick interface model. In the friction - slip model the real characteristics of the interface are considered whereas in the stick model the properties of the interface are chosen so that a perfect bond between the upper layer and the lower layer is guaranteed. Therefore, any difference between the distribution of shear stresses along the interfaces of the two models will be the result of occurrence of a slippage or debonding at the interface of the real structure.

4-4 Conclusions

Theoretical models developed for analysing a layered systems may be divided into four main groups. Among these, the finite element method is the most appropriate model for analysing a thin layered system. However the theory of layered systems in a repair application defined by Plum in [Plum Sept. 1990] is also directly relevant to the thin layered systems for evaluating of repair materials in a repair application.

In this study the behaviour of a thin layered system under the action of a rolling load with regard to the possible delamination defect at the interface between the two upper layers subjected to the load is of main interest. Therefore considering an appropriate thin layer of interface elements in the finite element model is a necessity. Owing to the existence of the vertical pressure at the contact area between a wheel and the surface of a thin layered system, the thin interface layer element proposed in [Desai et al. 1984] was introduced for this study. Any delamination at the interface of a thin layered system may occur as a result of a slippage or debonding at that zone. Consequently two failure criteria have to be considered for predicting the possible delamination, the Mohr Coulomb criteria and the normal stress at the interface.

Obviously for the implementation of the structural analysis, it is necessary to carry out appropriate tests regarding the material characteristics and the interface bond strength for each combination of different layers of materials.

CHAPTER 5

MATERIAL CHARACTERISTICS AND INTERFACE BOND STRENGTH

Material characteristics

Interface bond strength

5-1 Material characteristics

5-1-1 Types of materials

The materials used in this study consisted of Portland cement concrete (in the Steel Wheel Rolling Load experiment), steel fibre concrete (in the NUROLF experiment), one type of polymer cement concrete, two types of polymer concrete, and two types of primers as follows:

- Portland cement concrete
- Steel fibre concrete
- P4 system (polymer cement concrete)
- G1194 (polymer concrete)
- G1294 (polymer concrete)
- Gprime (primer)
- Pprime (primer)

In the following, each of the above materials and the corresponding tests and results, where applicable, will be illustrated.

5-1-2 Portland cement concrete

As it will be described later in chapter 6, Portland cement concrete slabs have been used in the Steel Wheel Rolling Load experiment. In this experiment all specimens consisted of small plain concrete slabs with one or two layers of other materials cast on top of them. For the student made specimens, the concrete substrate layers were of sizes 600 mm by 300 mm by 50 mm and were obtained from cutting precast concrete slabs of larger sizes. These precast slabs were supplied by a manufacturer and their performance under the prescribed loading conditions during the tests was satisfactory. However no accurate information regarding the strength and stress strain relationship of the concrete under load was available. Therefore it was decided to carry out some compressive strength and modulus of elasticity tests on the hardened concrete.

5-1-2-1 Preparation of plain concrete cube specimens for the measurement of compressive strength and modulus of elasticity

As it was said before, the concrete slabs used in the Steel Wheel Rolling Load experiment were provided by cutting larger precast slabs into smaller pieces of

the appropriate sizes. So the required number of cubes for carrying out the compressive strength test should be provided using the same slabs. Five cubes of size of 70 mm were provided using a concrete sawing machine. It should be added that for these specimens the ratio of aggregate size to the cube dimension was within the acceptable limits, i.e. less than 1:4 or 1:3. [Bungey 1989] [Neville 1983] However the effect of size on the strength of concrete will be considered in section 5-1-2-3-1.

5-1-2-2 Test procedure

To avoid introducing stress concentrations owing to unevenness of the upper and lower surfaces of the cubes during the test, faces of the cubes in contact with the platens of the testing machine were well ground before test. Then each cube was placed with the ground faces in contact with the platens of the testing machine. The load on the cube was applied at a constant rate of stress equal to 15 MPa/min. [BS 1881 : Part 4 : 1970] [Neville 1983]
The tests were carried out using a 5000 kN. hydraulically operated machine. The measurement of the axial force and displacements was made using a set of INTERCOLE data loggers and the Spectra lab software installed on a PC. The system was calibrated by carrying out similar compression tests and using two methods of displacement measurement, strain bridges and dial gauges.

5-1-2-3 Test results

5-1-2-3-1 Compressive strength

The crushing strength results have been reported to the nearest 0.5 MPa. [Neville 1983] The influence of size of specimens has been taken into account using the following equation: [Neville 1966]

$$\frac{f_c}{f_{cu,152}} = 0.56 + \frac{0.697}{\left(\frac{V}{152hd} + \frac{h}{d}\right)} \qquad (5\text{-}1)$$

Where: V = Volume of the specimen
h = The height of the specimen
d = The least lateral dimension of the specimen
f_c = Strength of the concrete specimens

$f_{cu,152}$ = Strength of 6 in. (150 mm) cube

The test results along with the dimensions of specimens have been reported in table 5-1-a. The values of mean strength, standard deviation, and coefficient of variation are shown in table 5-1-b.

In figure 5-1-a the stress - strain curves in compression are also depicted. The values of strains have been obtained by dividing the corresponding displacements by the height of each specimens.

Table 5-1: Results of compression tests on the small hardened concrete cubes related to the Steel Wheel Rolling Load experiment

a: Dimensions, compressive strengths, f_c, of the small cubes and their equivalent strengths of 150 mm cubes, $f_{cu,152}$

b: Mean strength, standard deviation, and coefficient of variation

Table 5-1-a:

Specimen Number	Dimensions (mm) Length-Width-Height	f_c (MPa)	$f_{cu,152}$ (MPa)
Specimen No. 1	72.8-71.6-72.4	59.0	57.5
Specimen No. 2	73.2-71.6-72.7	58.0	56.5
Specimen No. 3	73.1-71.8-72.3	60.5	59.0
Specimen No. 4	73.5-71.2-71.8	60.0	58.5
Specimen No. 5	73.5-71.3-71.9	63.5	62.0

Table 5-1-b:

Type of test	Total number of specimens	Mean strength $f_{cu,152}$ (MPa)	Standard deviation (MPa)	Coefficient of variation per cent
Compression cube test	5	58.5	2.08	3.6

From now onwards the mean value of $f_{cu,152}$ will be used as the compressive strength of the concrete.

5-1-2-3-2 Modulus of elasticity

Figure 5-1-a shows the stress - strain diagrams for the small cubes of concrete used in the Steel Wheel Rolling Load experiment. In these diagrams, the small concave - up parts of the curves at the start of loading which are due to the existing of fine shrinkage cracks, have been omitted. [Neville 1983] This has been done by projecting a tangent line to the end of the concave - up part of the curve and shifting the axis to meet it, without changing the values of the stresses.

From these diagrams the value of modulus of elasticity is obtainable. However there are basically two different types of this parameter, tangent modulus and secant modulus. The term Young's modulus of elasticity is applied only to the straight part of a stress - strain curve, or generally to the initial tangent modulus, i.e. to the tangent to the curve at the origin. The initial tangent modulus is of little practical importance, because it can only explain the behaviour of the material at the beginning of loading. [Neville 1983] Since the increase in strain due to the action of load partly depends on the creep of concrete, secant modulus of elasticity could be a more appropriate definition of the modulus of elasticity. Due to the fact that the behaviour of concrete at stresses less than 50 percent of the ultimate strength is nearly elastic, [Nilson et al. 1991] the secant modulus will be determined using this level of stress.

From the results of stress - strain relations for small concrete cubes and using the above criteria, the calculated values of modulus of elasticity for this type of concrete are listed in tables 5-2-a and 5-2-b. Although these values are related to the modulus of elasticity for concrete in compression, they could reasonably be used in tension wherever needed. [Galloway et al. 1976]

Using the concept of secant modulus and the diagrams shown in figure 5-1-a, an idealized stress - strain curve, based on the average values of stresses and strains at four points, has been introduced and shown in figure 5-1-b.

Table 5-2: Modulus of elasticity of the small concrete cubes related to the Steel Wheel Rolling Load experiment, E_c, in compression test

a: Value of modulus of elasticity for each specimen, E_c

b: Mean value of modulus of elasticity , standard deviation, and coefficient of variation

Table 5-2-a:

Specimen Number	Secant Modulus, E_c GPa
Specimen No. 1	27.8
Specimen No. 2	26.9
Specimen No. 3	22.0
Specimen No. 4	19.6
Specimen No. 5	20.1

Table 5-2-b:

Type of test	Total number of specimens	Mean value of modulus of elasticity E_c (GPa)	Standard deviation (GPa)	Coefficient of variation per cent
Compression cube test	5	23.3	3.84	16.5

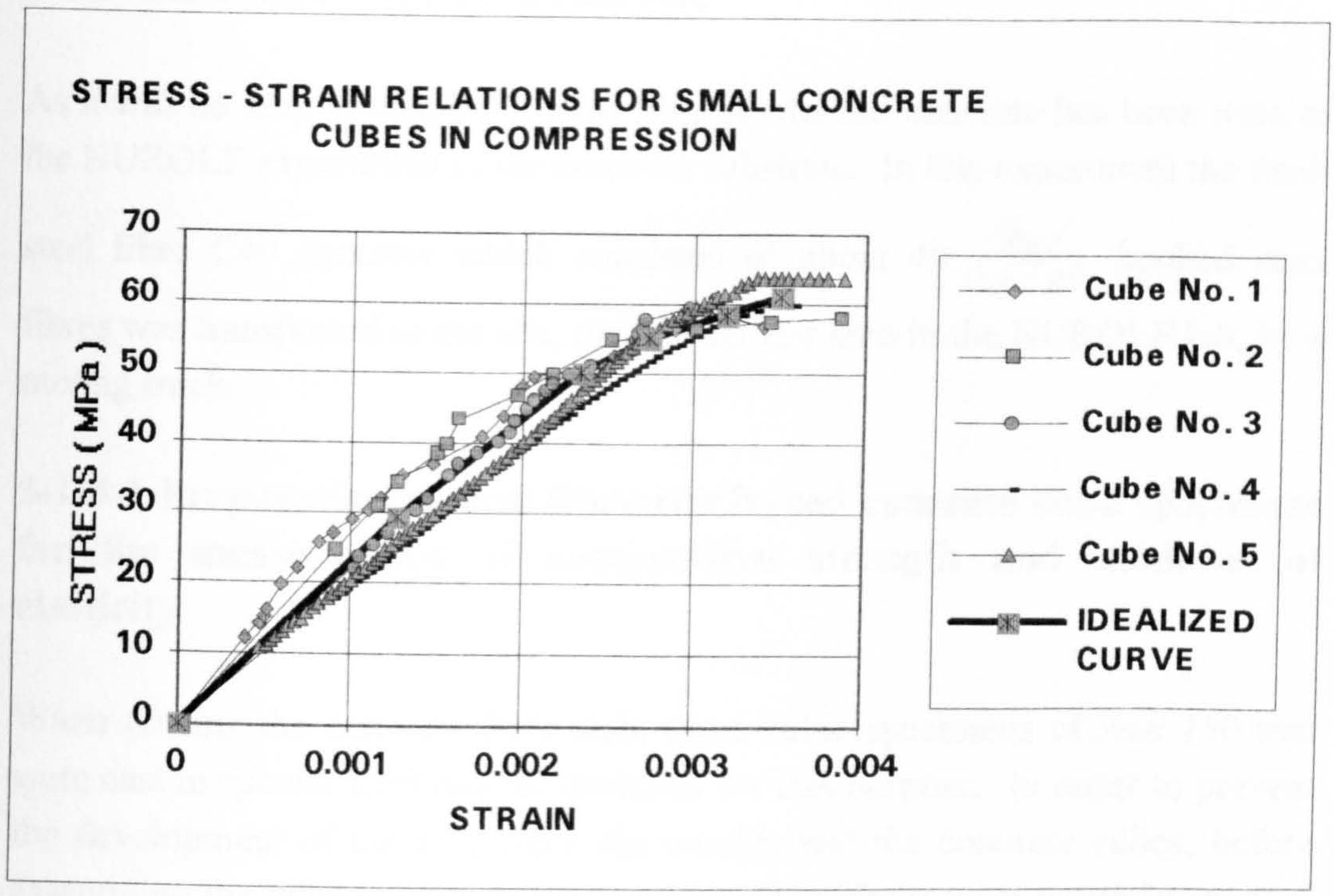

Figure 5-1-a: Stress- strain relations for small concrete cubes in compression related to the Steel Wheel Rolling Load experiment

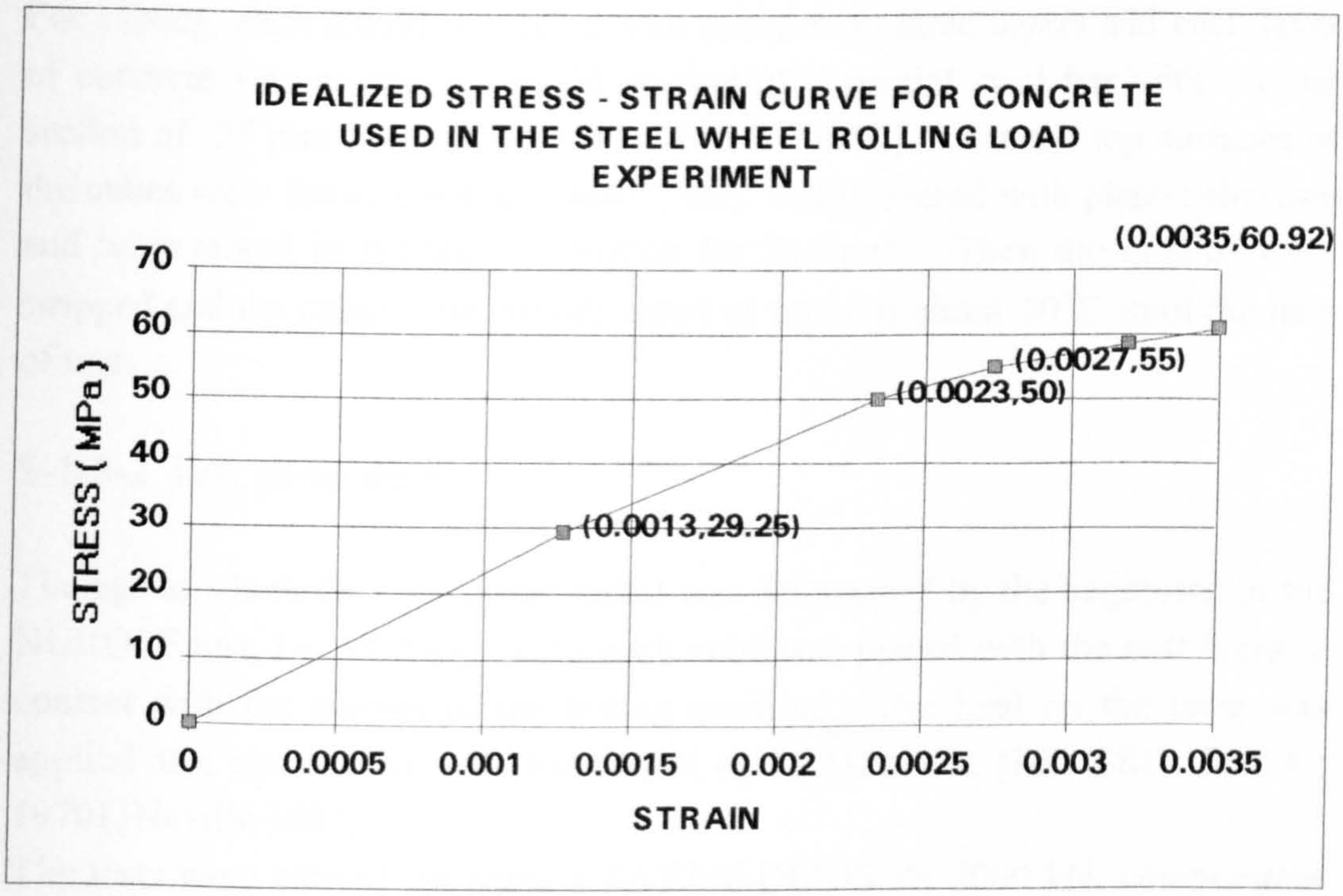

Figure 5-1-b: Idealized stress- strain curve for concrete used in the Steel Wheel Rolling Load experiment

5-1-3 Steel fibre reinforced concrete

As it will be seen in chapter 7, steel fibre reinforced concrete has been used in the NUROLF experiment as the concrete substrate. In this experiment the fresh steel fibre C40 concrete which consisted of about 40 kg/m^3 hooked steel fibres was transported to the site, the special test area in the NUROLF lab, by a mixing truck.

5-1-3-1 Preparation of steel fibre reinforced concrete cube specimens for the measurement of compressive strength and modulus of elasticity

When placing the concrete floor slab, three cubic specimens of size 150 mm were cast in special steel moulds designed for this purpose. In order to prevent the development of bond between the moulds and the concrete cubes, before assembling the moulds, their mating and inside surfaces were properly covered with a thin layer of mineral oil. The moulds and their bases were clamped together during casting to prevent the leakage of the concrete.
For casting, each mould was filled with concrete in three layers and each layer of concrete was compacted by 35 strokes of a special steel bar with a cross section of 25 mm square. [BS 1881: Part 3: 1970] After the top surfaces of the cubes were finished using a trowel, they were covered with plastic sheeting and were stored in the room condition for 24 hours. Then the moulds were stripped and the cubes were further cured in water at about $20^{\circ}C$ until the date of test.

5-1-3-2 Test procedure

The age at which the cubes were tested was determined by the beginning of the NUROLF test, i.e. 19 days. Then each cube was placed with the cast faces in contact with the platens of the testing machine. The load on the cube was applied at a constant rate of stress equal to 15 MPa/min. [BS 1881 : Part 4 : 1970] [Neville 1983]
The tests were carried out using a AVERY-DENISON 2000 kN. compression testing machine. For the purpose of the structural analysis, the measurement of the axial force and displacements was carried out using a dial gauge.

5-1-3-3 Test results

5-1-3-3-1 Compressive strength

The crushing strength results will be reported to the nearest 0.5 MPa. [Neville 1983] The test results along with the dimensions of the specimens have been reported in table 5-3-a. The values of mean strength, standard deviation, and coefficient of variation are shown in tables 5-3-b.
In figure 5-2-a the stress - strain curves in compression are also depicted. The values of strains have been obtained by dividing the corresponding displacements by the height of each specimens.

Table 5-3: Results of compression tests on the Steel fibre reinforced concrete cubes related to the NUROLF experiment
Grade and type of concrete: C40 concrete 40 kg / m^3 ZC 60/1.00 steel fibre [Knapton et al. 1994]
a: Dimensions, and compressive strength of each cube specimen, f_c
b: Mean strength, standard deviation, and coefficient of variation

Table 5-3-a:

Specimen Number	Dimensions (mm) Length-Width-Height	f_c (MPa)
Specimen No. 1	150.5-147.5-150.5	47
Specimen No. 2	150.5-150.0-150.0	46
Specimen No. 3	149.5-150.0-150.0	49

Table 5-3-b:

Type of test	Total number of specimens	Mean strength f_c (MPa)	Standard deviation (MPa)	Coefficient of variation per cent
Compression cube test	3	47.5	1.53	3.2

5-1-3-3-2 Modulus of elasticity

Figure 5-2-a shows the stress - strain diagrams for the steel fibre reinforced

concrete cubes used in the NUROLF experiment. Once again in these diagrams, the small concave - up parts of the curves at the start of loading which are due to the existing of fine shrinkage cracks [Neville 1983], have been omitted.

From the results of stress - strain relations for the steel fibre reinforced concrete cubes and using the same method as illustrated in section 5-1-2-3-2, the calculated values of modulus of elasticity for this type of concrete are listed in tables 5-4-a and 5-4-b. Although these values are related to the modulus of elasticity for concrete in compression, they could reasonably be used in tension wherever needed. [Galloway et al. 1976] Once again using the concept of secant modulus and the diagrams in figure 5-2-a, an idealized stress - strain curve, based on the average values of stresses and strains at four points, has been introduced and shown in figure 5-2-b.

Table 5-4: Modulus of elasticity of the steel fibre reinforced concrete cubes related to NUROLF experiment, E_c, in compression test

a: Value of modulus of elasticity for each specimen, E_c

b: Mean value of modulus of elasticity , standard deviation, and coefficient of variation

Table 5-4-a:

Specimen Number	Secant Modulus, E_c GPa
Specimen No. 1	16.4
Specimen No. 2	17.5
Specimen No. 3	15.9

Table 5-4-b:

Type of test	Total number of specimens	Mean value of modulus of elasticity E_c (GPa)	Standard deviation (GPa)	Coefficient of variation per cent
Compression cube test	3	16.6	0.82	4.9

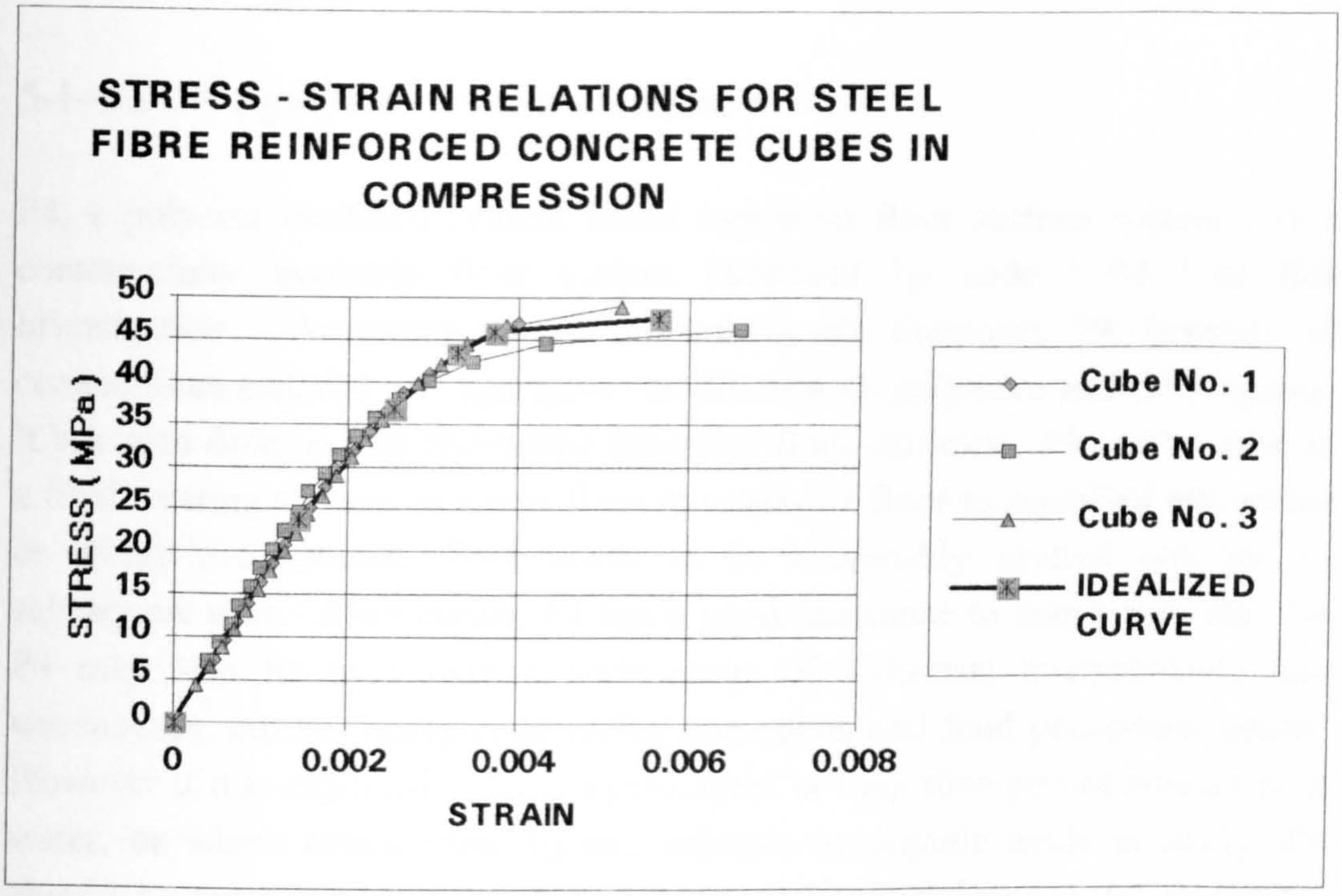

Figure 5-2-a: Stress- strain relations for steel fibre reinforced concrete cubes in compression

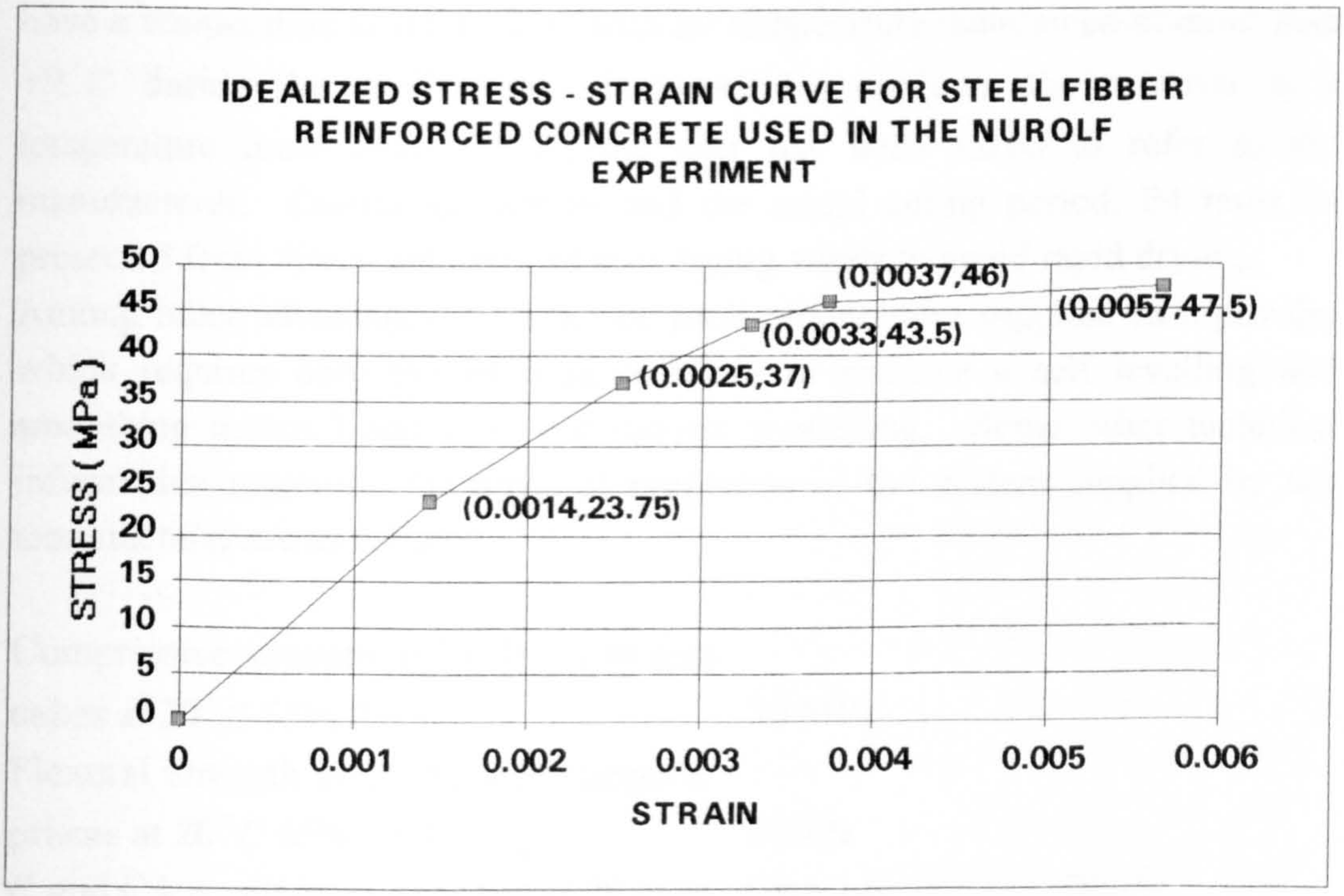

Figure 5-2-b: Idealized stress- strain curve for steel fibre reinforced concrete used in the NUROLF experiment

5-1-4 Flooring materials

5-1-4-a P4 (polymer cement concrete)

P4, a polymer modified cement based industrial floor surface system , is a commercially available floor system identified by code ' P4 ' in this investigation. According to the manufacturer's literature, P4 consists of cementitious material and aggregate modified with polymers and flow agents. It has been designed for reinstating industrial floor surfaces. P4 can be used as a final wearing surface on a new floor to achieve a floor to specified tolerances or where the concrete floor needs to be reasonably evened out for its subsequent uses. After curing, P4 has a good resistance to water and oils. So P4 may also be used over a wide range of industrial environments like warehouses, but not heavy engineering operations and food processing plants. However if it is expected to have a permanent or long time period contact with water, or where attack from organic solvents or organic acids is likely, P4 should be protected by a suitable resin based material like G1194 or G1294 which will be discussed later in this chapter. It has been specified that the surface of the concrete substrate onto which this material is to be applied must have a temperature at least $+5^{\circ}C$ with air temperature maintained at more than $+9^{\circ}C$ during the application. However for applying the material at a temperature more than $+25^{\circ}C$, the user has been asked to refer to the manufacturer. During application and the initial curing period, P4 must be protected from direct sunlight and also drying winds to avoid rapid drying.
Among other advantages, P4 is a one pack product and supplied as a powder which requires only the addition of water to produce a self levelling and smoothing material and does not require trowelling. Some other technical information regarding the physical properties of the system supplied by the manufacturer are as follows:

Compressive strength at 28 days (40 mm cubes at $20^{\circ}C$ 65% RH):	30 MPa	
Flexural strength at 28 days (rectangular prisms at $20^{\circ}C$ 65% RH):	8 MPa	
C and CA accelerated wear test at 28 days	Category Highest rating	Good

BRE impact resistance at 28 days:	Category	A
BS 8204: part 1 1987:	Highest rating	
Minimum thickness:	6 mm	
Maximum thickness:	12 mm	
TRRL slip resistance test-	Dry	Wet
4S rubber slider:	Excellent	Satisfactory
TRRL rubber slider:	Excellent	Satisfactory
Traffic time (20˚C), foot traffic:	4 hours	
Light traffic:	36 hours	

Based on the requirements for analysing the thin layered systems which will be discussed in chapters 6 to 7, the following mechanical tests were prescribed for this material: compressive strength test, modulus of elasticity in compression test, and flexural strength test.

5-1-4-b G1194 and G1294 (polymer concrete)

G1194 and G1294 are epoxy resin based floor topping systems, identified by codes ' G1194 ' and ' G1294 ' respectively in this investigation. G1194 is a commercially available floor system, but G1294 has not been approved to be supplied to the market yet, consequently there is not any published literature on the description of this material. However both of these materials have been designed for about the same purposes.

G1194 and G1294 are supplied as four and two component systems respectively and are pre - weighed for mixing on site.

According to the manufacturer's literature, G1194 consists of graded aggregates and a pigmented epoxy resin binder. This system is available in a wide variety of standard colours. After curing, G1194 provides a dense, smooth, impervious, coloured and chemically resistant floor surface which is light - reflective, hygienic and easy to clean. It can be used in a wide variety of light industrial environments as a lasting solution to floor maintenance problems. Some typical applications of this product have been enumerated as clean rooms, laboratories, plant rooms and light industrial plants. As a limitation, it has been specified that the surface of the substrate on to which G1194 is to applied should be dry and not to suffer from rising damp and should have a relative humidity not greater than 75 % at the time of installation, as measured

in accordance with BS 8203 Appendix A, or by a Vaisala thermohygrometer type HMI 31.

As it will be seen in chapter 6 and 7, G1194 or G1294 may be used as thin protecting layers on top of P4 system. Among other advantages, both G1194 and G1294 are flow applied flooring systems and are self levelling and self smoothing and do not require trowelling. These materials are also fast application, consequently minimise downtime.

Some other technical information regarding the physical properties of G1194 system supplied by the manufacturer are as follows:

Compressive strength (BS 6319):	50 MPa
Flexural strength (BS 6319):	34 MPa
Cure time:	
Foot traffic:	24 hours
Vehicular traffic:	48 hours
Chemicals:	7 days

Once again, based on the requirements for analysing the thin layered systems which will be discussed in chapters 6 to 7, the following mechanical tests were prescribed for this material: compressive strength test, modulus of elasticity in compression test, and flexural strength test.

5-1-4-c Primers

Two types of primers were supplied by the manufacturer, Gprime and Pprime. Primers should be applied at the interfaces of a layered system to improve the bond strength between different layers of materials. For the combination of P4/Concrete, the wrong primer was only used to provide the worst situation. For other combinations both of the two primers were examined. Gprime is a two pack product while Pprime is a one pack one.

According to the manufacturer's literature, Gprime is a standard curing solvent free epoxy primer which should be satisfactory for all the resin products. Pprime has been designed as a primer for P4 range and composed of acrylic copolymer and water.

In order to achieve the maximum bond strength at the interface of a two layered system, it is essential that the substrate surface is clean and dry before applying

any type of primer. Grit blasting or light scabbling have been recommended as the preferred methods of surface preparation. The mix ratios of Gprime product is as follows: (All ratios are given by weight)

Base (gr.)	Hardener (gr.)
35550	1470

5-1-4-1 Preparation of test specimens for measurement of compressive strength test, measurement of flexural strength test, and determination of modulus of elasticity in compression test

5-1-4-1-a P4 (polymer cement concrete)

As was said, P4 is a one pack product and supplied as a powder which requires only the addition of water to produce a self levelling and smoothing material and does not require trowelling. P4 powder and water were taken by weight as specified by the manufacturer, 18% water and 82% P4 powder and mixed properly for five minutes by hand. For each age and type of test the required number of specimens were cast in special steel moulds designed for this purpose. In table 5-5 minimum required number of samples for each test and dimensions of test specimens have been listed. [BS 6319 : Parts 2 and 3 : 1983 and part 6 : 1984]

All specimens of the same age and type of test were made from the same mix. In order to prevent the development of bond between the moulds and the specimens, before assembling the moulds, their mating and inside surfaces were properly covered with a thin layer of Vaseline. The moulds and their bases were clamped together during casting to prevent the leakage of the polymer cement concrete.

After casting the specimens, they were kept in their moulds for 24 hours in the room temperature, then the moulds were stripped and the cubes were further cured in the same conditions until the date of test.

Table 5-5: Minimum required number of samples and dimensions of test specimens for compressive strength test, flexural strength test, and modulus of elasticity in compression test

Table 5-5: Continued

Type of test	Min. number of samples	Dim. of test specimens
Compressive strength	3	40mm-40mm 160mm
Flexural strength	4	25mm-25mm-100mm
Modulus of elasticity	3	40mm-40mm 160mm

5-1-4-1-b G1194 and G1294 (polymer concrete)

As it was said, G1194 and G1294 are supplied as four and two component systems respectively. The mix ratios of each product is shown in the following table:

Table 5-6: Mix ratios of G1194 and G1294 floor topping materials: (All ratios are given by weight)

Mix ratios	Base	Hardener	Aggregate	Colour pot
G1194	22.44	16.33	58.31	2.92
G1294	84.50	15.50	-	-

Compounds of each material were taken by weight as specified in table 5-6 and mixed properly for five minutes by hand. For each age and type of test the required number of specimens were cast in special steel moulds designed for this purpose. In table 5-5 minimum required number of samples for each test and dimensions of test specimens have been listed. [BS 6319 : Parts 2 and 3 : 1983 and part 6 : 1984]

All specimens of the same age and type of test were made from the same mix. In order to prevent the development of bond between the moulds and the specimens, before assembling the moulds, their mating and inside surfaces were properly covered with a thin layer of Vaseline. The moulds and their bases were clamped together during casting to prevent the leakage of the polymer cement concrete.

After casting the specimens, they were kept in their moulds for 24 hours in the room temperature, then the moulds were stripped and the cubes were further cured in the same conditions until the date of test

5-1-4-2 Test procedure

5-1-4-2-1 Measurement of compressive strength

The ages at which the cubes were tested were generally 14, 28 and 56 days. However in some cases materials were also tested at the age of 6 days. The reason for choosing these ages is as follows. In the Steel Wheel Rolling Load experiment the main objective of the research was to investigate the behaviour of thin layered systems comprised of these materials at the normal ages of 14 and 28 days. However as it will be noted in chapter 6, some ready made specimens for this experiment were supplied by the manufacturer and were tested at the age of about two months. Finally the ages of 3 and 6 days were in fact the ages of top layer of the P4 and G1194 materials respectively in the NUROLF experiment.

The principle of this test is the subjection of test cubes to a compressive force up to the failure the specimen. The compressive force at the failure point is measured to determine the compressive strength.

Before carrying out the compression test, the surfaces of each cube were gently sandpapered. The bearing surfaces of the testing machine was wiped clean. Then the specimen was placed with the cast faces in contact with the platens of the testing machine. The load on the specimen was applied at a constant rate of approximately 45 MPa per minute. [BS 6319 : Part 2 : 1983]

5-1-4-2-2 Measurement of flexural strength test

The principle of this test is the subjection of test prisms in the form of a simple, freely supported beam to a three point loading up to the failure the specimen. The apparent surface stress in bending at the failure point is measured to determine the flexural strength.

The testing machine was equipped with a pair of steel rollers for applying the load. (figure 5-3) All three rollers were longer than the width of the specimens, 32 mm for the two supporting rollers and 48.5 mm for the loading roller, and had a nominal diameter of 10 mm. The distance between the axes of the supporting rollers was 76.2 mm. During the test, the rollers were positioned so that their axes were perpendicular to the specimen under test.

Before carrying out the flexural test, the surfaces of each prism were gently sandpapered. The bearing surfaces of the rollers the sides of the specimen were wiped clean. Then the specimen was located symmetrically on the

equipment for the measurement of the flexural strength. The loading roller was located midway between the supporting rollers and was free to rotate in the vertical plane through its axes. The load on the specimen was applied at a constant rate such that the strain rate was 3.75 mm/min. [BS 6319 : Part 3 : 1983]

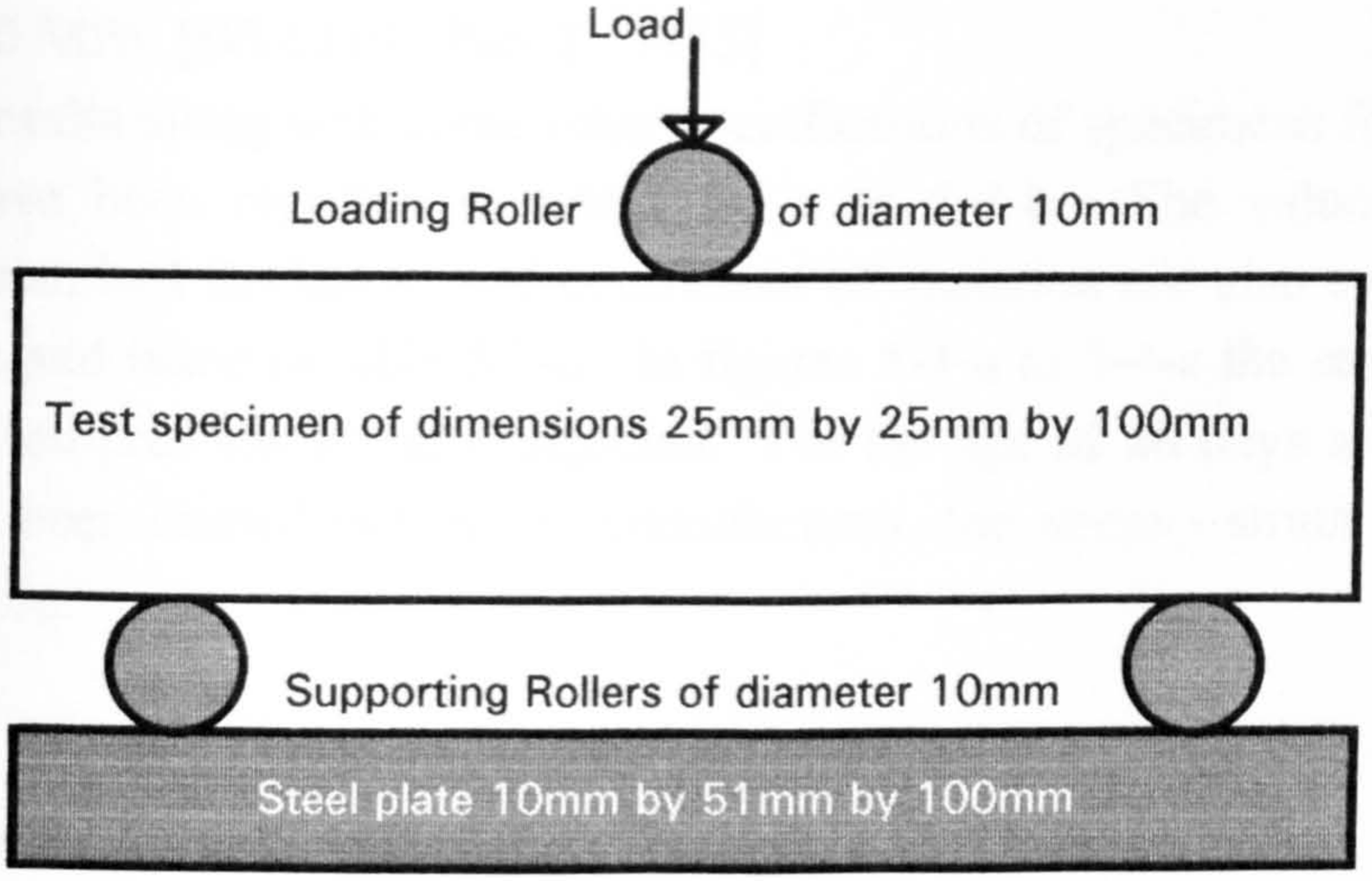

Figure 5-3 A schematic diagram of the flexural test equipment used in the flexural strength tests

5-1-4-2-3 Determination of modulus of elasticity in compression test

The principle of this test is the subjection of test prisms to a controlled axial load and measurement of their secant modulus by relating the compressive stress to the longitudinal strain induced by that stress. The measurement of the axial force and displacements was carried out using a set of INTERCOLE data loggers and the Spectra lab software installed on a PC.

Before carrying out the compression test, the surfaces of each prism were gently sandpapered. The bearing surfaces of the testing machine was wiped clean. Then the specimen was centrally placed on the lower machine platen in such a way that the load was parallel to the long axis of the test specimen. The load on the specimen was applied at a constant rate of approximately 2MPa/Sec. [BS 6319 : Part 6 : 1984]

5-1-4-3 Test results

5-1-4-3-1 P4 (polymer cement concrete)

5-1-4-3-1-a Measurement of compressive strength, P4

The compressive strength of each cube will be calculated by dividing the maximum load by the nominal cross - sectional area and will be reported to the nearest 1.0 MPa. [BS 6319 : Part 2 : 1983]

The test results along with some other specifications of specimens for each age of test have been reported in tables 5-7-a to 5-7-b. The values of mean strength, standard deviation, and coefficient of variation are also calculated at each stage and listed in table 5-7-c. In figures 5-4-a to 5-4-c the stress - strain curves in compression are also depicted. For the age of 28 days at which the tests have been carried out by the manufacturer, the stress - strain curves are not available.

Table 5-7: Results of the compressive strength tests at the ages of 6,14,28, and 56 days for the P4 cube specimens:

a: Ambient conditions during the preparation, curing and testing

b: Dimensions, mass of each specimen, compressive strength, and failure mode

c: Mean strength, standard deviation, and coefficient of variation

Table 5-7-a:

Age of the	Ambient conditions	
specimens at test	Temperature	Relative Humidity
6 Days	12.4˚ C - 20.5˚ C	48 % - 54 %
14 Days	14.8˚ C - 21.3˚ C	46 % - 54 %
28 Days *1	20˚ C	65 %
56 Days	10.2˚ C - 20.5˚ C	41 % - 56 %

*1: The results have been reported by the manufacturer.

Table 5-7-b:

Specimen Number	Age at the test (days)	Dimensions (mm) Length-Width-Height	Mass (gr.)	Compressive Strength (MPa)	Failure Mode
No. 1	6	40.0-40.3-40.2	125.3	22	Brittle
No. 2	6	40.3-39.9-40.2	125.4	22	Brittle

Table 5-7-b: Continued

Specimen Number	Age at the test (days)	Dimensions (mm) Length-Width-Height	Mass (gr.)	Compressive Strength (MPa)	Failure Mode
No. 3	6	40.3-40.3-40.1	124.7	22	Brittle
No. 4	6	40.2-40.6-39.9	125.3	21	Brittle
No. 1	14	40.1-40.3-40.3	123.9	25	Brittle
No. 2	14	40.8-40.2-40.7	127.2	26	Brittle
No. 3	14	40.0-40.8-39.9	124.2	25	Brittle
No. 1	28 *1	40 mm averaged	125.4	33	Brittle
No. 2	28 *1	40 mm averaged	125.0	32	Brittle
No. 3	28 *1	40 mm averaged	125.3	33	Brittle
No. 1	56	40.3-40.4-40.5	125.3	39	Brittle
No. 2	56	40.1-39.8-40.4	122.3	39	Brittle
No. 3	56	40.1-40.4-40.5	124.7	40	Brittle

*1: The results have been reported by the manufacturer.

Table 5-7-c:

Type of test	Age at the test (days)	Total number of specimens	Mean compressive strength (MPa)	Standard deviation (MPa)	Coefficient of variation (percent)
Compression cube test	6	4	22	0.50	2.3
Compression cube test	14	3	25	0.58	2.3
Compression cube test	28 *1	3	33	0.58	1.8
Compression cube test	56	3	39	0.58	1.5

*1: The results have been reported by the manufacturer.

5-1-4-3-1-b Measurement of flexural strength test, P4

The flexural strength of each prism, will be calculated using the following equation: [BS 6319 : Part 3 : 1983]

$$M = \frac{1.5WL}{BD^2} \qquad (5\text{-}2)$$

Where: M is the flexural strength, MPa
W is the maximum load of fracture, N
L is the span, mm
B is the breadth of specimen, mm
D is the height of specimen, mm

The values of flexural strength will be expressed to the nearest 0.2 MPa. The dimensions used in equation 5-2 will be those measured at the point of fracture. [BS 6319 : Part 3 : 1983]

The test results along with some other specifications of specimens for each age of test have been reported in tables 5-8-a to 5-8-b. The values of mean strength, standard deviation, and coefficient of variation are also calculated at each stage and listed in table 5-8-c.

Table 5-8: Results of the flexural strength tests at the ages of 7,14,28, and 56 days for the P4 prism specimens:
a: Ambient conditions during the preparation, curing and testing
b: The nominal sizes of each specimen before testing and the dimensions at the site of any fracture after carrying out the test , mass, flexural strength, and breaking load of each specimen.
c: Mean strength, standard deviation, and coefficient of variation

Table 5-8-a:

Age of the	Ambient conditions	
specimens at test	Temperature	Relative Humidity
7 Days *1	20˚ C	65 %
14 Days	14.8˚ C - 21.3˚ C	46 % - 54 %
28 Days *1	20˚ C	65 %
56 Days	10.2˚ C - 20.5˚ C	44 % - 56 %

*1: The results have been reported by the manufacturer.

Table 5-8-b:

Specimen Number	Age at the test (days)	Nominal sizes prior to test (mm)	Dim. at the site of fracture (mm)	Mass (gr.)	Flexural Strength (MPa)	Breaking load *3 (kN)
No. 1	7 *1	320-25-25	- *2	- *2	6.8	- *2
No. 2	7 *1	320-25-25	- *2	- *2	6.8	- *2
No. 3	7 *1	320-25-25	- *2	- *2	7.0	- *2
No. 1	14	25.0-25.3-100.0	25.3-25.2	120.3	6.2	871.5
No. 2	14	25.3-25.7-100.0	25.9-25.2	123.7	5.6	805.8
No. 3	14	25.0-25.5-100.0	25.6-25.2	123.3	6.4	910.3
No. 4	14	25.1-25.7-100.0	25.8-25.2	125.4	8.8	1261.4
No. 1	28 *1	320-25-25	- *2	- *2	10.4	- *2
No. 2	28 *1	320-25-25	- *2	- *2	11.6	- *2
No. 3	28 *1	320-25-25	- *2	- *2	10.8	- *2
No. 1	56	25.0-25.8-100.0	25.1-25.9	124.2	13.4	1973.9
No. 2	56	25.0-25.3-100.0	25.0-25.3	118.3	12.6	1764.0
No. 3	56	24.9-25.6-100.0	24.7-25.7	123.2	14.2	2026.8
No. 3	56	25.2-25.3-100.0	25.2-25.2	120.8	12.0	1680.1

*1: The results have been reported by the manufacturer.

*2: The information has not been reported by the manufacturer.

*3: For all the specimens fracture has occurred inside the middle third of the distance between the two supports.

Table 5-8-c:

Type of test	Age at the test (days)	Total number of specimens	Mean flexural strength (MPa)	Standard deviation (MPa)	Coefficient of variation (percent)
Flexural prism test	7 *1	3	6.8	0.12	1.8
Flexural prism test	14	4	6.8	1.4	20.0

Table 5-8-c: Continued

Type of test	Age at the test (days)	Total number of specimens	Mean flexural strength (MPa)	Standard deviation (MPa)	Coefficient of variation (percent)
Flexural prism test	28 *1	3	11.0	0.61	5.6
Flexural prism test	56	4	13.0	0.96	7.4

*1: The results have been reported by the manufacturer.

5-1-4-3-1-c Determination of modulus of elasticity in compression test, P4

The secant modulus of elasticity of each prism, will be calculated using the following equation: [BS 6319 : Part 6 : 1984]

$$E = \frac{(N_1 - N_2)}{(\varepsilon_1 - \varepsilon_2)bt} \qquad (5\text{-}3)$$

Where:

E is the secant modulus of elasticity, GPa

N_1 is the load corresponding to a strain of approximately 0.0022, kN

N_2 is approximately 10 % of N_1, kN

ε_1 is the strain under the load of N_1

ε_2 is the strain under the load of N_2

b is the width of the specimen at its centre to the nearest 0.1 mm

t is the thickness of the specimen at its centre to the nearest 0.1 mm

The values of secant modulus of elasticity will be expressed to the nearest 0.1 GPa. [BS 6319 : Part 6 : 1984]

The test results along with some other specifications of specimens for each age of test have been reported in tables 5-9-a to 5-9-b. The values of mean secant modulus of elasticity, standard deviation, and coefficient of variation are also calculated at each stage and listed in table 5-9-c.

The proposed idealized stress - strain curves for the P4 material at different ages have been also shown in figures 5-4-a to 5-4-c. The first part of each idealized curve is based on the results of the modulus of elasticity tests in compression on the prism specimens, whereas the other parts are based on the average values of stresses and strains at the corresponding idealized points obtained from the compressive strength tests on the cube specimens.

Table 5-9: Results of the modulus of elasticity in compression tests at the ages of 6, 14, 28, and 56 days for the P4 prism specimens:
a: Ambient conditions during the preparation, curing and testing
b: The Cross-sectional dimensions of the centre of each specimen, the upper (N_1) and lower (N_2) load levels used in equation (5-3), mean strain and the secant modulus of elasticity of each test specimen.
c: Mean secant modulus of elasticity, standard deviation, and coefficient of variation

Table 5-9-a:

Age of the	Ambient conditions	
specimens at test	Temperature	Relative Humidity
6 Days	21.0° C - 23.1° C	44 %-56 %
14 Days	14.8° C - 21.3° C	45 %-57 %
28 Days	14.6° C-21.6° C	42 %-54 %
56 Days	13.5° C-21.3° C	45 %-56 %

Table 5-9-b:

Specimen Number	Age at the test (days)	Cross - sectional Dim. at the centre (mm)	Upper (N_1) load (kN)	Lower (N_2) load (kN)	Mean strain	Modulus of elasticity (GPa)
No. 1	6	38.1-38.1	8.77	0.88	0.0005	12.1
No. 2	6	38.3-38.4	9.22	0.92	0.0005	11.2
No. 3	6	38.1-38.6	10.60	1.06	0.0005	14.0
No. 1	14	38.3-38.6	24.58	3.37	0.0010	14.6
No. 2	14	38.3-38.6	23.48	2.35	0.0011	12.8
No. 3	14	38.2-38.6	23.03	2.52	0.0009	15.5

Table 5-9-b: Continued

Specimen Number	Age at the test (days)	Cross - sectional Dim. at the centre (mm)	Upper (N_1) load (kN)	Lower (N_2) load (kN)	Mean strain	Modulus of elasticity (GPa)
No. 1	28	38.2-38.6	25.2	1.9	0.0012	13.8
No. 2	28	37.8-38.5	24.7	2.46	0.0010	15.0
No. 3	28	38.6-38.7	28.8	2.74	0.0012	14.9
No. 1	56	38.4-38.8	34.02	3.01	0.0013	16.0
No. 2	56	38.6-38.7	31.95	3.09	0.0014	14.3
No. 3	56	38.2-38.7	32.85	3.13	0.0012	16.2

Table 5-9-c

Type of test	Age at the test (days)	Total number of specimens	Mean secant modulus of elasticity (GPa)	Standard deviation (GPa)	Coefficient of variation (percent)
Modulus of elasticity test	6	3	12.4	1.43	11.5
Modulus of elasticity test	14	3	14.3	1.38	9.7
Modulus of elasticity test	28	3	14.6	0.67	4.6
Modulus of elasticity test	56	3	15.5	1.04	6.7

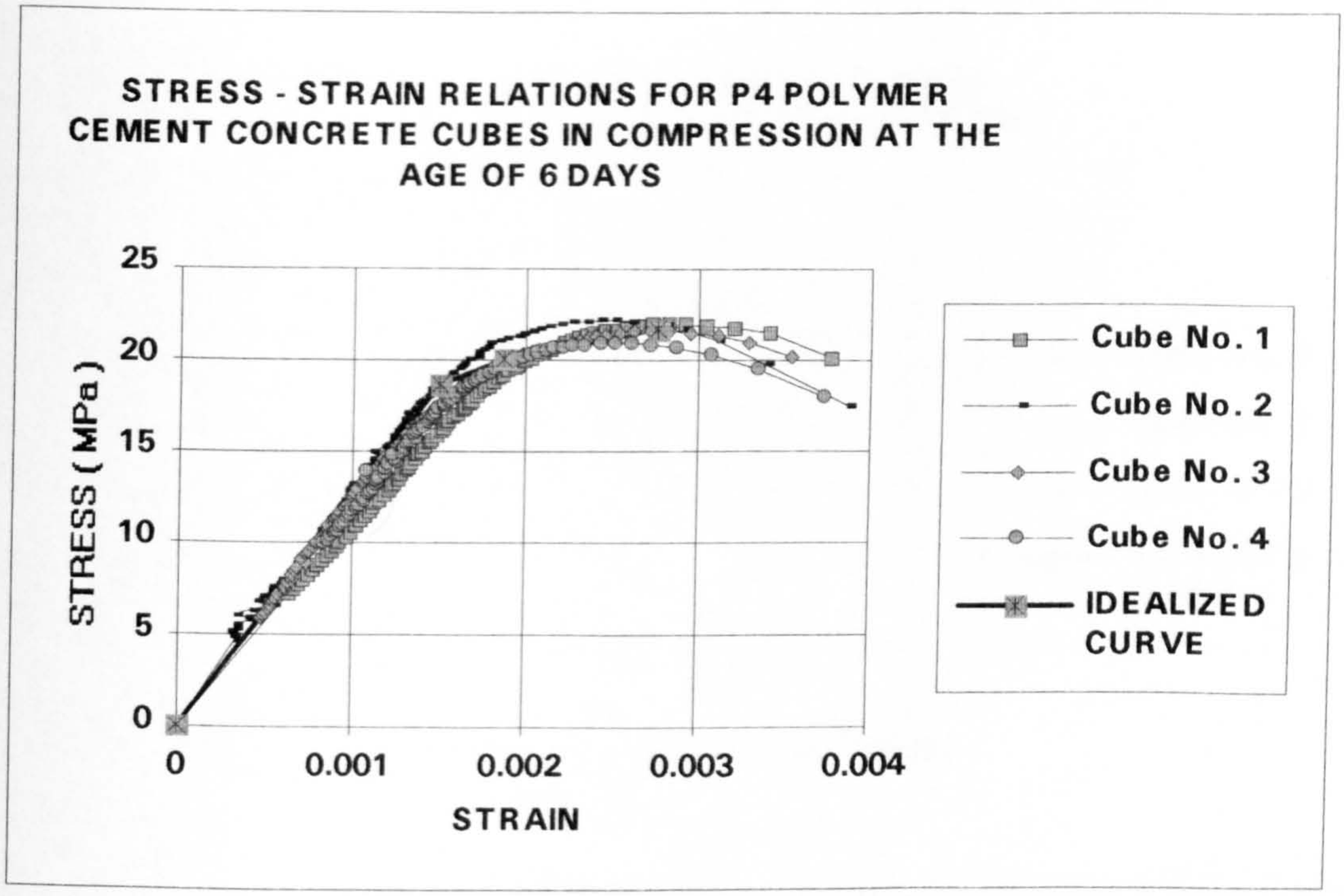

Figure 5-4-a-1: Stress- strain relations for P4 polymer cement concrete cubes in compression at the age of 6 days

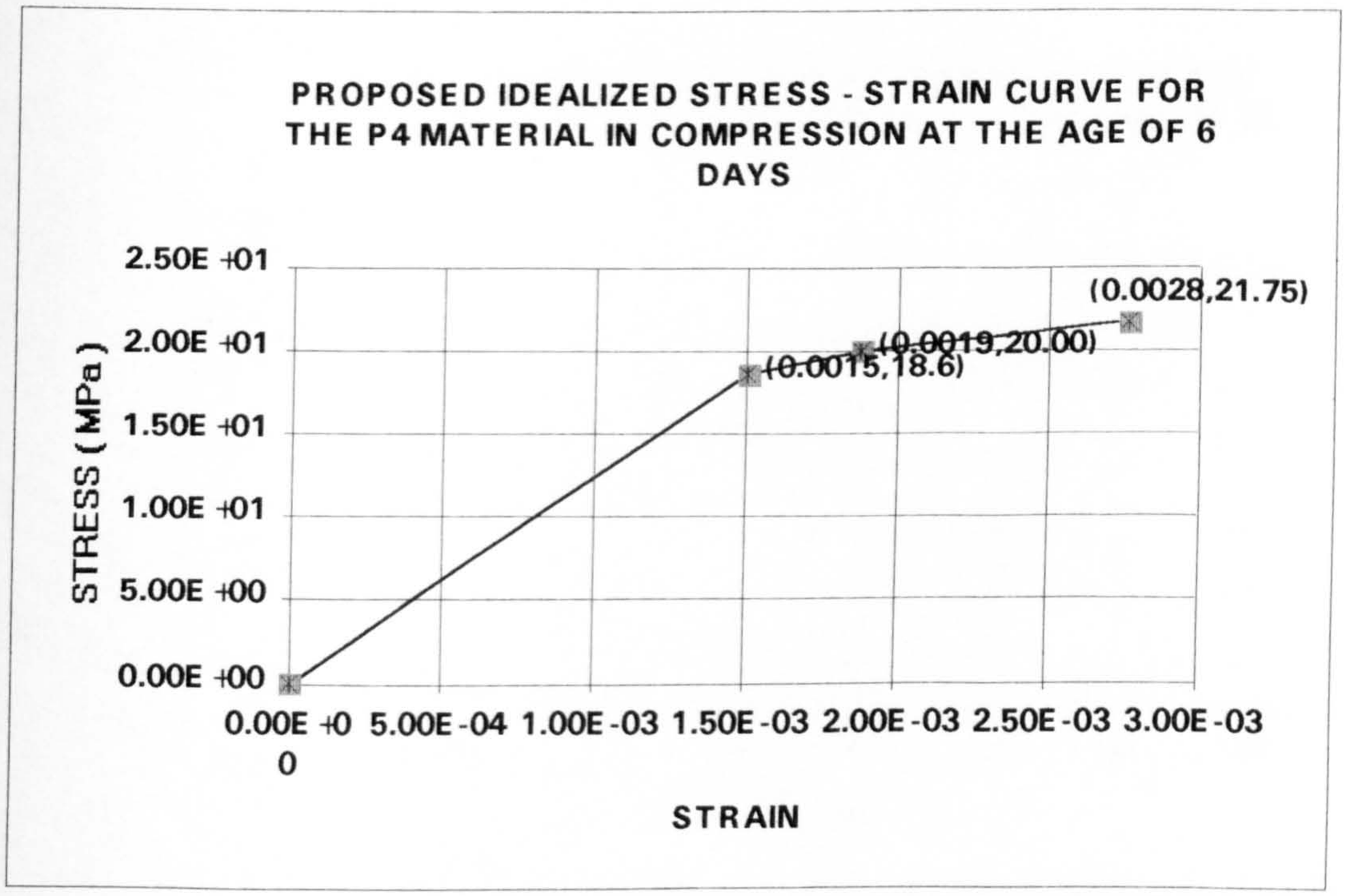

Figure 5-4-a-2: Proposed idealized stress- strain curve for the P4 material in compression at the age of 6 days

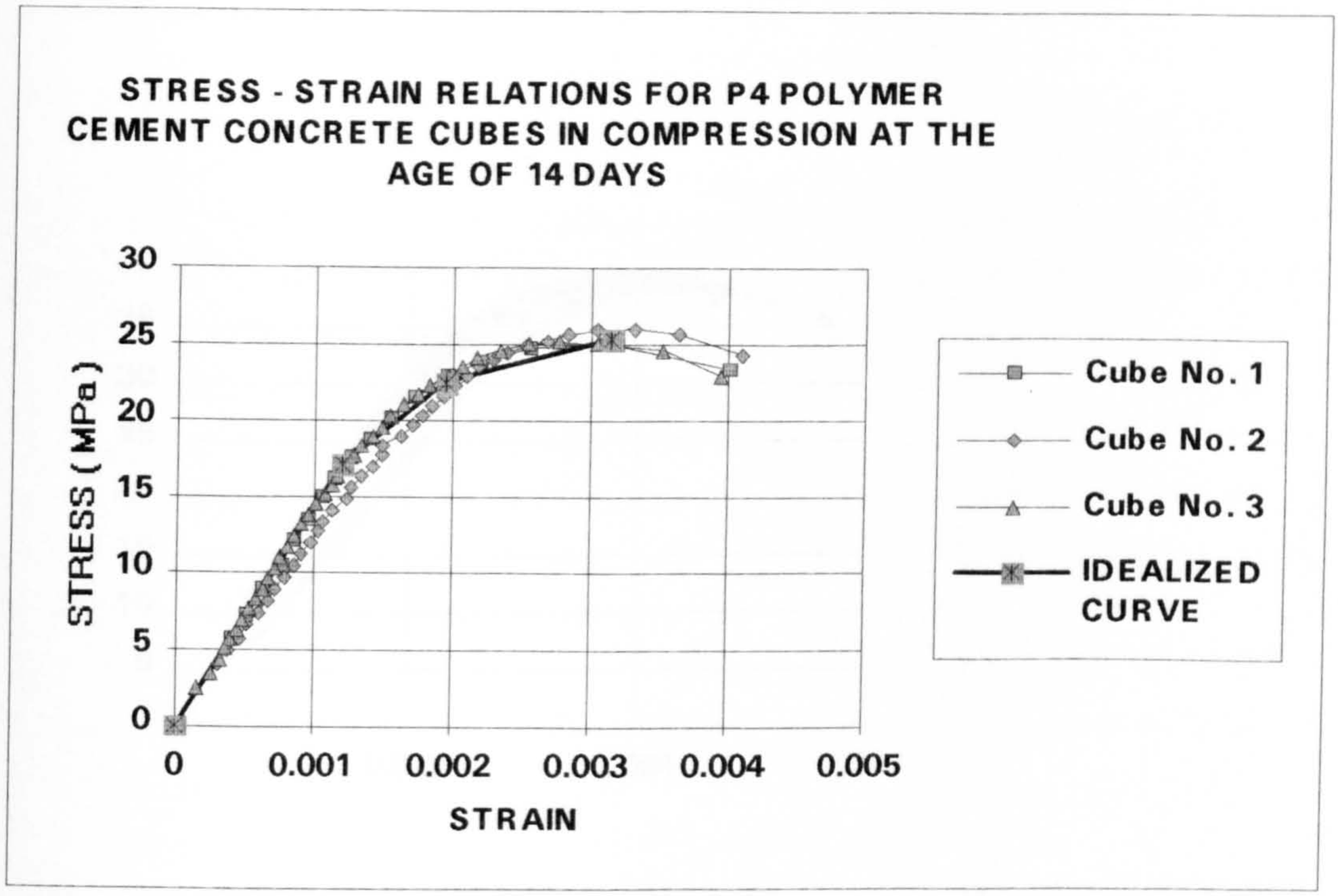

Figure 5-4-b-1: Stress- strain relations for P4 polymer cement concrete cubes in compression at the age of 14 days

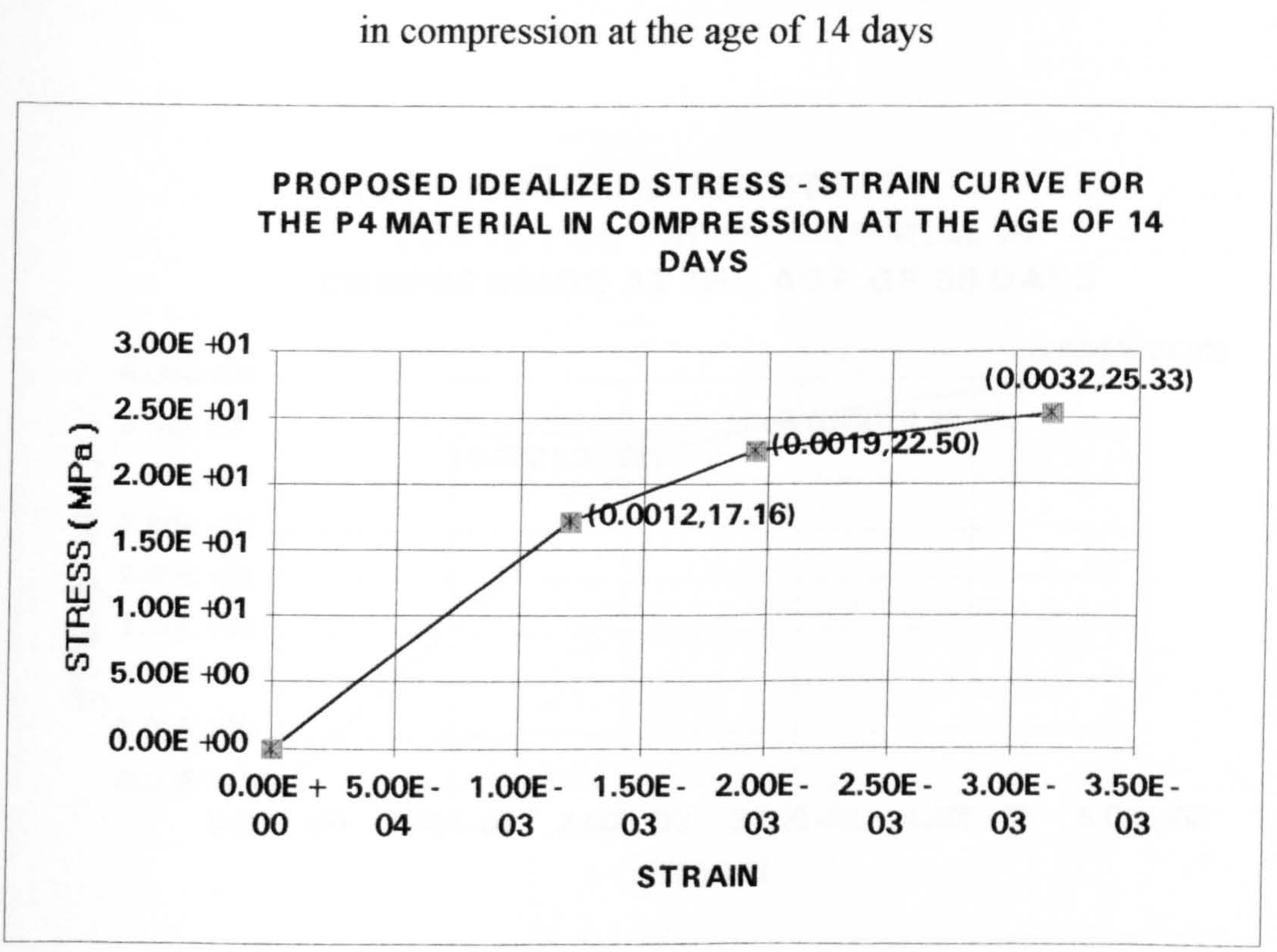

Figure 5-4-b-2: Proposed idealized stress- strain curve for the P4 material in compression at the age of 14 days

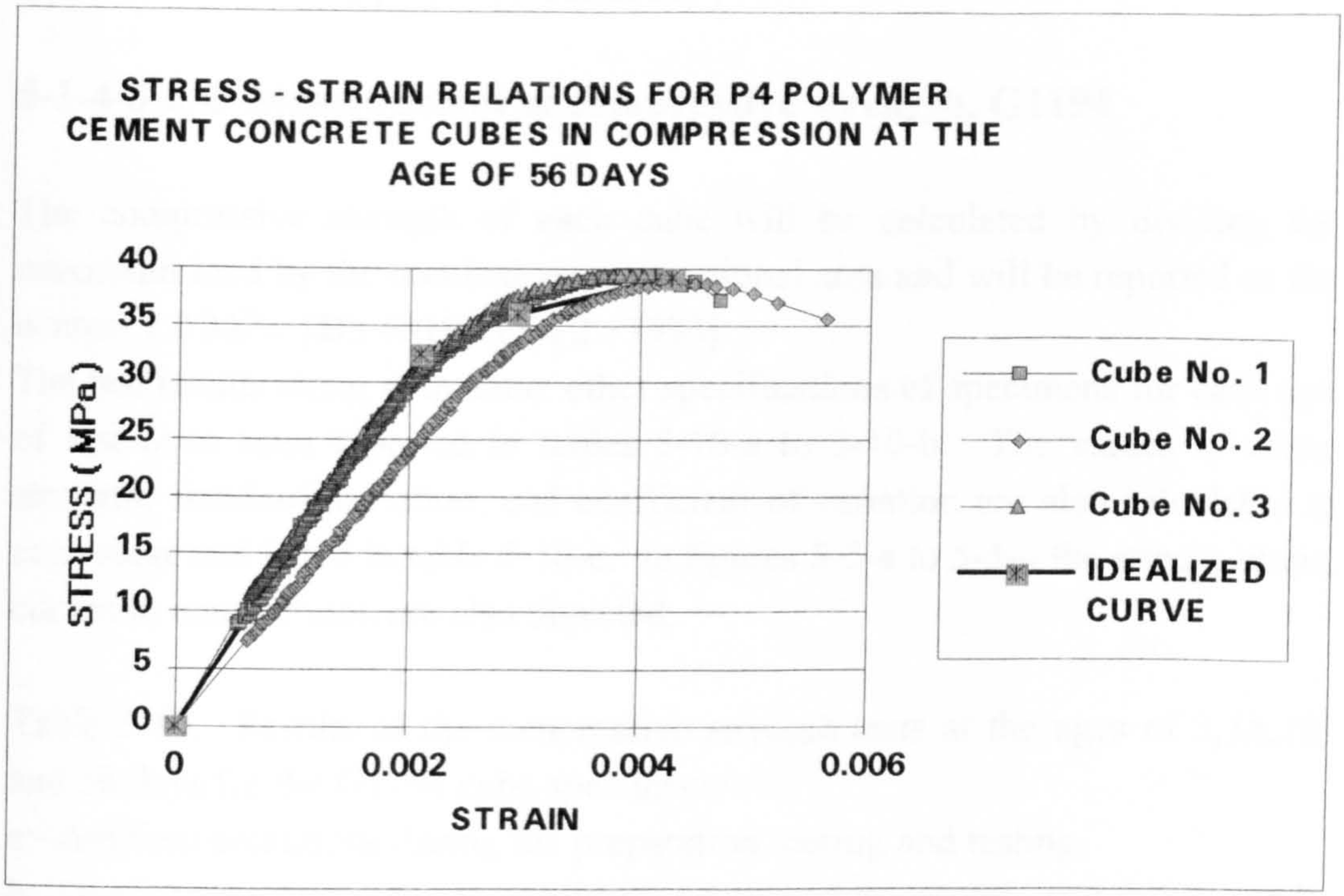

Figure 5-4-c-1: Stress- strain relations for P4 polymer cement concrete cubes in compression at the age of 56 days

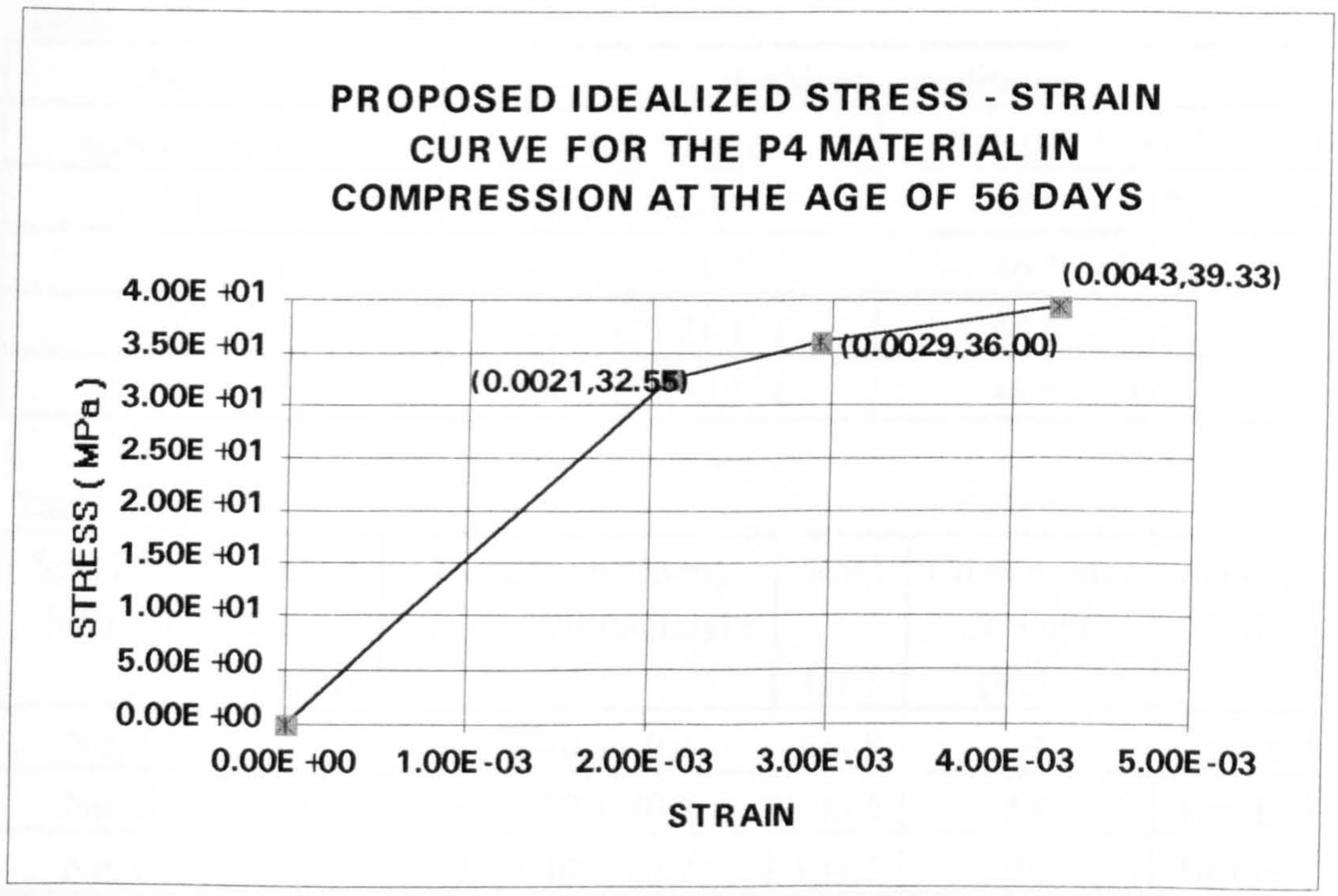

Figure 5-4-c-2: Proposed idealized stress- strain curve for the P4 material in compression at the age of 56 days

5-1-4-3-2 G1194 (polymer concrete)

5-1-4-3-2-a Measurement of compressive strength, G1194

The compressive strength of each cube will be calculated by dividing the maximum load by the nominal cross - sectional area and will be reported to the nearest 1.0 MPa. [BS 6319 : Part 2 : 1983]
The test results along with some other specifications of specimens for each age of test have been reported in tables 5-10-a to 5-10-b. The values of mean strength, standard deviation, and coefficient of variation are also calculated at each stage and listed in table 5-10-c. In figures 5-5-a to 5-5-c the stress - strain curves in compression are also depicted.

Table 5-10: Results of the compressive strength tests at the ages of 3,14,28, and 56 days for the G1194 cube specimens:
a: Ambient conditions during the preparation, curing and testing
b: Dimensions, mass of each specimen, compressive strength, and failure mode
c: Mean strength, standard deviation, and coefficient of variation

Table 5-10-a:

Age of the	Ambient conditions	
specimens at test	Temperature	Relative Humidity
3 Days	12.4˚ C - 20.5˚ C	48 % - 54 %
14 Days	14.8˚ C - 21.3˚ C	46 % - 54 %
28 Days	14.6˚ C - 21.1˚ C	45 % - 56 %
56 Days	10.2˚ C - 20.5˚ C	41 % - 56 %

Table 5-10-b:

Specimen Number	Age at the test (days)	Dimensions (mm) Length-Width-Height	Mass (gr.)	Compressive Strength (MPa)	Failure Mode
No. 1	3	39.4-40.1-40.1	104.9	54	Brittle
No. 3	3	40.2-39.1-40.1	103.6	54	Brittle
No. 3	3	38.9-40.3-40.2	104.1	56	Brittle
No. 1	14	40.3-39.9-40.1	106.8	60	Brittle
No. 2	14	40.9-40.4-40.2	108.3	60	Brittle

Table 5-10-b: Continued

Specimen Number	Age at the test (days)	Dimensions (mm) Length-Width-Height	Mass (gr.)	Compressive Strength (MPa)	Failure Mode
No. 3	14	40.2-39.6-40.3	105.6	61	Brittle
No. 1	28	40.4-40.0-40.1	107.1	69	Brittle
No. 2	28	40.8-40.3-40.2	108.0	66	Brittle
No. 3	28	40.2-40.0-40.3	106.4	70	Brittle
No. 1	56	39.9-39.9-39.9	105.8	80	Brittle
No. 2	56	40.0-40.0-40.0	107.1	82	Brittle
No. 3	56	40.0-40.0-40.0	107.2	79	Brittle

Table 5-10-c:

Type of test	Age at the test (days)	Total number of specimens	Mean compressive strength (MPa)	Standard deviation (MPa)	Coefficient of variation (percent)
Compression cube test	3	3	55	1.16	2.1
Compression cube test	14	3	60	0.58	1.0
Compression cube test	28	3	68	2.08	3.1
Compression cube test	56	3	80	1.53	1.9

5-1-4-3-2-b Measurement of flexural strength test, G1194

The flexural strength of each prism, will be calculated using equation (5-2). The values of flexural strength will be expressed to the nearest 0.2 MPa. The dimensions used in equation 5-2 will be those measured at the point of fracture. [BS 6319 : Part 3 : 1983] The test results along with some other specifications of specimens for each age of test have been reported in tables 5-11-a to 5-11-b. The values of mean strength, standard deviation, and coefficient of variation are also calculated at each stage and listed in table 5-11-c.

Table 5-11: Results of the flexural strength tests at the ages of 14,28, and 56 days for the G1194 prism specimens:

a: Ambient conditions during the preparation, curing and testing

b: The nominal sizes of each specimen before testing and the dimensions at the site of any fracture after carrying out the test , mass, flexural strength, and breaking load of each specimen.

c: Mean strength, standard deviation, and coefficient of variation

Table 5-11-a:

Age of the	Ambient conditions	
specimens at test	Temperature	Relative Humidity
14 Days	14.8˚ C - 20.5˚ C	50 % - 55 %
28 Days	14.6˚ C - 20.6˚ C	45 % - 54 %
56 Days	10.2˚ C - 20.5˚ C	44 % - 56 %

Table 5-11-b:

Specimen Number	Age at the test (days)	Nominal sizes prior to test (mm)	Dim. at the site of fracture (mm)	Mass (gr.)	Flexural Strength (MPa)	Breaking load *1 (N)
No. 1	14	24.7-25.0-100.0	24.9-25.1	102.8	37.8	5187.9
No. 2	14	24.8-25.0-100.0	24.5-25.2	103.0	32.2	4383.1
No. 3	14	25.0-25.0-100.0	24.9-25.1	104.0	37.8	5187.9
No. 3	14	25.0-25.0-100.0	24.8-25.3	103.1	33.4	4638.7
No. 1	28	25.0-25.2-100.0	25.1-25.5	106.7	35.8	5112.0
No. 2	28	24.8-25.0-100.0	24.8-25.3	104.1	38.0	5277.5
No. 3	28	24.6-25.0-100.0	24.8-25.1	103.6	38.0	5194.4
No. 4	28	24.9-25.0-100.0	25.0-25.1	104.1	38.0	5236.3
No. 1	56	25.0-25.1-100.0	25.2-24.8	101.6	37.6	5098.5
No. 2	56	24.9-25.5-100.0	24.9-25.5	101.7	40.6	5751.2
No. 3	56	24.9-25.1-100.0	24.8-25.3	100.6	39.2	5444.2
No. 4	56	24.7-25.1-100.0	24.7-25.1	101.0	35.0	4765.0

*1: For all the specimens fracture has occurred inside the middle third of the distance between the two supports.

Table 5-11-c:

Type of test	Age at the test (days)	Total number of specimens	Mean flexural strength (MPa)	Standard deviation (MPa)	Coefficient of variation (percent)
Flexural prism test	14	4	35.3	2.93	8.3
Flexural prism test	28	4	37.5	1.1	2.9
Flexural prism test	56	4	38.1	2.4	6.3

5-1-4-3-2-c Determination of modulus of elasticity in compression test, G1194

The secant modulus of elasticity of each prism, has been calculated using equation (5-3). The values of secant modulus of elasticity have been expressed to the nearest 0.1 GPa. [BS 6319 : Part 6 : 1984]

The test results along with some other specifications of specimens for each age of test have been reported in tables 5-12-a to 5-12-b. The values of mean secant modulus of elasticity, standard deviation, and coefficient of variation are also calculated at each stage and listed in table 5-12-c.

The proposed idealized stress - strain curves for the G1194 material at different ages have been also shown in figures 5-5-a to 5-5-d. The first part of each idealized curve is based on the results of the modulus of elasticity tests in compression on the prism specimens, whereas the other parts are based on the average values of stresses and strains at the corresponding idealized points obtained from the compressive strength tests on the cube specimens.

Table 5-12: Results of the modulus of elasticity in compression tests at the ages of 3, 14, 28, and 56 days for the G1194 prism specimens :

a: Ambient conditions during the preparation, curing and testing

b: The Cross-sectional dimensions of the centre of each specimen, the upper (N_1) and lower (N_2) load levels used in equation (5-3), mean strain and the secant modulus of elasticity of each test specimen.

c: Mean secant modulus of elasticity, standard deviation, and coefficient of variation

Table 5-12-a:

Age of the	Ambient conditions	
specimens at test	Temperature	Relative Humidity
3 Days	21.0° C - 23.1° C	48 % - 55 %
14 Days	14.8° C - 21.3° C	46 % - 54 %
28 Days	14.6° C - 21.1° C	44 % - 56 %
56 Days	10.2° C - 20.5° C	41 % - 56 %

Table 5-12-b:

Specimen Number	Age at the test (days)	Cross - sectional Dim. at the centre (mm)	Upper (N_1) load (kN)	Lower (N_2) load (kN)	Mean strain	Modulus of elasticity (GPa)
No. 1	3	37.8-38.1	15.66	1.57	0.0020	4.9
No. 2	3	37.7-38.2	18.79	1.88	0.0020	5.8
No. 3	3	37.9-38.0	18.99	1.91	0.0020	5.9
No. 1	14	38.0-38.2	24.00	2.55	0.0020	7.5
No. 2	14	37.8-38.4	25.20	2.20	0.0021	7.7
No. 3	14	38.1-38.2	24.50	2.35	0.0020	7.8
No. 1	28	38.0-38.1	30.40	3.30	0.0019	9.8
No. 2	28	37.9-38.5	30.90	3.18	0.0019	9.9
No. 3	28	37.8-38.2	33.50	3.41	0.0020	10.6
No. 1	56	37.9-37.9	38.80	3.49	0.0020	12.6
No. 2	56	37.6-38.4	38.20	4.02	0.0020	12.0
No. 3	56	38.0-38.3	44.00	6.37	0.0021	12.7

Table 5-12-c:

Type of test	Age at the test (days)	Total number of specimens	Mean secant modulus of elasticity (GPa)	Standard deviation (GPa)	Coefficient of variation (percent)
Modulus of elasticity test	3	3	5.5	0.55	10.0
Modulus of elasticity test	14	3	7.7	0.15	2.0
Modulus of elasticity test	28	3	10.1	0.44	4.4
Modulus of elasticity test	56	3	12.4	0.38	3.1

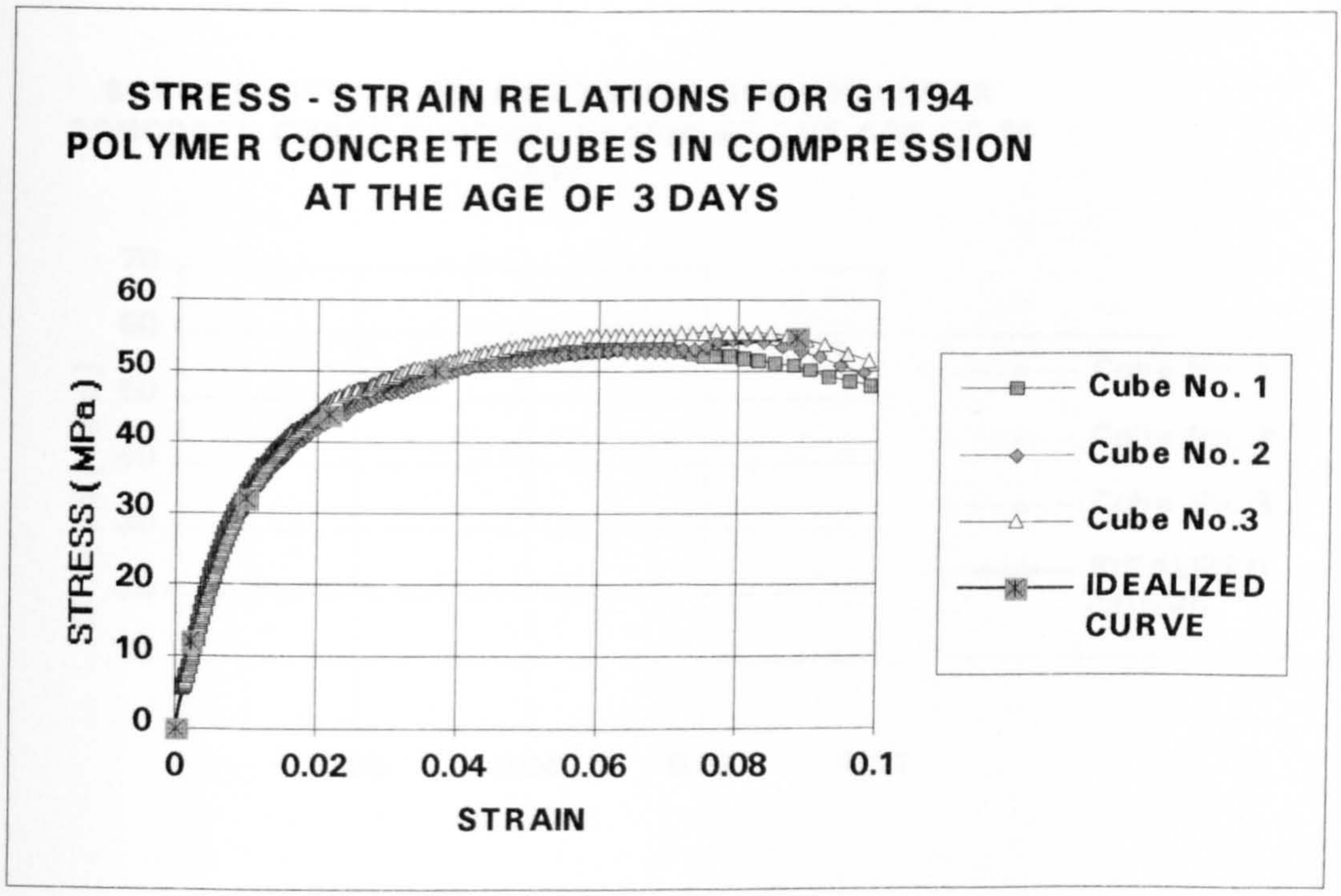

Figure 5-5-a-1: Stress- strain relations for G1194 polymer concrete cubes in compression at the age of 3 days

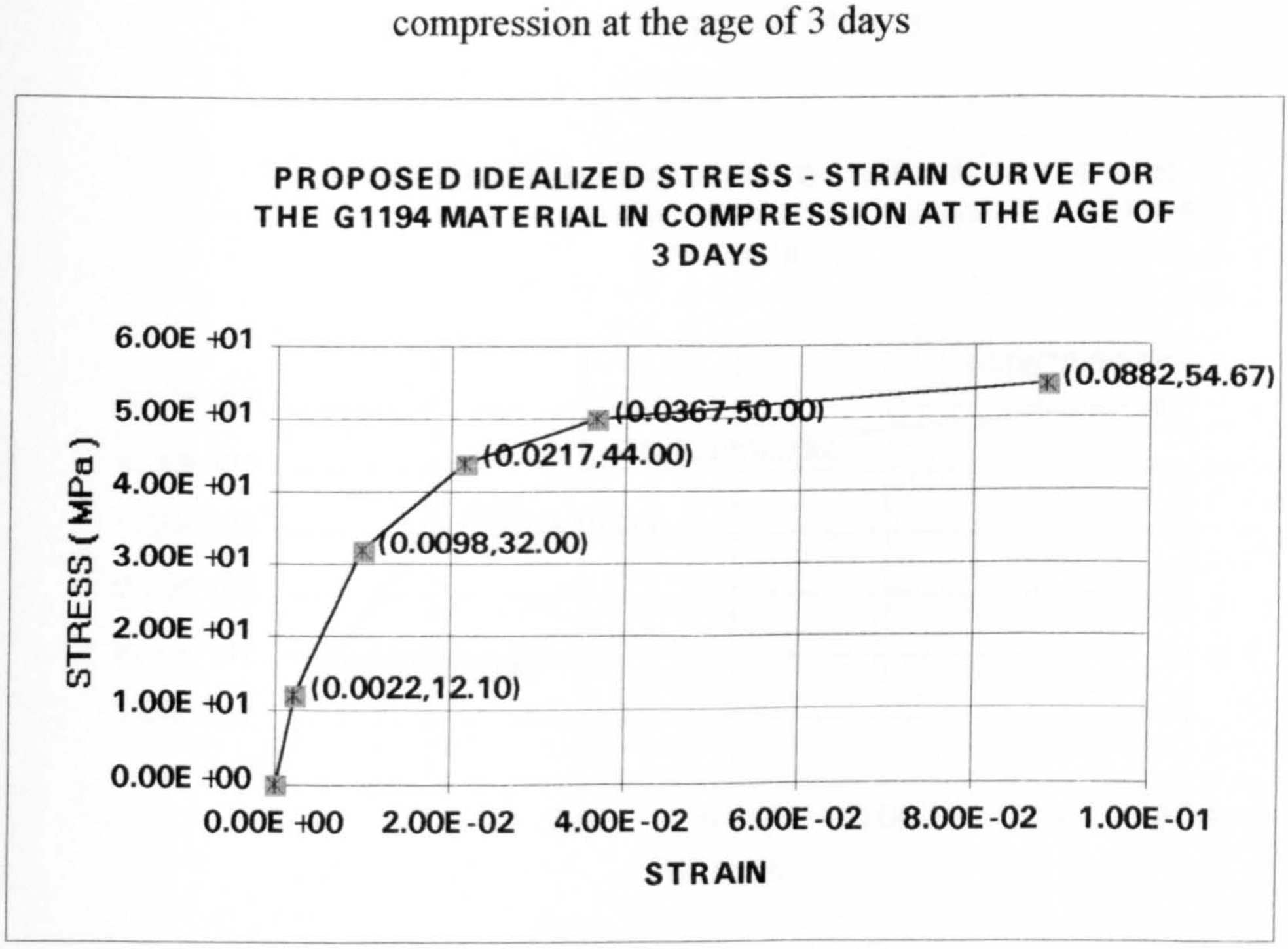

Figure 5-5-a-2: Proposed idealized stress- strain curve for the G1194 material in compression at the age of 3 days

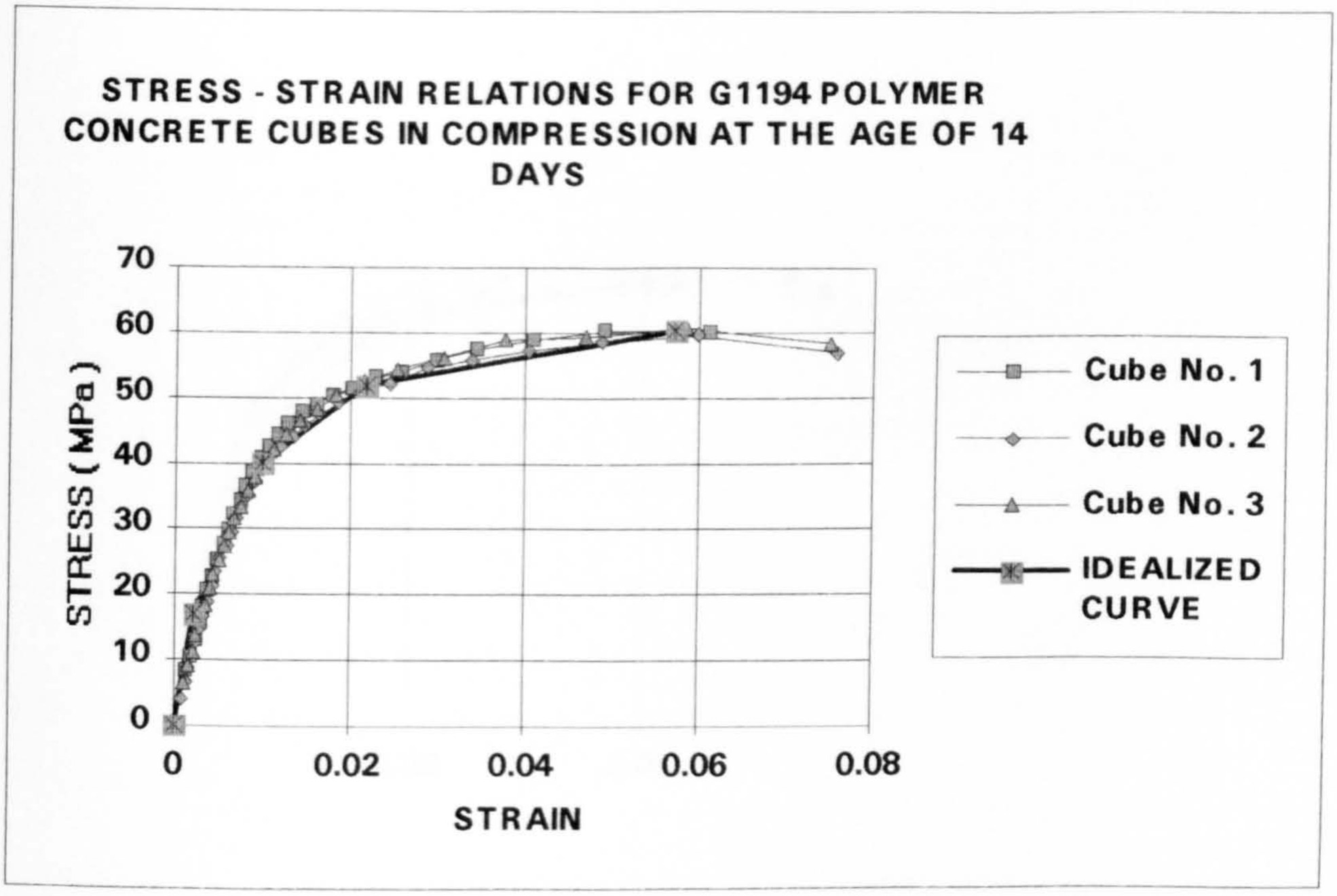

Figure 5-5-b-1: Stress- strain relations for G1194 polymer concrete cubes in compression at the age of 14 days

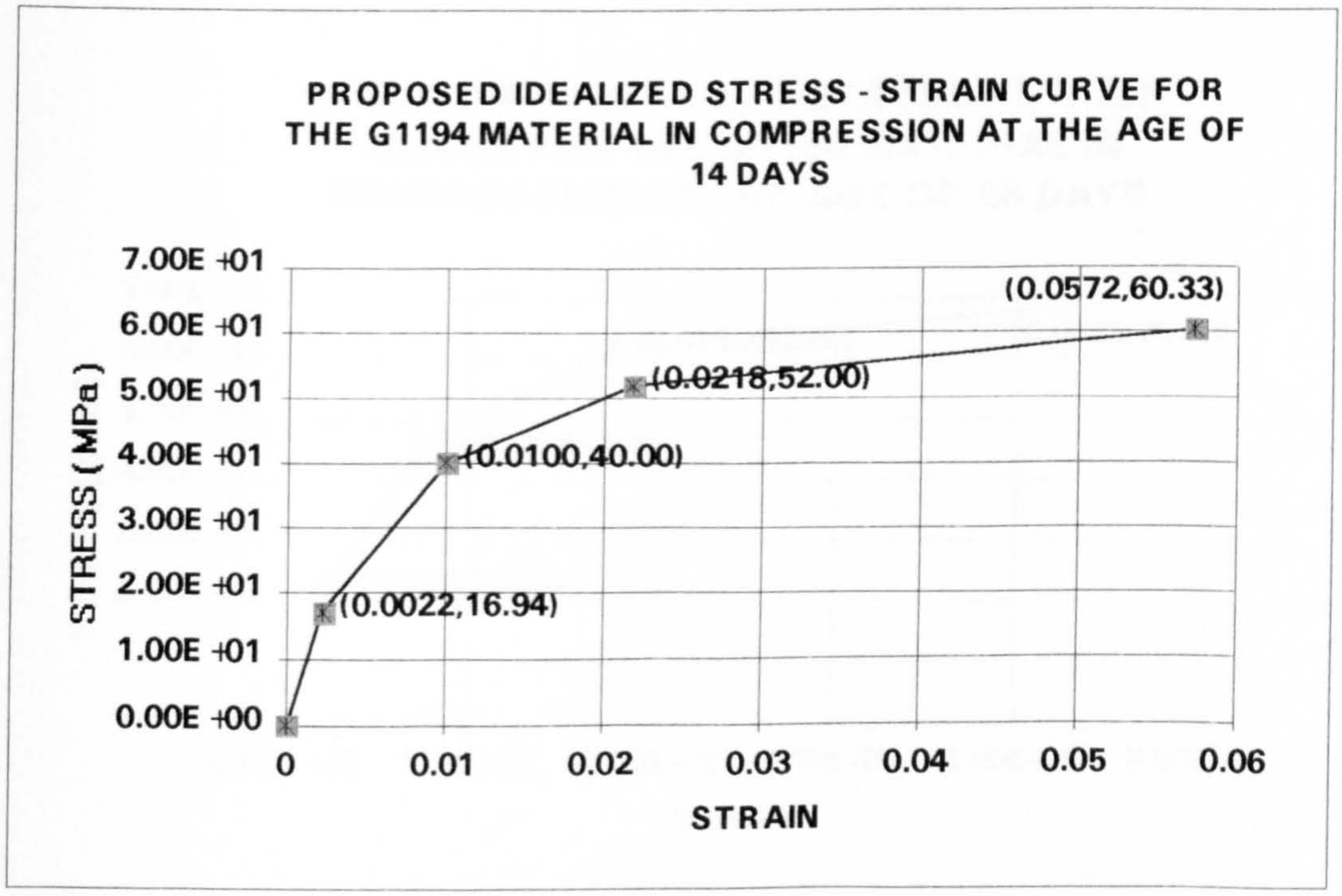

Figure 5-5-b-2: Proposed idealized stress- strain curve for the G1194 material in compression at the age of 14 days

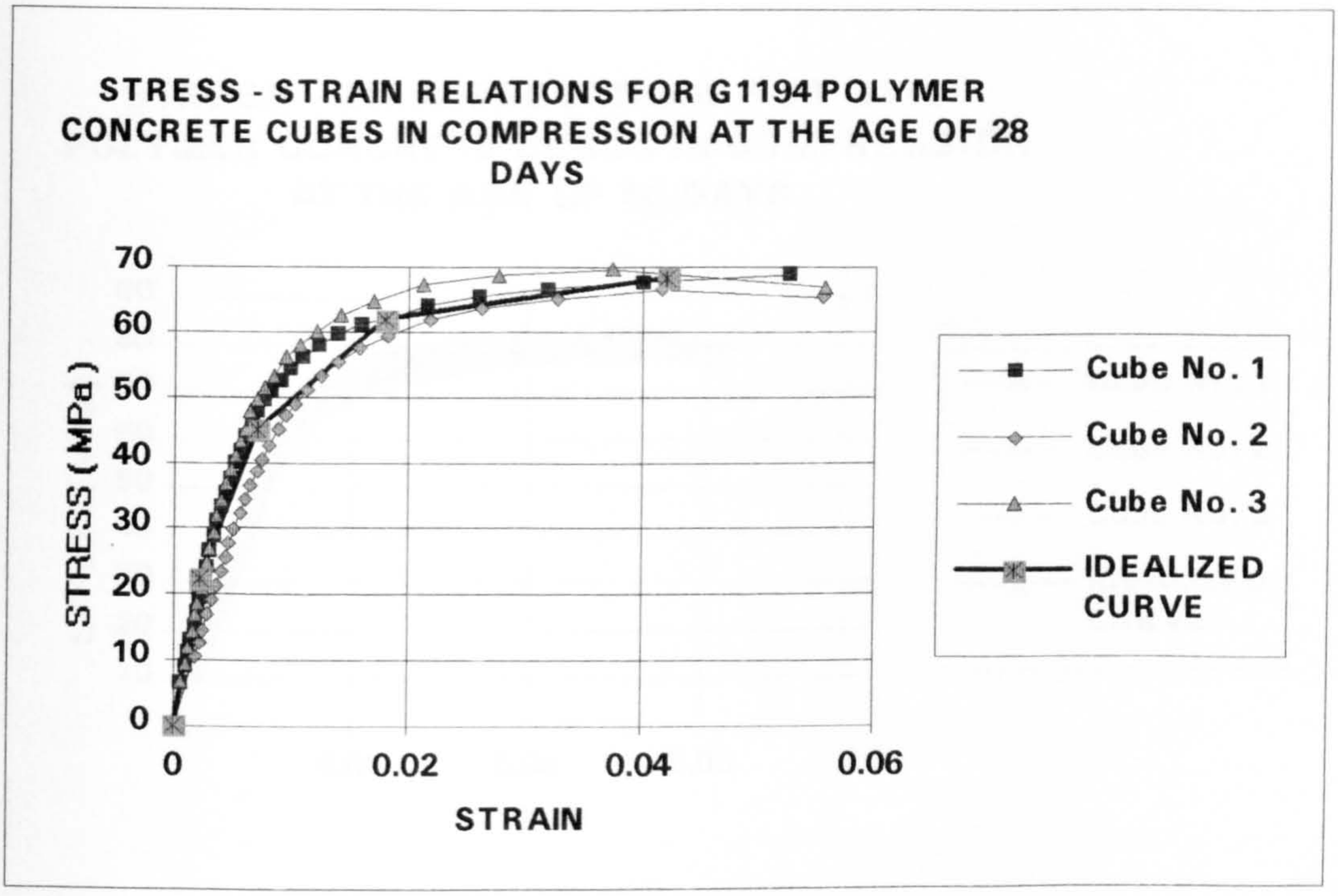

Figure 5-5-c-1: Stress- strain relations for G1194 polymer concrete cubes in compression at the age of 28 days

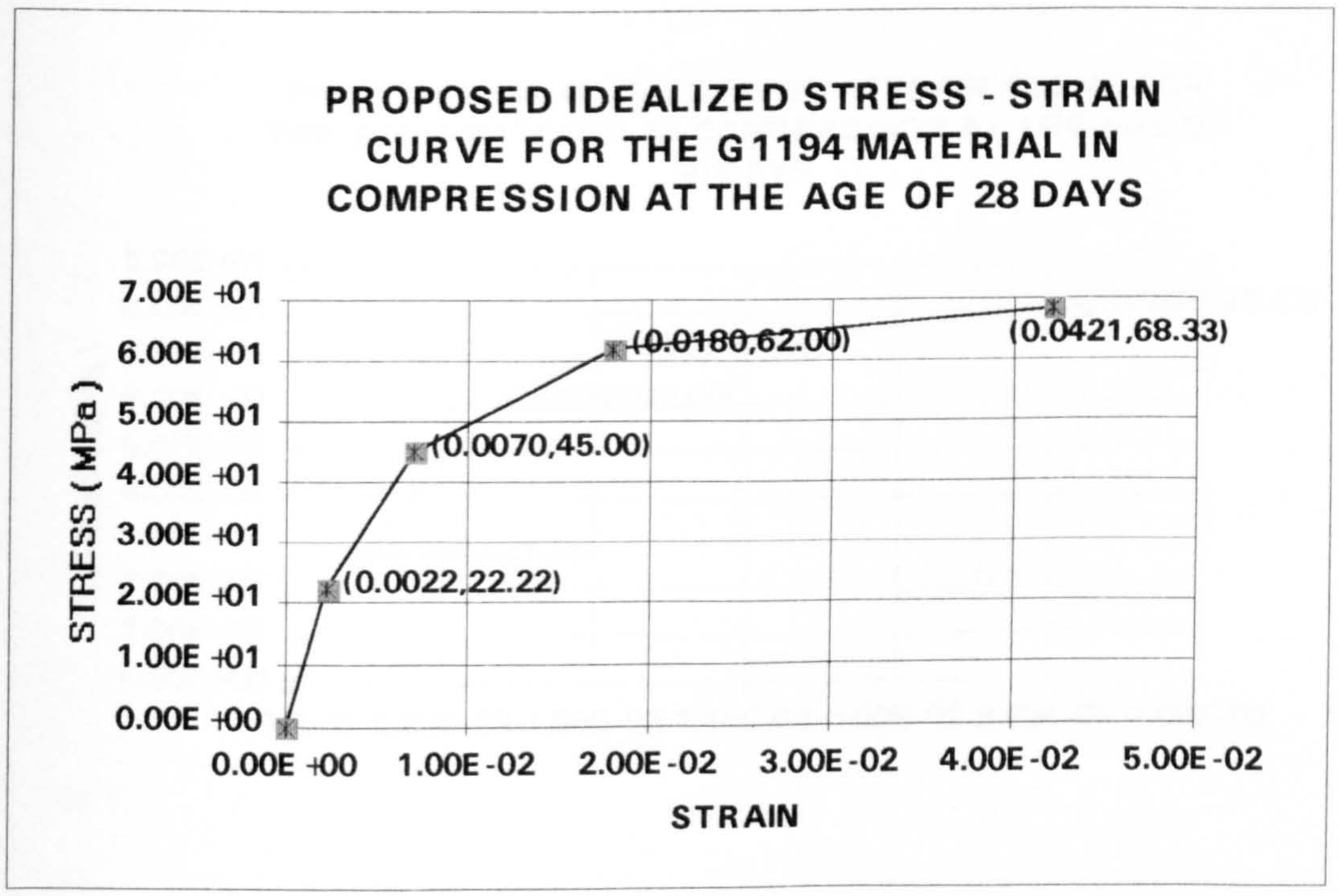

Figure 5-5-c-2: Proposed idealized stress- strain curve for the G1194 material in compression at the age of 28 days

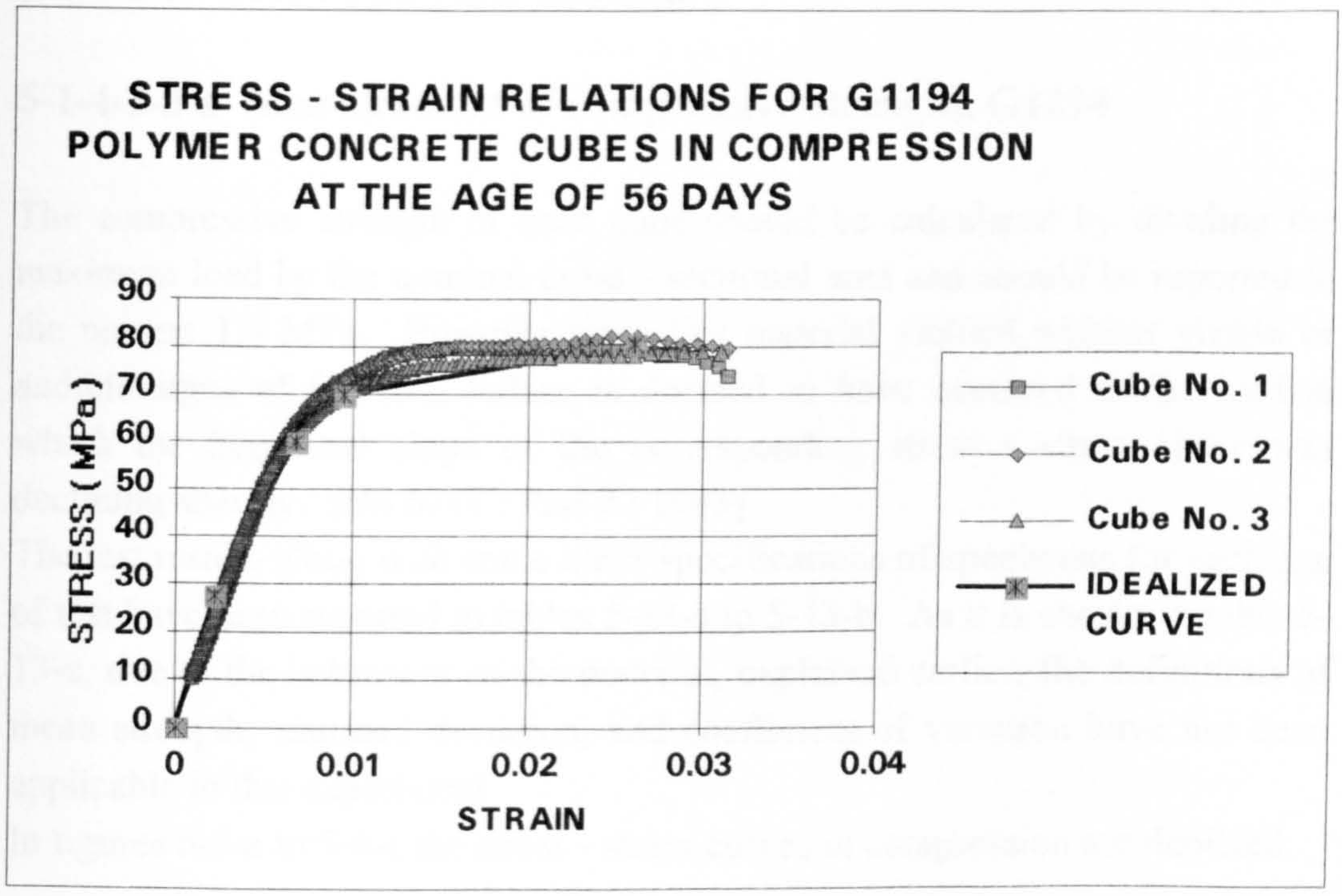

Figure 5-5-d-1: Stress- strain relations for G1194 polymer concrete cubes in compression at the age of 56 days

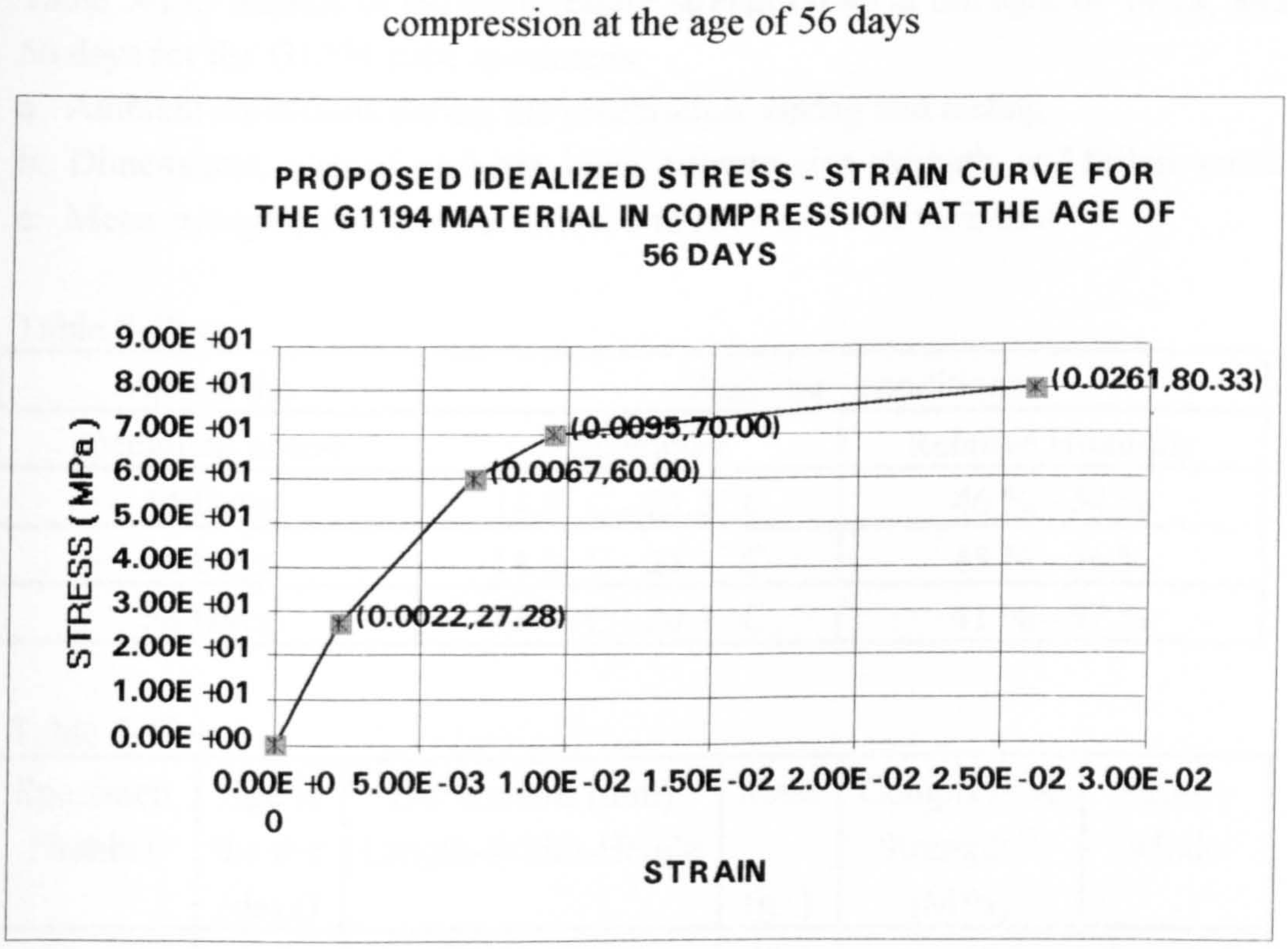

Figure 5-5-d-2: Proposed idealized stress- strain curve for the G1194 material in compression at the age of 56 days

5-1-4-3-3 G1294 (polymer concrete)

5-1-4-3-3-a Measurement of compressive strength, G1294

The compressive strength of each cube should be calculated by dividing the maximum load by the nominal cross - sectional area and should be reported to the nearest 1.0 MPa. However since this material yielded without visible or audible signs of fracture, failure is deemed to have occurred at the load at which the tangential slope of the corresponding stress - strain curve was declining sharply. [BS 6319 : Part 2 : 1983]

The test results along with some other specifications of specimens for each age of test have been reported in tables 5-13-a to 5-13-b. As it is shown in table 5-13-c, due to the behaviour of the material, explained earlier, the definitions of mean strength, standard deviation, and coefficient of variation have not been applicable in this experiment.

In figures 5-6-a to 5-6-c the stress - strain curves in compression are depicted.

Table 5-13: Results of the compressive strength tests at the ages of 14,28, and 56 days for the G1294 cube specimens:

a: Ambient conditions during the preparation, curing and testing

b: Dimensions, mass of each specimen, compressive strength, and failure mode

c: Mean strength, standard deviation, and coefficient of variation

Table 5-13-a:

Age of the	Ambient conditions	
specimens at test	Temperature	Relative Humidity
14 Days	14.8˚ C - 21.3˚ C	46 % - 54 %
28 Days	14.6˚ C - 21.1˚ C	45 % - 56 %
56 Days	11.7˚ C - 20.5˚ C	41 % - 57 %

Table 5-13-b:

Specimen Number	Age at the test (days)	Dimensions (mm) Length-Width-Height	Mass (gr.)	Compressive Strength *3 (MPa)	Failure Mode
No. 1	14	40.2-39.5-40.4	97.9	10 - 12 *1	Ductile *2
No. 2	14	40.3-39.9-39.9	97.8	10 - 12 *1	Ductile *2

Table 5-13-b: Continued

Specimen Number	Age at the test (days)	Dimensions (mm) Length-Width-Height	Mass (gr.)	Compressive Strength *3 (MPa)	Failure Mode
No. 3	14	40.0-39.5-40.1	96.9	10 - 12 *1	Ductile *2
No. 1	28	40.0-39.4-39.8	86.1	10 - 12 *1	Ductile *2
No. 2	28	40.1-39.8-40.0	88.1	10 - 12 *1	Ductile *2
No. 3	28	40.0-39.9-40.0	88.5	10 - 12 *1	Ductile *2
No. 1	56	40.0-39.9-39.9	97.9	10 - 12 *1	Ductile *2
No. 2	56	40.0-39.8-40.0	98.2	10 - 12 *1	Ductile *2
No. 3	56	39.9-39.6-40.3	97.7	10 - 12 *1	Ductile *2

*1 At this range the corresponding stress-strain curve changes slope, but it is not the yielding point nor the ultimate compressive strength.

*2 The material failed without visible sign of fracture, but with a large deformation.

*3 The material could bear up to about 45 MPa compressive stress at strain of 20%.

Table 5-13-c:

Type of test	Age at the test (days)	Total number of specimens	Mean compressive strength (MPa)	Standard deviation (MPa)	Coefficient of variation (percent)
Compression cube test	14	3	N / A *1	N / A	N / A
Compression cube test	28	3	N / A *1	N / A	N / A
Compression cube test	56	3	N / A *1	N / A	N / A

*1 The material could bear up to about 45 MPa compressive stress at strain of 20%.

5-1-4-3-3-b Measurement of flexural strength test, G1294

The flexural strength of each prism, should be calculated using equation (5-2). The values of flexural strength should be expressed to the nearest 0.2 MPa. However since the deflections obtained without any indication of fracture exceeded one fifteenth of the span, the tests were discontinued on the ground of

insufficient rigidity of the material for a meaningful value of flexural strength to be measured. [BS 6319 : Part 3 : 1983]

The test results along with some other specifications of specimens for each age of test have been reported in tables 5-14-a to 5-14-b. As it is shown in table 5-14-c, due to the behaviour of the material, explained earlier, the definitions of mean strength,, standard deviation, and coefficient of variation have not been applicable in this experiment.

Table 5-14: Results of the flexural strength tests at the ages of 14,28, and 56 days for the G1294 prism specimens:

a: Ambient conditions during the preparation, curing and testing

b: The nominal sizes of each specimen before testing and the dimensions at the site of any fracture after carrying out the test , mass, flexural strength, and breaking load of each specimen.

c: Mean strength, standard deviation, and coefficient of variation

Table 5-14-a:

Age of the	Ambient conditions	
specimens at test	Temperature	Relative Humidity
14 Days	15.1˚ C - 20.5˚ C	45 % - 54 %
28 Days	14.6˚ C - 20.6˚ C	44 % - 56 %
56 Days	10.2˚ C - 20.5˚ C	41 % - 56 %

Table 5-14-b:

Specimen Number	Age at the test (days)	Nominal sizes prior to test (mm)	Dim. at the site of fracture (mm)	Mass (gr.)	Flexural Strength (MPa)	Breaking load *1 (N)
No. 1	14	24.5-25.2-100.0	No. site *1	97.1	N / A *2	N / A
No. 2	14	24.8-25.1-100.0	No. site *1	97.9	N / A *2	N / A
No. 3	14	24.4-25.1-100.0	No. site *1	97.1	N / A *2	N / A
No. 3	14	24.4-25.2-100.0	No. site *1	95.8	N / A *2	N / A
No. 1	28	24.6-25.0-100.0	No. site *1	86.6	N / A *2	N / A
No. 2	28	24.7-25.0-100.0	No. site *1	87.0	N / A *2	N / A
No. 3	28	24.5-25.0-100.0	No. site *1	86.2	N / A *2	N / A

Table 5-14-b: Continued

Specimen Number	Age at the test (days)	Nominal sizes prior to test (mm)	Dim. at the site of fracture (mm)	Mass (gr.)	Flexural Strength (MPa)	Breaking load *1 (N)
No. 4	28	24.6-25.0-100.0	No. site *1	86.1	N / A *2	N / A
No. 1	56	24.5-25.0-100.0	No. site *1	95.8	N / A *2	N / A *3
No. 2	56	24.3-25.0-100.0	No. site *1	94.7	N / A *2	N / A *3
No. 3	56	24.6-25.0-100.0	No. site *1	96.8	N / A *2	N / A *3
No. 4	56	24.9-25.3-100.0	No. site *1	97.8	N / A *2	N / A *3

*1 No site of fracture occurred

*2 The deflection exceeded one fifteenth of the span of the specimen whereas no fracture occurred. So it was not possible to measure a meaningful value of flexural strength for the specimens. (BS 6319 : Part 3 : 1983)

*3 In this experiment for all the four specimens at maximum deflection, under an average load of 1810 N, some hair cracks appeared.

Table 5-14-c:

Type of test	Age at the test (days)	Total number of specimens	Mean flexural strength (MPa)	Standard deviation (MPa)	Coefficient of variation (percent)
Flexural prism test	14	4	N / A *1	N / A	N / A
Flexural prism test	28	4	N / A *1	N / A	N / A
Flexural prism test	56	4	N / A *1	N / A	N / A

*1 The deflection exceeded one fifteenth of the span of the specimen whereas no fracture occurred. So it was not possible to measure a meaningful value of flexural strength for the specimens. (BS 6319 : Part 3 : 1983)

5-1-4-3-3-c Determination of modulus of elasticity in compression test, G1294

The secant modulus of elasticity of each prism, will be calculated using equation (5-3). The values of secant modulus of elasticity will be expressed to the nearest 0.1 GPa. [BS 6319 : Part 6 : 1984]
The test results along with some other specifications of specimens for each age of test have been reported in tables 5-15-a to 5-15-b. The values of mean secant modulus of elasticity, standard deviation, and coefficient of variation are also calculated at each stage and listed in table 5-15-c.
The proposed idealized stress - strain curves for the G1294 material at different ages have been also shown in figures 5-6-a to 5-6-c. The first part of each idealized curve is based on the results of the modulus of elasticity tests in compression on the prism specimens, whereas the other parts are based on the average values of stresses and strains at the corresponding idealized points obtained from the compressive strength tests on the cube specimens.

Table 5-15: Results of the modulus of elasticity in compression tests at the ages of 14, 28, and 56 days for the G1294 prism specimens :
a: Ambient conditions during the preparation, curing and testing
b: The Cross-sectional dimensions of the centre of each specimen, the upper (N_1) and lower (N_2) load levels used in equation (5-3), mean strain and the secant modulus of elasticity of each test specimen.
c: Mean secant modulus of elasticity, standard deviation, and coefficient of variation

Table 5-15-a:

Age of the	Ambient conditions	
specimens at test	Temperature	Relative Humidity
14 Days	14.8˚ C - 21.3˚ C	44 % - 57 %
28 Days	14.6˚ C - 21.6˚ C	42 % - 57 %
56 Days	13.5˚ C - 21.3˚ C	45 % - 57 %

Table 5-15-b:

Specimen Number	Age at the test (days)	Cross - sectional Dim. at the centre (mm)	Upper (N_1) load (kN)	Lower (N_2) load (kN)	Mean strain	Modulus of elasticity (GPa)
No. 1	14	38.3-38.5	5.02	0.58	0.0021	1.5
No. 2	14	37.7-38.1	6.58	0.54	0.0023	1.9
No. 3	14	37.5-38.0	5.28	0.47	0.0020	1.7
No. 1	28	38.4-38.5	5.55	0.52	0.0020	1.7
No. 2	28	37.6-38.1	5.07	0.49	0.0020	1.6
No. 3	28	37.6-38.6	-*1	-*1	-*1	-*1
No. 1	56	37.6-38.3	5.33	0.50	0.0020	1.7
No. 2	56	37.6-38.6	6.43	0.48	0.0021	2.0
No. 3	56	37.5-38.4	6.50	0.62	0.0018	2.3

*1 Fail in recording the results

Table 5-15-c:

Type of test	Age at the test (days)	Total number of specimens	Mean secant modulus of elasticity (GPa)	Standard deviation (GPa)	Coefficient of variation (percent)
Modulus of elasticity test	14	3	1.7	0.2	11.8
Modulus of elasticity test	28	3	1.7	-	-
Modulus of elasticity test	56	3	2.0	0.30	13.6

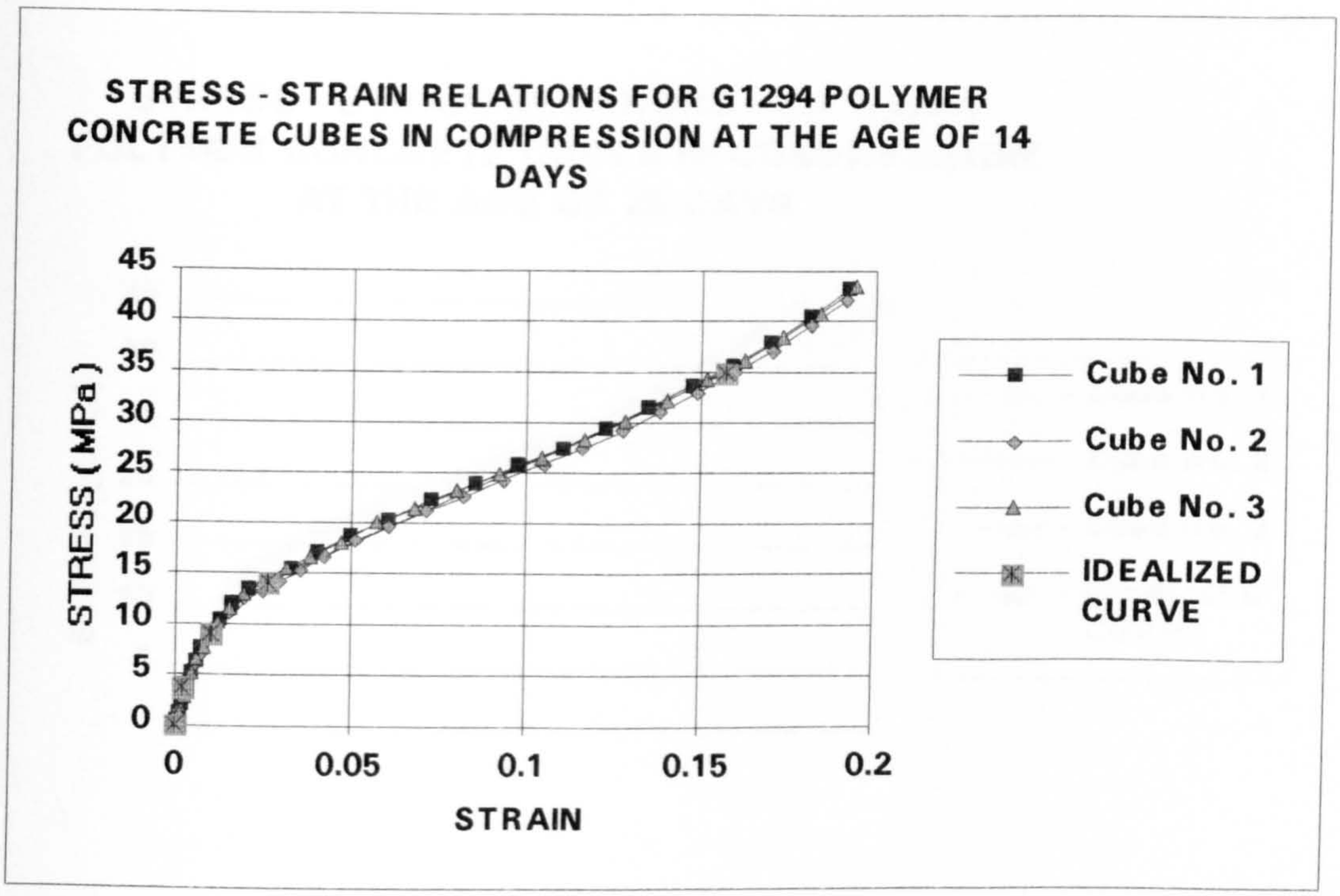

Figure 5-6-a-1: Stress- strain relations for G1294 polymer concrete cubes in compression at the age of 14 days

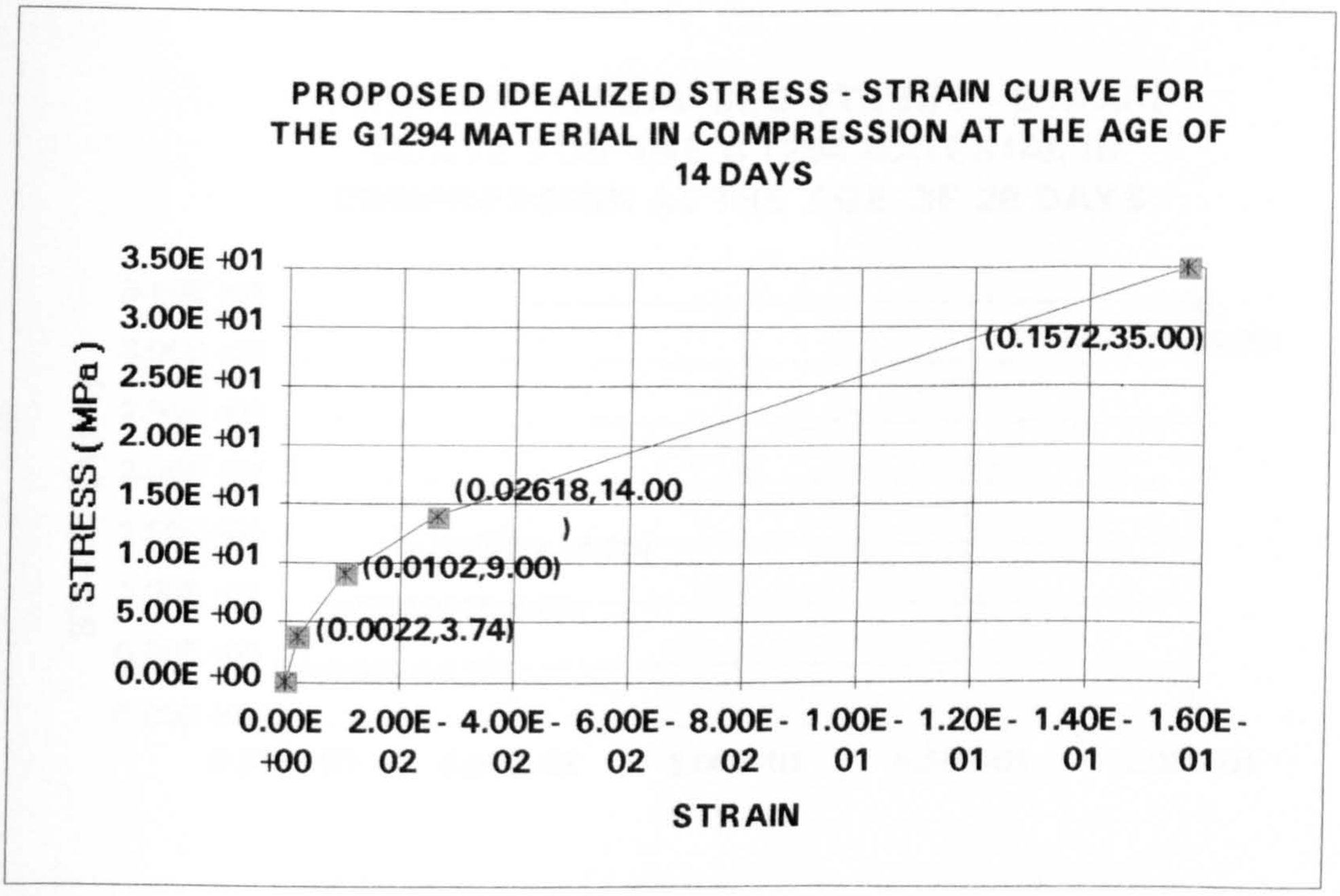

Figure 5-6-a-2: Proposed idealized stress- strain curve for the G1294 material in compression at the age of 14 days

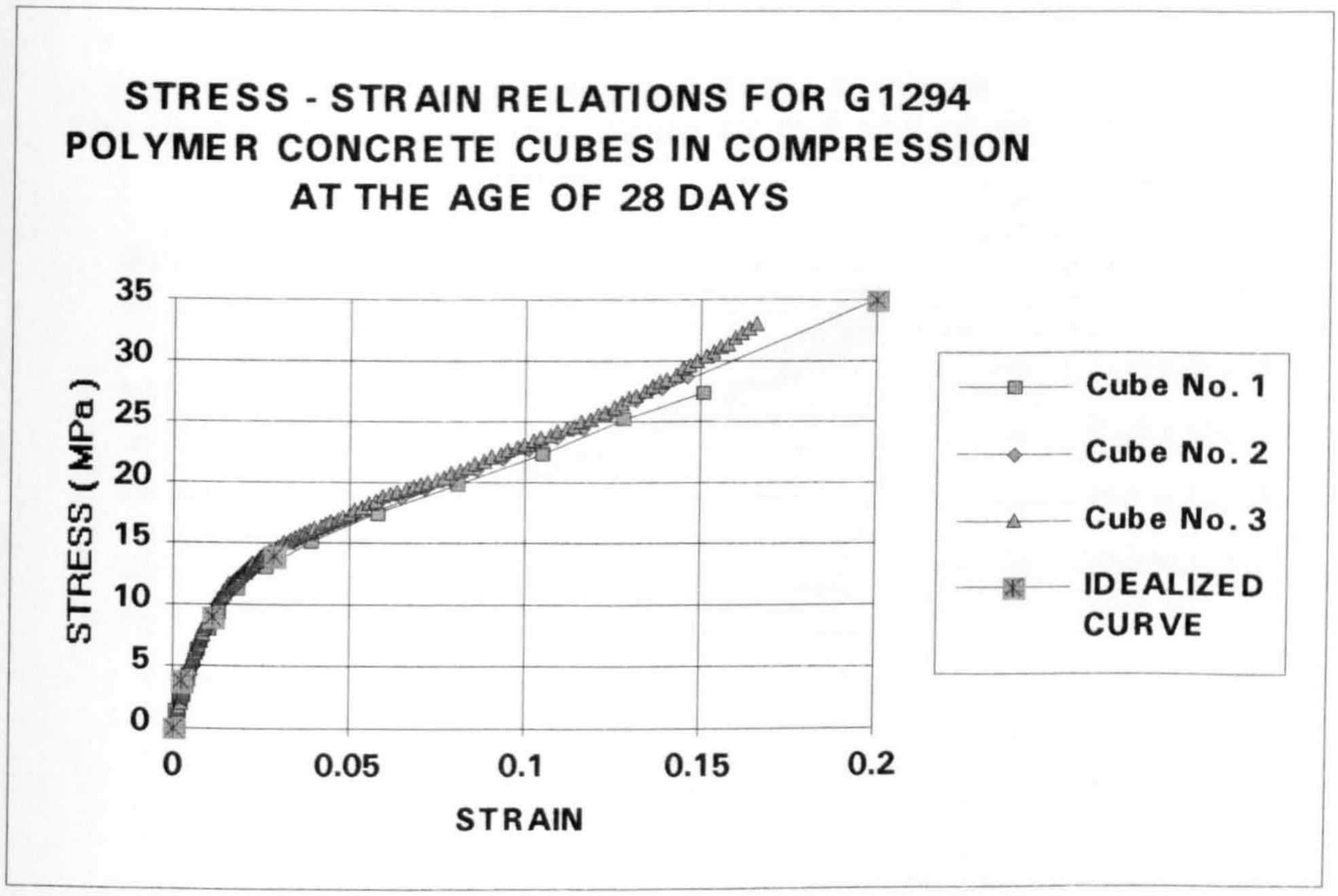

Figure 5-6-b-1: Stress- strain relations for G1294 polymer concrete cubes in compression at the age of 28 days

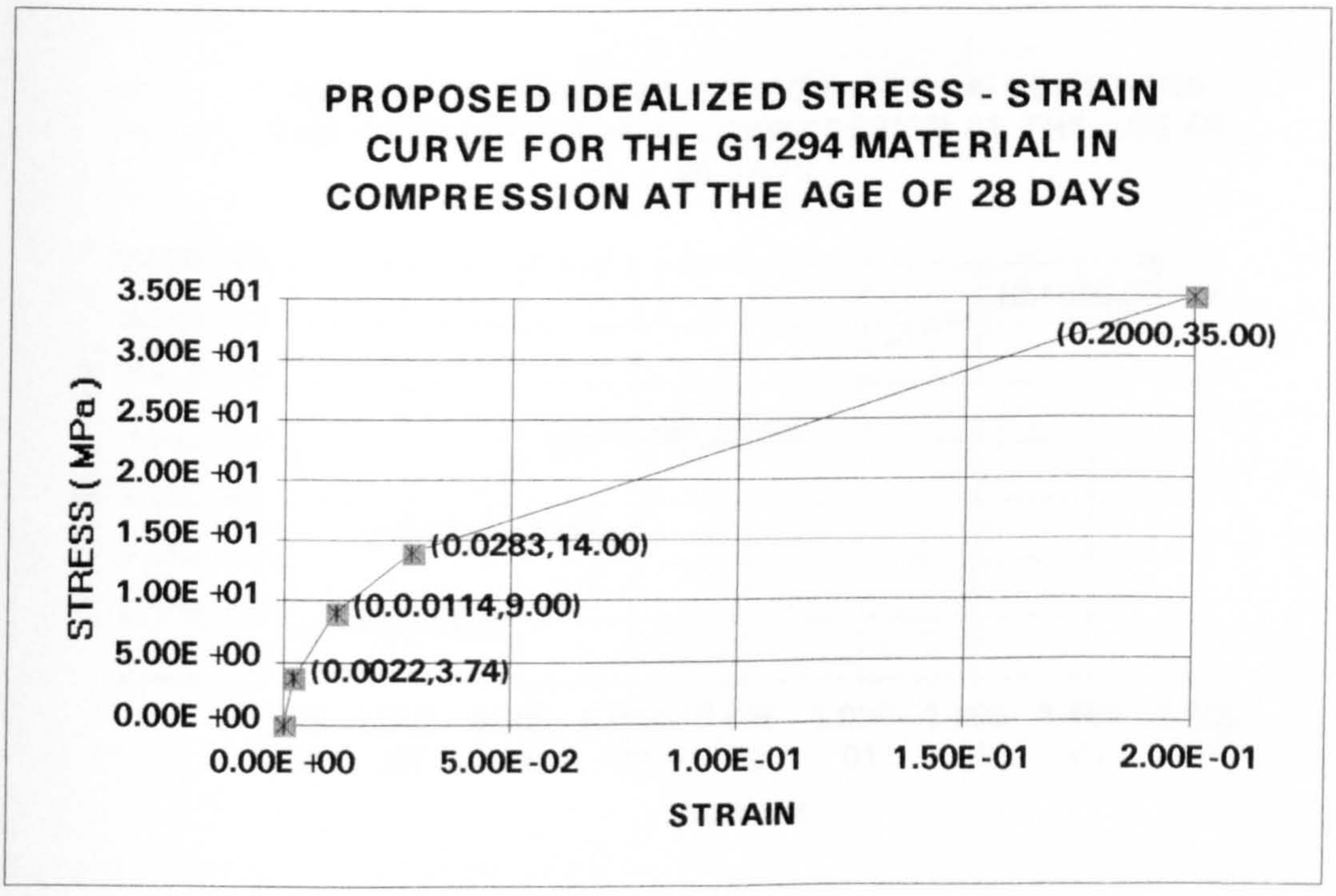

Figure 5-6-b-2: Proposed idealized stress- strain curve for the G1294 material in compression at the age of 28 days

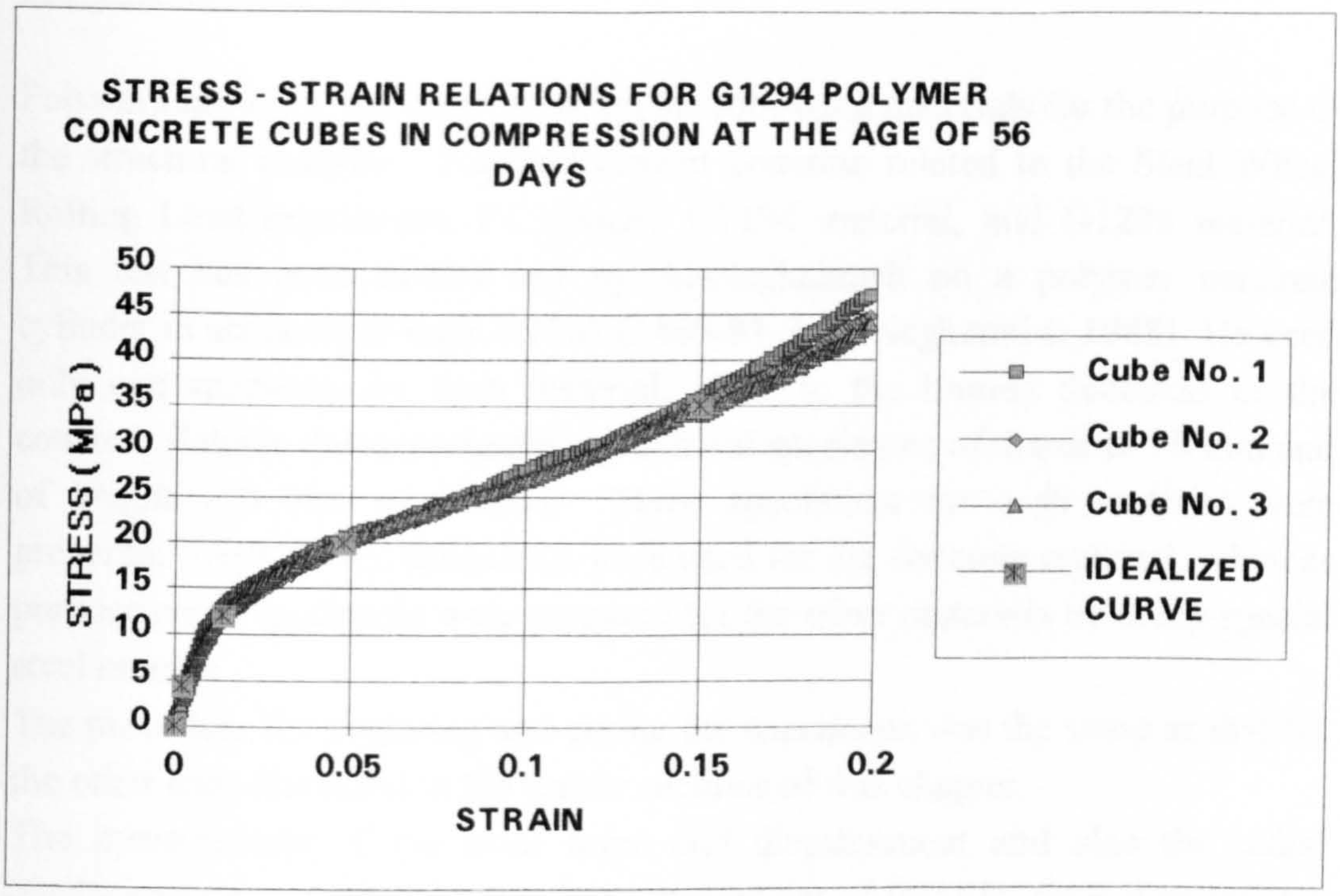

Figure 5-6-c-1: Stress- strain relations for G1294 polymer concrete cubes in compression at the age of 56 days

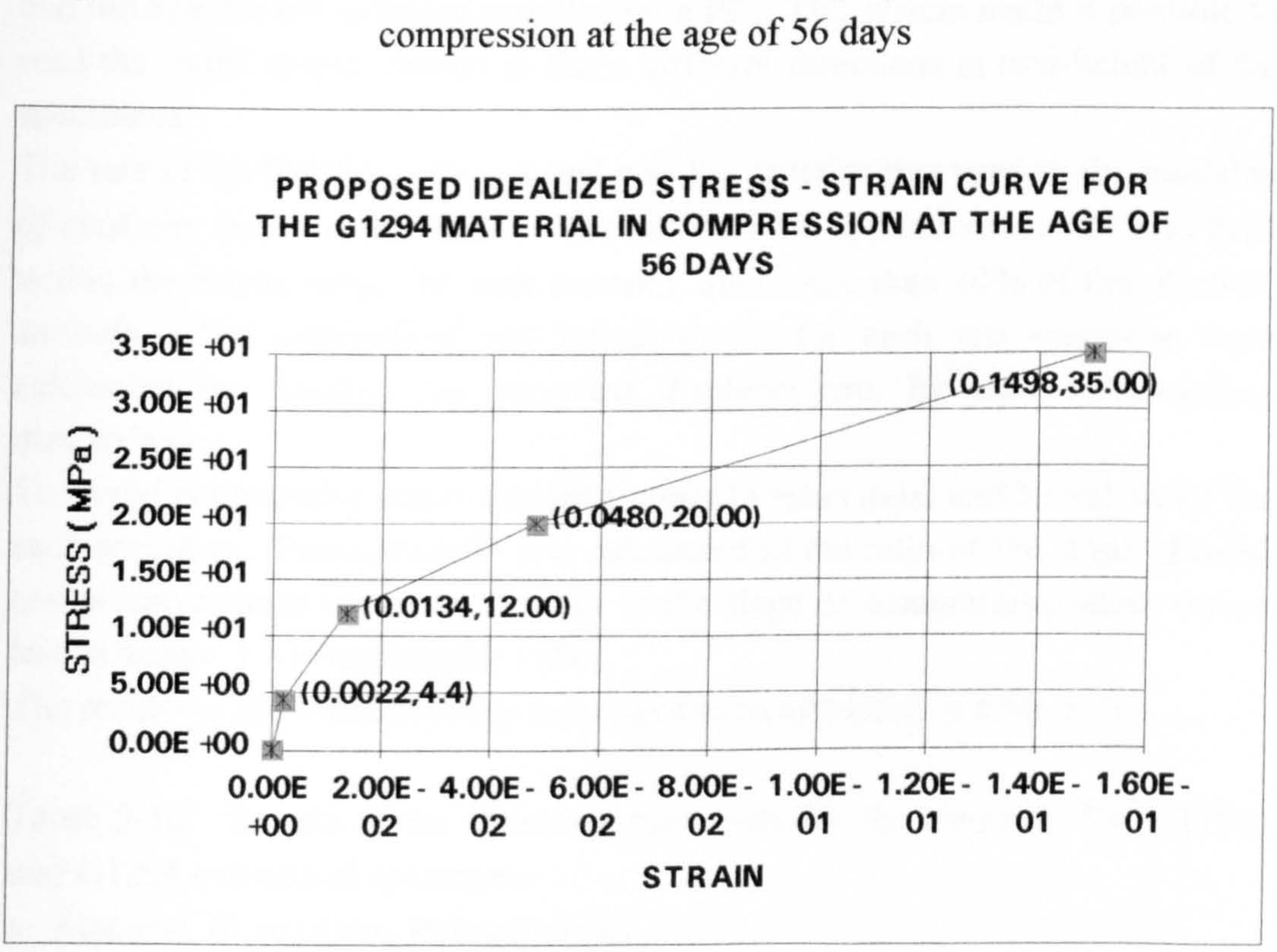

Figure 5-6-c-2: Proposed idealized stress- strain curve for the G1294 material in compression at the age of 56 days

5-1-5 Poisson's ratio

Poisson's ratio test was carried out on the following materials for the purpose of the structural analysis: Portland cement concrete related to the Steel Wheel Rolling Load experiment, P4 system, G1194 material, and G1294 material. This test has been carried out by Al-Negheimish on a polymer concrete cylinder in accordance with ASTM C 469-81. [Al-Negheimish 1988] He used only one specimen for each material. Due to the limited thickness of the concrete slabs in this experiment, cylindrical specimens of diameter 50 mm and of height 120 mm were used. Three specimens for each material were prepared. Drilled core specimens were used for the concrete material, whereas purpose made specimens were prepared for the other materials by using special steel moulds.

The procedure for preparing and curing the specimens was the same as that for the other tests discussed in the earlier sections of this chapter.

The measurement of the axial force and displacement and also the radial displacements was carried out using a special set of INTERCOLE data loggers and the Spectra lab software installed on a PC. The system made it possible to read the radial displacements in three different directions at mid-height of the specimens.

The rate of loading for each material was the same as that used in the modulus of elasticity test in compression. The range of the applied stress was also kept within the elastic range for each material, about less than 40% of the ultimate strength. The longitudinal and lateral strains for each test specimen were calculated by dividing the recorded displacements by the corresponding dimensions.

The axial compressive stress was then plotted versus axial and lateral strain for each specimen. Poisson's ratio was calculated as the ratio of the slope of axial compressive stress versus axial strain to the slope of compressive stress versus lateral strain. [Al-Negheimish 1988]

The results of the Poisson's ratio tests have been tabulated in table 5-16.

Table 5-16: Results of the Poisson's ratio tests for the concrete, P4, G1194, and G1294 cylindrical specimens

a: Material, dimensions, Poisson's ratio

b: Mean Poisson's ratio, standard deviation, and coefficient of variation

Table 5-16-a:

Specimen Number	Material	Age at the test (days)	Dimensions (mm) Length - Diameter	Poisson's ratio
NO 1	Concrete	-	120.0 - 50.8	0.15
NO 2	Concrete	-	120.2 - 50.8	0.21
NO 3	Concrete	-	120.1 - 50.8	-*1
NO 1	P4	28	120.1 - 50.0	0.25
NO 2	P4	28	120.5 - 50.1	0.19
NO 3	P4	28	120.9 - 50.1	0.30
NO 1	G1194	28	118.3 - 49.8	0.31
NO 2	G1194	28	118.4 - 49.8	-*1
NO 3	G1194	28	118.9 - 50.0	0.32
NO 1	G1294	28	117.6 - 50.0	0.37
NO 2	G1294	28	117.3 - 49.9	0.37
NO 3	G1294	28	117.4 - 49.9	0.39

*1 Fail in recording the results

Table 5-16-b:

Type of test	Material	Total number of specimens	Mean Poisson's ratio	Standard deviation	Coefficient of variation (percent)
Poisson's ratio test	Concrete	3	0.18	-	-
Poisson's ratio test	P4	3	0.25	0.06	22.0
Poisson's ratio test	G1194	3	0.32	-	-
Poisson's ratio test	G1294	3	0.38	0.01	2.6

5-2 Interface bond strength

The application of a thin layer for repair or protection of existing structures depends on the adhesion of the top layer material and its substrate. This adhesion is mainly due to chemical as well as physical interaction between the two materials. Stresses are induced at the interface of a thin layered systems as a result of the action of a rolling wheel load. Tensile and shear stresses are to be resisted by the interface bond strength if the upper layer must remain bonded.

The bond strength may be considered in the form of shear or tensile strength at the interface. There are many tests for measuring the bond strength of a two layered system have been used by different investigators, some of which will be summarised in the following section. These tests may be classified as direct tension tests, indirect tension tests, shear tests and shear and compression tests.

5-2-1 Interface bond strength test survey

5-2-1-1 Direct tension tests

The ' Limpet ' apparatus was used to assess the tensile bond strength of patch repair mortars for concrete. [Cleland et al. 1986] In this investigation slabs of 600 by 300 by 50 mm size were repaired using different repair materials and then were cored down into the old concrete using diamond tip coring drill producing 50 mm diameter cores at the required days. For measuring the bond strength, steel or aluminium probes of 50 mm diameter were glued on top of the cores and using ' Limpet ' the average tensile strength at failures was calculated by dividing the failure tensile force by the contact area of the probes. This equipment with a 10 kN. capacity is commercially available which applies a tensile force through a rod screwed axially into the probe. (figure 5-7) [Bungey 1989]

Similar " pull-off "test was done by Naderi as an in situ testing method for determining the tensile strength between a repair and its original concrete. [Naderi et al. 1986] Another type of pull-off test method, using the Elcometer pull-off tester was used by to measure the direct tensile strength of 20 mm diameter cores drilled into the slab test specimen. [Judge et al. 1986] In this investigation concrete paving slabs of 600 by 600 by 50 mm size were covered by a 20 mm deep repair mortar. After curing and coring the upper layer, the

special test ' dollies ' were adhered onto the surface of the cores and the average tensile strength at failures were measured for cores of similar conditions. Mwape [Mwape 1990] and Floros [Floros 1991] also carried out some tests using the Elcometer pull-off tester for evaluation the effect of ' Impact shock ' on the interface bond strength of a two layered system.

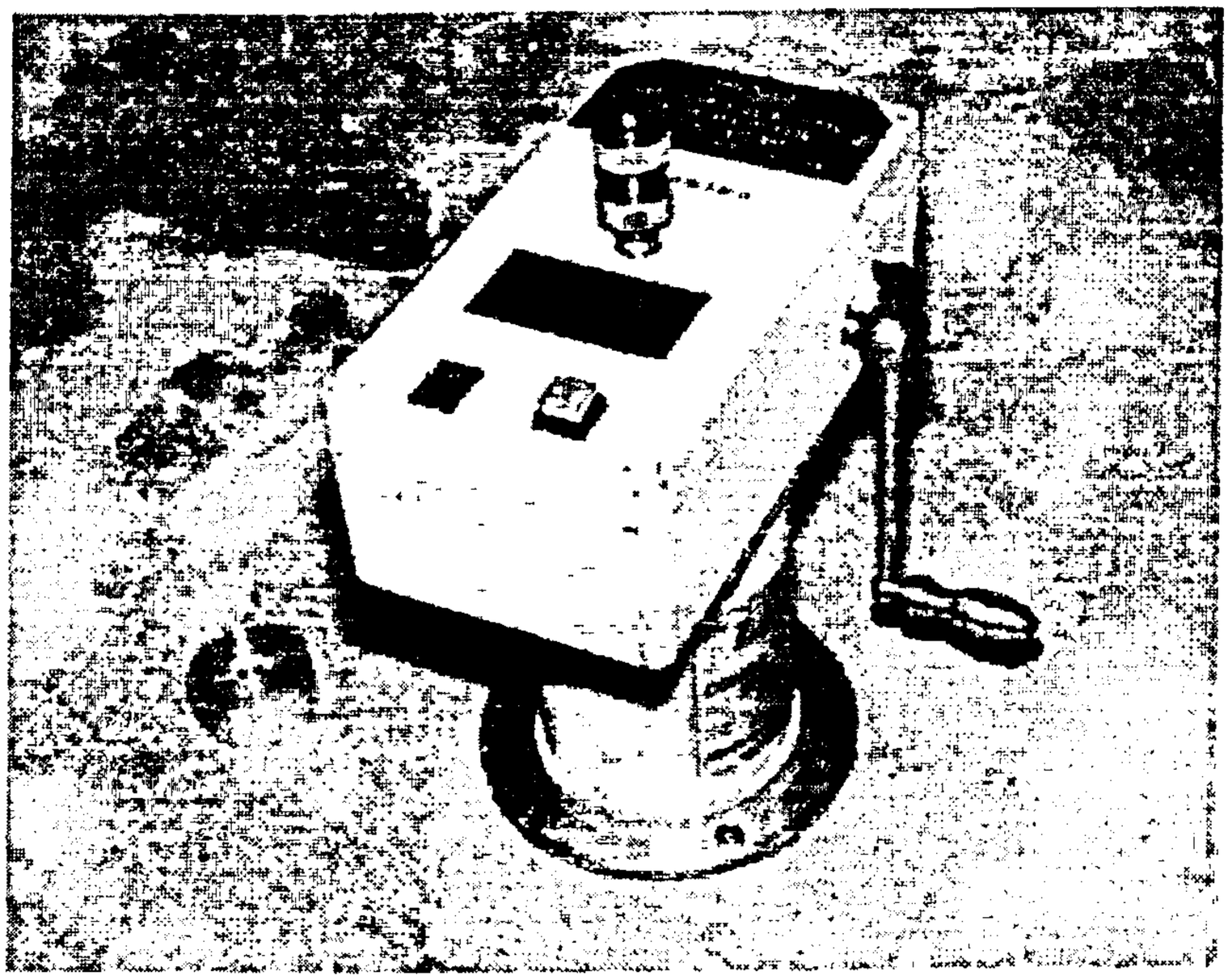

Figure 5-7: ' Limpet ' loading equipment [Bungey 1989]

Kwasny in Ref. [Kwasny 1986] introduced a similar pull-off test method as a qualification test on PCC systems for the repair of concrete road bridges. Al-Negheimish has studied the bond strength between polymer concrete and Portland cement concrete using Pull-out test in accordance with ACI Committee 503 report (1). (figure 5-8-a) [Al-Negheimish 1988] Bond strength pull-out tests were carried out by Rebeiz on an approximately 12 mm thick PC

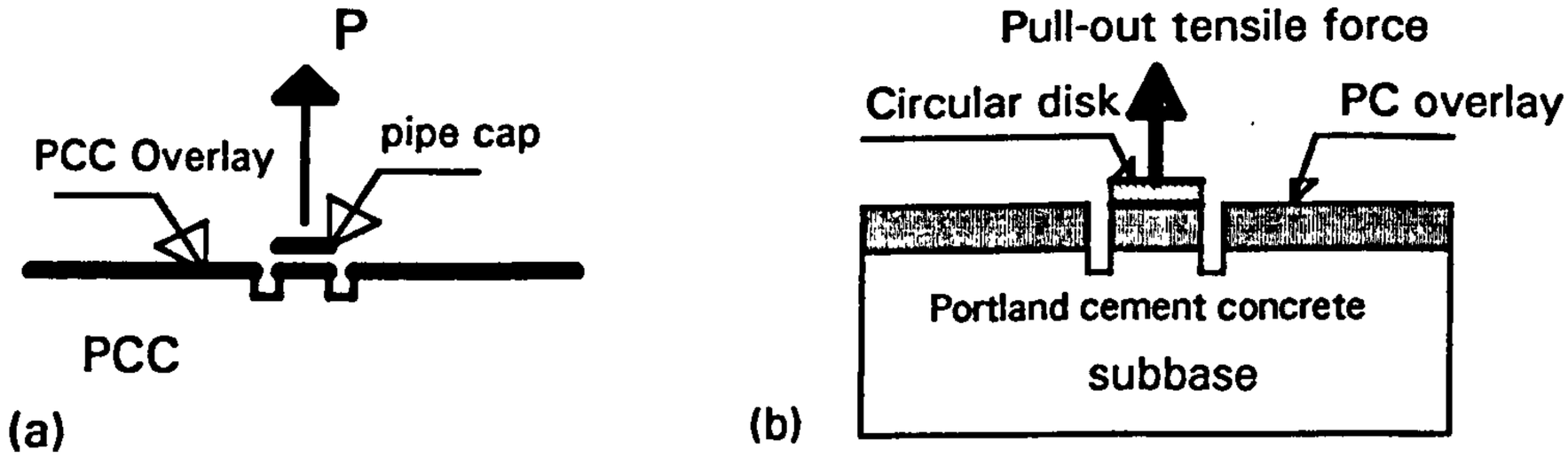

Figure 5-8: Schematic of pull-out bond test: a: [Al-Negheimish 1988], b: [Rebeiz et al. 1991] [Rebeiz and Fowler 1991] [Rebeiz et al. 1993]

overlay using 100 mm diameter cores in direct tension. (figure 5-8-b) [Rebeiz et al. 1991] [Rebeiz and Fowler 1991] [Rebeiz et al. 1993]

In an investigation for the adhesion of polymer-modified mortars to ordinary cement mortar, Ohama carried out some tests for adhesion in tension in accordance with JIS A 6915 (Wall Coatings for Thick Textured Finishes) and ASTM C 190 (Tensile Strength of Hydraulic Cement Mortars) respectively. (fig. 5-9) [Ohama et al. 1986]

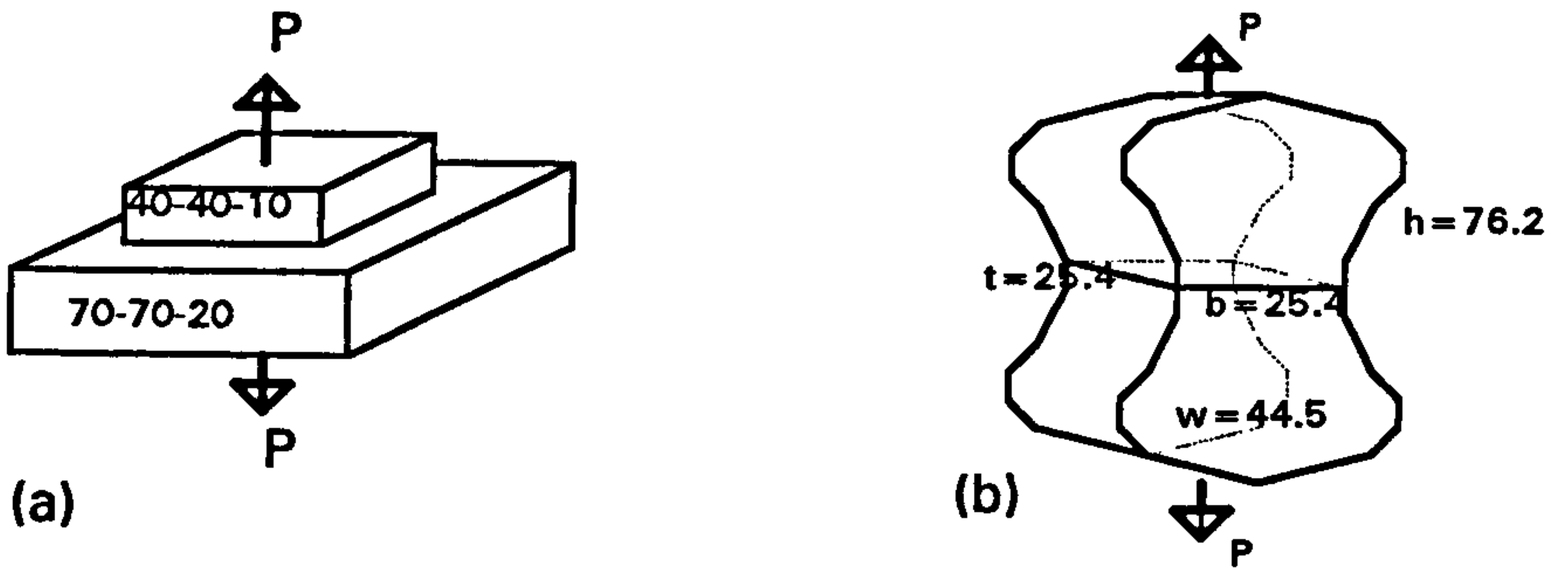

Figure 5-9: Adhesion test in tension [Ohama et al. 1986] a: JIS A 6915, b: ASTM C 190

Dogbone test method was also used by other investigators like Judge [Judge et al. 1986], in accordance with B S 6319 : Part 7 1985, for determination of tensile strength. In this test the cross sectional area at the waist is 645 mm^2. The shape of the specimen is schematically similar to that shown in figure 5-9-b. (figure 5-10) During the test, the specimen is held at each end by the use of specially designed jaws such that under tension it will break across its narrowest width.

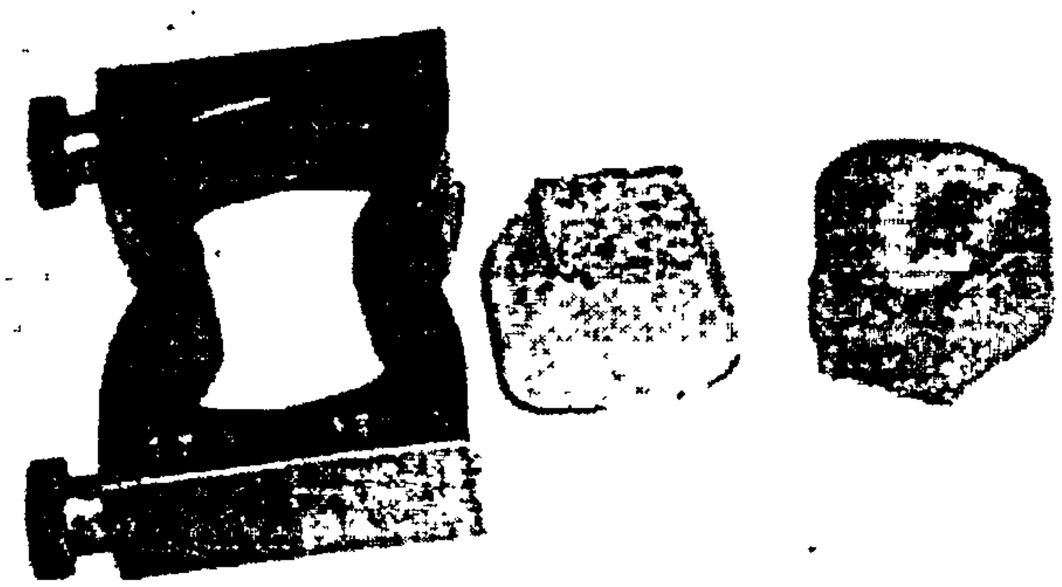

Figure 5-10: Dogbone mould and a tested specimen used in ref. [Judge et al. 1986]

Lundy used two forms of direct tension tests, a direct tensile test which was a

laboratory test done on cores or cylinder and the ACI 503 pullout test which again could be used in the laboratory or in the field. In the first test, tensile stress to failure was applied to the specimen through endcaps. In the second test the upper layer was cored to below the interface and a bonding cap was applied using epoxy. The diameter of cores were 2 or 4 inches. (figure 5-11) [Lundy 1990]

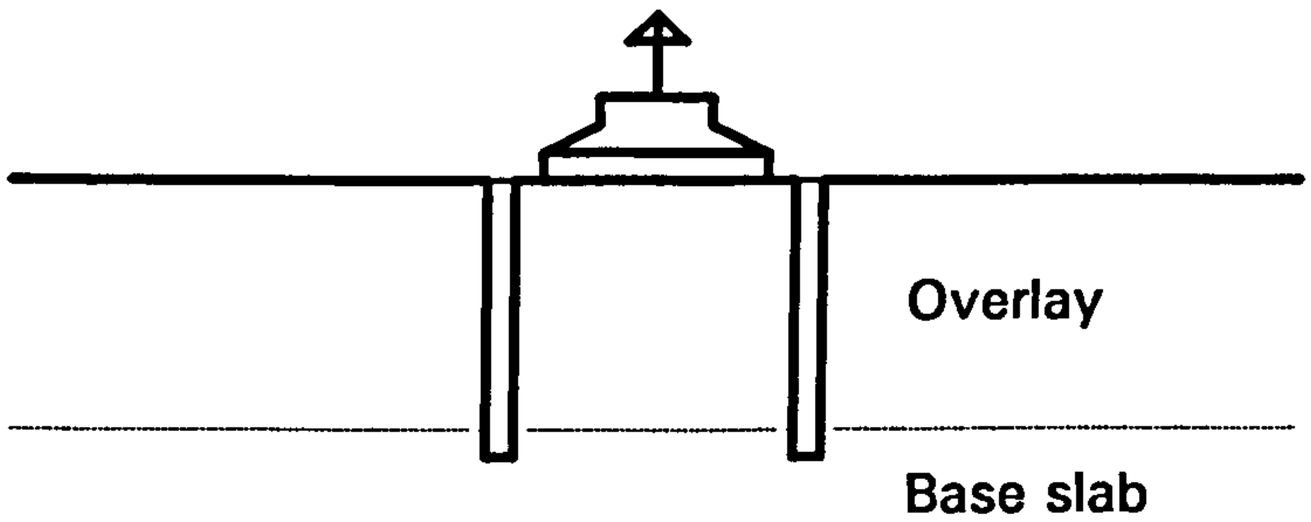

Figure 5-11: Schematic of pull-out test used by Lundy [Lundy 1990]

Finally Sprinkel has found the effects of age and air temperature on the tensile bond strength for some polymer overlays using the test method prescribed in ACI 503R. [Sprinkel 1993]

5-2-1-2 Indirect tension tests

Indirect tension tests may be used in the form of flexure tests or the Brazilian test (ASTM C496).
Flexural prism specimens were tested for adhesion in flexure in accordance with JIS A 1172 (Method of Test for Strength of Polymer - Modified Mortars). (Figure 5-12) [Ohama et al. 1986]

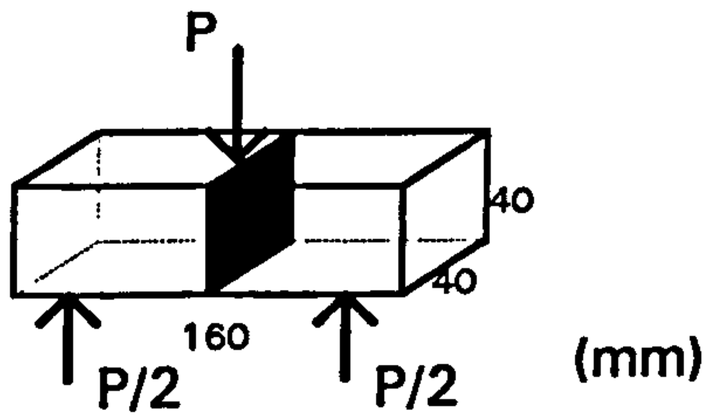

Figure 5-12: Adhesion test in flexure JIS A 1172 [Ohama et al. 1986]

Two other types of flexure tests, with bond planes at 45° and 60° relative to the horizontal using third point loading were chosen in ref. [Wall et al. 1986] for evaluating the flexural bond strength between the fresh and hardened concrete.

(figure 5-13-a and b) Moss and Batchelar had also used a similar test, with the bond plane at 30° in 1975 to determine the effectiveness of epoxy resins in bonding concrete. [Wall et al. 1986] Another indirect tension test similar to the standard ' Brazilian Test ', but using a prism specimen instead of a cylinder one to facilitate casting, was reported in ref. [Wall et al. 1986]. (figure 5-13-c) As it is depicted in figure 5-13-c, in this kind of test the plane of the bond is subjected to a biaxial principal stress state with tension directly across the bond. [Wall et al. 1986]

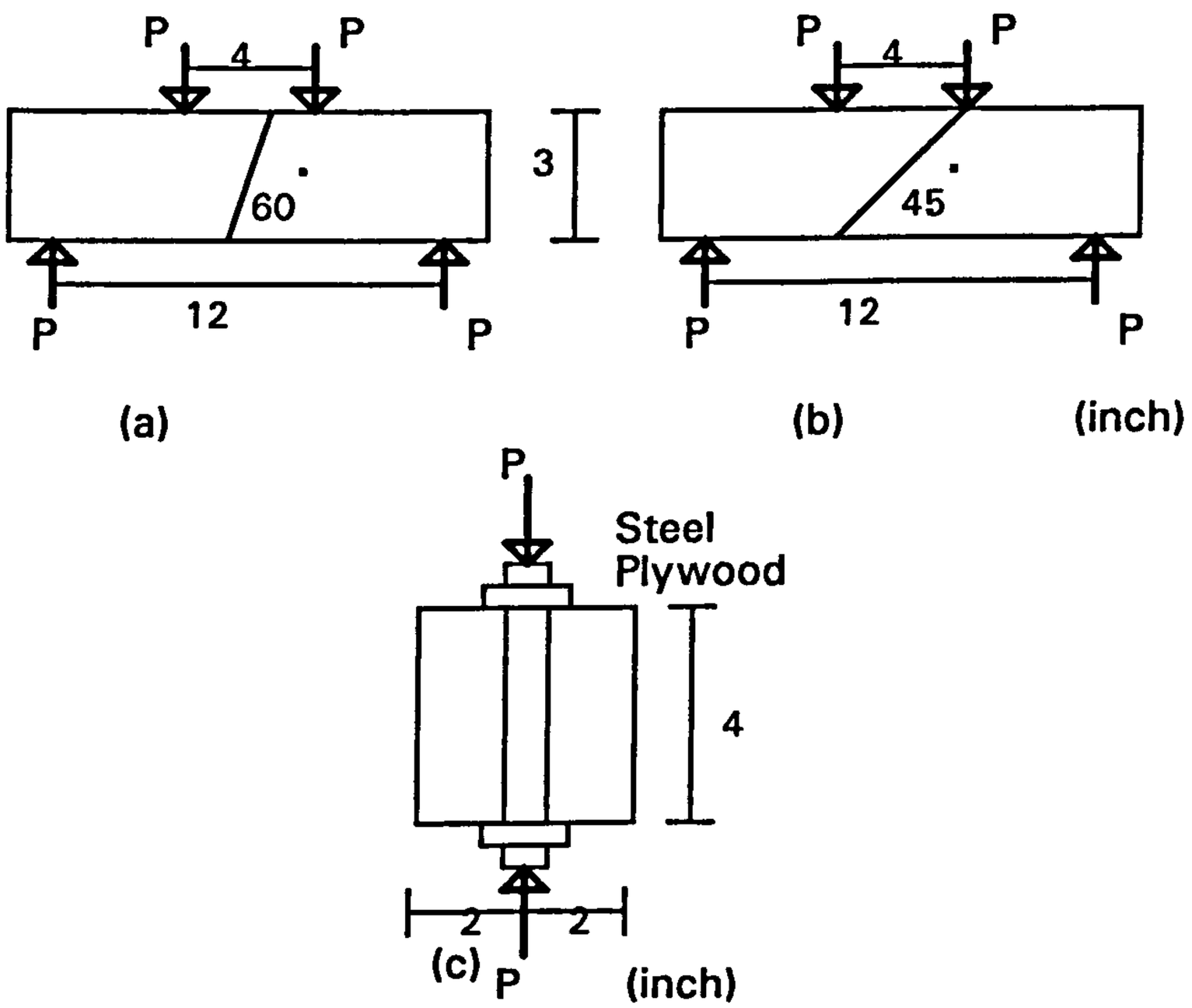

Figure 5-13: Indirect bond strength tests used in ref. [Wall et al. 1986]

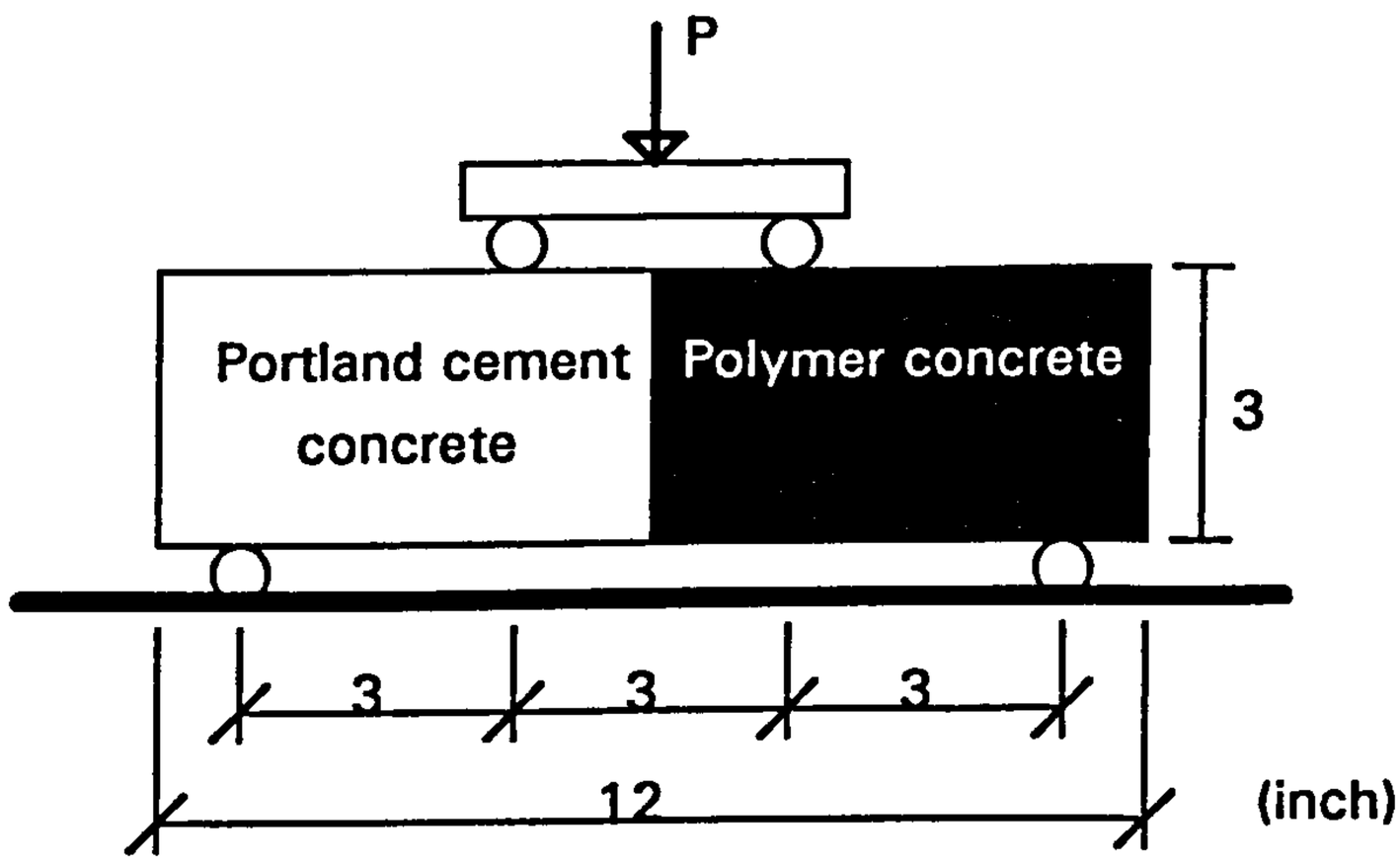

Figure 5-14: Flexural bond strength test used in ref. [Al-Negheimish 1988]

For carrying out flexure bond tests, Al-Negheimish prepared Portland cement concrete beams of 3 by 3 by 3 inch size in the same way as recommended in ASTM C78 for the standard modulus of elasticity test. Then he broke the cured beams in flexure using third point loading. At this stage three half beams were repaired and completed by polymer concrete using the rough end of the broken beams. For comparing the results, three specimens were also prepared using the smooth end of the broken beams. Finally the flexural bond strength of each composite were measured using third point loading. (figure 5-14) [Al-Negheimish 1988]

5-2-1-3 Shear tests and shear and compression tests

In an investigation into the effect of joint length on the failure bond shear strength of joints between precast hollow slabs, special shear and compression tests have been carried out. [Reinhardt 1982] In these series of tests real factory made precast elements have been used in order to increase the reliability of the corresponding results. Cross sectional dimensions of the

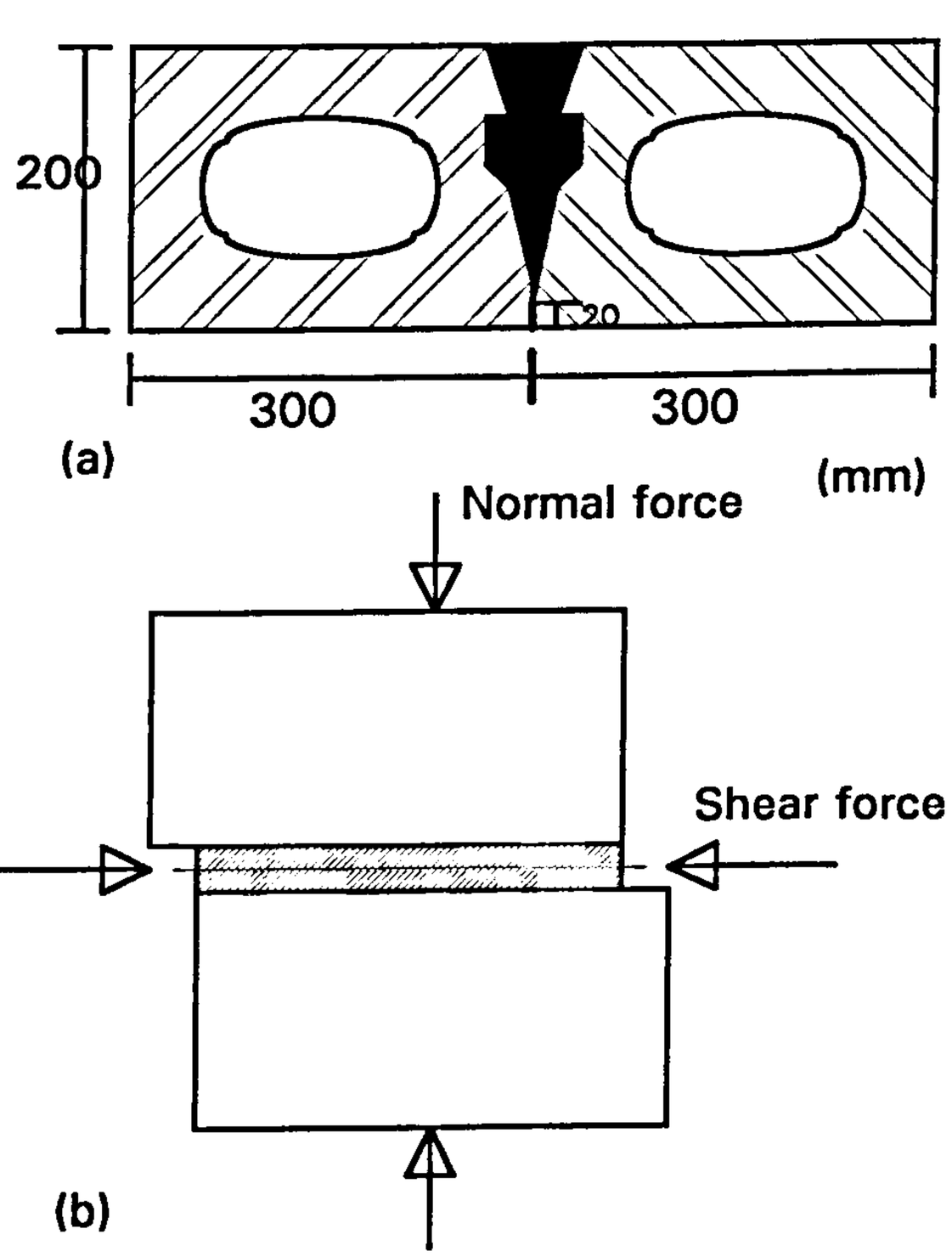

Figure 5-15: Shear and compression test used by Reinhardt [Reinhardt 1982]
a: Across section of investigated joint b: Schematic of the test

specimens are shown in figure 5-15. Joint lengths of the test specimens were o.3, 0.6, 1.2 and 2.0 m. For carrying out tests on specimens of these dimensions, a special equipment was designed. [Reinhardt 1982]

For evaluating the shear bond strength at the interface between PC overlays and the concrete substrate, cores were subjected to a shear force directed through the bond interface. [Sprinkel 1984] The shear bond strength for each specimen was calculated by dividing the failure shear force by the interface bonded area. (figure 5-16)

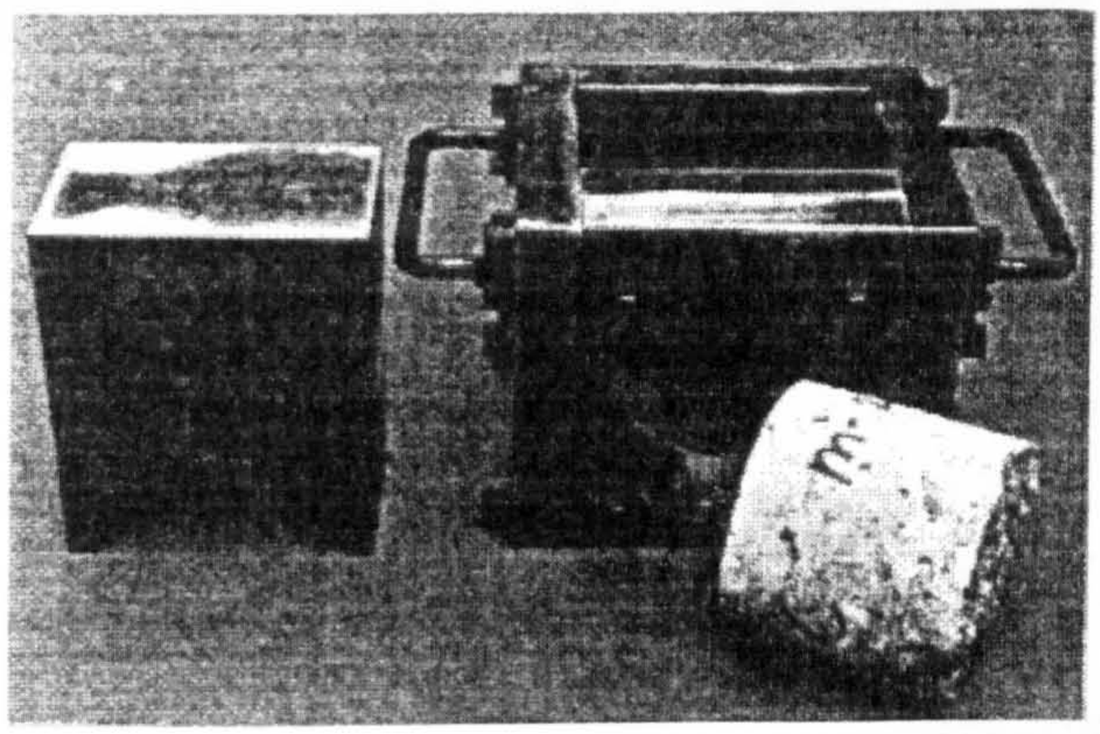

Figure 5-16: Apparatus for subjecting cores to shear used by Sprinkel [Sprinkel 1984]

Another direct shear test method, named " Friction Transfer " method, was used for measuring the bond strength between a patch repair mortar and the original concrete. In this method a specially devised apparatus was fitted on top of a previously prepared core, then by applying a torque, the maximum shear bond strength was recorded. The dimensions and other specification of the cores were the same as those required for the " limpet " test. [Cleland et al. 1986] This method of test which had been proposed and developed by Naderi [Naderi 1985], was also described in Ref. [Naderi et al. 1986] as an in situ test method for determining the shear bond strength between the repair and original concrete. (figure 5-17) Another torsion test method which has been developed at the University of Texas at Austin has been described as showing very erratic results to date. [Lundy 1990]

Slant compressive shear test has been used by many investigators. (figure 5-18) In this method of test composite specimen, cylinder or prism, is subjected to an axial compressive force, as a result of that both compressive and shear stresses develop along the interface. The magnitude of these stresses at failure may then be calculated. Prisms of 40 by 40 by 120 mm size and cylinders of

50 by 100 mm size with bond plane at 60° relative to the horizontal, in accordance with ASTM 882 (Standard Test Method for Bond Strength of Epoxy Resin Systems Used with Concrete), were used in Ref. [Ohama et al. 1986]. Slant compression/shear tests were conducted according BS6319 Part 4, using prism specimens of 100 by 100 by 500 mm size with the bond plane at 30°, 45° and 50° relative to the vertical. [Naderi et al. 1986] The shear failure envelope was produced for each combination of repair mortar and original concrete by plotting the average shear and normal compressive stresses at the interface. Considering the results, it was concluded that the credibility of the method was in serious doubts. [Naderi et al. 1986] This type of test was also reported in Ref. [Judge et al. 1986] using specimens of 50 by 55 by 150 mm, in Ref. [Wall et al. 1986] with a height : width ratio of 3:1, in Ref. [Al-Negheimish 1988] using 3 by 6 in. cylinders with a bond plane angle of 60° relative to the horizontal in accordance to ASTM C882-79, in Refs. [Kudlapur et al. 1989] and [Kudlapur 1990] using cylinders of 4 by 8 in. size and 45° slant, in Ref. [Lundy 1990] with a bond plane angle of 30° to the applied load.

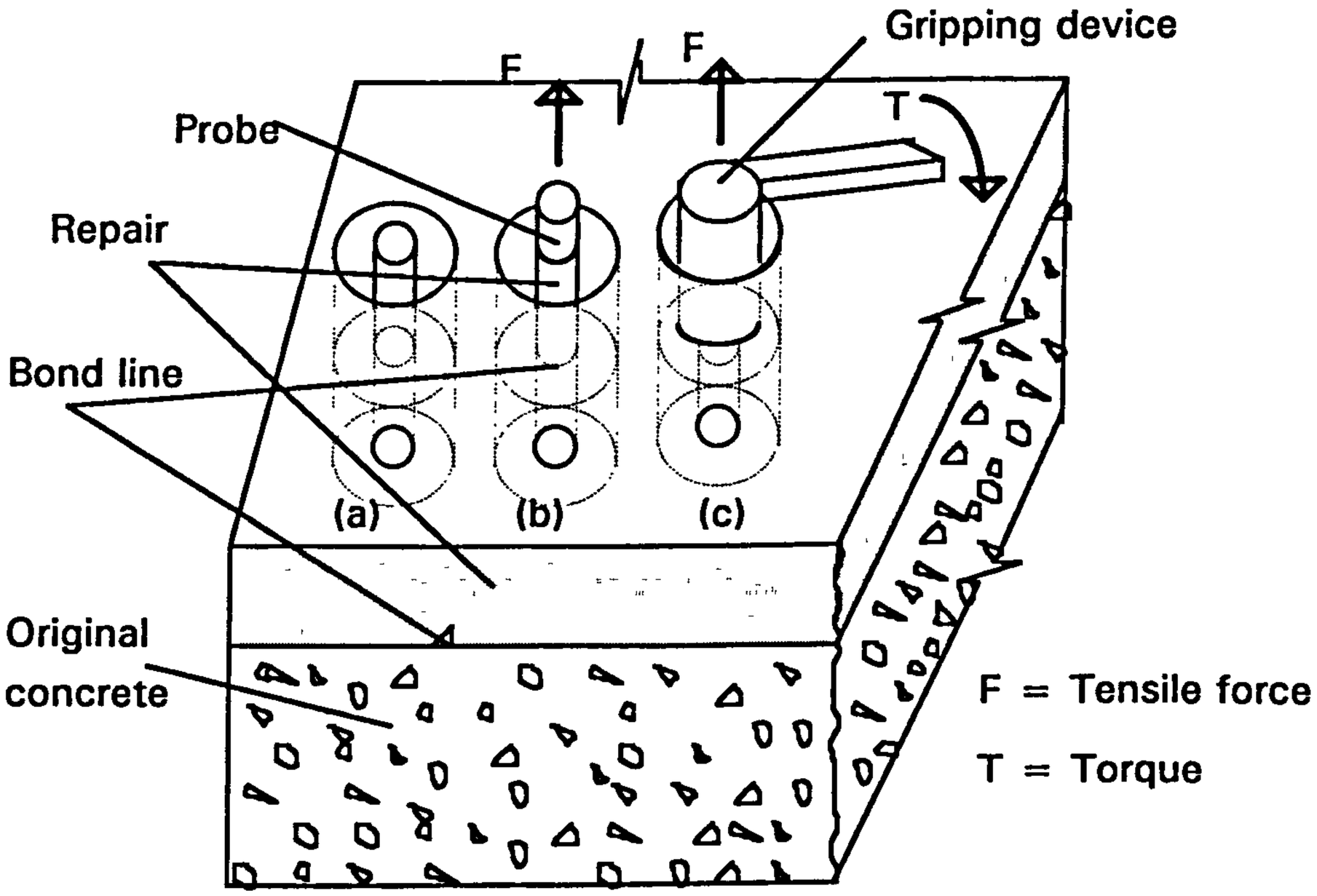

Figure 5-17: Schematic of in situ test arrangement described in ref. [Naderi et al. 1986] (a): Prepared core (b): Tensile bond test (c): Tensile and shear bond test

Another direct compressive shear test method, shown in figure 5-19, has been carried out in Ref. [Ohama et al. 1986].

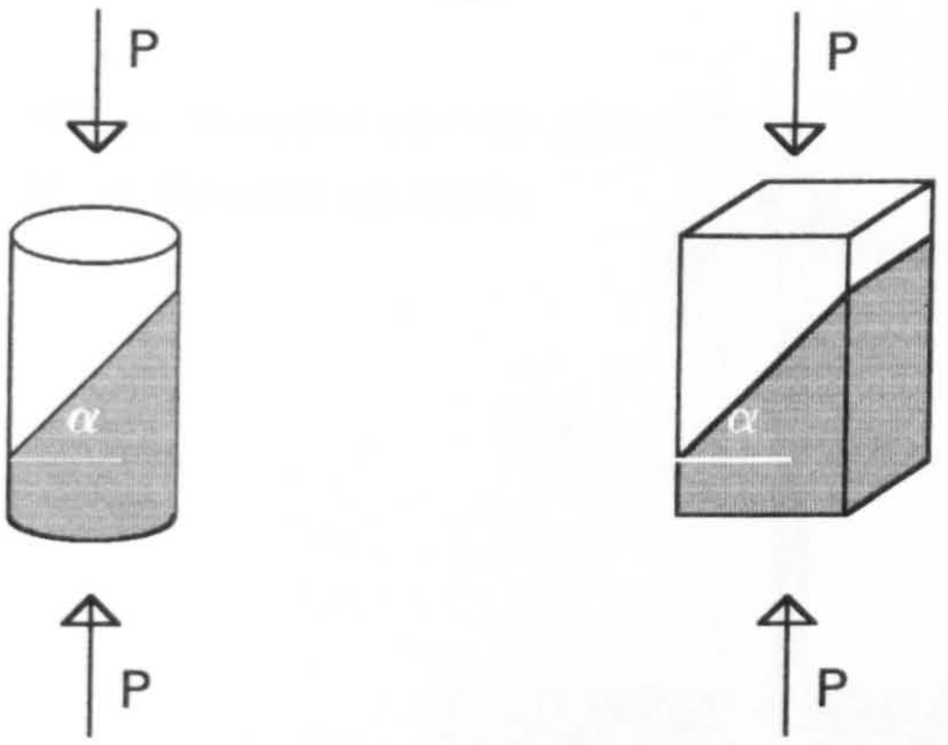

Figure 5-18: Schematic of slant shear compression test specimens

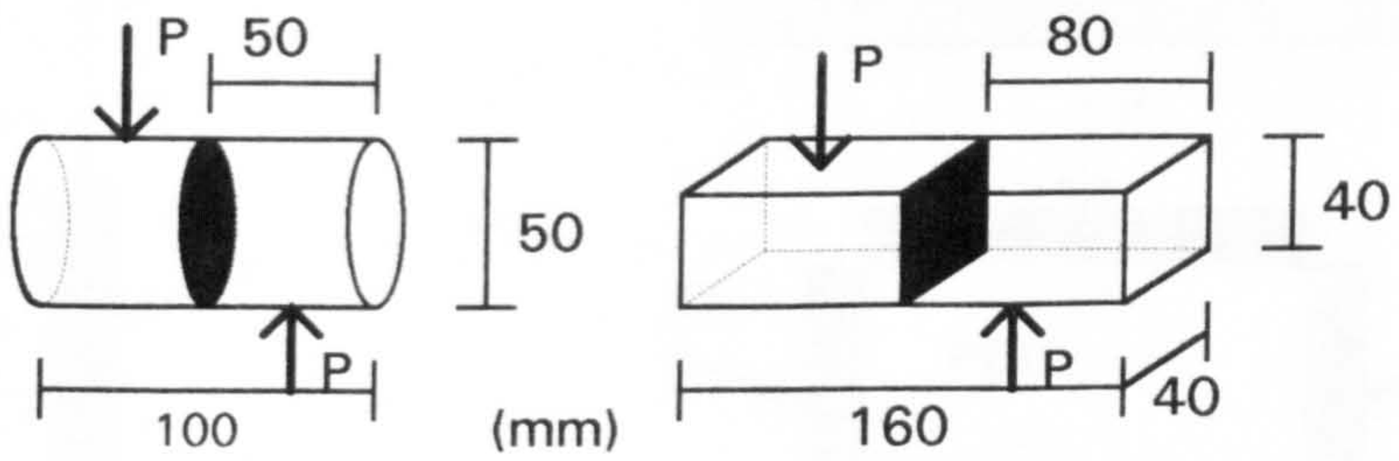

Figure 5-19: Direct shear test used in ref. [Ohama et al. 1986]

Bagate has carried out a kind of direct shear test method on concrete cores retrieved from overlaid pavements by applying a shearing load in compression " using an MST equipment at constant and uniform loading rate ". Further detail has not been given. [Bagate 1987]

Al-Negheimish has reviewed some more bond strength test methods used by previous investigators. These test methods are L-prism test, Plate shear bond test, double shear bond test and single shear test. (figure 5-20) [Al-Negheimish 1988]

The L - Prism test (figure 5-20-a) is also known as push - off shear test and has been used by many other investigators for measuring the shear strength at the interface of a new concrete layer cast against an older one. However in most cases transverse reinforcement across the composite interface has been used. [Al-Negheimish 1988] Reinforced specimens of L - Prism or push -off test method have been used by Kudlapur for investigating on the performance and shear strength of high - strength cold weather concrete repair materials in sub - freezing temperatures. [Kudlapur 1990] It has also been found that the results are size dependent and the shear stresses along the interface are not uniform. No one has reported this test for evaluating the bond strength between PC and concrete. The reason is probably the exothermic

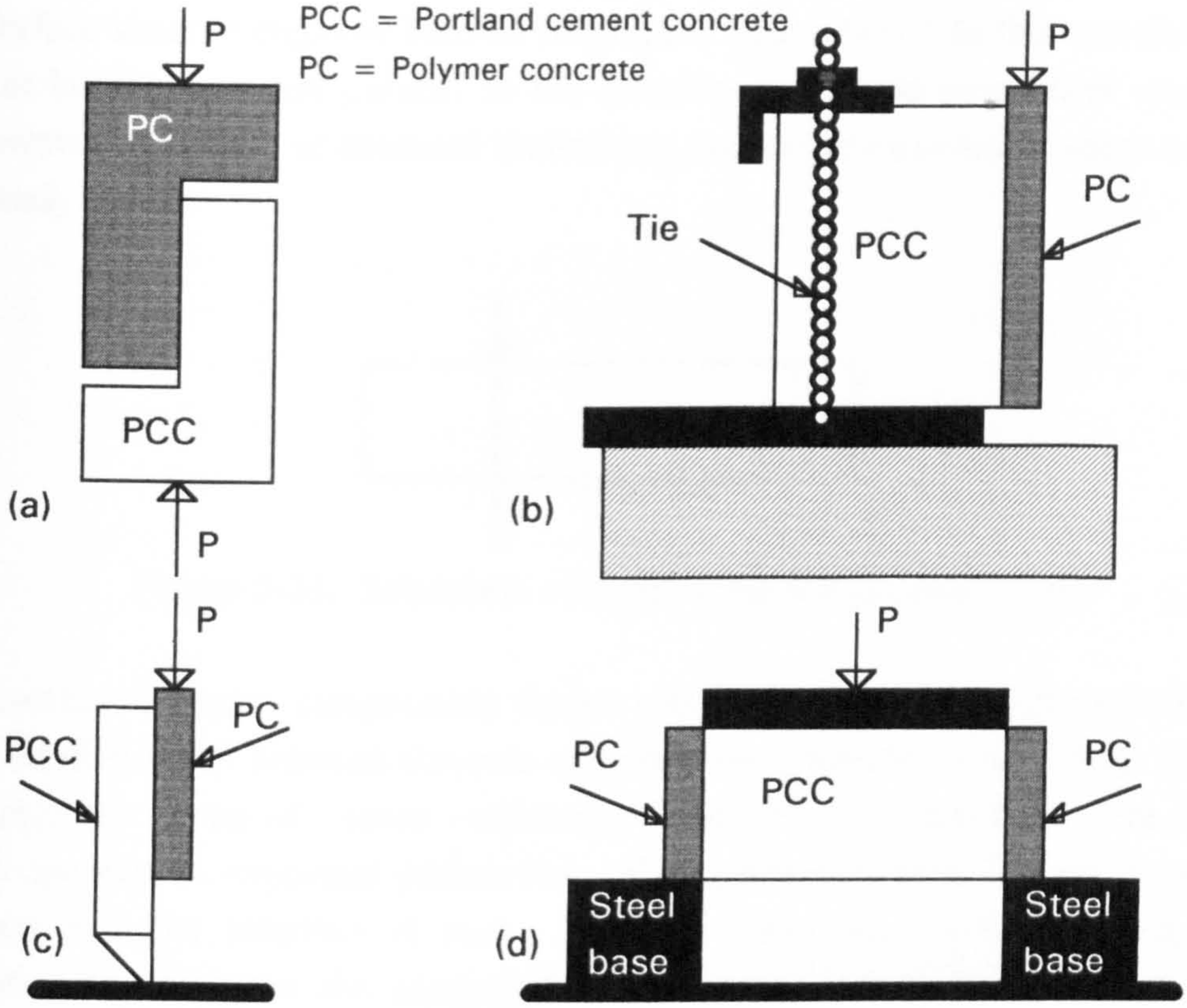

Figure 5-20: Shear bon tests methods a: L-prism test b: Single shear test c: Plate shear bond test d: Double shear bond test [Al-Negheimish 1988]

property of PC materials particularly when used in large volume. Single shear test and double shear test (figure 5-20-b & d) are direct shear tests and were widely used for measuring the bond strength between PC and Portland cement concrete in evaluating PC overlays. At last the plate shear test (figure 5-20-c) is a quick method of evaluating the shear bond strength of the interface and has been used by Al-Negheimish in his works. During the test a special steel specimen holder is needed so that the two layered system remains perpendicular to the loading surface. [Al-Negheimish 1988]

The behaviour at the interface between a concrete overlay and its reinforced concrete beam was simulated with a bilinear shear - slip relationship by using the push - off test data reported in Ref. [Saemman et al. 1964]. [Saiidi et al. 1990]

The results of shear block tests obtained from a previous study [Seible et al. 1988], were used for defining an interface constitutive behaviour for the structural analysing of concrete bridge overlays. [Seible and Latham 1990]

Lundy has used direct shear test using cored specimens for determining the interface shear strength of bonded overlays. (figure 5-21) In this test the load is to be coplanar and parallel to the interface to induce pure shear stresses. However as a result of practical limitations, eccentricity existed to some extent. [Lundy 1990]

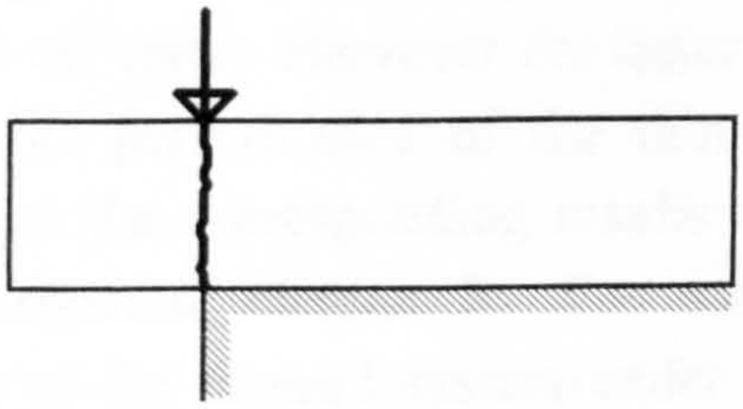

Figure 5-21: Schematic of direct shear test [Lundy 1990]

A combined shear - compression device was designed and used for measuring the bond strength between concrete and concrete. [Saucier et al. 1991] In this method the matter of " space - efficiency " and test - to - test time were taken into account as important parameters. The specimens were 75 mm concrete cubes with the interface at mid - height. Using this method of test, the relationship between the compressive and shear load at failure for a new concrete cast on dry - sawn concrete surface has been plotted. [Saucier et al. 1991]

Flexural patched beam or slab specimens have also been used for assessing the repair materials.(figure 5-22) [Kwasny 1986] [Kudlapur et al. 1989] [Kudlapur 1990]

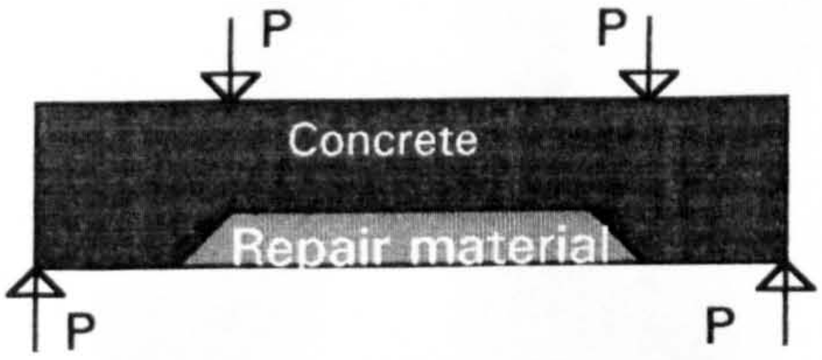

Figure 5-22: Schematic of a patched specimen in flexure

5-2-2 Interface bond strength test methods used in this study

In the previous section, most of the commonly used bond strength test methods were summarised. For analysing the behaviour of a layered system under the action of vertical or vertical and horizontal loads, the knowledge of bond characteristics at the interface is essential. This consists of the tensile bond

strength, where the normal tensile stress is dominant, and shear and compression bond strength, where the induced shear stress at the interface is dominant. Owing to the requirements of the analysis and availability of the equipment, two methods of tests were used in this investigation, the pull off test method and a new simple shear and compression test method. The Elcometer screed pull off tester (figure 5-23) or ' Limpet ' loading equipment were used for carrying out the pull off tests. However the latter was also employed as a way for evaluation of the performance of the thin layered systems in the NUROLF experiment and the corresponding results will be presented in the same part of this investigation, chapter 7. For measuring the shear bond strength at the interface of the layered system under the existence of normal compression stress, a special " shear box " test was developed using a shear box loading machine.

Two types of primers have been used in these series of tests, Gprime and Pprime. As it was thought that the ready made Rolling load specimens supplied by the manufacturer had been primed by Pprime, it was decided that all the bond strength specimens prepared for the age 56 days, but P4/Concrete specimens, must be primed with Pprime.

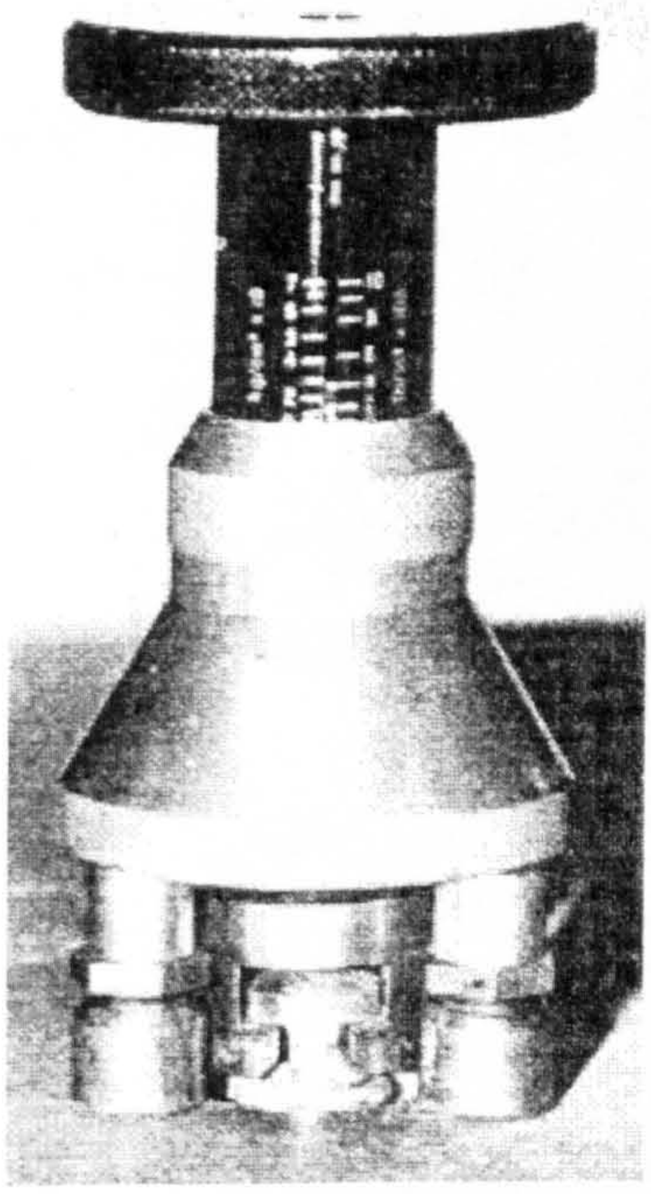

Figure 5-23: The Elcometer screed pull off tester [Judge et al. 1986]

5-2-2-1 Bond strength pull off tests

The Elcometer pull off tester was used for measuring the direst tensile strength of 20 mm diameter cores having a thickness of 5 mm , cast upon the lower layer surface. The samples were prepared using 600 by 300 by 50 mm concrete slabs. These slabs were the same as those used in the steel wheel rolling load tests. To avoid damaging the interface bonded plane during the drilling process, for the measurement of the bond strength between a desired material and concrete, the small cores of each material were cast upon the concrete slabs directly by using plastic rings. When testing the bond strength between G1194 or G1294 material and P4, a layer of P4 was to be cast on the concrete slab and cured for 14 days at the room conditions before casting the core specimens on top of that. Three specimens were used and tested for each condition, age and combination. At the time of testing, the special test dollies were adhered onto the core surfaces and then a tensile stress up to the bond failure were applied to the specimens.

A general layout of pull off test core specimens cast on the concrete slabs is shown in figure 5-24. As it was explained before, the layer of P4 in figure 5-24 is applicable when testing the bond strength between this material and G1194 or G1294 is concerned.

Figure 5-24: Layout for pull off tests on slab

5-2-2-1-1 Test results

The pull off test results along with some other specifications of core specimens for each age of test have been reported in parts a of tables 5-17 to 5-21.
The values of mean bond strength, standard deviation, and coefficient of variation are also calculated at each stage and listed in parts b of tables 5-16 to 5-20. The average results of pull off tests have also been shown in figures 5-23 to 5-25

Table 5-17: Results of pull off tests for the measurement of bond strength between G1194 and P4 at the ages of 14, 28 and 56 days:
a: Upper and lower layer material, age, interface condition and bond strength
b: Mean bond strength, standard deviation, and coefficient of variation

Table 5-17-a:

Specimen Number	Upper layer (core)	Lower layer (substrate)	Age (days)	Interface *1 Condition	Bond Strength (MPa)
1	G1194	P4	14	Gprime	1.4
2	G1194	P4	14	Gprime	1.4
3	G1194	P4	14	Gprime	1.1
1	G1194	P4	28	Gprime	1.7
2	G1194	P4	28	Gprime	2.7
3	G1194	P4	28	Gprime	2.9
1	G1194	P4	56	Pprime	2.0
2	G1194	P4	56	Pprime	1.8
3	G1194	P4	56	Pprime	1.7

*1 Position of failure for each specimen was in the P4 material, however the surface of delamination was perpendicular to the tensile force and the thickness of the delaminated layer of P4 was too thin to be measured.

Table 5-17-b:

Interface primer	Age at the test (days)	Total number of specimens	Mean bond strength (MPa)	Standard deviation (MPa)	Coefficient of variation (percent)
Gprime	14	3	1.3	0.17	13.1
Gprime	28	3	2.4	0.64	26.7
Pprime	56	3	1.8	0.15	8.3

Table 5-18: Results of pull off tests for the measurement of bond strength between G1194 and concrete at the ages of 14, 28 and 56 days:
a: Upper and lower layer material, age, interface condition and bond strength
b: Mean bond strength, standard deviation, and coefficient of variation

Table 5-18-a:

Specimen Number	Upper layer (core)	Lower layer (substrate)	Age (days)	Interface [*1] Condition	Bond Strength (MPa)
1	G1194	Concrete	14	Gprime	4.0
2	G1194	Concrete	14	Gprime	3.5
3	G1194	Concrete	14	Gprime	6.0
1	G1194	Concrete	28	Gprime	5.0
2	G1194	Concrete	28	Gprime	4.8
3	G1194	Concrete	28	Gprime	6.0
1	G1194	Concrete	56	Pprime	1.8
2	G1194	Concrete	56	Pprime	0.9
3	G1194	Concrete	56	Pprime	1.3

[*1]Position of failure for each specimen tested at the age of 14 or 28 days (using Gprime at the interface) was more than 75% in the Concrete and less than 25% at the bond surface, while for each specimen tested at the age of 56 days (using Pprime at the interface) failure occurred at the bond surface

Table 5-18-b:

Interface primer	Age at the test (days)	Total number of specimens	Mean bond strength (MPa)	Standard deviation (MPa)	Coefficient of variation (percent)
Gprime	14	3	4.5	1.32	29.3
Gprime	28	3	5.3	0.64	12.1
Pprime	56	3	1.3	0.45	34.6

Table 5-19: Results of pull off tests for the measurement of bond strength between G1294 and P4 at the ages of 14, 28 and 56 days:
a: Upper and lower layer material, age, interface condition and bond strength
b: Mean bond strength, standard deviation, and coefficient of variation

Table 5-19-a:

Specimen Number	Upper layer (core)	Lower layer (substrate)	Age (days)	Interface *1 Condition	Bond Strength (MPa)
1	G1294	P4	14	Gprime	1.0
2	G1294	P4	14	Gprime	1.0
3	G1294	P4	14	Gprime	1.5
1	G1294	P4	28	Gprime	1.3
2	G1294	P4	28	Gprime	1.0
3	G1294	P4	28	Gprime	0.8
1	G1294	P4	56	Pprime	0.8
2	G1294	P4	56	Pprime	0.8
3	G1294	P4	56	Pprime	1.3

*1Position of failure for each specimen was more than 75% in the P4 and less than 25% at the bond surface, however the surface of delamination was perpendicular to the tensile force and the thickness of the delaminated layer of P4 was too thin to be measured.

Table 5-19-b:

Interface primer	Age at the test (days)	Total number of specimens	Mean bond strength (MPa)	Standard deviation (MPa)	Coefficient of variation (percent)
Gprime	14	3	1.2	0.29	24.0
Gprime	28	3	1.0	0.25	25.0
Pprime	56	3	1.0	0.29	29.0

Table 5-20: Results of pull off tests for the measurement of bond strength between G1294 and concrete at the ages of 14, 28 and 56 days:
a: Upper and lower layer material, age, interface condition and bond strength
b: Mean bond strength, standard deviation, and coefficient of variation

Table 5-20-a:

Specimen Number	Upper layer (core)	Lower layer (substrate)	Age (days)	Interface Condition [*1]	Bond Strength (MPa)
1	G1294	Concrete	14	Gprime	1.6
2	G1294	Concrete	14	Gprime	1.5
3	G1294	Concrete	14	Gprime	1.5
1	G1294	Concrete	28	Gprime	1.5
2	G1294	Concrete	28	Gprime	1.0
3	G1294	Concrete	28	Gprime	2.0
1	G1294	Concrete	56	Pprime	1.6
2	G1294	Concrete	56	Pprime	1.5
3	G1294	Concrete	56	Pprime	2.0

[*1] Position of failure for each specimen was at the bond surface

Table 5-20-b:

Interface primer	Age at the test (days)	Total number of specimens	Mean bond strength (MPa)	Standard deviation (MPa)	Coefficient of variation (percent)
Gprime	14	3	1.5	0.06	4.0
Gprime	28	3	1.5	0.50	33.3
Pprime	56	3	1.7	0.26	15.3

Table 5-21: Results of pull off tests for the measurement of bond strength between P4 and concrete at the ages of 14, 28 and 56 days:
a: Upper and lower layer material, age, interface condition and bond strength
b: Mean bond strength, standard deviation, and coefficient of variation

Table 5-21-a:

Specimen Number	Upper layer (core)	Lower layer (substrate)	Age (days)	Interface *1 Condition	Bond Strength (MPa)
1	P4	Concrete	14	Gprime	0.4
2	P4	Concrete	14	Gprime	0.3
3	P4	Concrete	14	Gprime	0.4
1	P4	Concrete	28	Gprime	0.4
2	P4	Concrete	28	Gprime	0.4
3	P4	Concrete	28	Gprime	0.4
1	P4	Concrete	56	Gprime	0.4
2	P4	Concrete	56	Gprime	0.4
3	P4	Concrete	56	Gprime	0.4

*1 Position of failure for each specimen was at the bond surface

Table 5-21-b:

Interface primer	Age at the test (days)	Total number of specimens	Mean bond strength (MPa)	Standard deviation (MPa)	Coefficient of variation (percent)
Gprime	14	3	0.4	0.06	15.0
Gprime	28	3	0.4	0.00	0.0
Gprime	56	3	0.4	0.00	0.0

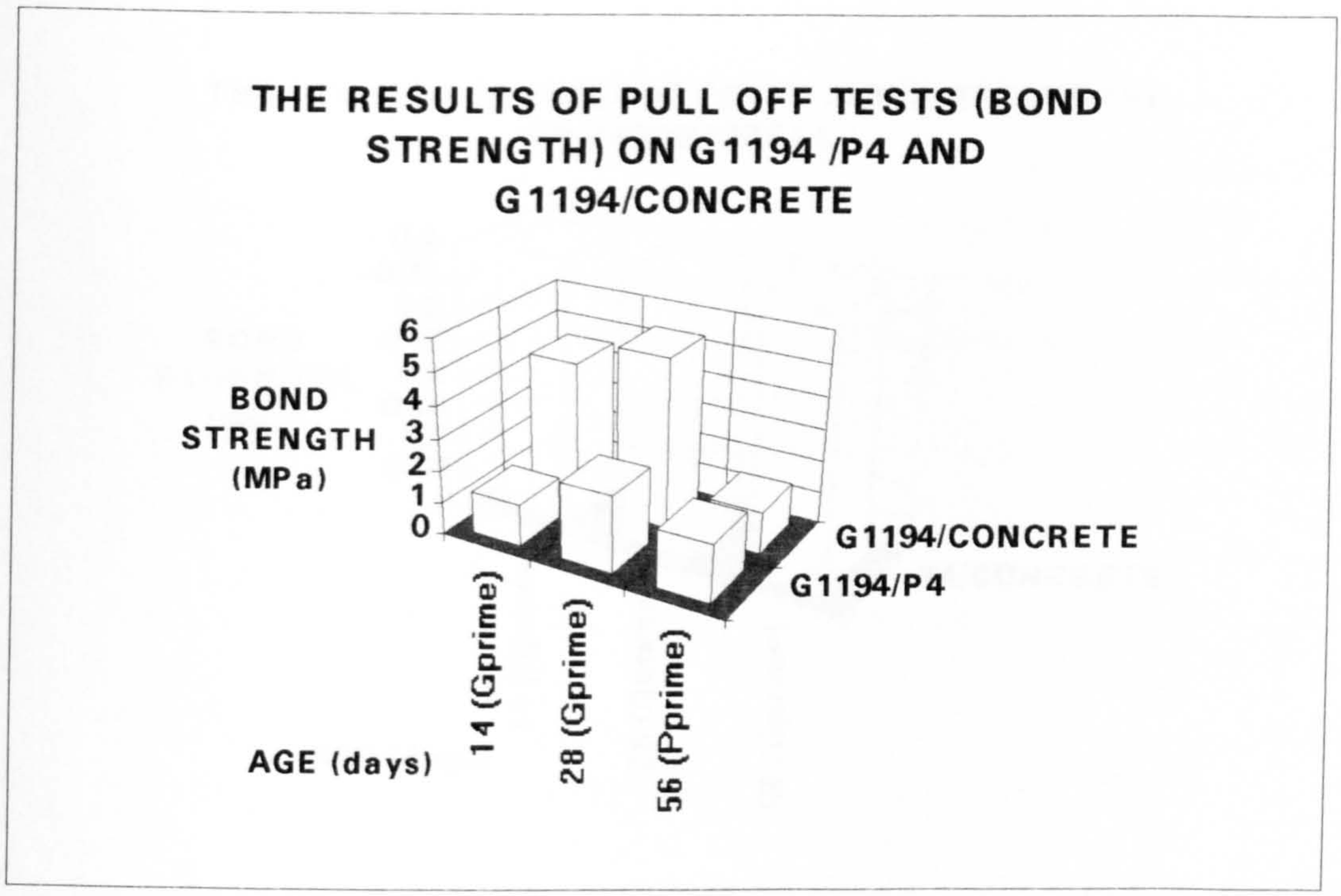

Figure 5-23: Pull off test results for G1194/P4 and G1294/Concrete systems at different ages using the Elcometer screed pull off tester

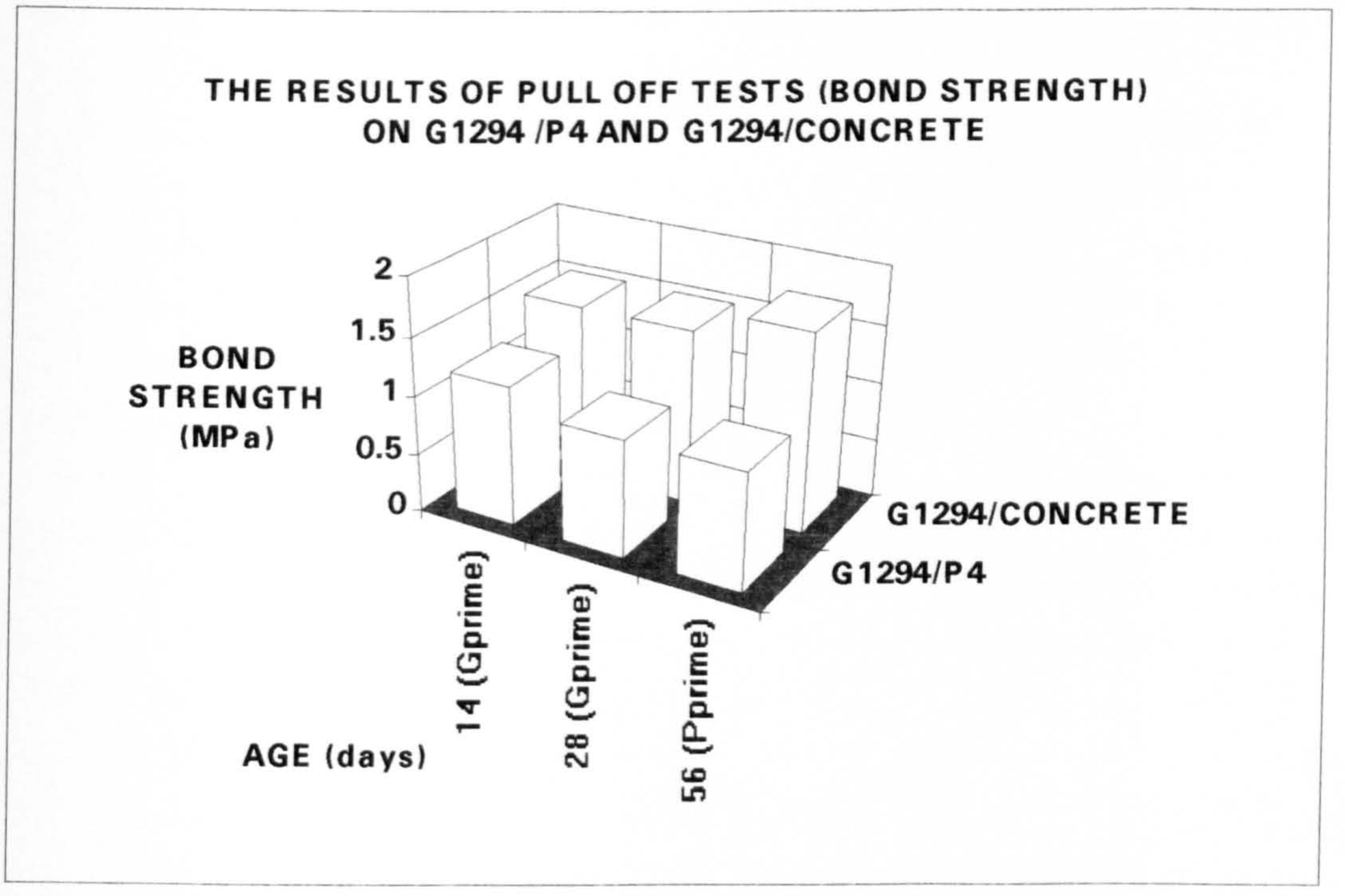

Figure 5-24: Pull off test results for G1294/P4 and G1294/Concrete systems at different ages using the Elcometer screed pull off tester

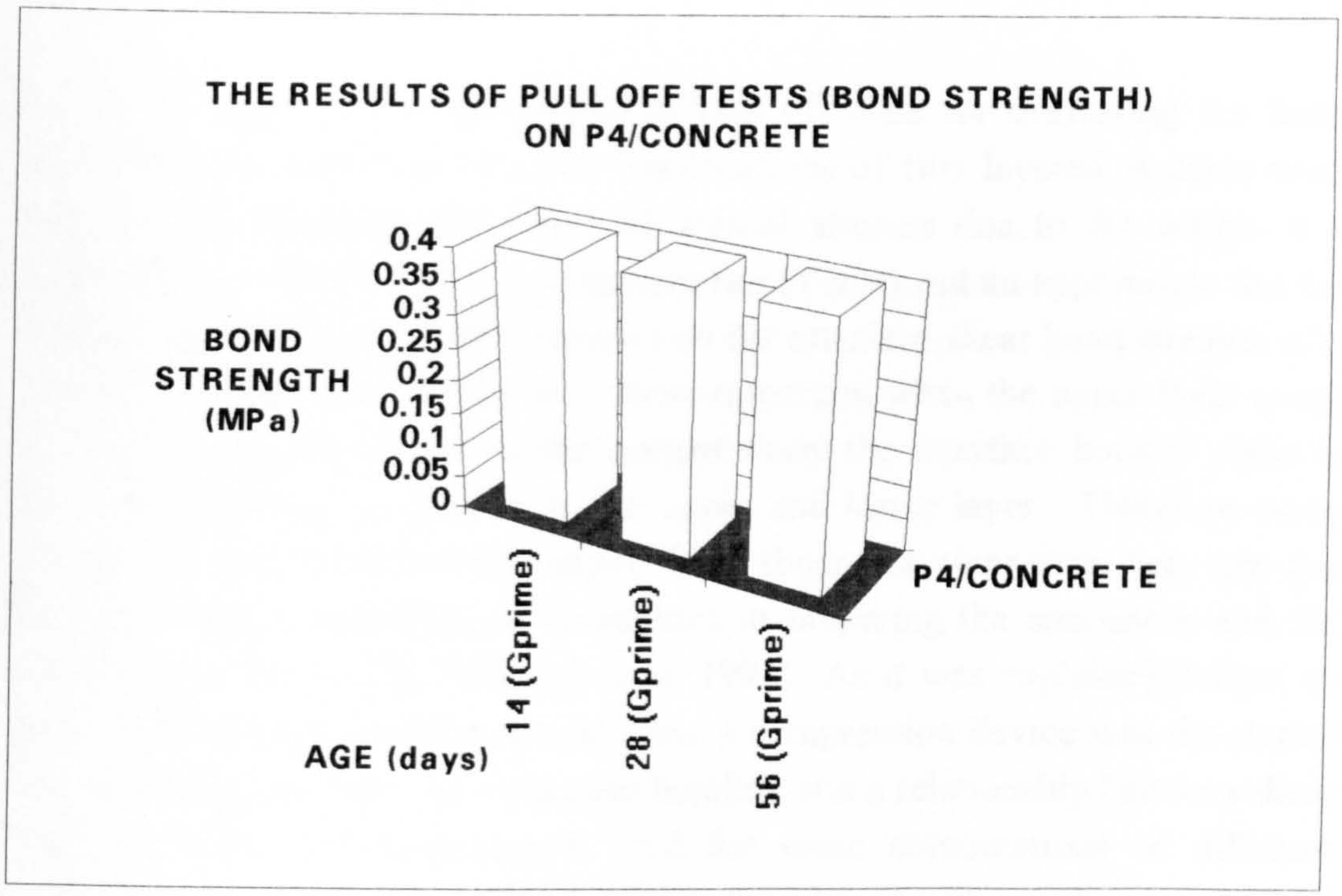

Figure 5-25: Pull off test results for P4/Concrete systems at different ages using the Limpet equipment

5-2-2-2 Shear box tests

In the previous section the results of pull off tests for evaluating the bond strength at the interface of some combinations of two layered systems were reported. Considering the effect of normal stresses due to the action of a vertical load, wheel load, an investigator has to carry out an appropriate test for measuring the results of these stresses on the interface shear bond strength of a layered system. This will be even more important when the upper layer is not thick. On the other hand, in the current study the interface bonded plane is always horizontal, i.e. parallel to the upper and lower layer. Therefore using the more common method of compression - shear test, slant shear test, may not be very helpful, regardless of difficulties in preparing the specimens and the scattering of the results. [Saucier et al. 1991] As it was explained before, in Ref. [Saucier et al. 1991] a special shear - compression device was developed for measuring concrete - to - concrete bonding and a relationship between shear load at failure and compressive load for some combinations of different concrete layers was concluded. However the idea of using such a test method in this investigation was based on the proposed thin layer element for analysing the behaviour of interfaces in rocks joints and soil - structure behaviour in Ref. [Desai et al. 1984] More details on the principles of the analysing method will be presented in the next chapter.

In the proposed shear box method, the cohesion and coefficient of friction for each combination of two materials are determined by using a standard shear box apparatus of plan dimensions 60 by 60 mm. (figure 5-26) Nevertheless, for testing the topping materials on top of concrete, due to the restriction in the load capacity of the testing machine, the plan dimensions of the box were reduced to 35 by 35 mm. According to Ref. [Saucier et al. 1991], " space - efficiency " of a specimen can easily be obtained by calculating the ratio between the bonded area subjected to the failure stress and the volume of the specimen. Considering a thickness of about 20 mm for each layer, one can realise that the value of " space - efficiency " for these specimens will be very satisfactory compared with other types of compression - shear tests. However this is largely a commercial matter but we are more interested, scientifically, in the site comparability problems, for instance exotherm and stress redistribution which are very important and at the same time very difficult subject in materials testing.

Five combinations of materials were considered with the use of different primers and at different ages. Test specimens were generally prepared in the following manner.

All specimens were prepared at two stages using the two parts of the split box. (figure 5-26) For the combinations of G1194/P4 and G1294/P4, the first layer of P4 was cast and cured in room conditions for 14 days, then its surface was brushed and primed using the desired primer. After curing the primer, the upper layer of the specimen was cast on it using both parts of the split box. For the combinations of G1194/Concrete, G1294/Concrete, and P4/Concrete, as it was mentioned before, the plan dimensions of the shear box were modified. For these cases small blocks of concrete of dimensions 35 by 35 by 20 mm were precisely cut out from the same slab specimens as used in the Steel Wheel Rolling Load experiment. The second step was the same as that for other combinations explained above. Two types of primers were used in this experiment, Gprime and Pprime. Before using each part of the split box, it was lubricated by Vaseline in order to facilitate the demoulding process.

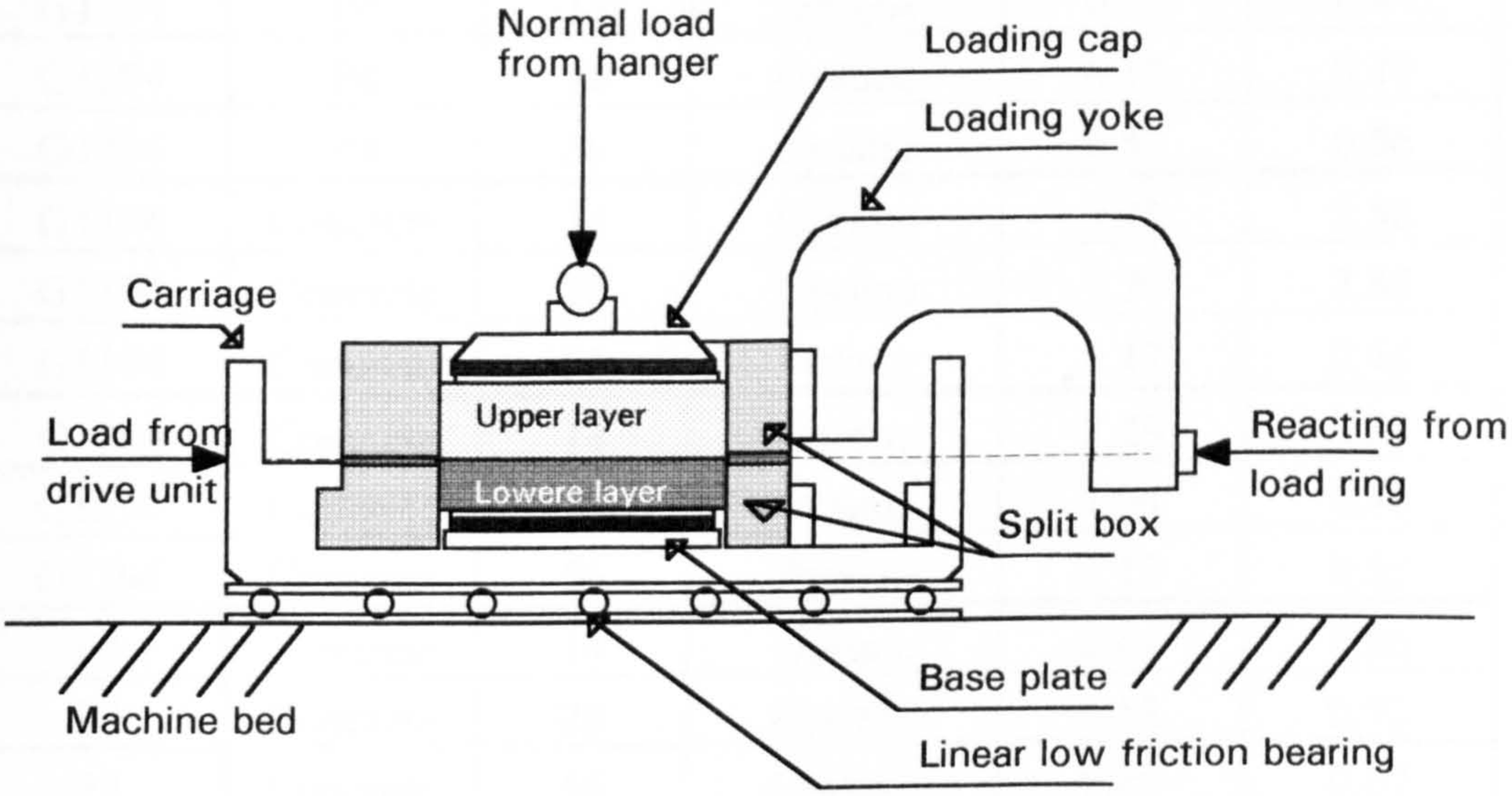

Figure 5-26: Schematic of the shear box test apparatus

5-2-2-2-1 Test results

As it was mentioned before, the main aim of these tests was to determine the effect of normal pressure on the interface shear bond strength. Therefore each combination of materials with the desired primer and age, was to be tested under different compression loads. The shear strength, under each normal

pressure, has been calculated by dividing the load at failure by the area of bonding (60 by 60 mm or 35 by 35 mm). The relationship between normal stress and shear bond strength has then been plotted in figures 5-27 to 5-41. By using the regression analysis, the values of cohesion and coefficient of friction have also been calculated in each case and summarised in table 5-22.

Table 5-22: The values of cohesion (shear strength at zero normal pressure) and coefficient of friction between different combinations of materials with different types of primers and at different ages:

Upper layer	Lower layer	Age (days)	Primer at the interface	Cohesion (MPa)	Coefficient of friction
G1194	P4	14	Gprime	1.23	0.72
G1194	P4	28	Gprime	1.30	0.89
G1194	P4	56	Pprime	1.04	0.70
G1294	P4	14	Gprime	0.70	0.47
G1294	P4	28	Gprime	0.58	0.49
G1294	P4	56	Pprime	0.53	0.56
G1194	Concrete	14	Gprime	3.48	2.58
G1194	Concrete	28	Gprime	4.20	2.88
G1194	Concrete	56	Pprime	1.47	0.44
G1294	Concrete	14	Gprime	2.29	0.29
G1294	Concrete	28	Gprime	1.94	0.40
G1294	Concrete	56	Pprime	1.15	0.18
P4	Concrete	14	Gprime	0.41	0.86
P4	Concrete	28	Gprime	0.58	0.72
P4	Concrete	56	Gprime	0.80	0.67

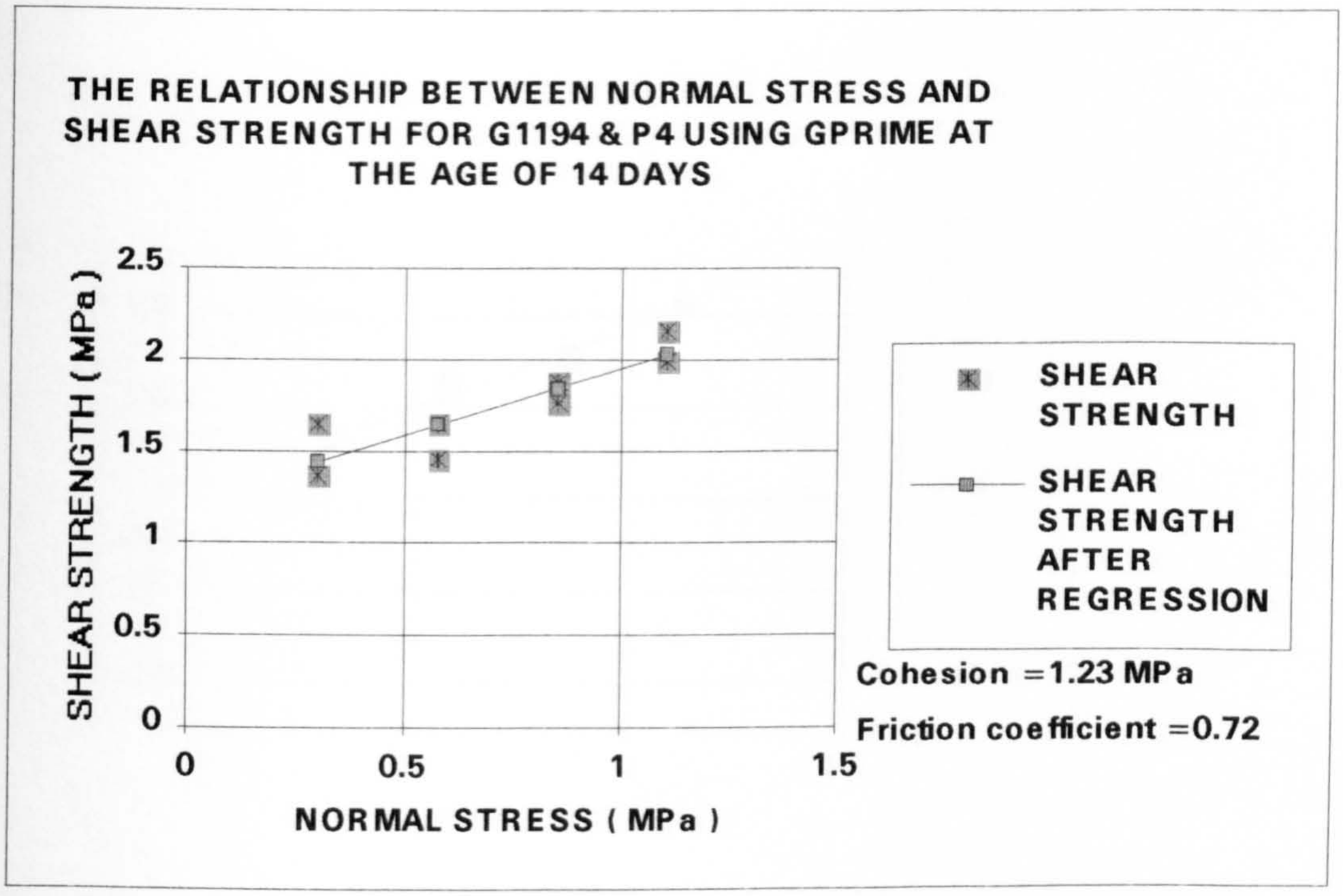

Figure 5-27: The relationship between normal stress and shear strength for G1194 & P4 using Gprime at the age of 14 days

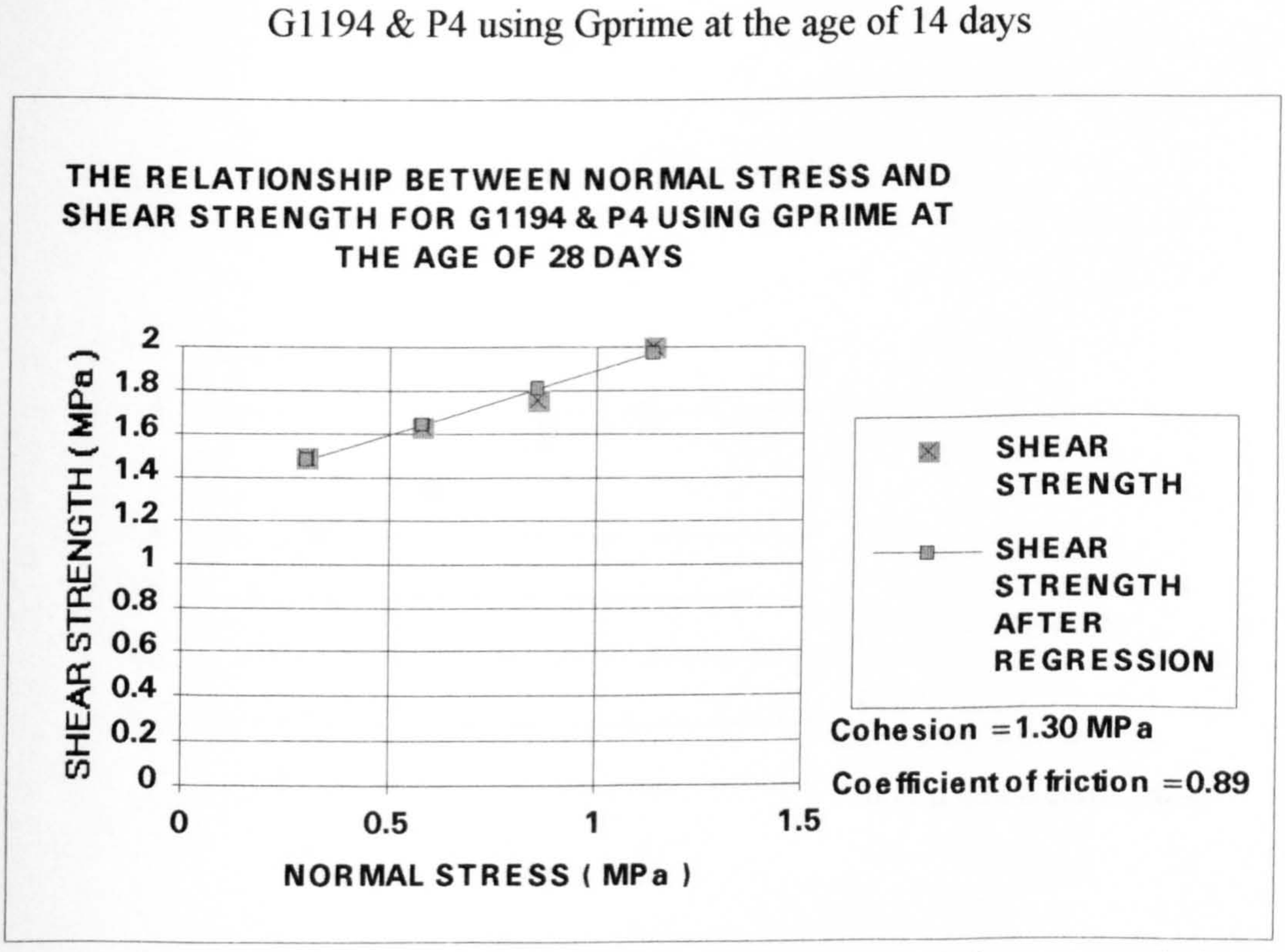

Figure 5-28: The relationship between normal stress and shear strength for G1194 & P4 using Gprime at the age of 28 days

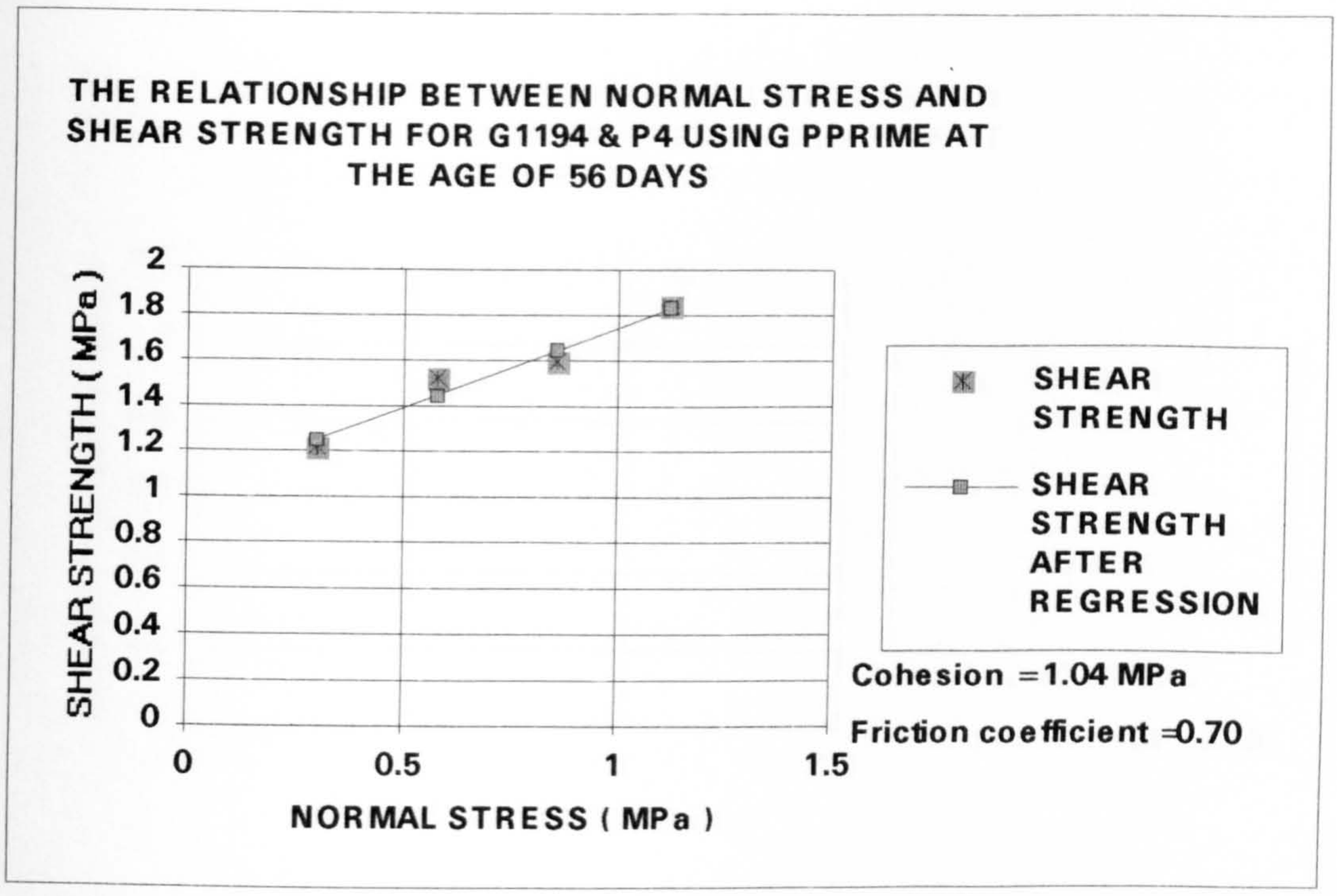

Figure 5-29: The relationship between normal stress and shear strength for G1194 & P4 using Pprime at the age of 56 days

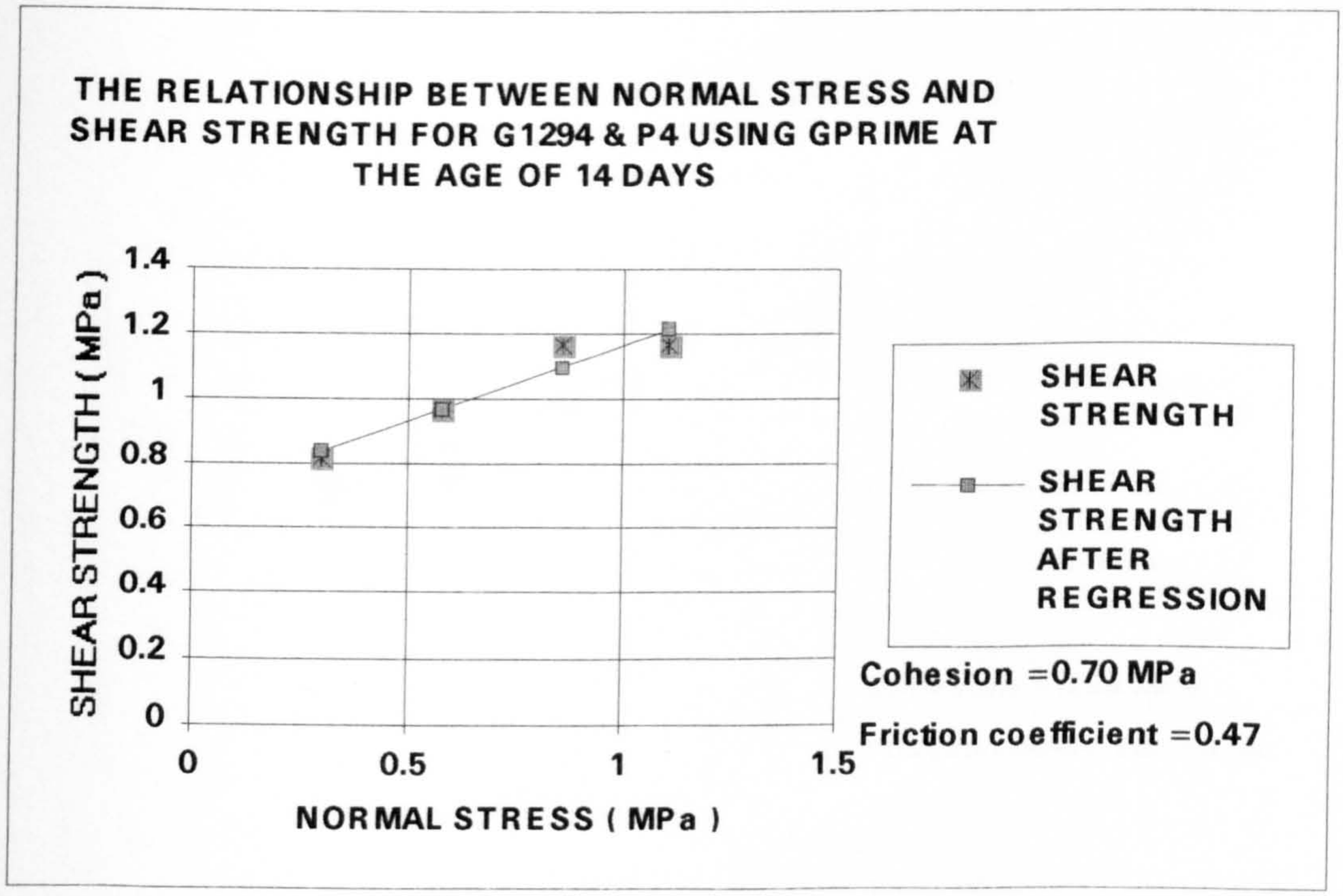

Figure 5-30: The relationship between normal stress and shear strength for G1294 & P4 using Gprime at the age of 14 days

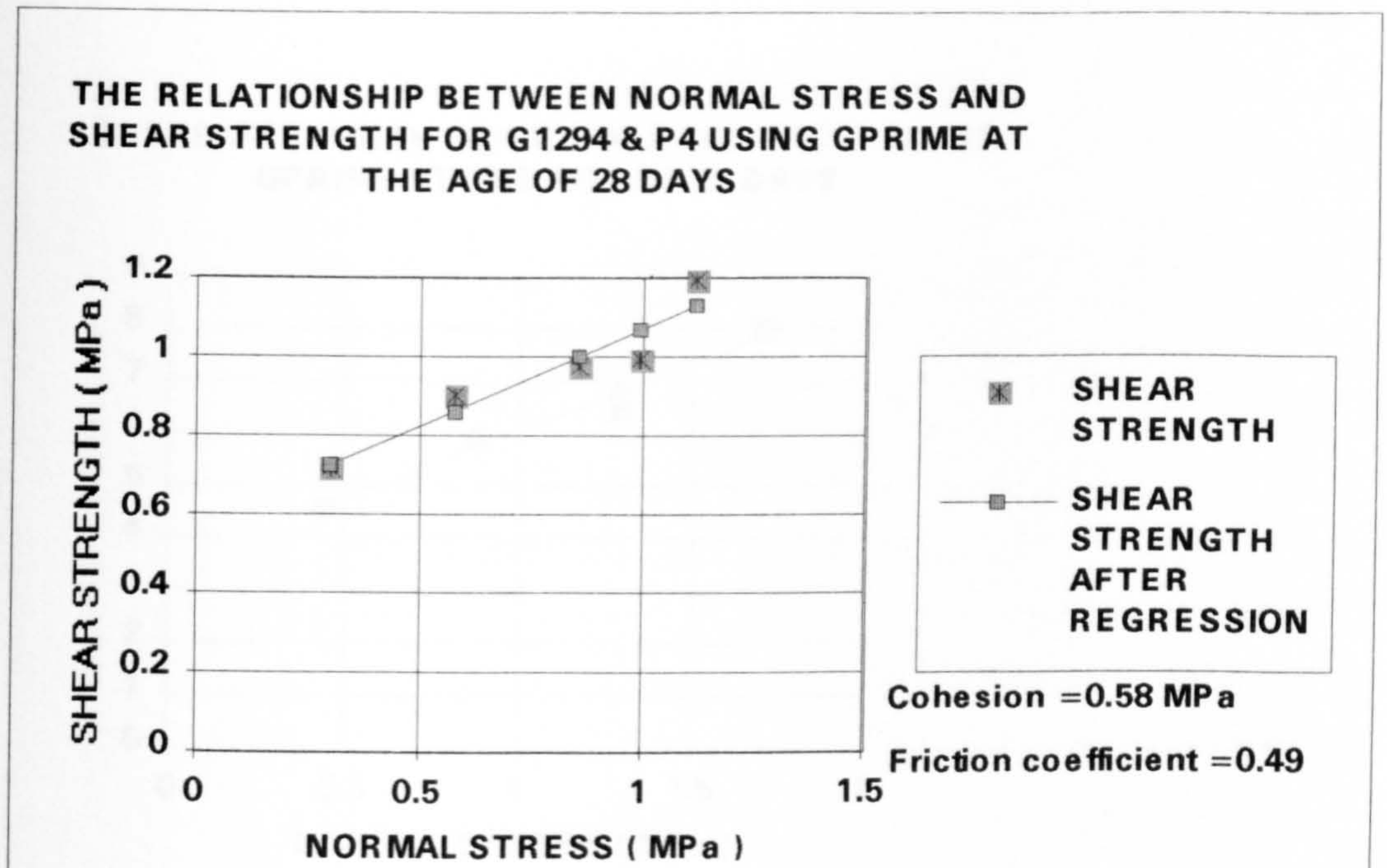

Figure 5-31: The relationship between normal stress and shear strength for G1294 & P4 using Gprime at the age of 28 days

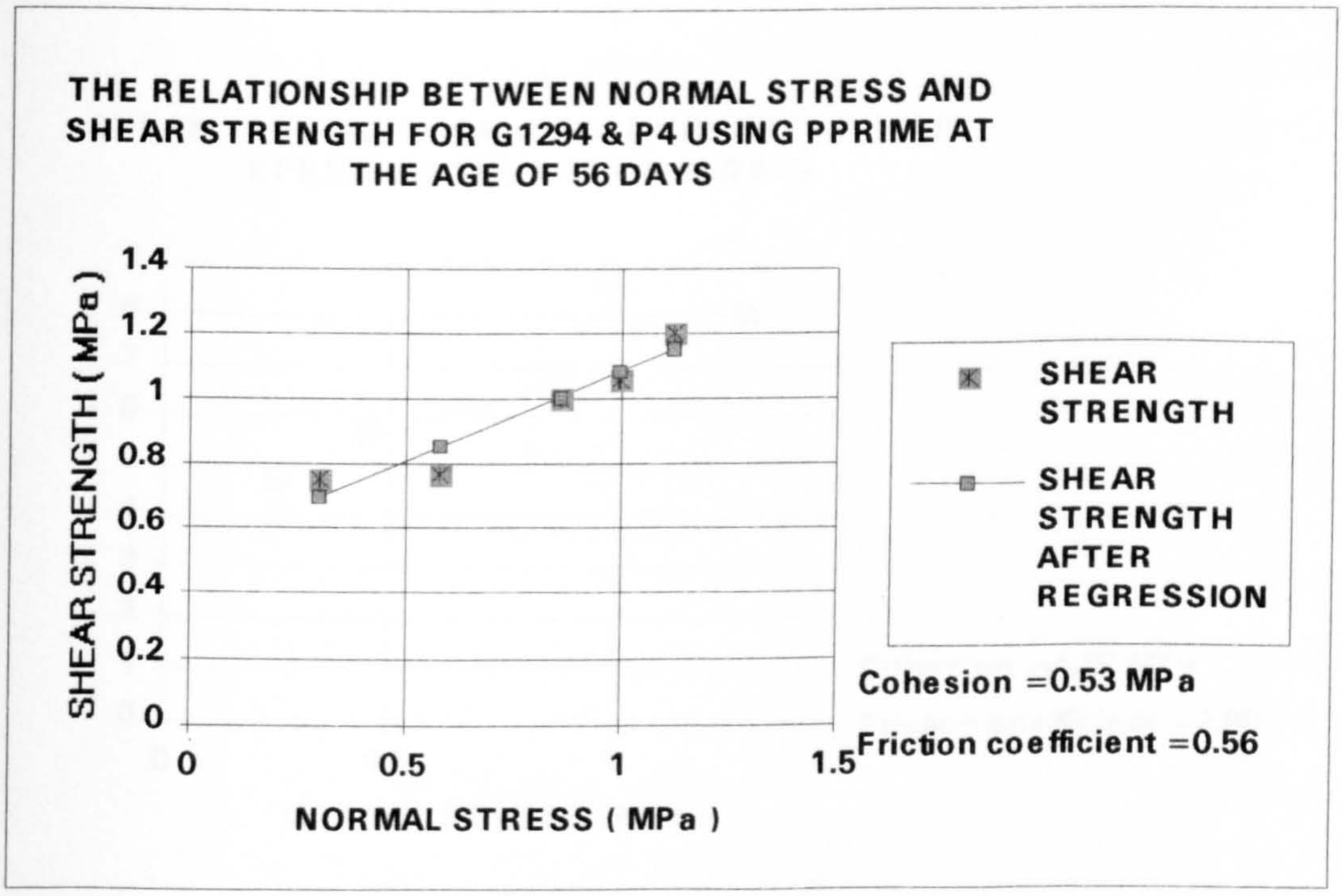

Figure 5-32: The relationship between normal stress and shear strength for G1294 & P4 using Pprime at the age of 56 days

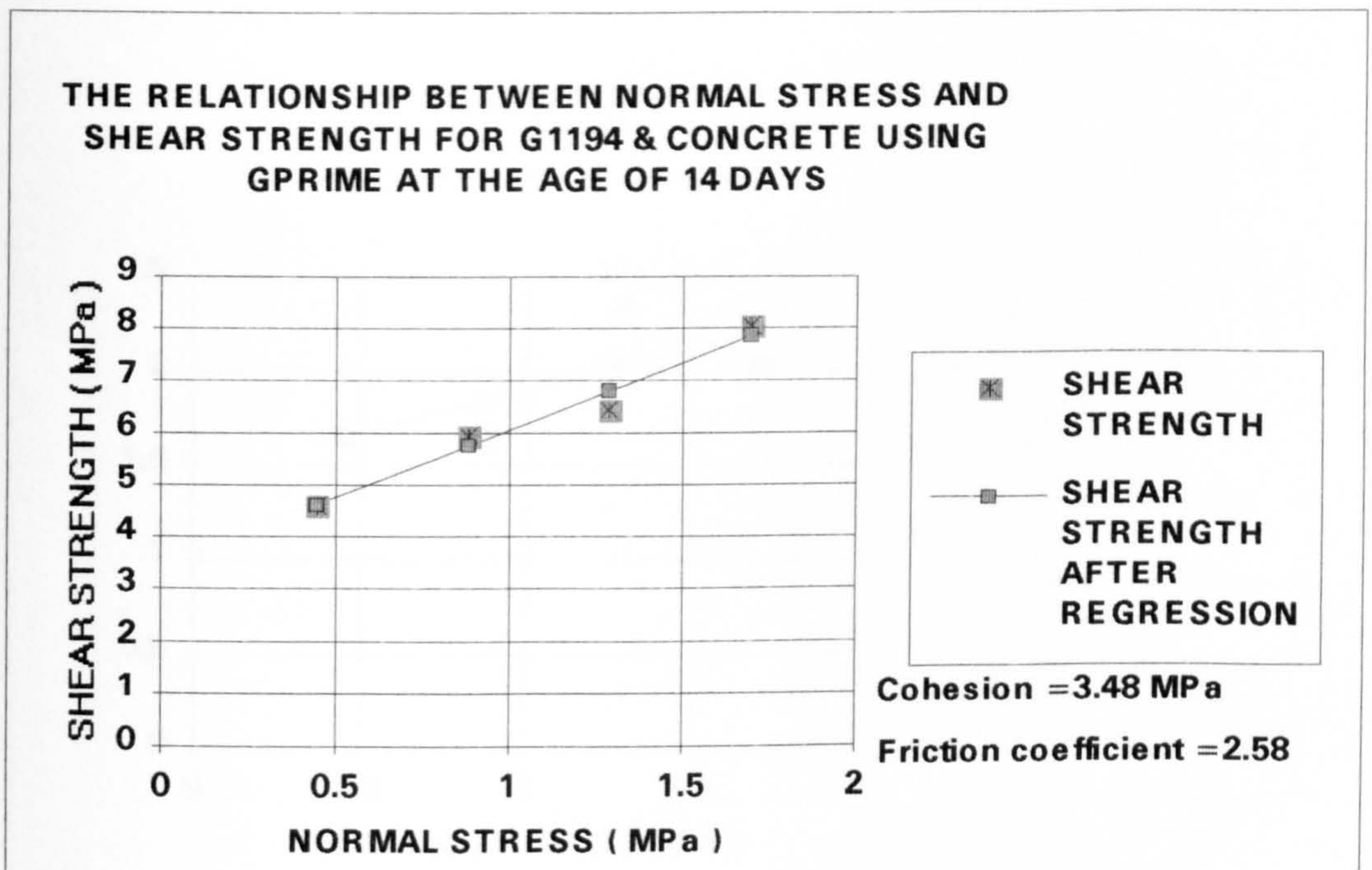

Figure 5-33: The relationship between normal stress and shear strength for G1194 & Concrete using Gprime at the age of 14 days

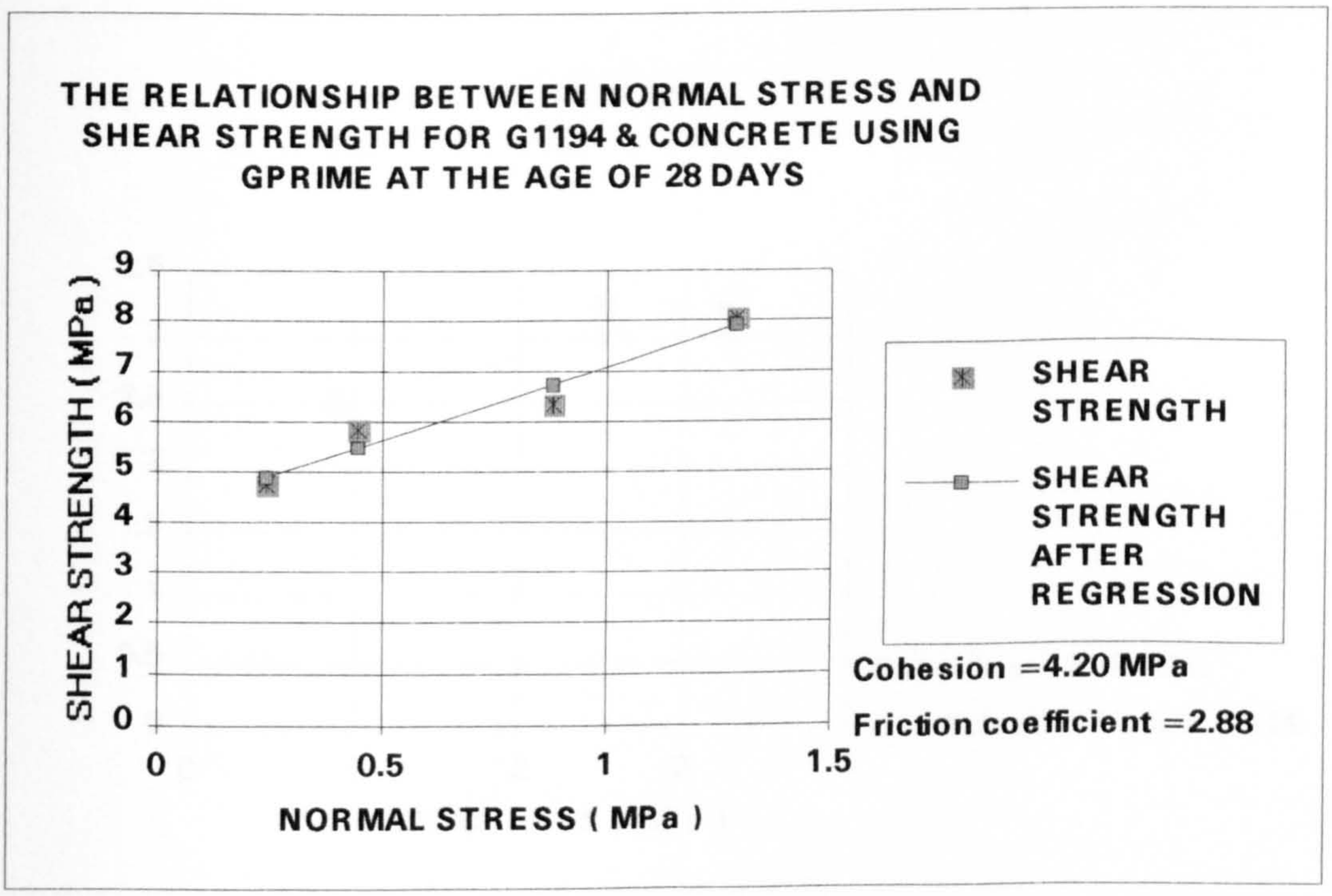

Figure 5-34: The relationship between normal stress and shear strength for G1194 & Concrete using Gprime at the age of 28 days

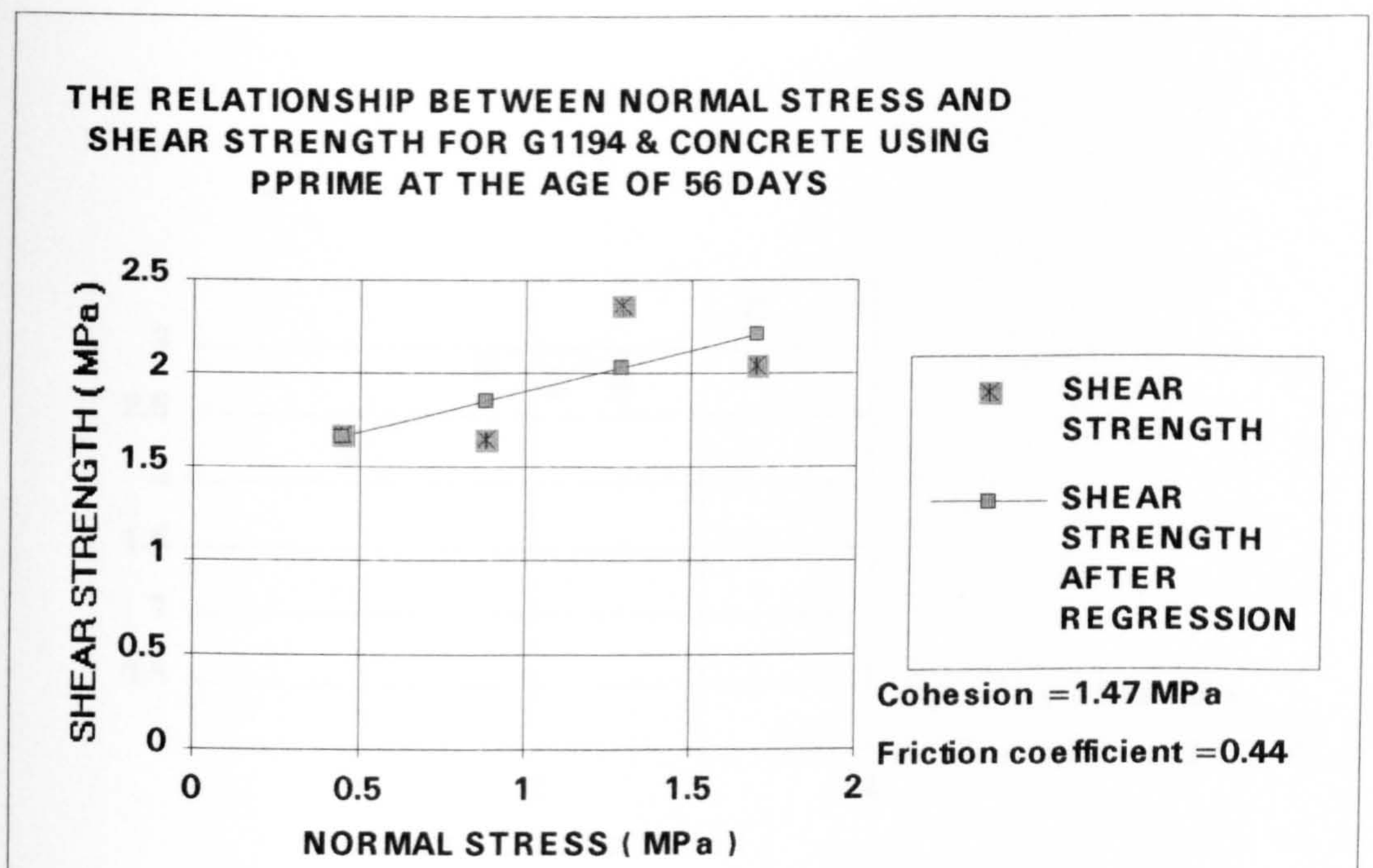

Figure 5-35: The relationship between normal stress and shear strength for G1194 & Concrete using Pprime at the age of 56 days

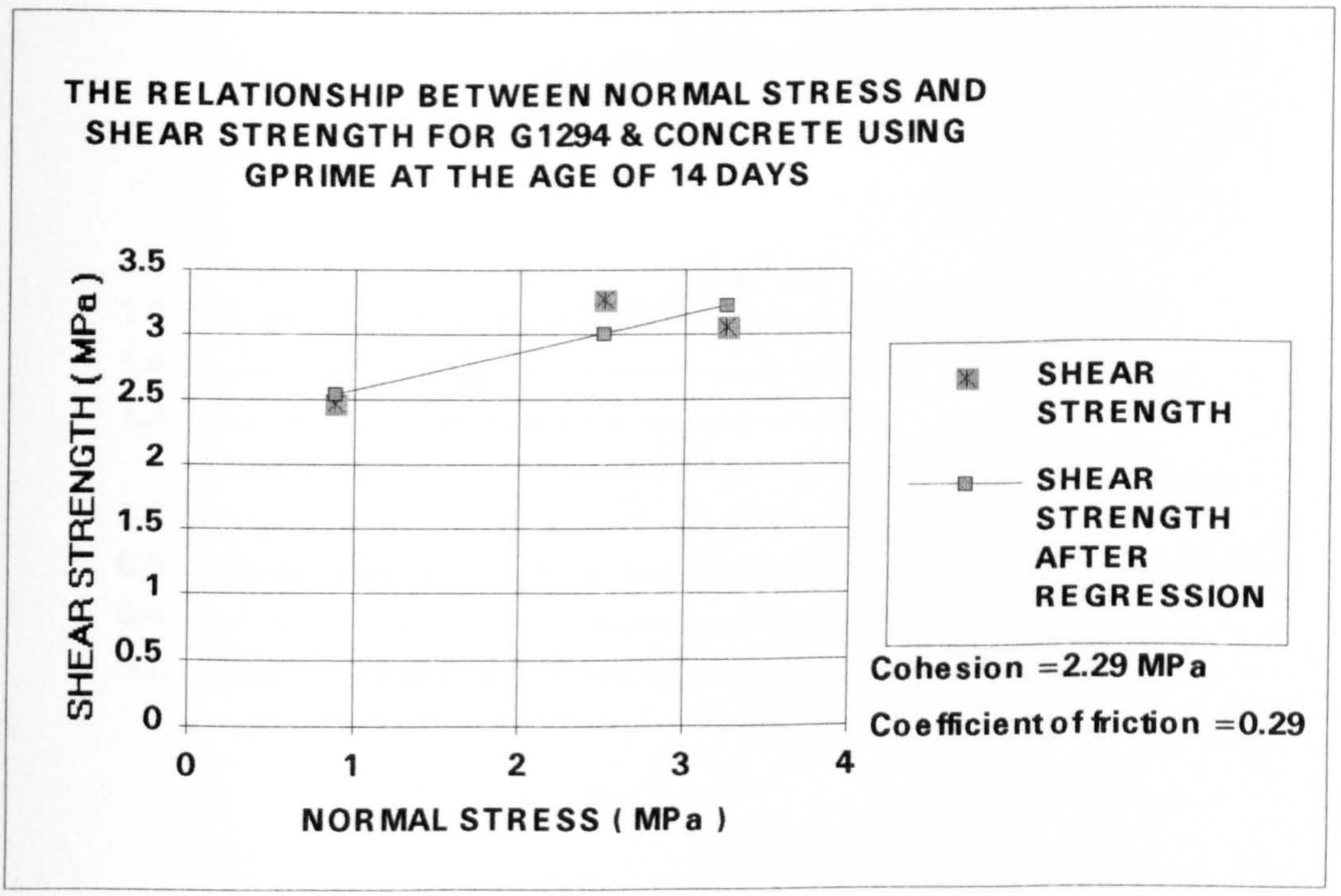

Figure 5-36: The relationship between normal stress and shear strength for G1294 & Concrete using Gprime at the age of 14 days

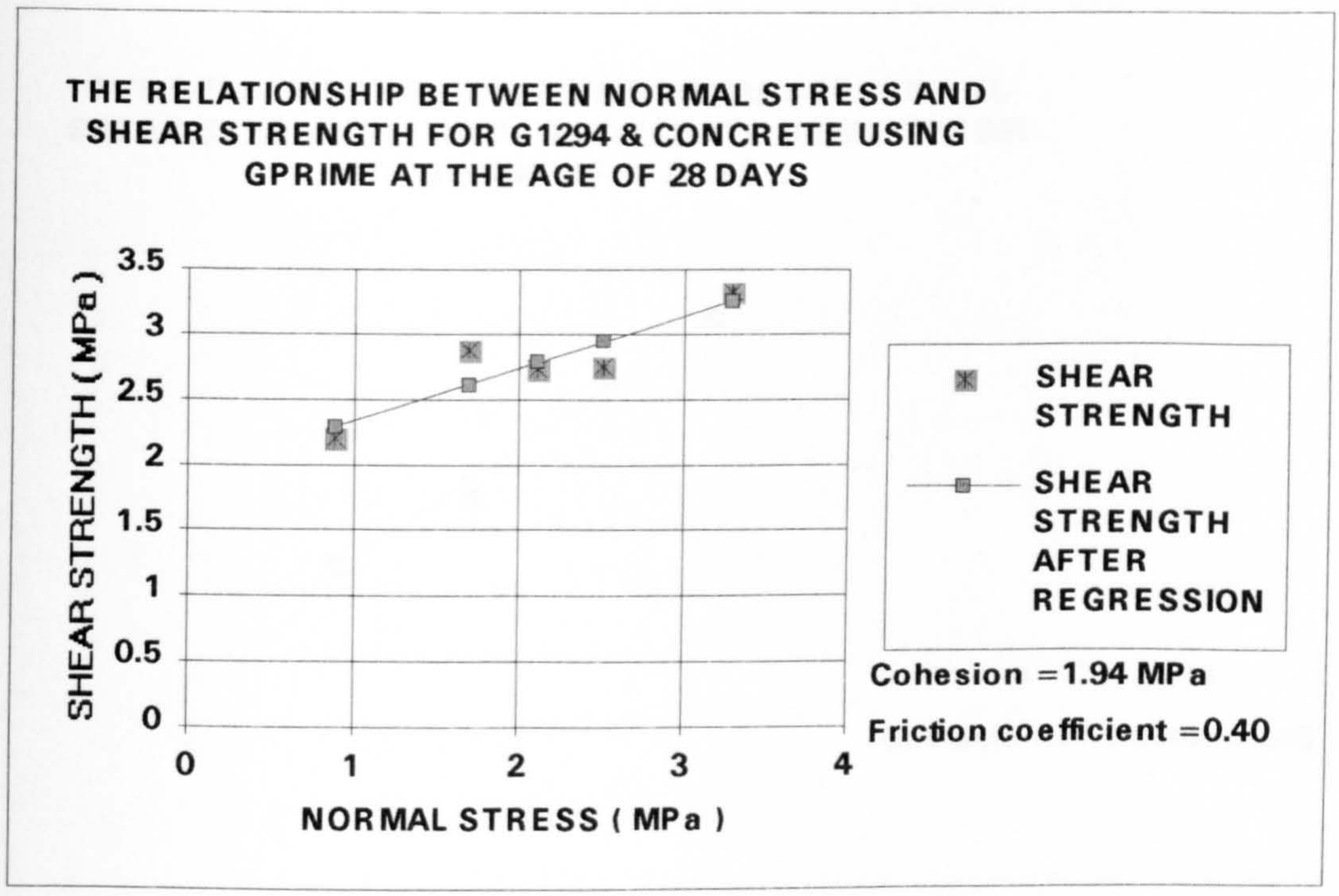

Figure 5-37: The relationship between normal stress and shear strength for G1294 & Concrete using Gprime at the age of 28 days

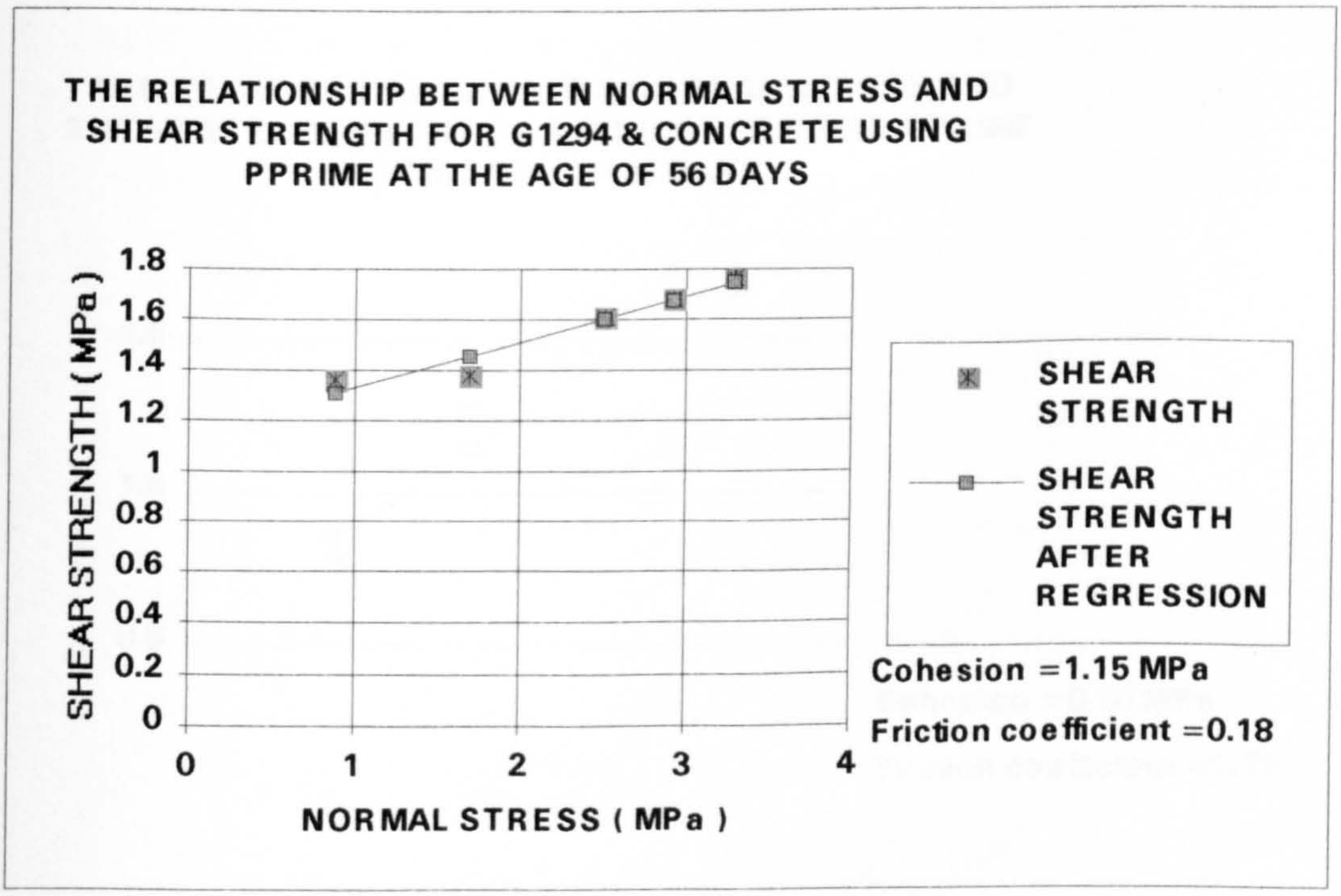

Figure 5-38: The relationship between normal stress and shear strength for G1294 & Concrete using Pprime at the age of 56 days

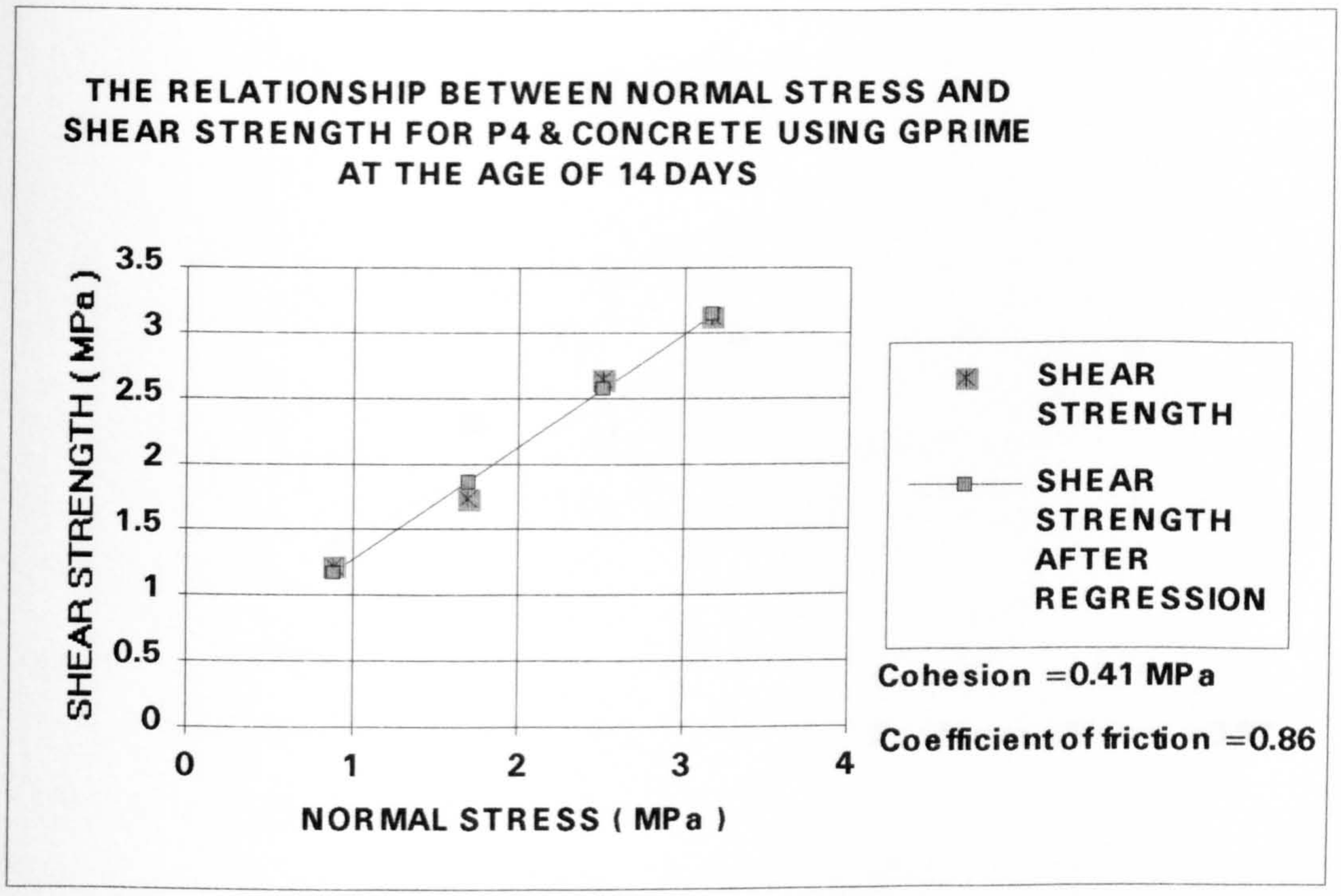

Figure 5-39: The relationship between normal stress and shear strength for P4 & Concrete using Gprime at the age of 14 days

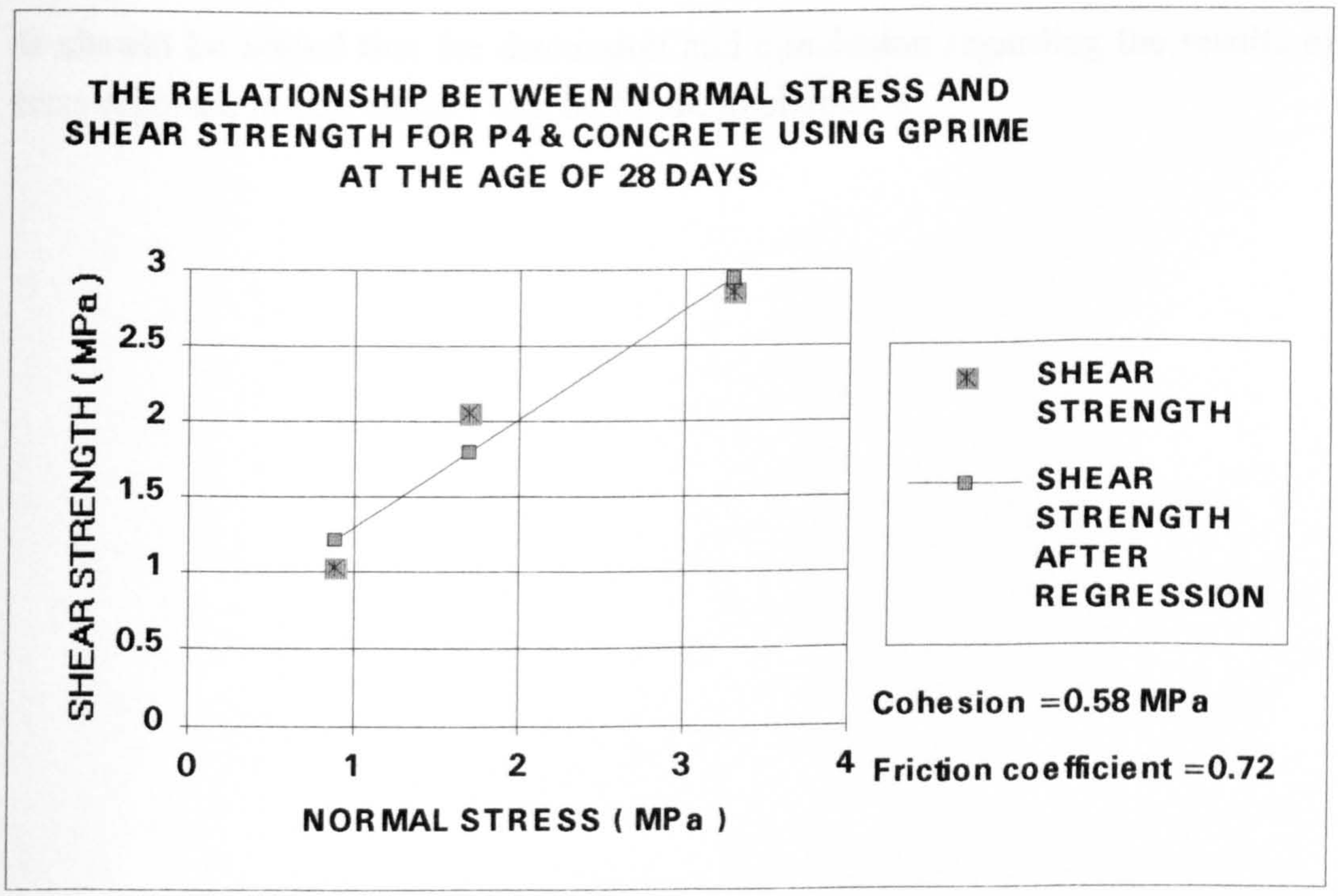

Figure 5-40: The relationship between normal stress and shear strength for P4 & Concrete using Gprime at the age of 28 days

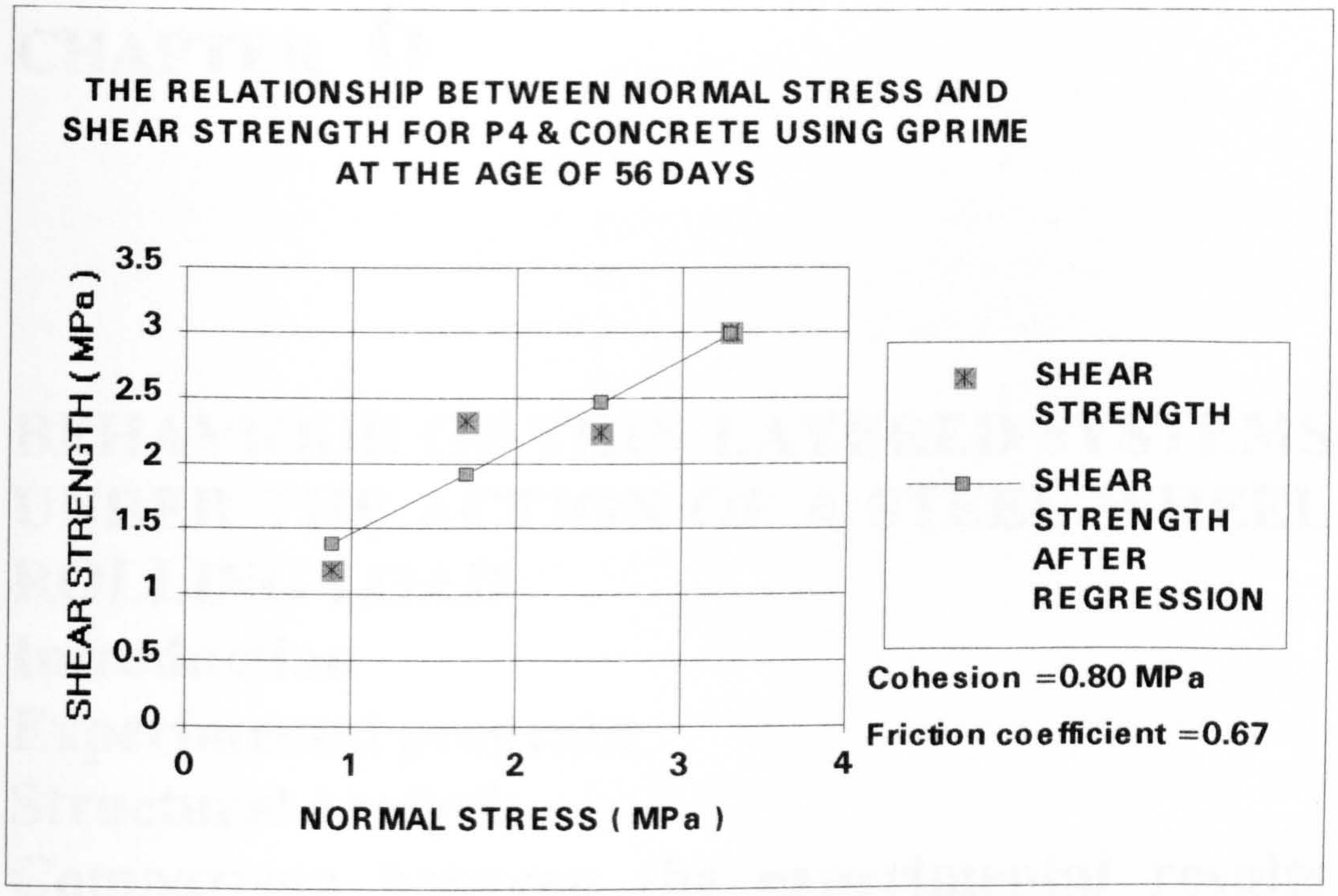

Figure 5-41: The relationship between normal stress and shear strength for P4 & Concrete using Gprime at the age of 56 days

It should be added that the discussion and conclusion regarding the results of tests reported in this chapter can be found in chapter 8.

CHAPTER 6

BEHAVIOUR OF THIN LAYERED SYSTEMS UNDER THE ACTION OF A STEEL WHEEL ROLLING LOAD

Introduction

Experimental program

Structural analysis

Comparison between the experimental results and theoretical analysis

Summary

6-1 Introduction

Industrial concrete floors, concrete floors of storage warehouses, superstores and hospitals may be protected or repaired by thin layered systems.
Each floor system, during its life of service, may be subjected to a number of different types of loads. These loads normally include uniformly distributed loads acting uniformly on relatively large areas like those resulted from general warehousing. The loads also include line loads which are uniform loads acting over extended lengths like partition walls, point loads or wheel loads, leg loads like raised storage platforms, horizontal loads which are generally resulted from mobile transporting and lifting equipment during braking and accelerating or cornering, thermal loads owing to thermal movements of the concrete floor and other loads like impact loads.
It is evident that most of these loads are taken into account by all standards for design purposes so that the concrete slab can resist the internal stresses arising from bending moments and shear forces. In other words, in a well designed concrete pavement, the slab will not completely fail under the action of these loads. However if the concrete substrate is to be protected or repaired by one or two layers of new materials, there may be another type of failure, namely delamination between two different subsequent layers. It could be said that the action of thermal loads and wheel loads are more important in this respect. Since work already carried out on the contribution of thermal movements to the delamination of composite systems is relatively considerable and moreover in indoor conditions these effects are not dominant, thermal stresses will not be considered in this research. By contrast, to the knowledge of the author, no one or at least very few people have tried to study the mechanism of delamination of a thin layered system under the action of a wheel load.
Vehicles used in most of factories or warehouses include fork - lift trucks and trolleys. In specific manufacturing process, special vehicles may be used. Loading areas are also designed to accommodate lorries and vans. [Plum, July 1990] Pallet transportation is a common way of mobile handling equipment in storage systems. Since the size of carrying wheels in these systems is small, load concentration can be very high. For example, for a polyurethane tyre, average contact pressure is about 9 MPa. [Concrete Society, Tech. Rep. No. 34] Clearly the use of steel wheels is a considerably worse case which may cause a delamination at an early age of the thin layered system.

The action of a rolling wheel load on the behaviour of a thin layered system will be investigated in this chapter and chapter 7. In this chapter the investigation is based on the use of a steel wheel load, whereas in the next chapter the behaviour of a thin layered under the action of pneumatic tyred vehicle wheel loads will be studied.

The objectives of this chapter may be summarised as follows:

- Introducing a test method for simulating the action of steel wheel load on a thin layered system.
- Examining some simple ways of detecting the possible delamination in the specimens.
- Structural analysis of the systems using the finite element method and the interface technique, based on the results of the material characteristics and interface bond strength tests reported in chapter 5.
- Comparing the results of the structural analysis and the experimental tests for different combinations of materials and at different ages and recognising the best combination which withstands a very heavy load up to 5000N.
- Introducing a constitutive model which is able to explain and predict the behaviour of the thin layered systems under the action of a steel wheel rolling load with particular interest in the delamination defect.

6-2 Experimental program

6-2-1 Materials

Materials used in the experimental program include concrete, polymer concrete, polymer cement concrete, and primer.

6-2-1-1 Concrete

Concrete was used as the substrate material in this experiment. As it will be explained later on in this chapter, two types of specimens were used in the Steel Wheel Rolling Load tests. The first group of the specimens were ready made and supplied by the manufacturer and unfortunately there was no information available regarding the properties of the concrete substrates. However the concrete slabs were strong enough to resist the load condition during the tests for most of the specimens. The second group of specimens were purpose made. The concrete substrate layers were of sizes 600 mm by

300 mm by 50 mm and were obtained from cutting precast slabs of longer sizes. These precast slabs were supplied by another manufacturer and their performance under the prescribed loading conditions during the tests was satisfactory. However as mentioned before in chapter 5, no accurate information regarding the strength and stress - strain relationship of the concrete under load was available. Therefore it was decided to carry out some compressive and modulus of elasticity tests on the hardened concrete and the corresponding results were tabulated in chapter 5.

6-2-1-2 P4 system (Polymer cement concrete)

As described in chapter 5, P4 system is a commercially available floor system identified by code ' P4 ' in this investigation. According to the manufacturer, P4 system consists of cementitious material and aggregates modified with polymers and flow agents. The main advantage of this material is that it is self levelling and smoothing and does not require trowelling. Other specifications of the P4 material have been given in chapter 5.

Polymer cement concrete, P4 system, was used in this experiment in two different ways. The main use of P4 system for the majority of the specimens was employing it as an intermediate layer on the concrete substrate and under one layer of polymer concrete systems, G1194 or G1294. Some specimens were also prepared and tested using P4 system as the final upper layer on the concrete substrate slabs.

6-2-1-3 G1194, G1294 (Polymer concrete)

As described in chapter 5, G1194 and G1294 are epoxy resin based floor topping systems identified by codes ' G1194 ' and ' G1294 ' respectively in this investigation. Both of the materials were also self levelling and smoothing and did not require trowelling. It should be mentioned that G1294 had not been approved to be supplied to the market at the time of tests. Other specifications of these materials can be found in chapter 5.

Polymer concrete systems, G1194 and G1294, were also used in this experiment in two different ways. For some specimens, G1194 or G1294 material was used as a thin protective layer on top of P4 system to increase the resistance of the layered system under the action of the very heavily concentrated load of the steel wheel in the Steel Wheel Rolling Load

experiment. For some other specimens, these materials were employed directly on concrete, without using P4 systems. Each combination was varied with the type of primer used at the interface.

6-2-1-4 Primers

Two types of primers were supplied by the manufacturer, Gprime and Pprime. Gprime and Pprime are priming systems identified by the codes given in this investigation. Gprime is a standard curing solvent free epoxy primer which has been recommended for all the resin products whereas Pprime is composed of acrylic copolymer and water and has been designed for P4 systems.
Although primers are generally to be applied at the interface of layered systems for improving the bond strength between different layers of materials, for the combination of P4 on concrete, the wrong primer, Gprime, was only used to provide the worst situation. For some combinations of layers of different materials, both of the primers were examined. (table 6-2-a)

6-2-2 Production of test specimens

6-2-2-1 Ready made specimens

Ready made specimens are those which were supplied by the manufacturer. (Figure 6-1) Materials used in these specimens included concrete as the substrate, P4 system, and G1194. The age of the specimens at the time of test was about 56 days. In these series of specimens different thicknesses of G1194 or P4 materials had been used. Although the material properties of the concrete substrate slabs of these specimens were not supplied, the performance of the specimens under the test conditions were more realistic because of the fact that they were manufactured specimens.
For all specimens the substrate concrete slabs were of sizes 450 mm by 220 mm by 40 mm. The thickness of P4 layer varied between 0 mm to 8 mm, while the thickness of G1194 layer varied between about 2 mm to 5 mm. The number of specimens and combinations of materials used in different layers are shown in table 6-1-a.

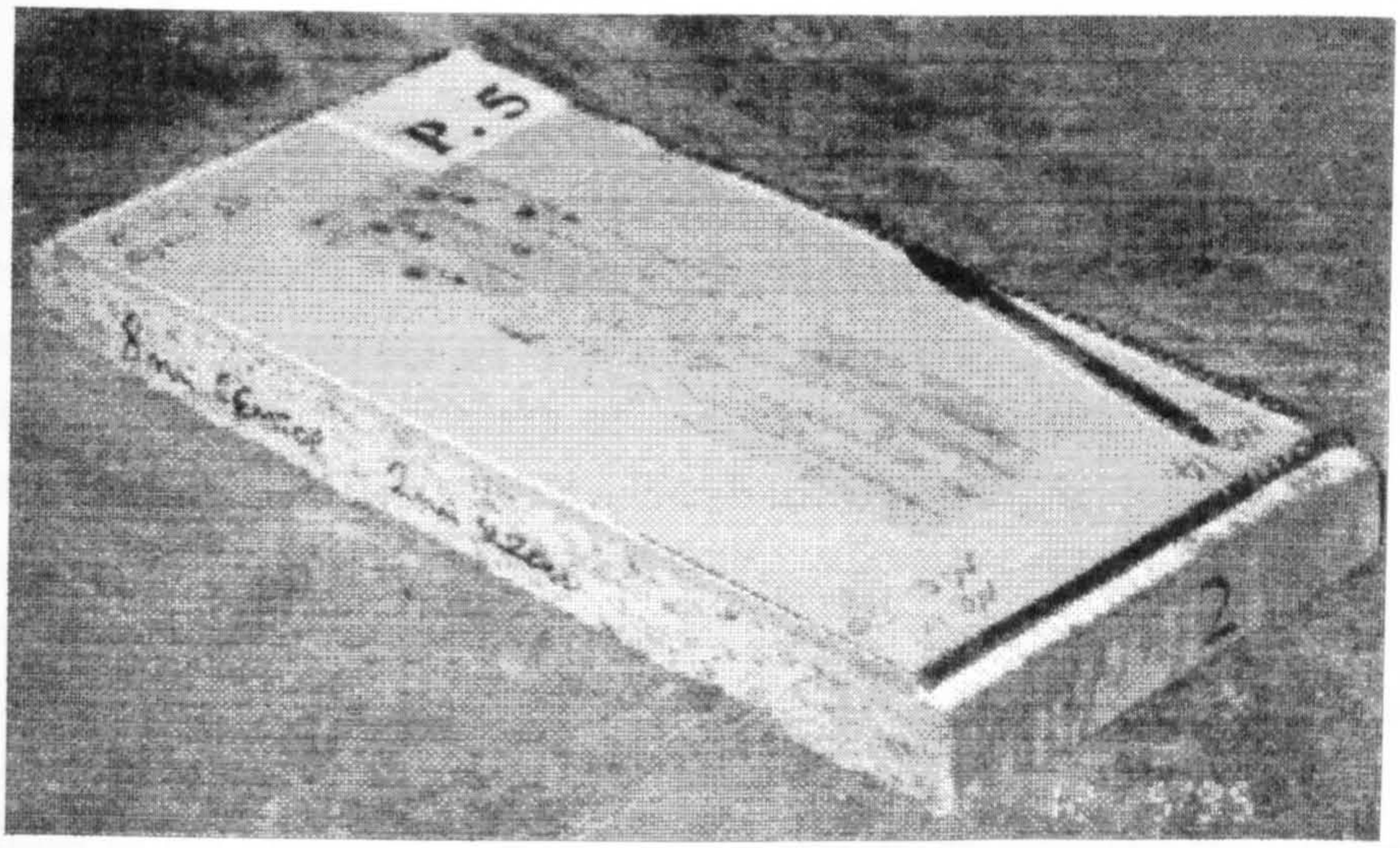

Figure 6-1: A sample of the ready made specimens

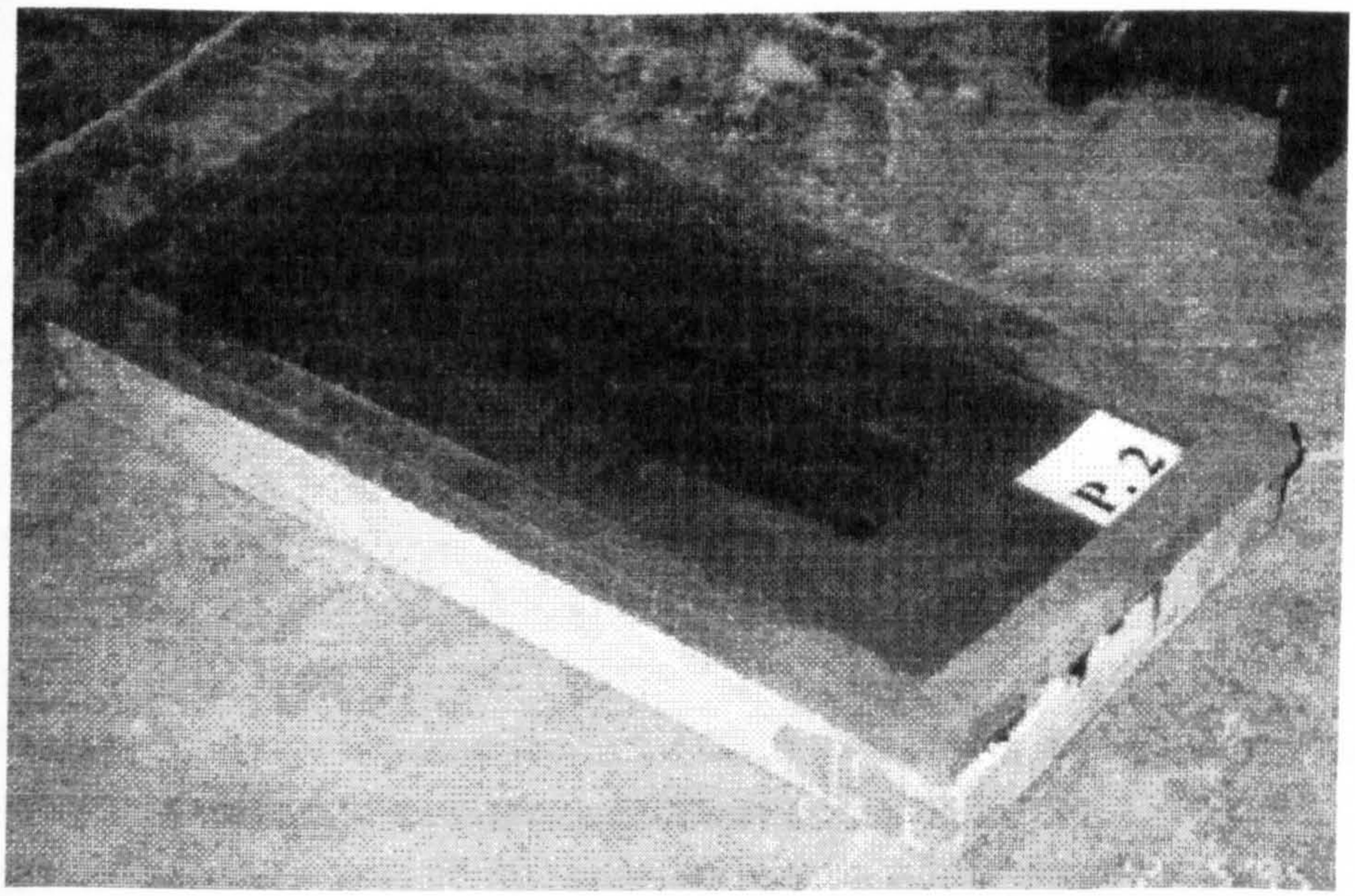

Figure 6-2: A sample of the purpose made specimens

6-2-2-2 Purpose made specimens

Although the ready made specimens showed the performances of some combinations of the layered systems, the main problem with them was the lack of information regarding the accurate mechanical properties of the constitutive materials for the purposes of a structural analysis. Moreover owing to the insufficient width and thickness of the concrete substrate slabs of the ready made specimens and consequently low bending strength, some of them were broken at a very early stage of test. For example most of the two layered systems could not resist the prescribed load and therefore were broken as the result of high tensile bending stresses at the bottom of the concrete substrate before giving any results.

In addition to the above reasons, it was necessary to examine the performance of the thin layered systems at different ages using both G1194 and G1294 materials.

As it was mentioned before, for the purpose made specimens the concrete substrate layers were of sizes 600 mm by 300 mm by 50 mm and were obtained from cutting precast concrete slabs of larger sizes. These precast slabs were supplied by another manufacturer and their performance under the prescribed loading condition during the tests was satisfactory.

6-2-2-2-1 Preparation of the purpose made specimens

There were totally five combinations of the four main materials (concrete, P4 system, G1194, and G1294) as follows: (table 6-2-a)

-G1194 material on top of a layer of P4 system on top of the concrete substrate, **G1194/P4/Concrete**. Gprime was used at the interface between the two layers of G1194 material and P4 system at different ages.

-G1294 material on top of a layer of P4 system on top of the concrete substrate, **G1294/P4/Concrete**. Gprime was used at the interface between the two layers of G1294 material and P4 system at different ages.

-G1194 material on top of the concrete substrate, **G1194/Concrete**. Two different types of primers were examined at the interface between the two layers of G1194 material and the concrete substrate at different ages.

-G1294 material on top of the concrete substrate, **G1294/Concrete**. Two different types of primers were examined at the interface between the two layers of G1294 material and the concrete substrate at different ages.

-P4 material on top of the concrete substrate, **P4/Concrete**, and only Gprime was used at the interface between the two layers of P4 system and the concrete substrate.

The ages at which the above tests have been carried out are tabulated in table 6-2. Two specimens have been tested at each specified age.

For the combination of P4/concrete and always between the two layers of P4 system and concrete substrate for all other combinations, only one primer was used, i.e. Gprime. For other interfaces of materials between two subsequent layers both of the primers, Gprime and Pprime, were examined.

In order to remove any dirt, dust or loose materials before the application of any type of the materials on top of the concrete substrate slabs or P4 layers, their surfaces were brushed using a wire brush and then well cleaned. After cleaning the surface of the lower layer, it was primed using the desired type of primer. Gprime was a two pack product and Pprime was a one pack one. The primers were prepared according to the manufacturer instructions and then applied to the surface of the lower layer using a stiff brush. The curing period for the Gprime was about 18 hours and for the Pprime was about one hour. In both cases the primers were allowed to dry before the application of the next layer.

After curing the applied primer, the components of the desired type of material were carefully weighed, mixed and applied on the previous layer according to the manufacturer's instructions. (Figure 6-2)

For the combinations of G1194/P4/Concrete and G1294/P4/Concrete, the P4 layer had to be cured for 14 days before applying the next flooring material on top of it. All materials were prepared, cured and tested in indoor conditions. The number of specimens and combinations of materials used in different layers are shown in table 6-2-a.

6-2-3 Steel Wheel Rolling Load Test

6-2-3-1 Test apparatus and equipment

6-2-3-1-1 Steel Wheel Rolling Load Test Rig

Owing to the lack of any standard test for the performance of a thin layered system under the action of a heavy rolling load, a Rolling Load Rig was developed at the Civil Engineering Department of the University of Newcastle Upon Tyne. It has been designed to simulate the action of a fork - lift truck tyre or a trolley wheel like those which are usually in use in the industrial floors or warehousing. (figure 6-3-a)

The test apparatus consists of a loaded wheel and a moving reciprocating table of size 600 mm by 500 mm on which the test specimens are placed. (figure 6-3-b) The wheel load can vary up to a maximum of 10 kN by adjusting the pressure value applied through a hydraulic pressure system. Figure 6-4 Shows the relationship between the oil pressure and the applied load. In this experiment the maximum value of the applied load was 5 kN.

The time taken for each cycle is also adjustable and on its average the wheel will travel at the speed of about 4.5 m/min. On operation, the wheel travels on a straight path of 310 mm long in each half cycle.

For the counting of cycles, the system is equipped with a lap counter.

6-2-3-1-2 The PUNDIT

As will be described later in this chapter, three different ways were used for detecting the possible delamination between the upper two layers in each Rolling Load test specimen:

- The ultrasonic pulse velocity method
- Tapping the surface of the upper layer using a piece of steel bar
- Breaking the specimen in two parts in some cases for verifying the results of the other two methods

As it is understood the latter two methods are very simple and do not require further explanation. The first method is also simple to carry out, however it would be worthwhile if the basis of this method is discussed in more details.

The ultrasonic pulse velocity method is carried out by measuring the travelling time of an ultrasonic pulse passing through the specimen to be examined.

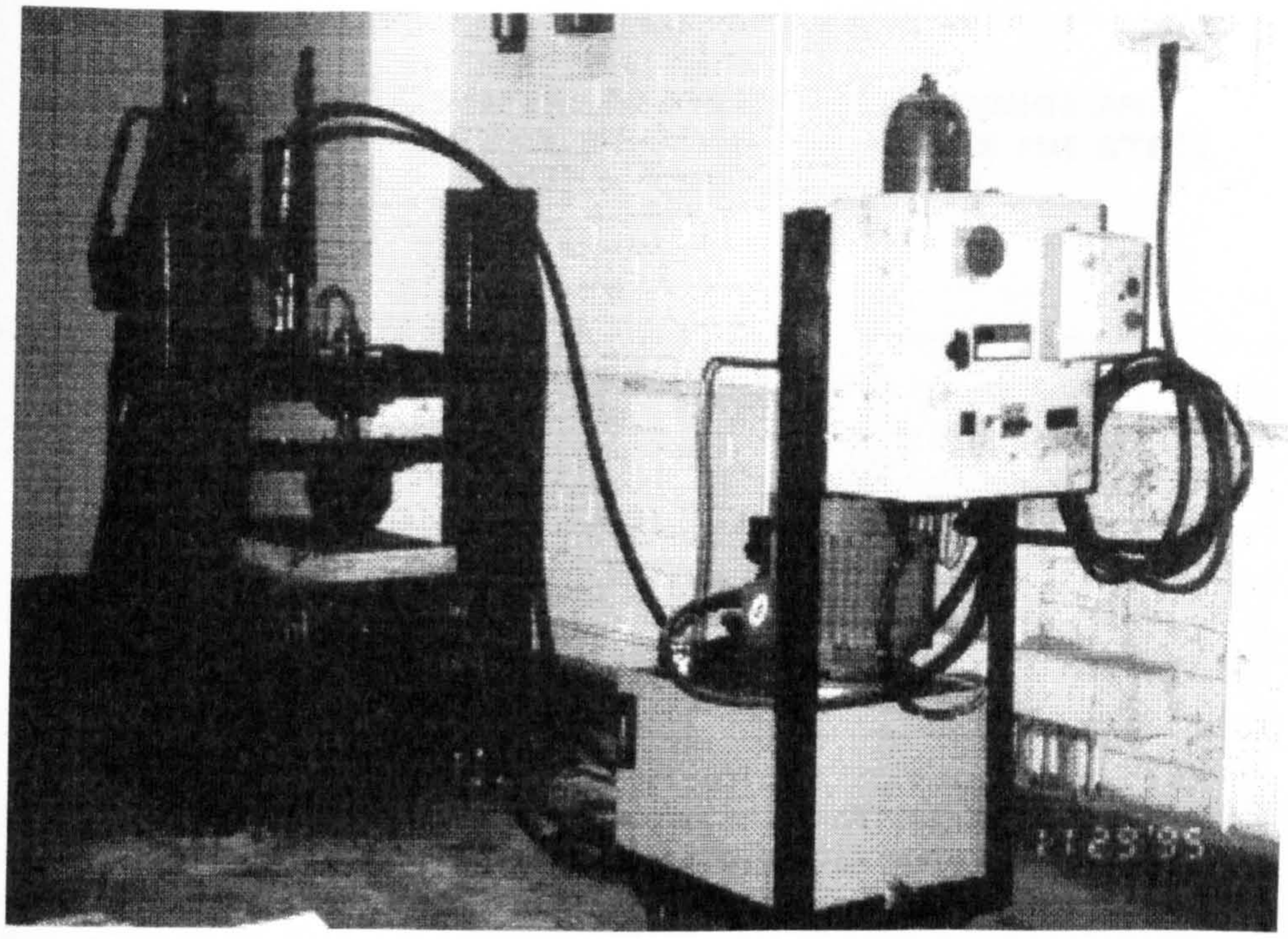

Figure 6-3-a: The Steel Wheel Rolling Load Rig

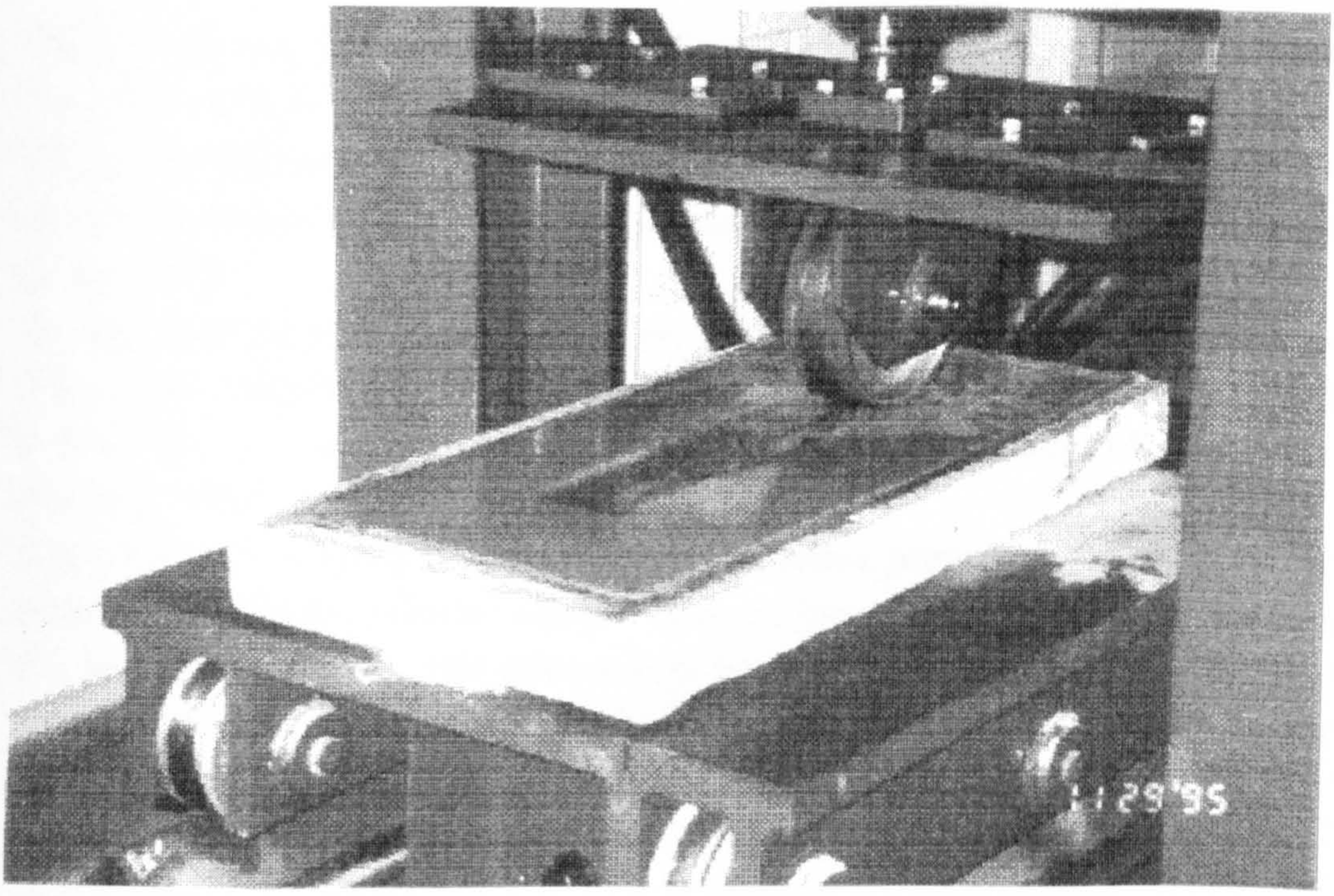

Figure 6-3-b: The reciprocating table and the steel wheel of the Rig

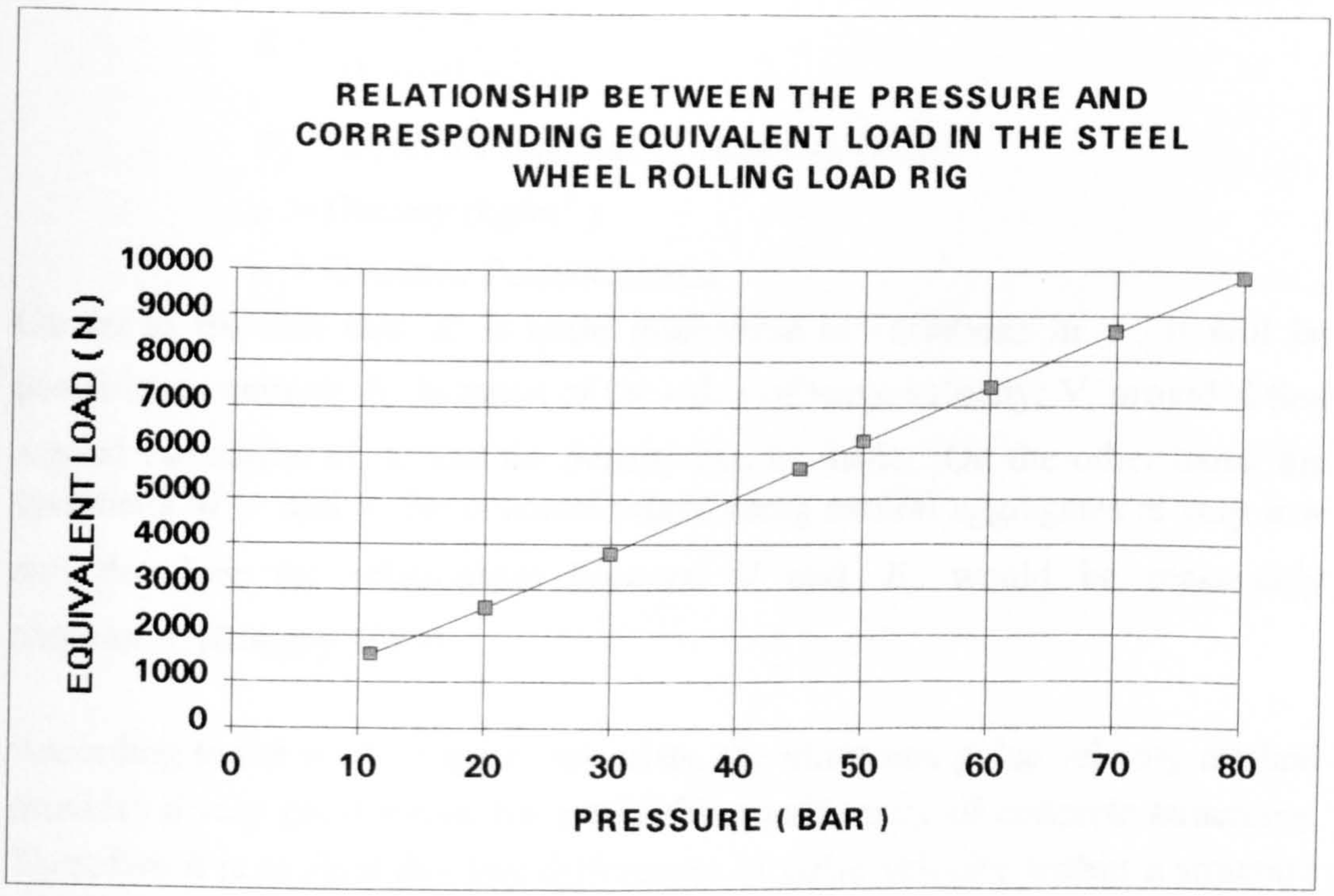

Figure 6-4: The relationship between the applied pressure and equivalent load in the Steel Wheel Rolling Load Rig

The first uses of this method dates to the mid 1940s in the USA. The fact that the pulse velocity depended primarily on the elastic modulus of the material, led the investigators in France, Canada, and the UK to develop equipment using electro - acoustic transducers for the measurement of the pulse velocity through the concrete.

Among three types of waves which are generated by an impulse applied to a solid mass, longitudinal waves (compression waves), are the most important and electro - acoustical transducers produce waves mainly of this type. [Bungey 1989]

Since the wave velocity is dependent on the elastic properties and mass of the material, if the wave velocity and the mass are known, it is possible to estimate the elastic properties. The relationship between the compression wave and modulus of elasticity for an infinite, homogeneous and isotropic elastic medium can be found using equation 6-1. [Bungey 1989]

$$V = \sqrt{\frac{K.E_d}{\rho}} \qquad (6\text{-}1)$$

Where: V = Compression wave velocity (km/s)

$$K = \frac{(1-v)}{(1+v)(1-2v)}$$

E_d = Dynamic modulus of elasticity (GPa)

ρ = Density (kg/m^3)

v = Dynamic Poisson's ratio

Owing to the fact that K is quite insensitive to variations in v, it will be possible to compute E_d in terms of the value of wave velocity, V, provided that a good estimation of K and the density can be made. On the other hand, the variations of v and ρ for concrete mixes using natural aggregates is very low and therefore the relationship between V and E_d would be reasonably consistent. [Bungey 1989]

According to the work of many scientists, the ultrasonic pulse velocity method provides a very good means for establishing uniformity of concrete structures. Therefore it is evident that any differences in pulse velocity within a structure for no acceptable reason could be a sign of discontinuity in that part of the structure. [Malhotra 1976] This was the basis for using this method for detecting any possible delamination in a thin layered system under the action of a steel wheel rolling load.

The testing apparatus used in this investigation was the PUNDIT, Portable Ultrasonic Nondestructive Digital Indicating Tester. The instrument weighs only 3.2 kg and is 180 mm by 110 mm by 160 mm. It consists of a pulse generator and a pulse receiver. (figure 6-5)

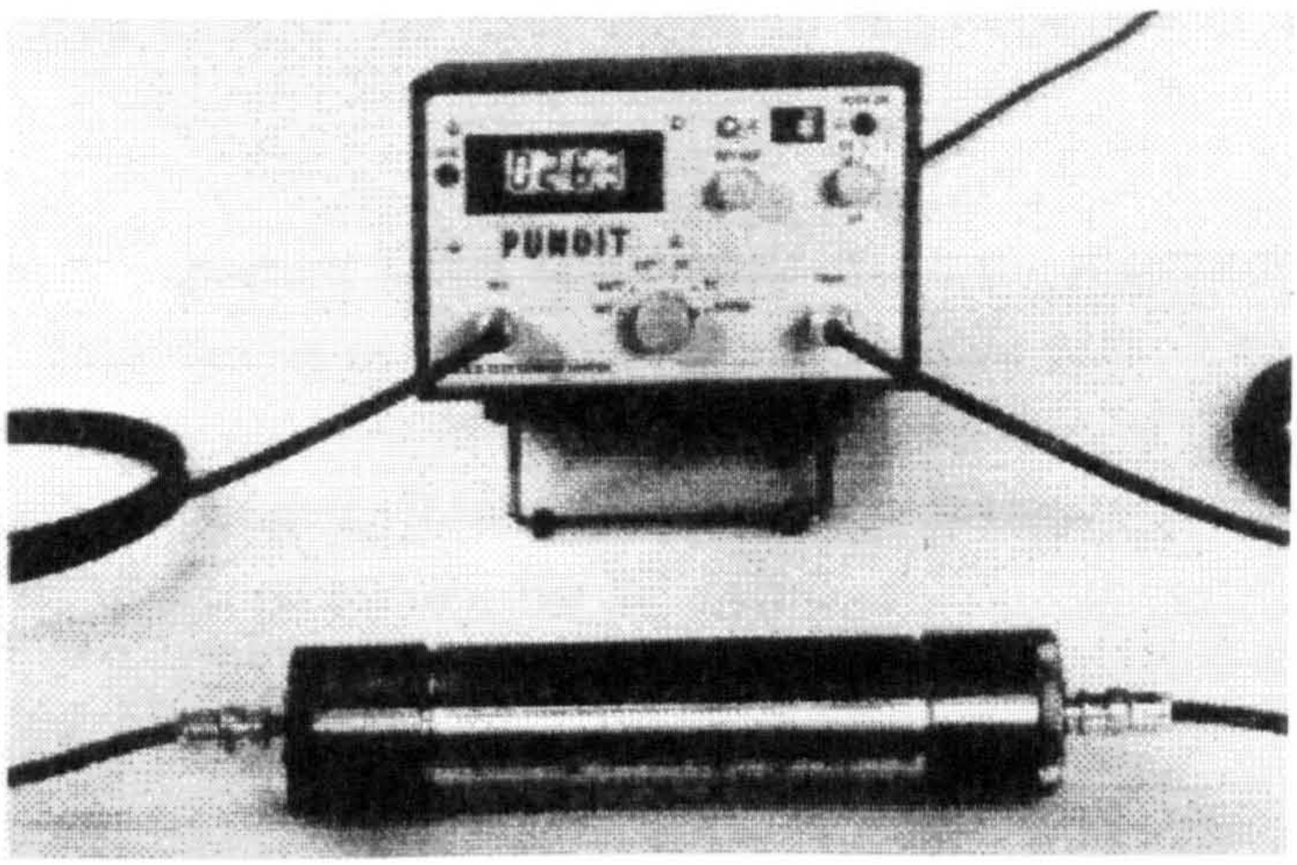

Figure 6-5: The PUNDIT [Bungey 1989]

The pulses are produced by shock - exciting piezoelectric crystals. Similar crystals are used in the receiver. The time taken for the ultrasonic pulse travelling through the specimen is measured by electronic measuring circuits. The resonant frequency of the transducers used with the PUNDIT is 50 kHz and can be used to test concrete specimens ranging up to about 22.7 m. The time for the pulse to travel between the two transducers is measured and displayed on a digital read out unit, by placing the transducers on opposite faces of the specimen.
The PUNDIT is incorporated with a nickel cadmium battery in the unit itself, which provides power for at least five hours use without requiring recharge.

Three ways may be used for measuring the transmit times, direct, semidirect, and indirect transmission method: [Malhotra 1976]
- Direct transmission method:
In this method the transducers are held on the opposite sides of the specimens, and therefore the best results may be obtained. (figure 6-6-a)
- Semidirect transmission method:
As it is seen in figure 6-6-b, this method may be appropriate where the first method is not possible. It is evident that this method will be less accurate that the direct method.
- Indirect transmission method:
In this method the pulse transmission along the surface of the mass is measured. Hence this method is used when only one surface of the structure is accessible. Obviously this method will result in the least accuracy among the three, because of the energy of the pulse is directed into the concrete. Moreover, in this method the path length of the pulse is not well defined. (figure 6-6-c)

Perhaps the most important factor which may affect the measurement of pulse velocity is the smoothness of the contact surface under test. This is related to the need for a good acoustical contact between the surface of the specimen and the face of each transducer. [Malhotra 1976] In the current investigation an appropriate jelly was used to improve the situation.

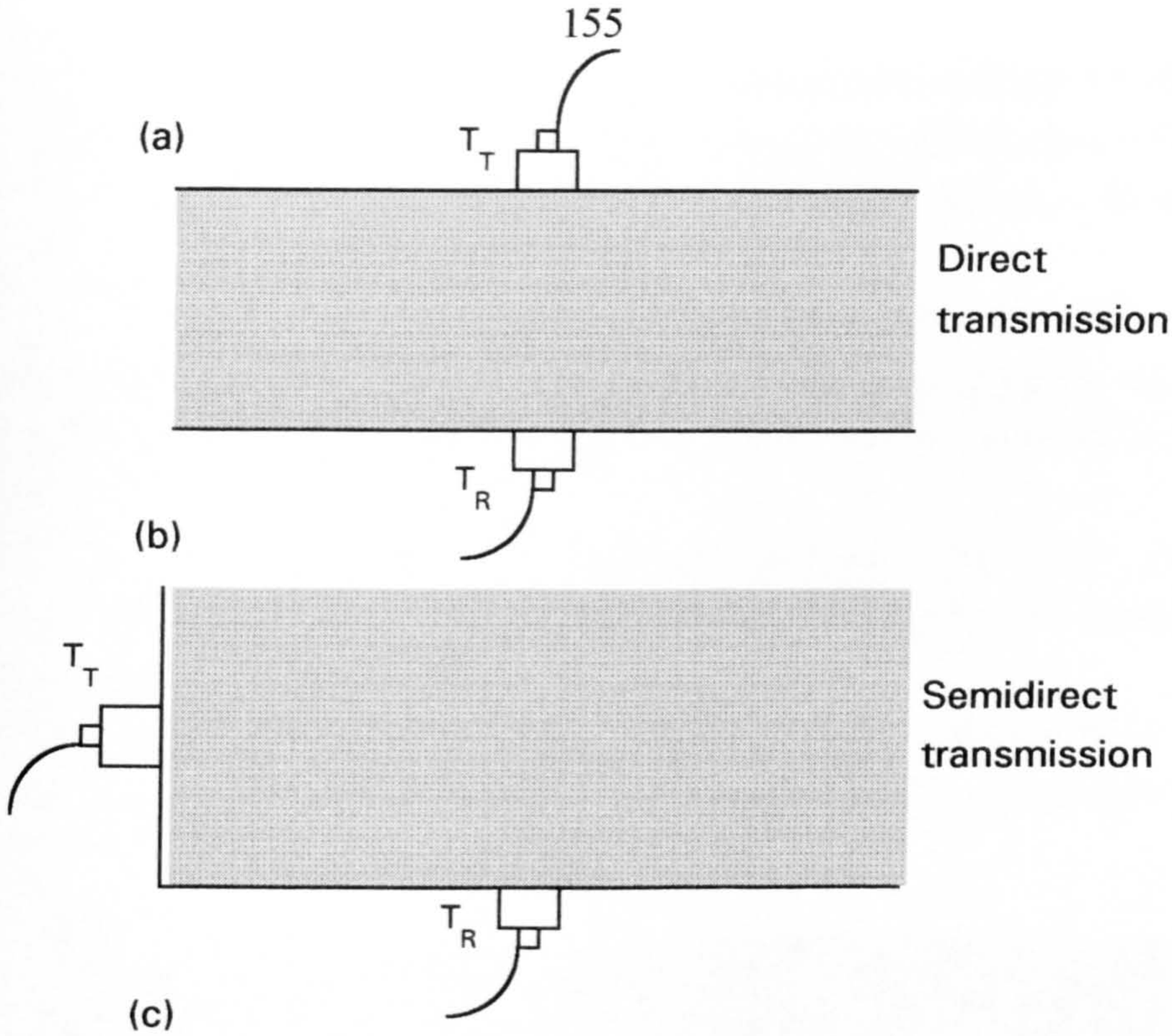

Figure 6-6: Tree methods of measuring the transmission time through a specimen: a: Direct transmission method b: Semidirect transmission method c: Surface transmission method [Malhotra 1976]

6-2-3-2 Test procedure

The aim of this test was to simulate the actual loading condition resulting from a free rolling steel wheel on a thin layered system, and to investigate the effect of this kind of load on the bond strength between the two upper layers which were immediately subjected to the load. In other words it was to be examined whether a free rolling load could cause a delamination at the interface of a thin layered system.

In this experiment, a constant rolling load of 3750 N was used for combinations G1194/P4/Concrete and G1294/P4/Concrete, while a 5000 N rolling load was used for other combinations. The steel wheel was made of cast iron with diameter and width of 150 mm and 45 mm respectively.

Sounding of the specimen surface was done manually by striking it with a steel rod. In a delaminated case, the upper layer would echo with a thud. [Van Dam et al. 1987] This seems to be as a result of loss of bond strength at the defected zone.

In the pulse velocity method, the pulse transmission time between the two transducers was measured and recorded before and after applying the load, a comparison between these two values may show the bond condition at the interface.

The third method was only used when the specimen was to be examined visually. This was done only for few specimens for verifying the results of the other two methods. (figure 6-7)

It is therefore concluded that the first two methods were used for all specimens while the third method was used for only few specimens for visualising any possible delamination.

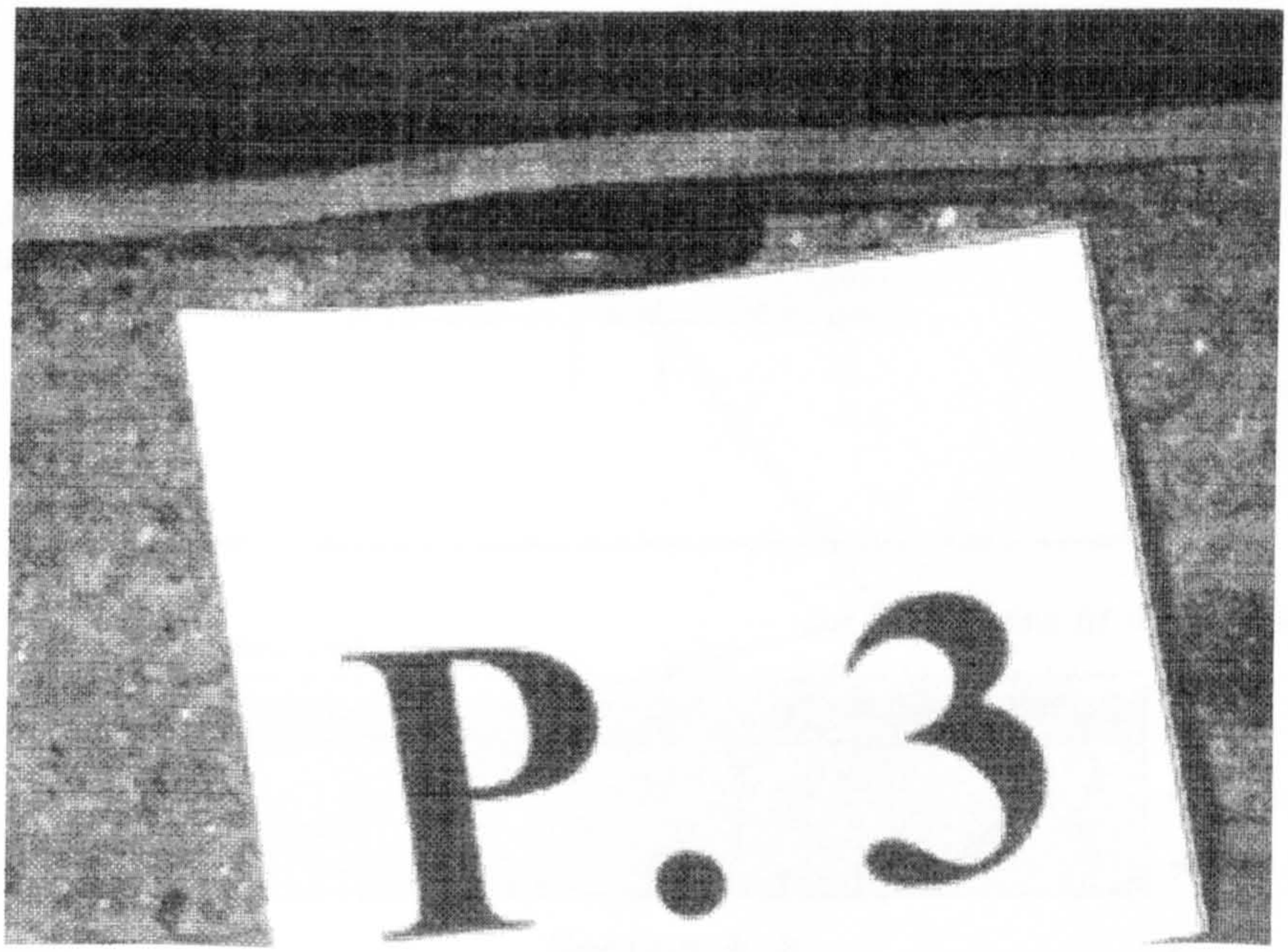

Figure 6-7: Visualising the delamination between G1294 and the concrete substrate by breaking the specimen into two parts

In order to facilitate the detecting of any possible delamination and at the same time to produce the worst loading condition, it was decided to apply the steel wheel rolling load on at least five adjacent paths on the specimen surface, with the same number of cycles in each path. In other words the width of the loading area became wider and this made possible to use transducers of diameter 50 mm for examining the interface bond in the pulse velocity method.

Before carrying out the rolling load test, the locations of the transducers onto the upper and lower surfaces of each specimens were to be determined. These locations were exactly in the center of the two upper and lower surfaces of the specimens, as the direct transmission method was to be used. (figure 6-8)
The initial pulse transmission time between the specified locations was measured and recorded for each specimen before test. After applying the desired number of rolling load cycles on the specimen, the specimen was examined using both the sounding method by tapping the surface and the pulse velocity method by recording and comparing the pulse transmission time between the specified points before and after the test. The procedure was to be continued until the end of the test.

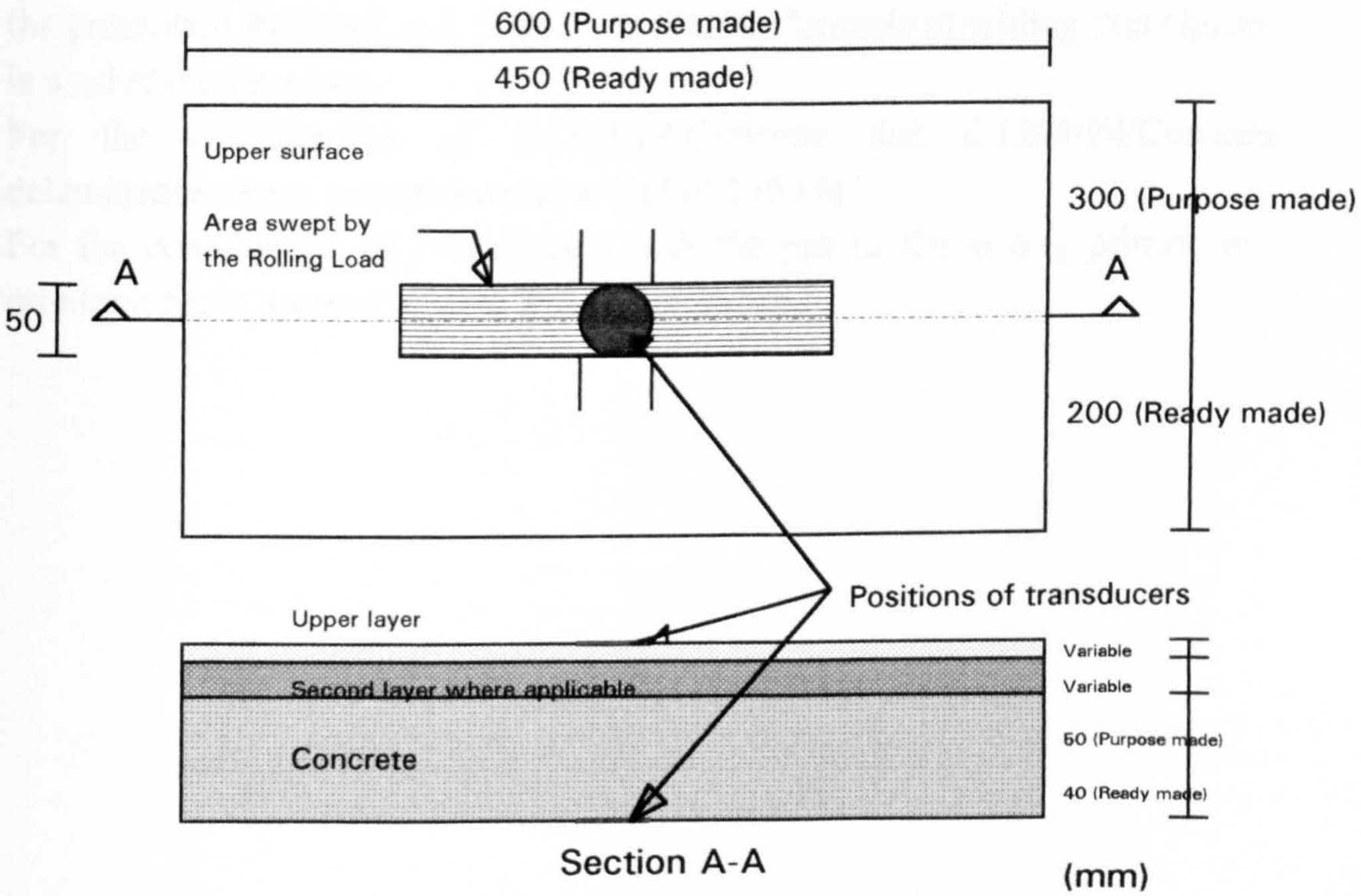

Figure 6-8: Schematic of the specimens in the Steel Wheel Rolling Load experiment

The number of the rolling load cycles to be applied on the specimens was different from one combination of materials to another. For some combinations of materials, e.g. G1194/P4/Concrete or G1294/P4/Concrete, the delamination occurred after applying a very low number of the rolling load cycles. In these circumstances, the final reading of the pulse transmission time was recorded

after debonding of the upper layer and then, the test for that specimen was to be terminated. For other specimens, the measurement of pulse transmission times was made at every 50 cycles until 200 cycles.

6-2-3-3 Test results:

The results of tests for the ready made and purpose made specimens have been tabulated in tables 6-1-b and 6-2-b respectively. The results include the performance of each combination of thin layered systems under the test, the normal change in the pulse transmission time, and the successful ways of the inspection for evaluating the layered system based on the corresponding experiment.

As it can be seen from the results, the only combination which can withstand the prescribed Rolling Load, 5000 N, is G1194/Concrete providing that Gprime is used at the interface.

For the combinations of G1194/P4/Concrete and G1294/P4/Concrete delaminations have occurred under a load of 3750 N.

For the combination of P4/Concrete with the use of the wrong primer, two problems arose, excessive wear and delamination.

Table 6-1-a: Details of the ready made specimens for the **Steel Wheel Rolling Load tests**

Specimen Number	Planar Dimensions (mm)	Concrete Thickness (mm)	P4 system Thickness (mm)	G1194 Thickness (mm)
No. 1	450-220	40	0	2-3
No. 2	450-220	40	0	2-3
No. 3	450-220	40	3	0
No. 4	450-220	40	3	0
No. 5	450-220	40	3	1.5-2
No. 6	450-220	40	3	1.5-2
No. 7	450-220	40	3	2-3
No. 8	450-220	40	3	2-3
No. 9	450-220	40	3	2.5-3
No. 10	450-220	40	3	2.5-3
No. 11	450-220	40	3	4.5-5
No. 12	450-220	40	3	4.5-5
No. 13	450-220	40	8	2
No. 14	450-220	40	8	2
No. 15	450-220	40	8	3
No. 16	450-220	40	8	3
No. 17	450-220	40	8	5
No. 18	450-220	40	8	5

Table 6-1-b: Results of the **Rolling Steel Wheel Test** on the ready made specimens supplies by the manufacturer

Specimen Number	Result of Test	Change in the pulse transmission time (μ sec.)	Successful ways of inspection
No. 1	Broken soon [1]	-	-
No. 2	**No Delamination** [2]	0.4	3 ways
No. 3	Broken soon [1]	-	-
No. 4	Broken soon [1]	-	-
No. 5	***Delamination*** [3]	1.4	3 ways
No. 6	***Delamination*** [3]	1.4	3 ways
No. 7	***Delamination*** [3]	1.5	3 ways
No. 8	***Delamination*** [3]	1.3	3 ways
No. 9	***Delamination*** [3]	1.6	3 ways
No. 10	***Delamination*** [3]	1.4	3 ways
No. 11	***Delamination*** [3]	1.2	3 ways
No. 12	***Delamination*** [3]	1.5	3 ways
No. 13	***Delamination*** [3]	1.6	3 ways
No. 14	***Delamination*** [3]	1.5	3 ways
No. 15	***Delamination*** [3]	1.3	3 ways
No. 16	***Delamination*** [3]	1.2	3 ways
No. 17	***Delamination*** [3]	1.5	3 ways
No. 18	***Delamination*** [3]	1.4	3 ways

1- Broken at less than 10 cycles.
2- Broken at about 60 cycles.
3- Delamination between the two upper layers at less than 10 cycles.

Table 6-2-a: Details of the purpose made specimens for the **Steel Wheel Rolling Load tests**

Specim. No.	Age (days)	Plan Dim. (mm)	Concrete Thick. (mm)	P4 Thickn. (mm)	Primer before coating	Coating Thick. (mm)	Coating Material Type
No. 1	28	600-300	50	10	Gprime	3	G1194
No. 1	28	600-300	50	10	Gprime	3	G1194
No. 3	28	600-300	50	10	Gprime	3	G1294
No. 4	28	600-300	50	10	Gprime	3	G1294
No. 5	14	600-300	50	0	Gprime	3	G1194
No. 6	14	600-300	50	0	Gprime	3	G1194
No. 7	14	600-300	50	0	Gprime	3	G1294
No. 8	14	600-300	50	0	Gprime	3	G1294
No. 9	28	600-300	50	0	Gprime	3	G1194
No. 10	28	600-300	50	0	Gprime	3	G1194
No. 11	28	600-300	50	0	Gprime	3	G1294
No. 12	28	600-300	50	0	Gprime	3	G1294
No. 13	56	600-300	50	0	Pprime	3	G1194
No. 14	56	600-300	50	0	Pprime	3	G1194
No. 15	56	600-300	50	0	Pprime	3	G1294
No. 16	56	600-300	50	0	Pprime	3	G1294
No. 17	28	600-300	50	0	Gprime	4	P4
No. 18	28	600-300	50	0	Gprime	4	P4

Table 6-2-b: Results of the **Rolling Steel Wheel Test** on the purpose made specimens at the University of Newcastle Upon Tyne

Specimen Number	Result of Test	Change in the pulse transmission time (μ sec.)	Successful ways of inspection
No. 1	***Delamination*** [1]	1.2	3 ways
No. 2	***Delamination*** [1]	1.5	3 ways
No. 3	***Delamination*** [1]	1.1	3 ways
No. 4	***Delamination*** [1]	1.3	3 ways
No. 5	**No Delamination** [2]	0.0	3 ways
No. 6	**No Delamination** [2]	0.1	3 ways
No. 7	***Delamination*** [3]	1.0	3 ways
No. 8	***Delamination*** [3]	1.2	3 ways
No. 9	**No Delamination** [2]	0.0	3 ways
No. 10	**No Delamination** [2]	0.0	3 ways
No. 11	***Delamination*** [3]	1.1	3 ways
No. 12	***Delamination*** [3]	1.2	3 ways
No. 13	***Delamination*** [4]	0.6	Breaking
No. 14	***Delamination*** [4]	0.5	Breaking
No. 15	***Delamination*** [3]	1.0	3 ways
No. 16	***Delamination*** [3]	1.1	3 ways
No. 17	***Delamination*** [5]	0.7	Breaking
No. 18	***Delamination*** [5]	0.6	Breaking

1- Delamination between the two upper layers at less than 10 cycles.
2- There was no sign of delamination after 200 cycles.
3- Obvious delamination between the two upper layers at about 50 cycles.
4- The delamination was detected by breaking the specimen after applying 200 cycles of load.
5- Rutting on the surface observed at the early stage of test, and after breaking the specimen the delamination revealed, however it was not very obvious.

6-3 Structural analysis

In the last sections, the experimental program regarding the behaviour of thin layered systems under the action of a steel wheel rolling load was presented. The main objective of that program was simulating any possible delamination at the interface between the coating and the second layer of the thin layered systems. In this part of study, it will be attempted to model and analyse the same systems in order to establish a proper method for predicting the behaviour of thin layered systems under the action of a Steel Wheel Rolling Load. The analysis will be based on the finite element method using a proper interface layer, as it was discussed in chapter 4.
Based on the results given in section 5-2, interface bond strength, and in the previous section of this chapter, the following combinations of layered systems will be analysed in this investigation as the most representative cases:

- **G1194/P4/Concrete** using **Gprime** at the interface between G1194 and P4 layer at the age of 28 days under the action of a 3750 N steel wheel load.
- **G1294/P4/Concrete** using **Gprime** at the interface between G1194 and P4 layer at the age of 28 days under the action of a 3750 N steel wheel load.
- **G1194/Concrete** using **Gprime** at the interface between G1194 and the concrete layer at the age of 28 days under the action of a 5000 N steel wheel load.
- **G1194/Concrete** using **Pprime** at the interface between G1194 and the concrete layer at the age of 56 days under the action of a 5000 N steel wheel load.
- **G1294/Concrete** using **Gprime** at the interface between G1294 and the concrete layer at the age of 28 days under the action of a 5000 N steel wheel load.

6-3-1 General assumptions and approximations

6-3-1-1 The finite element mesh and the constitutive materials

- For all the constitutive materials, nonlinear behaviour has been considered based on the corresponding idealized stress - strain curves defined in chapter 5. To achieve this, the implicit ('backward Euler')elasto - plastic von Mises yield surface model using the LUSAS finite element software has been employed.

" The implicit model allows the proper definition of a tangent stiffness matrix which maintains the quadratic convergence of the Newton -Raphson iteration scheme. " [LUSAS User Manual]

Although a three dimensional finite element mesh would be ideal for the analysis of a layered system, because of the restrictions in the computer memory and also saving the time of analysing, two dimensional plain strain finite element mesh has been used. However in order to keep the consistency with the interface elements, and at the same time to get a more accurate analysis, isoparametric quadrilateral 8 noded elements have been used for all layers of the thin layered systems.

6-3-1-2 The interface layer

- As was discussed in chapter 4, a thin elastic interface layer has been considered in each model of the thin layered systems to be analysed.

To define the interface layer, two parameters are required, the elastic shear modulus (G), and the thickness of the layer (t).

The G modulus is defined as follows: [Desai et al. 1984]

$$G_{K(\sigma_n,\tau,u_r)} = \frac{\partial\,[\tau_{(\sigma_r,u_r)}]}{\partial\,u_r} \times t\Big|_{\sigma_n} \qquad (6\text{-}1)$$

Where: G is the shear modulus of the interface layer, MPa

σ_n is the normal pressure in the direct shear test

τ is the shear stress, MPa

u_r is the deformation at the interface, mm

t is the thickness of the interface layer, mm

The ratio of $\frac{\partial\,[\tau_{(\sigma_r,u_r)}]}{\partial\,u_r}$ has been defined by analysing the appropriate plane strain finite element mesh of the shear box specimens reported in chapter 5. (figures 6-9-a & 6-10-a) Since the interface element layer has been assumed elastic, and isotropic, the above assumption would be acceptable.

The values of vertical load for the two models are the average figures which have been used in the shear box tests, i.e. 0.88 MPa for the small shear box model and 0.58 MPa for the large one. The value of the horizontal load is 1.00 MPa for both of the models. (figures 6-9, 6-10)

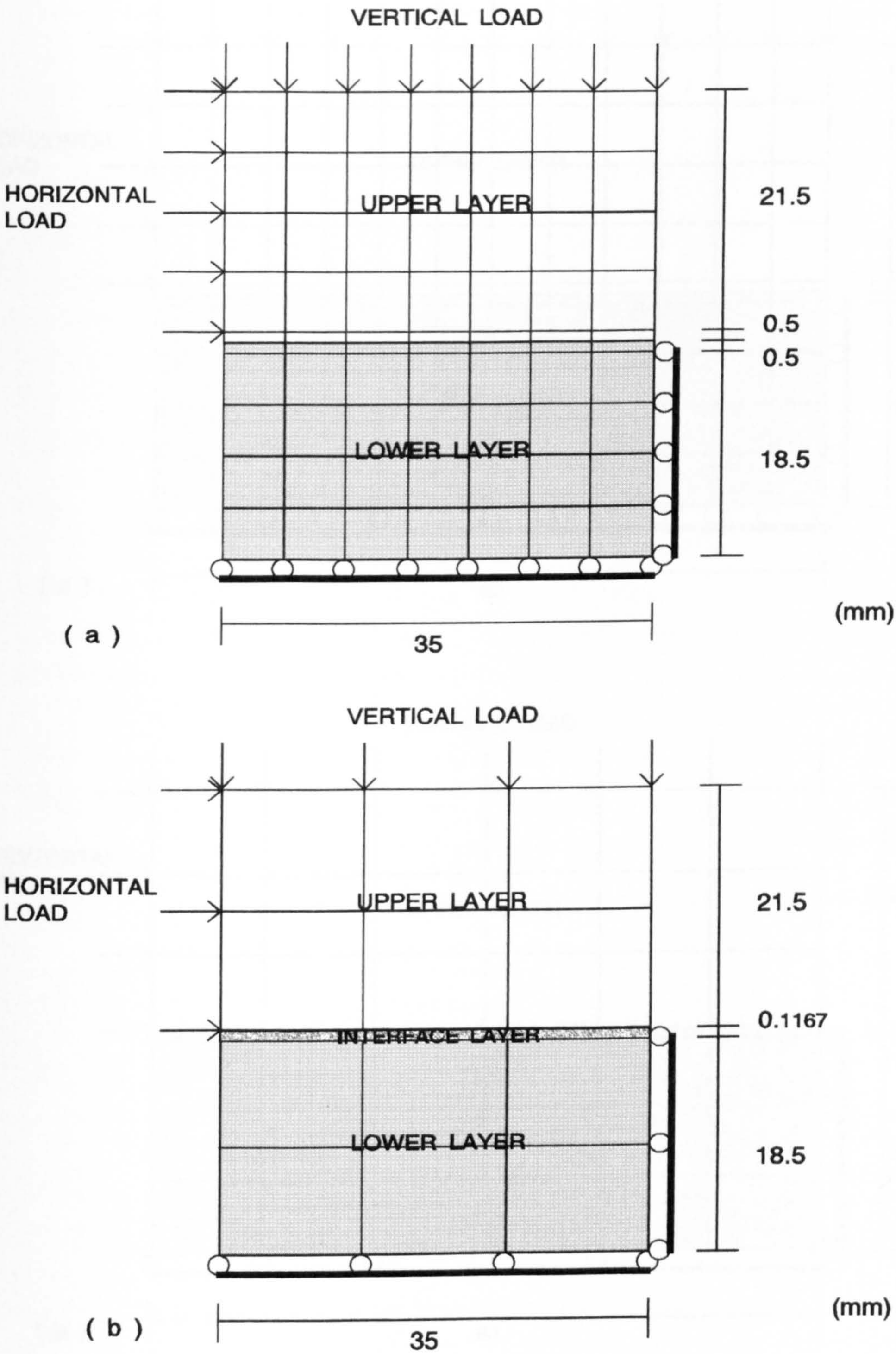

Figure 6-9: Small shear box finite element mesh
a: Without the interface layer b: With the interface layer

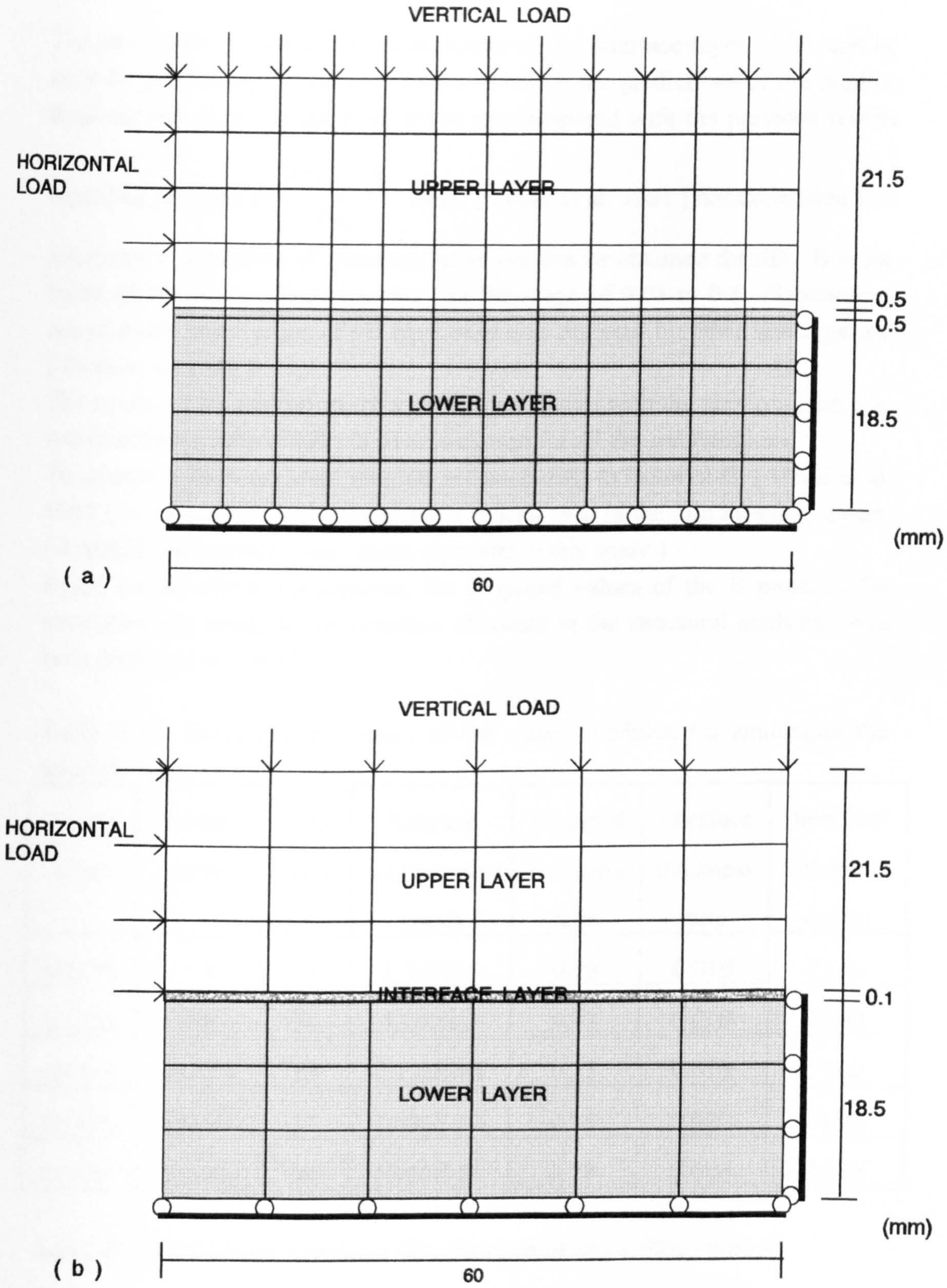

Figure 6-10: Large shear box finite element mesh
a: Without the interface layer b: With the interface layer

The other main parameter is the thickness of the interface layer. This can be done by performing parametric studies in which the predictions of the relative displacement from various thicknesses are compared with the previous results regarding the ratio of $\frac{\partial [\tau_{(\sigma_r, u_r)}]}{\partial u_r}$. Desai [Desai et al. 1984] has concluded that satisfactory simulation of interface behaviour can be obtained for t/B (B is the width of the surrounding elements) in the range of 0.01 to 0.1. Satisfactory use of much lower ratios of t/B have been also reported by other investigators. [Desai et al. 1984]

The results of the current study were also consistent with the previous findings, and therefore a ratio of t/B = 0.01 was chosen for all the combinations.

To achieve a more accurate solution and according to Desai et al. [Desai et al. 1984], isoparametric solid elements have been used in the thin interface layers. (8 noded quadrilateral plane strain elements in this study)

Based on the above assumptions, the proposed values of the E modulus for simulating the required thin interface elements in the structural analysis, have been tabulated in table 6-3.

Table 6-3: The proposed values of the elastic modulus for simulating the interface layer

Upper layer	Lower layer	Age (days)	Relative displacement (mm)	Assumed Poisson's ratio	Interface thickness ratio	Interface E modulus (MPa)
G1194	P4	28	2.500E-4	0.29	0.01B	5120t
G1294	P4	28	1.260E-3	0.32	0.01B	2100t
G1194	Concrete	28	3.130E-04	0.25	0.01B	5780t
G1194	Concrete	56	2.680E-04	0.25	0.01B	6150t
G1294	Concrete	28	1.460E-03	0.28	0.01B	2420t

6-3-1-3 The contact pressure distribution of the rolling wheel

The steel wheel in the Steel Wheel Rolling Load experiment was a roller bearing one, and therefore the contact area with the surface of the specimens

was elliptical. For the purpose of the structural analysis which will be presented in due course in this chapter, it was necessary to measure the contact area between the steel wheel and the surface of the specimens. This was done by spraying paint on the surface of the steel wheel and then the image of the contact area was obtained on a piece of paper placed on the specimen under the wheel.

Now the important question for the purpose of a structural analysis is the contact pressure distribution.

Experimental tests using finite strain gauges have shown that the contact pressure distribution of a pneumatic or solid tyre in motion is uneven. [Concrete Society, Technical Report No. 34] This has been also confirmed by other investigators. (figure 6-11) [Zeid et al. 1981] [Padovan et al. 1984]

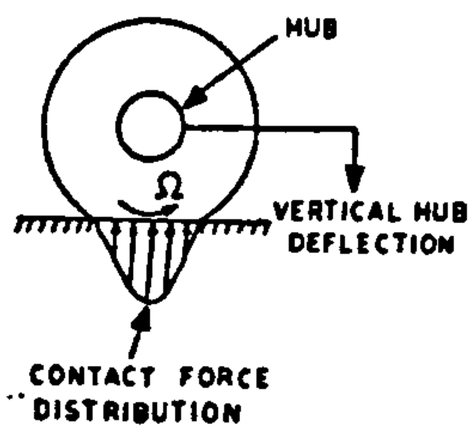

Figure 6-11: Schematic of a contact pressure distribution under a wheel in motion [Padovan et al. 1984]

In fact for an elastic surface the contact pressure pattern will be symmetrical. If however the stress strain curve of the material shows hysterisis, the stress distribution under the wheel becomes asymmetric. The horizontal component of the stress resultant in this case may vary from 10% to 20% depending on the corresponding factors. [Plum 1995]

However considerable simplifying assumptions have been made in most contact studies. For example in many problems, the frictional forces which are induced in the contact zone have not been taken into account. [Conway et al. 1966]

In this investigation a symmetrical contact pressure distribution will be assumed. Apart from the simplicity, owing to the lack of the presence of the above complex horizontal component of the stress resultant, this assumption would make the analysis to be more conservative.

Since plain strain analysis will be used, for each model of the thin layered systems, two central strips along the two diameters of the elliptic contact area will be considered. The pressure distribution along the strips will follow equation (6-2) in two perpendicular directions. This equation is the exact

solution, obtained by Hertz, in 1895, for the pressure distribution over a strip compressed by a rigid circular roller for the ratio of $a/h=0$. The results of studies made by Conway et al. showed that the pressure distributions vary but little with changes in a/h. (Figure 6-12) [Conway et al. 1966]

$$p=\frac{2P}{\pi a^2 t}(a^2-x^2)^{1/2} \qquad (6\text{-}2)$$

Where: p is the contact pressure at point x, MPa (Figure 6-12)

P is the load which acts on the strip, N

a is the half width of the indented area, mm

t is the thickness of the strip, mm (here t = 1 mm)

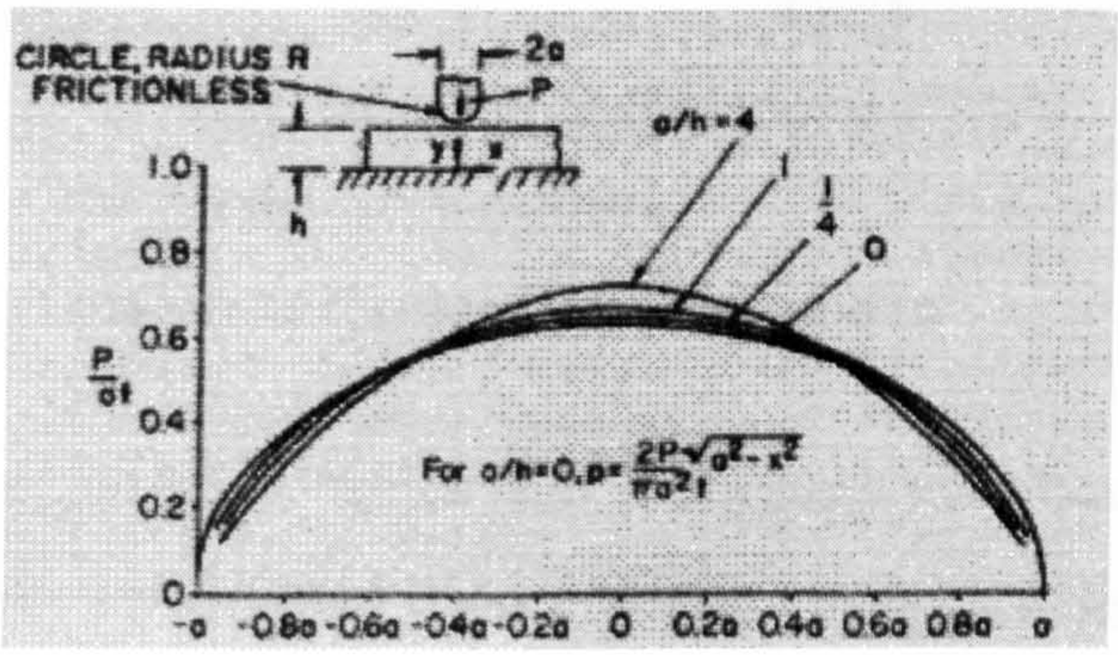

Figure 6-12: Normal stress distributions under circular frictionless roller applied to isotropic strip [Conway et al. 1966]

The nonlinear pressure distribution will be approximately represented by a series of pressures which are constant over the incremental lengths. (figure 6-13)

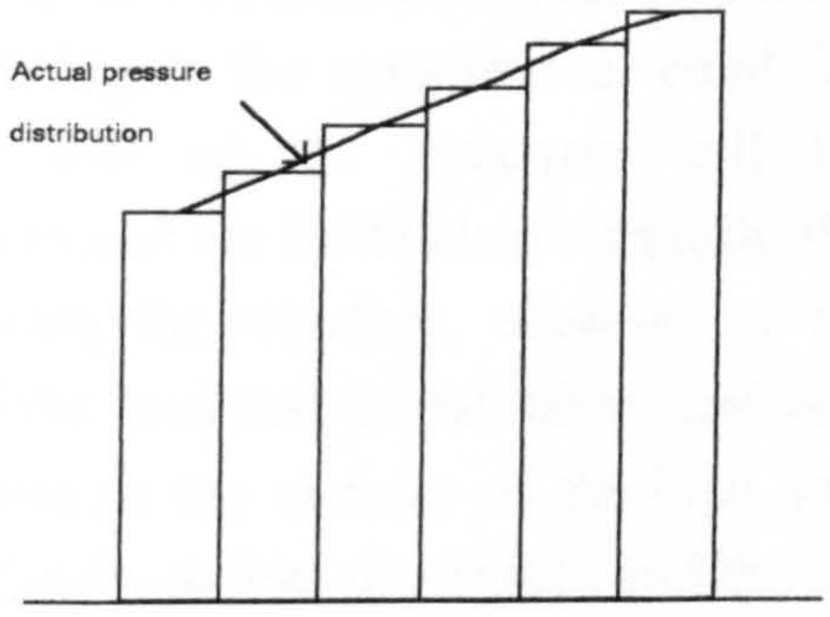

Figure 6-13: Approximate pressure distribution representation

6-3-1-4 The failure criteria

Two failure criteria for predicting the possible delamination at the interface layer will be considered, the Mohr Coulomb criteria and the normal stress at the interface. For this purpose, the distribution of shear stress, τ_{xy}, and normal stress, σ_y, along the interface will be drawn and compared with the corresponding values of shear strength and normal pull off bond strength. The value of shear strength will be calculated from equation (6-3). [Zienkiewicz et al.] [Desai et al. 1984]

$$\textit{Shear strength} = C + \sigma_n \tan \Phi \qquad (6\text{-}3)$$

Where: C is the cohesion at the interface, MPa

σ_n is the normal stress

$\tan \Phi$ is the coefficient of friction

When $\tau_{xy} > C + \sigma_n \tan \Phi$, it means that a slippage may occur. Similarly if $\sigma_y >$ *Bond strength*, a debonding at the interface will be predictable.

It should be noted that after a failure occurs at any node, a new distribution of the stresses will take place within the whole volume of the structure. Therefore the results of the following analysis for each model could predict the interface nodes at which the first horizontal cracks may appear.

6-3-2 The results of the stress - strain analysis

The stress strain analysis will be carried out for five models, five combinations of different layers. Owing to the symmetrical condition of the load and the finite element mesh, half of the structure will be analysed for each combination. For each model the finite element mesh, the distribution of shear and normal stresses along the interface, contours of the maximum principal stress in the vicinity of the load and the interface, and finally the distribution of maximum principal stress in the vicinity of the load and the interface will be presented. By comparing the values of stresses and the corresponding values of strengths, the potential delamination zone for each case will be shown in a clear way.

6-3-2-1 Model 1: G1194/P4/Concrete

Age: 28 days
Load: 3750 N
Contact area: An elliptic area of diameters a= 18 mm & b = 12 mm

Specifications of the materials and layers:

G1194:

E = 10100 MPa (table 5-12)
υ = 0.32 (table 5-16)
Thickness = 3 mm
Nonlinear properties idealisation: (figure 5-5-c-2)

Interface between G1194 and P4 using Gprime as the primer:

E = 5120 t (table 6-3)
t = 0.01B (table 6-3)
υ = 0.29 (table 6-3)
Cohesion = 1.3 MPa (table 5-22)
Coefficient of friction = 0.89 (table 5-22)
where t is the interface thickness (mm), and B is the width of the finite elements at the interface.

P4:

E = 15100 MPa (table 5-9)
υ = 0.25 (table 5-16)
Thickness = 10 mm
Nonlinear properties idealisation: (figure 5-4-c-2)

Concrete:

E = 23300 MPa (table 5-2)
υ = 0.18 (table 5-16)
Thickness = 50 mm
Nonlinear properties idealisation: (figure 5-1-b)

Pressure distribution representation over the incremental lengths, MPa:

Model No.	Length 1	Length 2	Length 3	Length 4	Length 5	Length 6
Model 1-a	35.6	34.1	31.0	25.5	15.6	-
Model 1-b	35.6	34.6	32.5	29.0	23.6	14.3

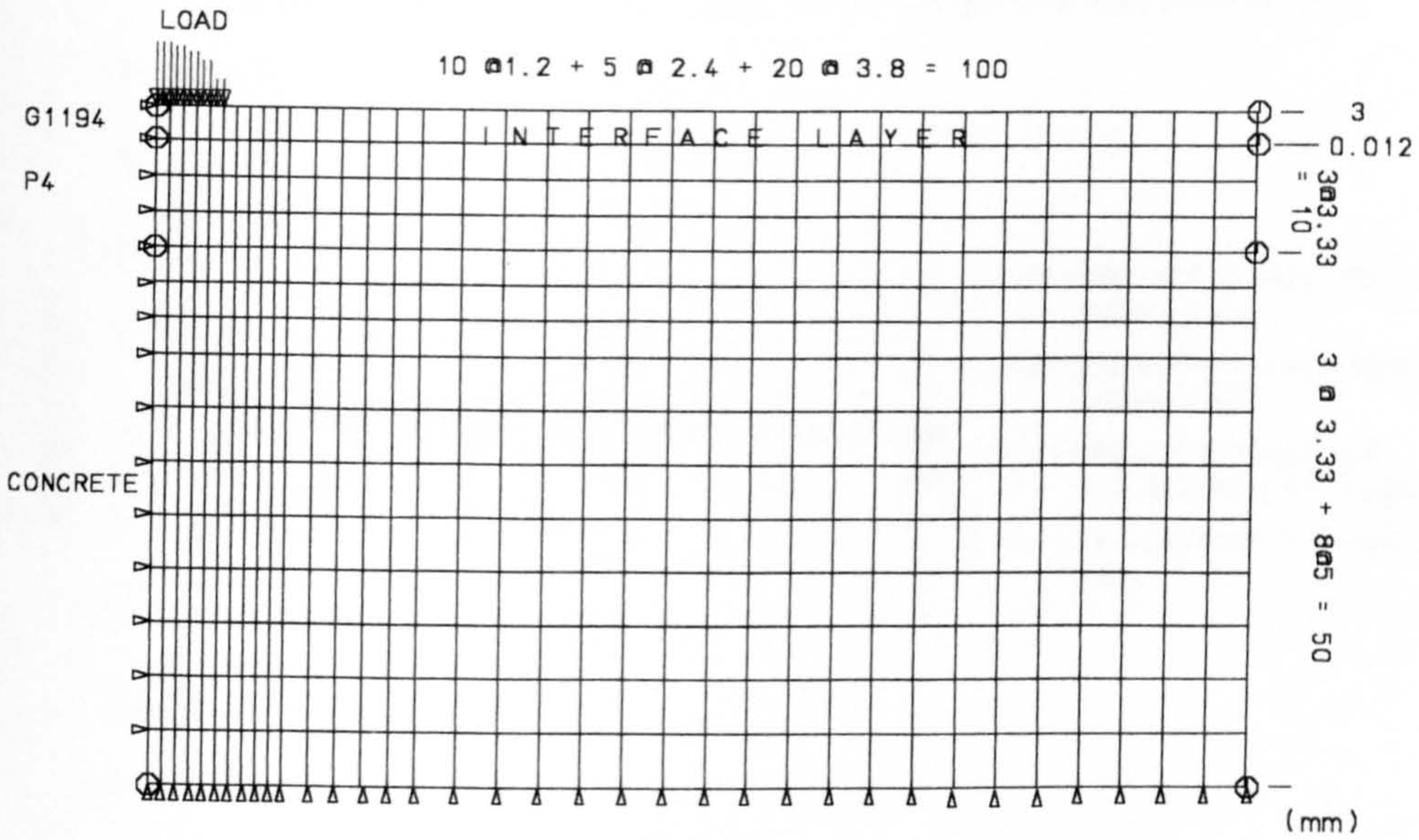

Figure 6-14-a: The finite element mesh for Model 1-a
(Load distribution over the short diameter of the contact area is considered)

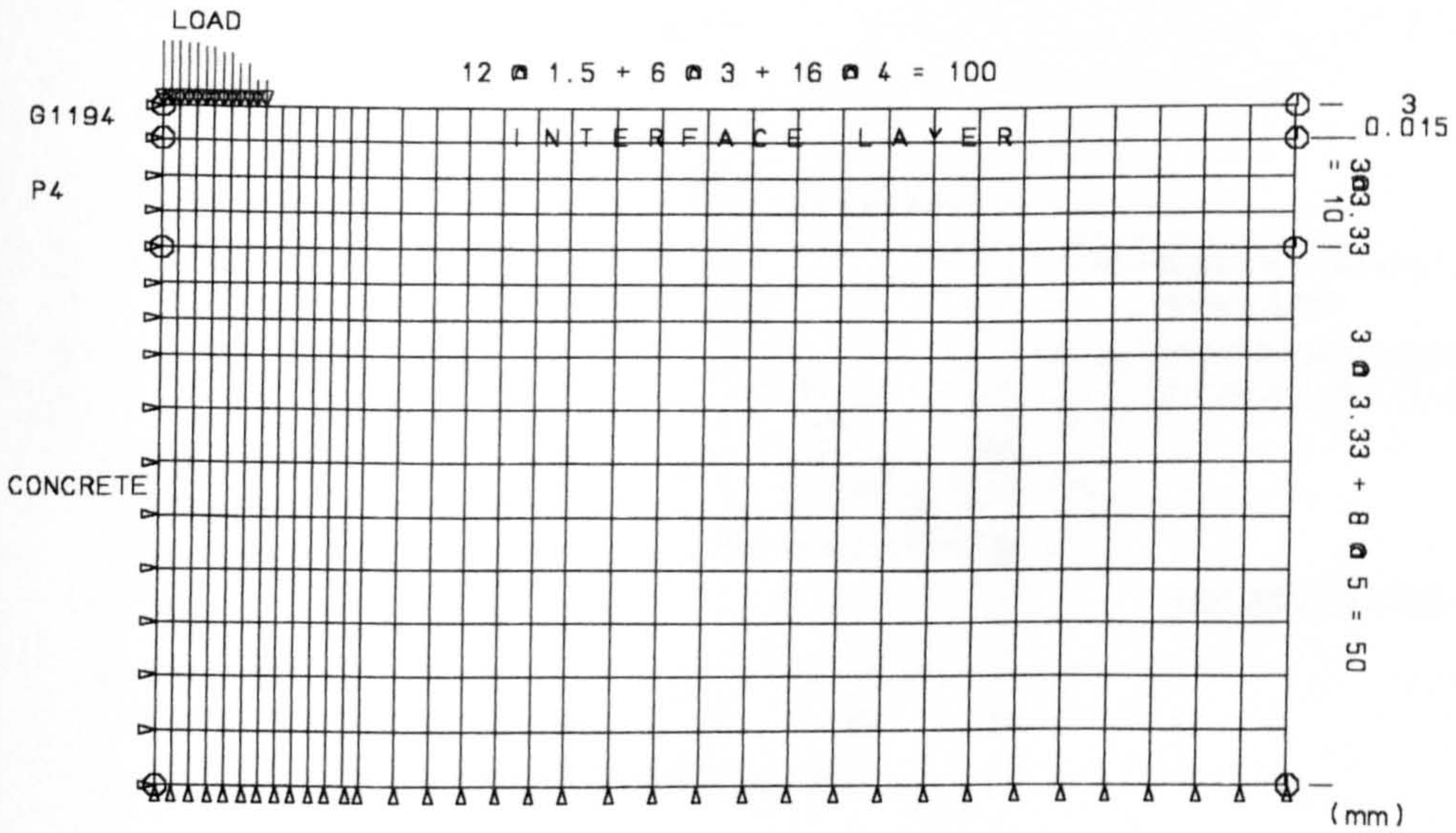

Figure 6-14-b: The finite element mesh for Model 1-b
(Load distribution over the long diameter of the contact area is considered)

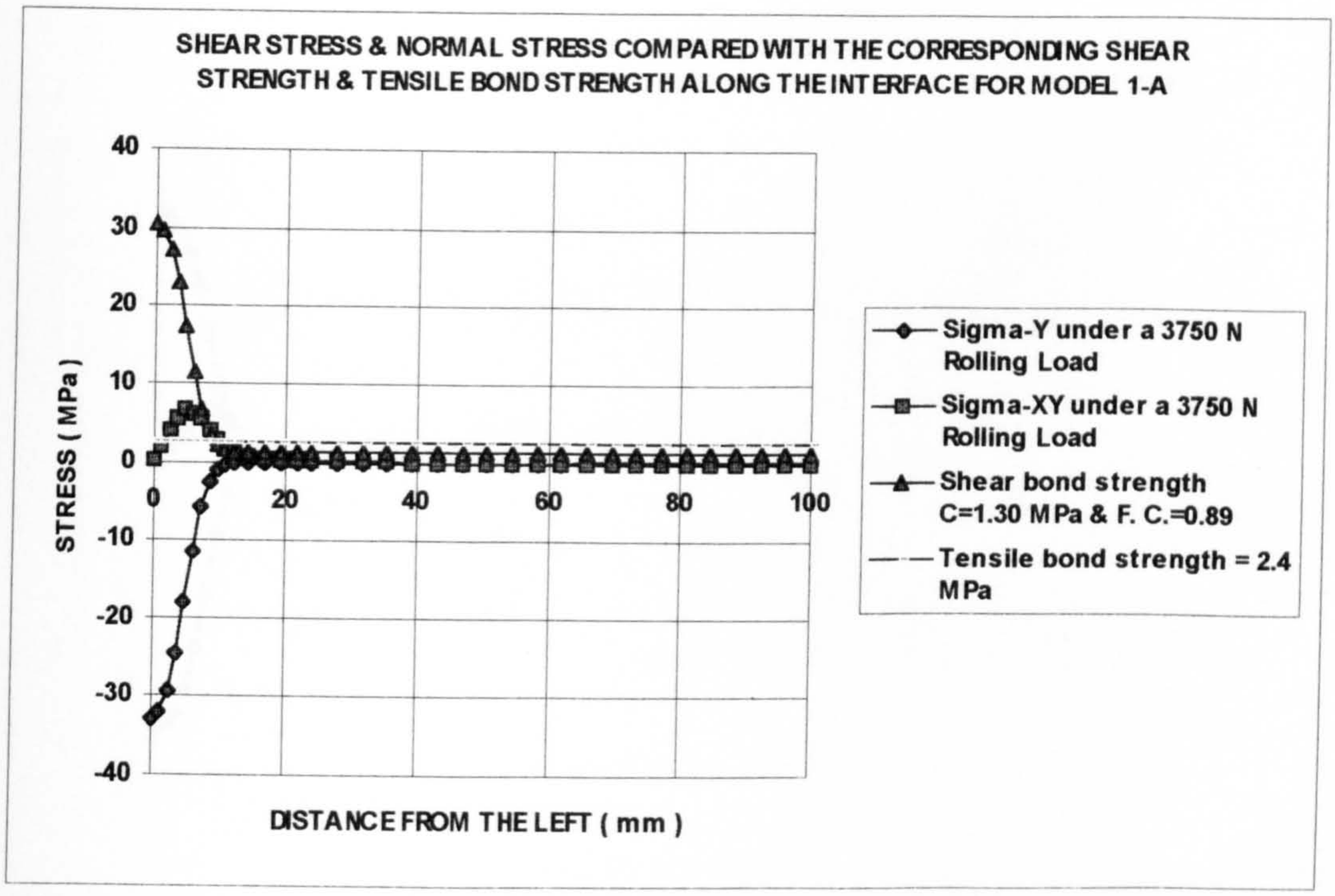

Figure 6-14-a-1: Model 1-a, G1194/P4/Concrete {Compression (-), Tension (+)}

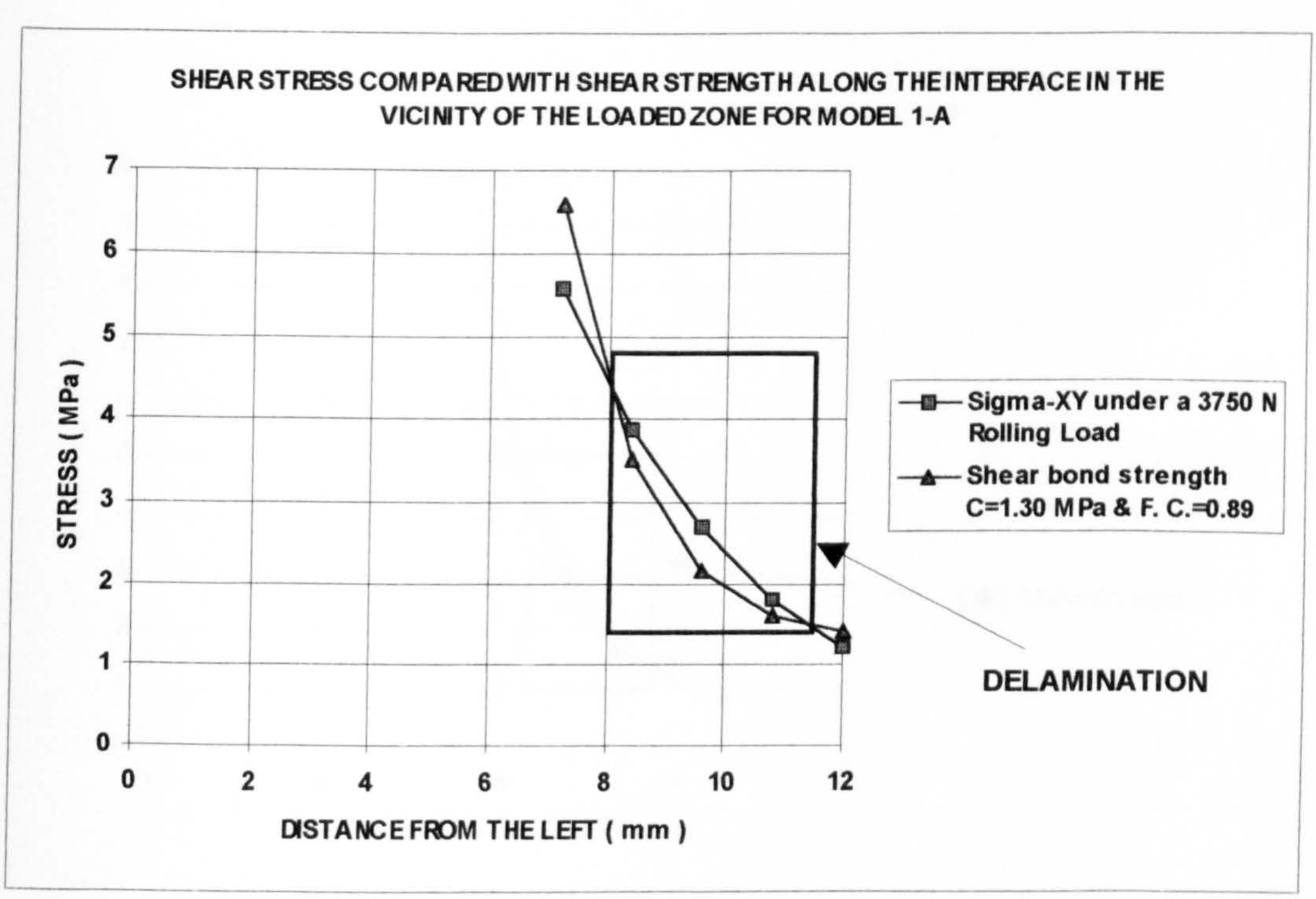

Figure 6-14-a-2 (Zoom): Model 1-a, G1194/P4/Concrete
(Delamination due to shear stress occurs) ***AGREEMENT***

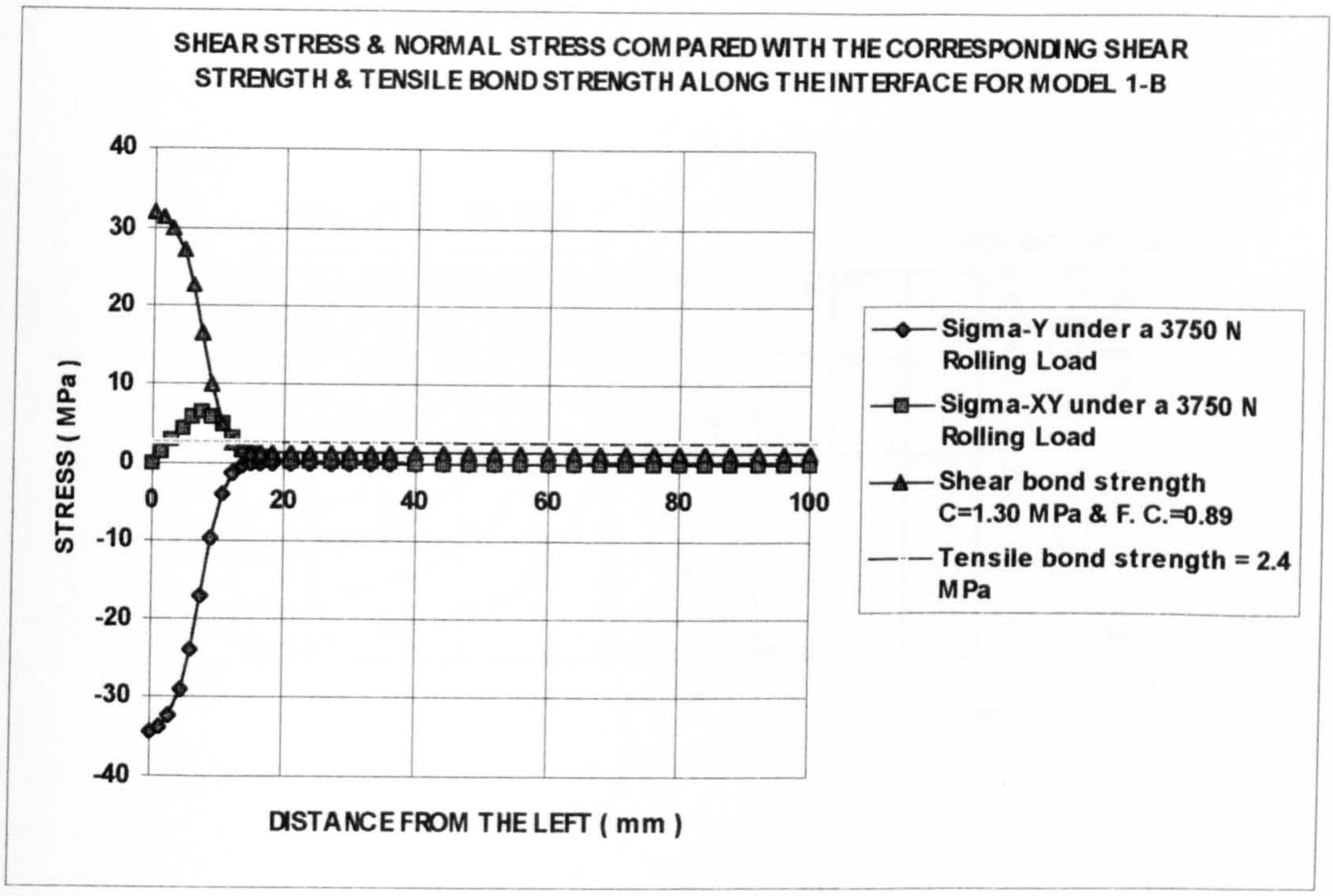

Figure 6-14-b-1: Model 1-b, G1194/P4/Concrete {Compression (-), Tension (+)}

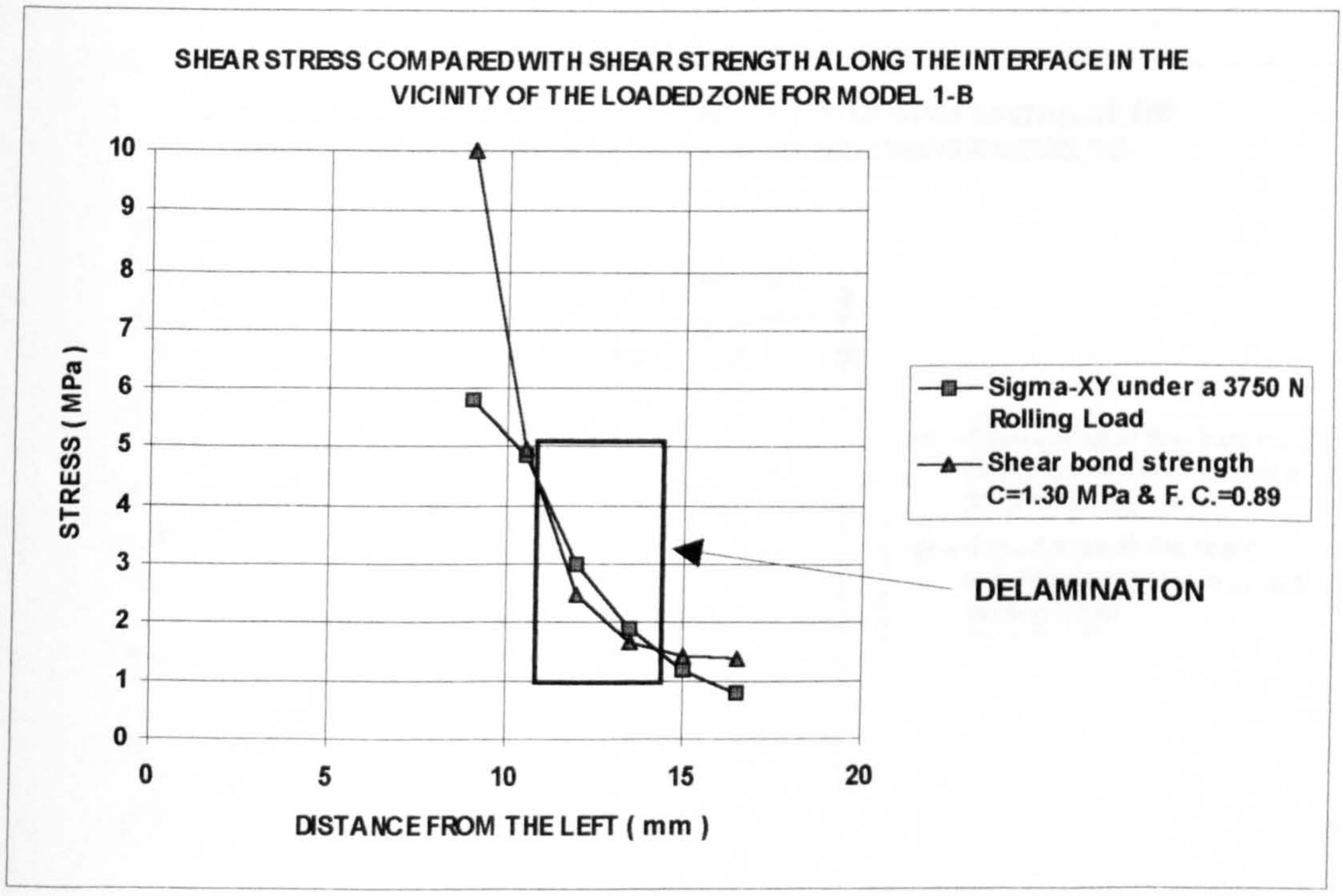

Figure 6-14-b-2 (Zoom): Model 1-b, G1194/P4/Concrete
(Delamination due to shear stress occurs) ***AGREEMENT***

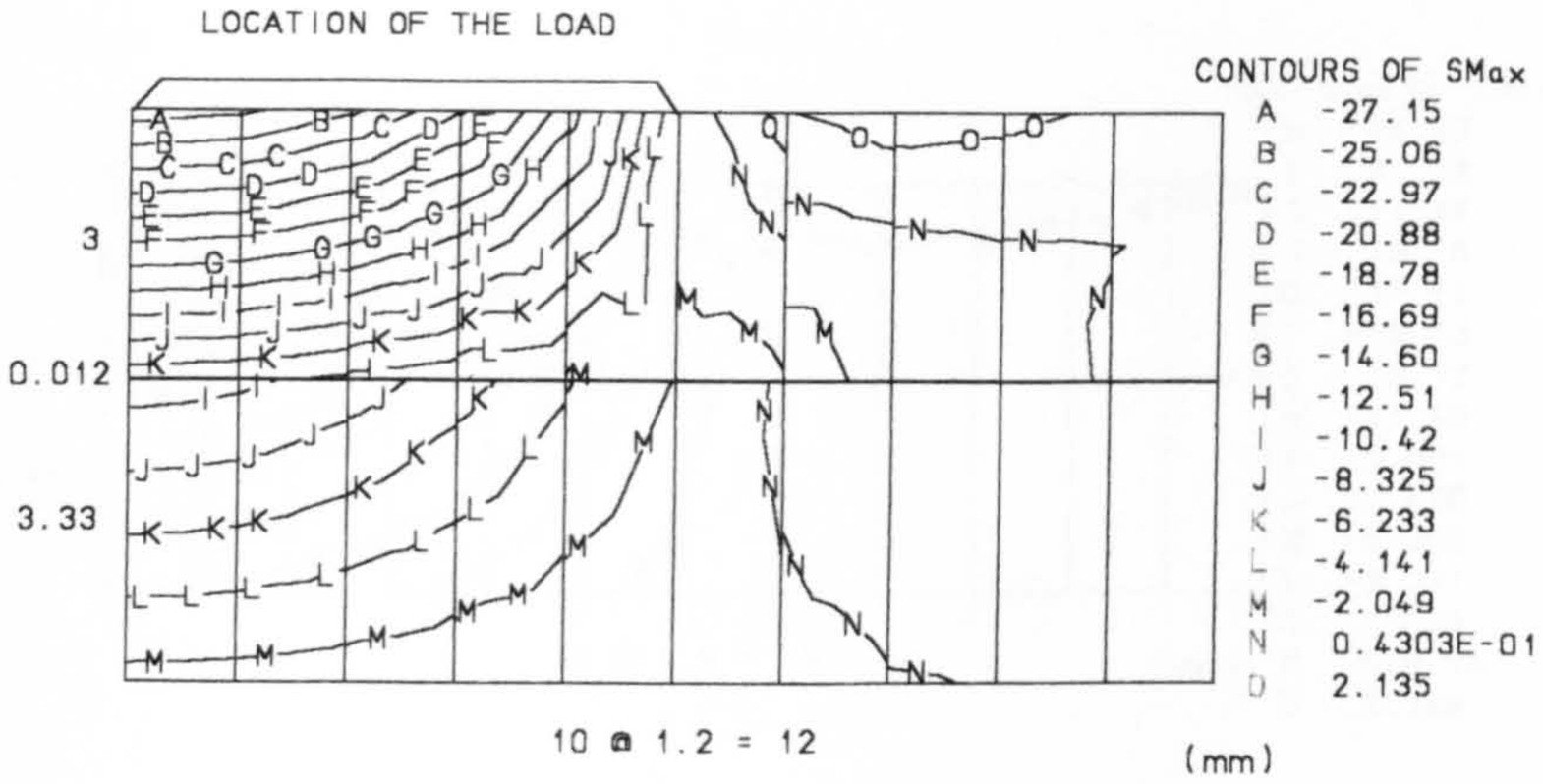

Figure 6-14-a-3: Contours of Sigma-1 (maximum) in the vicinity of the load and the interface for Model 1-a

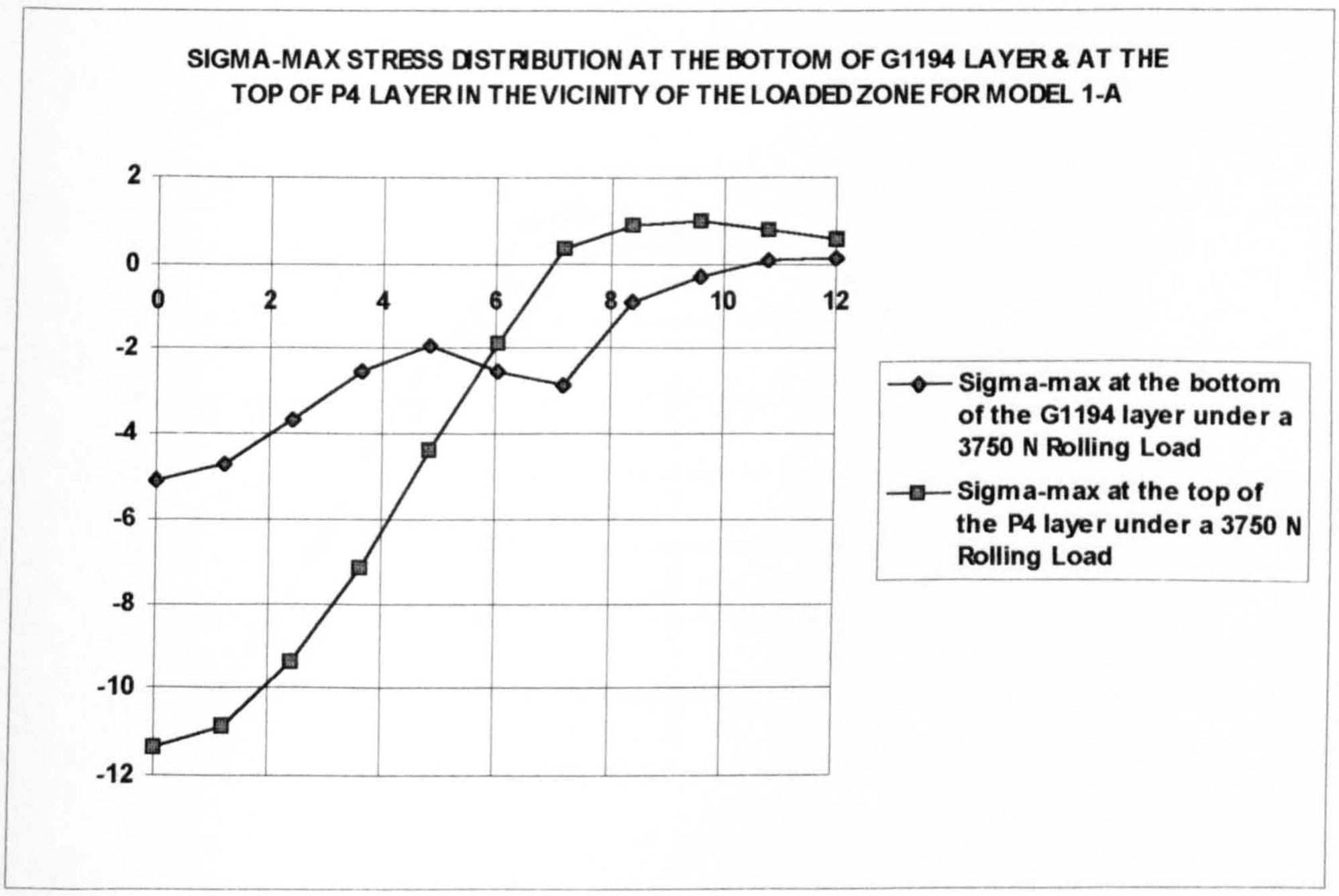

Figure 6-14-a-4: Sigma-1 (maximum) stress distribution in the vicinity of the load and the interface for Model 1-a {Compression (-), Tension (+)}

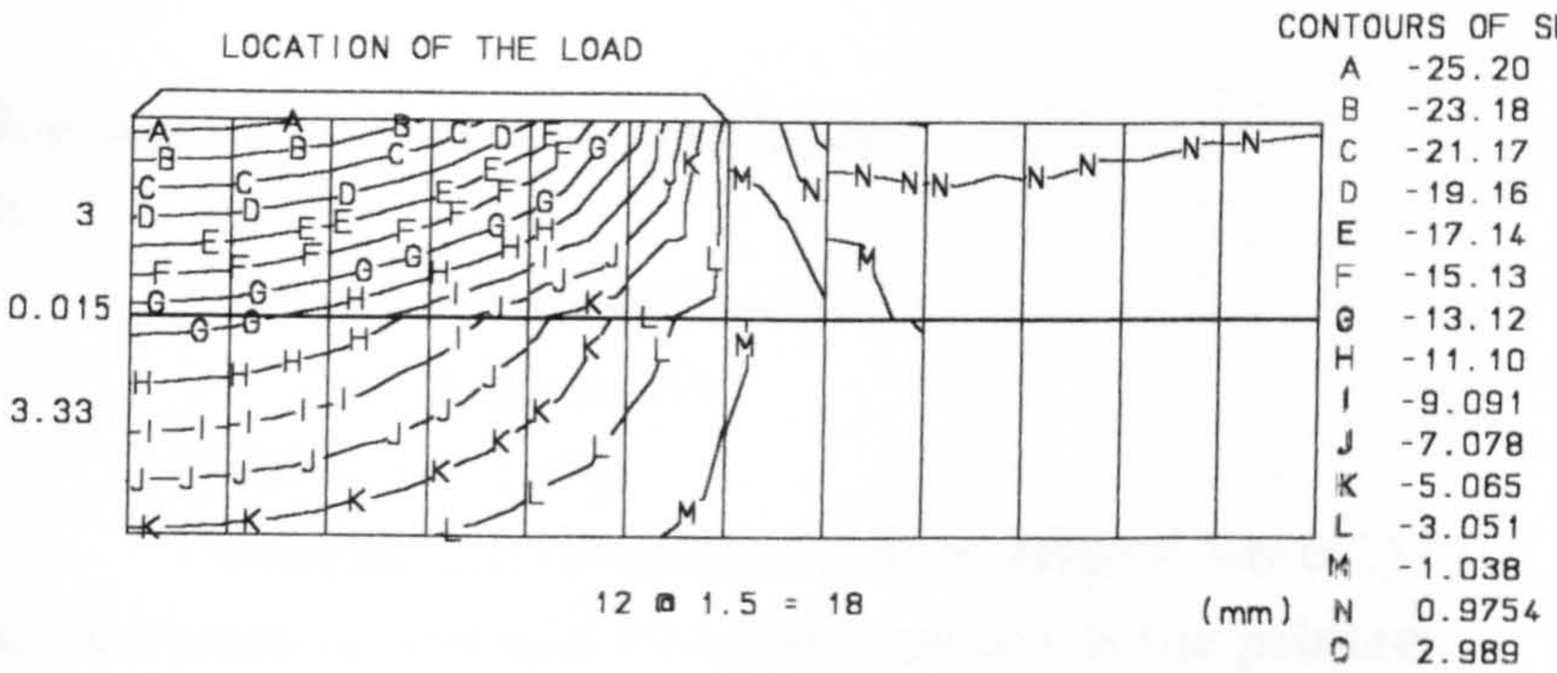

Figure 6-14-b-3: Contours of Sigma-1 (maximum) in the vicinity of the load and the interface for Model 1-b

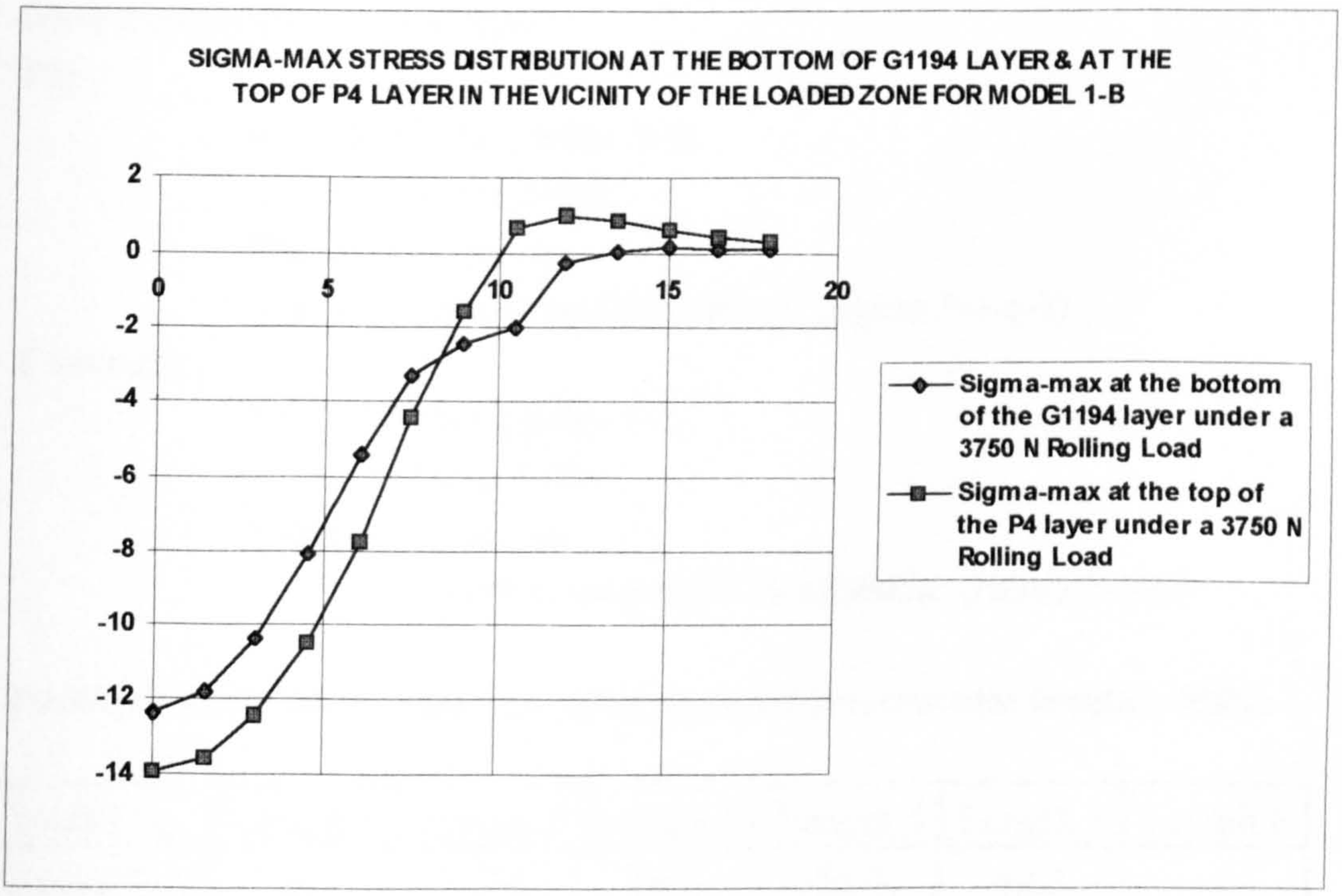

Figure 6-14-b-4: Sigma-1 (maximum) stress distribution in the vicinity of the load and the interface for Model 1-b {Compression (-), Tension (+)}

6-3-2-2 Model 2: G1294/P4/Concrete

Age: 28 days
Load: 3750 N
Contact area: An elliptic area of diameters a= 19.5 mm & b = 14 mm

Specifications of the materials and layers:

G1294:

E = 1700 MPa (table 5-15)
υ = 0.38 (table 5-16)
Thickness = 3 mm
Nonlinear properties idealisation: (figure 5-6-b-2)

Interface between G1294 and P4 using Gprime as the primer:

E = 2100 t (table 6-3)
t = 0.01B (table 6-3)
υ = 0.32 (table 6-3)
Cohesion = 0.58 MPa (table 5-22)
Coefficient of friction = 0.49 (table 5-22)
where t is the interface thickness (mm), and B is the width of the finite elements at the interface.

P4:

E = 15100 MPa (table 5-9)
υ = 0.25 (table 5-16)
Thickness = 10 mm
Nonlinear properties idealisation: (figure 5-4-c-2)

Concrete:

E = 23300 MPa (table 5-2)
υ = 0.18 (table 5-16)
Thickness = 50 mm
Nonlinear properties idealisation: (figure 5-1-b)

Pressure distribution representation over the incremental lengths, MPa:

Model No.	Length 1	Length 2	Length 3	Length 4	Length 5	Length 6
Model 2-a	28.1	27.0	24.5	20.2	12.3	-
Model 2-b	28.1	27.4	25.7	23.0	18.7	11.3

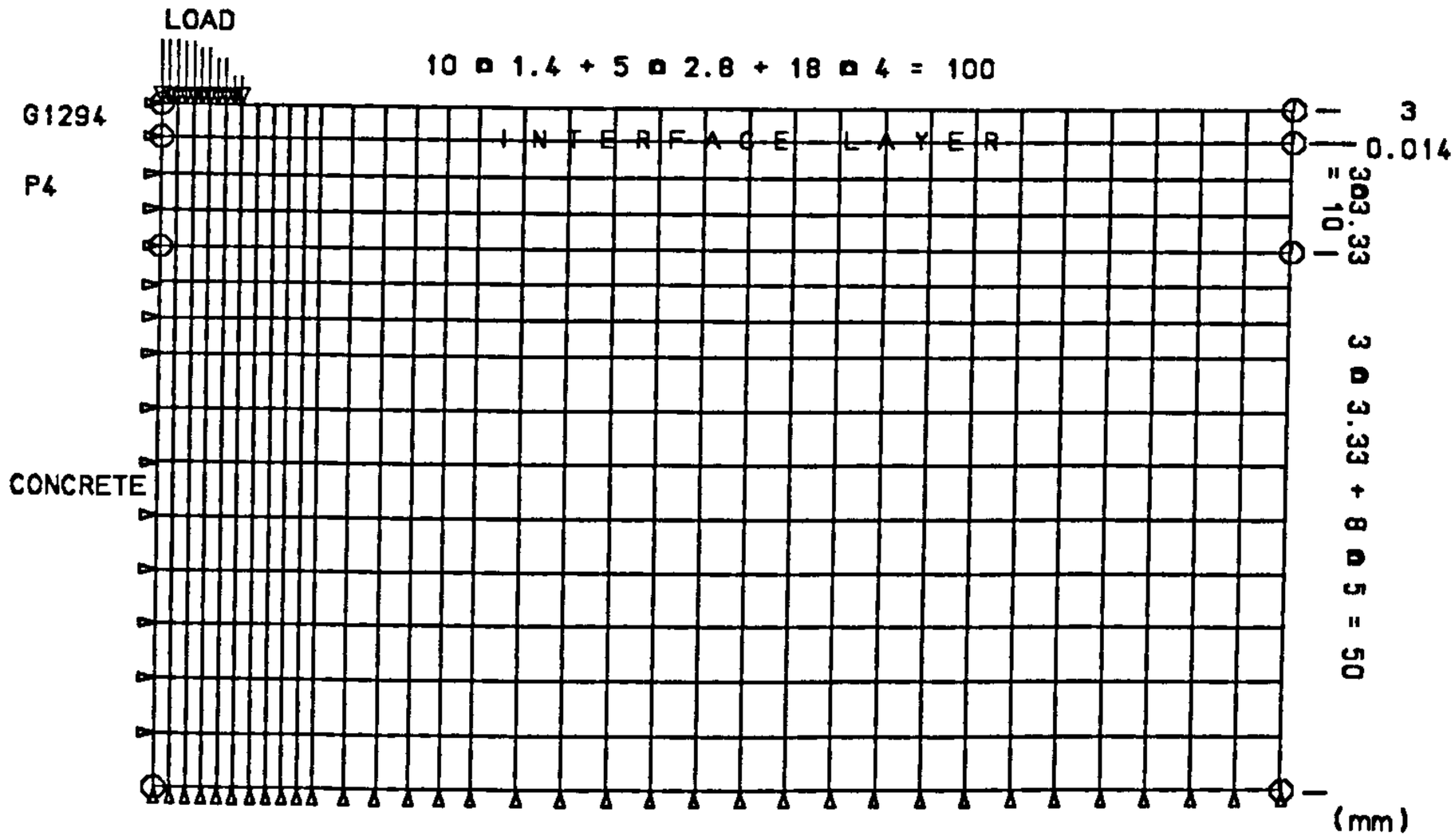

Figure 6-15-a: The finite element mesh for Model 2-a
(Load distribution over the short diameter of the contact area is considered)

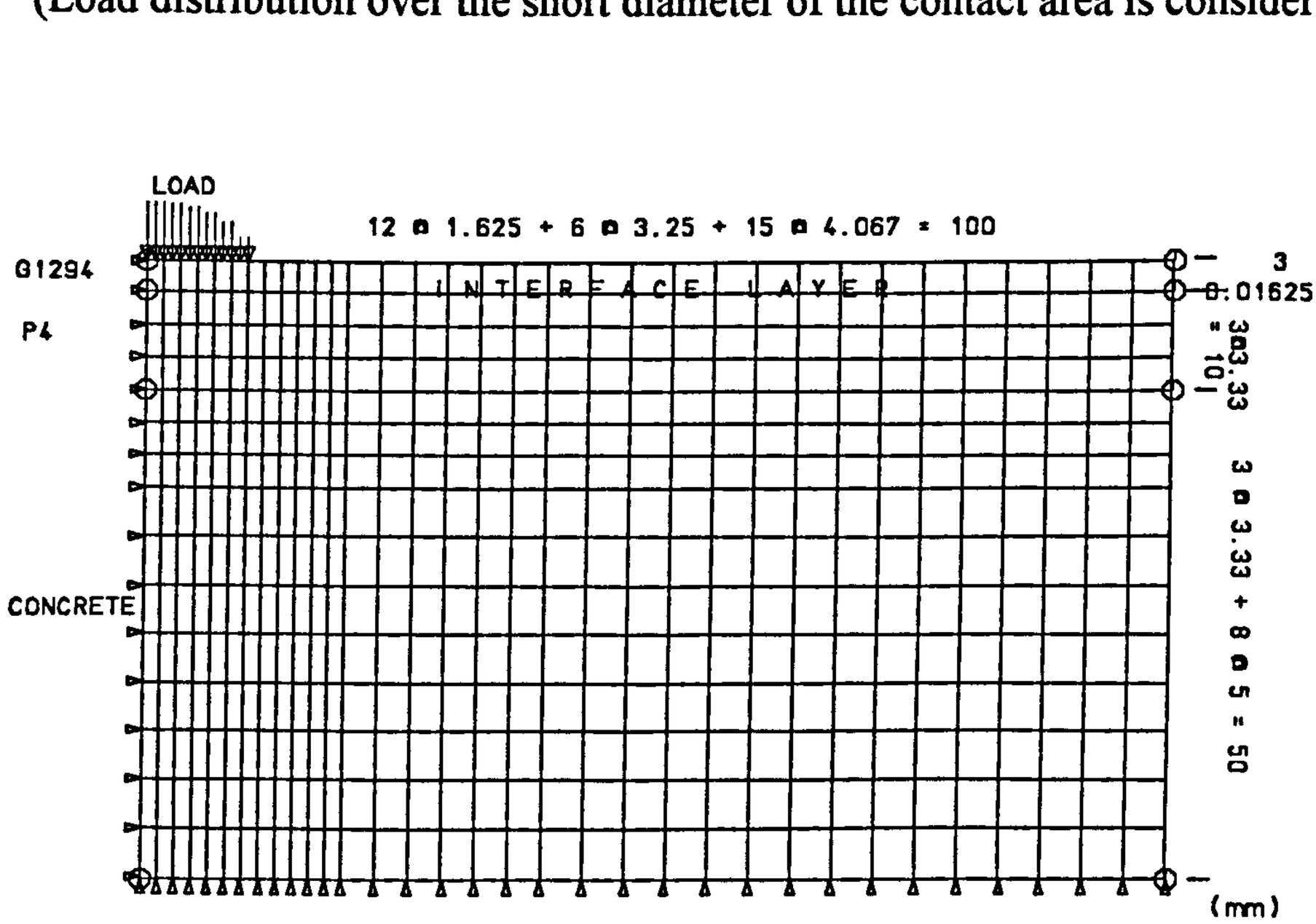

Figure 6-15-b: The finite element mesh for Model 2-b
(Load distribution over the long diameter of the contact area is considered)

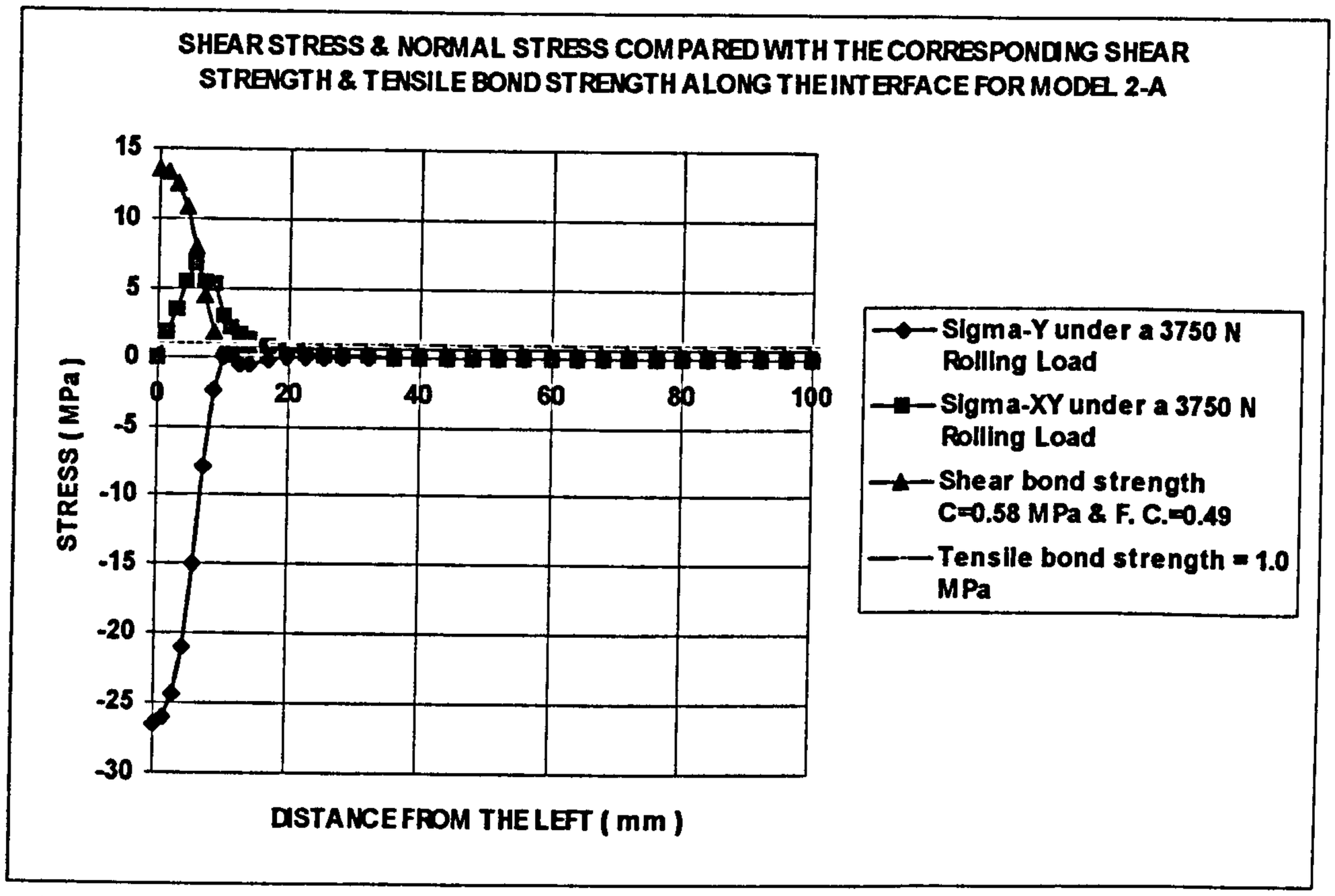

Figure 6-15-a-1: Model 2-a, G1294/P4/Concrete {Compression (-), Tension (+)}

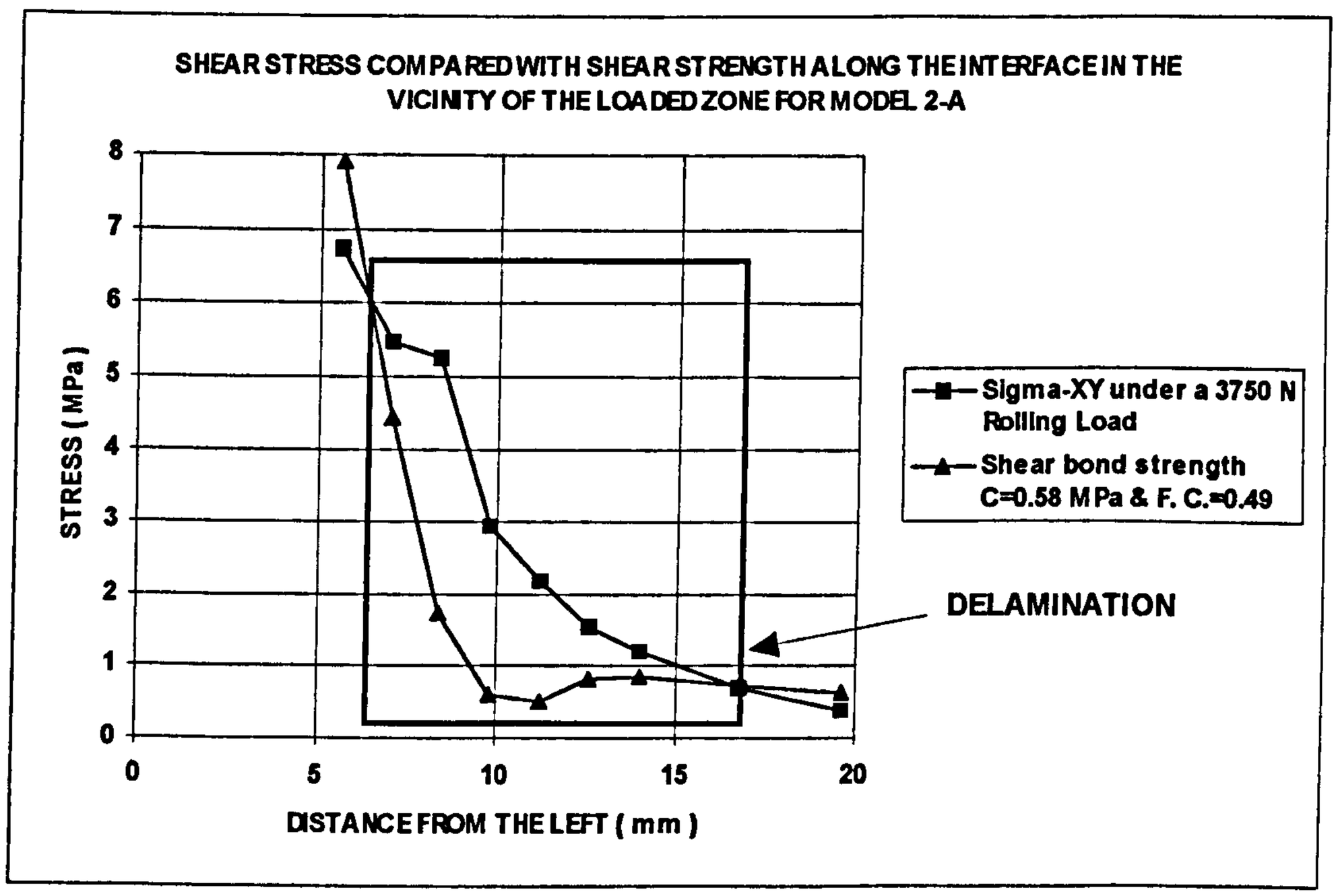

Figure 6-15-a-2 (Zoom): Model 2-a, G1294/P4/Concrete
(Delamination due to shear stress occurs) ***AGREEMENT***

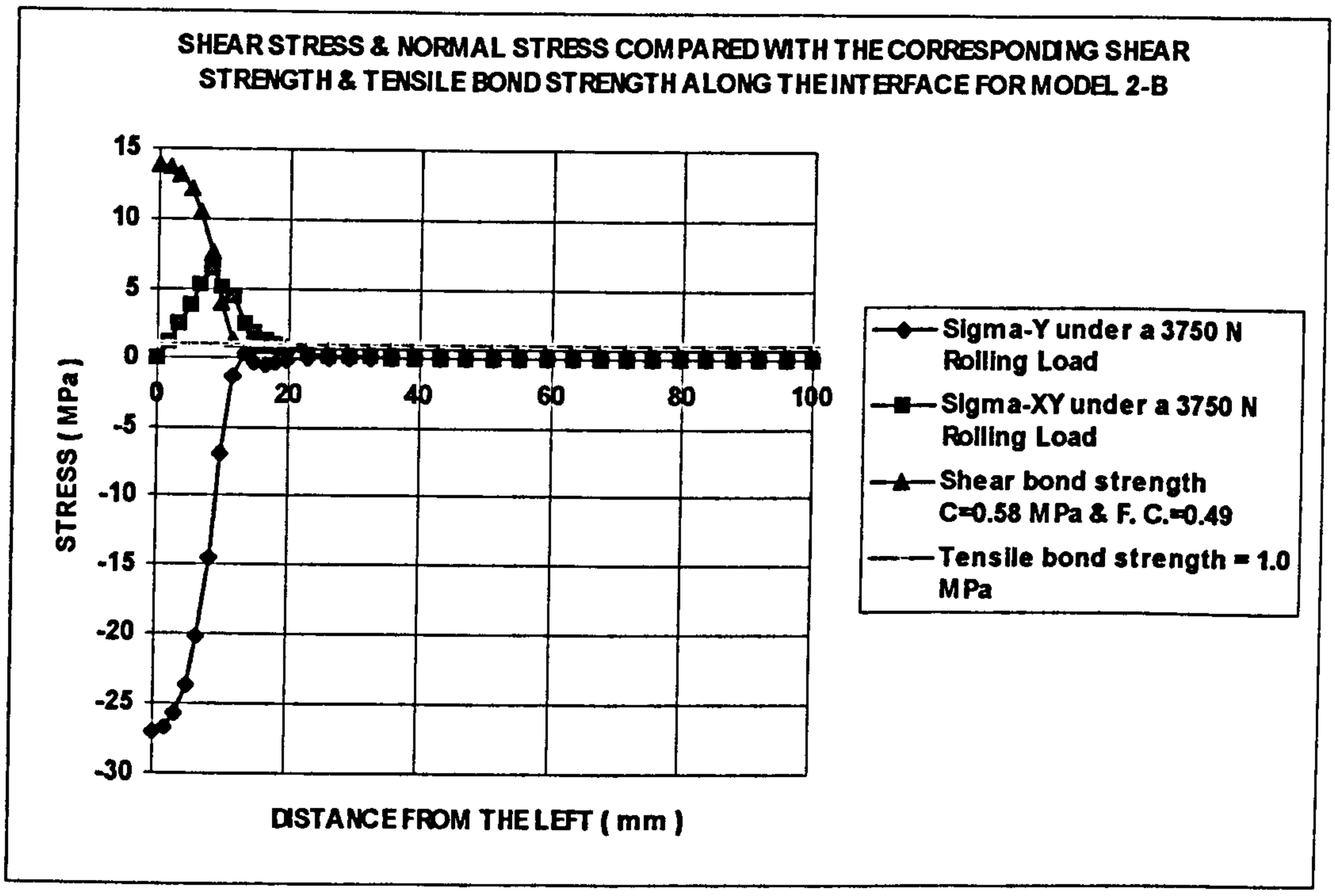

Figure 6-15-b-1: Model 2-b, G1294/P4/Concrete {Compression (-), Tension (+)}

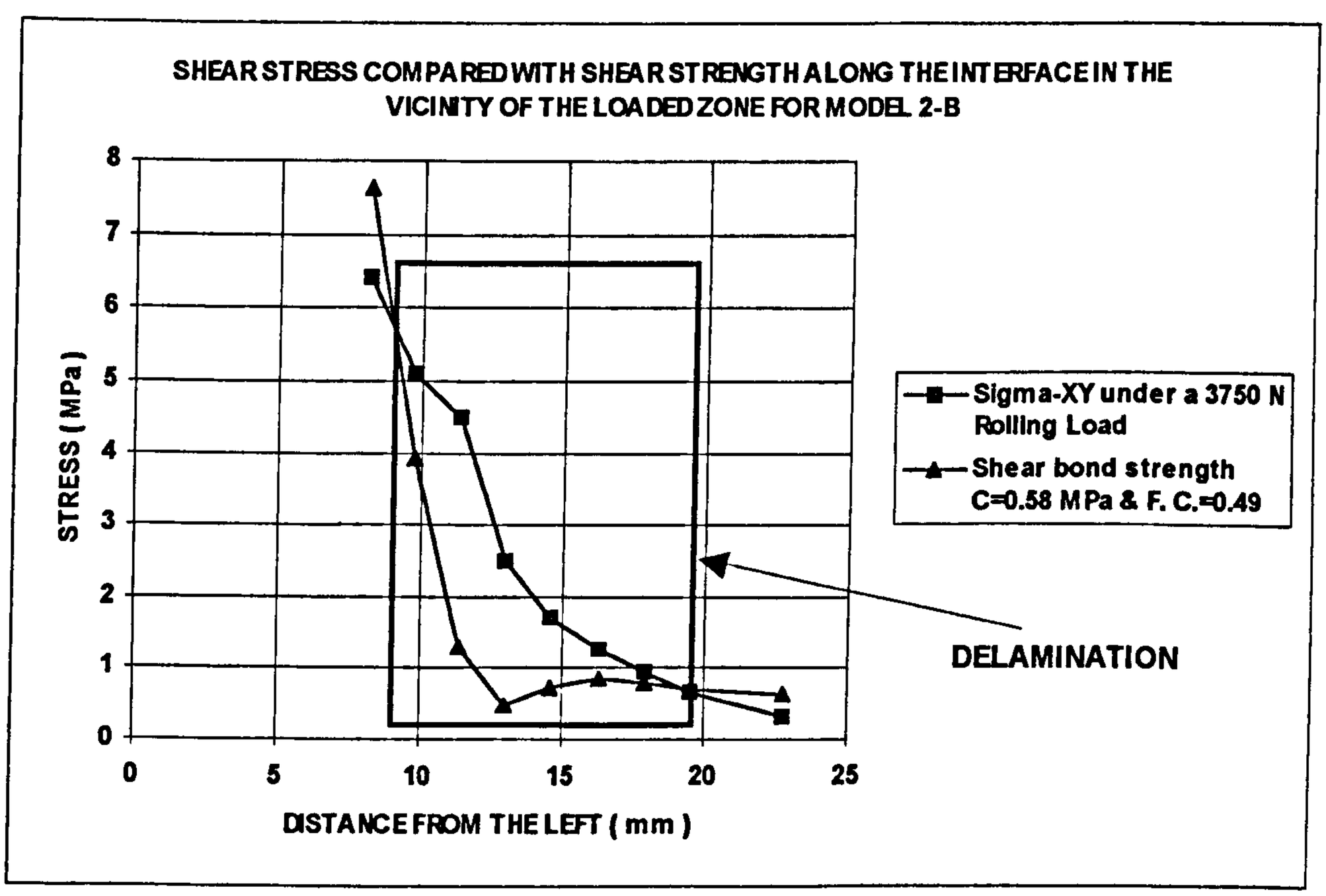

Figure 6-15-b-2 (Zoom): Model 2-b, G1294/P4/Concrete
(Delamination due to shear stress occurs) ***AGREEMENT***

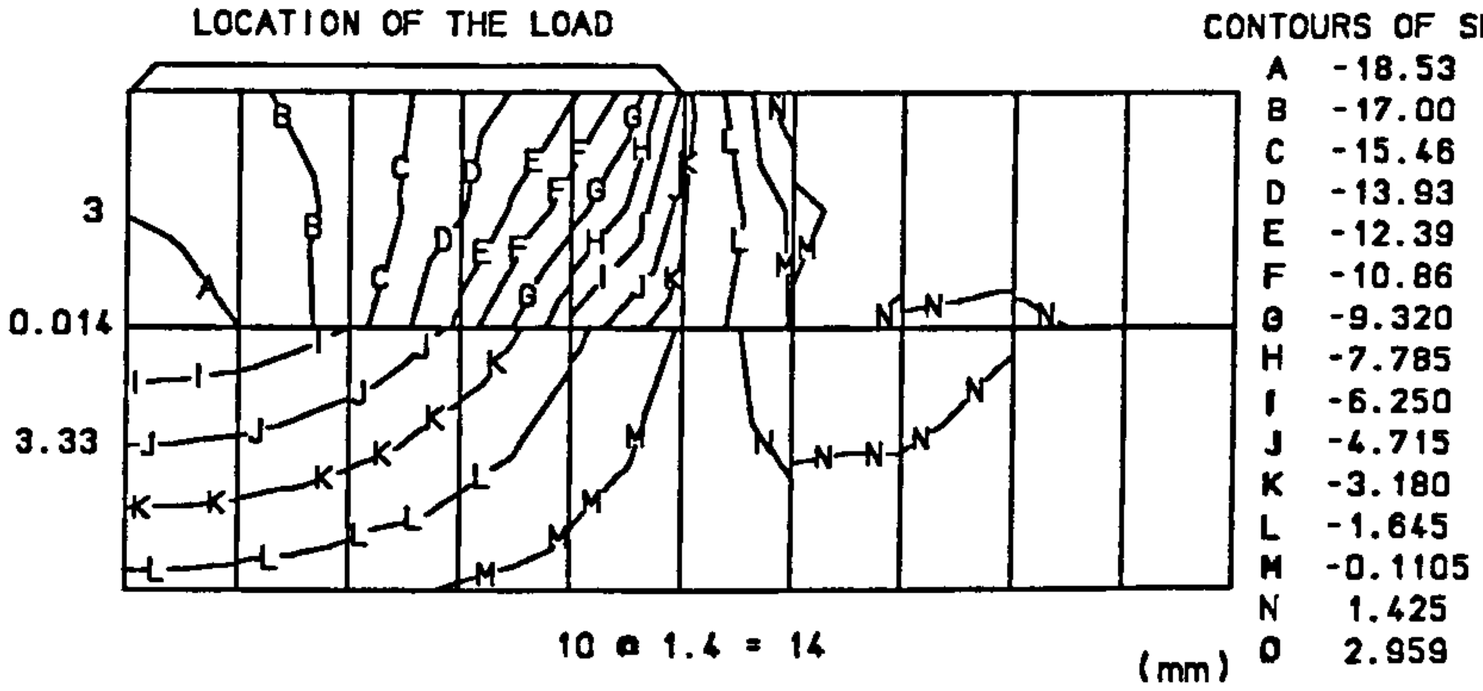

Figure 6-15-a-3: Contours of Sigma-1 (maximum) in the vicinity of the load and the interface for Model 2-a

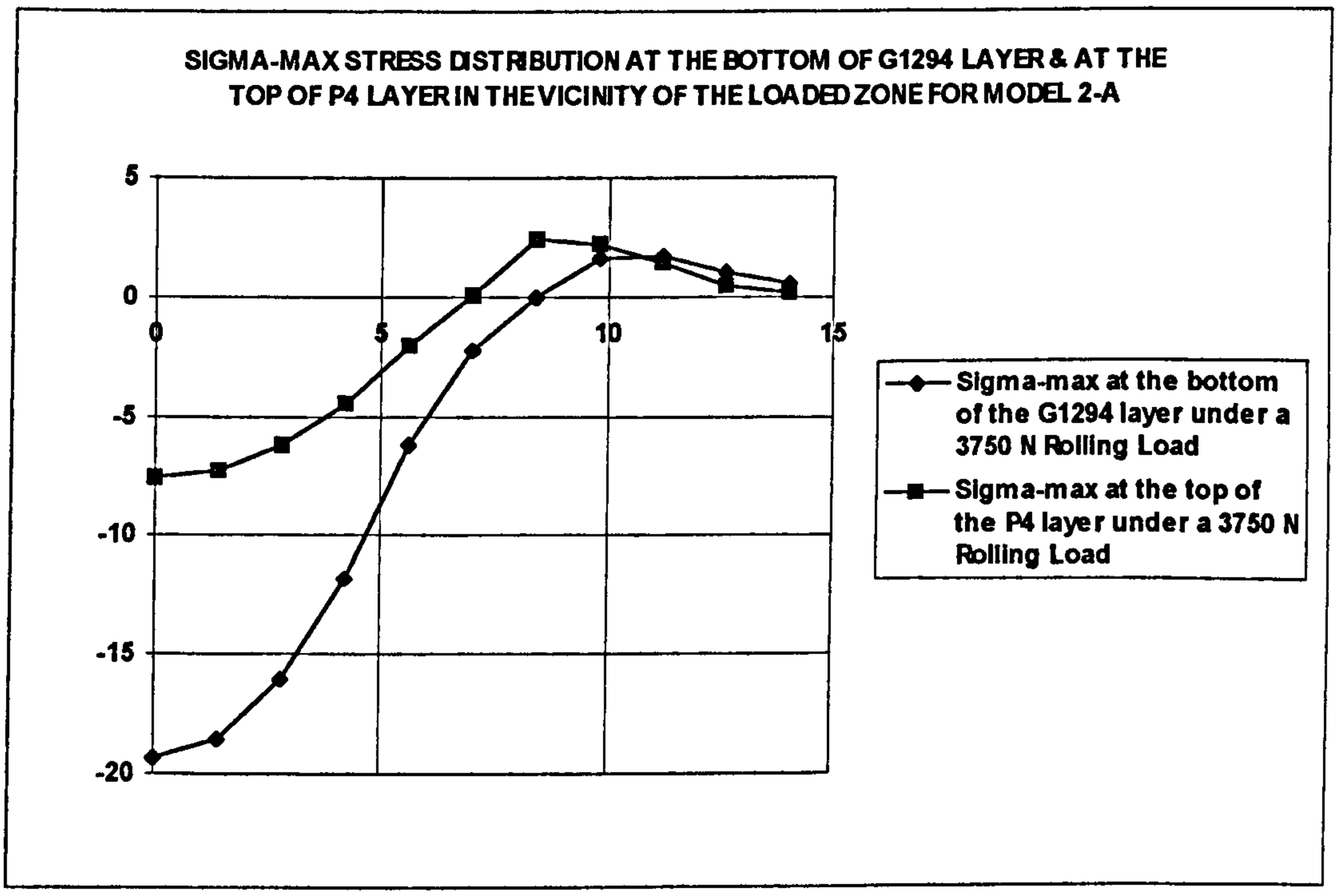

Figure 6-15-a-4: Sigma-1 (maximum) stress distribution in the vicinity of the load and the interface for Model 2-a {Compression (-), Tension (+)}

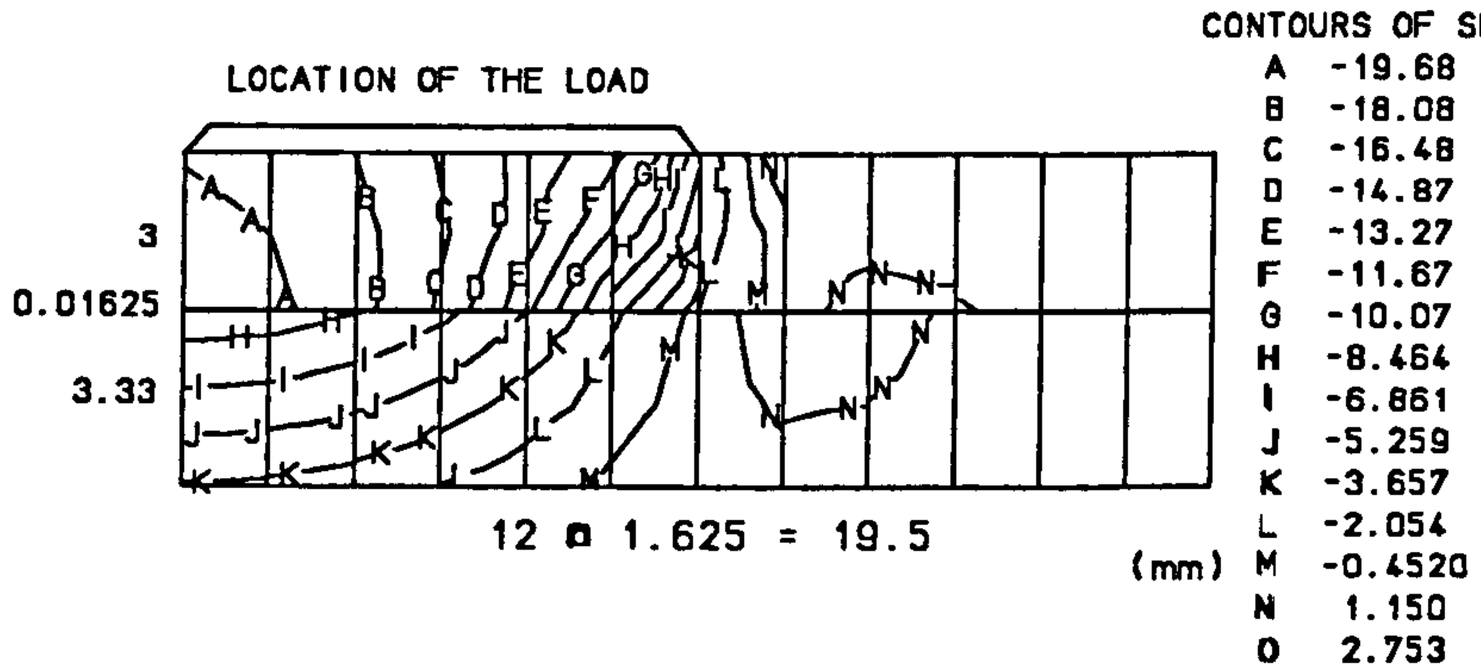

Figure 6-15-b-3: Contours of Sigma-1 (maximum) in the vicinity of the load and the interface for Model 2-b

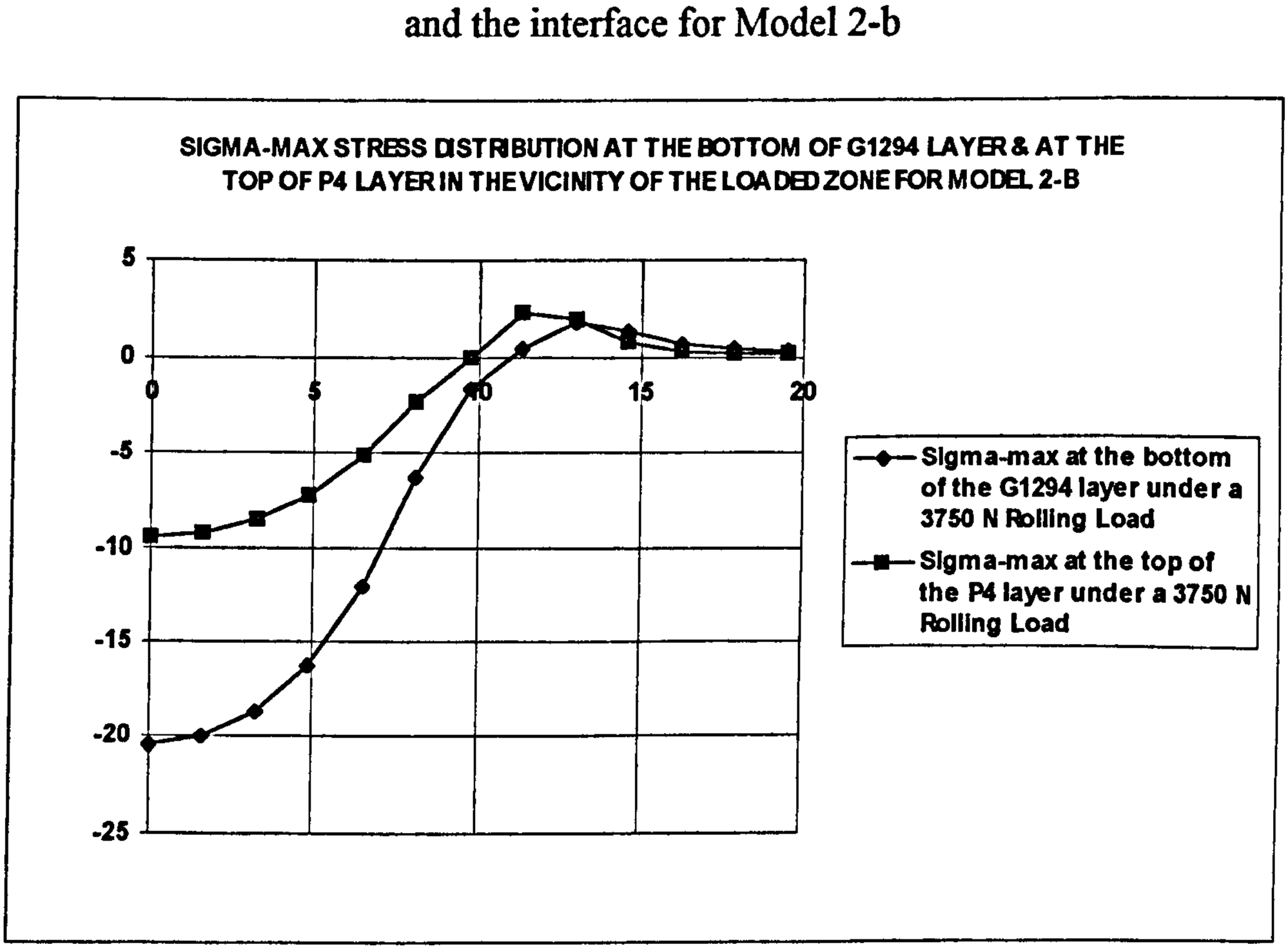

Figure 6-15-b-4: Sigma-1 (maximum) stress distribution in the vicinity of the load and the interface for Model 2-b {Compression (-), Tension (+)}

6-3-2-3 Model 3: G1194/Concrete

Age: 28 days
Load: 5000 N
Contact area: An elliptic area of diameters a= 15.5 mm & b = 11.5 mm

Specifications of the materials and layers:

G1194:

E = 10100 MPa (table 5-12)
υ = 0.32 (table 5-16)
Thickness = 3 mm
Nonlinear properties idealisation: (figure 5-5-c-2)

Interface between G1194 and concrete using Gprime as the primer:

E = 5780 t (table 6-3)
t = 0.01B (table 6-3)
υ = 0.25 (table 6-3)
Cohesion = 4.20 MPa (table 5-22)
Coefficient of friction = 2.88 (table 5-22)
where t is the interface thickness (mm), and B is the width of the finite elements at the interface.

Concrete:

E = 23300 MPa (table 5-2)
υ = 0.18 (table 5-16)
Thickness = 50 mm
Nonlinear properties idealisation: (figure 5-1-b)

Pressure distribution representation over the incremental lengths, MPa:

Model No.	Length 1	Length 2	Length 3	Length 4	Length 5	Length 6
Model 3-a	57.4	55.1	50.0	41.2	25.2	-
Model 3-b	57.5	55.9	52.5	46.9	38.2	23.1

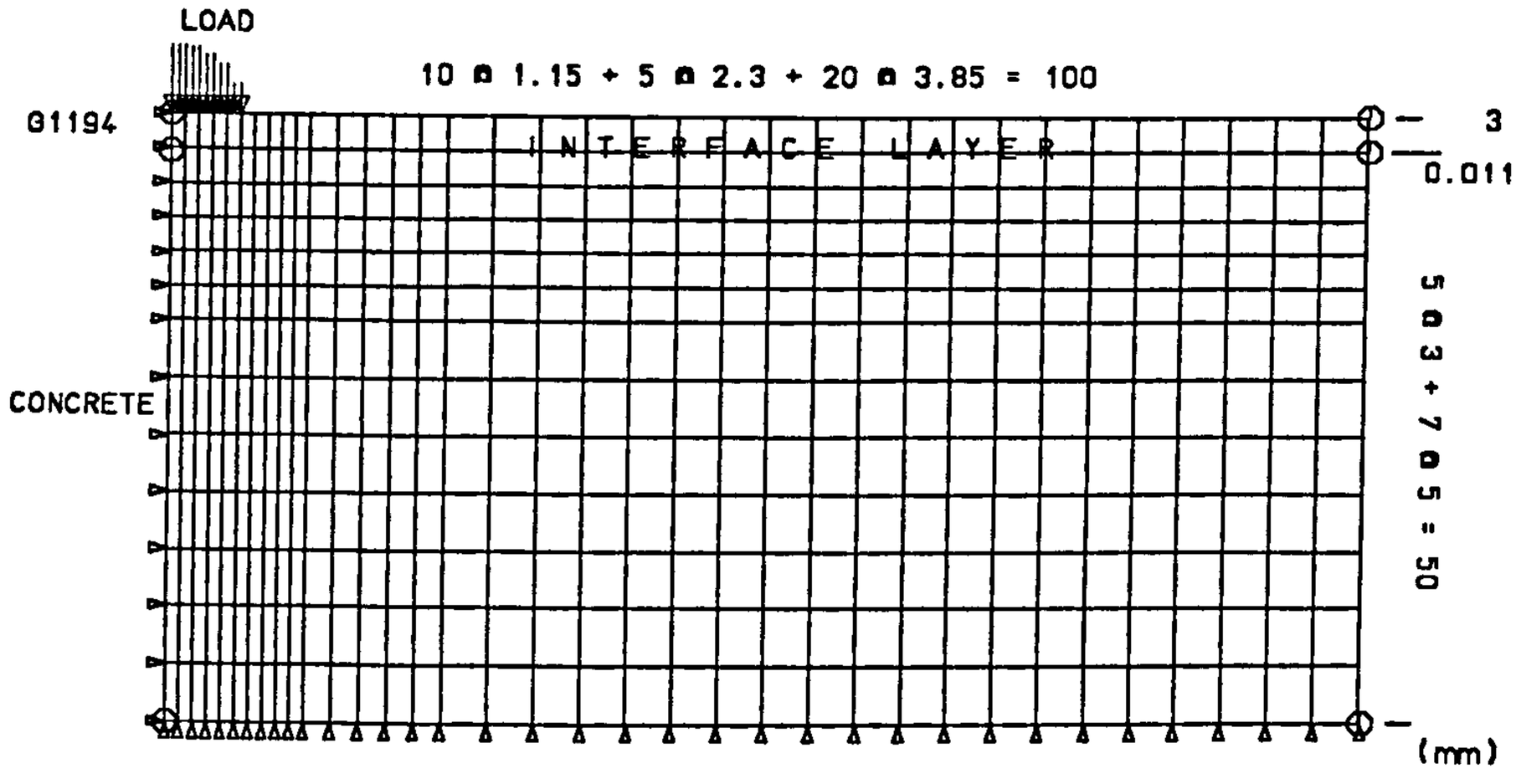

Figure 6-16-a: The finite element mesh for Model 3-a
(Load distribution over the short diameter of the contact area is considered)

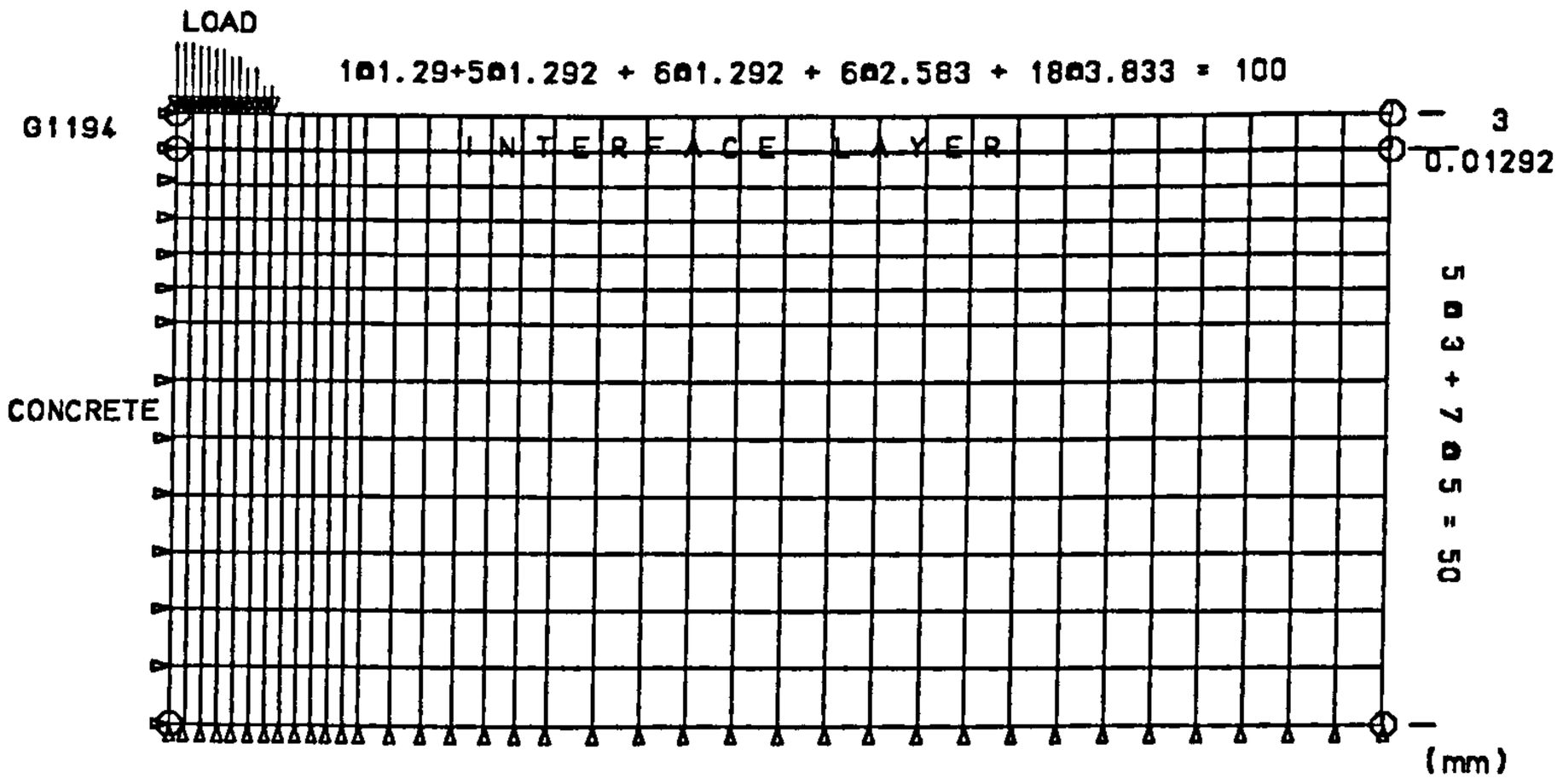

Figure 6-16-b: The finite element mesh for Model 3-b
(Load distribution over the long diameter of the contact area is considered)

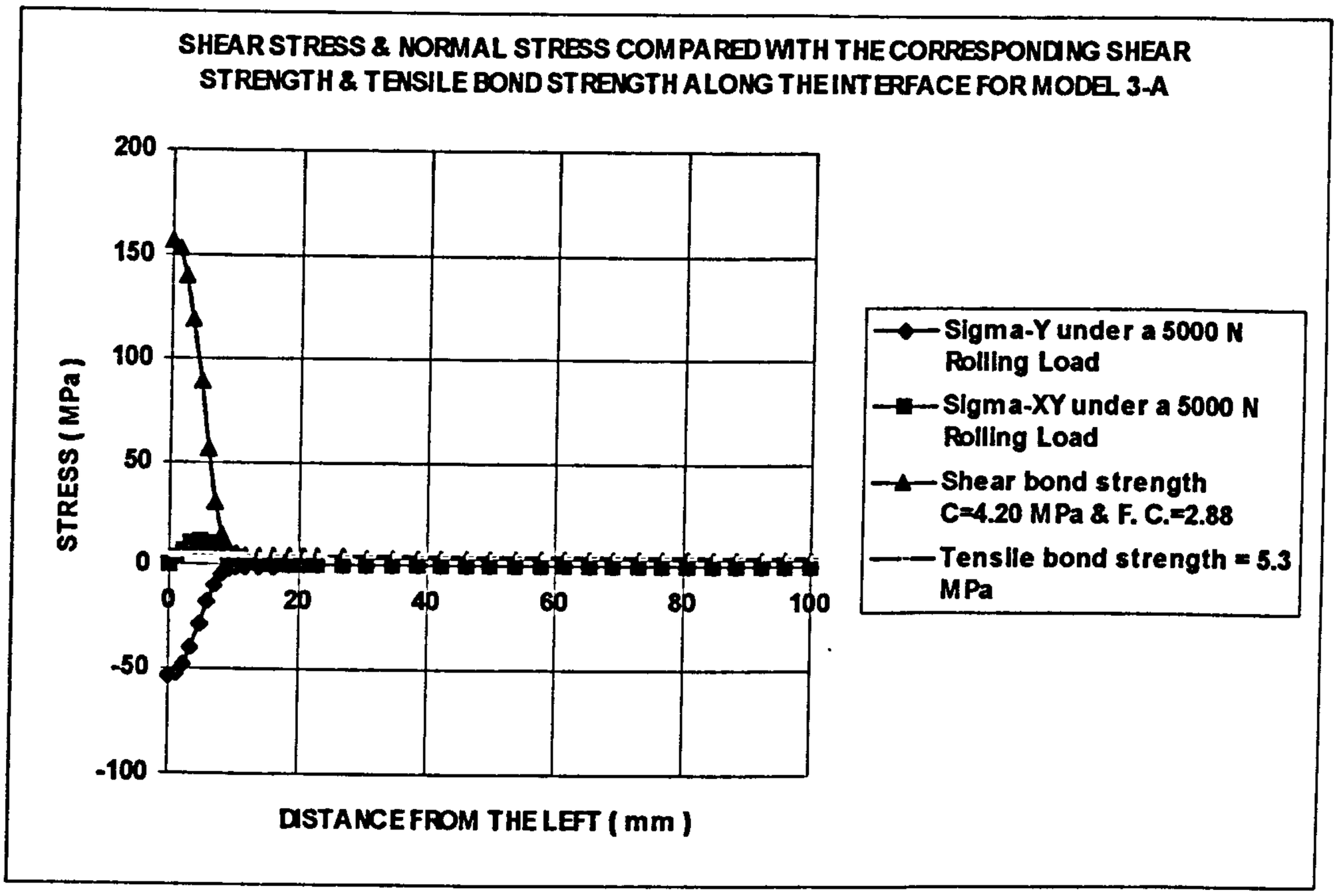

Figure 6-16-a-1: Model 3-a, G1194/Concrete {Compression (-), Tension (+)}

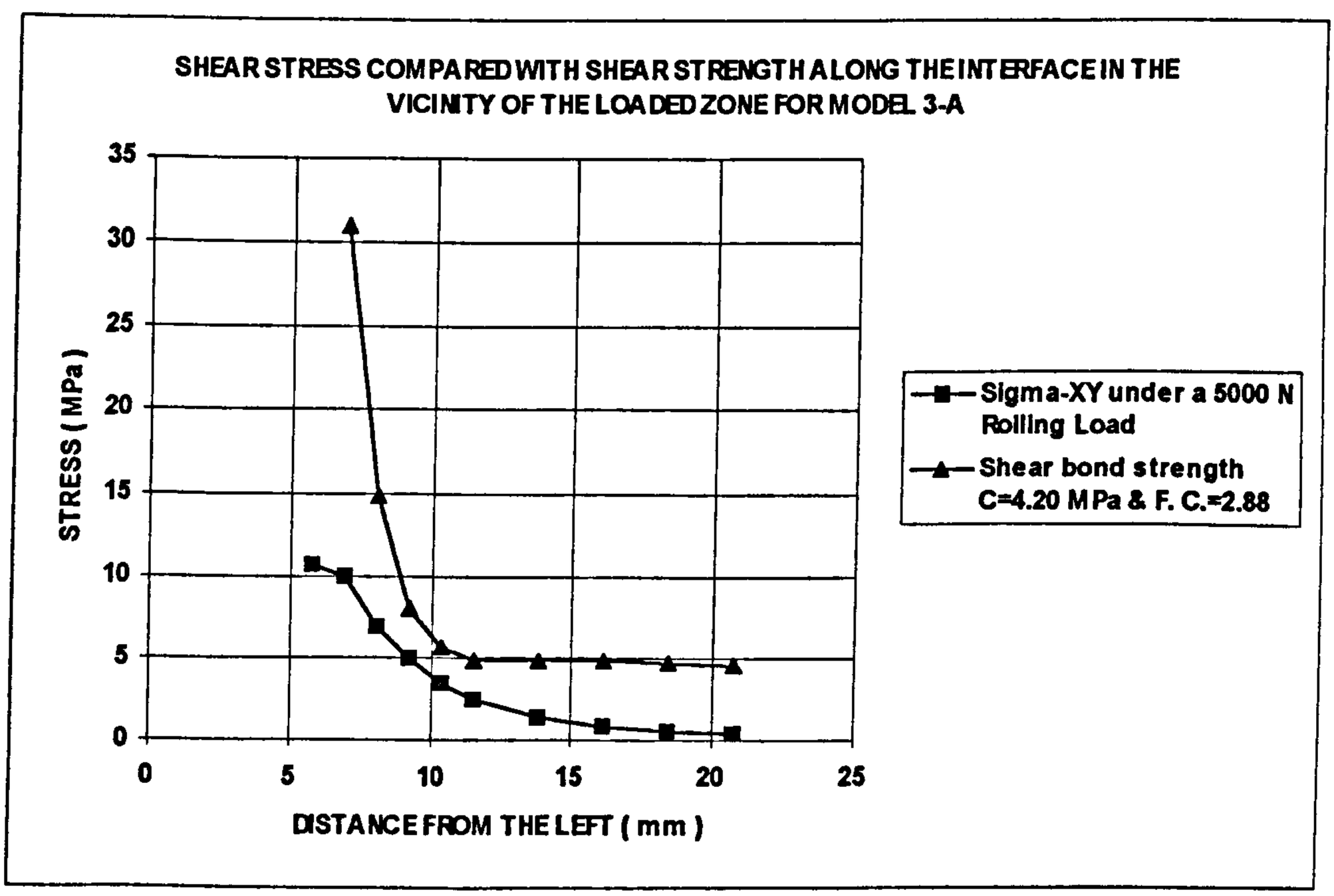

Figure 6-16-a-2 (Zoom): Model 3-a, G1194/Concrete
(No delamination occurs) ***AGREEMENT***

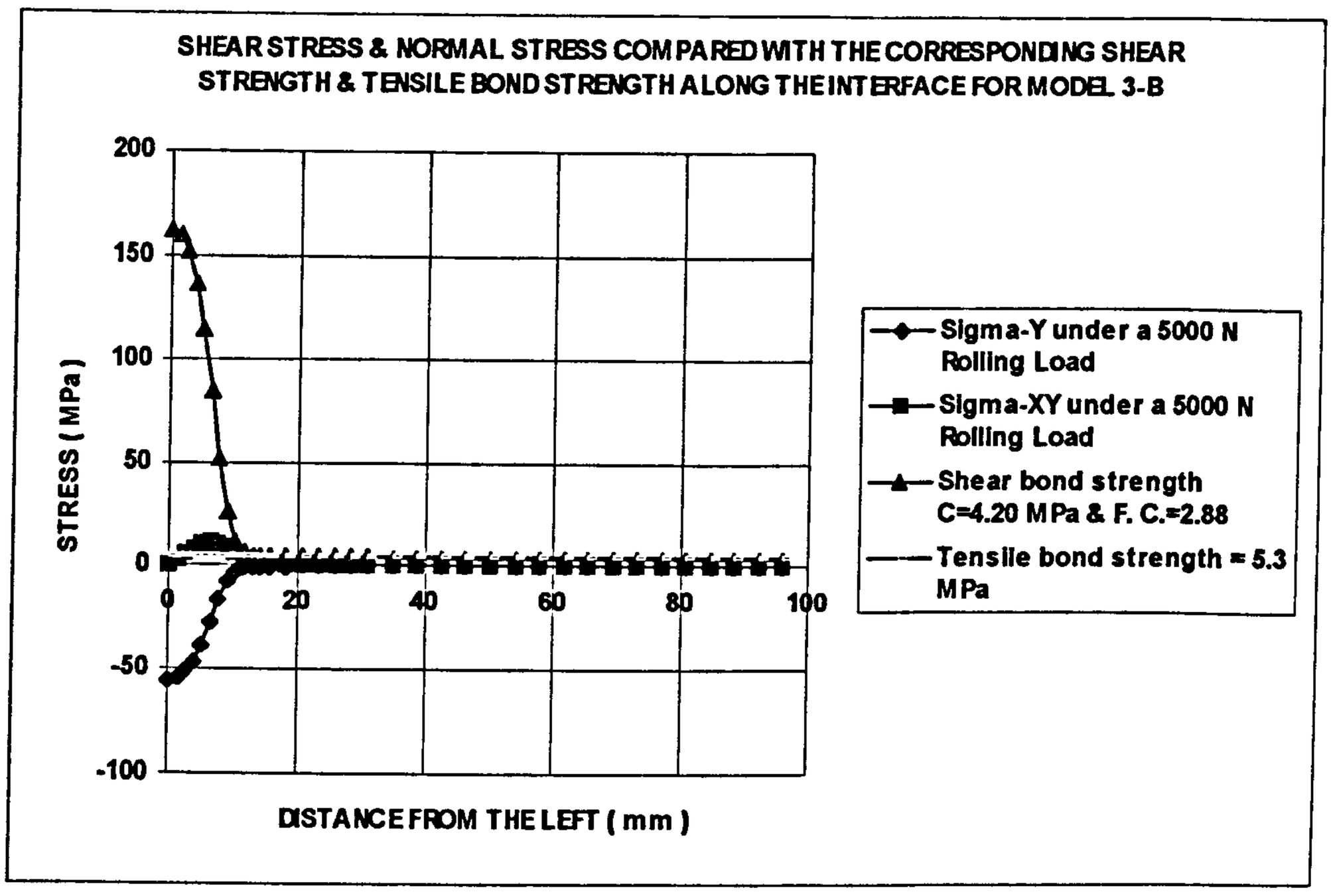

Figure 6-16-b-1: Model 3-b, G1194/Concrete {Compression (-), Tension (+)}

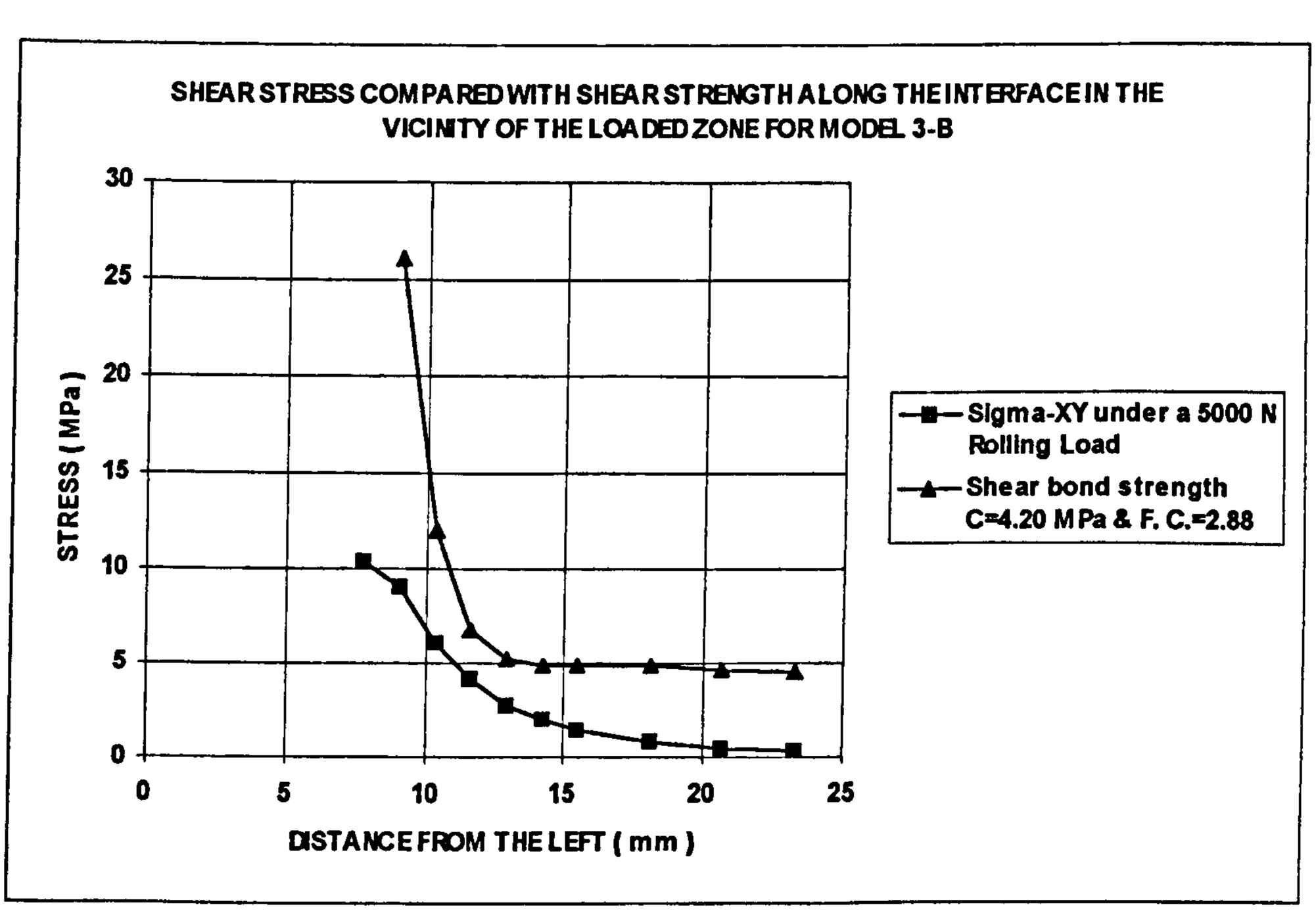

Figure 6-16-b-2 (Zoom): Model 3-b, G1194/Concrete
(No delamination occurs) ***AGREEMENT***

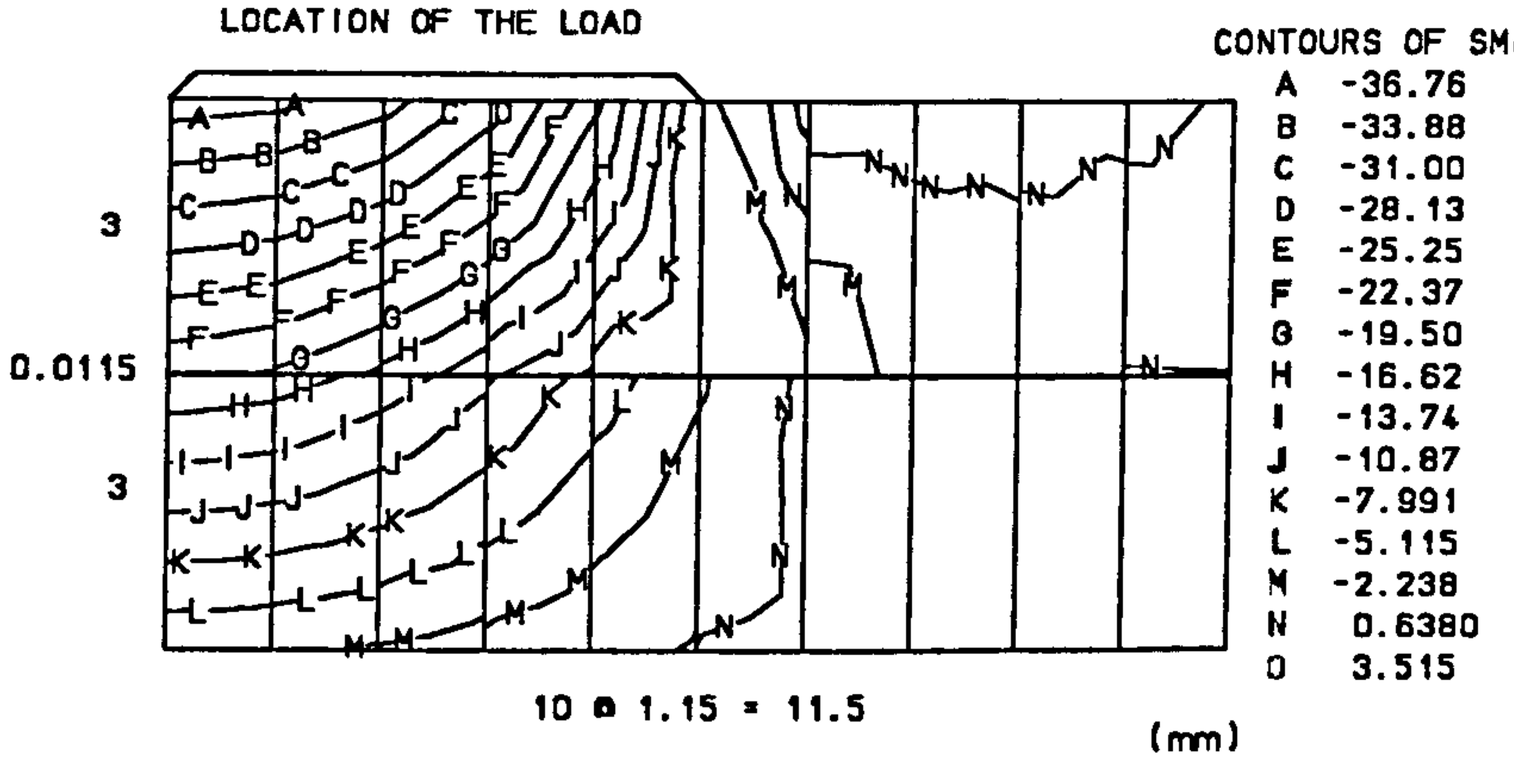

Figure 6-16-a-3: Contours of Sigma-1 (maximum) in the vicinity of the load and the interface for Model 3-a

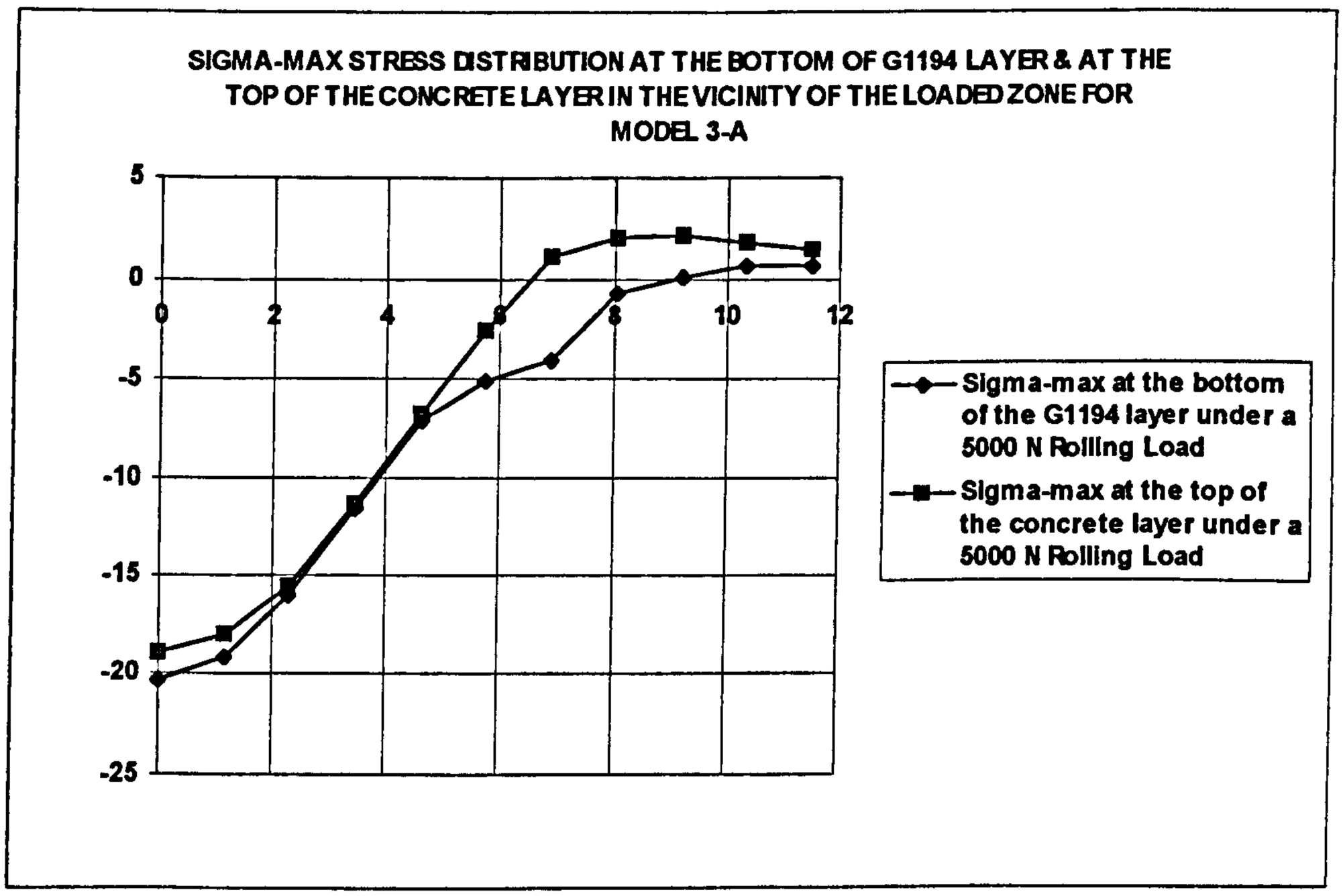

Figure 6-16-a-4: Sigma-1 (maximum) stress distribution in the vicinity of the load and the interface for Model 3-a {Compression (-), Tension (+)}

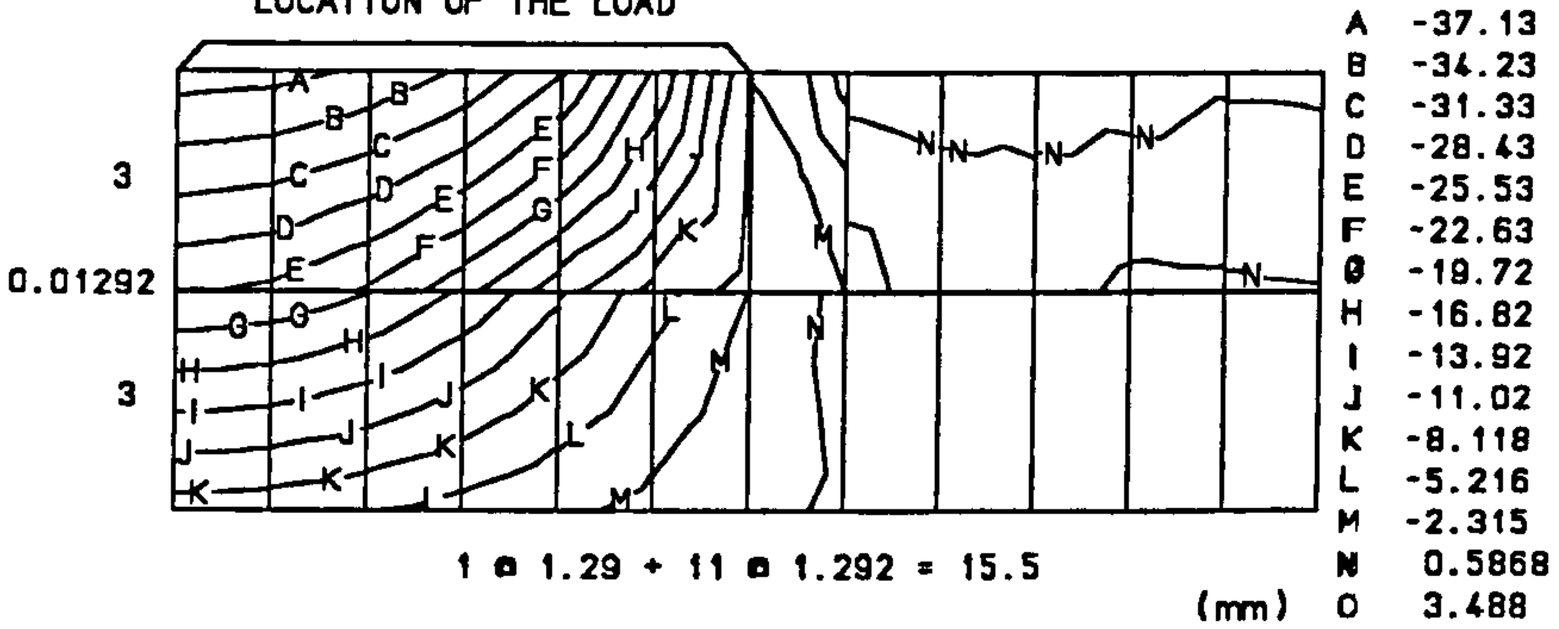

Figure 6-16-b-3: Contours of Sigma-1 (maximum) in the vicinity of the load and the interface for Model 3-b

Figure 6-16-b-4: Sigma-1 (maximum) stress distribution in the vicinity of the load and the interface for Model 3-b {Compression (-), Tension (+)}

6-3-2-4 Model 4: G1194/Concrete

Age: 56 days
Load: 5000 N
Contact area: An elliptic area of diameters a= 15.0 mm & b = 11.5 mm

Specifications of the materials and layers:

G1194:

E = 12400 MPa (table 5-12)
υ = 0.32 (table 5-16)
Thickness = 3 mm
Nonlinear properties idealisation: (figure 5-5-d-2)

Interface between G1194 and concrete using Pprime as the primer:

E = 6150 t (table 6-3)
t = 0.01B (table 6-3)
υ = 0.25 (table 6-3)
Cohesion = 1.47 MPa (table 5-22)
Coefficient of friction = 0.44 (table 5-22)
where t is the interface thickness (mm), and B is the width of the finite elements at the interface.

Concrete:

E = 23300 MPa (table 5-2)
υ = 0.18 (table 5-16)
Thickness = 50 mm
Nonlinear properties idealisation: (figure 5-1-b)

Pressure distribution representation over the incremental lengths, MPa:

Model No.	Length 1	Length 2	Length 3	Length 4	Length 5	Length 6
Model 3-a	59.4	56.9	51.7	42.6	26.0	-
Model 3-b	59.5	57.8	54.3	48.5	39.5	23.9

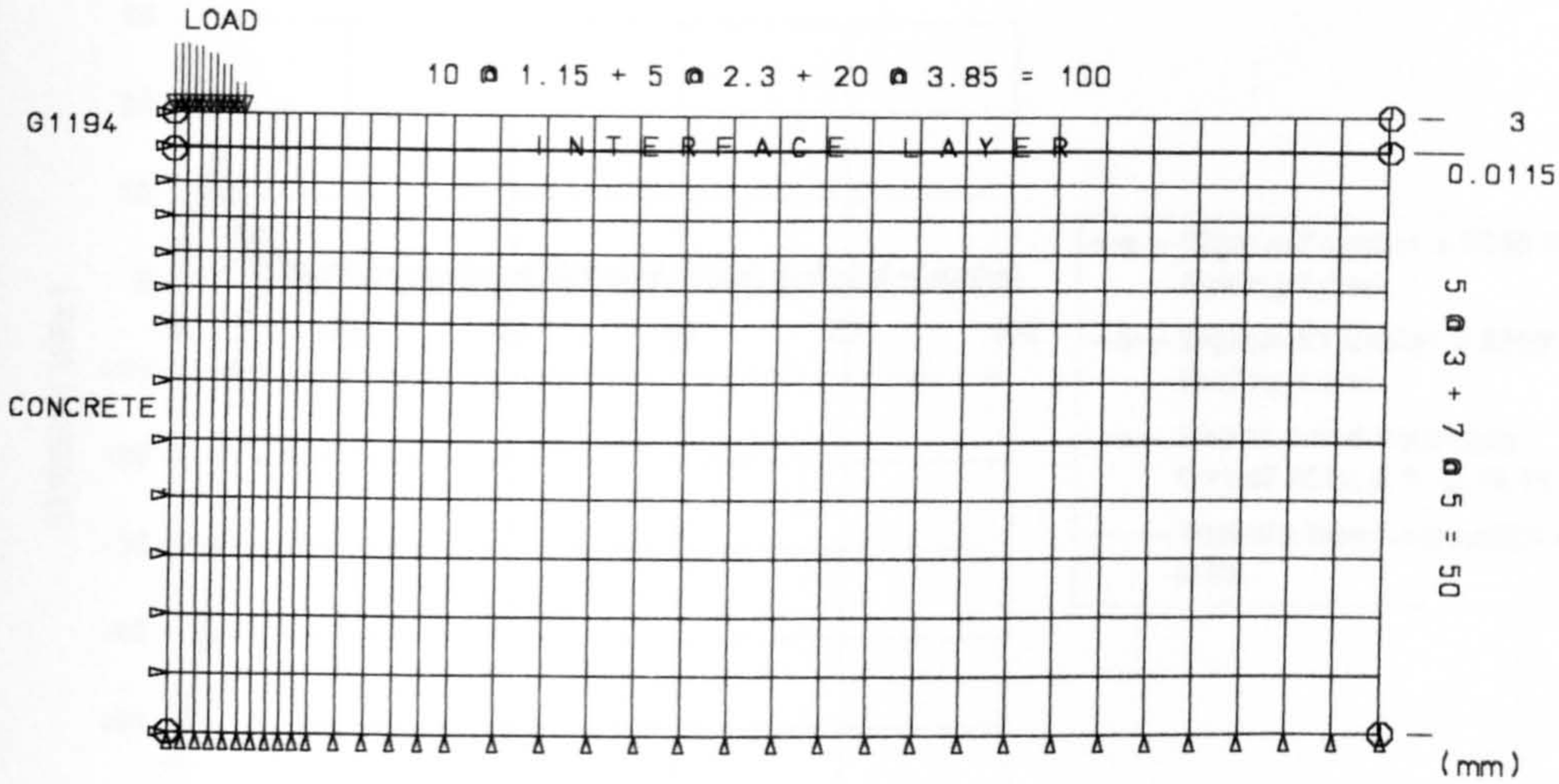

Figure 6-17-a: The finite element mesh for Model 4-a
(Load distribution over the short diameter of the contact area is considered)

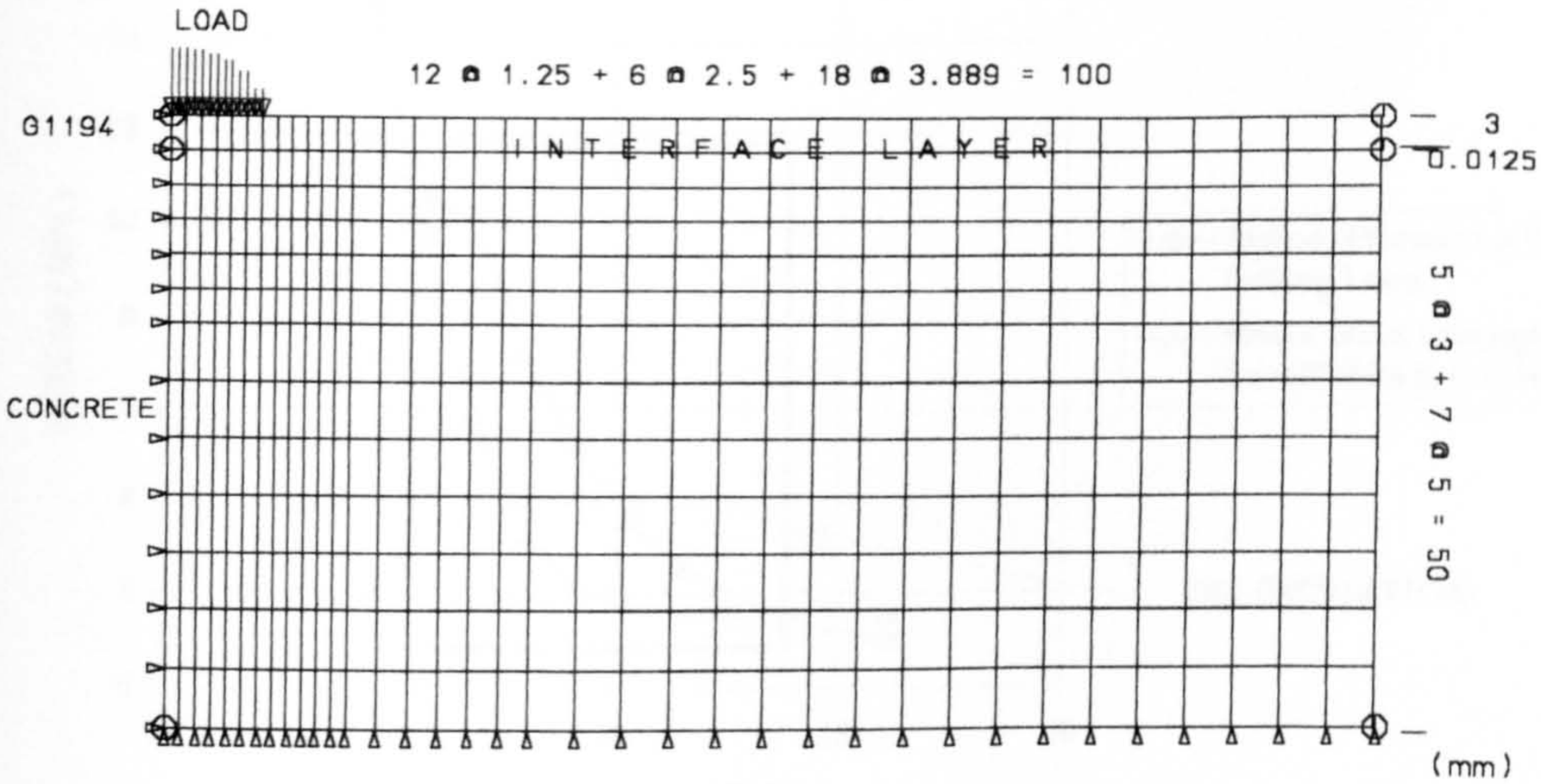

Figure 6-17-b: The finite element mesh for Model 4-b
(Load distribution over the long diameter of the contact area is considered)

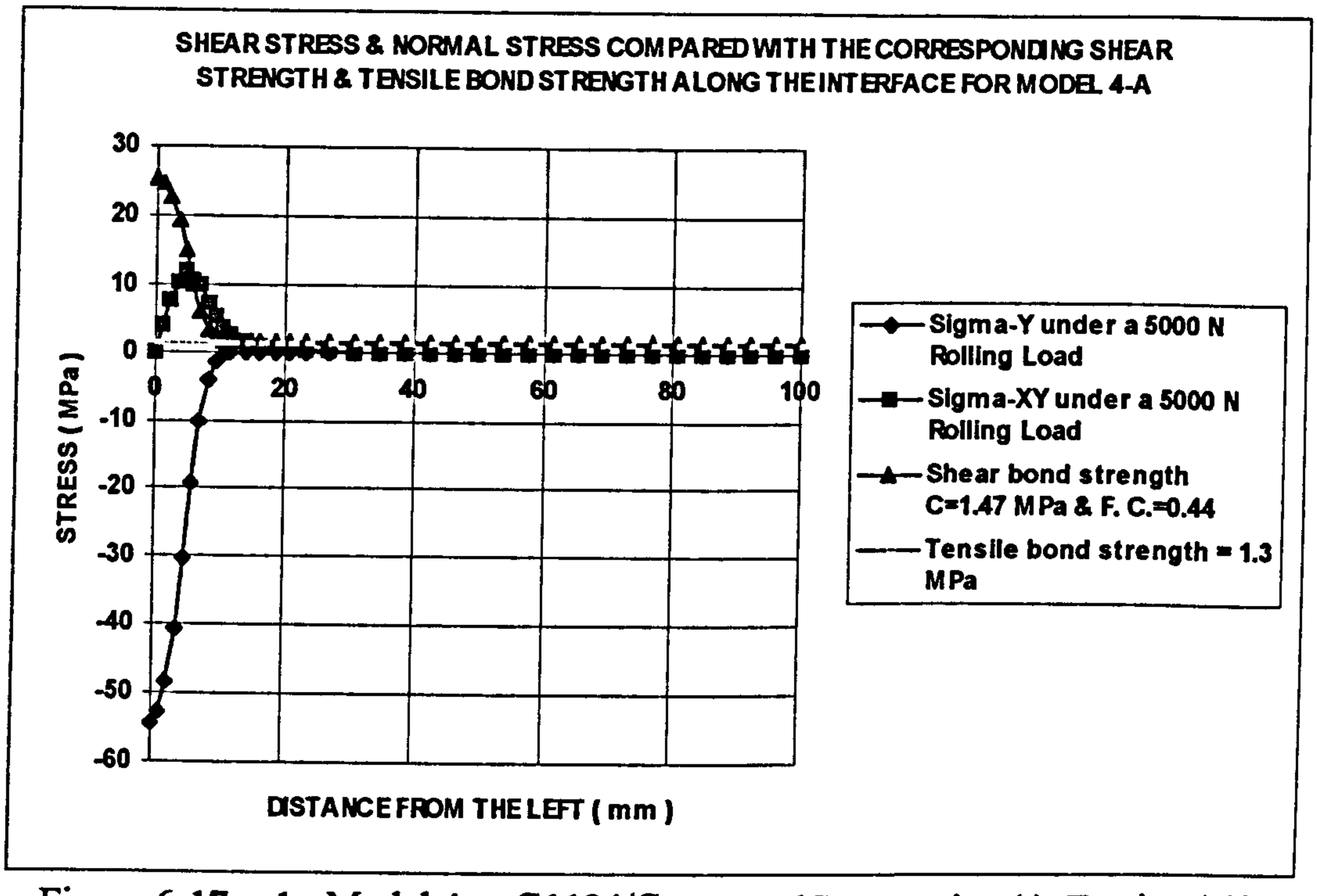

Figure 6-17-a-1: Model 4-a, G1194/Concrete {Compression (-), Tension (+)}

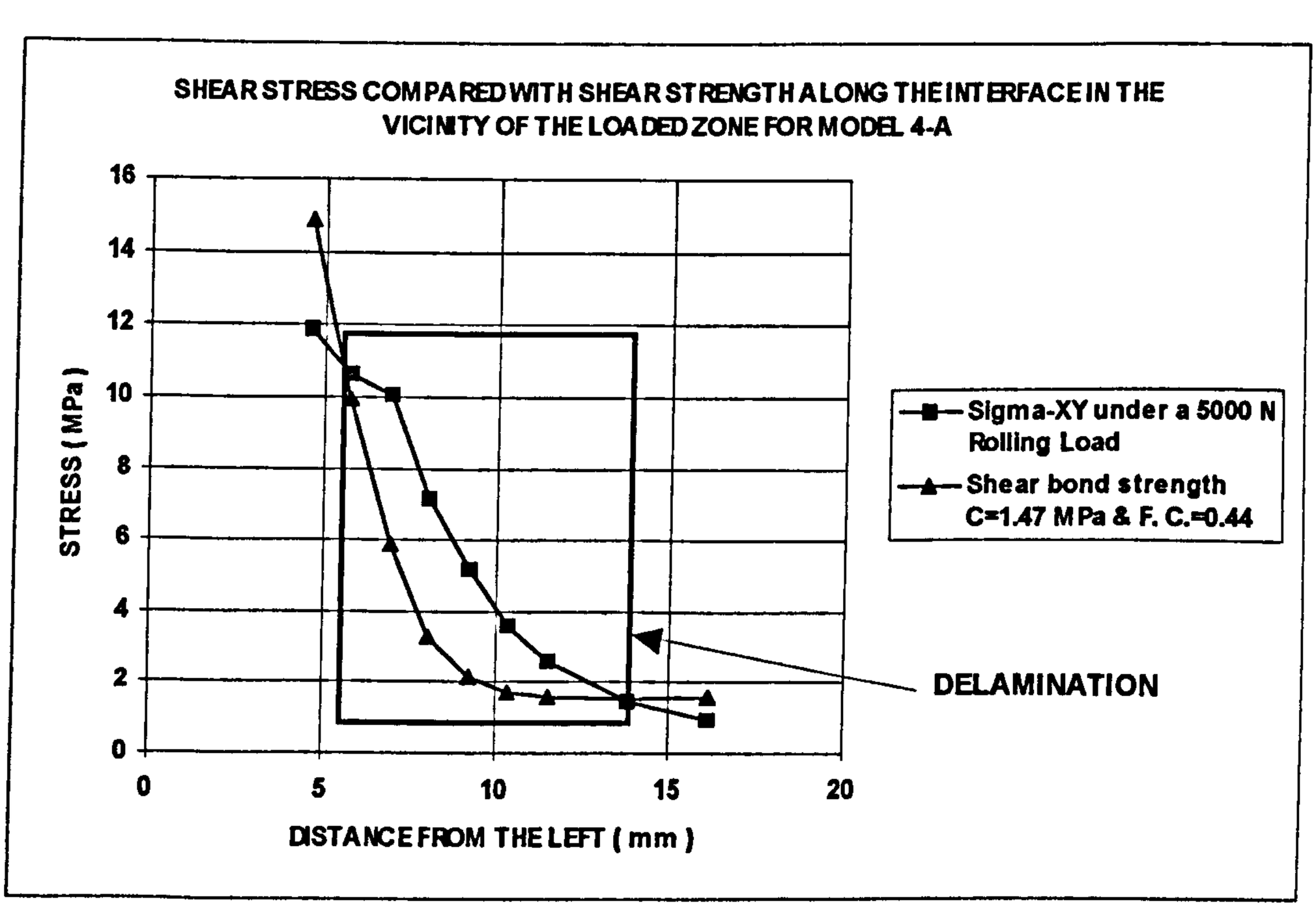

Figure 6-17-a-2 (Zoom): Model 4-a, G1194/Concrete
(Delamination occurs) ***AGREEMENT***

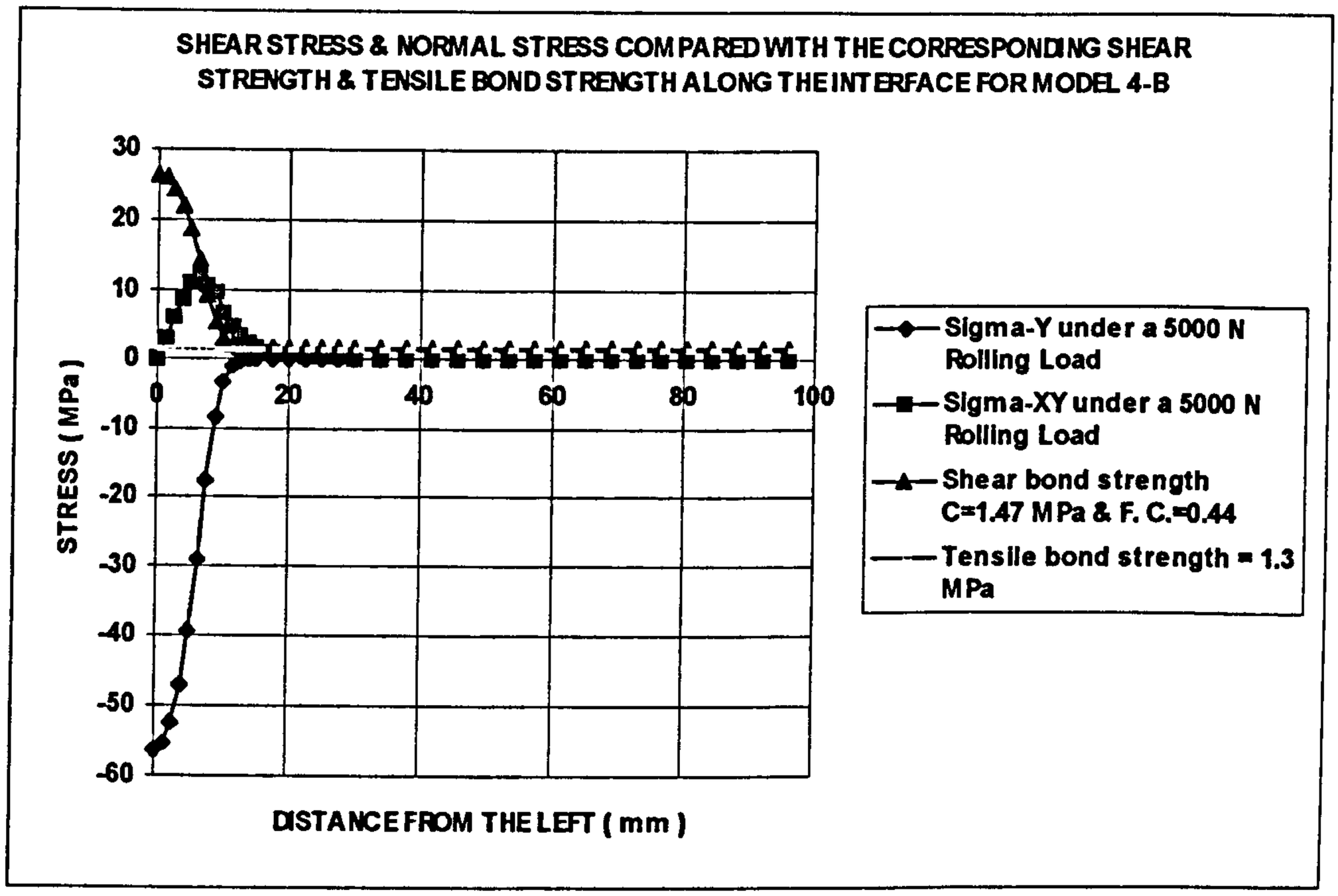

Figure 6-17-b-1: Model 4-b, G1194/Concrete {Compression (-), Tension (+)}

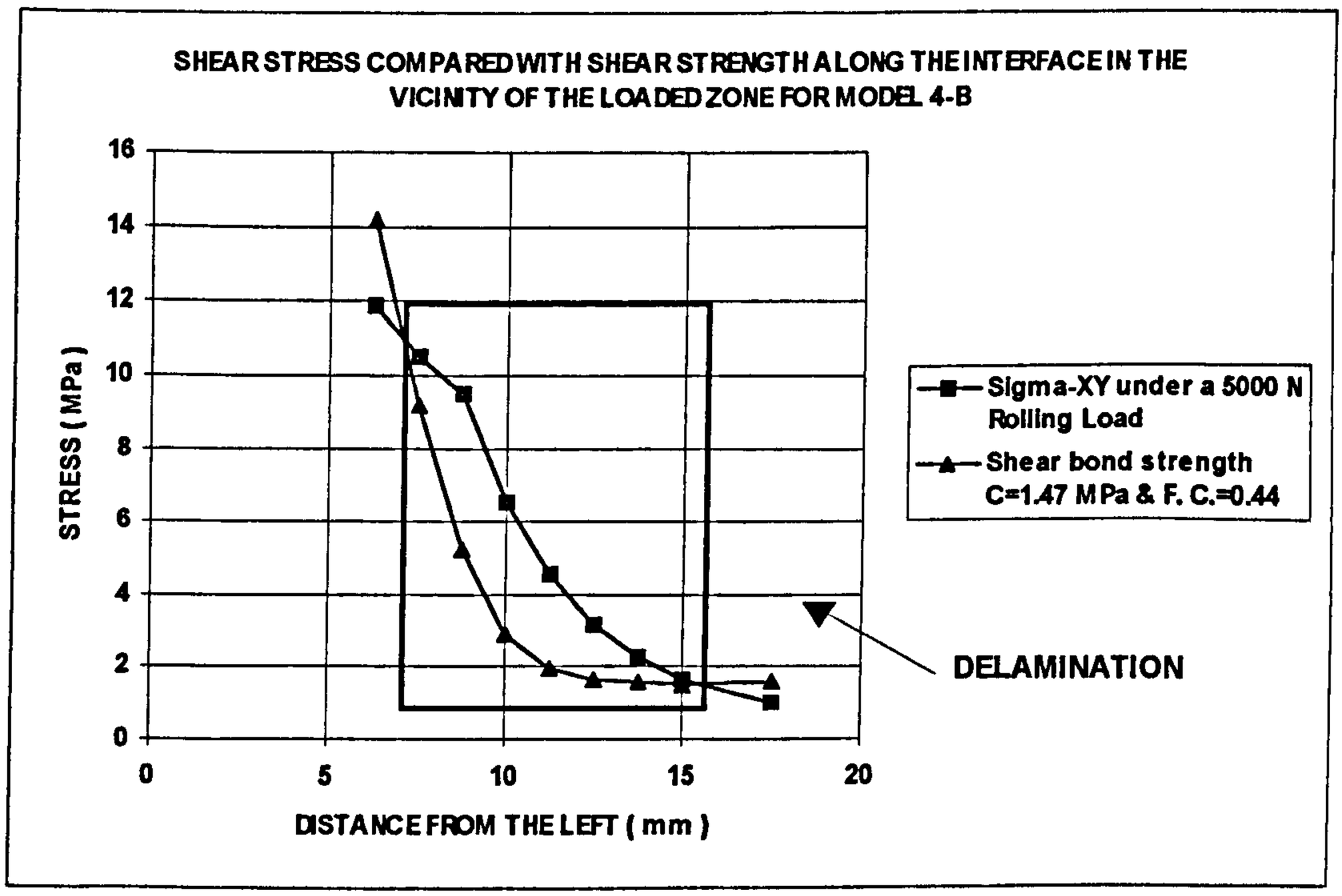

Figure 6-17-b-2 (Zoom): Model 4-b, G1194/Concrete
(Delamination occurs) ***AGREEMENT***

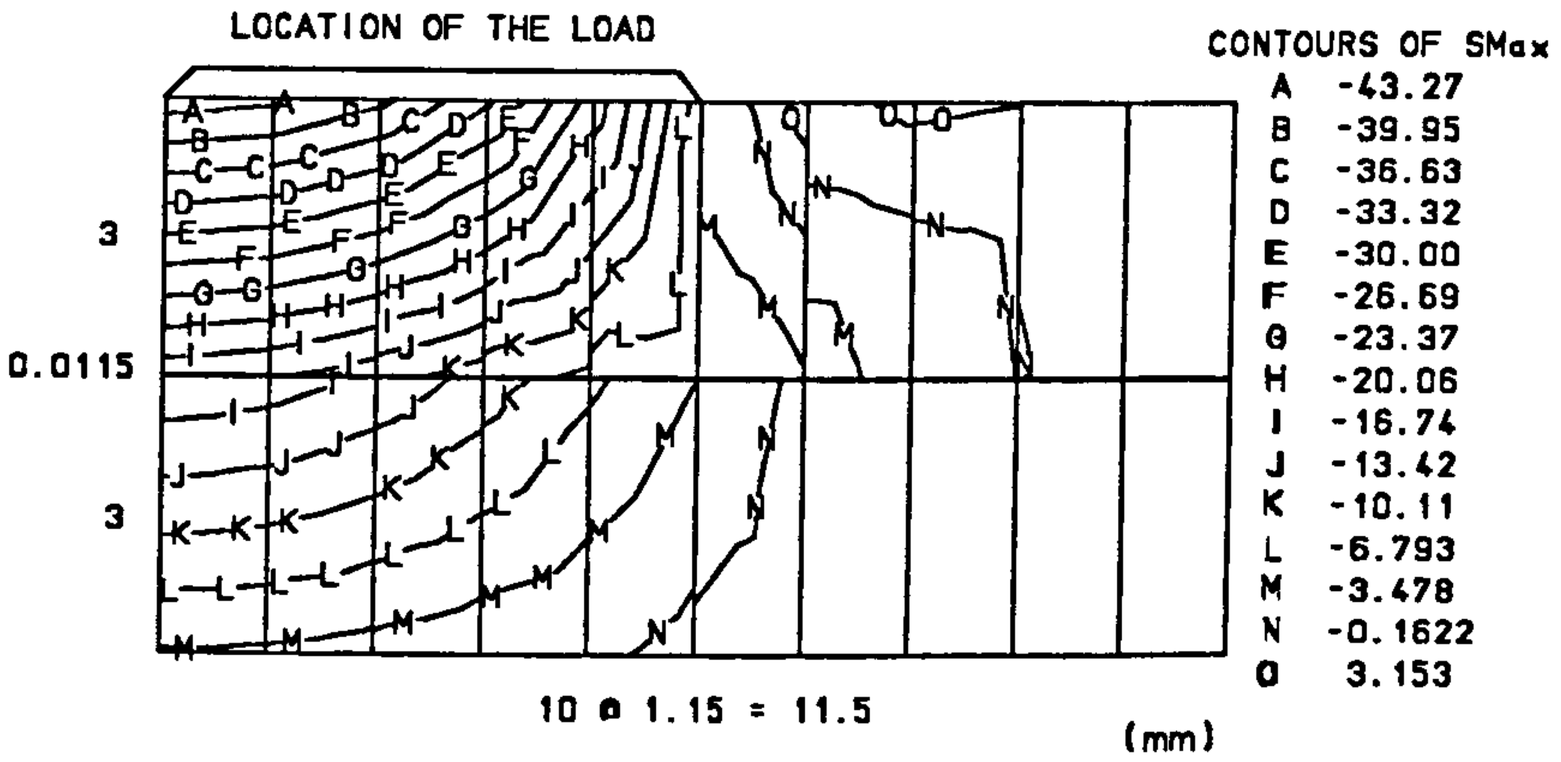

Figure 6-17-a-3: Contours of Sigma-1 (maximum) in the vicinity of the load and the interface for Model 4-a

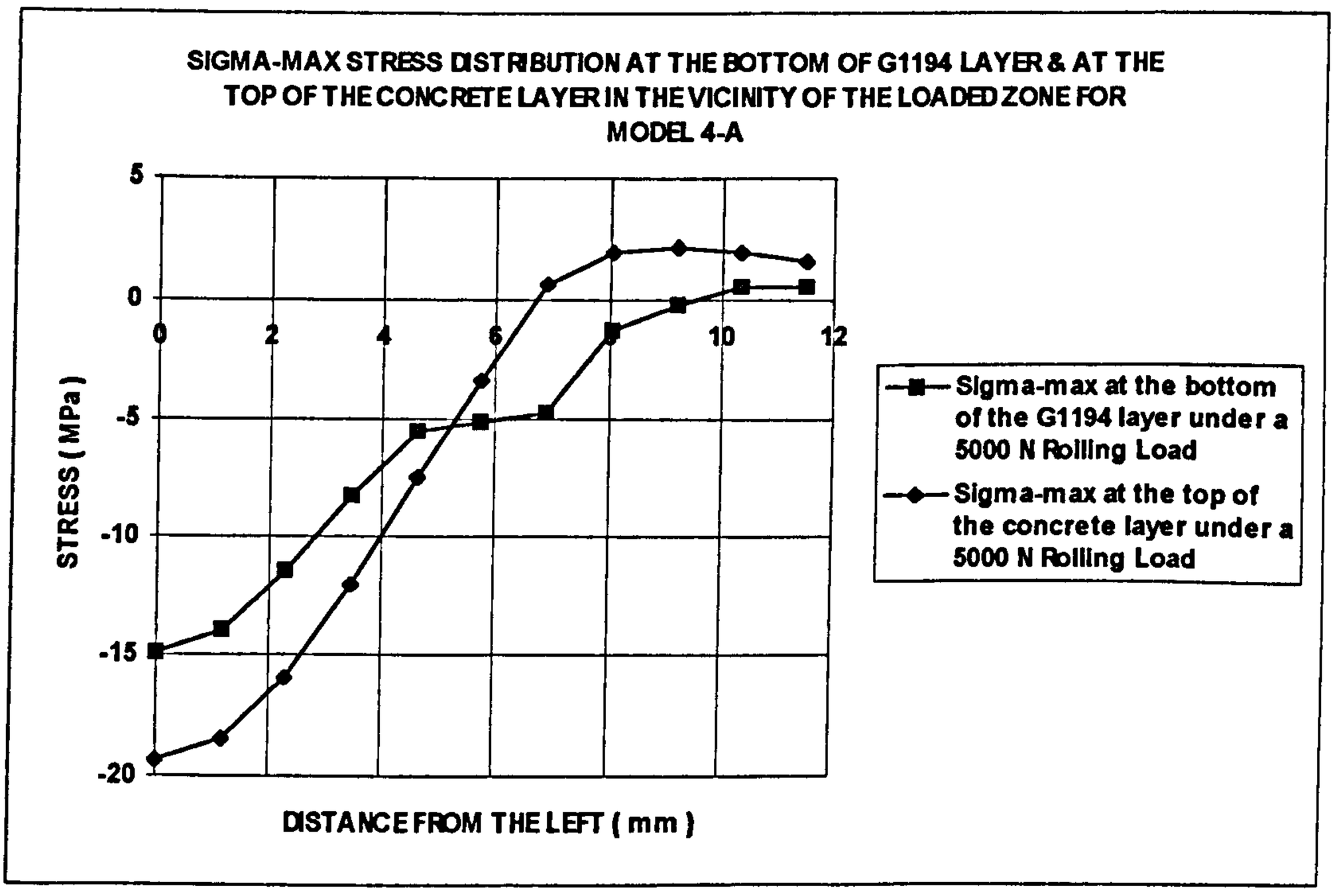

Figure 6-17-a-4: Sigma-1 (maximum) stress distribution in the vicinity of the load and the interface for Model 4-a {Compression (-), Tension (+)}

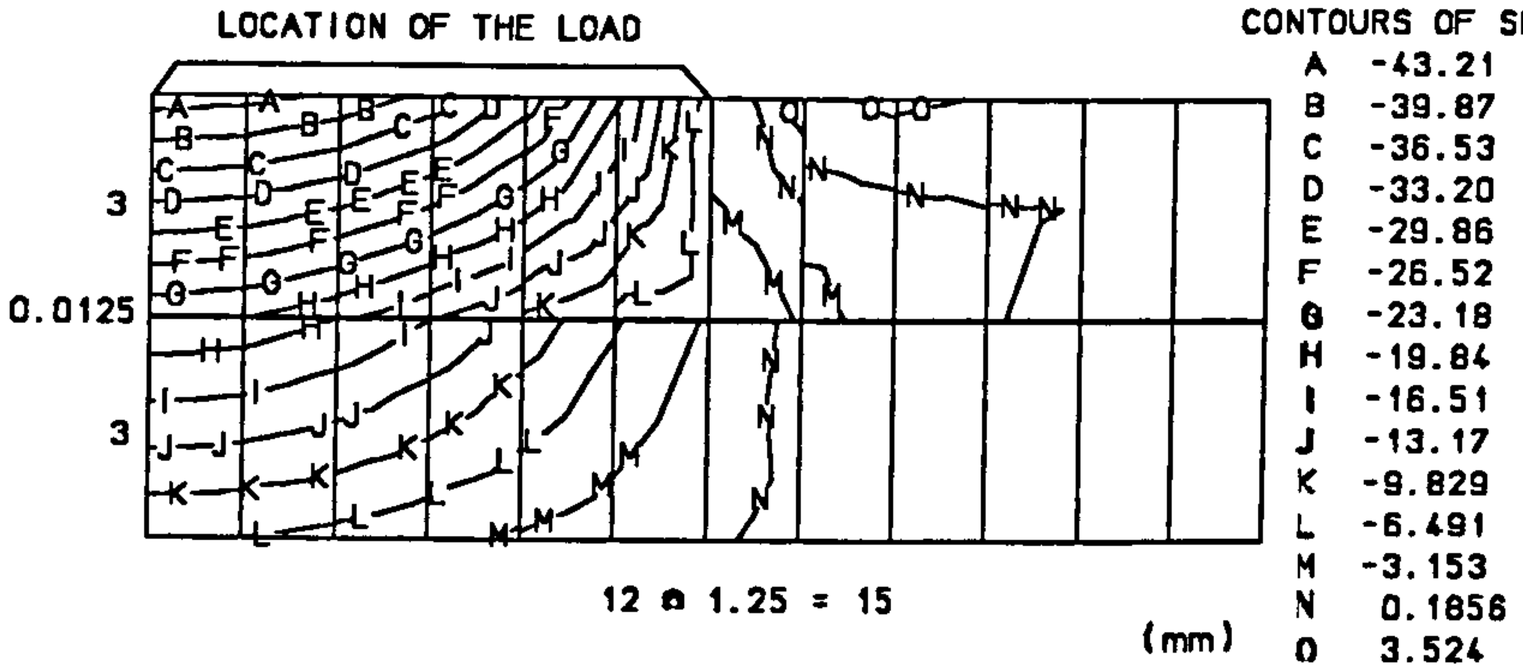

Figure 6-17-b-3: Contours of Sigma-1 (maximum) in the vicinity of the load and the interface for Model 4-b

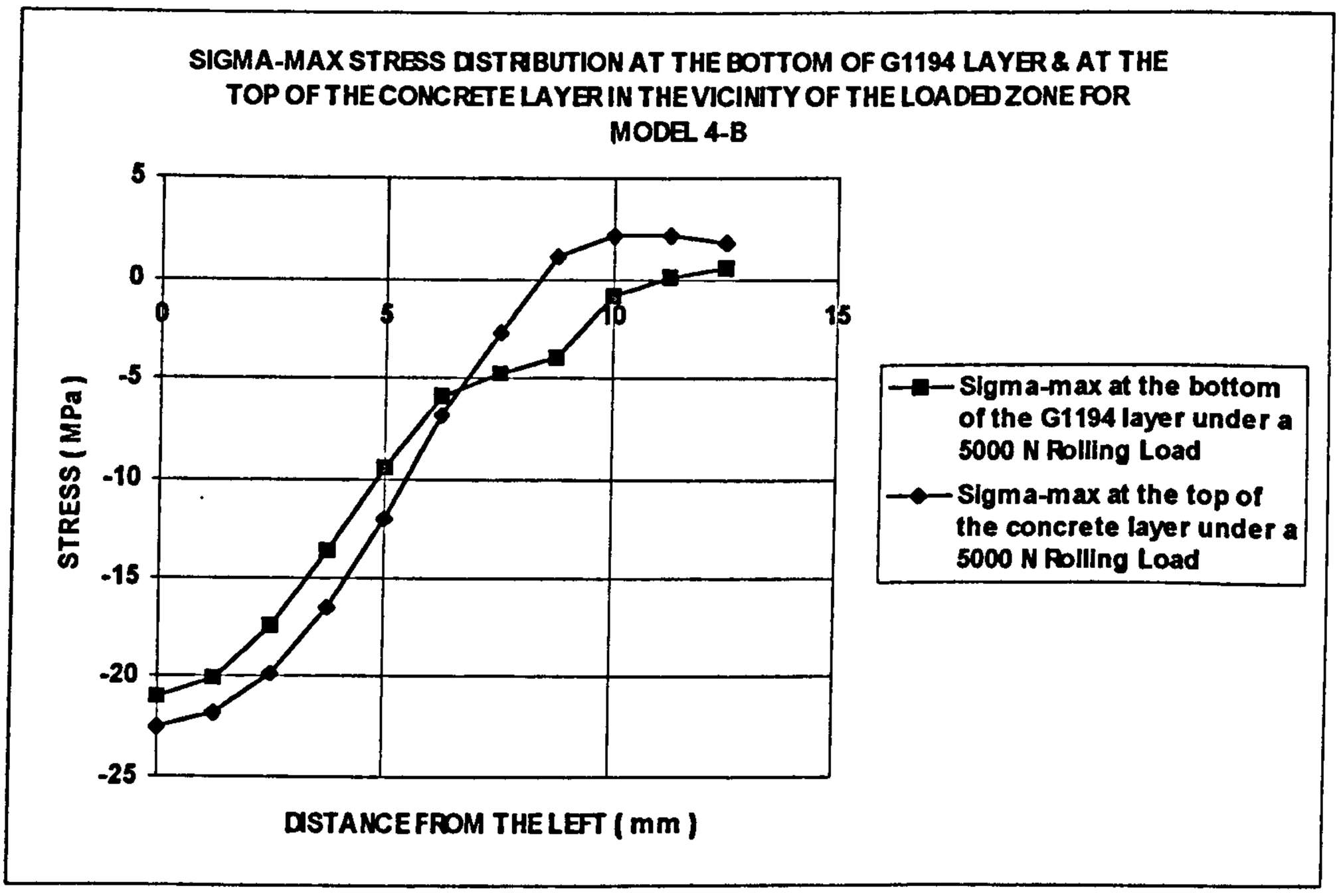

Figure 6-17-b-4: Sigma-1 (maximum) stress distribution in the vicinity of the load and the interface for Model 4-b {Compression (-), Tension (+)}

6-3-2-5 Model 5: G1294/Concrete

Age: 28 days
Load: 5000 N
Contact area: An elliptic area of diameters a= 21 mm & b = 15 mm

Specifications of the materials and layers:

G1294:

E = 1700 MPa (table 5-15)
υ = 0.38 (table 5-16)
Thickness = 3 mm
Nonlinear properties idealisation: (figure 5-6-b-2)

Interface between G1194 and concrete using Gprime as the primer:

E = 2420 t (table 6-3)
t = 0.01B (table 6-3)
υ = 0.28 (table 6-3)
Cohesion = 1.94 MPa (table 5-22)
Coefficient of friction = 0.40 (table 5-22)
where t is the interface thickness (mm), and B is the width of the finite elements at the interface.

Concrete:

E = 23300 MPa (table 5-2)
υ = 0.18 (table 5-16)
Thickness = 50 mm
Nonlinear properties idealisation: (figure 5-1-b)

Pressure distribution representation over the incremental lengths, MPa:

Model No.	Length 1	Length 2	Length 3	Length 4	Length 5	Length 6
Model 3-a	32.5	31.2	28.3	23.3	14.2	-
Model 3-b	32.5	31.6	29.7	26.5	21.6	13.1

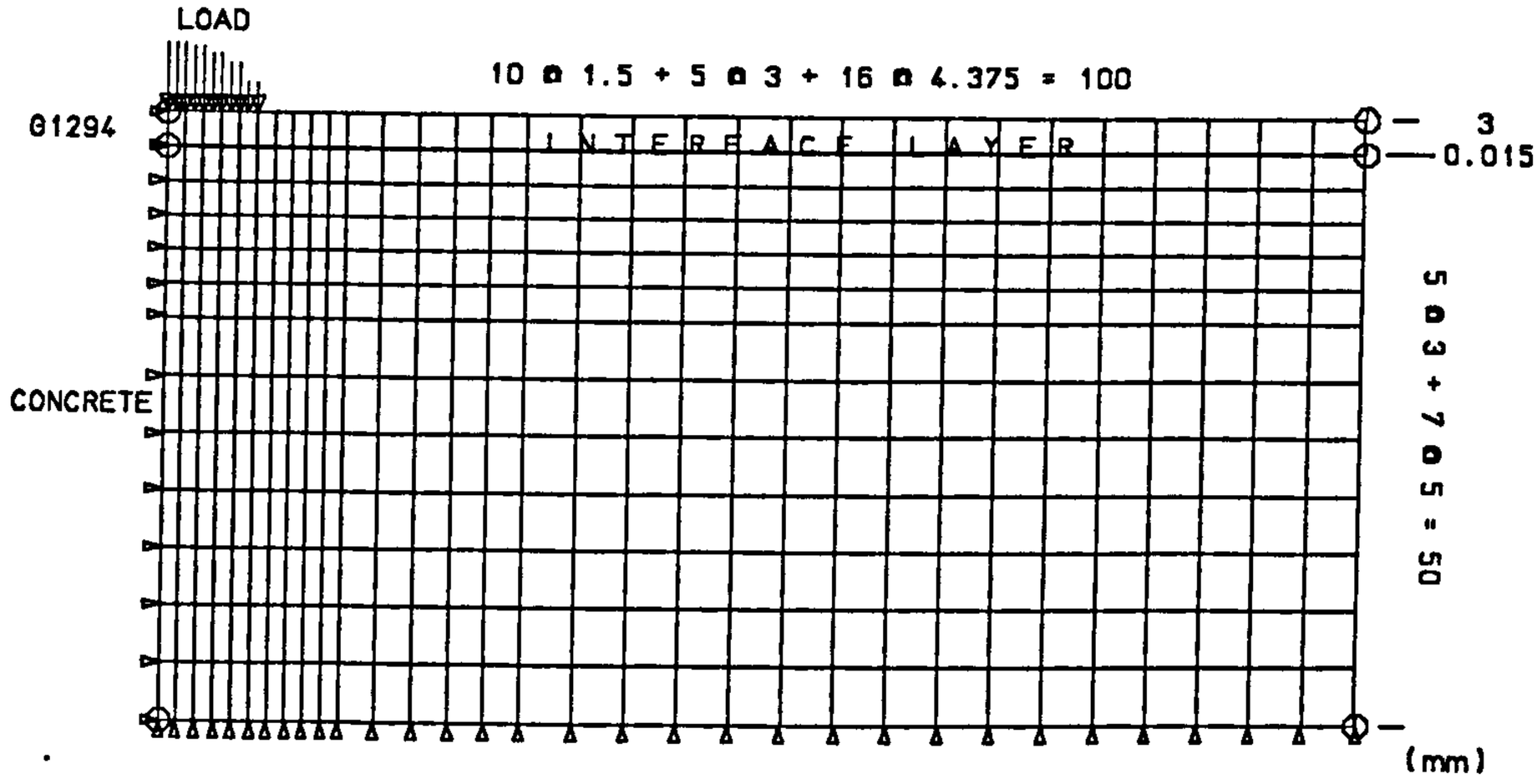

Figure 6-18-a: The finite element mesh for Model 5-a
(Load distribution over the short diameter of the contact area is considered)

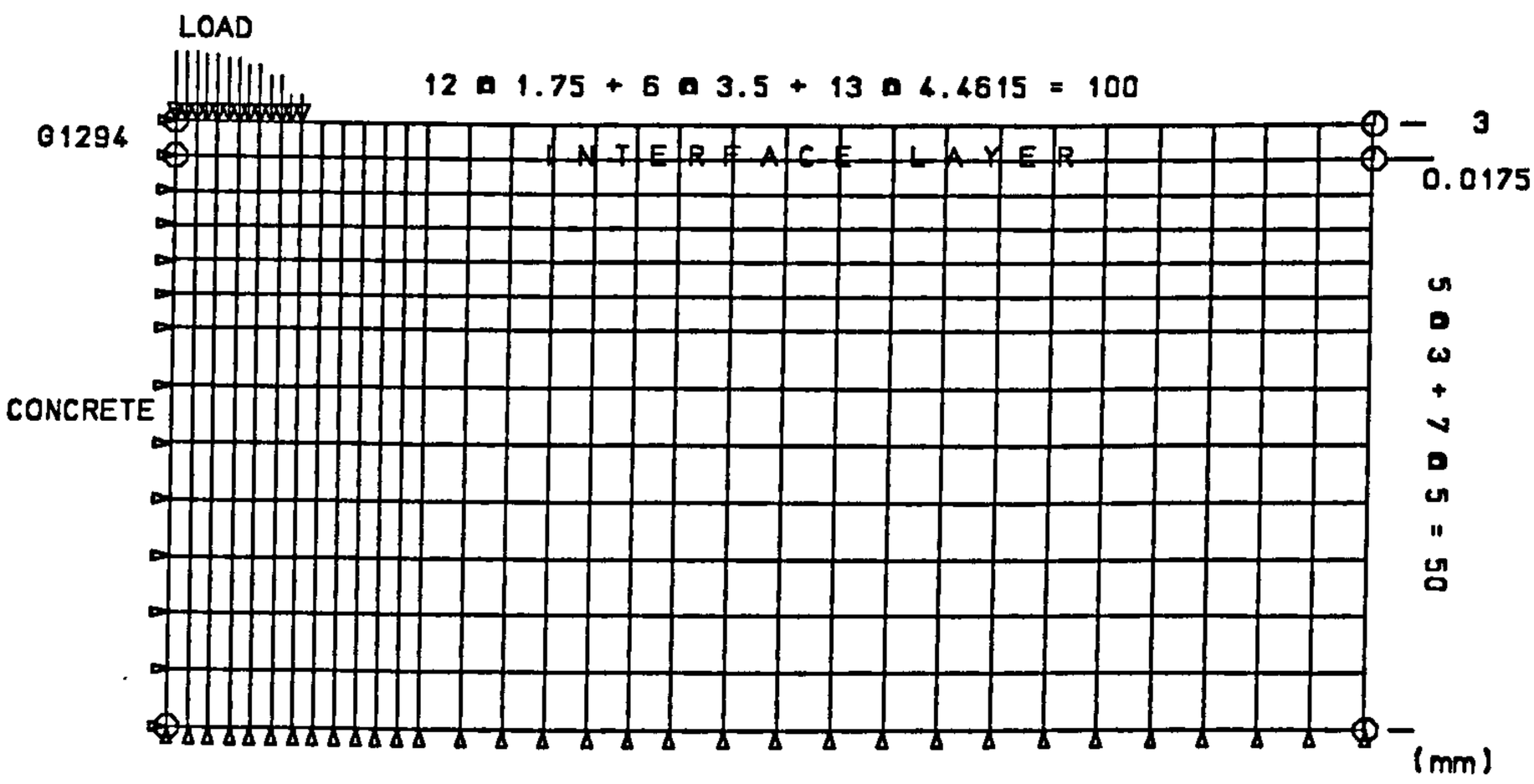

Figure 6-18-b: The finite element mesh for Model 5-b
(Load distribution over the long diameter of the contact area is considered)

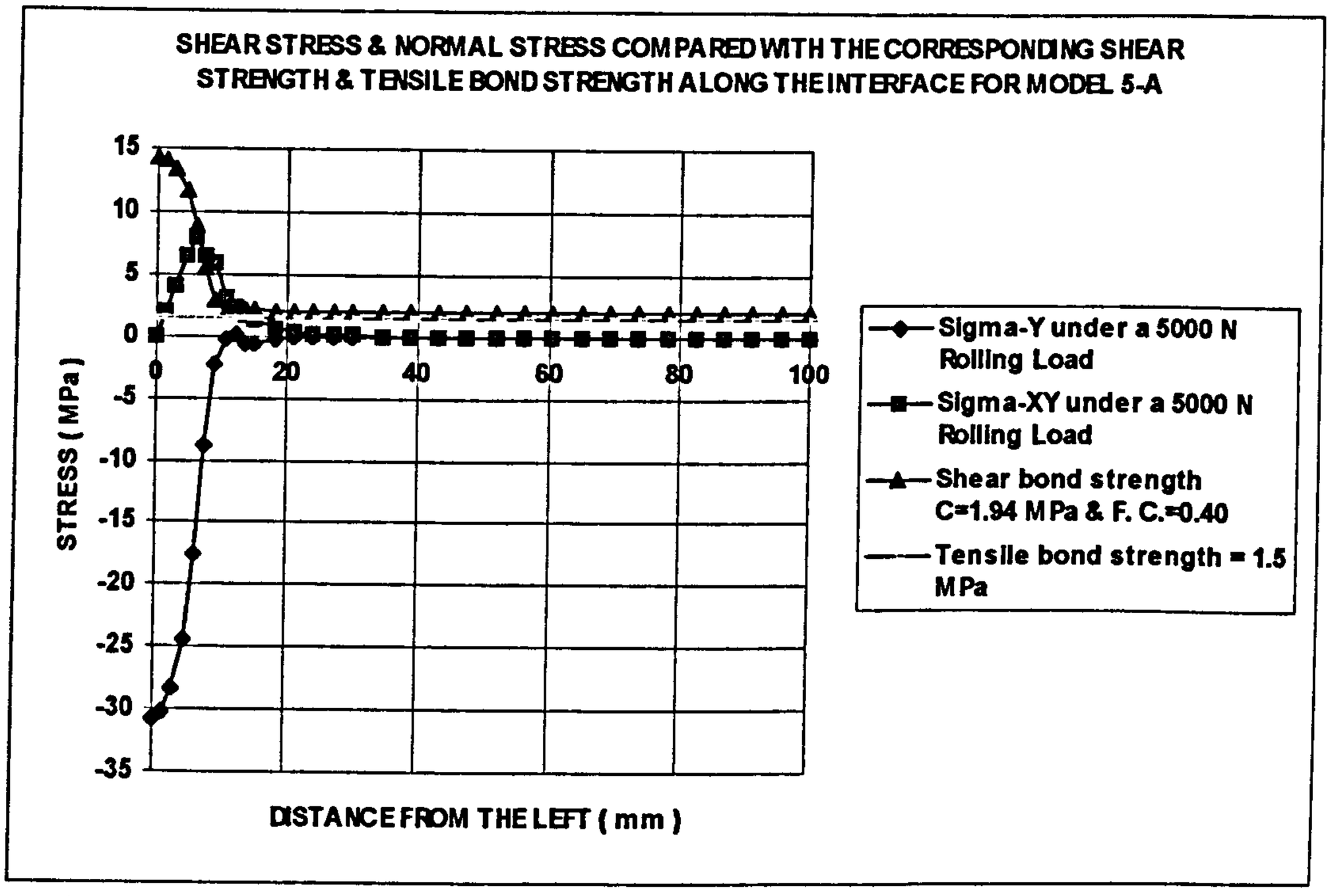

Figure 6-18-a-1: Model 5-a, G1294/Concrete {Compression (-), Tension (+)}

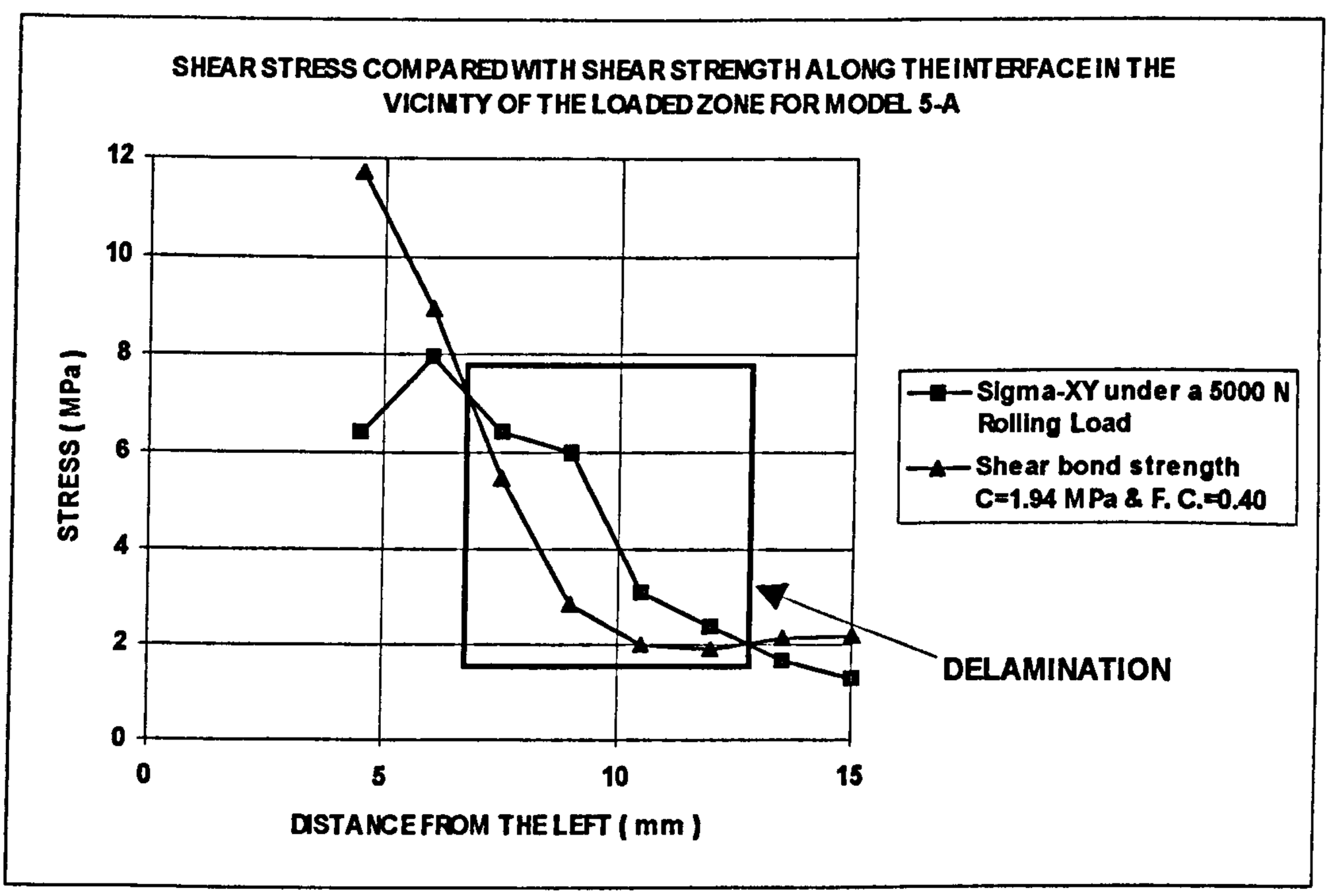

Figure 6-18-a-2 (Zoom): Model 5-a, G1294/Concrete
(Delamination occurs) ***AGREEMENT***

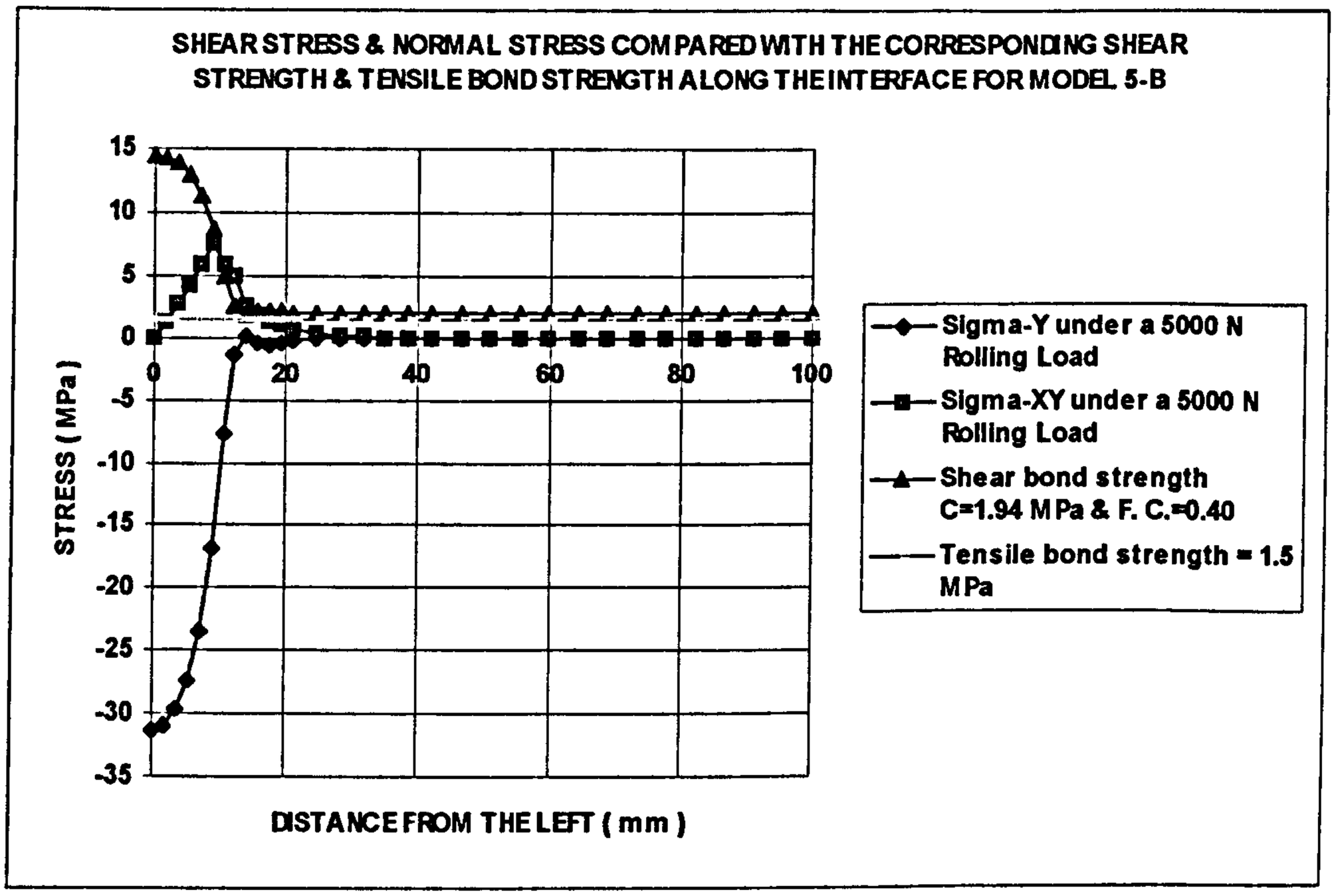

Figure 6-18-b-1: Model 5-b, G1294/Concrete {Compression (-), Tension (+)}

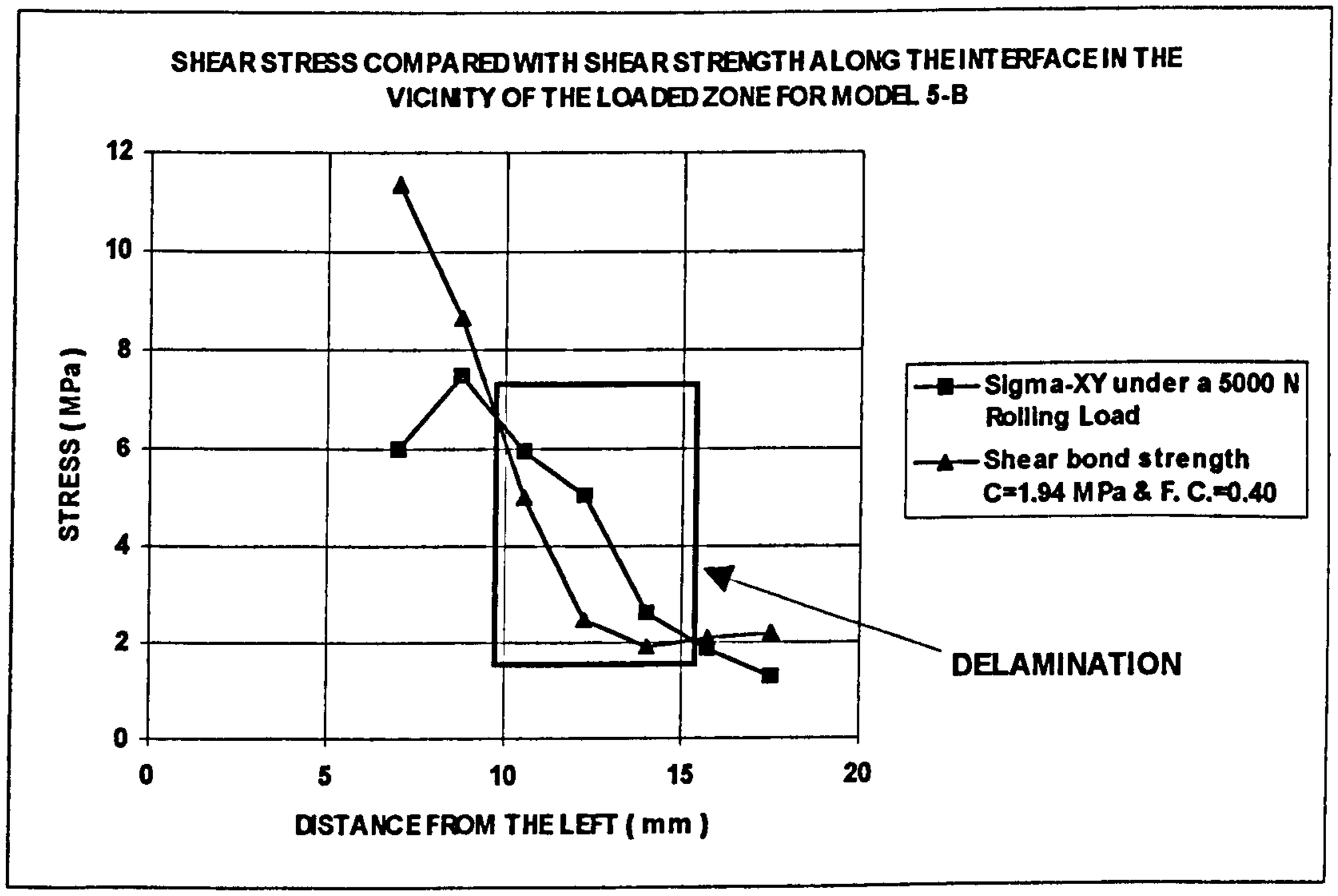

Figure 6-18-b-2 (Zoom): Model 5-b, G1294/Concrete
(Delamination occurs) ***AGREEMENT***

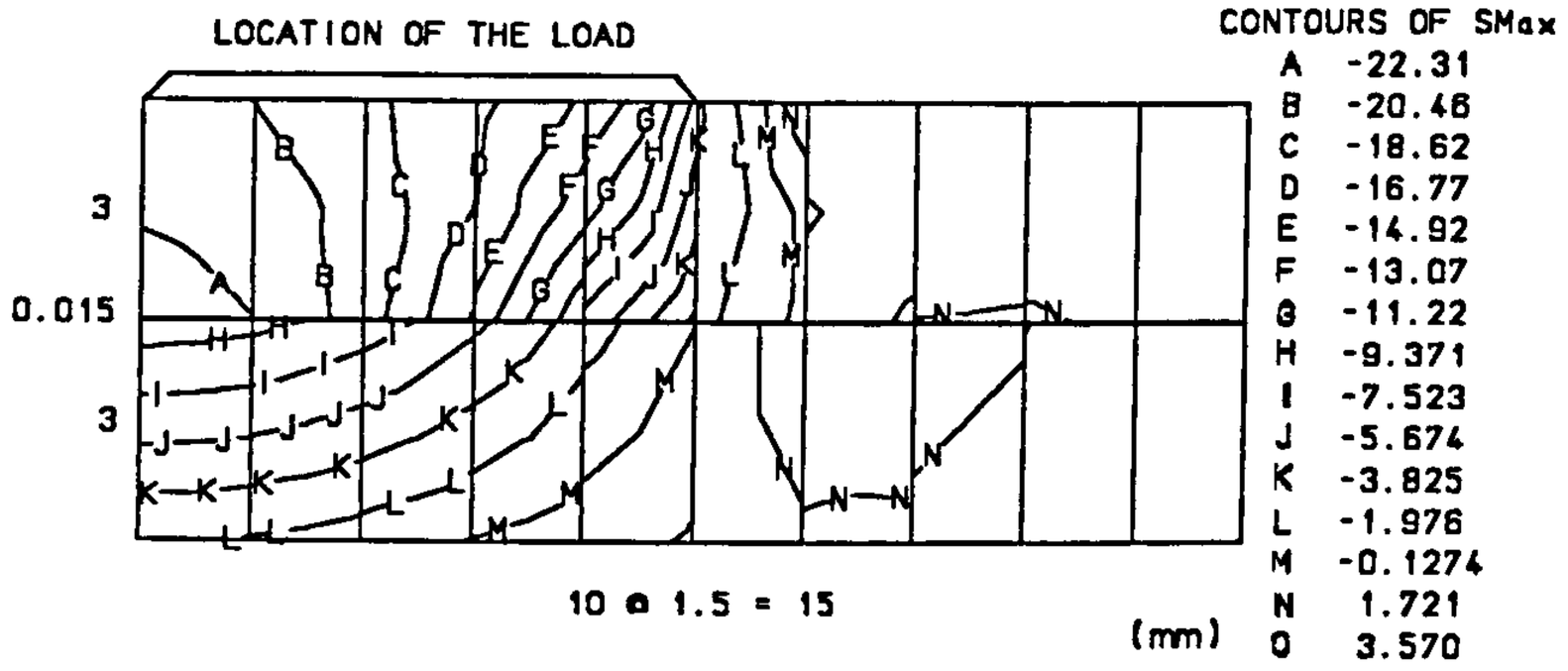

Figure 6-18-a-3: Contours of Sigma-1 (maximum) in the vicinity of the load and the interface for Model 5-a

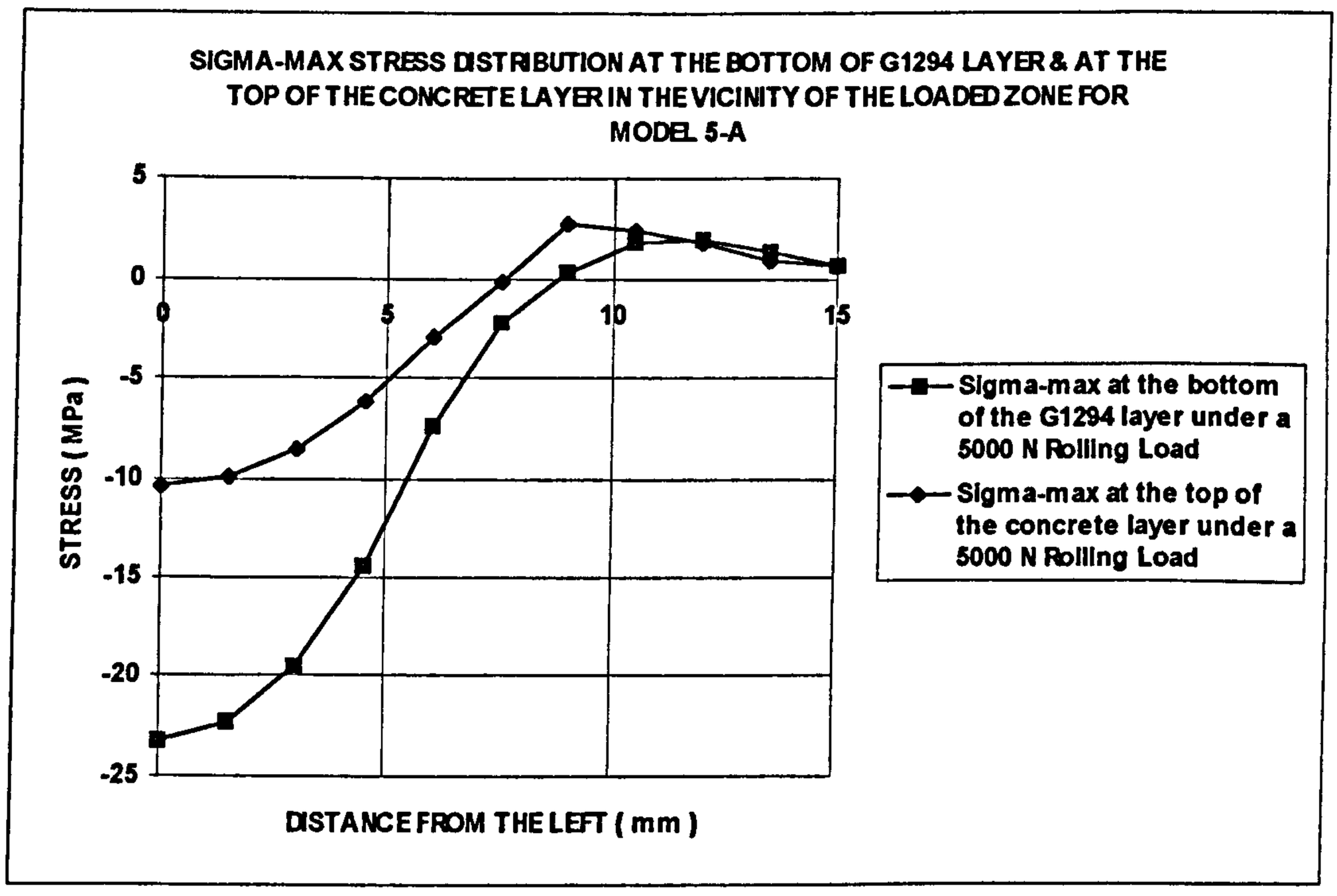

Figure 6-18-a-4: Sigma-1 (maximum) stress distribution in the vicinity of the load and the interface for Model 5-a {Compression (-), Tension (+)}

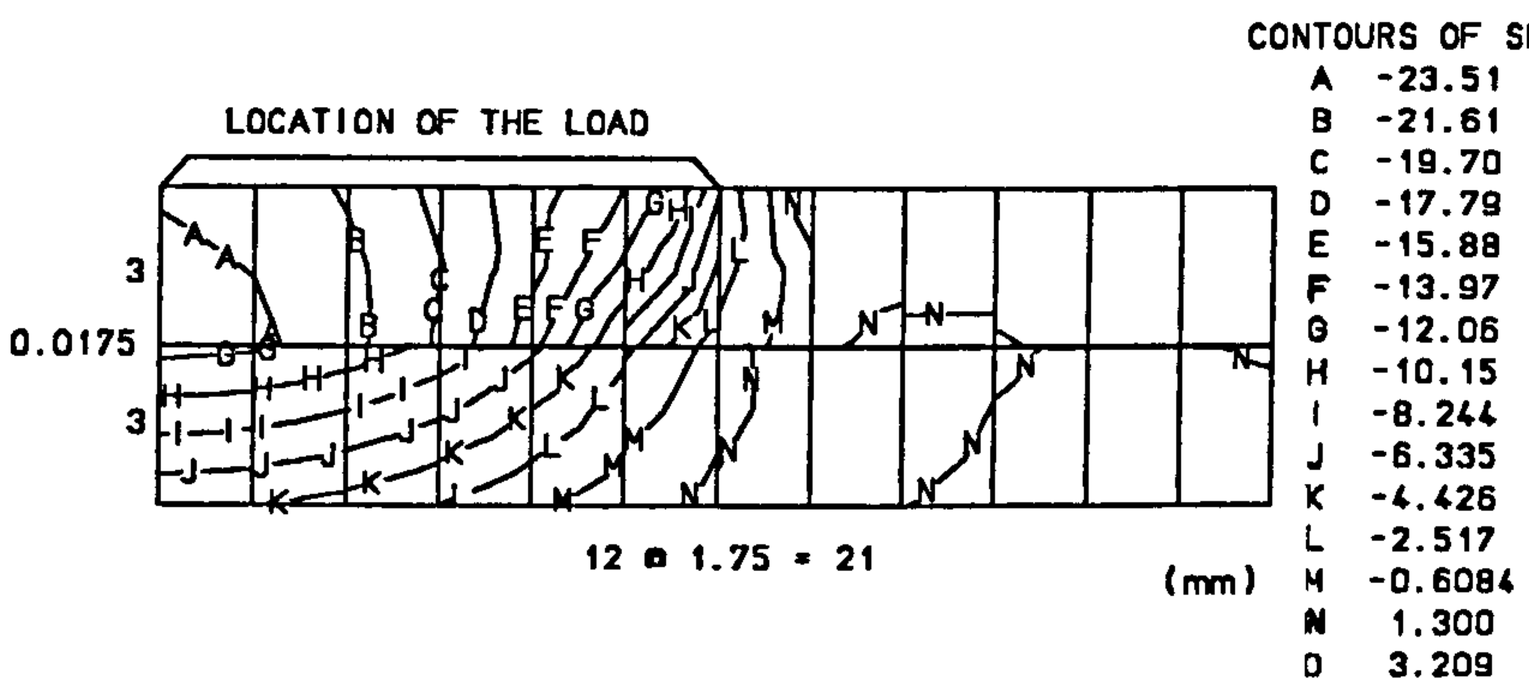

Figure 6-18-b-3: Contours of Sigma-1 (maximum) in the vicinity of the load and the interface for Model 5-b

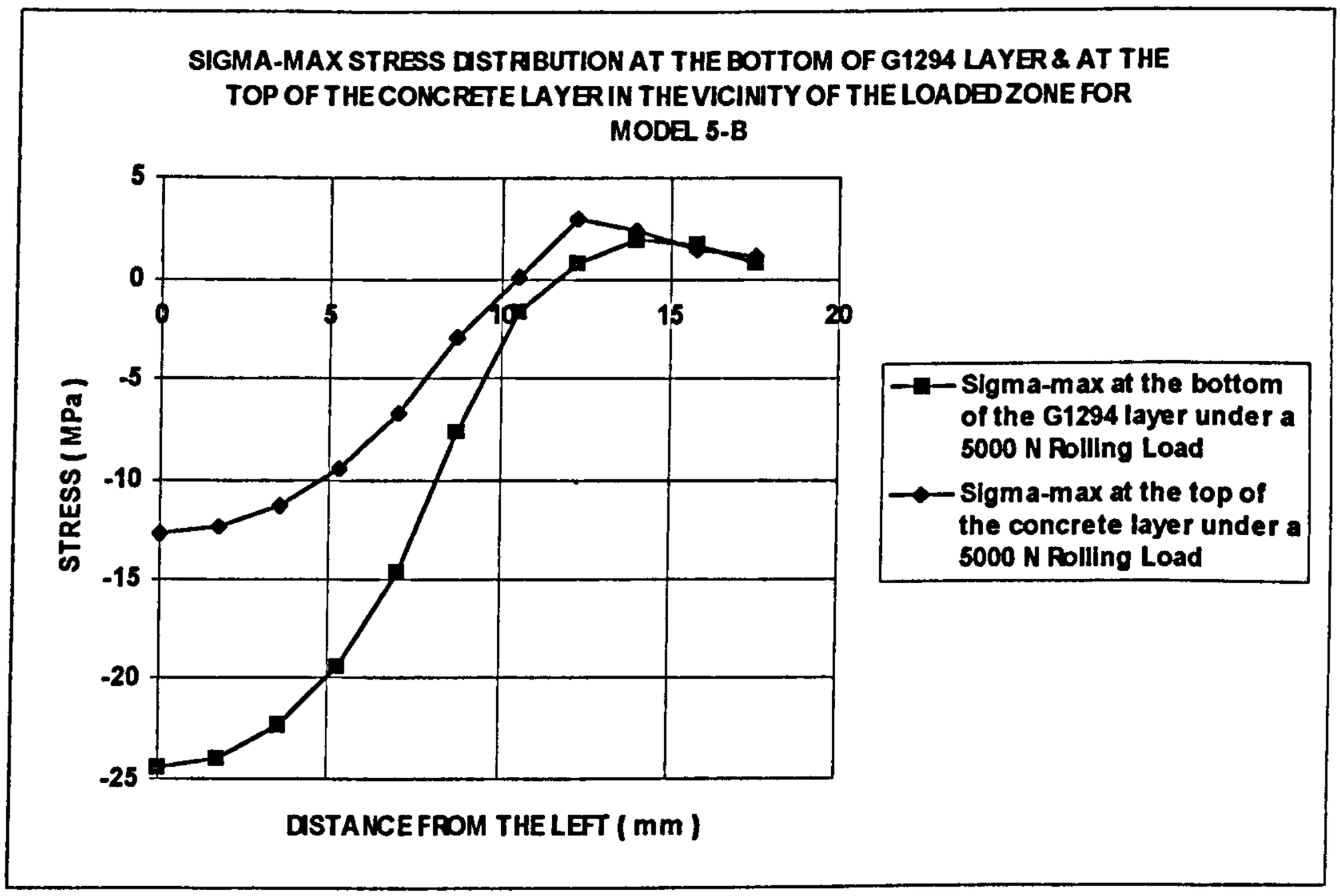

Figure 6-18-b-4: Sigma-1 (maximum) stress distribution in the vicinity of the load and the interface for Model 5-b {Compression (-), Tension (+)}

6-4 Summary

In this chapter the behaviour of thin layered systems under the action of a steel wheel load was studied.

The first part of the study was the implementation of the experimental program. In this experiment two types of specimens were used, the ready made specimens supplied by the manufacturer, and the purpose made specimens prepared in the Department of Civil Engineering of the University of Newcastle Upon Tyne. Both types of the specimens showed similar behaviour under the test conditions. The action of a steel wheel rolling load was well simulated using the Steel Wheel Rolling Load Rig. Three ways were used for detecting the possible delamination at the interface between the upper layer and the second layer. For most of the specimens all the detecting methods were satisfactory, however for few cases breaking the specimens was the only solution. The best combination of the thin layered systems used in this investigation was G1194/Concrete with the use of Gprime at the interface. This system could resist the maximum 5000 N without any sign of delamination or wear.

The second part of the study was the modelling of the thin layered systems in order to predict their behaviour under the prescribed load condition using the finite element method. The prediction of the slippage and debonding of the coating layer was tried by defining a thin interface layer between the two upper layers of each system. Two failure criteria, slippage due to shear stresses and debonding due to normal stresses were considered. The results of shear box and bond strength tests were used in this respect. The idealized stress strain curves for the constitutive materials were used in the implicit elasto plastic von Mises model, using the LUSAS finite element software. Elastic behaviour was assumed for the interface layer. The analytical results were consistent with the

experiment to a considerable extent. Considering the maximum principal stress distribution and contours in the vicinity of the load and the interface, one may conclude that the above method would be a better way for predicting the possible delamination in a thin layered system.

CHAPTER 7

BEHAVIOUR OF THIN LAYERED SYSTEMS UNDER THE ACTION OF PNEUMATIC TYRED VEHICLE ROLLING LOADS

Introduction

Experimental program

Structural analysis

Comparison between the experimental results and theoretical analysis

Summary

7-1 Introduction

Some floors are subjected to loads more accurately represented by a rolling pneumatic tyred wheel. In chapter 6, the behaviour of thin layered systems under the action of a free steel wheel rolling load was studied. In this chapter the behaviour of the thin layered systems under the action of a pneumatic tyred vehicle wheel load will be studied.

The main difference between the two investigations is that the contact pressure in the current situation will be very low.

The objectives of this chapter may be summarised as follows:

- Introducing and using the NUROLF, Newcastle University Rolling Load Facility, as a test method for simulating the action of a pneumatic tyred vehicle wheel load on a thin layered system.
- Examining some simple ways of detecting the possible delamination in a thin layered floor system.
- Structural analysis of the systems using the finite element method and the interface technique, based on the results of the material characteristics and interface bond strength tests reported in chapter 5.
- Comparing the results of the structural analysis and the experimental tests for different combinations of materials and evaluating the performances of the materials and the thin layered systems under test.
- Extending the use of the constitutive model used in chapter 6 to explain and predict the behaviour of the thin layered systems under the action of a pneumatic tyred vehicle wheel rolling load with particular interest in the delamination defect.

7-2 Experimental program

7-2-1 Materials

Materials used in the experimental program include steel fibre reinforced concrete, polymer concrete, polymer cement concrete, and primer.

7-2-1-1 Steel fibre reinforced concrete

Steel fibre reinforced concrete was used as the substrate layer in this experiment. The fresh concrete was of type C40 included of about 40 kg / m^3 hooked steel fibres and was transported to the site, the special test area in the

NUROLF lab by a mixing truck. The values of compression strength and modulus of elasticity of the concrete were reported in chapter 5.

7-2-1-2 P4 system (Polymer cement concrete)

The specifications of the P4 material have been given in chapter 5.
Polymer cement concrete, P4 system, was used in this experiment in two different ways as follows:
- Using P4 system as an intermediate layer on the steel fibre reinforced concrete substrate and under one layer of polymer concrete systems, G1194 or G1294.
- Using P4 system as the final upper layer on top of the steel fibre reinforced concrete substrate.

7-2-1-3 G1194, G1294 (Polymer concrete)

The specifications of these materials have been given in chapter 5.
Polymer concrete systems, G1194 and G1294, were also used in this experiment in two different ways as follows:
- Using G1194 or G1294 material as a thin protective layer on top of P4 system to enhance the quality of the surface of the thin layered system against the destructive factors arisen in an industrial floor system.
- Using these materials directly on top of a concrete substrate, without the use of any P4 system.
Each combination might vary with the type of primer used at the interface.

7-2-1-4 Primers

As was done in chapter 6, two types of primers were used at the interfaces of the thin layered systems in this experiment, Gprime and Pprime. The type of primer used at the interface of each two adjacent layers of materials has been shown in figure 7-13.

7-2-2 Preparation of the thin layered systems

As was mentioned, the NUROLF was used in this investigation for simulating the large scale Rolling Load resulted from a pneumatic tyred vehicle

wheel. (figure 7-14)

Therefore it was necessary to design and construct the concrete slab in order to provide a substrate for the subsequent layers of materials. The testing bed was of dimensions 5000 mm by 2000 mm in the NUROLF lab.

7-2-2-1 Design of the concrete slab pavement for carrying out the large scale Truck Tyre Rolling Load Test using the NUROLF

7-2-2-1-1 Assumptions and recommendations

- Planar dimensions of the new concrete slab : 5000 mm ×2000 mm
- Maximum rear axle load: 14000 kg
- Maximum front axle load: 14000/4 kg = 3500 kg
- Distance between the front and rear load: 3400 mm
- Only the right hand side wheel of each axle is running on the testing bed.
- CBR value for the subgrade is 7% and for the granular subbase is about 40%. The thickness of subbase layer is about 800 mm.
- Tire pressure: 105 psi ≈ 0.735 MPa
- Number of repetitions of loading: less than 8000.
- Grade and type of concrete (Steel fibre reinforced concrete): C40 concrete 40 kg / m^3 ZC 60/1.00 steel fibre. [Knapton et al. 1994]
- Minimum cement content = Between 320 and 350 kg / m^3 [Knapton et al. 1994]
- Sand: Between 750 to 850 kg / m^3 good quality and well graded sharp sand with a maximum size of 4 mm should be used. [Knapton et al. 1994]
- Coarse aggregate: A continuous aggregate graded with a maximum size of 28 mm for rounded gravel and 32 mm for crushed stone should be used. The fraction larger than 14 mm to 15 mm should be limited to 20%. [Knapton et al. 1994]
- Slump: About 50 mm [Knapton et al. 1994]
- Water/cement ratio should be about 0.50 and should be kept less than 0.55. To obtain a better workability, an appropriate superplasticizer may be used. [Knapton et al. 1994]
- Because of the steel fibres in the concrete, admixtures of chloride or chloride containing additives are not permitted. [Knapton et al. 1994]

Notation:

σ_{MAX} = flexural stress (MPa)

υ = Poisson's ratio of concrete $\approx$ 0.17 [Nilson et al. 1991]

h = depth of slab (mm)

E = static modulus of elasticity $\approx$ 20000 MPa [Knapton et al. 1994]

K = modulus of subgrade reaction (N/mm^3)

P = point load = wheel load $\times$load safety factor [Knapton et al. 1994]

l = radius of relative stiffness (mm)

M_t = tangential moment

b = Radius of equivalent circular loading area (mm) $\approx$

$$\left(\frac{wheel\ load(N)}{\pi \times tyre\ \text{pressure(MPa)}}\right)^{0.5}$$ [Knapton et al. 1994]

s = distance between load patch centres [Knapton et al. 1994]

7-2-2-1-2 Design procedure:

For a C40 concrete 40 kg/m^3 ZC 60/1.00 steel fibre, from table 7-1, the 28-day design flexural strength value is 4.5 MPa.

Table 7-1: 28-day design flexural values for some concrete mixes [Knapton et al. 1994]

Type of Concrete	Flexural Strength (MPa)
Plain C40 concrete	2.4
C40 concrete 30 kg/m^3 ZC 60/1.00 steel fibre	3.8
C40 concrete 40 kg/m^3 ZC 60/1.00 steel fibre	4.5

Now for wheel loading from table 7-2, we can choose the value of load safety factor:

Load safety factor = 1.5

From figure 7-1, the modulus of subgrade reaction is 45 MN/m^3(0.045 N/mm^3) that is equivalent to a CBR value of 7%. [Chandler 1982]

The existing granular subbase of thickness 800 mm will increase the 'apparent' modulus of subgrade reaction. This effect can be taken into account by using table 7-3, which suggests an enhanced value of k$\approx$0.136 N/mm^3. [Knapton et al. 1994]

Table 7-2: Load safety factor for a given number of repetitions of loading [Chandler 1982]

Maximum number of load repetitions	Load safety factor
> 400000	2.00
...	...
< 8000	1.5

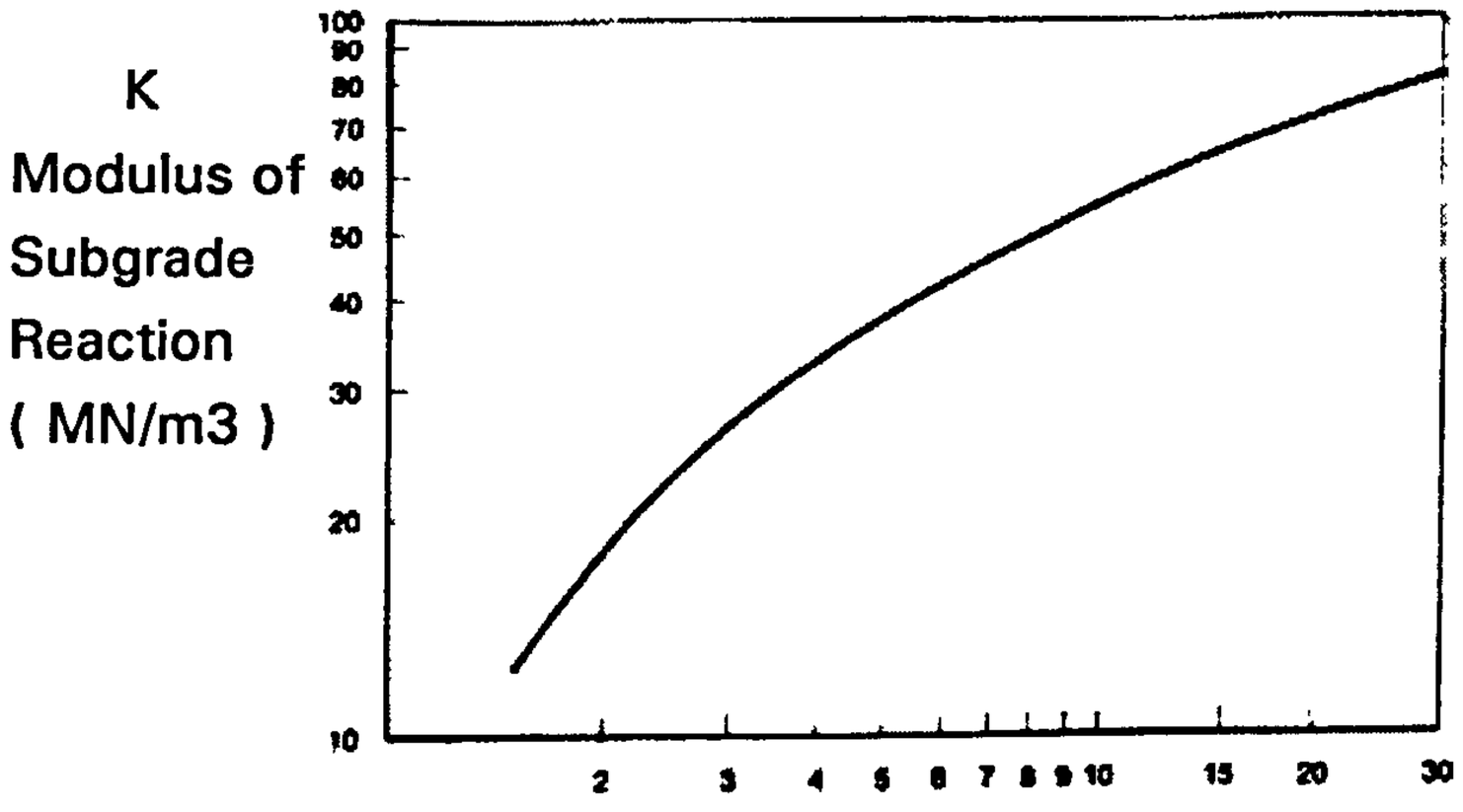

Figure 7-1: Approximate relationship between CBR and modulus of subgrade reaction. [Chandler 1982]

Table 7-3: Enhanced value of K (N/mm^3) when a subbase is used. [Knapton et al. 1994]

K value of subgrade alone	Thickness of granular subbase			
	150 mm	200 mm	250 mm	300 mm
0.020	0.026	0.030	0.034	0.038
0.027	0.034	0.038	0.044	0.049
0.040	0.049	0.055	0.061	0.066
0.054	0.061	0.066	0.073	0.082
0.060	0.066	0.072	0.081	0.090

Load cases:

1- Internal loading with the rear wheels:

Design load per dual wheel, assuming two dual wheels per axle =14 / 2 ×1.5 =10.5 tones=105000 N (7-1)

$$\text{Contact area} \approx \frac{load}{tyre\ pressure} = \frac{105000}{0.735} = 142857 mm^2$$

So: Radius of equivalent circular loading area = 213 mm (7-2)

From equation 7-3, proposed by Westergaard and Timoshenko for calculating the internal stress due to an internal point load, and trying a 150 mm deep slab, we have: [Knapton et al. 1994]

$$\sigma_{max} = \frac{0.275(1+\upsilon)P}{h^2} \log(0.36Eh^3 / Kb^4) \qquad (7\text{-}3)$$

$$\sigma_{max} = \frac{0.275(1+0.15)105000}{150^2} \log(0.36 \times 20000 \times 150^3 / (0.136 \times 213^4))$$

So, Tensile stress internally due to a rear wheel (dual) is:

$\sigma_{max} = 2.86$ MPa ≤ 4.5 MPa

This stress is well inside the allowable stress.

2- Edge loading with the rear wheel (dual):

Design load per wheel (dual) = 105000 N (7-1)

Radius of equivalent circular loading area = 213 mm (7-2)

From equation 7-4, proposed by Westergaard and Timoshenko for calculating the edge stress due to an edge point load, and trying a 150 mm deep slab, we have: [Knapton et al. 1994]

$$\sigma_{max} = \frac{0.529(1+0.54\upsilon)P}{h^2} \log(0.20Eh^3 / Kb^4) \qquad (7\text{-}4)$$

$$\sigma_{max} = \frac{0.529(1+0.54 \times 0.15)105000}{150^2} \log(0.20 \times 20000 \times 150^3 / (0.136 \times 213^4))$$

So, tensile stress at edge due to a rear wheel (dual) becomes:

$\sigma_{max} = 4.49$ MPa ≤ 4.5 MPa

It is seen that the calculated edge stress is just inside the allowable stress of 4.5 MPa.

3- Combinations of loading:

3-1- Combination of the front and rear wheel loads both acting internally:

From equation 7-5, for a 150 mm slab with the above specifications, the value of radius of relative stiffness (l) is obtained: [Knapton et al. 1994]

$$l=(Eh^3/(12(1-\upsilon^2)K))^{1/4} \quad (7\text{-}5)$$

$$l=(20000\times150^3/(12(1-0.15^2)0.136))^{1/4}$$

$$l=453.4 \text{ mm}$$

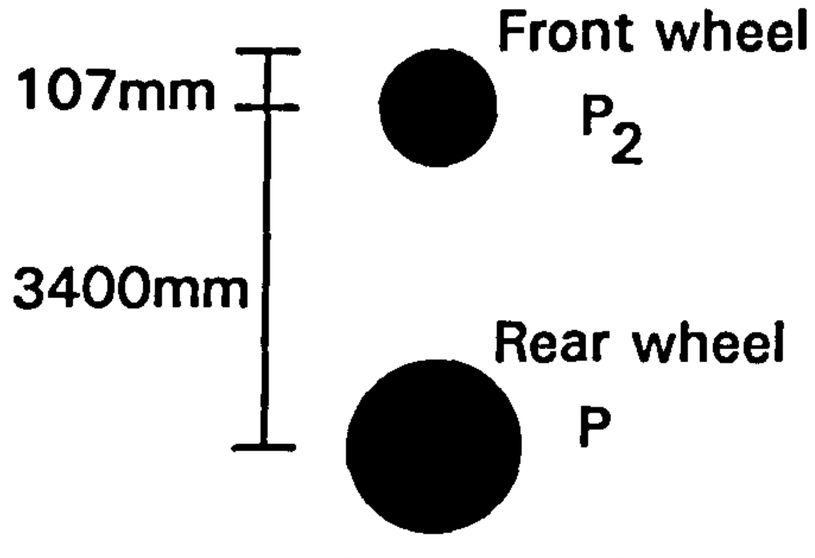

Figure 7-2: Loading combination (Both internally)

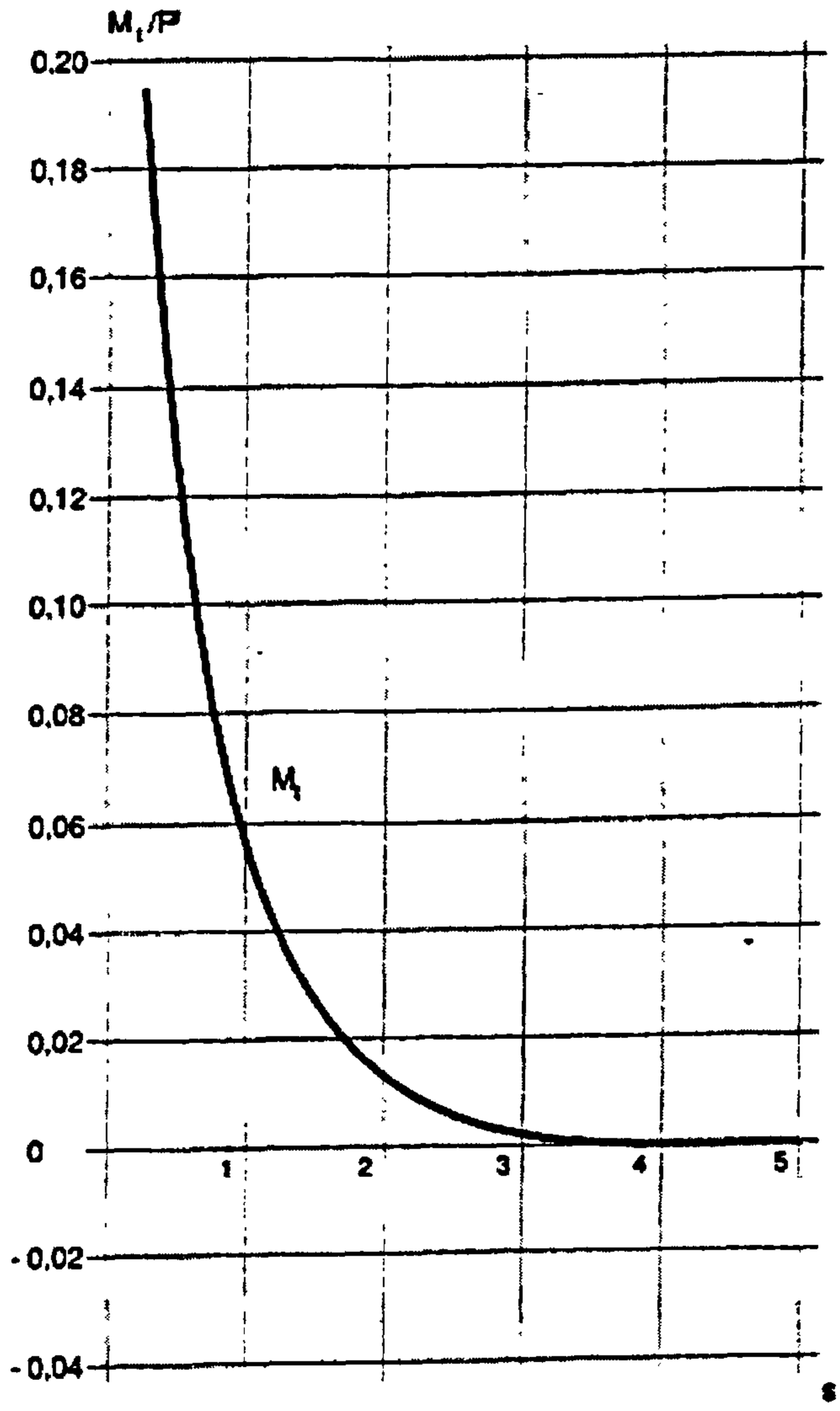

Figure 7-3: Relationship between ratio M_t/P and ratio s/l [Knapton et al. 1994]

$$\text{Contact area (front wheel)} \approx \frac{load}{tyre\ pressure} = \frac{35000\times0.5\times1.5}{0.735} = 35714\ mm^2$$

Radius of equivalent circular loading area (front wheel) ≈ 107 mm

Radius of equivalent circular loading area (rear wheel) = 213 mm

Distance between the centre of rear load and front load (figure 7-2):

s = 3400 mm ⇒ s/l = 3400/453.4 = 7.5

The stress at position P (the greatest point load) due to a load at position P_2 (the other point load) may be determined by using equation 7-6 and figure 7-3. [Knapton et al. 1994]

$$\sigma_{add} = \frac{M_t}{P}\frac{6}{h^2}P_2 \qquad (7\text{-}6)$$

The relationship between ratio M_t/P and ratio s/l has been plotted in figure 7-3. From figure 7-3, it is obvious that the presence of the front wheel in this case has not any effect on the tensile stress due to the rear wheel (dual). [Knapton et al. 1994]

3-2- Combination of the front wheel load (at the edge) and rear wheel load (at an internal point):

Again with the same ratio of s/l=7.5 , from figure 7-3, it is obvious that the presence of the front wheel in this case has not any effect on the tensile stress due to the rear wheels (dual). [Knapton et al. 1994]

It is seen from the above calculations that the edge loading condition for the rear wheel (dual) controls the design and that the calculated edge stress is inside the allowable stress. Hence the slab thickness will be 150 mm.

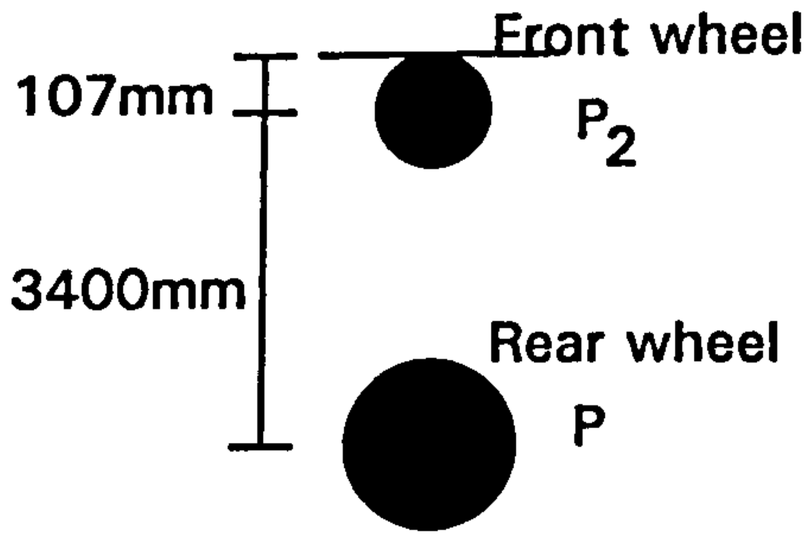

Figure 7-4: Loading combination (Internally and at the edge)

7-2-2-1-3 Shrinkage and temperature effects:

Shrinkage and temperature effects may result in two kinds of stresses, the first is tensile stress due to a uniform contraction and the second is warping stress due to a variation of temperature or concrete shrinkage through the slab depth.

[Nilson et al. 1991]

1- Tensile stress due to a uniform contraction:

To calculate the tensile stress due to a uniform concrete shrinkage or decrease in temperature, we can use the following equation: [Nilson et al. 1991]

$$f_t = \frac{\gamma \mu l}{2} \qquad (7\text{-}7)$$

Where:

f_t = the resulting uniform tensile stress, in MPa

γ = specific gravity of concrete, about 2.4×10^5 N/mm^3

μ = Coefficient of friction between slab and subgrade (Varies between 1.0 and 2.5 and for design of highway pavements, the AASHTO Interin Guide assumes a value of 1.5. [Nilson et al. 1991])

l = length between contraction or construction joints, here is 5000 mm

Assuming a specific gravity of 2.4×10^5 N/mm^3 for concrete and μ=1.5, we have:

$$f_t = \frac{2.4 \times 10^{-5} \times 1.5 \times 5000}{2} = 0.09 \text{ MPa}$$

Therefore: $f_t/f_r = \frac{0.09}{4.9} \approx 0.02$

This means that the value of tensile stress due to a uniform contraction of the concrete slab in comparison with the flexural strength of concrete is negligible.

2- Warping stress due to a variation of temperature or concrete shrinkage through the slab depth:

According to Ref. [Nilson et al. 1991], for indoor slabs, the tensile stress due to warping effects is about 0.35 MPa (50 psi) at the top surface. The warping stresses generally superimpose on the uniform tensile stresses calculated by equation (7-7). However because in this project the corner loading condition will not occur, the warping stress should not superimpose on the uniform stress. Considering the above results, slab reinforcement appears unnecessary here, and a C40 concrete slab floor (40 kg/m^3 ZC 60/1.00 steel fibre) 150 mm thick will be used. (figures 7-5 and 7-6)

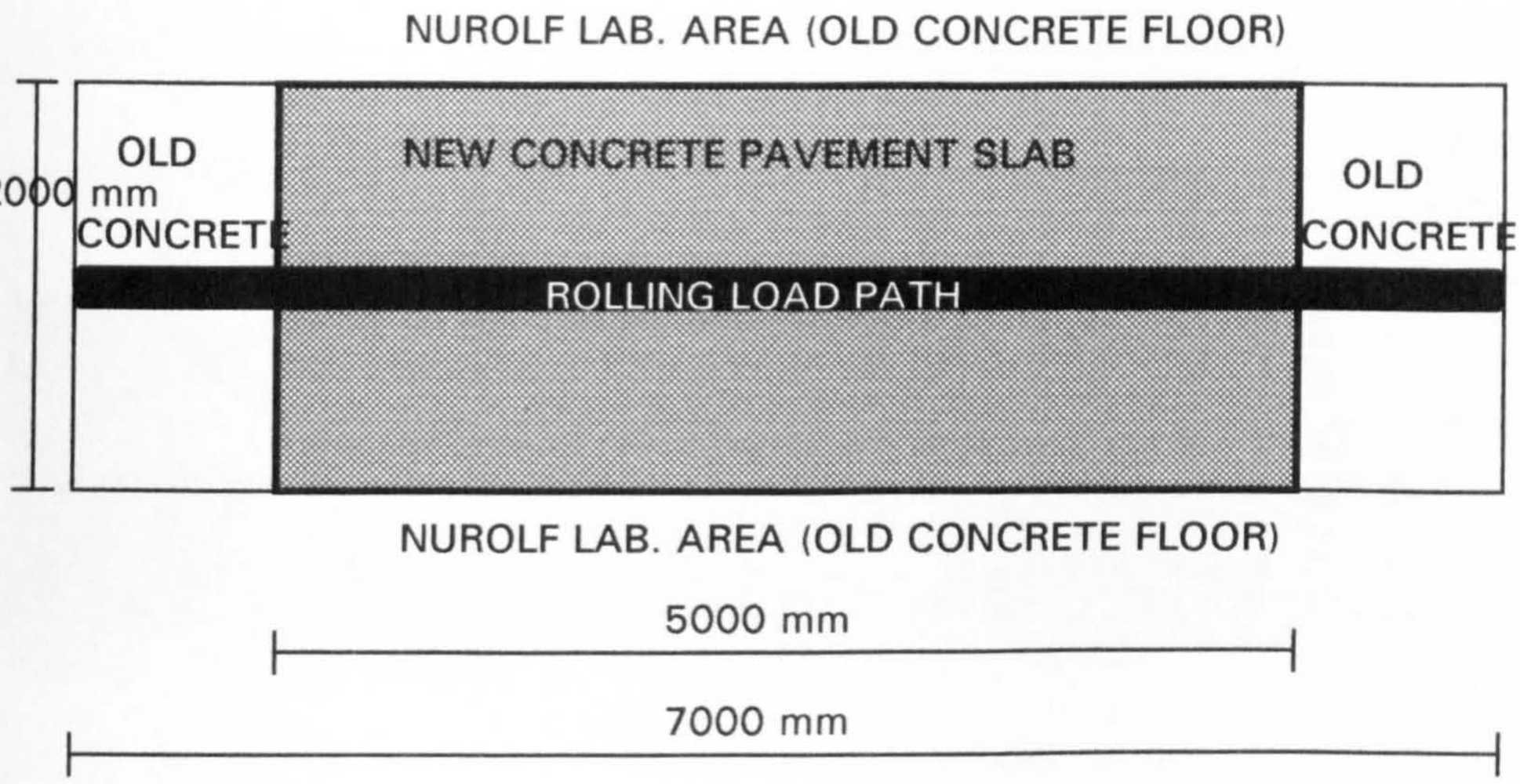

Figure 7-5: The overall plan of the testing area

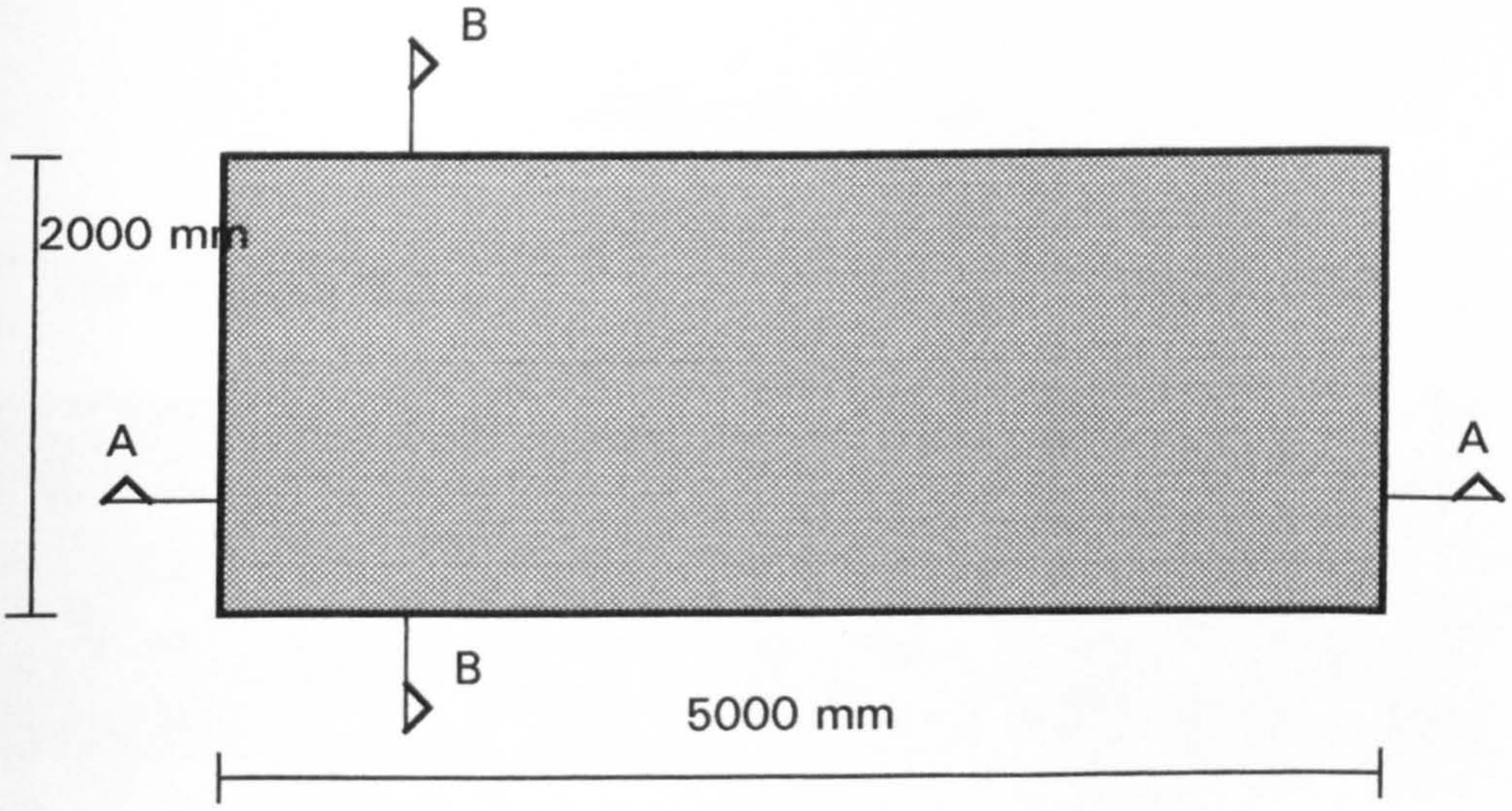

Figure 7-6: The new steel fibre reinforced concrete pavement plan

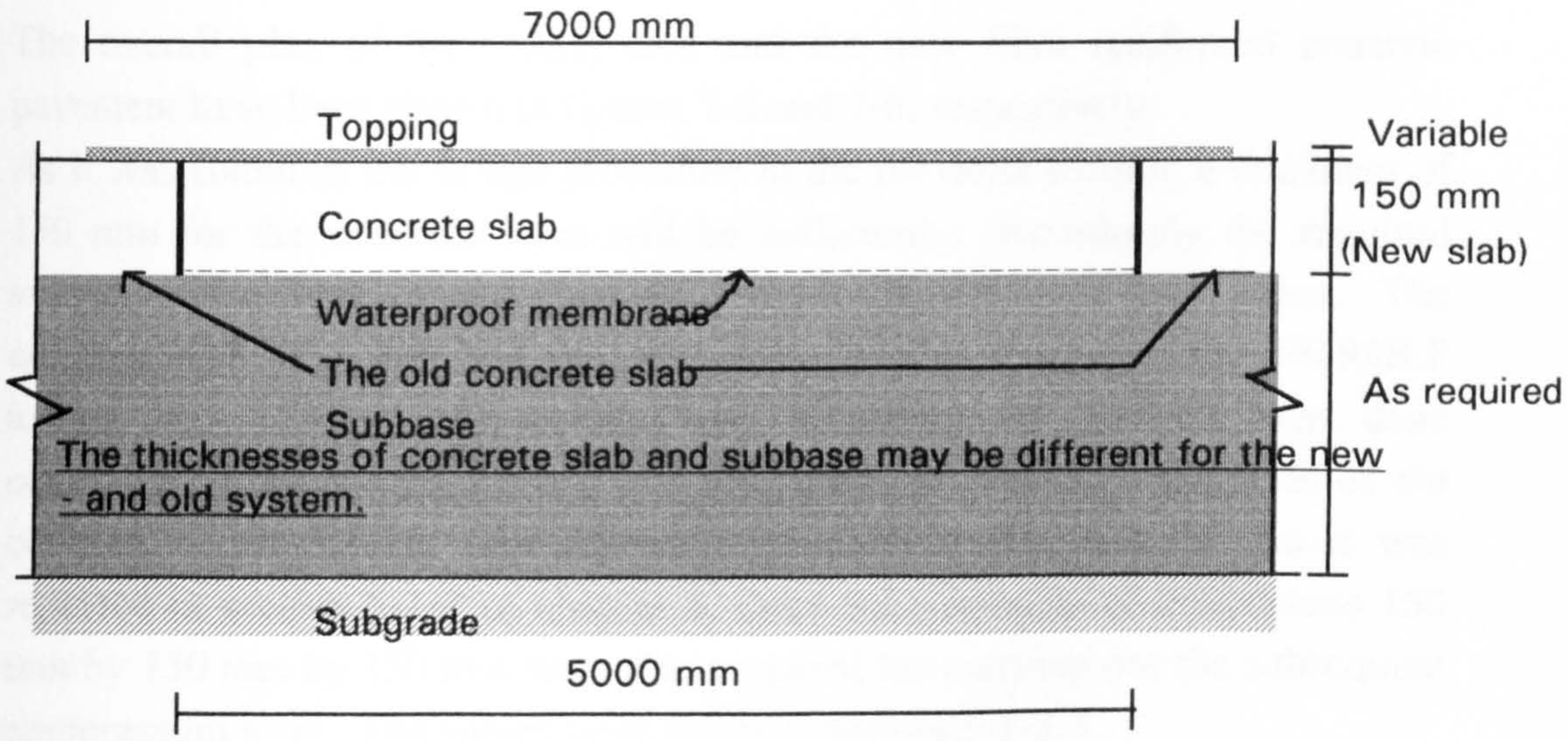

Figure 7-6-a: Section A-A

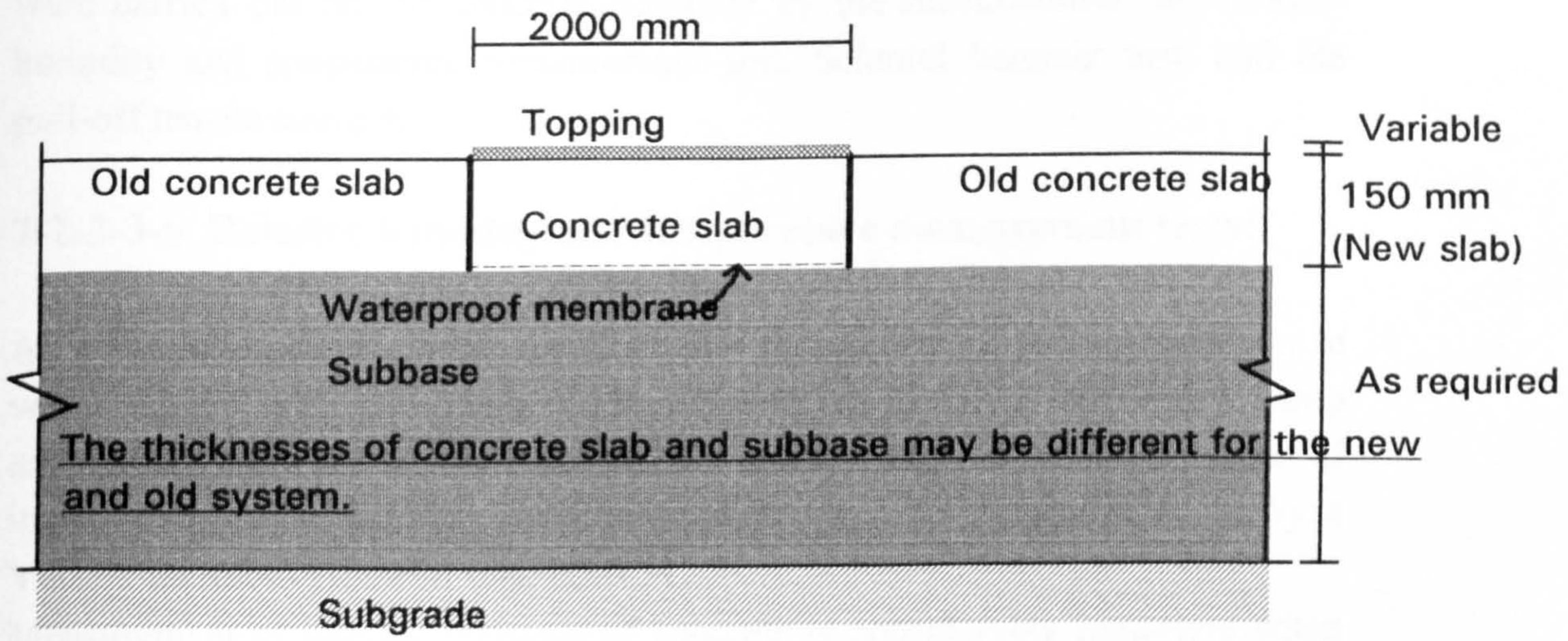

Figure 7-6-b: Section B-B

7-2-2-2 Construction of the steel fibre reinforced slab

The overall plan of the testing area and the new fibre reinforced concrete pavement have been shown in figures 7-5 and 7-6, respectively.
As it was found in the design procedure in the previous section, a thickness of 150 mm for the concrete layer will be sufficient. Accordingly the required volume of the fresh concrete was delivered to the site by a truck mixer. The concrete slab was then laid properly in the predicted area of the NUROLF testing bed. During the construction, spreading the concrete was done manually. Timber screed board was also used for correcting the level of the concrete. Compacting was achieved using a vibrating poker. As it was reported in section 5-1-3 of chapter 5, three cube samples of dimensions 150 mm by 150 mm by 150 mm were also prepared for carrying out the subsequent compression tests. The values were given in section 5-1-3-3.

7-2-2-3 Pre examinations of the concrete substrate

As it is shown in figure 7-5, the concrete substrate consisted of the new steel fibre reinforced concrete slab and a part of the old concrete pavement of the NUROLF lab.
Due to some limitations and recommendations for the use of the G1194 or P4 materials, before the application of any flooring material, three type of tests were carried out on the concrete substrate by the manufacturer, the relative humidity and temperature measurement test, Schmidt hammer test, and the pull-off tensile strength test.

7-2-2-3-a Relative humidity and temperature measurement tests:

As a limitation, it has been specified that the surface of the substrate on to which G1194 is to applied should be dry and not to suffer from rising damp and should have a relative humidity not greater than 75 % at the time of installation, as measured in accordance with BS 8203 Appendix A, or by a Vaisala thermohygrometer type HMI 31.
Measurement of internal moisture of concrete is considerably important when assessing the durability performance. There are different ways for the measurement of moisture of the concrete. A simple method for this purpose is using a hand held electronic equipment for site usage which is now available

in the market. The equipment normally consists of a digital meter which is connected to an electronic probe sealed into a 60 mm deep surface-drilled 25 mm diameter hole. The probe which is influenced by the relative humidity of the air in the hole, is in the form of a small plastic capacitor in a protective cover. The range of measurements may vary between 20% to 90%. The accuracy will vary with the difference in reading from the value of 75% RH and $\pm$15% of the difference is claimed, for example $\pm$3.75% at 50% RH. It should be added that since the value of 75% RH is critical for the alkali-silica reactions, calibration is based on providing a maximum accuracy at around this value. [Bungey 1989]

In this experiment, the relative humidity and temperature of the new steel fibre reinforce concrete surface were measured using VAISALA equipment. (figure 7-7)

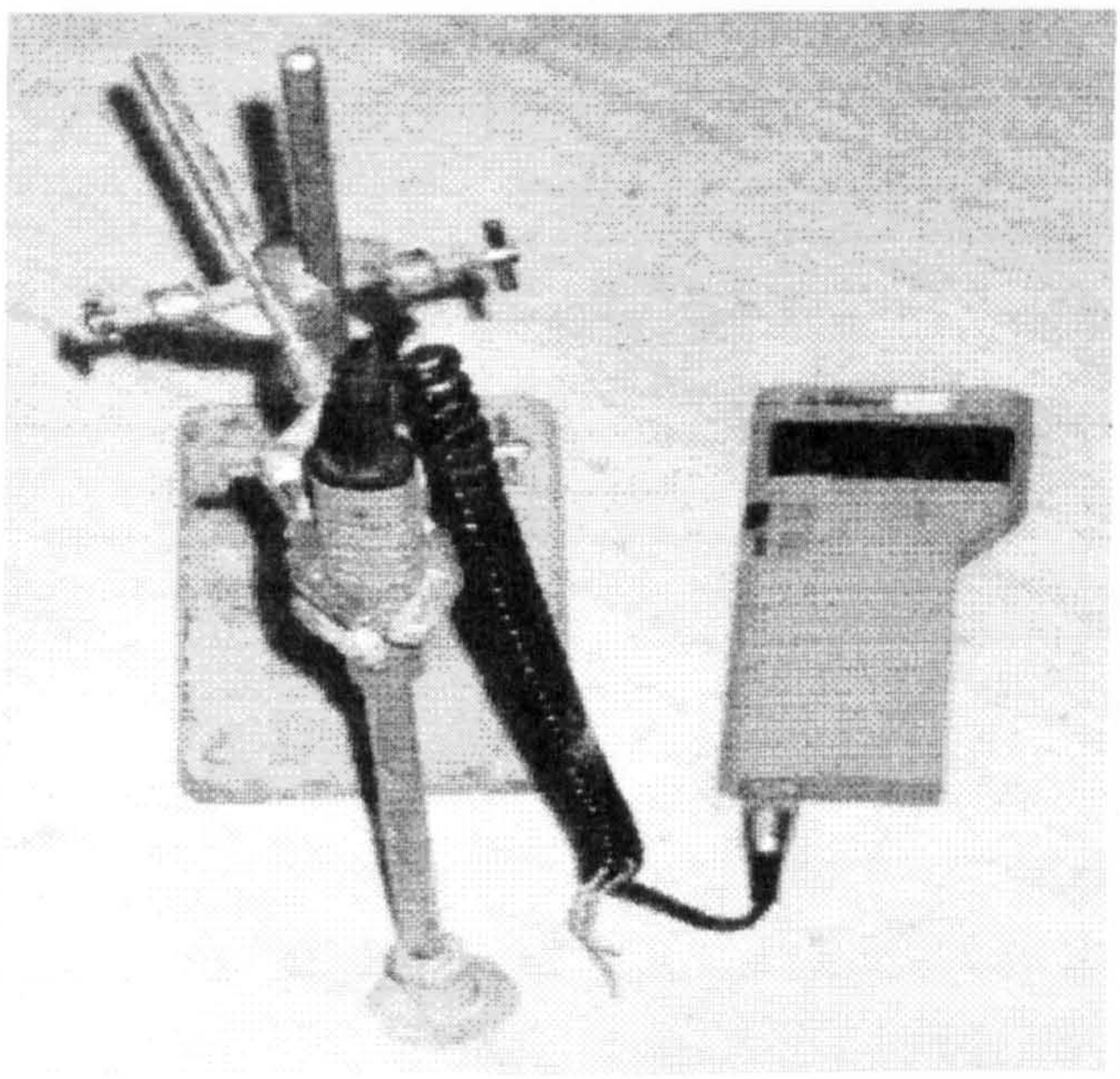

Figure 7-7: VAISALA equipment for measuring the R. H. & temperature

The values obtained at the age of 13 days for the concrete slab were as follows:

RH $\approx$85% and Temperature $\approx$17.7 $^{\circ}$C

Due to the limited time for using the NUROLF lab., the condition was evaluated as satisfactory by the manufacturer.

7-2-2-3-b Rebound test using Schmidt hammer

As a design criteria, the P4 system can be applied onto a concrete substrate which has either a minimum 25 MPa compressive strength or a surface tensile

strength value in excess of 1.25 MPa.

To consider the above criteria two different tests were carried out, Schmidt hammer test and pull-off tensile strength test.

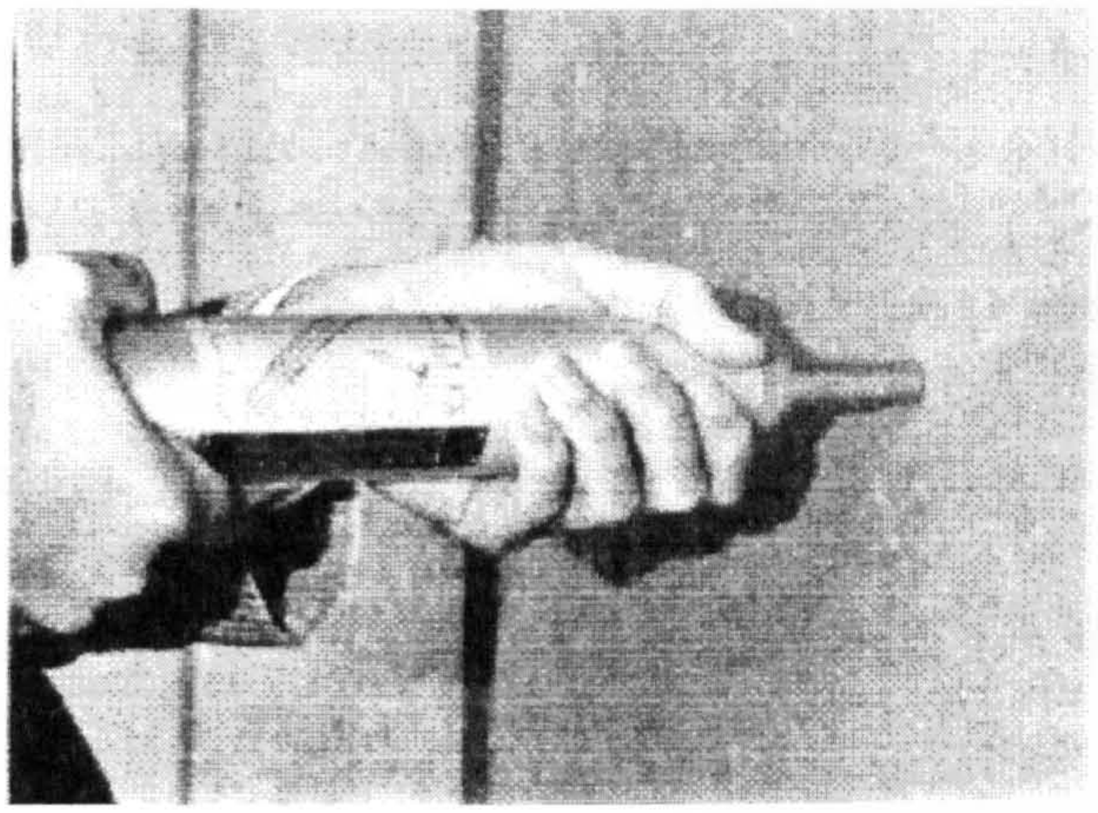

Figure 7-8: Schmidt hammer in use [Bungey 1989]

2000 mm

800 mm	49	39	41	Old concrete
1250 mm	26	25	25	New concrete
1250 mm	25	22	23	New concrete
1250 mm	23	23	26	New concrete
1250 mm	28	25	24	New concrete
1000 mm	57	25	50	Old concrete

2000 mm

Figure 7-9: The estimated values of compressive strength resulted from the Schmidt hammer test on the concrete substrate (MPa)

Schmidt hammer test was first developed in the mid 1940, by the Swiss engineer Ernst Schmidt. Modern types of the equipment are also based on the first model. (figure 7-8) By using Schmidt hammer, one relates the hardness of the concrete surface to its compressive strength. The equipment is very simple to use. However the reading will be very sensitive to local variations in the concrete mass, particularly to aggregate particles which may be located near to the surface. For this reason it is necessary to take the average of several readings at each location. According to BS 1881 : Part 202 (21), 12 readings

are recommended to be taken over an area not exceeding 300 mm square, and also the impact points should not be less than 20 mm apart from each other or from the edge. [Bungey 1989]

The reading taken by using a Schmidt hammer is known as the rebound number and should be converted to the compressive strength using the appropriate rebound number/strength relationship. [Bungey 1989]

It should be mentioned that Schmidt hammer test was used in this experiment as an approximate way for the evaluation of the compressive strength of the concrete substrate. Figure 7-9 shows the average values of the compressive strength for the new and old concrete substrates. The age of the new concrete slab at the time of the test was 13 days.

As it is seen from figure 7-9 , the concrete strength for the application of G1194 is acceptable.

7-2-2-3-c Pull-off tensile strength test using ' Limpet ' equipment

The use of ' Limpet ' equipment for the measurement of the bond strength at the interface of a thin layered system was described in chapter 5-2-1-1. (figure 5-7)

In this experiment the surface tensile strength of the concrete substrate was to be measured. The special dollies of diameter 50 mm were first glued to the surface of the concrete, using Araldite, and then after the curing time they were jacked off to measure the force necessary to pull a piece of the concrete away from the surface. (figure 7-10)

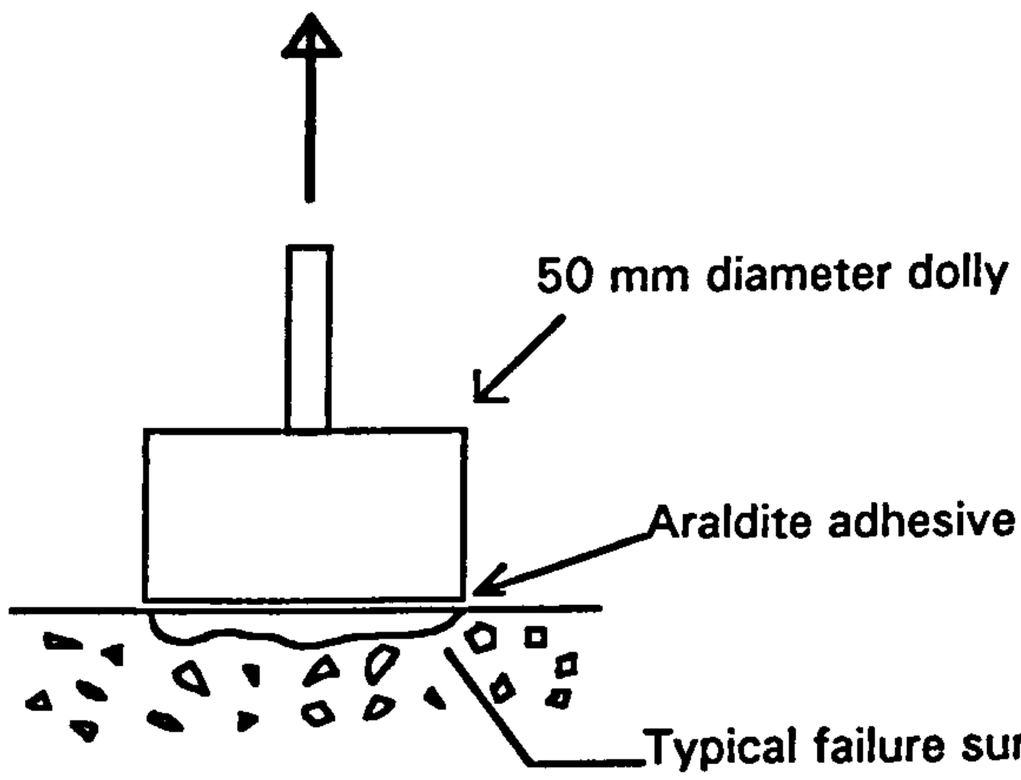

Figure 7-10: Surface tensile strength pull-off test method [Bungey 1989]

The results of the surface tensile strength test are tabulated in table 7-4. Once again it is seen that the average value of the tensile bond strength tests, 1.15,

would be acceptable for the application of the G1194 layer on top of the concrete substrate.

It should be added that it is also possible to correlate the results of this test with the corresponding values of compressive strengths by using an appropriate calibration curve like that which is shown in figure 7-11. (figure 7-11)

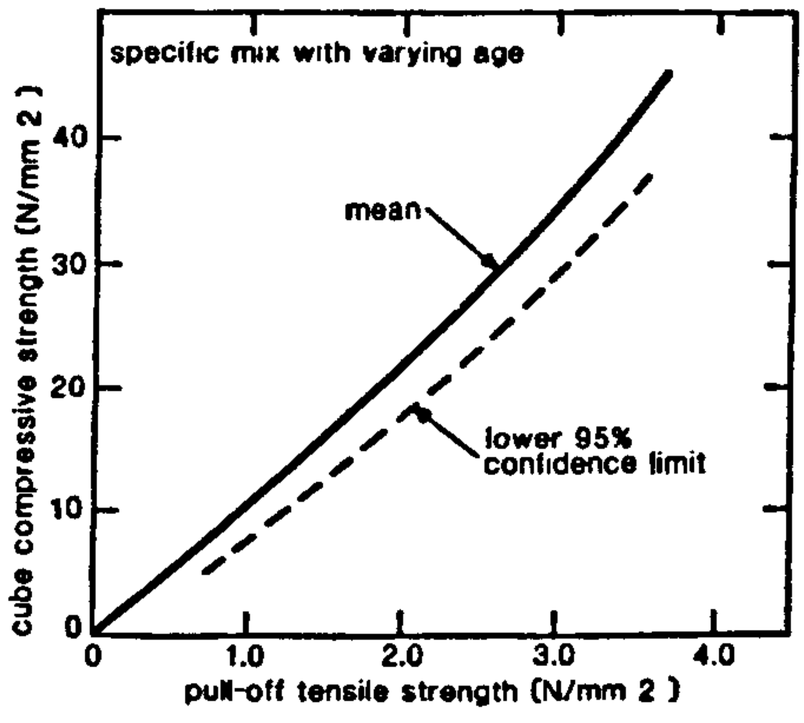

Figure 7-11: A typical pull-off tensile strength and compressive strength correlation [Bungey 1989]

Table 7-4: The results of the surface tensile strength tests on the concrete substrate in the NUROLF experiment

Specimen Number	Tensile Bond Force (kN)	Tensile Bond Strength (MPa)
1	2.00	1.02
2	2.34	1.19
3	1.62	0.83
4	3.05	1.55
Average of the four	2.25	1.15

7-2-2-4 Surface preparation

To obtain a high bond strength, concrete substrate surface must be sound, clean, and dry. This can be achieved by shot blasting the surface of the concrete substrate. In this experiment a Blastrac 1-7 D series surface preparation machine was used. The Blastrac 1-7 D has been designed for using on small or inaccessible surfaces. The cleaning path was 200 mm and the rate of preparing was 15 m^2 per hour. The system can work within 1 cm of an edge and is electrically powered and manually propelled for simplicity of

operation and the process is dust free, environmentally friendly and cost effective. [Blastrac] The machine has been shown in figure 7-12.

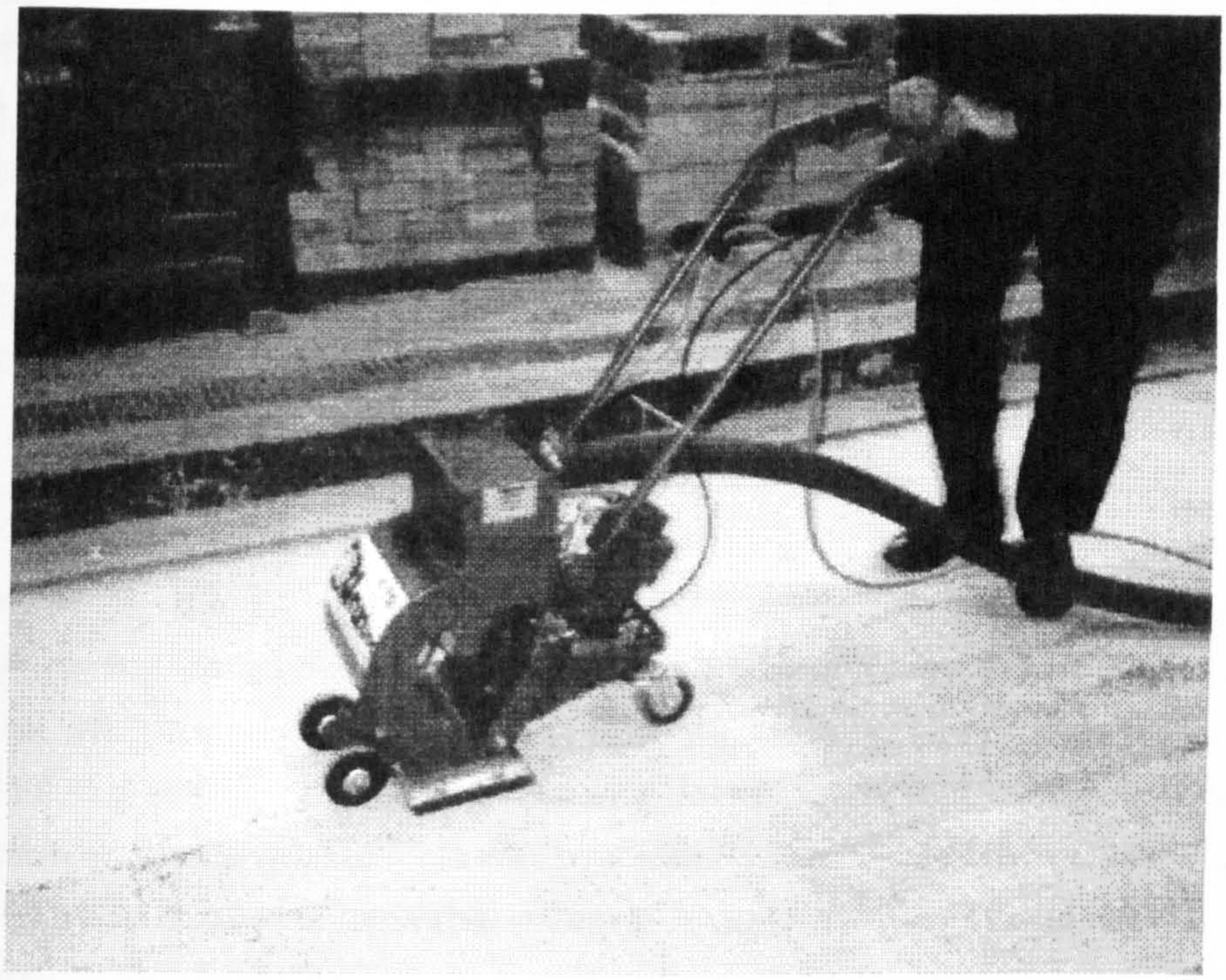

Figure 7-12: The Blastrac 1-7 D shot blasting machine in use

7-2-2-5 Construction of the thin layered flooring materials on top of the concrete substrate

Figure 7-13 shows the layout of the combinations of thin layered systems laid on the testing area.

In this experiment there were totally five combinations of the four main materials (concrete, G1194, G1294, and the primers) as follows: (figure 7-13)

-G1194 material on top of a layer of P4 system on top of the new concrete substrate, **G1194/P4/Concrete**, and only Gprime was used at the interface between the two layers of G1194 material and P4 system. (Bay No. 5)

-G1294 material on top of a layer of P4 system on top of the new concrete substrate, **G1294/P4/Concrete**, and only Gprime was used at the interface between the two layers of G1294 material and P4 system. (Bay No. 4)

-G1194 material on top of the old concrete substrate, **G1194/Concrete**. Two different types of primers were examined at the interface between the two layers of G1194 material and the concrete substrate. (Bays Nos. 1 & 7)

-G1294 material on top of the new concrete substrate, **G1294/Concrete.** Two different types of primers were examined at the interface between the two layers of G1294 material and the concrete substrate. (Bay Nos. 2 & 6)
-P4 material on top of the new concrete substrate, **P4/Concrete,** and only Pprime was used at the interface between the two layers of P4 system and the concrete substrate. (Bay No. 3)

The age of each combination at which the NUROLF tests have been carried out is reported in table 7-8.

As it is shown in figure 7-13, a thin layer of P4 system was to be laid on bays nos. 3,4, and 5, This was done at the age of 13 days of the new concrete layer. Before laying the P4 system, the cleaned shot blasted substrate was primed properly using Pprime. After drying out the primer (after about 2 hours), P4 material was properly mixed with the appropriate percentage of water by using a powerful portable mixing machine in a large plastic bin. After pouring P4 material on to the surface of the concrete substrate, the fresh layer of the material was gently compacted using a special rolling plastic brush. The thickness of this layer was about 6 mm.

G1194 and G1294 were to be applied on the appropriate bays in accordance with the layout shown in figure 7-13. This was done at the age of 16 of the new concrete substrate and at the age of 3 days of the P4 layer. Before laying G1194 or G1294 material, the cleaned shot blasted substrate was primed properly using the desired primer. After drying out the primer (after about 2 hours for Pprime and after about 16 to 18 hours for Gprime), the components of the flooring material were properly mixed by using a powerful portable mixing machine in a large plastic bin. After pouring G1194 or G1294 material on to the surface of the concrete substrate, the fresh layer of the material was gently compacted using a special rolling plastic brush. The thickness of this layer was about 3 mm.

Figure 7-13: The layout of the testing area

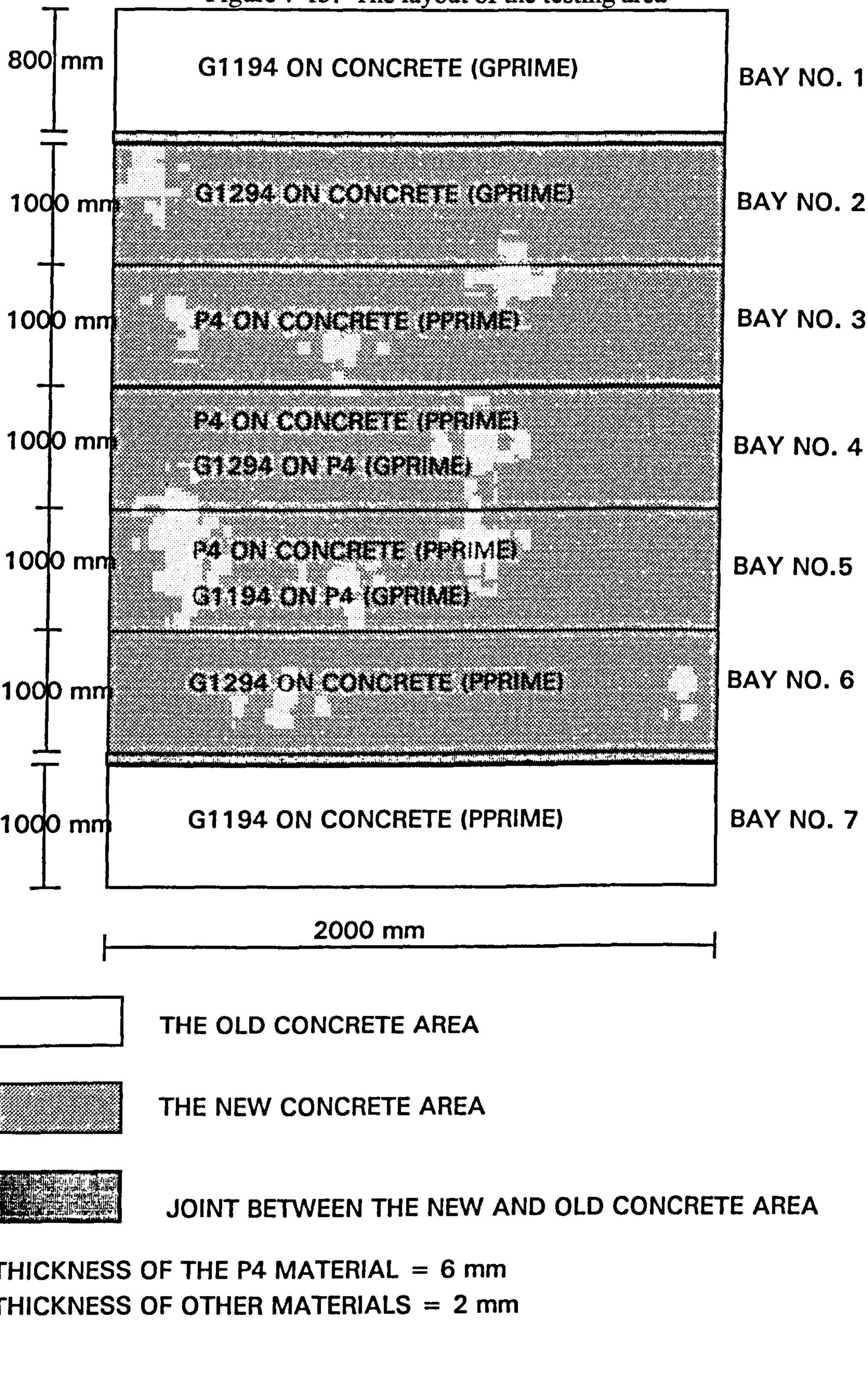

THICKNESS OF THE P4 MATERIAL = 6 mm
THICKNESS OF OTHER MATERIALS = 2 mm

7-2-3 Pneumatic Tyre Rolling Load Test

7-2-3-1 Test apparatus and equipment

7-2-3-1-1 NUROLF

NUROLF, Newcastle University Rolling Load Facility, was designed and constructed by Professor John Knapton's Structural Engineering group within the Department of Civil Engineering at the University of Newcastle Upon Tyne during 1991-1992.

NUROLF can provide a realistic full scale laboratory simulation of any kind of traffic loading.

The test vehicle (figure 7-14) in NUROLF is powered by a 60 HP computer controlled electric motor accelerating the rear axle through the original vehicle's differential gears. By using the computerized system, it is possible to simulate the prescribed levels of acceleration, deceleration and constant speed.

The vehicle consists of dual water ballast tanks and panniers load lockers which make it possible to apply vertical axle loads up to 14000 kg and horizontal tyre-pavement loads by acceleration up to 2000 kg.

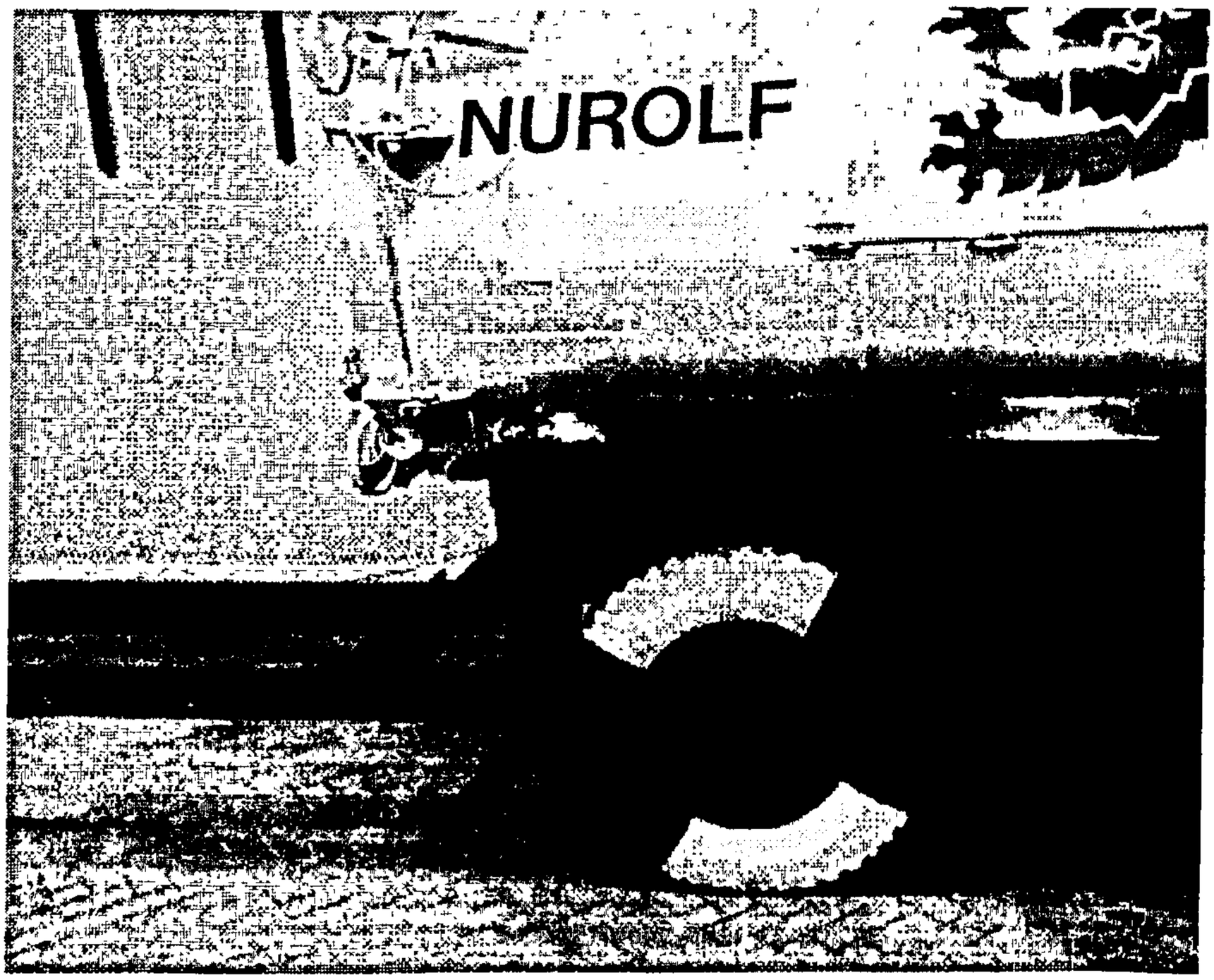

Figure 7-14: The NUROLF vehicle [NUROLF]

The load application position is kept constant by the vehicle system. Having the above specifications and other built in facilities, NUROLF can be used in a wide range of testing applications. [NUROLF]

7-2-3-1-2 PUNDIT

As it will be described later on in this chapter, three different ways were used for detecting the possible delamination between the upper two layers in each combination of the thin layered systems in the NUROLF experiment:

- The ultrasonic pulse velocity method
- Tapping the surface of the upper layer using a piece of steel bar
- Tensile bond strength pull off test using Limpet.

The ultrasonic pulse velocity method using the PUNDIT was described in chapter 6-2-3-1-2. The second method is very simple and does not require further explanation. The third method will also be referred to in the next section of this chapter.

7-2-3-1-3 Limpet

Limpet loading equipment (figure 5-7) was used in this experiment for carrying out some comparative tensile bond strength tests for detecting any possible delamination at the interface between the upper two layers in each combination of the thin layered systems.
The apparatus and its uses were described in chapter 5-2-1-1 and 7-2-2-3.

7-2-3-2 Test procedure

The aim of this test was to simulate the actual loading condition resulted from a relatively free pneumatic tyre rolling load on a thin layered system, and to investigate the effect of this kind of load on the bond strength between the two upper layers which were directly subjected to the load. In other words it was to be examined whether a relatively free tyre rolling load could cause a delamination. The NUROLF test vehicle was used for this purpose.
In this experiment two constant rolling loads of 4.625 ton and 6.5 ton applied on a rear dual wheel were used. The inflation pressure was 100 psi. (figure 7-15)

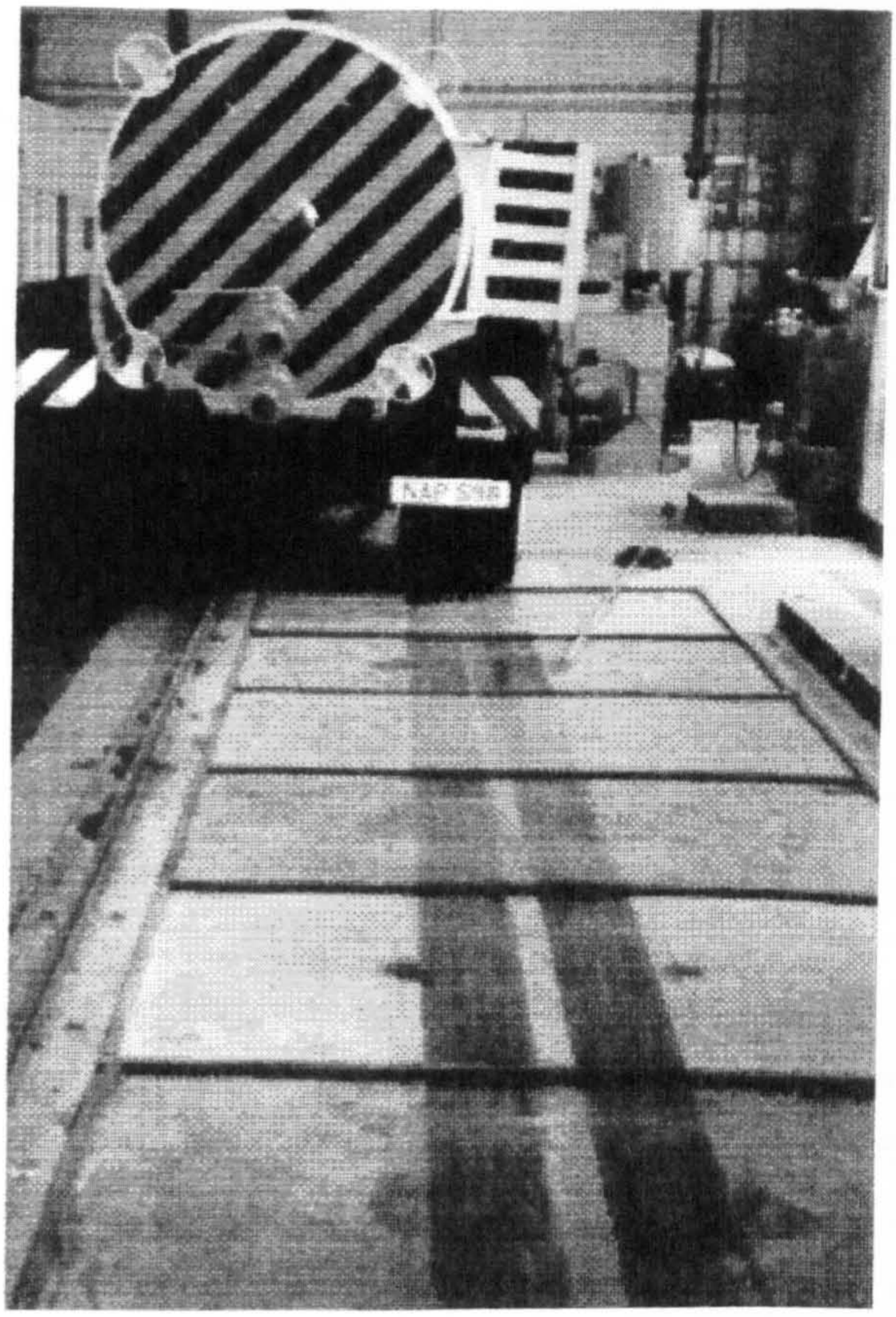

Figure 7-15: The thin layered systems under the rolling load test

As stated before, three methods were used for detecting any possible delamination, sounding of the upper layer surface, pulse velocity method, and tensile bond strength test.

Sounding of the upper layer surface was done manually by striking it with a steel rod. In a delaminated case, the upper layer would echo with a thud. [Van Dam et al. 1987]

In the pulse velocity method, the pulse transmission time between the two transducers was measured and recorded before and after applying the load, a comparison between these two values would show the bond condition at the interface.

The third method was measuring the tensile bond strength between the two upper layers of each thin layered system, both on the tyre path and on the free loading area of each Bay. By comparing the two series of results, the performance of the layered system under the action of the load was to be examined.

Before carrying out the rolling load test, the locations of the transducers onto the surface of each combination of layers (each bay) were to be determined. These locations were on the two opposite sides of the tyre path, as the surface transmission method (figure 6-6-c) was to be used in this experiment. (figure 7-16)

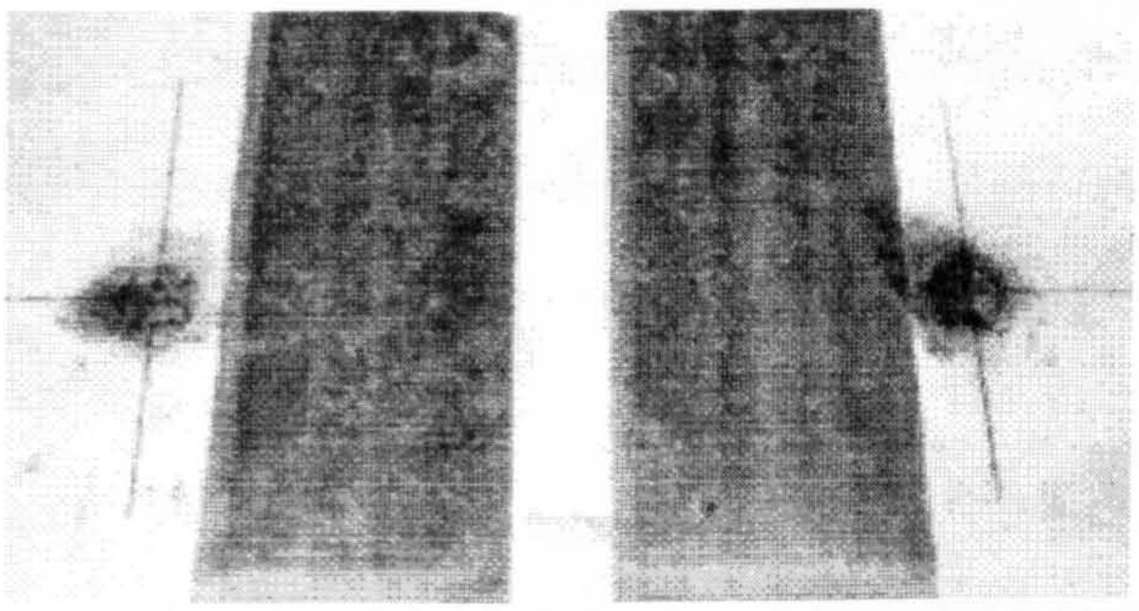

Figure 7-16: Locations of the transducers on the surface of a thin layered system

The initial pulse transmission time between the specified locations was measured and recorded for each combination (each bay) before test. After applying the desired number of rolling load cycles on the test area, the combinations were examined using both the sounding method by tapping the surface and the pulse velocity method by recording the pulse transmission time between the specified points. The procedure was to be continued until the end of the test. After completing all stages of the Rolling load test, the thin layered systems were also examined by the third method, the tensile bond strength test method, using Limpet. (figure 7-17)

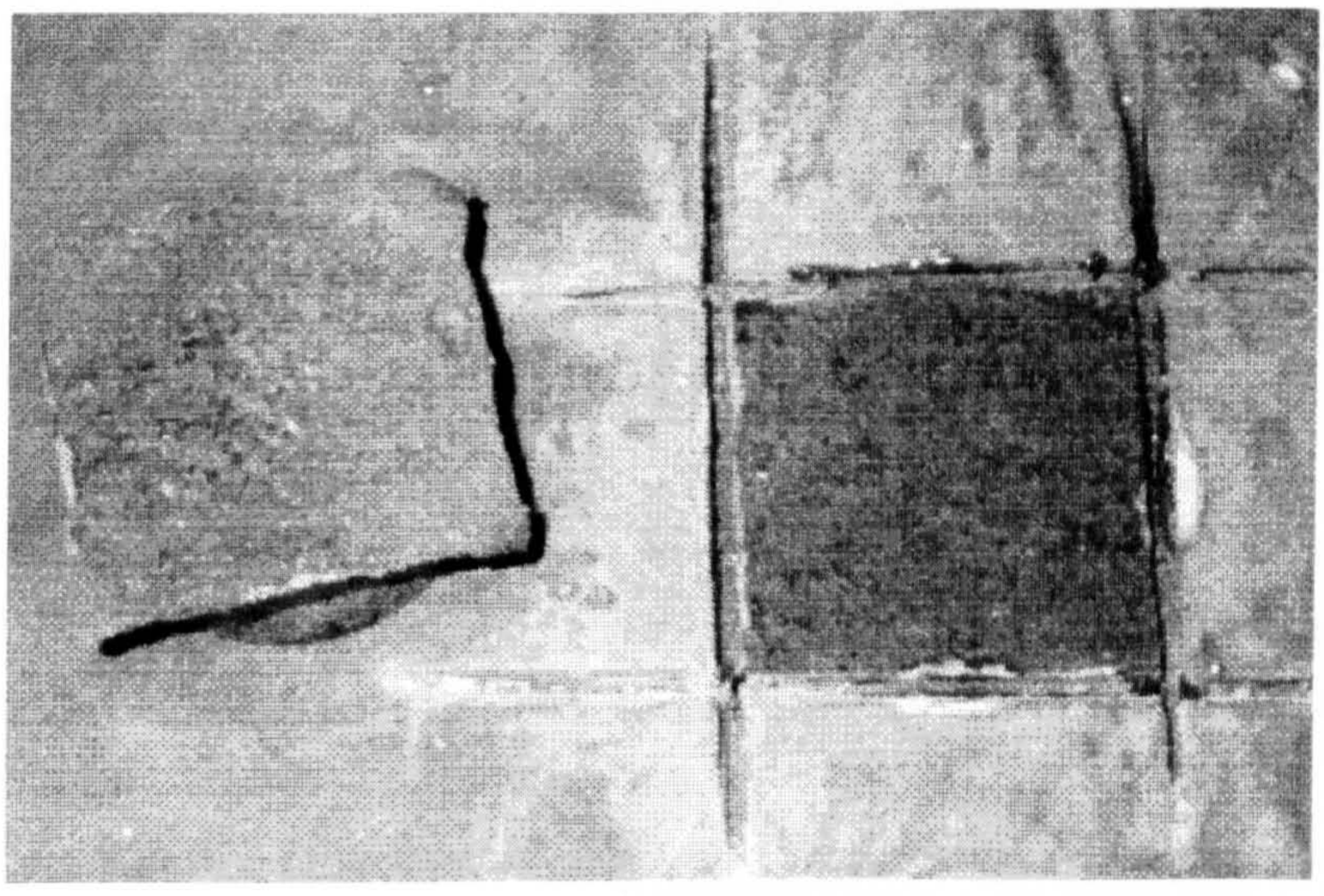

Figure 7-17: Tensile bond strength test using Limpet equipment

The total number of applied load cycles, values of the corresponding rolling loads on two tyres, and methods of surface examinations used for the thin layered systems at each stage are tabulated in table 7-5.

Table 7-5: Information on the total number of applied load cycles, rolling load values , and methods of surface examinations used for the thin layered systems at each stage of the test

Total number of applied load cycles	Maximum vertical load (Tyre inflation = 100 psi)	Methods of surface examination		
		Sounding test	PUNDIT test	Limpet test
100	4.625 ton	+	+	-
200	4.625 ton	+	+	-
500	4.625 ton	+	+	-
1000	4.625 ton	+	+	-
1400	6.500 ton	+	+	+

7-2-3-3 Test results

Information on the total number of applied load cycles, and the rolling load values at each stage of the test was given in table 7-5. As stated in that table, after each stage of the test, the surfaces of the thin layered systems were examined using the sounding method. At none of these stages was any sign of delamination detected by this method.

The results of the pulse transmission method are summarized in table 7-6. As it is seen from the results of this table, the change in the transmission time in each case is not considerable, and therefore it can be concluded that there has been no delamination in the thin layered systems.

At the end of the Rolling Load Tests, the thin layered systems were also examined by the tensile bond strength method using Limpet. The corresponding results are shown in table 7-7. As it is seen, once again the results show no evidence of delamination.

Although it was the objective of this investigation, to evaluate the polymer concrete materials under dry condition, the test area was made wet all over and

then, the rear wheel of the NUROLF vehicle was placed on G1294 and G1194 for a period of 24 and 48 hours respectively. As a result of this test, G1294 was badly damaged so that the image of the tyres were obvious. (figure 7-18) By contrast the behaviour of G1194 was very good and there was not any change on the appearance of the material surface.

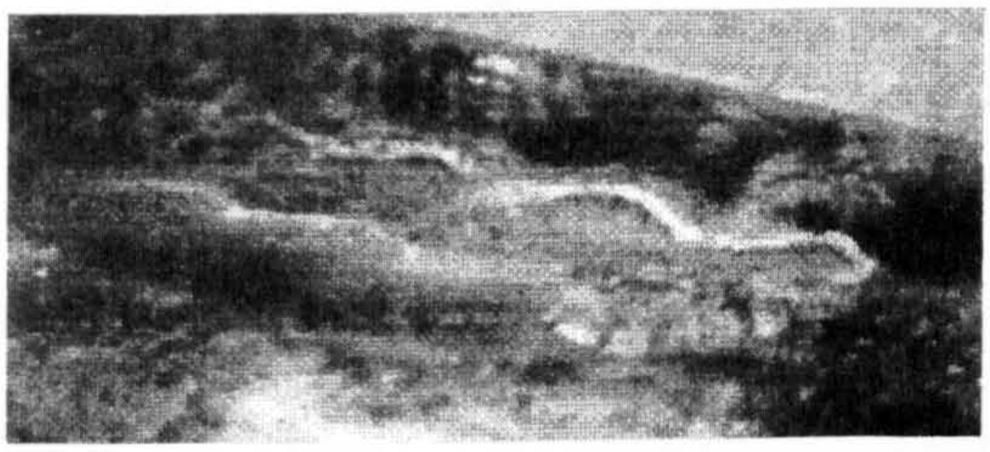

Figure 7-18: The performance of G1294 material under wet condition

Table 7-6: The results of the pulse velocity method using the PUNDIT on the surface of the thin layered systems in the NUROLF experiment

Bay Number	Distance (mm)	Pulse transm. time (μ sec) after applying the following load cycles				
		0 cycles	200 cycles	500 cycles	1000 cycles	1400 cycles
1	620	207	208	208	207	208
2	625	155	155	155	155	156
3	620	157	157	158	157	156
4	660	160	160	161	150	159
5	655	158	158	158	158	157
6	635	156	156	155	156	155
7	630	197	198	197	198	198

Table 7-7: The results of the tensile bond strength tests using Limpet on the thin layered systems in the NUROLF experiment

Bay Number	Location of the specimen	Bond strength (Mpa)[1]	Layers adjacent to the interface of failure		Primer at the interface
1	On the path	0.38[2]	G1194	Concrete	Gprime
1	Off the path	2.92	G1194	Concrete	Gprime
2	On the path	1.26	G1294	Concrete	Gprime
2	Off the path	1.26	G1294	Concrete	Gprime
3	On the path	1.23	P4	Concrete	Pprime
3	Off the path	1.34	P4	Concrete	Pprime
4	On the path	1.05	G1294	P4	Gprime
4	Off the path	1.31	G1294	P4	Gprime
5	On the path	1.91	P4	Concrete	Pprime
5	Off the path	1.68	P4	Concrete	Pprime
6	On the path	0.29	G1294	Concrete	Pprime
6	Off the path	0.17	G1294	Concrete	Pprime
7	On the path	0.45	G1194	Concrete	Pprime
7	Off the path	0.79	G1194	Concrete	Pprime

1- Results have been taken from the average of three tests on each bay.

1- The failure occurred within the concrete substrate. However due to the excellent background of combination G11/Concrete, the corresponding low value of bond strength can not be assigned to the interface behaviour, as the concrete was an old concrete which had been being used under the action of the NUROLF vehicle for the life of the NUROLF.

7-3 Structural analysis

In the last sections, the experimental program regarding the behaviour of thin layered systems under the action of a pneumatic tyred vehicle wheel rolling load was presented. The main objective of that program was examining whether any delamination at the interface between the coating and the second layer of the thin layered systems would occur. The results showed that no delamination had occurred at the interface between the two layers of each system. In this part of study, it will be attempted to model and analyse the same systems in order to establish a proper method for predicting the behaviour of thin layered systems under the action of a Tyre Wheel Rolling Load. The analysis will be based on the finite element method using a proper interface layer, as it was discussed in chapter 4 and used in chapter 6.
Based on the results given in section 5-2, interface bond strength, and in the previous section of this chapter, the following combinations of layered systems will be analysed in this investigation as the most representative cases:

- **G1194/P4/Concrete** using **Gprime** at the interface between G1194 and P4 layer at the age of 3 days under the action of a 32500 N pneumatic tyre load. (Bay No. 5)

- **G1294/P4/Concrete** using **Gprime** at the interface between G1294 and P4 layer at the age of 3 days under the action of a 32500 N pneumatic tyre load. (Bay No. 4)

- **G1194/Concrete** using **Pprime** at the interface between G1194 and the concrete layer at the age of 3 days under the action of a 32500 N pneumatic tyre load. (Bay No. 7)

- **G1294/Concrete** using **Pprime** at the interface between G1294 and the concrete layer at the age of 3 days under the action of a 32500 N pneumatic tyre load. (Bay No. 6)

- **P4/Concrete** using **Pprime** at the interface between P4 and the concrete layer at the age of 6 days under the action of a 32500 N pneumatic tyre load. (Bay No. 3)

7-3-1 General assumptions and approximations

7-3-1-1 The finite element mesh and the constitutive materials

- Owing to the low tyre contact pressure, for all the constitutive materials, linear elastic behaviour has been considered based on the corresponding results of the modulus of elasticity tests in chapter 5.
- It is the manufacturer's claims that most of the bond strength at the interface between the different layers of materials is developed within about three days of construction and in fact the results of tests reported in chapter 5 showed that the bond strength is not very susceptible to the age. For this reason further bond strength and shear box tests were not carried out specifically for the purpose of the analysis in this part of work, and therefore the most appropriate results from the available data given in chapter 5 have been used in the following analysis.

As the main concern of this investigation was the behaviour of the thin layered systems at the interface, only 25 mm of the depth of the concrete substrate has been considered in the finite element mesh. The appropriateness of this thickness has been inferred from the study carried out by Zollinger et al. [Zollinger et al. 1994]. The length of the finite element mesh will also be the same as assumed by the above researchers.

Although a three dimensional finite element mesh would be ideal for the analysis of a layered system, because of the restrictions in the computer memory and also saving the time of analysing, once again two dimensional plain strain finite element mesh has been assumed. This assumption has been also made by other investigators. [Zollinger et al. 1994] [Lundy 1990] However in order to keep the consistency with the interface elements, and at the same time to get a more accurate analysis, isoparametric quadrilateral 8 noded elements have been used for all layers of the thin layered systems. Once again the LUSAS finite element software will be employed for the analysis in this chapter.

7-3-1-2 The interface layer

- As it was discussed in chapter 4 and 6, a thin elastic interface layer has been considered in each model of the thin layered systems to be analysed.

To define the interface layer, two parameters are required, the elastic shear modulus (G), and the thickness of the layer (t). The procedure for defining these parameters will be exactly the same as it was discussed in section 6-3-1-2 of chapter 6.

Therefor the G modulus is defined as follows: [Desai et al. 1984]

$$G_{i(\sigma_n,\tau,u_r)} = \frac{\partial\,[\tau_{(\sigma_r,u_r)}]}{\partial\,u_r} \times t\Big|_{\sigma_n} \qquad (6\text{-}1)$$

The ratio of $\frac{\partial\,[\tau_{(\sigma_r,u_r)}]}{\partial\,u_r}$ has been defined by analysing the appropriate plane strain finite element mesh of the shear box specimens reported in chapter 5. (figures 6-9-a & 6-10-a) Since the interface element layer has been assumed elastic, and isotropic, the above assumption would be acceptable.

Table 7-8: The proposed values of the elastic modulus for simulating the interface layer

Upper layer	Lower layer	Bay No.	Relative displacement (mm)	Assumed Poisson's ratio [3]	Interface thickness ratio	Interface E modulus (MPa)
G1194 [1]	P4	5	4.400E-04	0.29	0.01B	3500t
G1294 [1]	P4	4	1.265E-03	0.32	0.01B	1980t
G1194 [1]	Concrete	1	4.960E-04	0.25	0.01B	5360t
G1194 [1]	Concrete	7	5.110E-04	0.25	0.01B	4730t
G1294 [1]	Concrete	2	1.492E-03	0.28	0.01B	2150t
G1294 [1]	Concrete	6	1.492E-03	0.28	0.01B	2150t
P4 [2]	Concrete	3	3.060E-04	0.21	0.01B	4710t

1- Age at the time of test = 3 days

2- Age at the time of test = 6 days

3- As an assumption, the average value for the materials used in the adjacent layers has been considered in the analysis.

The values of vertical load for the two models are the average figures which have been used in the shear box tests, i.e. 0.88 MPa for the small shear box

model and 0.58 MPa for the large one. The value of the horizontal load is 1.00 MPa for both of the models. (figures 6-9-b, 6-10-b)

The other main parameter is the thickness of the thin interface layer. As it was discussed in section 6-3-1-2 of chapter 6, once again the ratio of t/B = 0.01 has been considered for all the combinations in this chapter.

To achieve a more accurate solution and according to Desai et al. [Desai et al. 1984], isoparametric solid elements have been used in the thin interface layers. (8 noded quadrilateral plane strain elements in this study)

Based on the above assumptions, the proposed values of the E modulus for simulating the required thin interface elements in the structural analysis, have been tabulated in table 7-8.

7-3-1-3 The contact pressure distribution of the rolling tyre

Although the NUROLF vehicle was capable of simulating much higher values of acceleration and deceleration, due to the limited travelling distance in this experiment, the value of acceleration was about 1 $m/\sec^2$. For a tyre pressure of 100 psi (0.7 MPa), the above acceleration will result in producing a shear stress of about 0.07 MPa. As it will be referred to in due course in this section, the longitudinal contact shear pressure due to a free rolling tyre is about 25 psi (0.175 MPa). Comparing the above figures, we could reasonably consider the situation as a free rolling tyre. This assumption will also be very helpful with regard to the size of the structure to be analysed, as in this case the structure can be considered as symmetrical.

The distribution of stresses between the tread and the road for freely rolling tyres have been studied by many investigators. [Lippmann et al. 1974] [Tielking et al. 1987] According to these researches, the real contact stress between a free rolling tyre and the pavement is nonuniform and very complicated. (figure 7-19)

The contact pressure may be divided into three components, normal pressure, longitudinal shear pressure and transverse shear pressure. Factors affecting the normal component of the contact pressure may be speed, tyre inflation, tyre load, and pavement friction. Tielking and Roberts have discussed the above factors and concluded that due to the small effects of speed and pavement friction on normal pressure distribution for a free - rolling tyre, normal contact pressures resulted from a nonrotating tyre deflected against a frictionless surface are realistic representations of the normal pressure under a real tyre

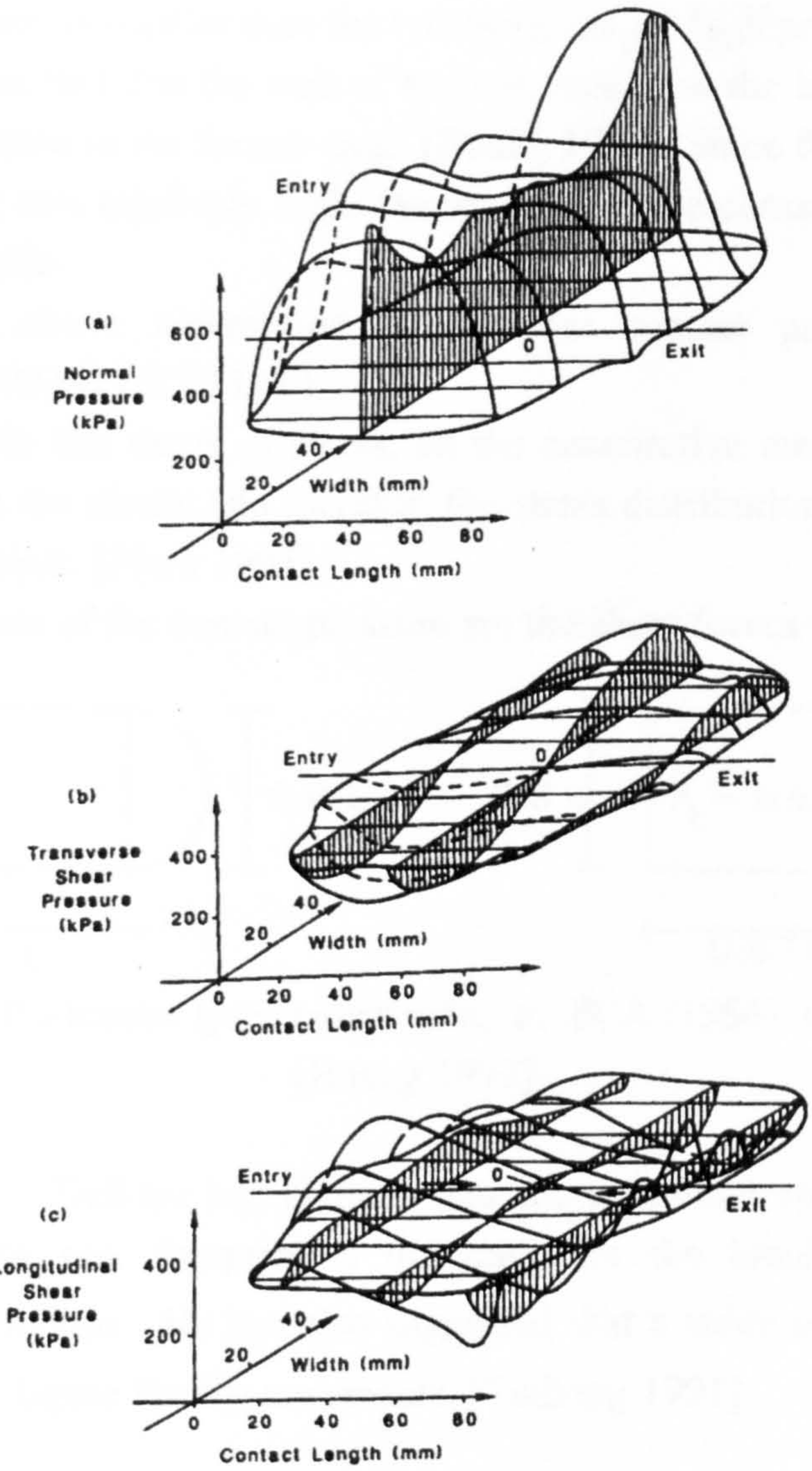

Figure 7-19: A typical laboratory measurement of tyre contact pressure for a tyres size 165 SR 13 with the inflation pressure of 24 psi under a load of 3532 N at a speed of 16.7 m/sec.: a: Normal pressure; b: Transverse shear pressure; c: Longitudinal shear pressure [Tielking et al. 1987]

travelling at highway speeds. [Tielking et al. 1987] Moreover owing to the complexity of the real tyre contact pressure, many investigators have used a uniform distribution of contact pressure in their researches. [Zollinger et al. 1994] [Lau et al. 1994] The assumption of using a uniform normal contact pressure distribution will also be considered in this investigation.

Basically the normal contact pressure is greater than the tyre pressure for low pressure tyres and is smaller than the tyre pressure for high pressure tyres. This is because of the fact that the wall of tyres is tension in the latter case whereas it is in compression in the former case. [Huang 1993] Since the tyre pressure in this experiment was relatively high, the use of it as the contact pressure would be on the safe side.

Based on the above assumption, the normal contact pressure has been considered as 100 psi (0.7 MPa).

Obviously within this range of stress, all the constitutive materials in the thin layered systems are elastic and therefor, the stress distribution under the wheel will be symmetrical. [Plum 1995]

Other components of the contact pressure are the shear forces produced by

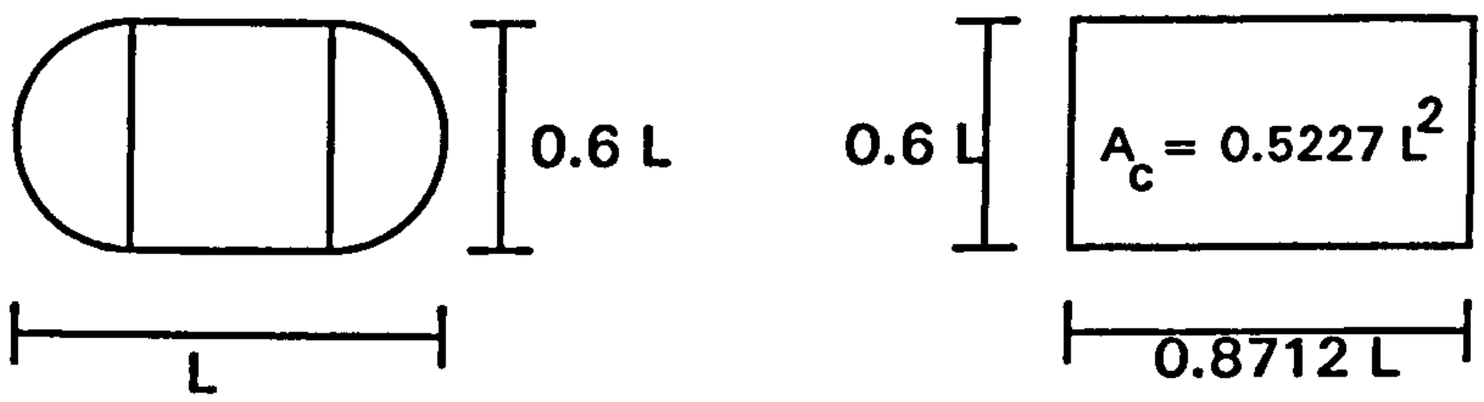

Figure 7-20: Pneumatic tyre contact area; a: PCA (1966) b: PCA (1984) [Huang 1993]

pneumatic tyres. Tielking has showed that the maximum shear stress in the free rolling truck tyre footprint is the same for the longitudinal and the transverse distributions. He has also suggested that a value of " $\tau_m = 25\ psi$ " can be a realistic figure for dry pavements. [Tielking 1991]

7-3-1-4 Contact area

The appropriate shape of contact area for a pneumatic tyre has been shown in figure 7-20-a which is based on PCA (1966). As it is seen in the figure, the contact area is composed of a rectangular and two semicircles. The length L in figure 7-20-a can be calculated from equation 7-8: [Huang 1993]

$$A_c = \pi(0.3L)^2 + (0.4L)(0.6L) = 0.5227L^2$$

$$L = \sqrt{\frac{A_c}{0.5227}} \qquad (7\text{-}8)$$

Where: A_c = The contact area $\approx \frac{\text{load on each tyre}}{\text{tyre pressure}}$

In PCA (1984) which is based on the finite element method, a rectangular area of dimensions 0.8712L by 0.6L is assumed. (figure 7-20-b)
Accepting the latter assumption for a 6.5 ×0.5 =3.25 ton pneumatic tyre, we have:

$$A_c = \frac{0.5 \times 6.5 \times 10^4}{100 \times 0.007} \approx 46429\ mm^2$$

$$L = \sqrt{\frac{46429}{0.5227}} \approx 298$$

Contact area ≈ 260 mm by 179 mm

7-3-1-5 The failure criteria

As it was discussed in section 6-3-1-4 of chapter 6, two failure criteria for predicting the possible delamination at the interface layer will be considered, the Mohr Coulomb criteria and the normal stress at the interface. However there will be a difference between the presentation of the results of the structural analysis in this chapter and those given in chapter 6. Since the behaviour of the constitutive materials in the NUROLF experiment is assumed as perfectly elastic, it makes it possible to use a special two dimensional elasto - plastic interface model which is available in the LUSAS finite element system. [LUSAS User Manual]
The elasto - plastic interface model may be used for representing the friction - contact relationship within planes of weakness between two discrete two dimensional bodies. As it was mentioned, nonlinear behaviour is governed by an elasto - plastic constitutive law, which is formulated with a Mohr - Coulomb criteria tangential to the interface plane, and a limited tension criteria normal to the interface plane.
The solution for this elasto - plastic interface model will be based on an incremental - iterative procedure using Newton - Raphson iterations. [LUSAS User Manual]
Four modes of deformation are incorporated with this model for the thin interface layer, stick mode, slip mode, debonding mode, and rebonding mode. The program automatically will modify the values of normal and shear stresses after each iteration and equilibrium as follows: [Desai et al. 1984]

Modes of deformation	computed
Before iteration and equilibrium	After iteration and equilibrium
Stick mode:	
$\sigma_n \langle 0$ (Compression)	Same as computed
$\tau \langle$ *Shear strength*	
Slip mode:	
$\sigma_n \langle 0$ (Compression)	$\sigma_n \langle 0$ (Compression)
$\tau \geq$ *Shear strength*	$\tau =$ *Shear strength*
Debonding mode:	
$\sigma_n \langle 0$ (Compression), $\tau \langle$ Shear strength on A_c	$\sigma_n \langle 0$ (Compression), $\tau \langle$ Shear strength on A_c
$\sigma_n \langle 0$ (Compression), $\tau \geq$ Shear strength on A_s	$\sigma_n \langle 0$ (Compression), $\tau =$ Shear strength on A_s
$\sigma_n \geq 0$ (Tension), $\tau \geq$ Shear strength on $A - A_c - A_s$	$\sigma_n = 0$, $\tau = 0$ on $A - A_c - A_s$
Rebonding mode:	
$\sigma_n \langle 0$ (Compression)	$\sigma_n \langle 0$ (Compression)
$\tau \geq 0$	$\tau \geq 0$

As an approximation full contact is assumed at this time.

Where: A = total area, A_c = contact area, A_s = area of slip which is usually assumed to be zero.

As it is seen from the above expressions, in this method, when a failure occurs at any node, the redistribution of stresses and strains within the structure would be taken into account. For evaluating a thin layered system with regard to the delamination defect, it is therefor necessary to carry out the analysis on two models of the structure simultaneously, one with a friction - slip interface model and the other with a stick interface model. In the friction - slip model

the real characteristics of the interface are considered whereas in the stick model the properties of the interface are chosen so that a perfect bond between the upper layer and the lower layer is guaranteed. Therefore, any difference between the distribution of shear stresses along the interfaces of the two models will be the result of occurrence of a slippage or debonding at the interface of the real structure.

7-3-2 The results of the stress - strain analysis

The stress strain analysis will be carried out for five models, five combinations of different layers. Owing to the symmetrical condition of the load and the finite element mesh, half of the structure will be analysed for each combination. For each model the finite element mesh, the distribution of shear stress along the interface, contours of the maximum principal stress in the vicinity of the load and the interface, and finally the distribution of maximum principal stress in the vicinity of the load and the interface will be presented. Two models of interfaces are to be considered for each combination, a friction - slip model and a stick model. By comparing the values of shear stresses along the interface for the two cases, any possible delamination can be easily detected.

7-3-3 Discussion of the results

The results of the structural analysis carried out for five combinations of different layers, Models 1 to 5, have been presented in sections 7-3-2-1 to 7-3-2-5. Two models of interfaces have been considered for each combination, a friction -slip model and a stick model. It is clearly seen that for graphs representing the distributions of shear stresses along the interface of each combination, all the constitutive points for both cases of the friction -slip model and the stick model are coincident. This means that no delamination has occurred in any combination of the thin layered systems.

From the contours and distribution of maximum principal stress in the vicinity of the load and the interface of each combination, it can be also concluded that the values of these stresses have not been critical in any case. In figure 7-25-6, the distributions of maximum principal stress at the bottom of the P4 layer and at the top of the concrete substrate have crossed each other. This is because of the fact that their modulus of elasticities have been relatively close to each other, and therefore it is not a sign of delamination at the interface.

7-3-2-1 Model 1: G1194/P4/Steel fibre reinforced concrete

Age: 3 days
Load: 32500 N
Contact area: An equivalent rectangular area of diameters a = 260 mm & b = 179 mm

Specifications of the materials and layers:

G1194:

E = 5500 MPa (table 5-12)
υ = 0.32 (table 5-16)
Thickness = 3 mm

Interface between G1194 and P4 using Gprime as the primer:

E = 3500 t (table 7-8)
t = 0.01B (table 7-8)
υ = 0.29 (table 7-8)
where t is the interface thickness (mm), and B is the width of the finite elements at the interface.
Cohesion, coefficient of friction, and tensile bond strength:
(tables 5-16 & 5-21)

Interface model	Cohesion (MPa)	Coefficient of friction	Tensile bond strength (MPa)
Friction - slip model	1.23	0.72	1.30
Stick model	5.00	5.00	5.00

P4:

E = 12400 MPa (table 5-9)
υ = 0.25 (table 5-16)
Thickness = 6 mm

Steel fibre reinforced concrete:

E = 16600 MPa (table 5-4)
υ = 0.17 (section 7-2-2-1)
Thickness = 25 mm (section 7-3-1-1)

Contact Pressure, MPa: (section 7-3-1-3)

Vertical uniform contact pressure = 100 psi = 0.7 MPa
Horizontal uniform contact pressure = 25 psi = 0.175 MPa

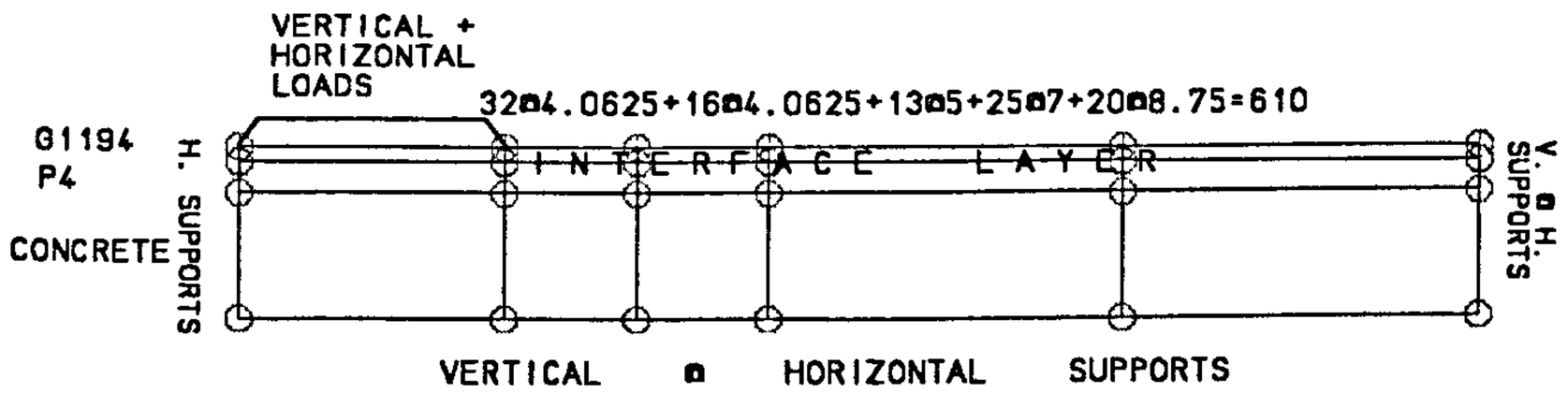

Figure 7-21-1: Half of the structure considered for the analysis of Model 1

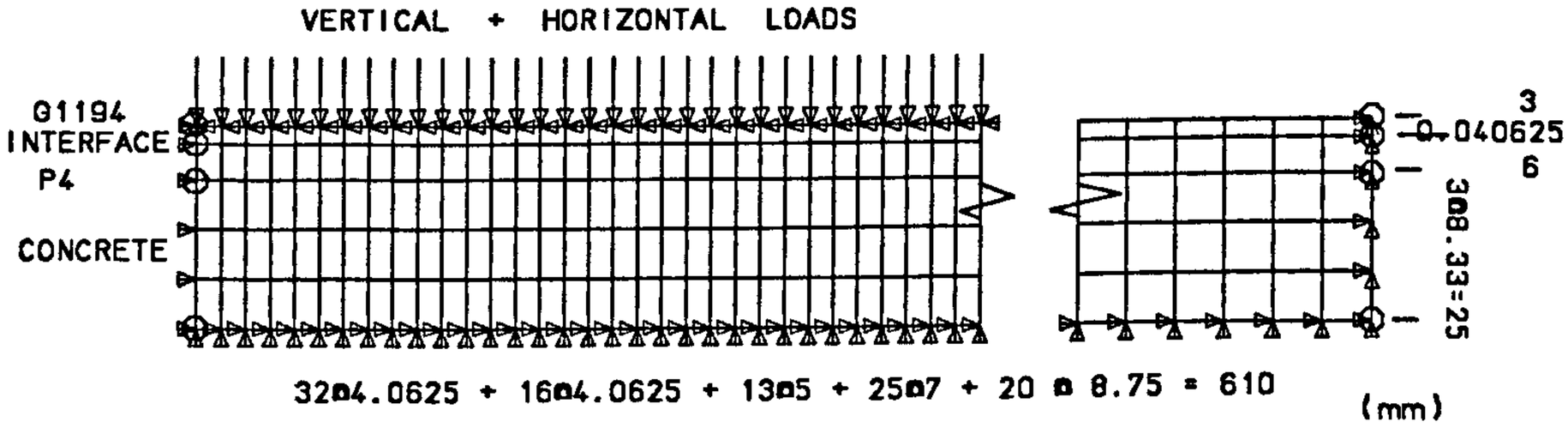

Figure 7-21-2: The finite element mesh for Model 1

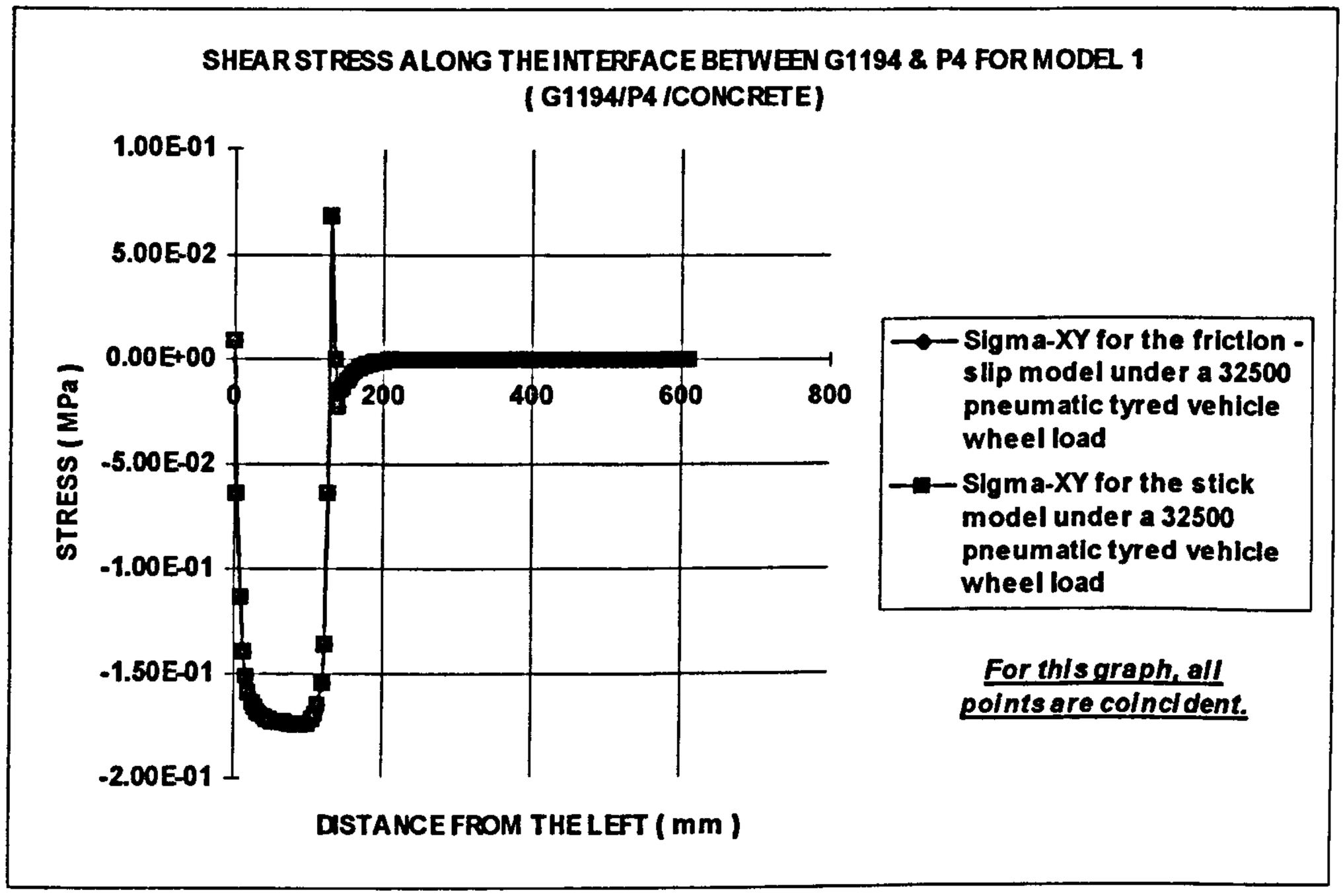

Figure 7-21-3: Model 1, G1194/P4/Concrete {Compression (-), Tension (+)}

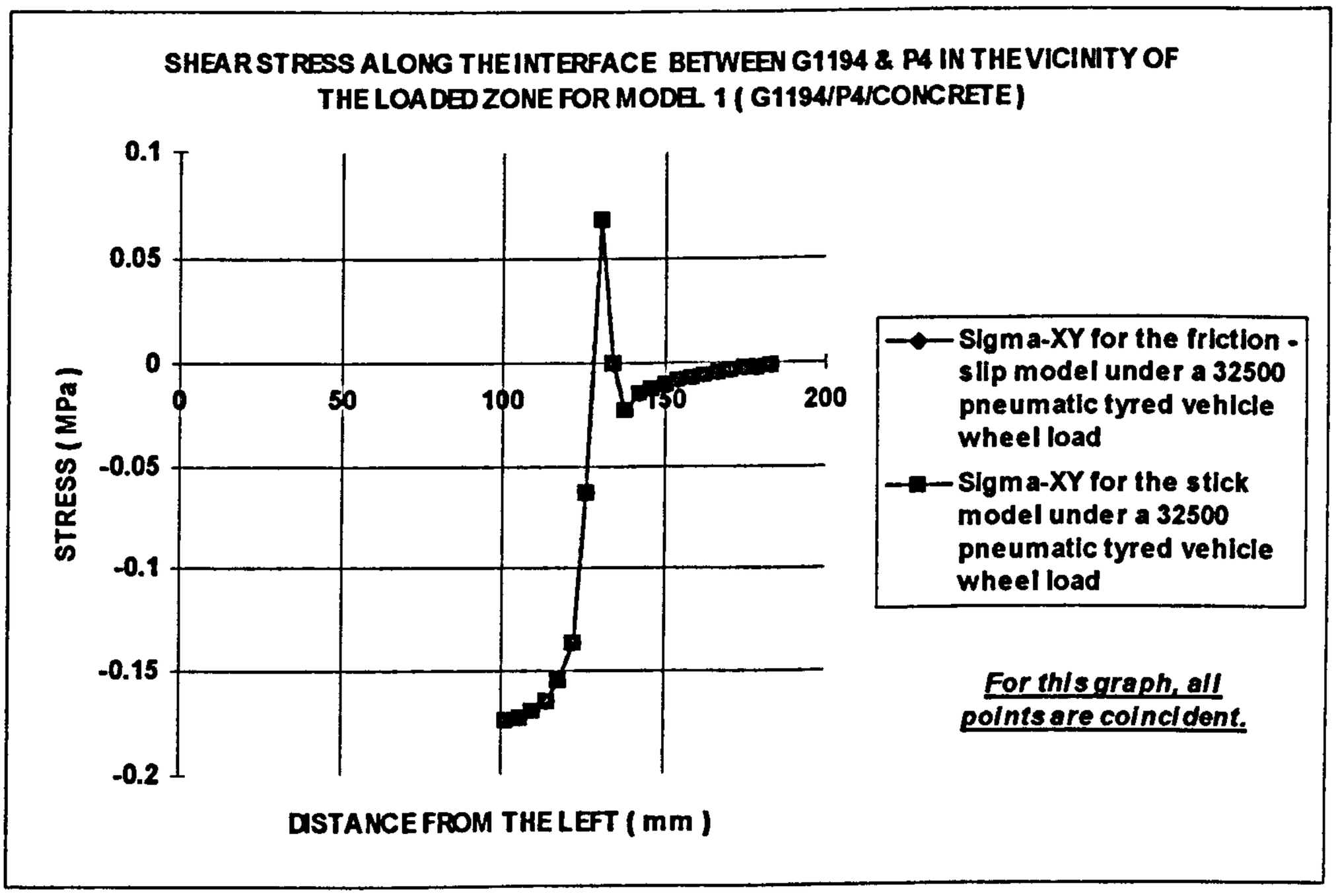

Figure 7-21-4 (Zoom): Model 1, G1194/P4/Concrete {Compression (-), Tension (+)} (No delamination occurs) ***AGREEMENT***

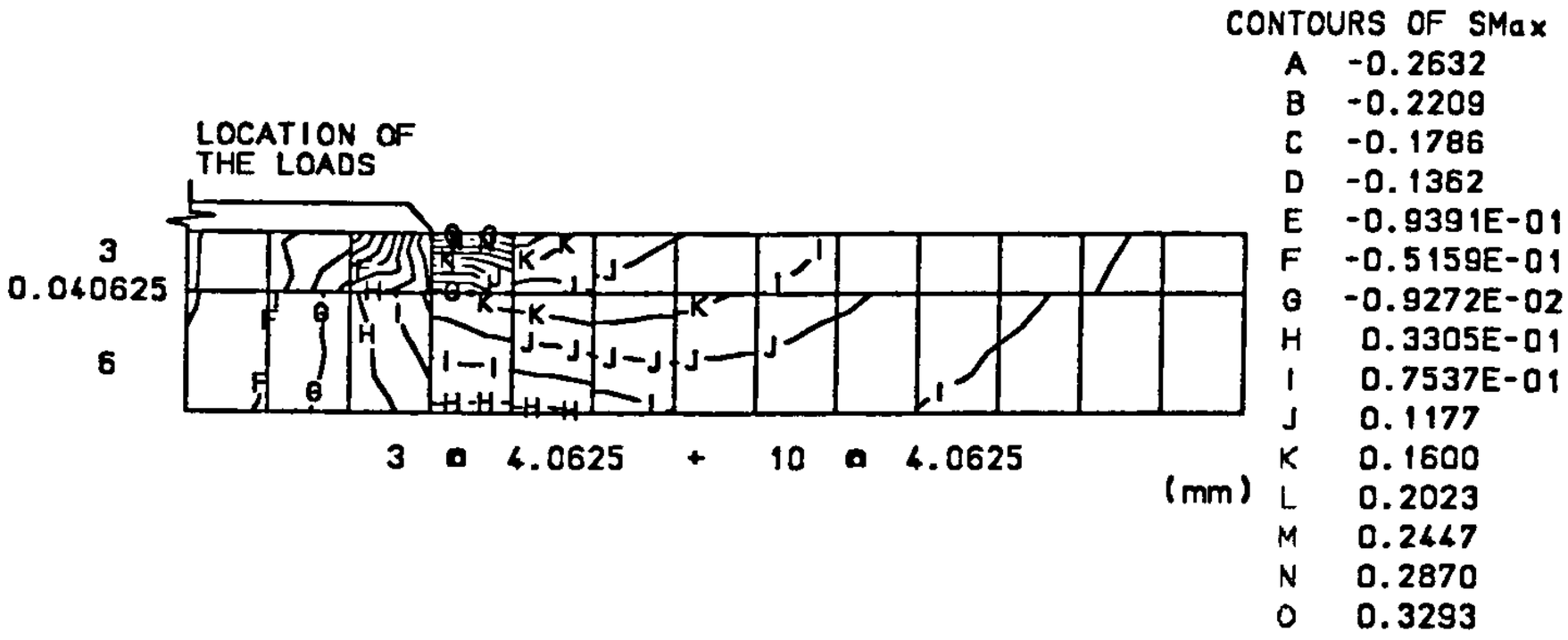

Figure 7-21-5: Contours of Sigma-1 (maximum) in the vicinity of the load and the interface for Model 1 {Compression (-), Tension (+)}

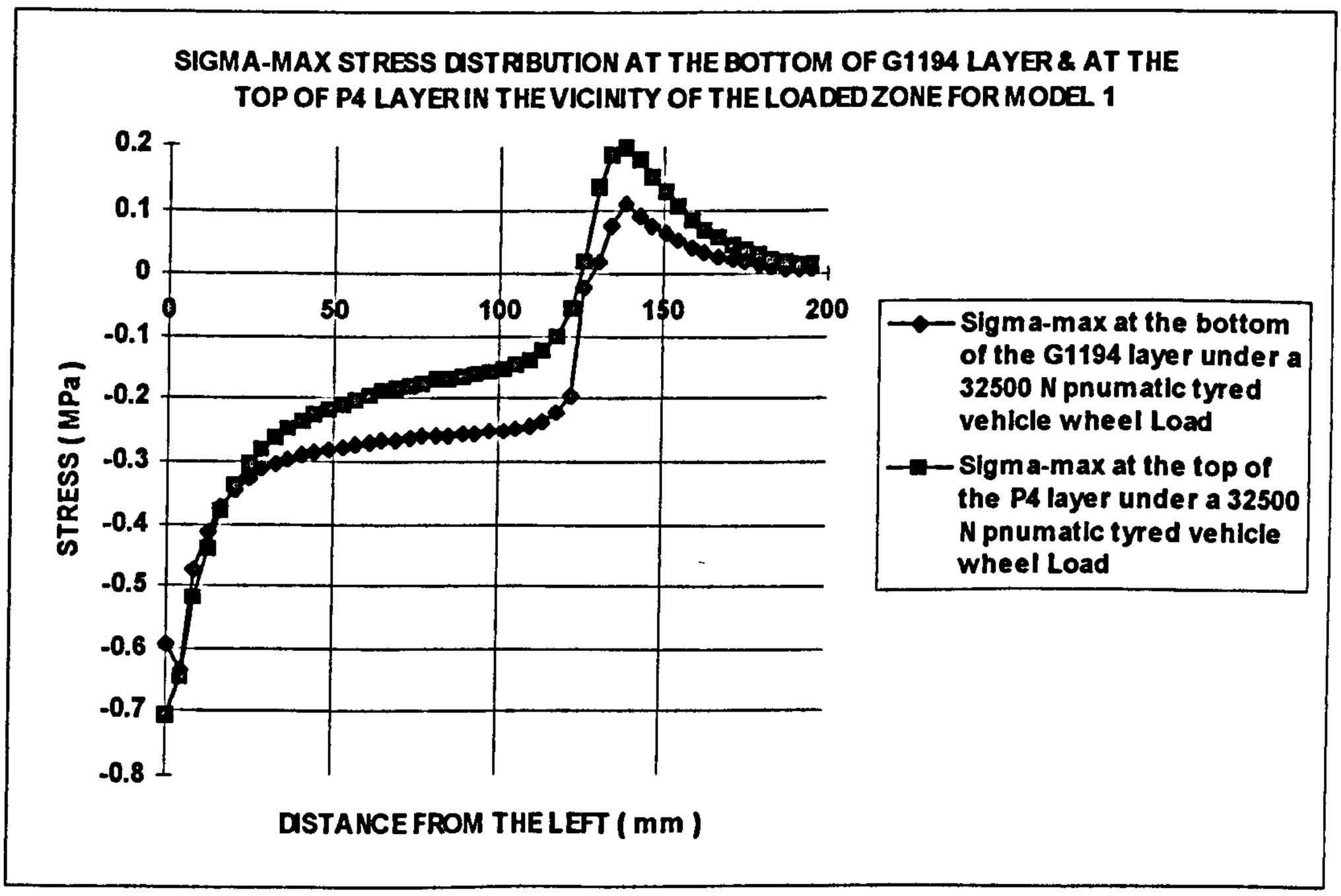

Figure 7-21-6: Sigma-1 (maximum) stress distribution in the vicinity of the loads and the interface for Model 1 {Compression (-), Tension (+)}

7-3-2-2 Model 2: G1294/P4/Steel fibre reinforced concrete

Age: 3 days

Load: 32500 N

Contact area: An equivalent rectangular area of diameters a = 260 mm & b = 179 mm

Specifications of the materials and layers:

G1294:

E = 1700 MPa (table 5-15)

υ = 0.38 (table 5-16)

Thickness = 3 mm

Interface between G1294 and P4 using Gprime as the primer:

E = 1980 t (table 7-8)

t = 0.01B (table 7-8)

υ = 0.32 (table 7-8)

where t is the interface thickness (mm), and B is the width of the finite elements at the interface.

Cohesion, coefficient of friction, and tensile bond strength: (tables 5-18 & 5-21)

Interface model	Cohesion (MPa)	Coefficient of friction	Tensile bond strength (MPa)
Friction - slip model	0.70	0.47	1.20
Stick model	5.00	5.00	5.00

P4:

E = 12400 MPa (table 5-9)

υ = 0.25 (table 5-16)

Thickness = 6 mm

Steel fibre reinforced concrete:

E = 16600 MPa (table 5-4)

υ = 0.17 (section 7-2-2-1)

Thickness = 25 mm (section 7-3-1-1)

Contact Pressure, MPa: (section 7-3-1-3)

Vertical uniform contact pressure = 100 psi = 0.7 MPa

Horizontal uniform contact pressure = 25 psi = 0.175 MPa

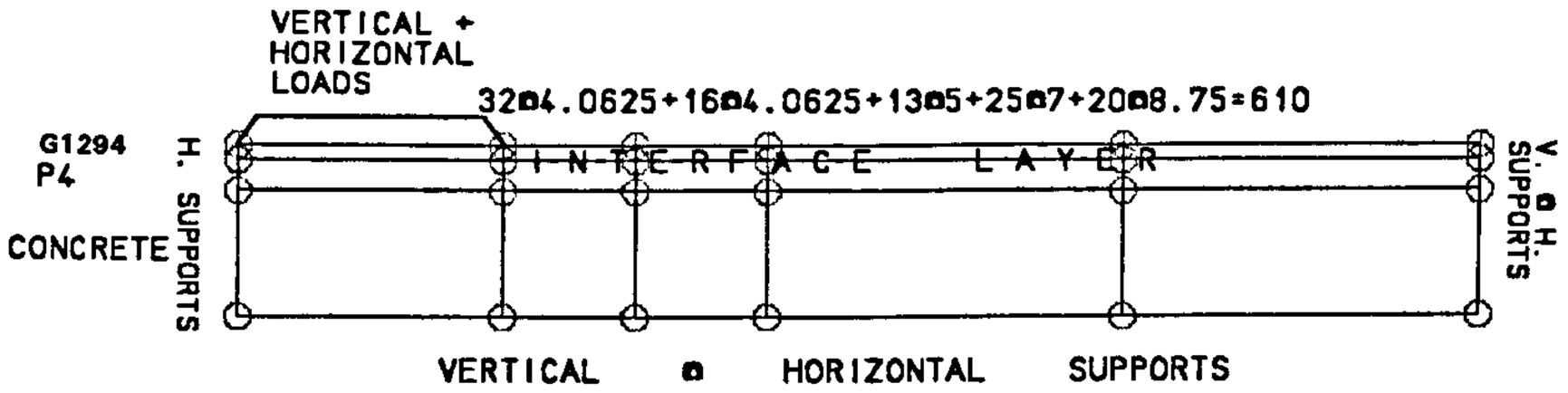

Figure 7-22-1: Half of the structure considered for the analysis of Model 2

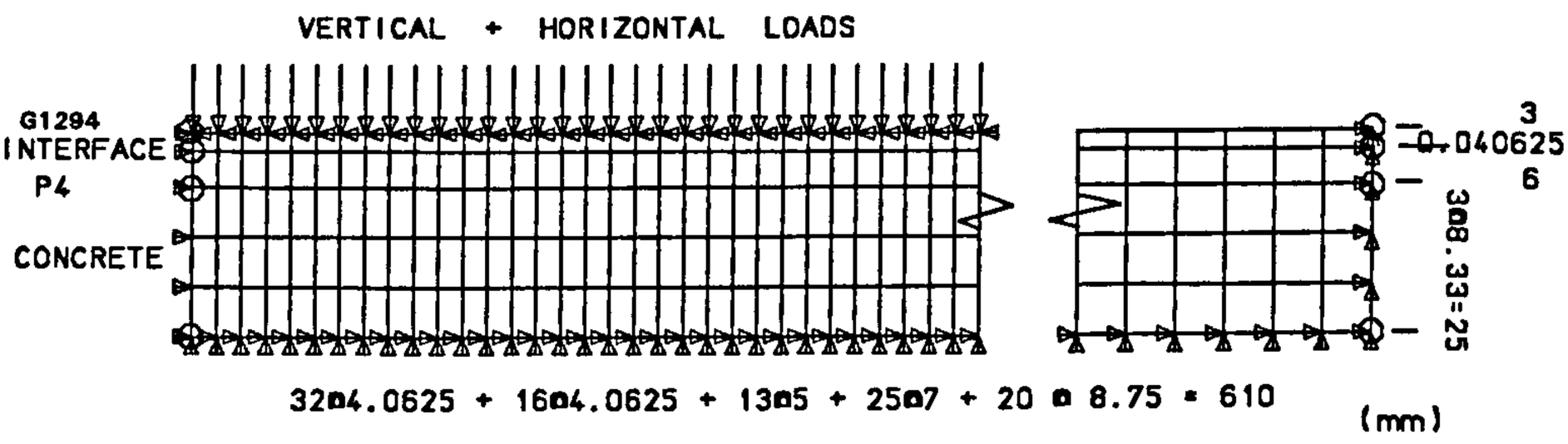

Figure 7-22-2: The finite element mesh for Model 2

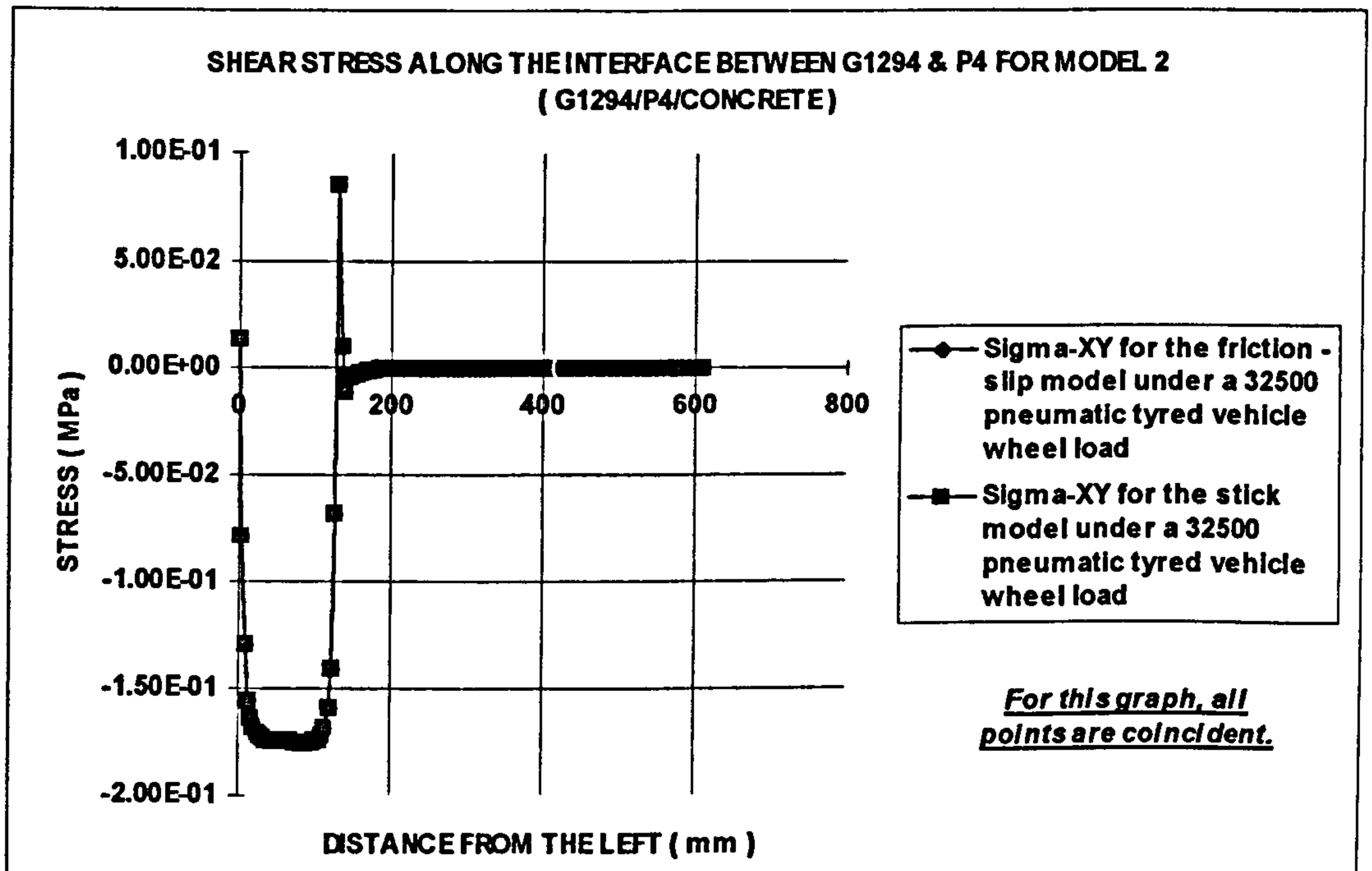

Figure 7-22-3: Model 2, G1294/P4/Concrete {Compression (-), Tension (+)}

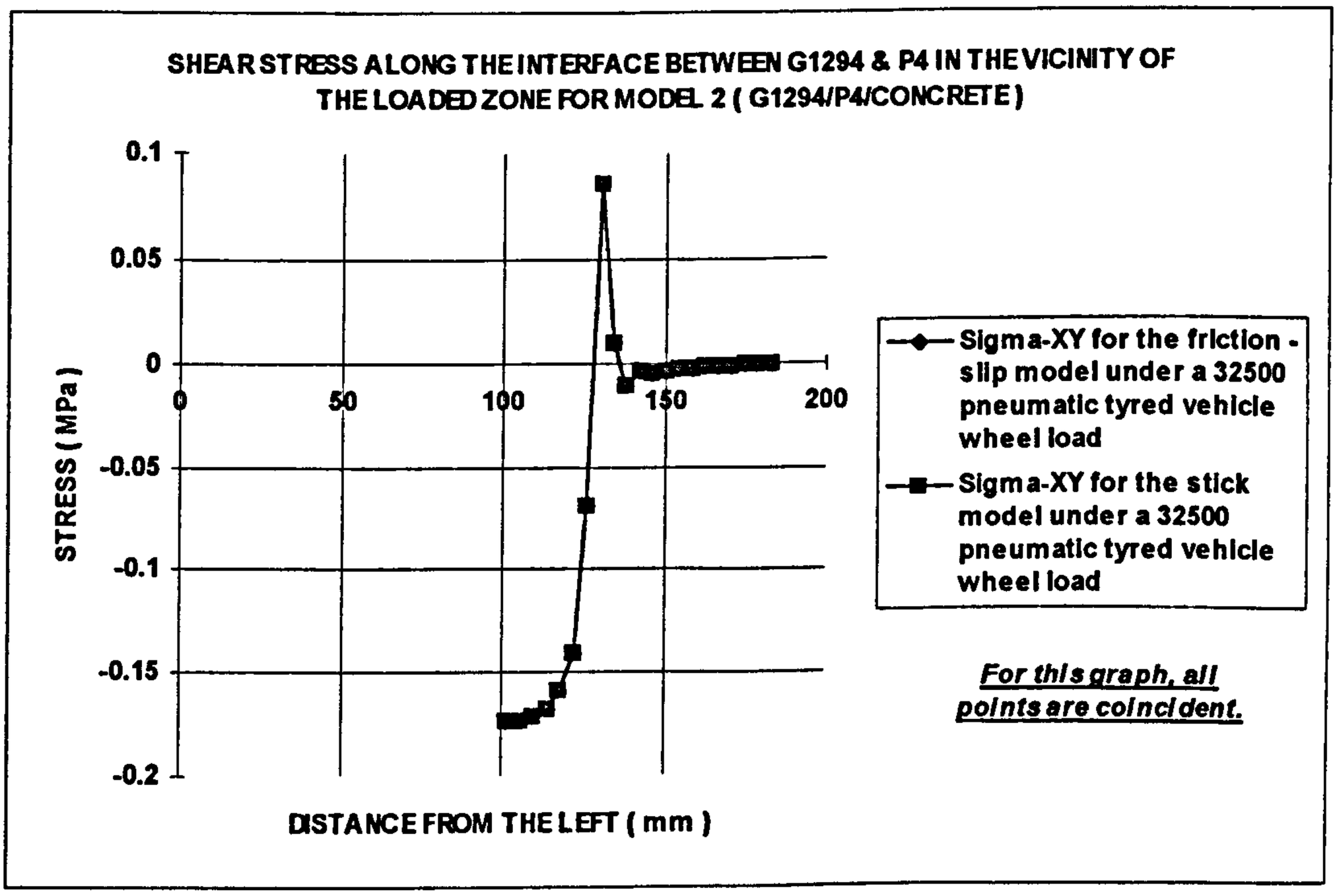

Figure 7-22-4 (Zoom): Model 2, G1294/P4/Concrete {Compression (-), Tension (+)} (No delamination occurs) ***AGREEMENT***

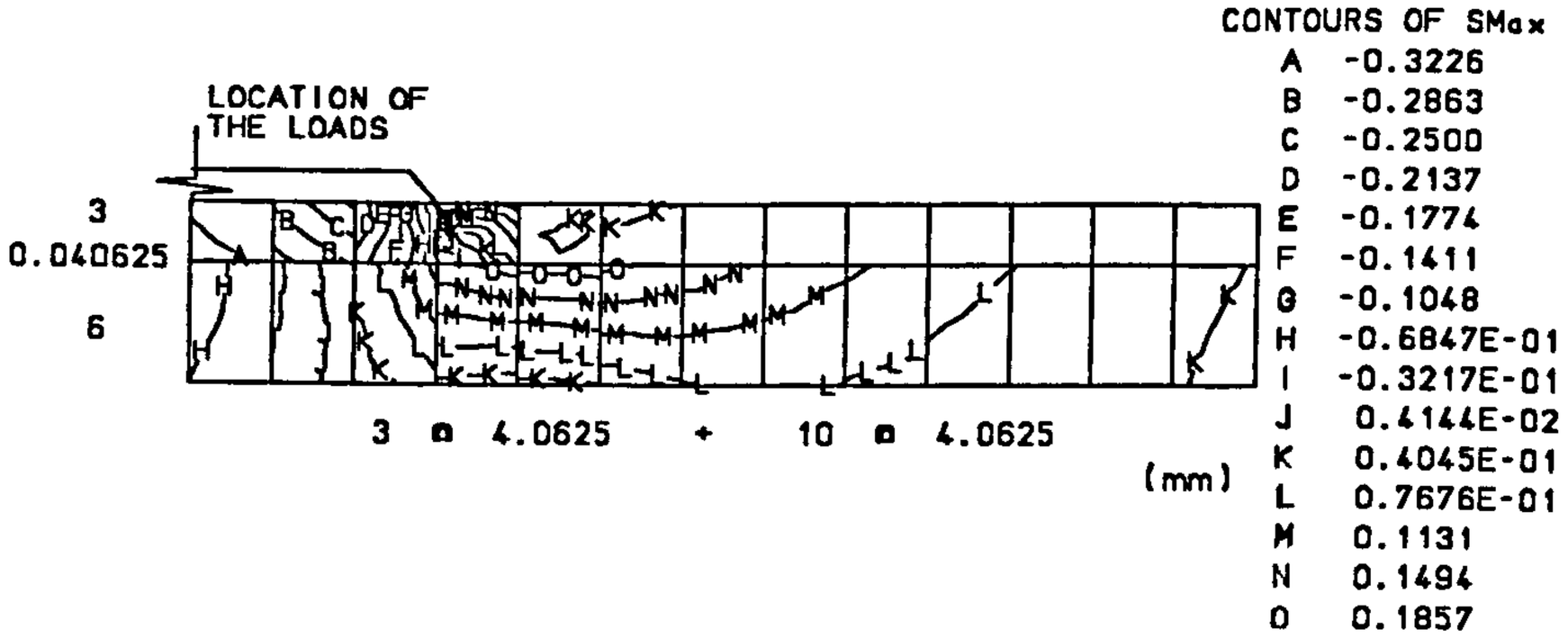

Figure 7-22-5: Contours of Sigma-1 (maximum) in the vicinity of the load and the interface for Model 2 {Compression (-), Tension (+)}

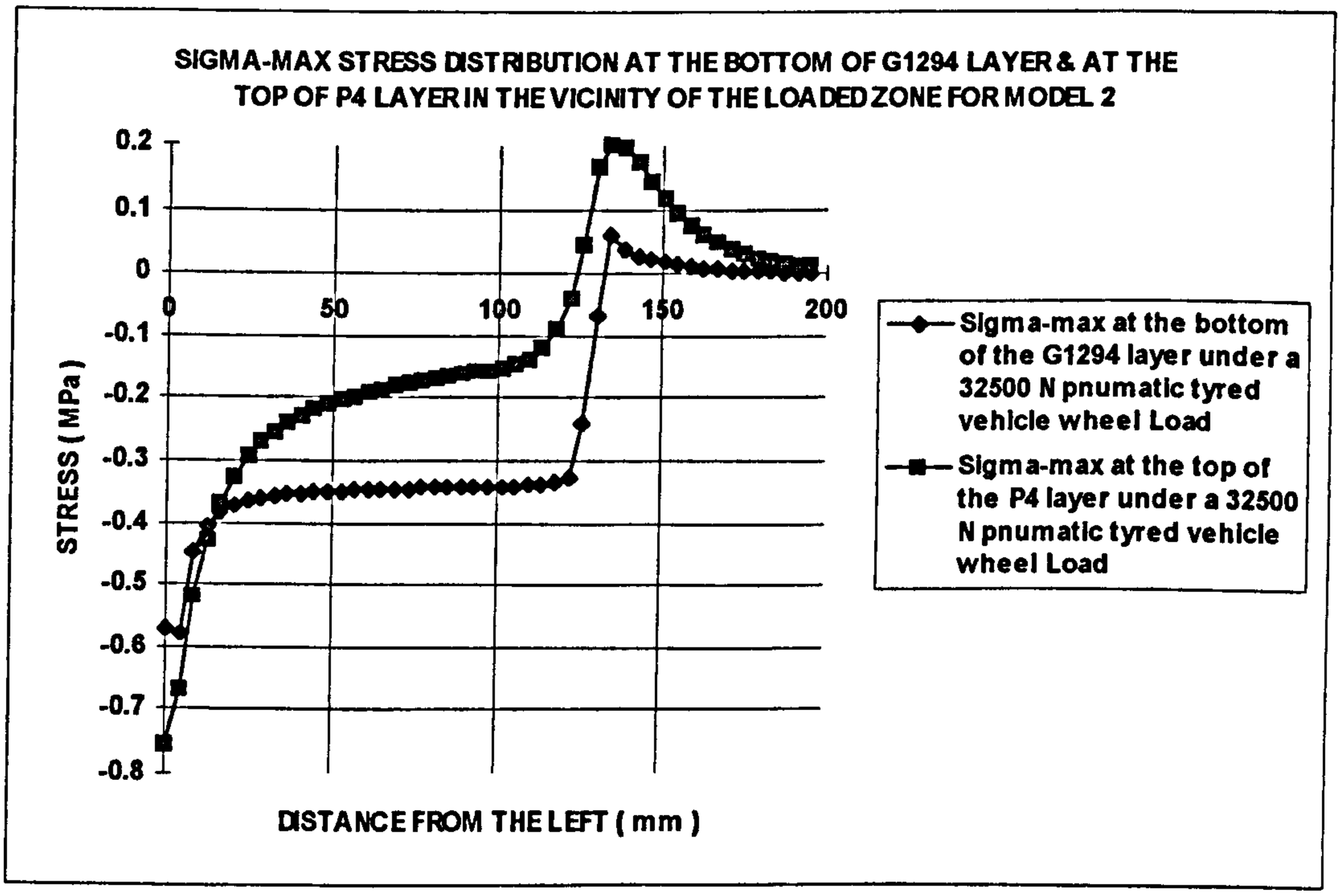

Figure 7-22-6: Sigma-1 (maximum) stress distribution in the vicinity of the loads and the interface for Model 2 {Compression (-), Tension (+)}

7-3-2-3 Model 3: G1194/Concrete

Age: 3 days
Load: 32500 N
Contact area: An equivalent rectangular area of diameters a = 260 mm & b = 179 mm

Specifications of the materials and layers:

G1194:

E = 5500 MPa (table 5-12)
υ = 0.32 (table 5-16)
Thickness = 3 mm

Interface between G1194 and concrete using Pprime as the primer:

E = 4730 t (table 7-8)
t = 0.01B (table 7-8)
υ = 0.25 (table 7-8)
where t is the interface thickness (mm), and B is the width of the finite elements at the interface.
Cohesion, coefficient of friction, and tensile bond strength:
(tables 5-17 & 5-21)

Interface model	Cohesion (MPa)	Coefficient of friction	Tensile bond strength (MPa)
Friction - slip model	1.47	0.44	1.30
Stick model	5.00	5.00	5.00

Concrete:

E = 23900 MPa (as an assumption based on figure 7-9 and equation $E_c = 57000\sqrt{f_c'}$ (psi) [Nilson et al. 1991])
υ = 0.17 (section 7-2-2-1)
Thickness = 25 mm (section 7-3-1-1)

Contact Pressure, MPa: (section 7-3-1-3)

Vertical uniform contact pressure = 100 psi = 0.7 MPa
Horizontal uniform contact pressure = 25 psi = 0.175 MPa

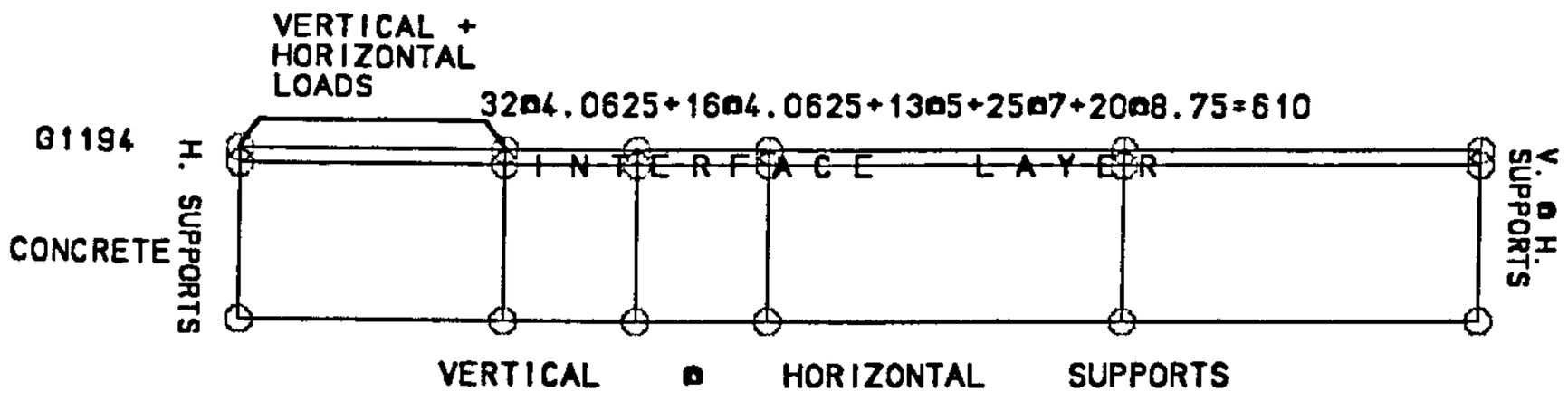

Figure 7-23-1: Half of the structure considered for the analysis of Model 3

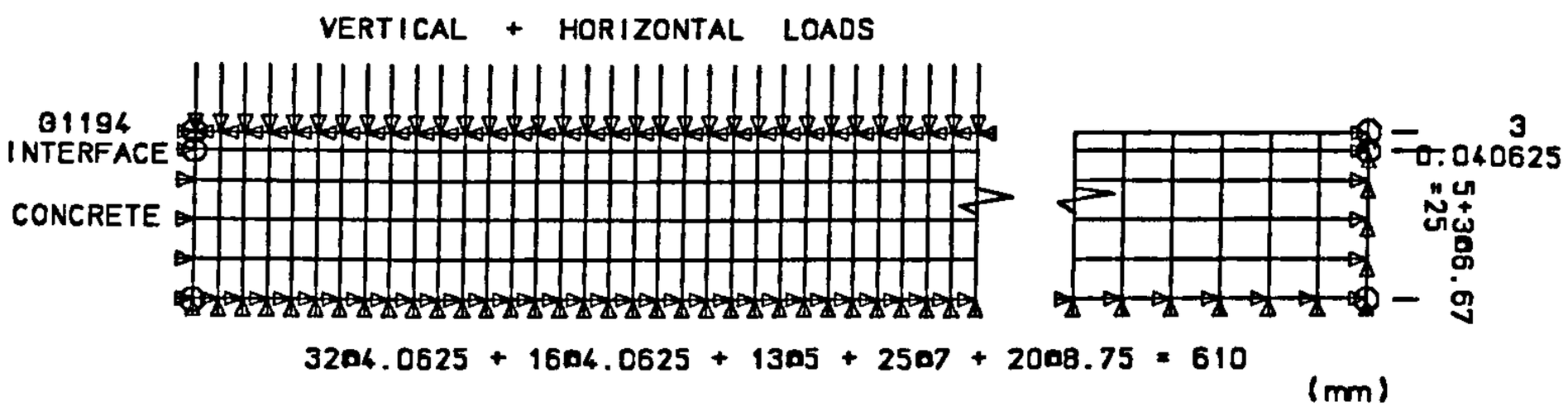

Figure 7-23-2: The finite element mesh for Model 3

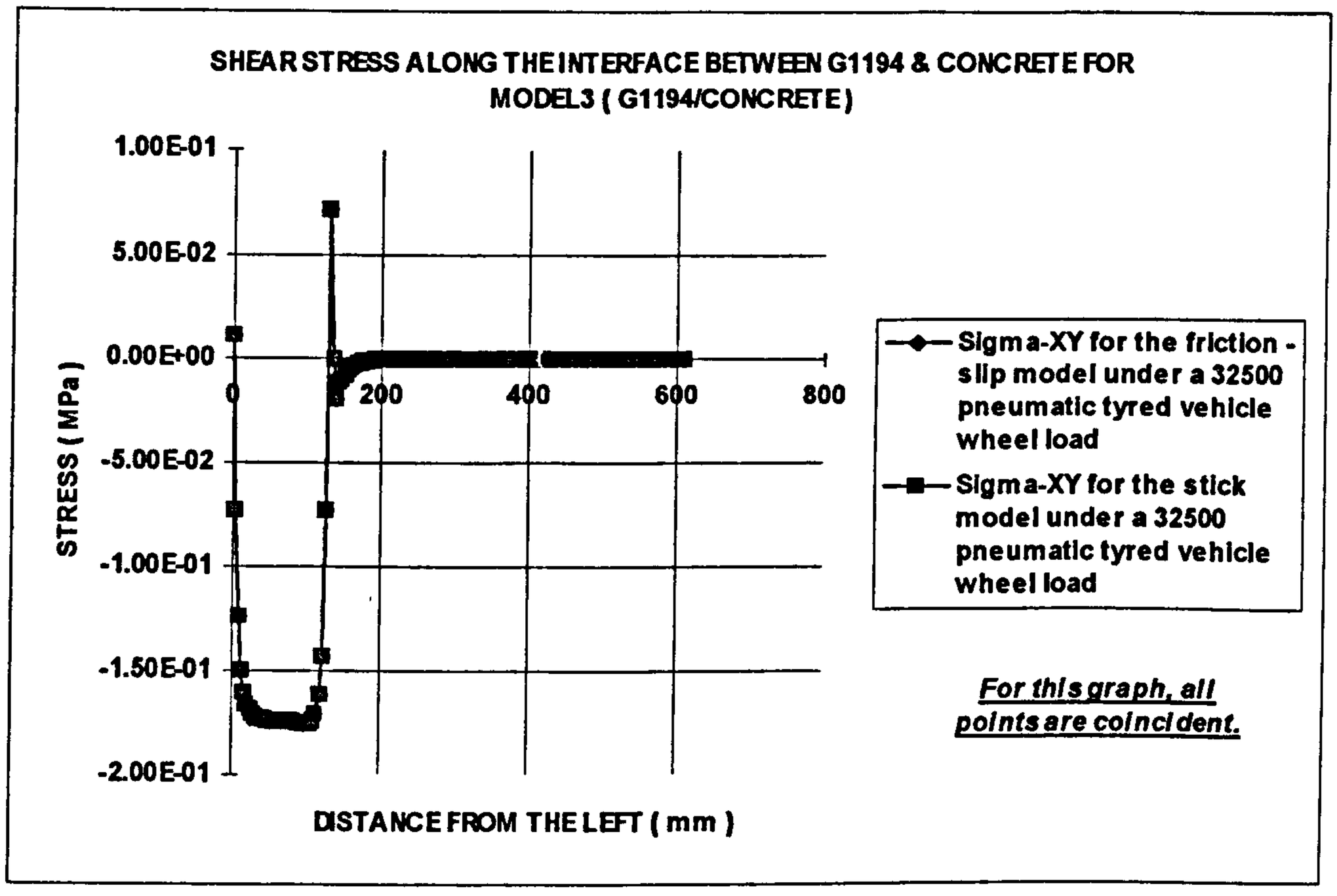

Figure 7-23-3: Model 3, G1194/Concrete {Compression (-), Tension (+)}

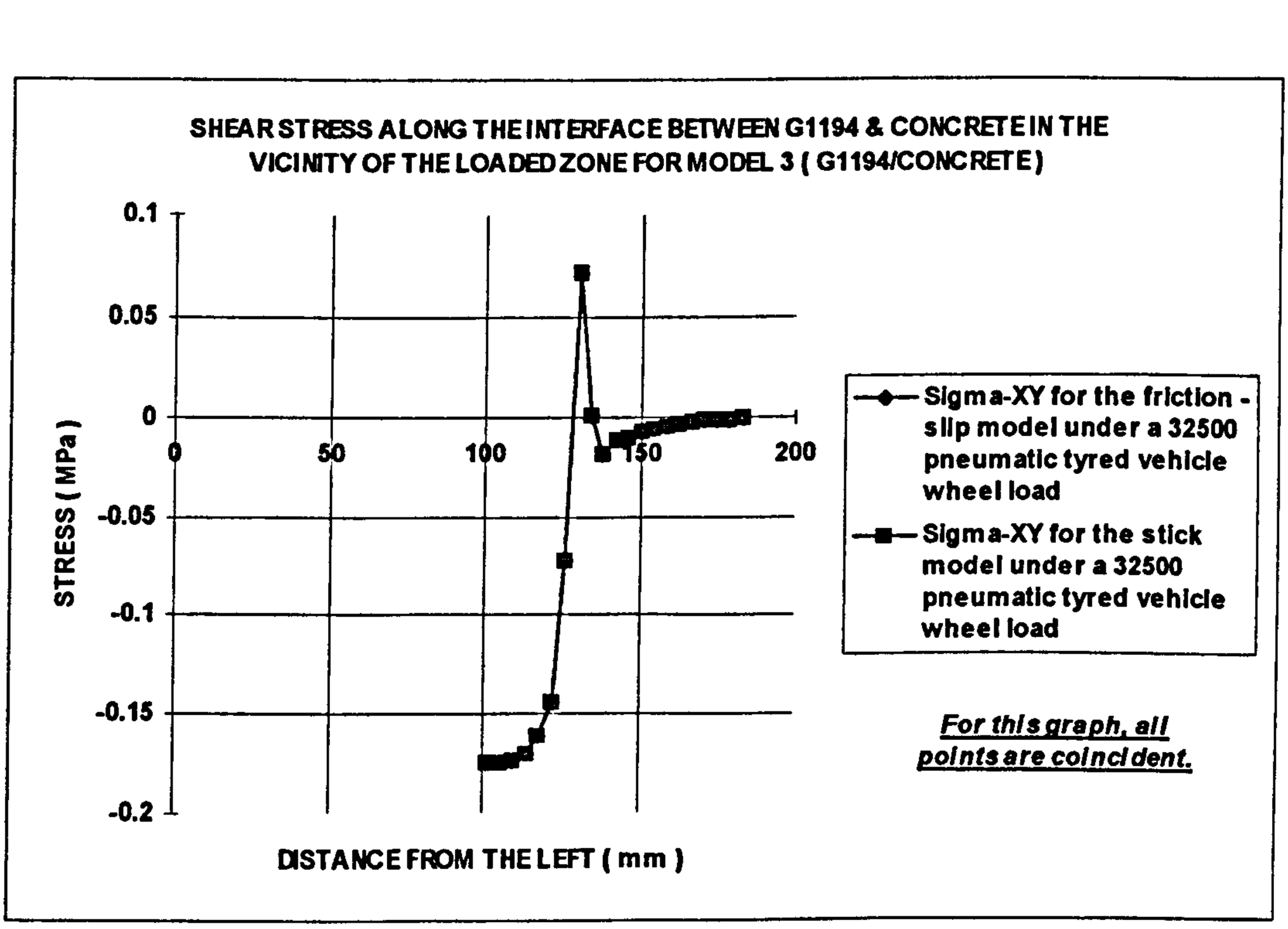

Figure 7-23-4 (Zoom): Model 3, G1194/Concrete {Compression (-), Tension (+)} (No delamination occurs) ***AGREEMENT***

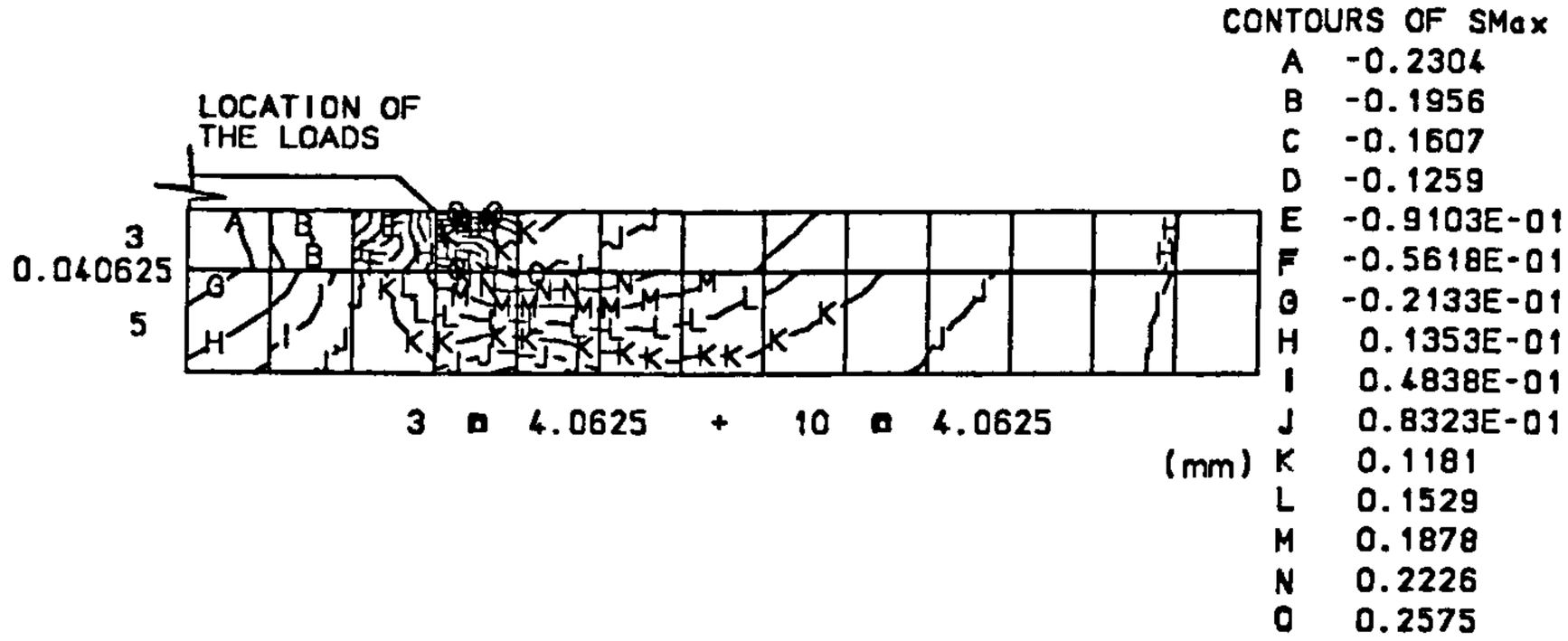

Figure 7-23-5: Contours of Sigma-1 (maximum) in the vicinity of the load and the interface for Model 3 {Compression (-), Tension (+)}

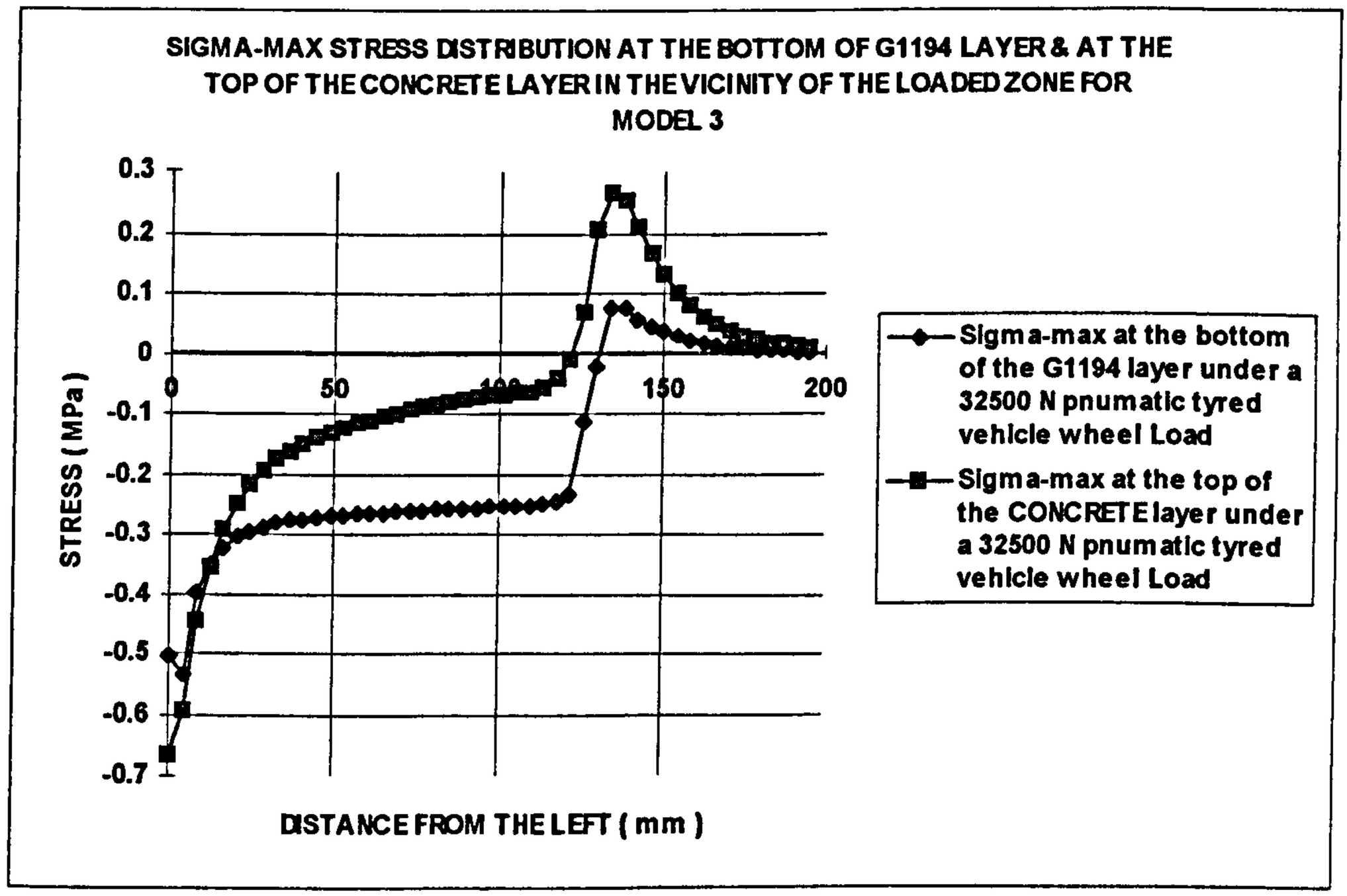

Figure 7-23-6: Sigma-1 (maximum) stress distribution in the vicinity of the loads and the interface for Model 3 {Compression (-), Tension (+)}

7-3-2-4 Model 4: G1294/Steel fibre reinforced concrete

Age: 3 days

Load: 32500 N

Contact area: An equivalent rectangular area of diameters a = 260 mm & b = 179 mm

Specifications of the materials and layers:

G1294:

E = 1700 MPa (table 5-15)

υ = 0.38 (table 5-16)

Thickness = 3 mm

Interface between G1294 and concrete using Pprime as the primer:

E = 2150 t (table 7-8)

t = 0.01B (table 7-8)

υ = 0.28 (table 7-8)

where t is the interface thickness (mm), and B is the width of the finite elements at the interface.

Cohesion, coefficient of friction, and tensile bond strength: (tables 5-19 & 5-21)

Interface model	Cohesion (MPa)	Coefficient of friction	Tensile bond strength (MPa)
Friction - slip model	1.15	0.18	1.70
Stick model	5.00	5.00	5.00

Steel fibre reinforced concrete:

E = 16600 MPa (table 5-40

υ = 0.17 (section 7-2-2-1)

Thickness = 25 mm (section 7-3-1-1)

Contact Pressure, MPa: (section 7-3-1-3)

Vertical uniform contact pressure = 100 psi = 0.7 MPa

Horizontal uniform contact pressure = 25 psi = 0.175 MPa

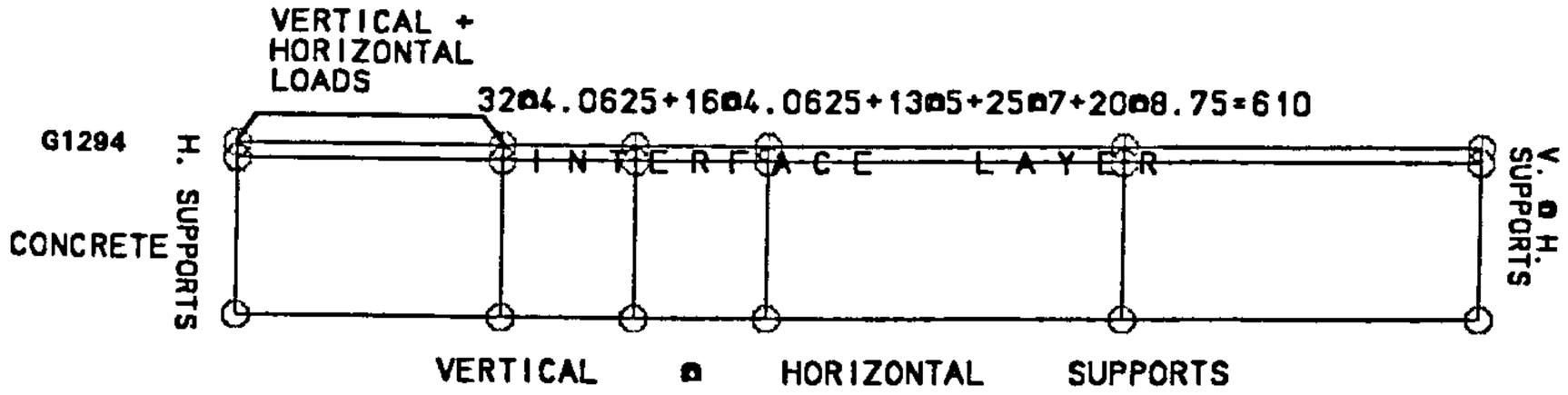

Figure 7-24-1: Half of the structure considered for the analysis of Model 4

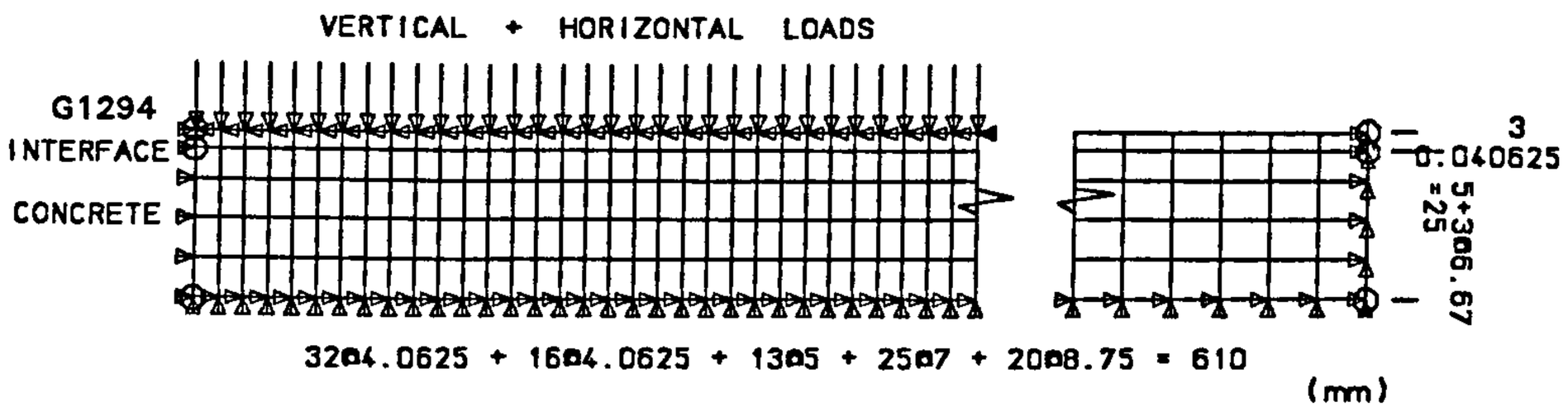

Figure 7-24-2: The finite element mesh for Model 4

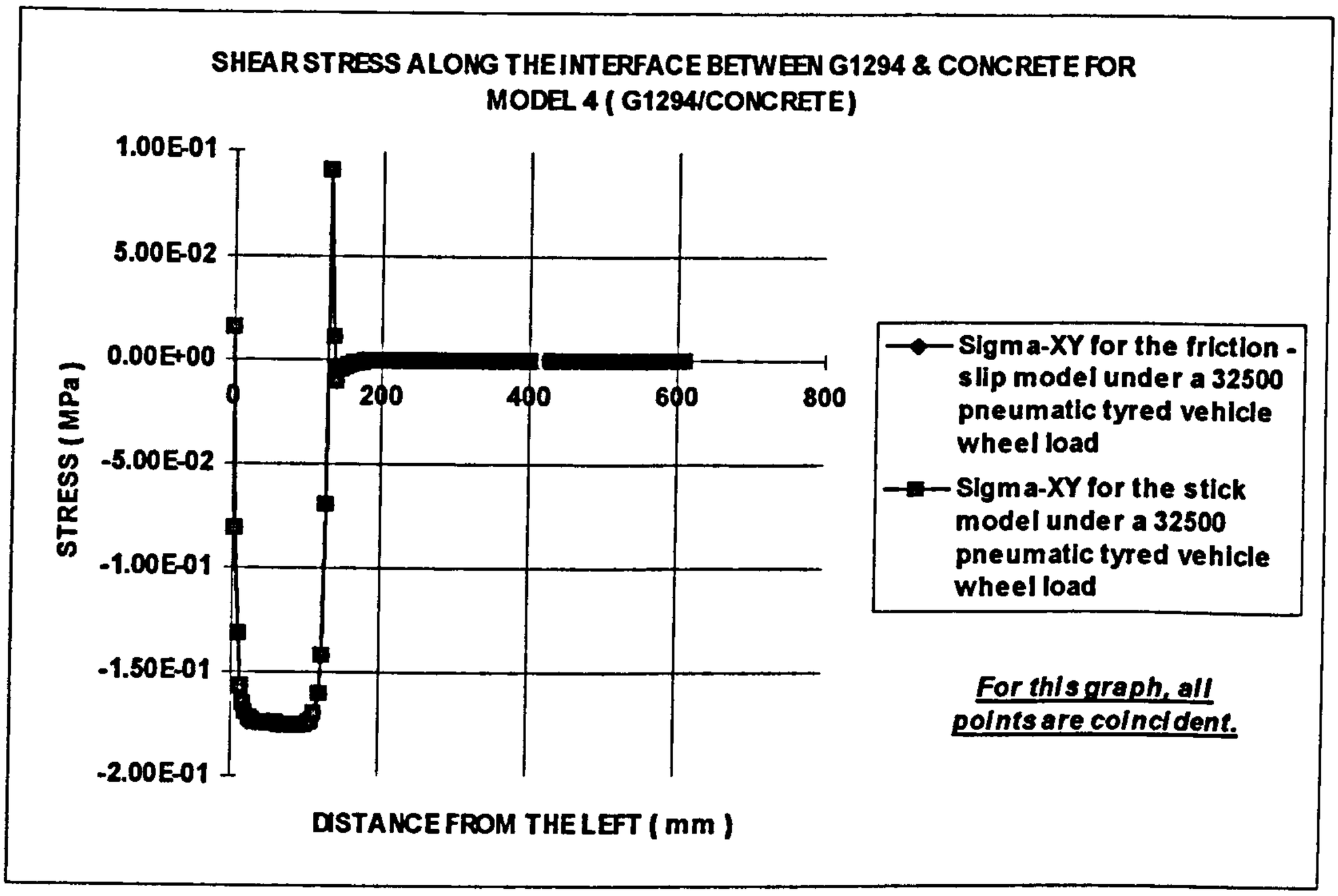

Figure 7-24-3: Model 4, G1294/Concrete {Compression (-), Tension (+)}

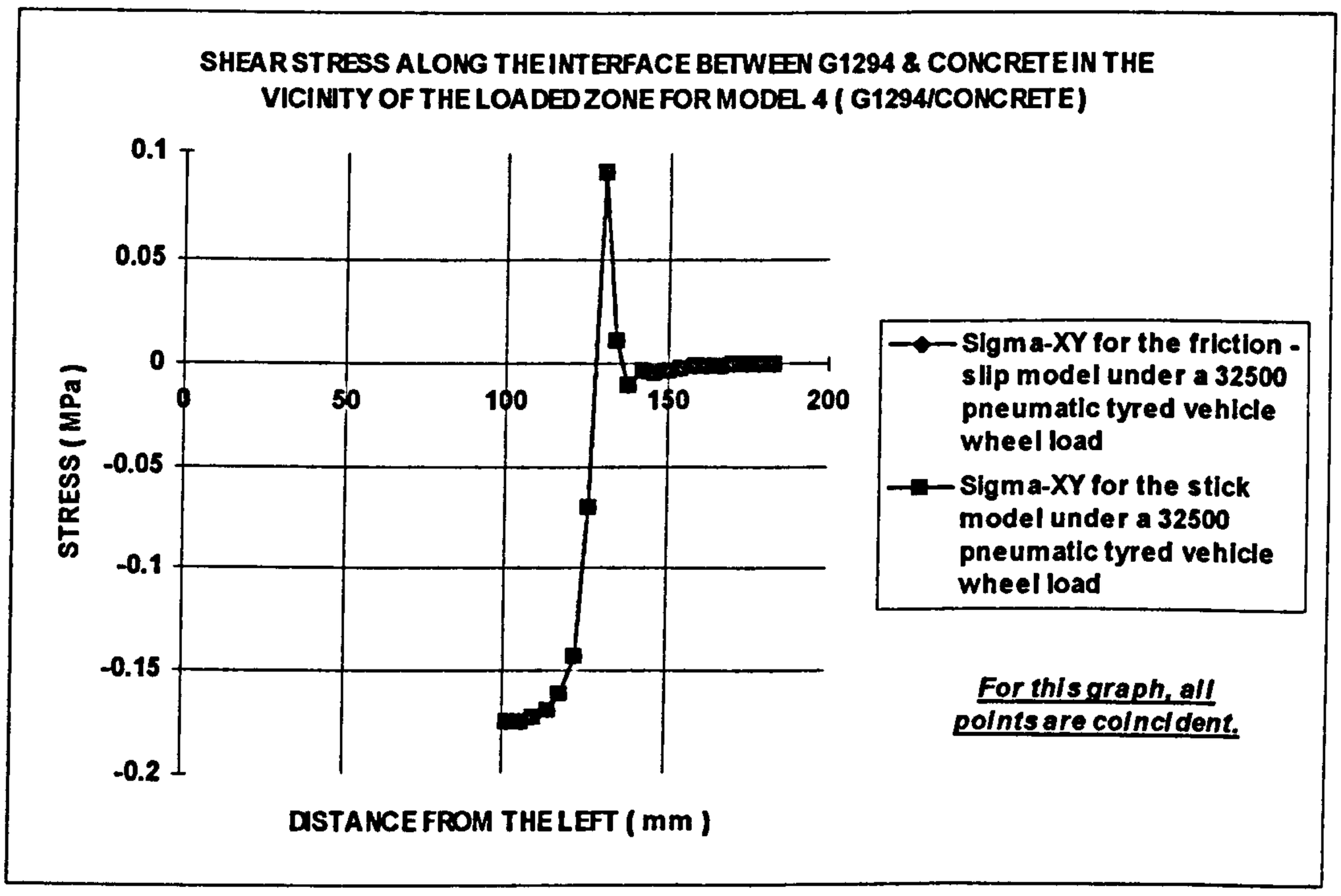

Figure 7-24-4 (Zoom): Model 4, G1294/Concrete {Compression (-), Tension (+)} (No delamination occurs) ***AGREEMENT***

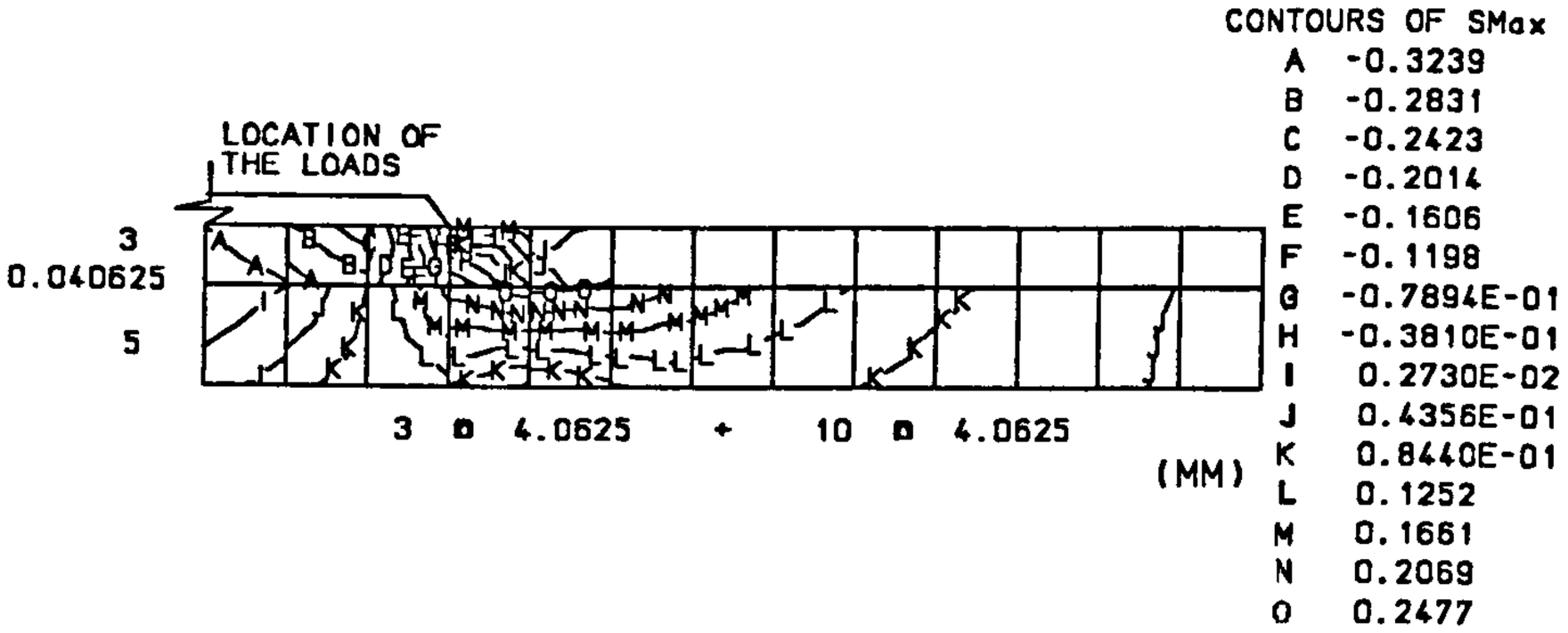

Figure 7-24-5: Contours of Sigma-1 (maximum) in the vicinity of the load and the interface for Model 4 {Compression (-), Tension (+)}

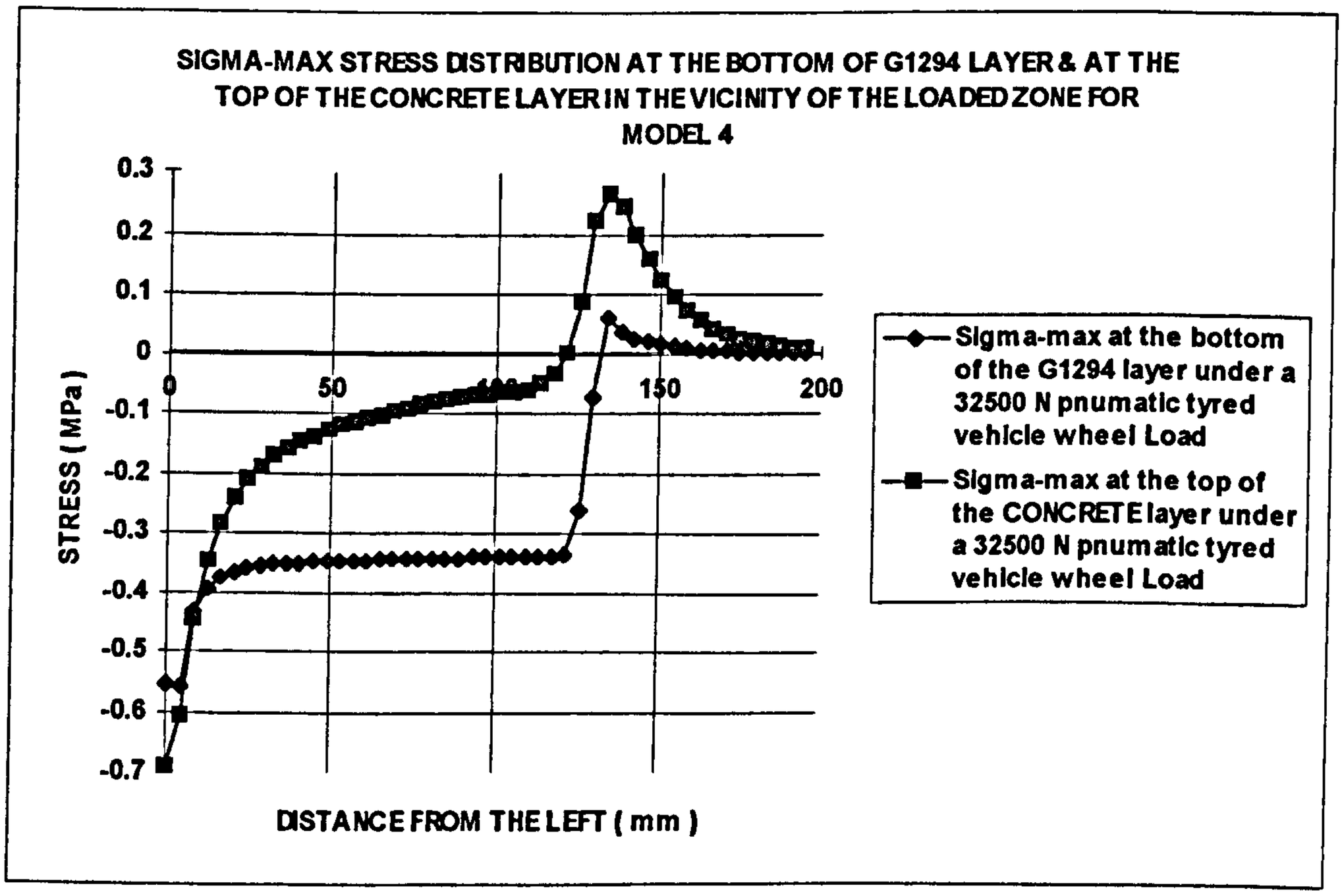

Figure 7-24-6: Sigma-1 (maximum) stress distribution in the vicinity of the loads and the interface for Model 4 {Compression (-), Tension (+)}

7-3-2-5 Model 5: P4/Steel fibre reinforced concrete

Age: 6 days
Load: 32500 N
Contact area: An equivalent rectangular area of diameters a = 260 mm & b = 179 mm

Specifications of the materials and layers:

P4:

E = 12400 MPa (table 5-9)
υ = 0.25 (table 5-16)
Thickness = 3 mm

Interface between P4 and concrete using Pprime as the primer:

E = 4710 t (table 7-8)
t = 0.01B (table 7-8)
υ = 0.21 (table 7-8)
where t is the interface thickness (mm), and B is the width of the finite elements at the interface.
Cohesion, coefficient of friction, and tensile bond strength:
(tables 5-20 & 5-21)

Interface model	Cohesion (MPa)	Coefficient of friction	Tensile bond strength (MPa)
Friction - slip model	0.41	0.86	0.50
Stick model	5.00	5.00	5.00

Steel fibre reinforced concrete:

E = 16600 MPa (table 5-4)
υ = 0.17 (section 7-2-2-1)
Thickness = 25 mm (section 7-3-1-1)

Contact Pressure, MPa: (section 7-3-1-3)

Vertical uniform contact pressure = 100 psi = 0.7 MPa
Horizontal uniform contact pressure = 25 psi = 0.175 MPa

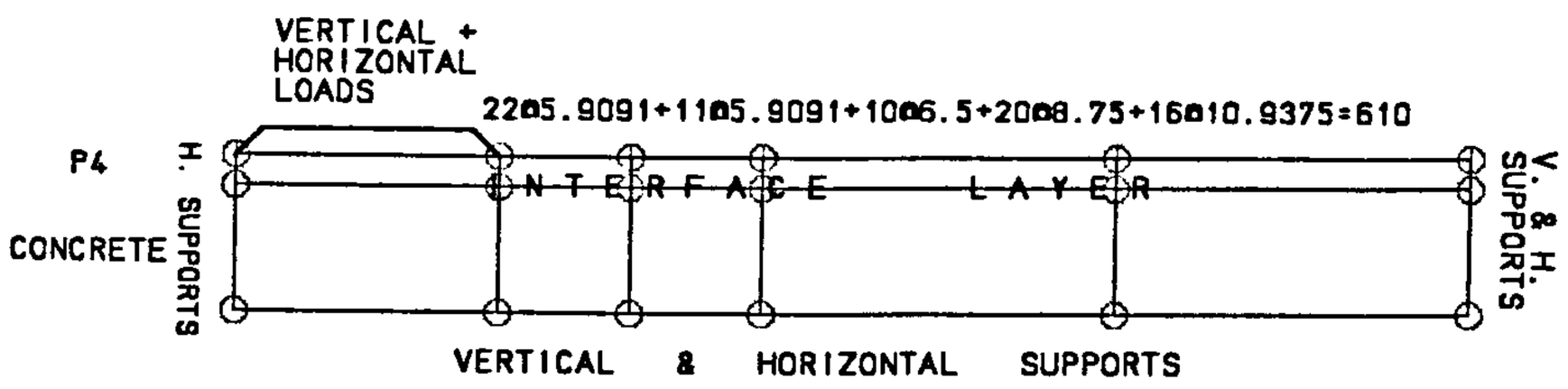

Figure 7-25-1: Half of the structure considered for the analysis of Model 5

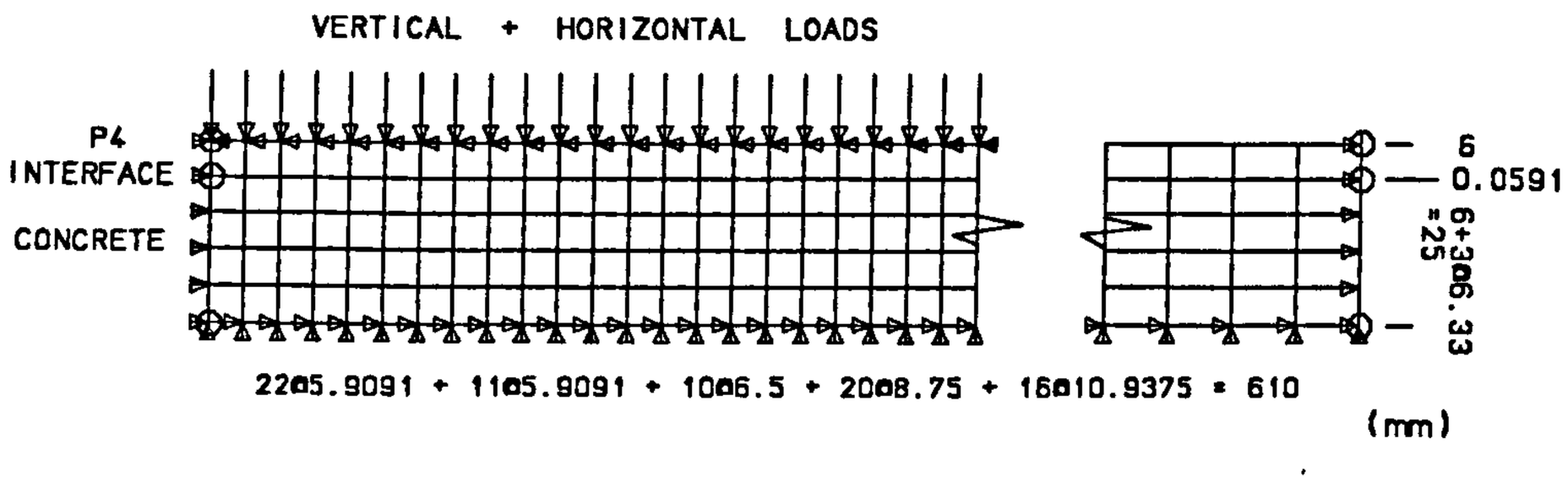

Figure 7-25-2: The finite element mesh for Model 5

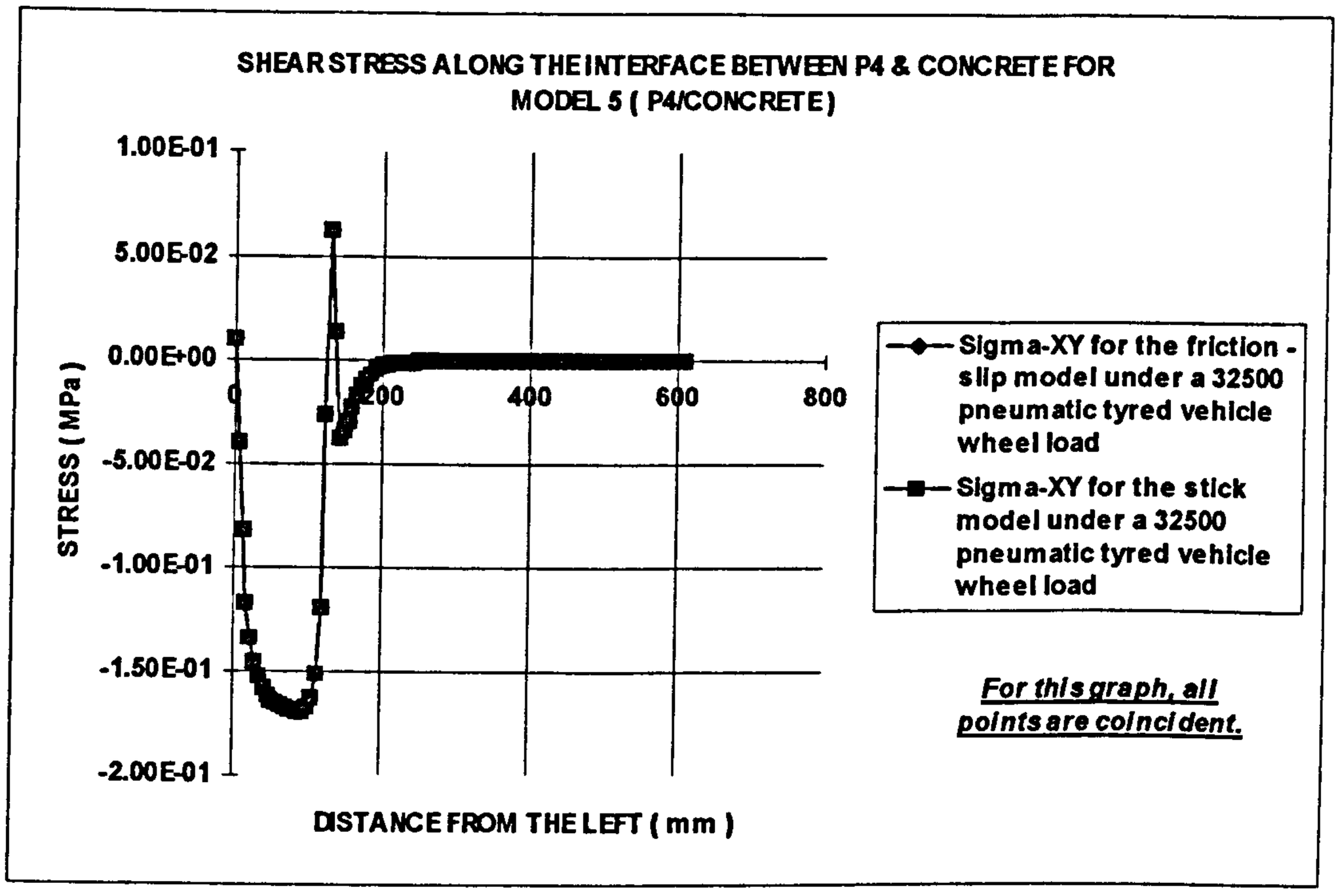

Figure 7-25-3: Model 5, P4/Concrete {Compression (-), Tension (+)}

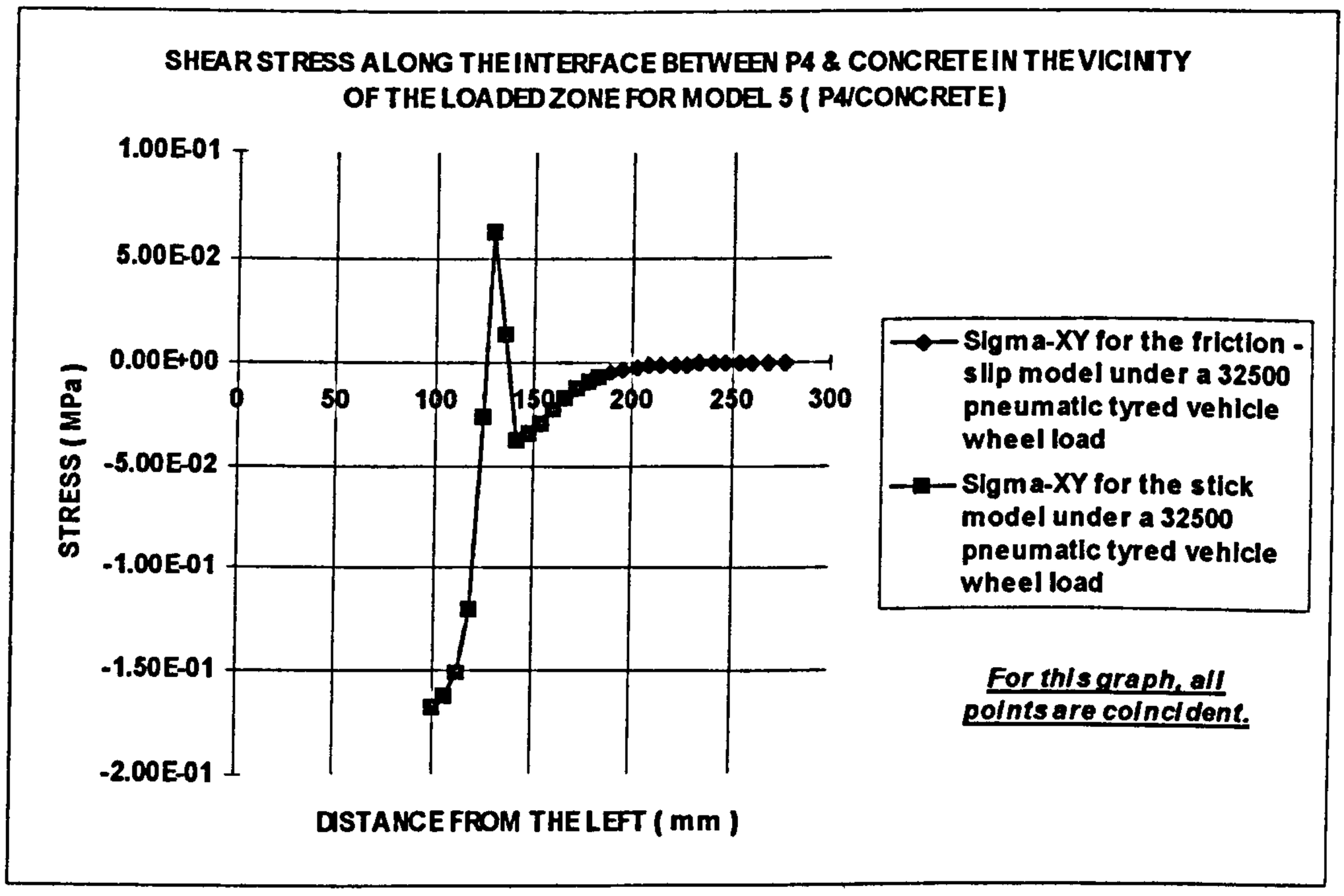

Figure 7-25-4 (Zoom): Model 5, P4/Concrete {Compression (-), Tension (+)}
(No delamination occurs) ***AGREEMENT***

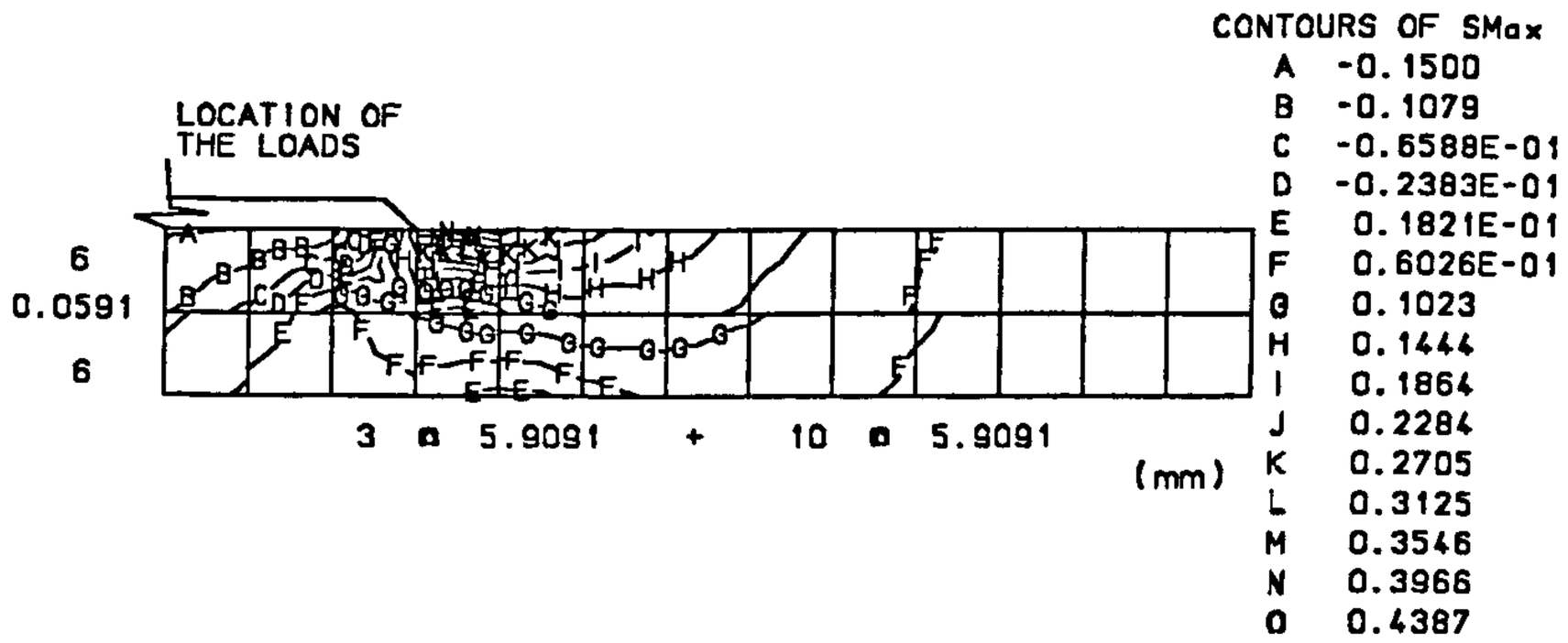

Figure 7-25-5: Contours of Sigma-1 (maximum) in the vicinity of the load and the interface for Model 5 {Compression (-), Tension (+)}

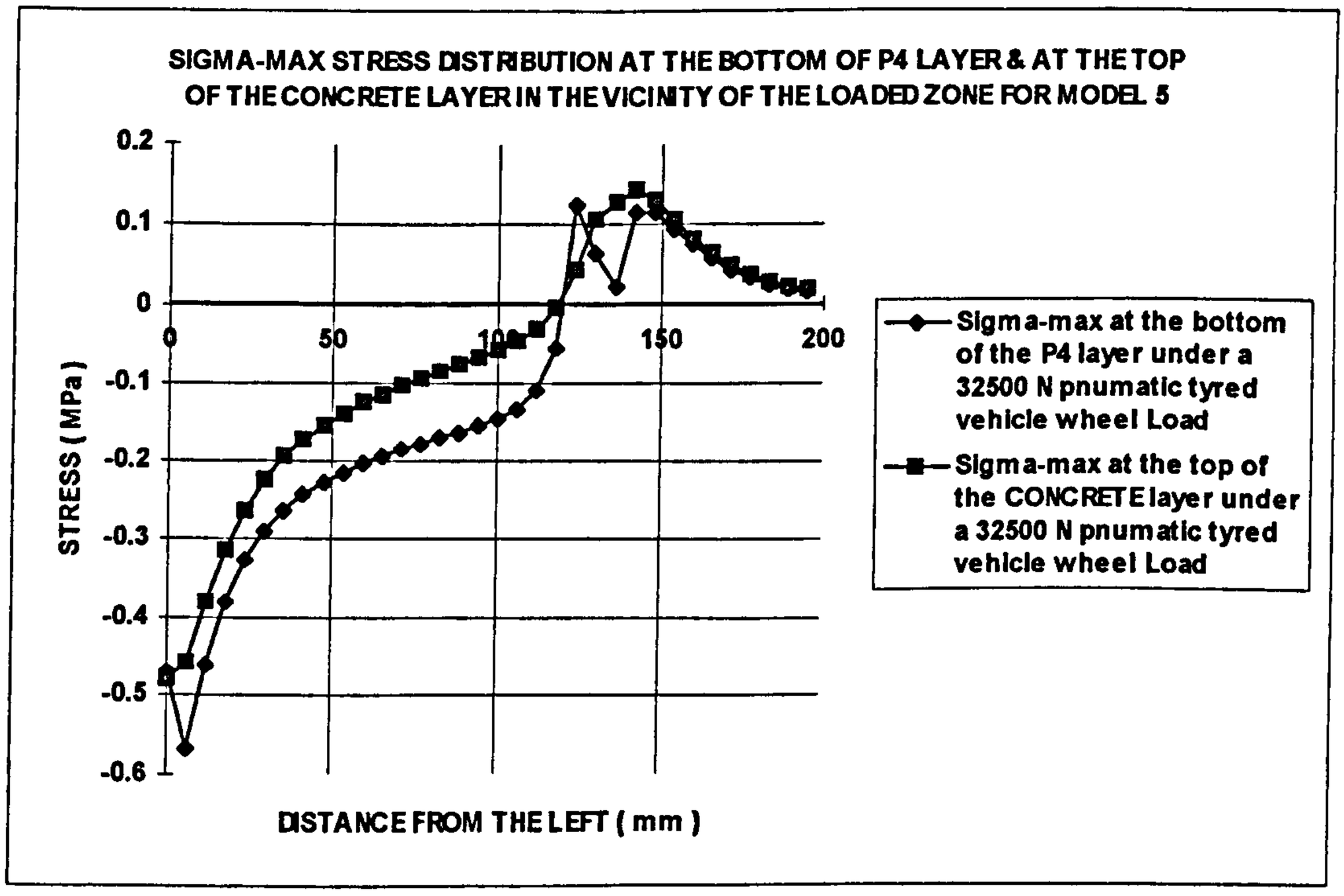

Figure 7-25-6: Sigma-1 (maximum) stress distribution in the vicinity of the loads and the interface for Model 5 {Compression (-), Tension (+)}

7-4 Summary

In this chapter the behaviour of thin layered systems under the action of a pneumatic tyred vehicle wheel load was studied.

The first part of the study was the implementation of the experimental program. In this experiment seven combinations of the four main materials and two different primers were prepared and tested. The action of a pneumatic tyred vehicle wheel rolling load was well simulated using the NUROLF, Newcastle University Rolling Load Facility. Three ways were used for detecting the possible delamination at the interface between the upper layer and the second layer. For most of the combinations all the detecting methods were satisfactory. Although the ages of the upper layer materials at which the rolling load tests started were very early, three days for six combinations and six days for one combination, all the thin layered systems could resist the maximum 6.5 ton dual tyre load without any sign of delamination. Owing to the lack of a highly concentrated load, P4 material also performed well under the tests. However G1294 was badly damaged as a result of being under load in wet conditions so that the image of the tyres were on the surface of the material was obvious even after unloading.

The second part of the study was the modelling of the thin layered systems in order to predict their behaviour under the prescribed load condition using the finite element method. The prediction of the slippage and debonding of the coating layer was tried by defining a thin interface layer between the two upper layers of each system. Two failure criteria, slippage due to shear stresses and debonding due to normal stresses were considered. The results of shear box and bond strength tests were used in this respect. The value of the tyre contact pressure made it possible to use a linear elastic behaviour for all the constitutive materials and the interface layer in the thin layered systems. This

made it possible to use a special two dimensional elasto - plastic interface model which is available in the LUSAS finite element system. In this method, when a failure occurs at any node, the redistribution of stresses and strains within the structure would be taken into account. Therefore in order to evaluate each thin layered system, two models of the structure were to be analysed simultaneously, one with a friction - slip interface model and the other with a stick interface model and any difference between the distribution of shear stresses along the interfaces of the two models was to be interpreted as the result of occurrence of a slippage or debonding at the interface of the real structure. The analytical results were consistent with the experiment to a considerable extent.

The maximum principal stress distribution and contours in the vicinity of the load and the interface of each thin layered system also showed low values of this type of stress.

CHAPTER 8

SUMMARY, DISCUSSION, CONCLUSION, RECOMMENDATIONS FOR FURTHER RESEARCH

Summary

Discussion

Conclusion

Recommendations for further research

8-1 Summary

Thin layered systems may be used in repair, protection or strengthening of concrete structures in various fields of the construction industry.
A thin layered system in this study is understood as a system with one or more thin layers of different physical and mechanical properties which lies on a surface of a main substrate.
Each of the two other dimensions of a thin layered system may vary from a very small quantity in an isolated patch repair on an individual member of a structure, to a very large amount in a coating layer on a warehouse floor. Since the latter case was the main subject of this study, the substrate layer was considered as a concrete slab.

The action of a rolling wheel load on the behaviour of a thin layered system was investigated in this study. Two types of wheel loads were used in this investigation: a steel wheel load and a pneumatic wheel load.

As was mentioned in chapter 1, the main objectives of this study may be summarised as follows:
- Introducing thin layered systems in general, simulating the action of rolling wheel loads on different combinations of thin layered systems and detecting any possible delamination at the interfaces of these structures.
- Modelling and analysing the systems using the finite element method, based on the results of the material properties tests.
- Comparing the results of the structural analysis and the experimental tests, and introducing a constitutive model for explaining and predicting the behaviour of thin layered systems under the action of a rolling load with particular interest in the delamination defect.

The following materials were used in this program:
- Portland cement concrete as the substrate material for the thin layered systems used in the Steel Wheel Rolling Load experiment
- Steel fibre reinforced concrete as the substrate material for the thin layered systems used in the NUROLF experiment
- P4 system (polymer cement concrete)
- G1194 (polymer concrete)
- G1294 (polymer concrete)

- Gprime (primer)
- Pprime (primer)

In the Steel Wheel Rolling Load experiment, the Rolling Load Rig was used which had been previously developed for simulating the action of an arbitrary rolling wheel. The load applied in this experiment was nearly a free rolling load and its maximum value was 5 kN. Two types of specimens were used in the experiment, the ready made specimens and the purpose made specimens. The specimens consisted of totally five combinations of the flooring materials. Both types of the specimens showed similar behaviour under the test conditions.

Three methods were used for detecting the possible delamination at the interface between the upper layer and the second layer:

- The ultrasonic pulse velocity method using the PUNDIT
- Tapping the surface of the upper layer using a piece of steel bar
- Breaking the specimen in two parts in some cases for verifying the results of the other two methods

For most of the specimens all the detecting methods were satisfactory, however for few cases breaking the specimens was the only solution. The best combination of the thin layered systems used in this experiment was G1194/Concrete with the use of Gprime at the interface. This system could resist the maximum 5000 N without any sign of delamination or wear. Other combinations were delaminated in the tests, some of them even under a lower value of load.

In the pneumatic tyred vehicle wheel rolling load experiment, the action of the load was well simulated using the NUROLF. The load applied in this experiment was nearly a free rolling load and its maximum value was 6.500 ton with a tyre inflation of 100 psi (0.7 MPa). The thin layered systems consisted of totally five combinations of the flooring materials.

Three methods were used for detecting the possible delamination at the interface between the upper layer and the second layer:

- The ultrasonic pulse velocity method
- Tapping the surface of the upper layer using a piece of steel bar
- Tensile bond strength pull off test using the Limpet loading equipment

For most of the combinations all the detecting methods were satisfactory. Although the ages of the upper layer materials at which the rolling load tests

started were very early, three days for six combinations and six day for one combination, all the thin layered systems could resist the maximum 6.5 ton dual tyre load without any sign of delamination. However G1294 was badly damaged as a result of being under load in wet conditions so that the image of the tyres were on the surface of the material was obvious even after unloading.

With regard to the material characteristics, the following tests were carried out as the least required types of tests for the subsequent structural analysis:

Portland cement concrete:	Compressive strength and modulus of elasticity tests, Poisson's ratio test
Steel fibre concrete:	Compressive strength and modulus of elasticity tests
P4, G1194, and G1294:	Compressive strength test, flexural strength test, modulus of elasticity in compression test, Poisson's ratio test

For the determination of interface bond strength, two types of tests were carried out: the conventional pull off test using the Elcometer or Limpet equipment, and a special proposed shear - compression test using the shear box apparatus. In the shear box test, which was a relatively new test method, the relationship between normal stress and the corresponding shear strength was defined for each combination of the materials at each age of the test.

The final part of the study was the modelling and analysing of the thin layered systems in order to predict their behaviour under the prescribed load condition using the finite element method. The prediction of the slippage and debonding of the coating layer was tried by defining a thin interface layer between the two upper layers of each system. Two failure criteria, slippage due to shear stresses and debonding due to normal stresses were considered. The results of shear box and bond strength tests were used in this respect. In the Steel Wheel Rolling Load experiment, the idealized stress strain curves, proposed in chapter 5 for the constitutive materials, were used in the implicit elasto plastic von Mises model, using the LUSAS finite element software. In the NUROLF experiment owing to the low value of the tyre contact pressure, a linear elastic behaviour was assumed for all the constitutive materials. Elastic behaviour was assumed for the interface layer. The analytical results were consistent with the experiment to a considerable extent in both cases.

8-2 Discussion

According to the survey of applications of the thin layered systems carried out by Choi in 1991, the most likely environment anticipated was internal ambient with dry condition. [Choi 1991] Moreover, according to the manufacturer, the flooring materials used in this investigation (P4, G1194, and G1294) had been mainly designed for indoor conditions such as warehouses. Because of the above reasons, all tests in this study including the material characteristics tests, the interface bond strength tests, and the rolling load tests were carried out in internal ambient and dry conditions.

8-2-1 Material characteristics and interface bond strength

8-2-1-1 Material characteristics

8-2-1-1-1 Portland cement concrete

As was mentioned in section 5-2-1 of chapter 5, portland cement concrete slabs of sizes 600 mm by 300 mm by 50 mm were used for the purpose made specimens in the Steel Wheel Rolling Load experiment. The precast slabs were supplied by a manufacturer and there was no accurate information regarding their properties. Therefore it was decided to carry out some compressive strength and modulus of elasticity tests on the hardened concrete, using the same slabs. Because of this limitation, five cubes of size 70 mm were provided using a concrete sawing machine. The values of the axial force and displacements were measured and recorded during the tests. This measurement was then used for defining the modulus of elasticity and the stress - strain relations in compression. For the purpose of carrying out a more realistic structural analysis, an idealized stress - strain curve for the concrete material based on the average values of stresses and strains was also defined. Coefficient of variations for the compressive strength and modulus of elasticity were 3.6% and 16.5%, respectively which were acceptable. With the relatively high average value of compressive strength of 58.5 MPa, the performance of the concrete slabs under the prescribed loading conditions during the Steel Wheel Rolling Load tests was also satisfactory. Also Poisson's ratio test was carried out on this material. Once again owing to the limited thickness of the concrete slabs, cylindrical specimens of diameter 50 mm and of height 120 mm

were used.

8-2-1-1-2 Steel fibre reinforced concrete

Steel fibre reinforced concrete was used in the NUROLF experiment as the concrete substrate. The main reason for using this type of concrete was to reduce the required thickness of the concrete slab as the testing area for NUROLF. As was explained in section 5-1-3-1, three cubic specimens of size 150 mm were prepared for the compressive strength tests in this experiment. The mean strength at the age of 19 days (the age at which the NUROLF tests were to be started) was relatively high, 47.5 MPa. The coefficient of variation of 3.2% was very good. The values of modulus of elasticity and the idealized stress - strain curve were defined in the same way as was done for the portland cement concrete slabs. The coefficient of variation of 4.9% for the modulus of elasticity was again very good. The performance of the slab under the action of the maximum 6.5 ton rear dual tyre load resulted from NUROLF vehicle was satisfactory.

8-2-1-1-3 Flooring materials

As was mentioned before, the following tests were carried out as the least required types of tests for the subsequent structural analysis: Compressive strength test, flexural strength test, modulus of elasticity in compression test, and Poisson's ratio test.

- Compressive strength:

As it has been shown in figure 8-1, both the P4 and G1194 materials have a relatively high initial compressive strength at their early ages. The G1194 material shows much higher compressive strength in comparison with the P4 material.

The values of coefficients of variation are very low for both systems at the different ages.

Both of the materials showed a brittle mode of failure. For the G1294 material, the specimens did not show any visible sign of fracture under the tests, and therefore no value of mean compressive strength was given in the corresponding table of results in chapter 5 (table 5-13-c). However it could bear up to about 45 MPa compressive stress, but with a large deformation.

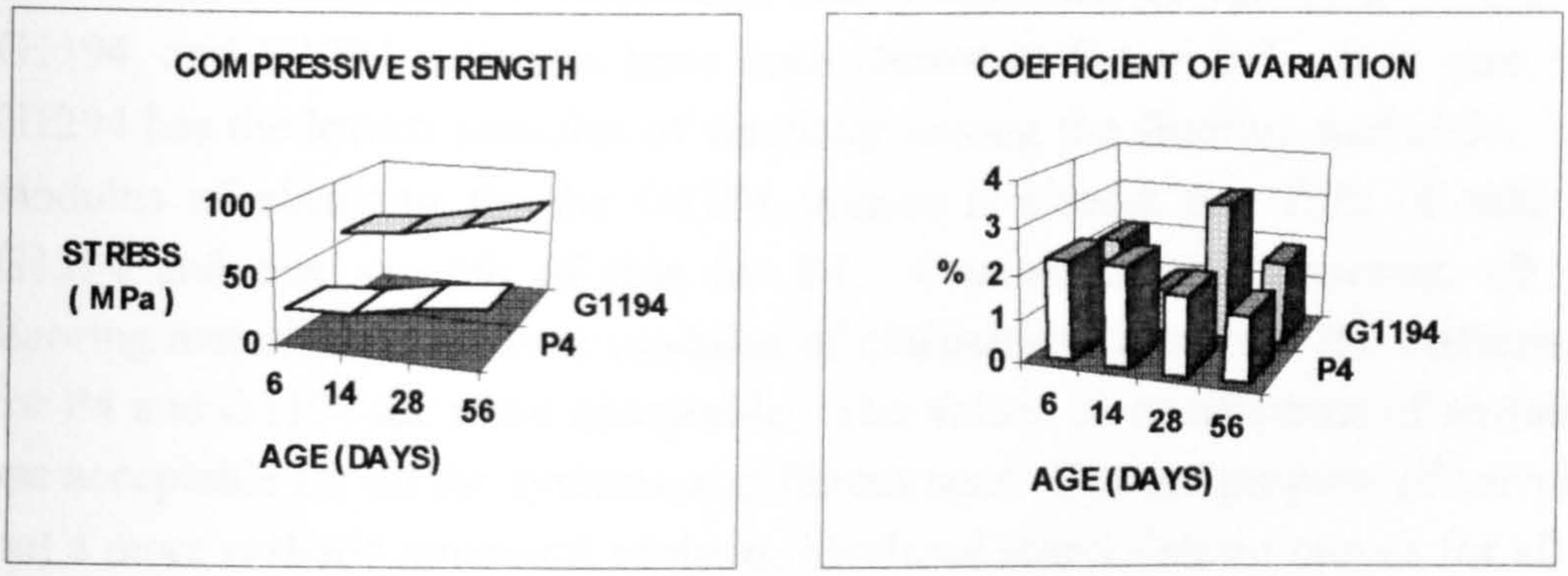

Figure 8-1: Values of strengths and coefficients of variations in the compressive strength tests

- Flexural strength test

The values of flexural strengths and coefficients of variation for the P4 and G1194 materials have been shown in figure 8-2. It is seen that the flexural strength for each of these flooring materials is greater than any normal concrete. The flexural strength for G1194 is nearly more than three times higher than that for the P4 material. Both of the materials showed a brittle behaviour at failure. The values of coefficients of variation are low for both systems at the different ages except for P4 at the age of 14 days which is poor. As reported in table 5-14-c for the G1294 material, the deflection exceeded one fifteenth of the span of each specimen during the test whereas no fracture occurred. Therefore it was not possible to measure a meaningful value of flexural strength for the specimens. This however means that there will be no flexural crack for the material under any circumstances.

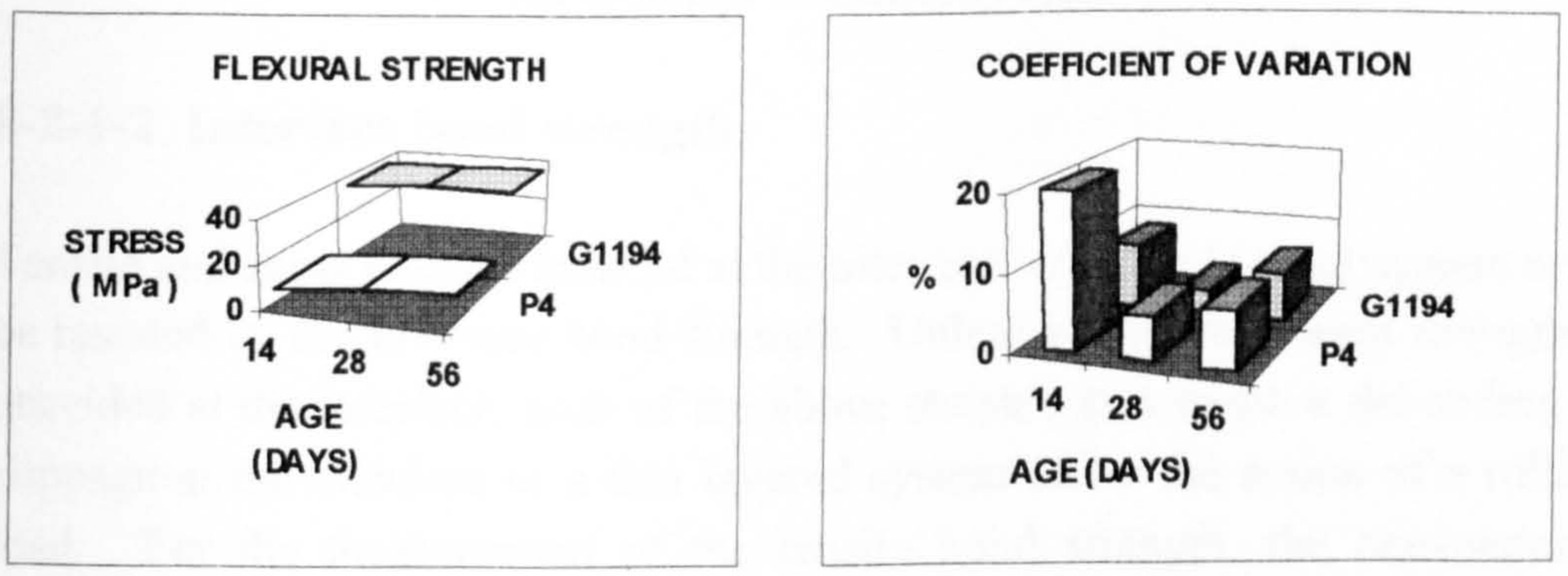

Figure 8-2: Values of strengths and coefficients of variations in the flexural strength tests

- Modulus of elasticity test:

The values of modulus of elasticities and coefficients of variation for the P4, G1194, and G1294 materials have been shown in figure 8-3. It is seen that G1294 has the lowest modulus of elasticity among the flooring materials. The modulus of elasticity for the G1294 system is almost one fifth of that for G1194 and one seventh of that for P4. Compared with concrete, all the flooring materials have lower modulus of elasticities. However the differences for P4 and G1194 are more acceptable. The values of coefficients of variation are acceptable for all the systems at different ages. For the purpose of carrying out a more realistic structural analysis, idealized stress - strain curves for all of the above materials and at different ages of tests, based on the average values of stresses and strains, have been also defined and depicted in figures 5-4, 5-5, and 5-6 in chapter 5. From these figures it can be realised that the behaviour of the P4 system is similar to concrete while both of G1194 and G1294 materials are more ductile. This may be a good advantage of these systems under heavily concentrated loads such as the Steel Wheel Rolling Load.

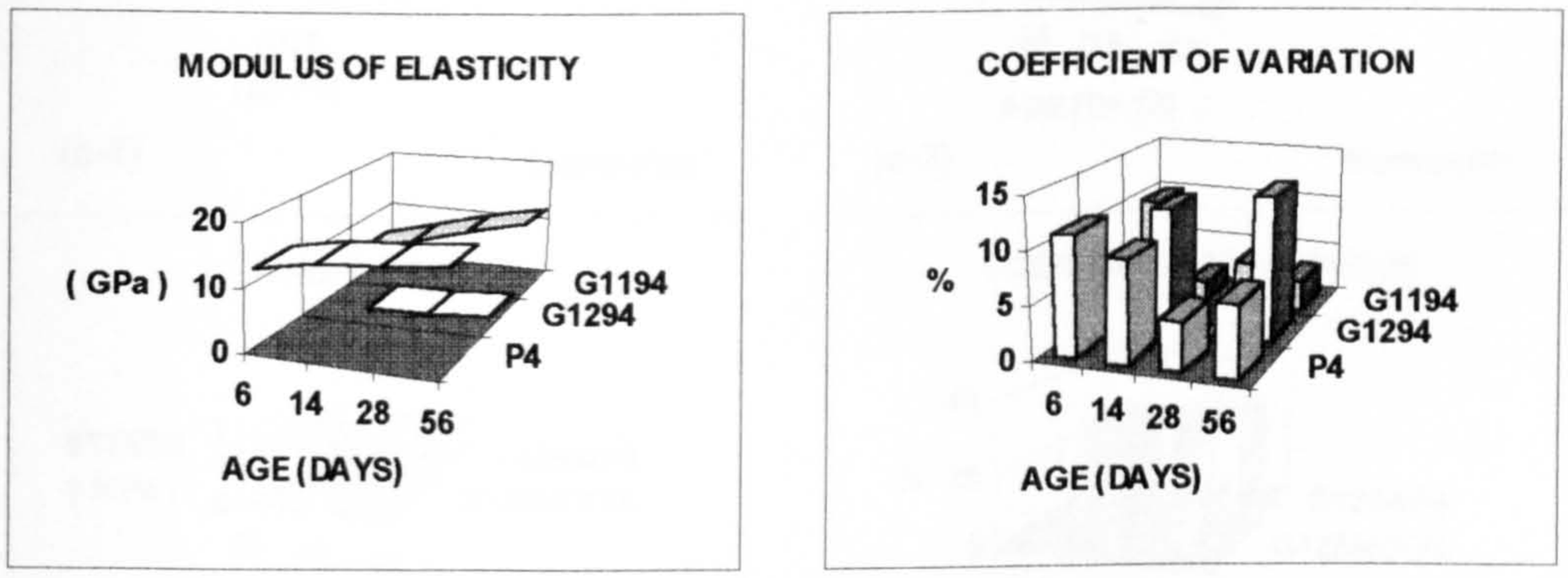

Figure 8-3: Values of modulus of elasticities and coefficients of variations in the modulus of elasticity tests

8-2-1-2 Interface bond strength

Tensile and shear stresses induced at the interface of a thin layered system must be resisted by the interface bond strength. Unless a sufficient bond strength is provided at the interface, each of the above stresses may cause a debonding or slippage at the interface of a thin layered system under the action of a rolling load. For the measurement of the tensile bond strength, the conventional method of pull off test was used, while for the measurement of the interface shear strength a new simple shear - compression test was proposed using the shear box apparatus.

8-2-1-2-1 Pull off tests

Pull off tests were carried out using the Elcometer screed pull off tester or the Limpet loading equipment. Two types of primers were used, Gprime and Pprime. For combination P4/Concrete, all the interfaces of the specimens at all ages were primed with the wrong primer (Gprime). For the rest of the combinations, Gprime was used at the ages of 14 and 28 days, while Pprime was only used at the age of 56 days. The results of the tensile bond strength tests (pull off tests) along with the coefficients of variation have been shown in figure 8-4.

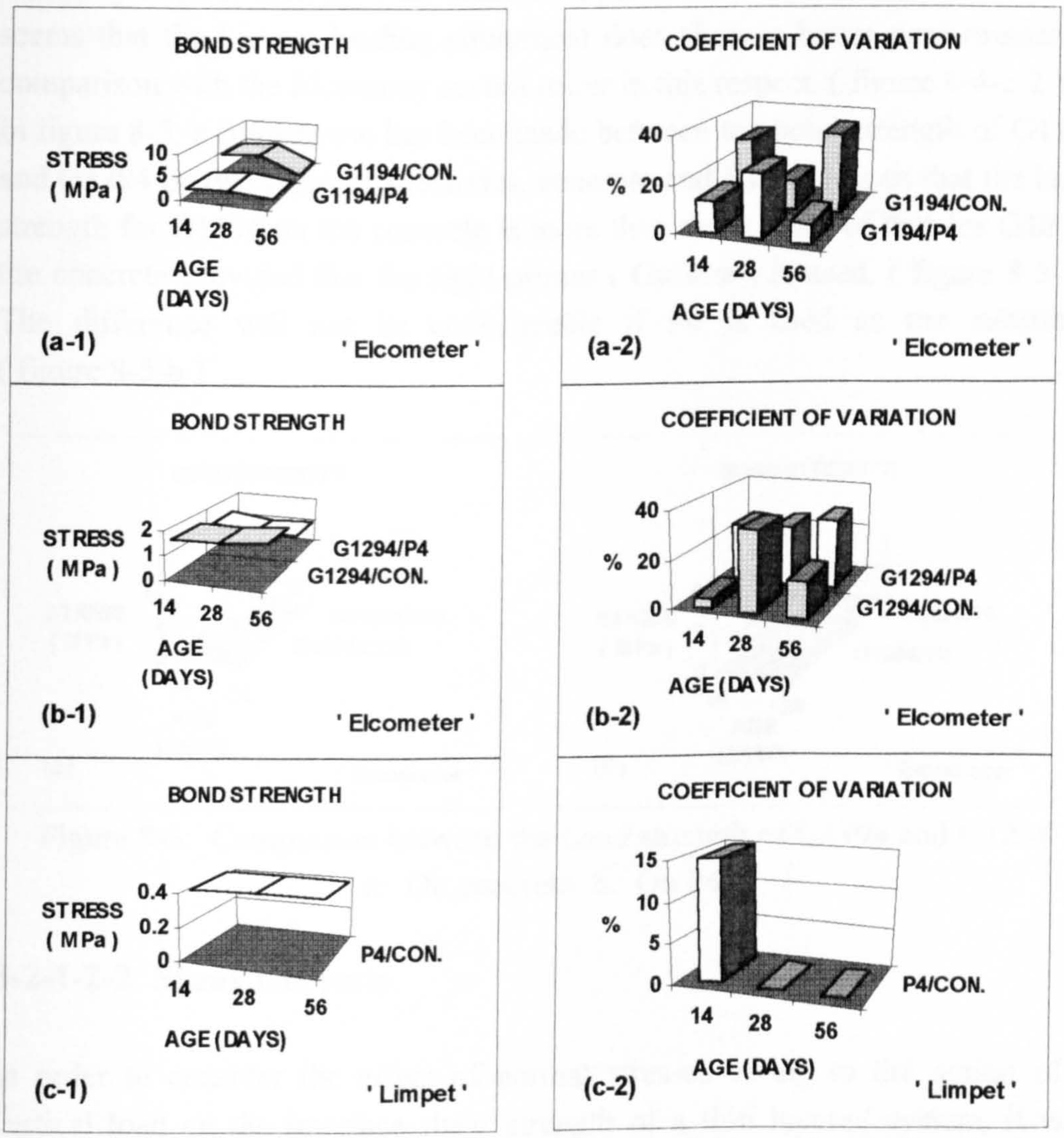

Figure 8-4: Values of bond strengths and coefficients of variations in the tensile bond strength tests (pull off tests)

From figure 8-4, it is seen that the value of bond strength is not very susceptible to the age, but to the interface primer. For example in figure 8-4-a-1, the bond strength has decreased considerably at the age of 56 day when Pprime has been used as the primer. The strongest bond has been provided in combination G1194/Concrete by using Gprime at the interface. The bond strength between G1194 or G1294 and concrete is stronger than that between G1194 or G1294 and P4 provided that the right primer (Gprime) is used. The main reason for the very low bond strength between P4 and concrete in figure 8-4-c-1 is that the wrong primer (Gprime) has been used at the interface. The main disadvantage of the pull off test method in this experiment has been the relatively large scattering of the results. (figures 8-4-a-2, b-2, c-2) However it seems that the Limpet loading equipment does show a better performance in comparison with the Elcometer screed tester in this respect. (figure 8-4-c-2)
In figure 8-5, a comparison has been made between the bond strength of G1194 and G1294 on two types of substrates, concrete and P4. It is seen that the bond strength for G1194 on the concrete is more than three times of that for G12 on the concrete provided that the right primer (Gprime) is used. (figure 8-5-a) The difference will not be considerable if P4 is used as the substrate. (figure 8-5-b)

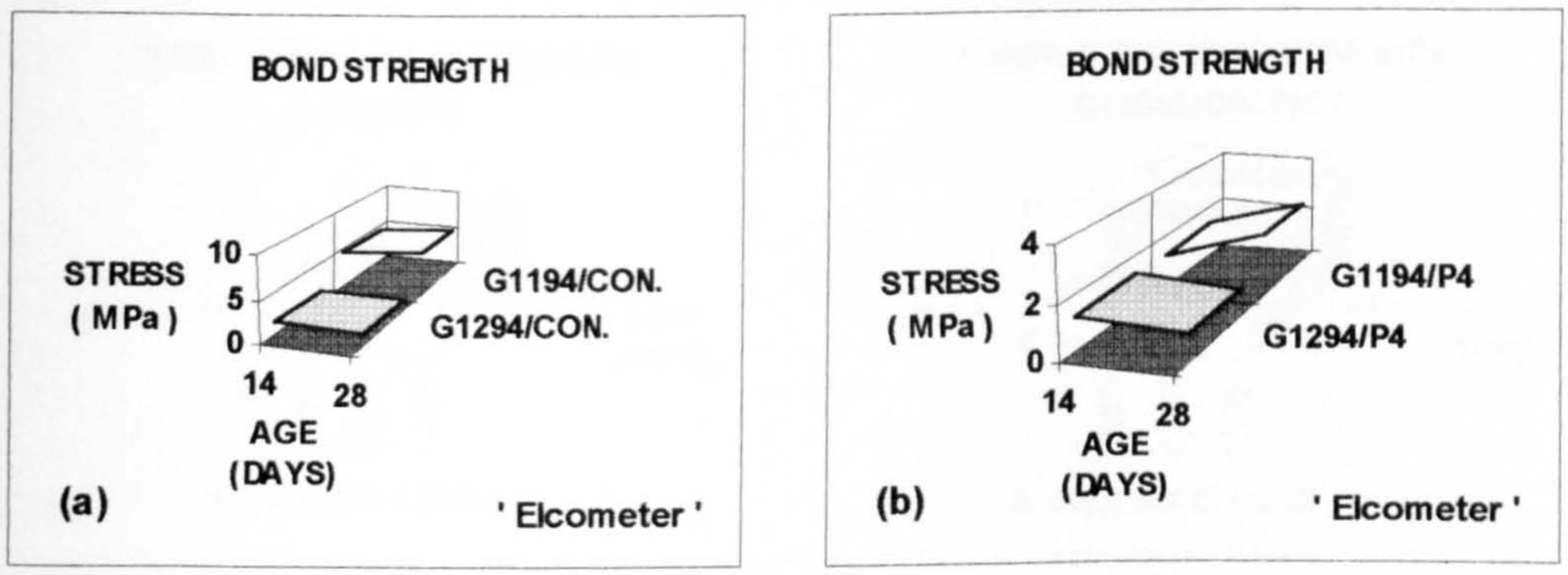

Figure 8-5: Comparison between the bond strength of G1194 and G1294
a: On concrete b: On P4

8-2-1-2-2 Shear box tests

In order to consider the effect of normal stresses owing to the action of a vertical load on the interface shear strength of a thin layered system, it was necessary to carry out the shear box tests. As was mentioned in section 5-2-2, in the proposed shear box test, the cohesion and coefficient of friction for each

combination of two materials are determined by using a shear box apparatus. The two types of primers were used in the same way as done in the pull off tests. For combination P4/Concrete, all the interfaces of the specimens at all ages were primed with the wrong primer (Gprime). For the rest of the combinations, Gprime was used at the ages of 14 and 28 days, and Pprime was only used at the age of 56 days.

Comparative charts showing the relationships between normal stresses and shear bond strengths for different combinations at different ages have been shown in figure 8-6. The relationship between normal stress and shear bond for each single combination of the materials and at each age was also plotted in figures 5-27 to 5-41, and the values of cohesion and coefficient of friction were

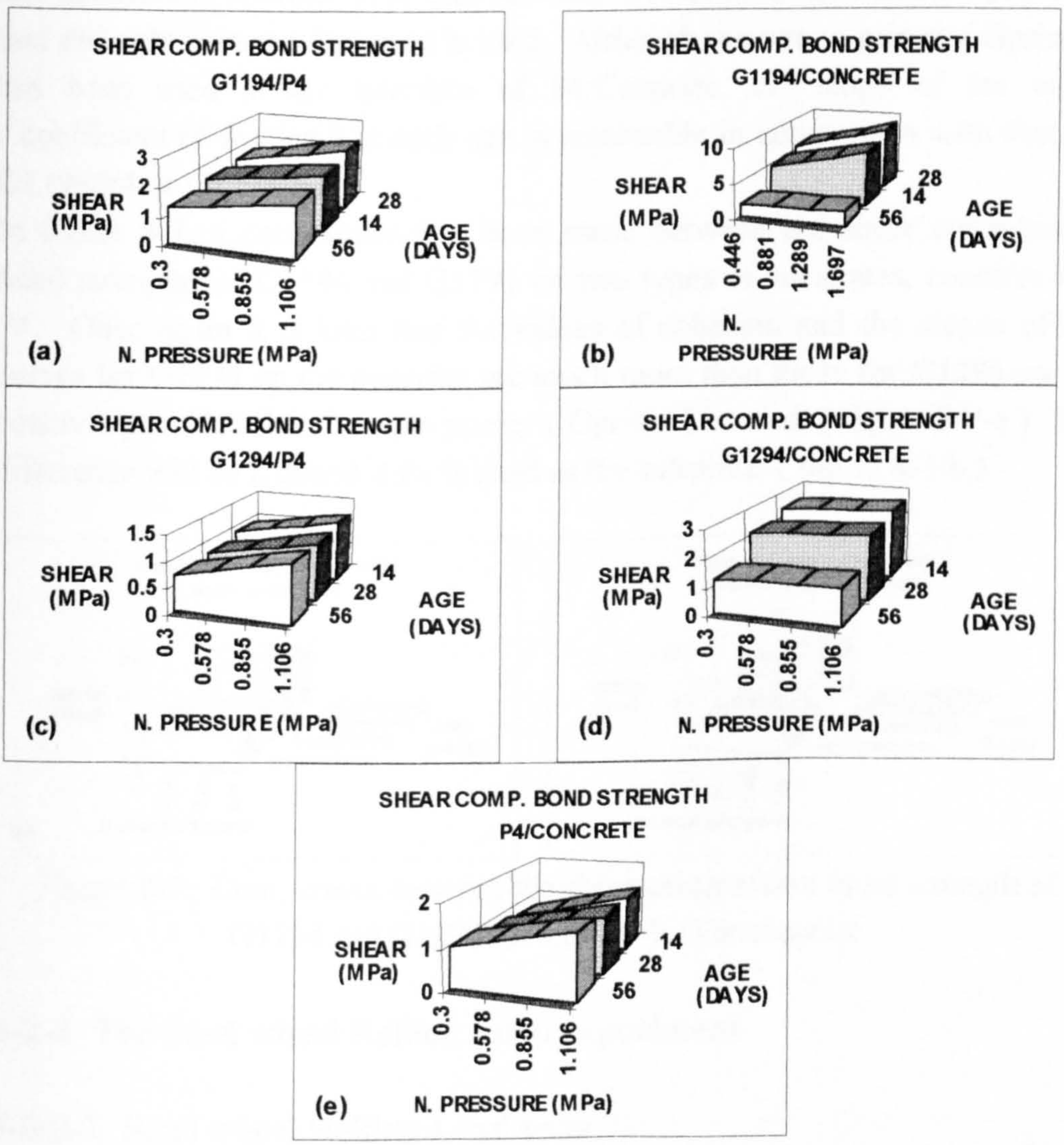

Figure 8-6: Comparative charts showing the relationships between normal stresses and shear strengths for different combinations at different ages

reported in table 5-22 of chapter 5. From figures 5-27 to 5-41, it is seen that the scattering of the results is acceptable, despite the fact that only a few number of tests have been carried out for each case. From table 5-22, it is revealed that the values of cohesion and coefficient of friction are not very susceptible to the age, but to the interface primer. The comparative charts in figure 8-6 also show the above criteria. This is more evident for G1194/Concrete and G1294/Concrete where there is a large reduction both in cohesion and coefficient of friction at the age of 56 days as a result of using Pprime at the interface. (figures 8-6 -b & d) Similar to the results of pull off tests, the strongest bond has been provided in combination G1194/Concrete by using Gprime at the interface. The bond strength between G1194 or G1294 and concrete is stronger than that between G1194 or G1294 and P4 provided that the right primer (Gprime) is used. Although the wrong primer (Gprime) has been used at the interface of P4/Concrete, the slope of the curve (coefficient of friction) at each age is reasonable in comparison with that for G1194/P4 or G1294/P4.

In figure 8-7, a comparison has been made between the shear compression bond strengths of G1194 and G1294 on two types of substrates, concrete and P4. Once again it is seen that the values of cohesion and the slopes of the curves for G1194 on the concrete are much more than those for G1294 on the concrete provided that the right primer (Gprime) is used. (figure 8-7-a) The difference will be reduced if P4 is used as the substrate. (figure 8-7-b)

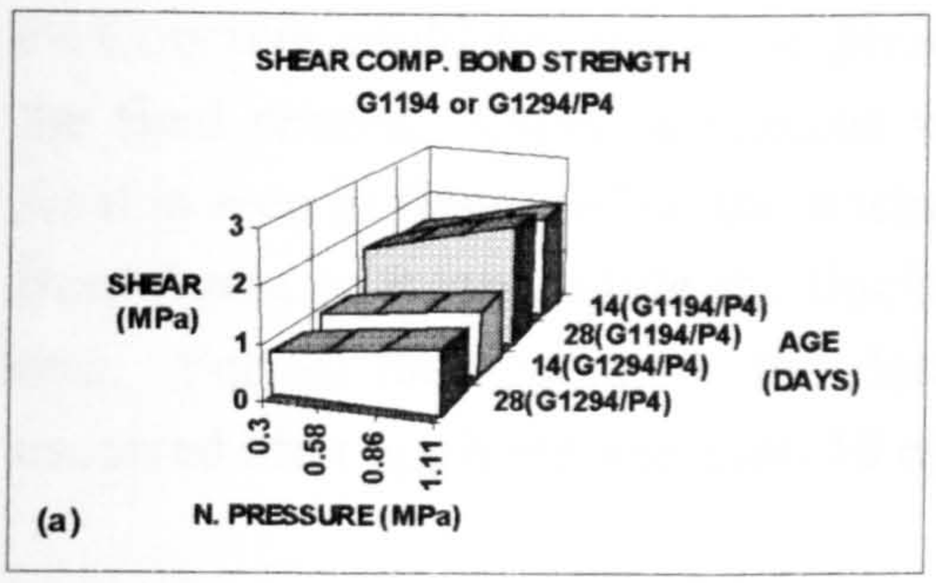

Figure 8-7: Comparison between the shear compression bond strength of G1194 and G1294 a: On P4 b: On concrete

8-2-2 The Steel wheel Rolling Load experiment

8-2-2-1 Steel wheel Rolling Load tests

Two types of specimens were used in this experiment; the ready made specimens, and the purpose made specimens.

The specifications and the results of the Steel Wheel Rolling Load tests on the ready made and purpose made specimens were tabulated in tables 6-1 and 6-2 of chapter 6, respectively. The thickness of the concrete substrate for the ready made specimens was 40 mm and for the purpose made specimens was 50 mm. Thickness of each layer of the flooring materials along with the ages at which the tests were carried out are also shown in figure 8-7. Two specimens were provided at each age of the test.

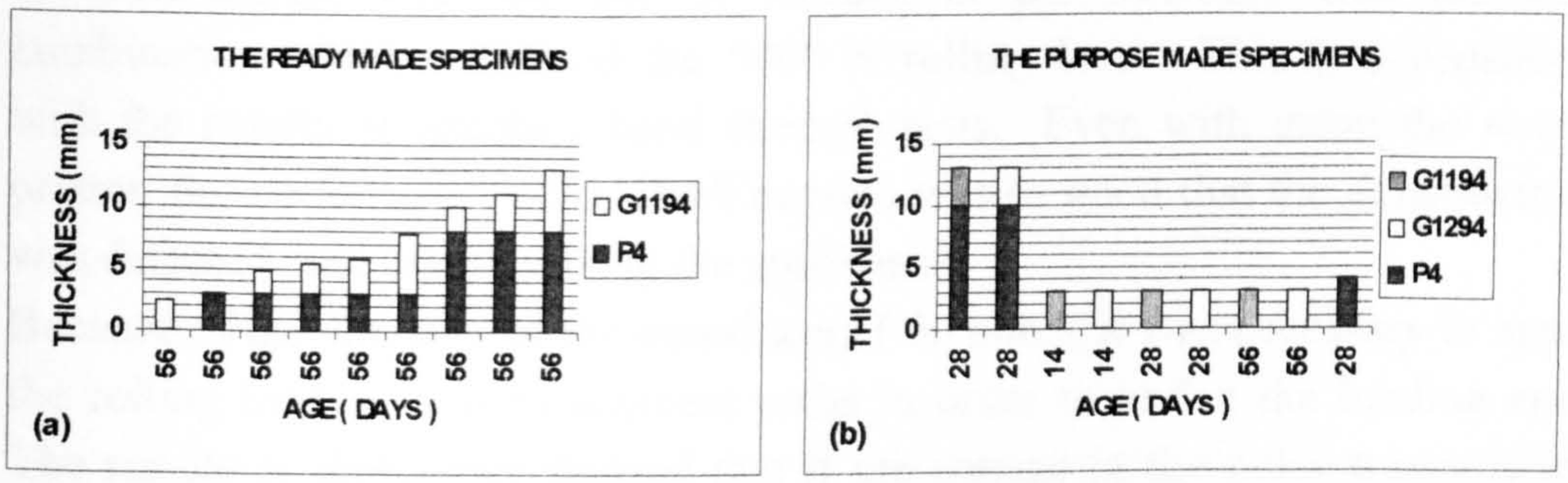

Figure 8-7: Thickness of each layer of the flooring materials and ages of tests in the Steel Wheel Rolling Load specimens

The ready made specimens included three combinations; G1194/Concrete, P4/Concrete, and G1194/P4/Concrete. As indicated in table 6-1-b, owing to the low thickness of the concrete layer, combinations of G1194/Concrete and P4/Concrete could not resist the prescribed loading condition and did not give the final results. Other specimens were of combination G1194/P4/Concrete. As it is seen in figure 8-7-a, the thickness of P4 layer in these specimens varied from 3 mm to 8 mm, while the thickness of G1194 layer varied from 1.5 to 5 mm. For all the specimens the delamination between the two upper layers occurred after applying less than 10 cycles of a 3750 N load .

For the purpose made specimens there were totally five different combinations; G1194/P4/Concrete, G1294/P4/Concrete, G1194/Concrete, G1294/Concrete, and P4/Concrete. As is seen in figure 8-7-b, the thickness of G1194 or G1294 in these specimens, where applied, was 3 mm while the thickness of P4 layer was 10 mm as the second layer and 4 mm as the upper layer. Similar to the ready made specimens, for the purpose made specimens of combinations of G1194/P4/Concrete and G1294/P4/Concrete, the delamination between the two upper layers occurred at less than 10 cycles under a load of 3750 N. For the

specimens of combination of G1294/Concrete, delamination was detected at about 50 cycles under a load of 5000 N. The delamination for these combinations could be detected by using both ways of sounding the surface or the pulse velocity method. However for G1194/Concrete using Pprime at the interface the delamination was detected by breaking the specimens after applying 200 cycles of 5000 N load. In the combination of P4/Concrete, rutting on the surface was observed at the early stage of the test. Delamination also occurred at the interface due to the use of the wrong primer at the interface, but was detected only after breaking the specimens.

G1194/Concrete with the use of Gprime at the interface was the only combination which withstood the 5000 N rolling load. This was consistent with the results of interface bond strength tests. Even with using the wrong primer, the performance of G1194/Concrete was so good that the delamination was detected only after breaking the specimens.

Because of the diameter of the transducers (50 mm), it was necessary to apply the rolling load on several adjacent paths in order to widen the loading area. The results of these tests showed that if the change in the pulse transmission time exceeds one μ sec., it means that a delamination has occurred providing that the direct transmission method is used. As was mentioned before, sounding the surface was also proved to be a reliable method for detecting most of the delaminations.

8-2-2-2 Structural analysis

In this part of the study, it was attempted to model and analyse the thin layered systems used in the Steel Wheel Rolling Load tests in order to predict their behaviour under the prescribed load condition. The analysis was based on the finite element method and a frictionless contact was assumed between the wheel and the surface. The prediction of the slippage and debonding of the coating layer was tried by defining a thin interface layer between the two upper layers of each system. Two failure criteria, slippage due to shear stresses and debonding due to normal stresses were considered. The results of the shear box and bond strength tests were used in this respect. The idealized stress strain curves, proposed in chapter 5 for the constitutive materials, were used in the implicit elasto plastic von Mises model, using the LUSAS finite element software. A nonlinear normal pressure distribution was approximated under the steel wheel. Elastic behaviour was assumed for the interface layer. Despite

the simplifications made in the solution, the analytical results were consistent with the experiment to a considerable extent.

Compared with the values of flexural strength for the constitutive materials, the values of maximum principal stress in the vicinity of the load and the interface of the delaminated systems were not critical. In fact, the delaminated surfaces of the specimens used in the Steel Wheel Rolling Load experiment were also relatively even. This means that a delamination at the interface of a thin layered system may occur without inducing any internal crack in the constitutive materials. It also indicates that the use of the interface layer for studying the behaviour of the thin layered systems with regard to the delamination defect is a necessity.

8-2-3 The NUROLF experiment

8-2-3-1 Pneumatic Tyred Vehicle Rolling Load tests

The NUROLF test vehicle was used in this experiment for simulating the actual loading condition resulted from a relatively free pneumatic tyre rolling load on a thin layered system. The layout of the testing area was in figure 7-13 and the results of the rolling load tests on the systems were tabulated in tables 7-6 and 7-7 of chapter 7. The thickness of the new steel fibre reinforced concrete substrate slab was 150 mm. Thickness of each layer of the flooring materials on each bay of the testing area along with the ages at which the tests were carried out are also shown in figure 8-8.

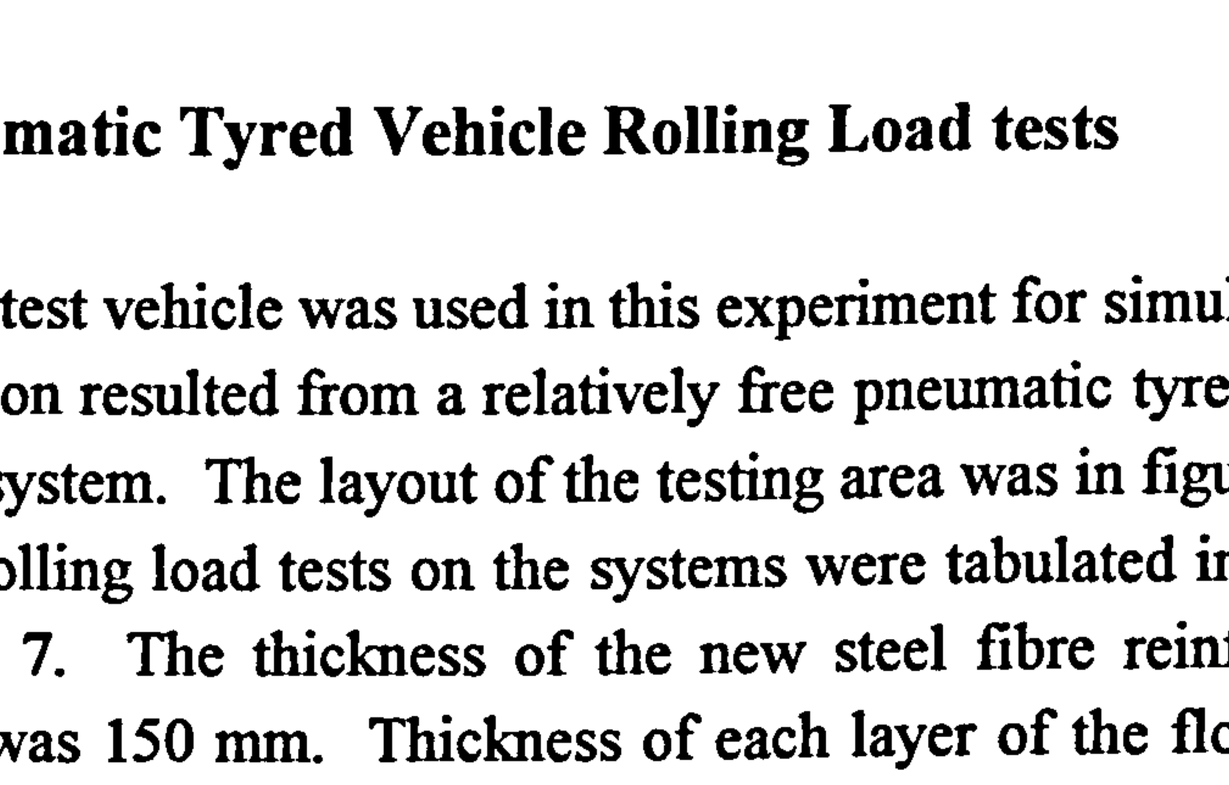

Figure 8-8: Thickness of each layer, age of the upper layer, and type of the primer used in the NUROLF experiment

The thin layered systems included five combinations; G1194/P4/Concrete, G1294/P4/Concrete, G1194/Concrete, G1294/Concrete, and P4/Concrete. As

the simplifications made in the solution, the analytical results were consistent with the experiment to a considerable extent.

Compared with the values of flexural strength for the constitutive materials, the values of maximum principal stress in the vicinity of the load and the interface of the delaminated systems were not critical. In fact, the delaminated surfaces of the specimens used in the Steel Wheel Rolling Load experiment were also relatively even. This means that a delamination at the interface of a thin layered system may occur without inducing any internal crack in the constitutive materials. It also indicates that the use of the interface layer for studying the behaviour of the thin layered systems with regard to the delamination defect is a necessity.

8-2-3 The NUROLF experiment

8-2-3-1 Pneumatic Tyred Vehicle Rolling Load tests

The NUROLF test vehicle was used in this experiment for simulating the actual loading condition resulted from a relatively free pneumatic tyre rolling load on a thin layered system. The layout of the testing area was in figure 7-13 and the results of the rolling load tests on the systems were tabulated in tables 7-6 and 7-7 of chapter 7. The thickness of the new steel fibre reinforced concrete substrate slab was 150 mm. Thickness of each layer of the flooring materials on each bay of the testing area along with the ages at which the tests were carried out are also shown in figure 8-8.

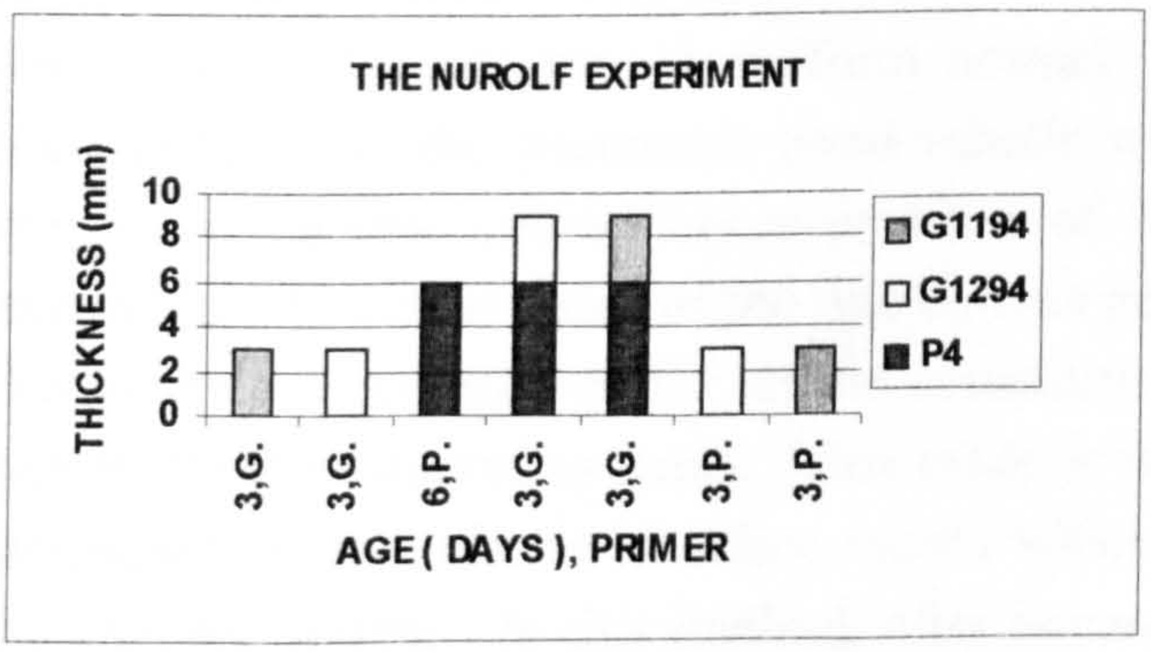

Figure 8-8: Thickness of each layer, age of the upper layer, and type of the primer used in the NUROLF experiment

The thin layered systems included five combinations; G1194/P4/Concrete, G1294/P4/Concrete, G1194/Concrete, G1294/Concrete, and P4/Concrete. As

it is seen in figure 8-8, the thickness of G1194 or G1294 was 3 mm while the thickness of P4 was 6 mm, where applicable, in these systems. The maximum vertical load was 6.500 ton applied on a rear dual wheel, and the tyre inflation was 100 psi. Three methods were used for detecting any possible delamination, sounding of the upper layer surface, pulse velocity method, and tensile bond strength test. Although the ages of the upper layer materials at which the rolling load tests started were very early, all the three methods indicated that there was no delamination in the thin layered systems after applying 1400 load cycles. Unlike in the previous experiment, owing to the lack of a highly concentrated load, P4 material also performed well under the tests. However G1294 was badly damaged as a result of being under wet conditions so that the image of the tyres were on the surface of the material was very obvious even after unloading. By contrast the behaviour of G1194 was very good and there was not any sign of damage or change in the appearance of the material surface.

8-2-3-2 Structural analysis

In this part of the study, it was attempted to model and analyse the thin layered systems used in the NUROLF tests in order to predict their behaviour under the prescribed load condition. The analysis was based on the finite element method. The prediction of the slippage and debonding of the coating layer was tried by defining a thin interface layer between the two upper layers of each system. Two failure criteria, slippage due to shear stresses and debonding due to normal stresses were considered. The results of the shear box and bond strength tests were used in this respect. A uniform normal contact pressure distribution was assumed under the pneumatic tyred vehicle wheel. As a free rolling truck tyre, a longitudinal contact shear pressure of 25 psi was also considered in each model. Since the value of the tyre contact pressure was low, a linear elastic behaviour was considered for all the constitutive materials and the interface layer in the thin layered systems. This made it possible to use a special two dimensional elasto - plastic interface model which is available in the LUSAS finite element system. In this method, after occurring a failure at any node, the redistribution of stresses and strains within the structure would be taken into account. For evaluating each combination of the thin layered systems, it was therefore necessary to carry out the analysis on two models of the structure simultaneously, one with a friction - slip interface model and the

other with a stick interface model. In the friction - slip model the real characteristics of the interface were considered whereas in the stick model very high values of cohesion, coefficient of friction, and tensile bond strength were assumed. The results given in section 7-3-2 of chapter 7 showed that there was no difference between the distribution of shear stresses along the interfaces of the two models for each combination. This means that no slippage or debonding had occurred at the interfaces of the thin layered systems. Therefore in spite of the simplifications made in the solution, the analytical results were consistent with the experiment to a considerable extent. It is also consistent with the results given by other investigators. [Lau et al. 1994]

The values of maximum principal stresses in the vicinity of the load and the interface of the delaminated systems were also very low compared with the values of flexural strength for the constitutive materials. This indicates that the safety margin against the inducing of internal cracks in the vicinity of the interface and the load for these systems has been very high.

8-3 Conclusion

This study was undertaken to introduce thin layered systems as a solution to the repair and protection of concrete structures. The materials which are more commonly in use for constructing these systems were reviewed. The most known failure causes of these systems were enumerated. The possibility of using these systems for protecting the concrete slabs in large areas such as warehouses under the action of a free rolling load and indoor conditions was studied. Some special flooring materials were used in this investigation. Two types of rolling load were considered, a steel wheel rolling load and a pneumatic tyred vehicle rolling load. Detecting and predicting any possible delamination between the upper two layers in the thin layered systems were in particular interest. The study necessitated to simulate the action of the rolling loads on the thin layered systems and also to establish a proper method of analysis in order to explain and predict the behaviour of these systems under the prescribed loading conditions.

On the basis of the investigation carried out here, the following conclusions can be drawn:

- Thin layered systems have been used in repair, protection or strengthening of concrete structures in various fields of the construction industry. Protection, upgrading and rehabilitation of the floor slabs, restoration of appearance of the concrete structures, protection of the reinforcing steel of the concrete structure against atmospheric or chemical attack are some common uses of these systems. They may also offer impermeability, skid resistance, wear resistance, and water shedding properties. Some of theses systems may have the capability of being installed with minimal disruption to traffic.

- Among the three flooring materials used in this investigation, the G1194 showed the best performance, particularly with regard to the Steel Wheel Rolling Load experiment. The compressive strength for this material varied from 55 MPa (about the same as for the concrete substrate) at the age of 3 days to about 1.5 times that value at the age 56 days. It also showed the highest value of flexural strength among the flooring materials. Its modulus of elasticity was less than half of that for the concrete substrate at the age of 28 days. However it showed a ductility more than 10 times of that for the concrete or the P4 system in compression.

- With regard to the tensile bond strength tests (pull off tests), the use of the Elcometer screed tester showed a relatively large scattering of results while the Limpet loading equipment seemed to offer a better performance in comparison with the Elcometer screed tester in this respect.

- The results of the tensile bond strength tests showed that the value of bond strength was not very susceptible to the age, but to the interface primer. The strongest bond strength was recorded for combination G1194/Concrete with the use of Gprime at the interface. It was also seen that the bond strength for G1194 on the concrete was more than three times of that for G1294 on the concrete provided that the right primer (Gprime) had been used. The difference was not considerable where P4 was used as the substrate.

- The proposed simple shear box test method was successfully used for considering the effect of normal stresses due to the action of a vertical load on the interface shear strength of a thin layered system. Despite carrying out a few number of tests for each combination, the scattering of the results was acceptable. The accessibility of the shear box apparatus may be a big advantage of this test method. The results of the shear box tests were in general agreement with those of the pull off tests. For example the strongest bond was provided in combination G1194/Concrete by using Gprime at the interface. Similar to the results of the pull off tests, the values of cohesion and coefficient of friction obtained from the shear box tests were not very susceptible to the age, but to the interface primer. Also the bond strength between G1194 or G1294 and concrete was stronger than that between G1194 or G1294 and P4 provided that the right primer (Gprime) had been used.

- The Steel Wheel Rolling Load Rig proved to be a reliable apparatus for simulating the action of a steel wheel rolling load.
The results of the rolling load tests showed that G1194/Concrete with the use of Gprime at the interface was the only combination which withstood the maximum 5000 N load without any sign of delamination or wear. This is consistent with the results of bond strength and shear box tests. All other combinations of the thin layered systems and even G1194/Concrete, with the use of the wrong primer, were delaminated under the action of such a load sooner or later in the tests. Some of them were delaminated even under a lower value of load. The interesting point was that the quality of the delaminated

surfaces at the interface of each combination was the same as that observed in the interface bond strength tests and also in the shear box tests. With regard to the above, it could be concluded that the interface bond strength is the most important factor in resisting a thin layered system against any possible delamination under the action of a rolling load.

The combination of P4/Concrete is not recommended to be used under such a steel wheel rolling load as rutting on the surface observed at the early stage of test.

The type of the primer used at the interface has a vital role in the performance of a thin layered system under a solid wheel rolling load. For example a system having excellent performance under a heavy solid wheel rolling load can still be delaminated with the use of a wrong primer under the same loading condition.

- The NUROLF offered a realistic method for simulating the action of a pneumatic tyred vehicle wheel rolling load.

From the NUROLF experiment, it can be concluded that all combinations of the thin layered systems have been able to resist a maximum 6.5 ton dual tyre load without any delamination, even when tested a relatively short time after construction.

Owing to the lack of a highly concentrated load, P4 material also showed very good performance under the action of the pneumatic tyred vehicle wheel load. This means that the performance of the P4 system in dependent on the type of the rolling wheel load.

G1294 is not recommended to be used unless it is adequately modified, as it was badly damaged as a result of being under load in wet condition.

- The pulse velocity method, tensile bond strength test, and sounding the surface were all used successfully for detecting any possible delamination for most of the thin layered systems in this investigation. However it could be said that the sounding method is the simplest and most economical way of examining a thin layered system in this respect. It could be also said that a bigger difference between the modulus of elasticities of the upper layer and the second layer of a thin layered system will result in an easier detecting of any possible delamination.

- Despite the simplifications made in the solution, the analytical results were

consistent with the experimental results to a considerable extent in both of the experiments. It is therefore concluded that the following steps could be followed in order to predict the behaviour of a thin layered system under the action of a rolling load with regard to the delamination defect:

1- Carrying out the required types and number of tests for defining the properties of the constitutive materials. The number and also the types of the tests will be based on many factors among which the characteristics of the materials themselves, loading conditions, environmental conditions, type and place of the application of the thin layered system are very important.

2- Carrying out a series of tensile bond strength (pull off) tests preferably using the Limpet loading equipment.

3 - Carrying out a series of shear box tests in order to define the relationship between the normal pressure and the shear strength at the interface.

4- Defining the thin interface layer as illustrated in section 4-3-3 of chapter 4 and implemented in section 6-3-1-2 of chapter 6 and in section 7-3-1-2 of chapter 7.

5- Defining the contact pressure distribution.

6- Defining an appropriate finite element mesh with regard to the basic requirements for a finite element modelling.

7- Implementing the structural analysis of the finite element model using an appropriate finite element system such as LUSAS or PAFEC. In sections 6-3-2 of chapter 6 and 7-3-2 of chapter 7, two different ways of presentation and interpretation of the results have been given, each of them is based on the specifications of the problem and limitations of the analysis.

8- As a final check for each project, carrying out at least one experimental test on each case using facilities such as the Steel Wheel Rolling Load or the NUROLF, is recommended.

8-4 Recommendations for further research

8-4-1 Inclusion of the horizontal forces in the rolling load experiment

In the current study, particularly in the Steel Wheel Rolling Load experiment, the behaviour of the thin layered systems was examined under the action of a free rolling load. Although the Steel Wheel Rolling Load itself was very heavy and a highly concentrated load, its consequences would be even more severe if it is capable of simulating the action of a braking load as well. Recently modifications were carried out to the rig so that it is now capable of applying horizontal braking force as well as the vertical force on the specimen under test.

With this regard, as mentioned in section 3-2-2 of chapter 3, recently an experimental investigation was also carried out into the effect of steel wheel braking forces on the behaviour of the thin layered systems used in chapter 6 of this study. The results proved that very severe damage may occur due to the action of braking loads caused by a steel wheel load on the thin layered systems. The failure modes included delamination, wave or carpet effect (figure 3-2), and tearing or cracking of the upper layer directly subjected to the load. [Samin 1996] Using such a facility, the investigator is able to simulate any combinations of vertical and horizontal loads which are of interest. Obviously the same steps which were taken in this investigation and summarized at the end of the previous section will be valid for the analysis and predicting the behaviour of the thin layered system under such combinations of loads . The only difference would be that in case of the presence of a braking load, the finite element mesh will not be considered as symmetrical.

8-4-2 Modifying the flooring materials

As it was seen in this investigation, the P4 material showed a very good performance in the NUROLF experiment, both as a substrate for G1194 and as the upper layer in a thin layered system. As it was partly a cementitious material, its cost was perhaps less than G1194 and G1294. Therefore, it would be a good base for G1194 or G1294, providing that the bond strength between the two layers is sufficient for the purpose of the application. However it was seen that two problems may arise when using this material in the Steel Wheel Rolling Load experiment; excessive wear, and debonding. Also delamination

occurred in all combinations of G1194/P4/Concrete and G1194/P4/Concrete. Therefore, based on the above facts, the following recommendations seem to be pertinent to the application of the P4 material:

1- The P4 material may be used as the upper layer or as the intermediate layer on a concrete substrate where a highly concentrated load is not expected.

2- If the P4 material is to be used as the intermediate layer under a thin layer of G1194 under the action of a solid wheel rolling load, research must be done in order to increase the bond strength between G1194 and P4 so that any possible delamination is avoided.

As G1294 was badly damaged as a result of being under load in wet condition, it must not be used unless it is adequately modified.

The combination of G1194/Concrete with the use of Gprime at the interface showed the best performance under the action of the steel wheel rolling load, so the possibility of its use in other fields of construction, repair or protection of concrete structures should be also studied. Obviously in different cases of applications, different types of tests, and different curing and testing conditions are to be defined. Even for a new application, the material may still need to be modified in order to meet some additional special requirements.

8-4-3 Modifying the method of tests and the analysis

As a matter of comparability, a further research into the effect of the confinement of the upper layer in the proposed shear box test on the shear compression bond strength is recommendable. This may be more important, if the horizontal braking force of the wheel load is to be considered in the analysis.

As it was mentioned in the previous section, G1194/Concrete may has the capability of being used in a broader field of the construction industry, for example in the repair and protection of concrete bridges. With this regard the G1194 material may need to be modified to meet the required specifications for that purpose. If it is so, the test methods have to be improved or even changed or completed. For example in a bridge repair or protection application, carrying out appropriate fatigue tests and compatibility tests are required. As a result of the change in the loading conditions, there may be a need for carrying

out dynamic tests instead of the static ones, both for the material characteristics and the interface bond strength. New ambient conditions must be considered. When the speed of a rolling wheel is very high the effect of tyre impact should be also taken into account.

REFERENCES

A

Al-Negheimish, Abdulaziz Ibrahim, " Bond strength, long term performance and temperature induced stresses in polymer concrete-Portland cement concrete composite members ", Ph.D. dissertation, The University of Texas at Austin, 1988

Allen, R. T. L., Edwards, S. C., and Shaw, J. D. N., " The Repair of Concrete Structures ", Second edition, Blackie Academic & Professional, an imprint of Chapman & Hall, Glasgow, UK, 1993

Anon, " Maintenance and repair of roads and bridges ", Concrete (London), Vol. 24, No. 4, Apr. 1990 3p

Anon, " Solving decontaminable flooring problems ", Nuclear Engineering International, Vol. 34, No. 421, Aug. 1989 p. 37

B

Bagate, Moussa, " A mechanistic design for thin - bonded concrete overlay pavements", Ph.D. dissertation, The University of Texas at Austin, 1987

Barksdale, R. D., " Analysis of layered systems ", Final report of Project B-607, National Science Foundation Grant No. GK-1583, Georgia Institute of Technology, 1969

Bendeddouche, O., " The mechanical and physical properties of epoxy resins and their influence on the performance of screeds ", MSc thesis, University of Newcastle Upon Tyne, 1985

Boussinesq, J. " Application des potentials, Paris ", 1885.

Bundies, F.J., " Adhesion of modern barrier coats on concrete motorway bridges and troughs under tarmac ", Proceedings of an international symposium organised by RILEM Technical Committee 52 - Resin Adherence to Concrete and Laboratoive Central des Ponts et Chauss'ees, Paris, September 16-19, 1986

Bungey, J. H., " The Testing of Concrete in Structures ", Second edition, Chapman and Hall, New York, 1989

Burmister, D. M., " The Theory of Stresses and displacements in layered systems and application to the Design of Airport Runways ", proc. HBR, 1954

C

Carter, P.d., " Thin Polymer Wearing Surfaces for Preventive Maintenance of Bridge Decks ", Proc. polymer concrete: 9th Symposium Fall convention: Papers, 1993, American concrete Inst./USA ACI Special Publications 137

Cather, B., and Leeming, M., " A coat of many colours ", January/February 1995 Concrete pp. 10-12

Chandler, J. W. E., " Design of floors on ground ", Technical report, Cement and Concrete Association, no. 550, June 1982

Choi, K. S., " Failure modes in layered systems ", University of Newcastle Upon Tyne, MPhil thesis, December 1991 (Draft only)

CIRIA, PRACTICE NOTE, " Thin flooring on solid floors - Visual imperfections ", CIRIA, SPECIAL PUBLICATION 37, 1985

Cleland, D.J., Naderi, M., and Long, A.E., " Bond strength of patch repair mortars for concrete ", Proceedings of an international symposium organised by RILEM Technical Committee 52 - Resin Adherence to Concrete and Laboratoive Central des Ponts et Chauss'ees, Paris, September 16-19, 1986

Concrete Society, Technical Report No. 39, " POLYMERS IN CONCRETE ", A Technical Report of The Concrete Society's Technical Development Centre, prepared by a Working Party of its Materials Group

Concrete Society, Technical Report No. 34, " CONCRETE INDUSTRIAL GROUND FLOORS ", The Concrete Society in association with the British Industrial Truck Association and the Storage Equipment Manufacturers Association, 1988

Conway, H. D.; Vogel, S. M.; Farnham, K. A.; and So, S., " Normal and shearing contact stresses in indented strips and slabs ", International Journal of Engineering Science, Vol. 4, pp. 343-359, 1966

Cook, R. D.; Malkus, D. S.; and Plesha, M. E., " Concepts and Applications of Finite Element Analysis ", Third edition, John Wiley & Sons, New York, 1989.

D

Desai, C. S., and Zaman, M. M., " Thin layer element for interfaces and joints ", Int. j. for numerical and analytical methods in geomechanics, Vol. 8, 19-43, 1984.

Desai, C. S., " Behavior of interfaces between structural and geologic media ", Proc. Intl. Conf. on Recent Advances in Geotech. Earthquake Eng. and Soil Dynamics, St. Louis Mo., 1981

Dorsch, David F., " Assessment and repair of fire - damaged concrete structures ", Innovation in Repair Techniques of Concrete Structures, Procs 1993, ASCE, ANNU CONV EXPO 1993, Edited by Ghafoori, Nader

E

Eberline, Donita K.; Klaiber, F. Wayne; Dunker, Kenneth, " Bridge strengthening with epoxy-bonded steel plates ", Transportation Research Record, No. 1180, 1988,

pp. 7-11

F

FEA, LUSAS Finite Element Analysis System, Version 11," LUSAS User Manual ", FEA Ltd., UK

Floros, T., " Repair of compression zones in R.C. beams and the effect of interface bond strength ", MPhil thesis, The university of Newcastle Upon Tyne, Dec. , 1991

Fukushima, T., Tomosawa, F., Fukushi, I., and Tanaka, H, " Protection effects of polymeric finishes on the carbonation of concrete and corrosion of reinforcement ", Proceedings of an international symposium organised by RILEM Technical Committee 52 - Resin Adherence to Concrete and Laboratoive Central des Ponts et Chauss'ees, Paris, September 16-19, 1986

G

Galloway, J. W.; and Harding, H. M., " Elastic moduli of a lean and a pavement quality concrete under uniaxial tension and compression ", Materials and structures, 9, No. 49, pp. 13-18, Paris, Jan.-Feb. 1976.

H

Hamoush, S. A.; and Ahmad, S. H., " Static strength tests of steel plate strengthened concrete beams ", Materials and Structures, March 1990, Vol. 23, No. 134, pp. 116-125

Hazen, Fred E., " Monolithic Linings and Coatings for Secondary Containment Structures ", Materials Performance, Vol. 30, No. 8, Aug. 1991, pp. 36-41

Hogg, A. H. A., " Equilibrium of a Thin Plate Symmetrically Loaded, Resting on an Elastic Subgrade of Infinite Depth ", Philosophical Mag., Ser. 7, Vol. 25, March 1938

Holl, D. L., " Equilibrium of a Thin Plate Symmetrically Loaded on a Flexible Subgrade ", J. Sci., Vol. 12, no. 4, Iowa State College, July 1938

Holl, D. L., " Thin Plates on Elastic Foundations ", Proc. Int. Congr. Appl. Mech., 5th, Cambridge, Mass., 1938

Holl, D. L., " Plane - Strain Distribution of Stress in Elastic Media ", Iowa Engineering Station, Bulletin 148, Ames, Iowa, 1941.

Holtgreve, K., " A contribution in regard to behaviour of reinforced Tee-Beams with bonded flat steel components under fatigue loads ", Proceedings of an international symposium organised by RILEM Technical Committee 52 - Resin Adherence to Concrete and Laboratoive Central des Ponts et Chauss'ees, Paris, September 16-19, 1986

Huang, Yang H., " Finite - element analysis of slabs on elastic solids ", ACE Journal of Transportation Engineering, Vol. 100, TE2, May 1974

Huang, Yang H., " Pavement Analysis and Design ", Prentice Hall, Inc., Englewood Cliffs, New Jersey, 1993.

Huang, D. J., " Structural Analysis of Cementitious System ", Research report, University of Newcastle Upon Tyne, Oct., 1990

Hudson, W. R., " Discontinuous Orthotropic Plates and Pavement Slabs ", University of Texas, PhD. Dissertation, August 1965

Hudson, W. R.; and Matlock, H., " Analysis of discontinuous orthotropic pavement slabs subjected to combined loads ", Highway research record, No. 131, 1966

J

Jones, A., " Tables of Stresses in Three - layer Elastic Systems ", HRB Bull., 342, 1962

Judge, A. I., Cheriton, L. W., Lambe, R. W., " Bonding systems for concrete repair - An assessment of commonly used materials ", Proceedings of an international symposium organised by RILEM Technical Committee 52 - Resin Adherence to Concrete and Laboratoive Central des Ponts et Chauss'ees, Paris, September 16-19, 1986

K

Kawakami, M., H. Tokuda, M. Kagaya, and Nasu, R., " Precast reinforced concrete pipe with polymer mortar ", Proc. polymer concrete: 9th Symposium Fall convention: Papers, 1993, American concrete Inst./USA ACI Special Publications 137

Kennedy, J. C.; and Prause, R. H., " Development of multi - layer analysis model for tie/ballast track structures ", Paper presented at the 57th Annual Meeting of the TRB, January 1978.

Khazanovich, L.; and Ioannides, Anastasios M., " Structural analysis of unbonded concrete overlays under wheel and environmental loads ", Transportation research record, No. 1449, pp. 174-181, 1994

Knapton, J., and Ellerton, J., " Single Pour Industrial Floor Slabs, Their specification, Design, Construction and Monitoring ", Newcastle University Ventures Ltd., Newcastle Upon Tyne, 1994.

Krauss, Paul D., " Polymer concrete helps to keep the traffic moving, with minimal maintenance ", Modern plastics, 1988 Vol. 65 No. 12 pp. 92,95

Kudlapur, Shivaprasad; Hanaor, Ariel; Balaguru, P. N.; Nawy, Edward G., " Evaluation of Cold-Weather Concrete Patching Materials ", ACI Materials Journal

(American Concrete Institute), Vol. 86 no. 1 Jan-Feb 1989 pp. 36-44

Kudlapur, Shivaprasad T., " Performance and shear interaction in two-layered systems of high- strength cold weather concrete repair materials in sub-freezing temperatures ", Ph.D. dissertation, The State University of New Jersey, May 1990

Kwasny, R., " Qualification tests on PCC systems for the repair of concrete road bridges ", Proceedings of an international symposium organised by RILEM Technical Committee 52 - Resin Adherence to Concrete and Laboratoive Central des Ponts et Chauss'ees, Paris, September 16-19, 1986

L

Lau, C. M., Fwa, T. F., and Paramasivam, P., " Interface Shear Stress In Overlaid Concrete Pavements ", Journal of Transportation Engineering, March/April 1994, Vol. 120, No. 2, pp. 163-177

Li, T. Q., ' Pioneer test report on thin polymer layered system under the action of line load ', University of Newcastle Upon Tyne, Sept., 1990

Lippmann, S. A., and Oblizajek, K. L., " The distributions of stress between the tread and the road for freely rolling tires ", SAE, Automotive Engineering Congress, Detroit, Mich., February 25 - March 1,1974.

Love, A. E. H., " A treatise on the mathematical theory of elasticity ", 4th Ed., Cambridge University Press, London, England, 1927

Lundy, James Ray, " Delamination of bonded concrete overlays at early ages ", Ph.D. dissertation, The university of Texas at Austin, 1990

LUSAS, FEA LUSAS Finite Element Analysis System, Version 11," LUSAS User Manual ", FEA Ltd., UK

M

Majidzadeh, K., " A Mechanistic Approach to Rigid Pavement Design ", CONCRETE PAVEMENTS, Edited by A. F. Stock, ELSEVIER APPLIED SCIENCE PUBLISHERS LTD, Essex, England 1988

Malhotra, V. M., " TESTING HARDENED CONCRETE: NONDESTRUCTIVE METHODS ", First edition, The Iowa State University Press, Ames, Iowa, and American Concrete Institute, Detroit, Michigan, USA, 1976

Mays, G. C., and Hutchinson, A. R., " Adhesives in civil engineering ", Cambridge University Press, Cambridge, 1992

Mays, Dr G., and Calder, A., " External plates extend reinforcement's reach ", Concrete (London), Vol. 22, No. 11, Nov. 1988, pp. 25-28,

McCullough, B. F., " A Pavement Overlay Design System Considering Wheel Loads, Temperature Changes, and Performance ", PhD. Dissertation, University of California at Berkeley, July 1969

Mehta, P. Kumar, and Monteiro, Paulo J. M., " CONCRETE Structure, Properties, and Materials " Second edition, Prentice - Hall, Inc., New Jersey, 1993

Mwape, A.L., " Durability of concrete and its protection ", MSc dissertation, The university of Newcastle Upon Tyne, Sept., 1990

N

Naderi, M., Cleland, D., and Long, A.E., " Insitu test methods for Repaired concrete structures ", Proceedings of an international symposium organised by RILEM Technical Committee 52 - Resin Adherence to Concrete and Laboratoive Central des Ponts et Chauss'ees, Paris, September 16-19, 1986

Naderi, M., " Internal research report ", Civil Engineering Department, The Queen's University of Belfast, Oct. 1985.

Neville, A. M., " Properties of Concrete ", 3rd edition, Pitman, London, 1983

Neville, A. M., " A general relation for strengths of concrete specimens of different shapes and sizes ", Journal of American Concrete Institution, 63, pp. 1095-109, Oct. 1966.

Nilson, Arthur H.; and Winter, George, " Design of concrete structures ", Eleventh Edition, McGraw-Hill, Inc., New York, 1991.

O

O'connor, Jerome P.; Kline, Thomas R., " Case studies in concrete repair technology ", Construction Specifier, Vol. 43, No. 12, Dec. 1990, pp. 84-90, 92-93

O'connor, D. N., and Saiidi, M., " Compatibility of Polyester - Styrene Polymer Concrete Overlays With Portland Cement Concrete Bridge Decks " ACI Material Journal (AME . Concrete INS), 1993, Vol. 90, No. 1, Jan. - Feb. pp. 59-68

Ohama, Y., Demura, K., Nagao., H., and Ogi, T., " Adhesion of polymer - modified mortars to ordinary cement mortar by different test methods ", Proceedings of an international symposium organised by RILEM Technical Committee 52 - Resin Adherence to Concrete and Laboratoive Central des Ponts et Chauss'ees, Paris, September 16-19, 1986

P

Padovan, J.; Tovichakchaikul, S.; and Zeid, I., " Finite element analysis of steadily moving contact fields ", Computers & structures, Vol. 18, No. 2, pp. 191-200, 1984

Peattie, K. R., " Stresses and Strain Factors for Three-Layer Elastic Systems ", HBR Bull. 342, 1962

Peattie, K. R., " Stress distribution in layered systems ", Lectures at the University of Newcastle Upon Tyne, Oct. 1980

Perkins, Philip H., " REPAIR, PROTECTION AND WATERPROOFING OF CONCRETE STRUCTURES ", Elsevier applied science publishers, London and New York, 1986

Pickett, G.; and Ray, G. K., " Influence Charts for Concrete Pavements ", Transactions, ASCE, Vol. 116, 1951, pp. 49-73

Pickett, G.; Raville, M. E.; Jones, W. C.; and Mc Cormick, F. J., " Deflections, Movements, and Reactive Pressures for Concrete Pavements ", Kansas State College Bulletin No. 65, October 1951

Plevris, N.; Triantafillou, T. C., and Veneziano, D., " Reliability of RC Members Strengthening With CFRP Laminates ", Journal of Structural Engineering, Vol. 121, No. 7, July 1995, pp. 1037-1044

Plum, David R., and Morton, R., " Special materials - their use and appraisal ", Highways, Vol. 56, No. 1936, April 1988, pp. 46-50

Plum, D. R., " The behaviour of polymer materials in concrete repair and factors influencing selection " The Structural Engineer, Journal of the Institution of Structural Engineers, vol. 68, no. 17, September 1990, pp. 337-345

Plum, D. R., " POLYMER MODIFIED MATERIALS AND THE CURING ENVIRONMENT ", Proceedings of the International Conference on Structural Faults and Repairs 89, vol. I, pp. 99-101, June 1989

Plum, D. R., " Epoxy resin repair materials - In the laboratory and insitu ", Proceeding of the International Conference on Structural Faults and Repairs, 1987, vol. 1, pp. 335-341

Plum, D. R., " Thin layer cementitious systems for FOSROC CCD LIMITED ", July 1990

Plum, D. R., " Horizontal loading in layered system ", Internal report, Dept. of civil engineering, University of Newcastle Upon Tyne, August 1995

Plum, D. R., " Materials- What to specify? ", Construction Maintenance and Repair, vol. 5, no. 4, pp. 3-7, July/August 1991

Plum, D. R., " Environmental effects on polymer modified materials ", Proceedings of the International Conference on Highrise Buildings, Vol. II, pp. 726-731, Nanjing, March 1989

Plum, D. R., " Materials-Why they fail ", Construction Maintenance and Repair, vol. 5, no. 5, pp. 4-8, September/October 1991

Plum, D. R., " Materials - how to select ", Construction Maintenance and Repair, vol. 5, no. 5, pp. 27-30, November/December 1991

R

Ranisch, E. -H., and Rostasy, F.S., " Bonded steel plates for the reduction of fatigue stresses of coupled tendons in multispan bridges ", Proceedings of an international symposium organised by RILEM Technical Committee 52 - Resin Adherence to Concrete and Laboratoive Central des Ponts et Chauss'ees, Paris, September 16-19, 1986

Reagan, F., " Performance Characteristics of Traffic Deck Membranes ", Concrete International: Design and Construction, Vol. 14, No. 6, pp. 48-51, 1992

Rebeiz, K. S., Fowler, D. W., and Paul, D. R., " Making polymer concrete with recycled pet ", Plastics engineering, 1991, Vol. 47 No. 2, pp. 33-34

Rebeiz, K. S., and Fowler, D. W., " Recycling plastics in polymer concrete systems for engineering applications ", Polymer - Plastics Technology and Engineering, Vol. 30 No. 8, 1991, pp. 809-825

Rebeiz, K. S., Fowler, D. W., and Paul, D. R., " Recycling plastics in polymer concrete for construction applications ", J. of Materials in Civil Engineering Vol. 5 No. 2, May 1993, pp. 237-248

Reinhardt, H. W., " Length influence on bond strength of joints in composite precast concrete slabs ", The International Journal of Cement Composites and Lightweight Concrete, Volume 4, Number 3, August 1982, pp 139-143

Rigo J. M.; Degeimbre R.; and Francken L. (the editors), " Reflective Cracking Pavements ", Proc. of the second International RILEM Conference, Liege, Belgium, March 10-12, 1993, E & FN SPON

S

Saemman, J. C., and Washa, George W., " Horizontal Shear Connections Between Precast Beams and Cast - in - Place Slabs ", ACI Journal, Proceedings V. 61, No. 11, Nov. 1964, pp. 1383 - 1409

Saiidi, M., Vrontinos, S., and Douglas, B., " Model for the Response of Reinforced Concrete Beams Strengthened by Concrete Overlays ", ACI Structural Journal (American Concrete Institute), Vol. 87, No. 6, Nov. - Dec. 1990, pp. 687-695

Samin, I. S. P., " Behaviour of thin layered systems (Braking loads) ", Final year project for B.Eng. (Hon.) in The University of Newcastle Upon Tyne, June 1996

Saucier, F., Bastien, J., Pigeon, M., and Fafard, F., ' A combined shear - compression device to measure concrete - to -concrete bonding ', Experimental

techniques, 1991, Vol. 15 no. 5 pp. 50-55

Saxena, S. K., " Foundation mats and pavement slabs resting on an elastic foundation - analysed through a physical model ", Dorham, Duke University, Department of Civil Engineering, 1971, Doctoral Dissertation

Schiffman, R. L., " General Analysis of Stresses and Displacements in Layered Elastic Systems ", proc. Int. Conf. Struct. Design Asphalt Pavements, Ann Arbor, Mich., pp. 365-375, 1962

Seible, F., Latham, C., and Krishnan, K., 1988, " Structural concrete overlays in bridge deck rehabilitation - summary of experimental results, analytical studies and design recommendations ", Structural Systems Research Project, Report No. SSRP-88/04, University of California, San Diego, Calif.

Seible, F., and Latham, C. T., 1990, " Analysis and design models for structural concrete bridge deck overlays ", Journal of Structural Engineering, 1990, Vol. 116, No. 10, pp. 2711-2728

Sohrabi, M. R., " Investigation 1, Report on Thin Layered Cementitious Systems ", University of Newcastle Upon Tyne, Nov. , 1993.

Sohrabi, M. R., " Investigation 2, Report on Thin Layered Cementitious Systems ", University of Newcastle Upon Tyne, Jan. , 1994.

Sprinkel, M. M., " Polymer Concrete Bridge Overlays ", Transportation research record, 1993 No. 1392 pp. 107-116

Sprinkel, M. M., " Thin Polymer Concrete Overlays for Bridge Deck Protection ", Transportation Research Record 950, 1984, Vol. 1, pp 193-201

Sprinkel, M. M., " Thermal Compatibility of Thin Polymer Concrete Overlays ", Taken from TRANSPORTATION RESEARCH RECORD 899, titled 'Bridge Inspection and Rehabilitation', published by Transportation Research Board, National Academy of Science

Spyrakos, Constantine C., " Finite Element Modeling in Engineering Practice ", West Virginia University Press, USA, 1994.

Surat, M., " Thermal shock of screeds ", B. Eng. project, University of Newcastle Upon Tyne, January, 1990

T

Tielking, J.T., and Roberts, F.L., " Tire contact pressure and its effect on pavement strain ", J. of Transp. Engrg. ASCE, 1987, 113(1), 56-71

Tielking, J.T., " Pavement shear forces produced by truck tires ", Texas Transportation Institute, College station, TX 77843-3135, February 1991.

Timoshenko, S., " Theory of Elasticity ", McGraw - Hill Company, Inc. New York 1934

V

Van Dam, T.; Blackmon, E.; and Shahin, M. Y., " Effect of concrete overlay debonding on pavement performance ", Transportation Research Record, 1987, No. 1136, pp. 119-129

Van Gemert, D., Vanden Bosch, M., and Leuven, K.U., " Long - term performance of epoxy bonded steel - concrete joints ", Proceedings of an international symposium organised by RILEM Technical Committee 52 - Resin Adherence to Concrete and Laboratoive Central des Ponts et Chauss'ees, Paris, September 16-19, 1986

W

Wall, J.S., Shrive, N.G., and Gamble, B.R., " Testing of bond between fresh and hardened concrete ", Proceedings of an international symposium organised by RILEM Technical Committee 52 - Resin Adherence to Concrete and Laboratoive Central des Ponts et Chauss'ees, Paris, September 16-19, 1986

Westergaard, H. M., " Stresses in concrete pavements computed by theoretical analysis ", Bureau of Public Roads, Vol. 7, no. 2, April 1926

Wilson, E. L., " Structural analysis of axisymmetric solids ", American Institute of Aeronautics and Astronautics Journal, Vol. 3, 1965.

Wilson, E. L., " Solid SAP, a static analysis program for three dimensional solid structures ", Berkeley, Structure Engineering Laboratory, University of California, 1969. Report SESM 71-19.

X

Xian-Neng, L., " Study of the use of crack resistant polymer mortars as anticorrosion coating for outdoor concrete ", Proceedings of an international symposium organised by RILEM Technical Committee 52 - Resin Adherence to Concrete and Laboratoive Central des Ponts et Chauss'ees, Paris, September 16-19, 1986

Y

Yang, N. C., " Design of functional pavements ", 1972, McGraw-Hill Book Company

Yoder, E. J., " PRINCIPLES OF PAVEMENT DESIGN ", 1959, John Wiley & Sons, Inc.

Z

Zeid, Ibrahim; and Padovan, Joseph, " Finite element modelling of rolling contact ", Computers & Structures, Vol. 14, No. 1-2, pp. 162-170, 1981

Zienkiewicz et al., O. C., " Analysis of nonlinear problems with particular reference to jointed rock systems ", Proc. 2nd Intl. Conf. Society of Rock Mech., Belgrade, Vol. 3, 1970, pp. 501-509

Zollinger, D.G., Senadheera, S.P., and Tang, T., " Spalling of continuously reinforced concrete pavements ", J. of Transportation Engineering, American Society of Civil Engineering, Vol. 120, No. 3, May/Jun. 1994

APPENDIX

The behaviour of a thin layered cementitious system under the condition of impact shock

THE BEHAVIOUR OF A THIN LAYERED CEMENTITIOUS SYSTEM UNDER THE CONDITION OF IMPACT SHOCK

M. R. Sohrabi, PhD student, June 1994, University of Newcastle Upon Tyne

INTRODUCTION

Impact shock is the effect of falling a heavy object or tool on the screed, which might result in a delamination at the interface. This phenomenon may happen as a result of roughly handled crane operation, as well. [P1]

"Because of the random nature of these kind of events, they are difficult to quantify, and most reports of screeds failing in this way are somewhat hearsay. However, laboratory simulation is a real possibility under impact shock." [P1]

Accepting the random nature of the impact shock, it is intended, in this investigation, to look further at this event as a structural dynamic problem.

In spite of its apparent simplicity of form, the event of an object falling on a screed and the subsequent interaction between them is very complex. Basically, these kind of events might be divided into two groups. The first is the falling of an object from a height of about zero, which may produce a rectangular impulsive load. The second is the falling an object from a height of more than zero. In this paper the latter case has been studied. To achieve a more realistic conclusion, it has been tried to review the two previous experimental investigations into impact shock from a theoretical point of view. Although in this study the elastic behaviour has been assumed for the constitutive materials, it could give the engineer a good understanding of the behaviour of thin layered systems in this field. [S1]

Response to a rectangular impulsive load in a single degree of freedom system

In an impulsive load, damping has very little importance in controlling the maximum response of the system. [C1] In an impulsive load, the maximum response may happen in a very short time, before the damping forces can absorb a considerable amount of energy of the system. For this reason, it will be reasonable to ignore the effect of damping forces in analysing an impact shock problem.

Impact shock may result in an impulsive load which might have, in the least case a rectangular distribution in terms of time. (fig 1)

For a single degree of freedom system (fig 2), the differential equation of motion becomes:

$$m\ddot{v}+c\dot{v}+kv=p_{(t)} \qquad (1)$$

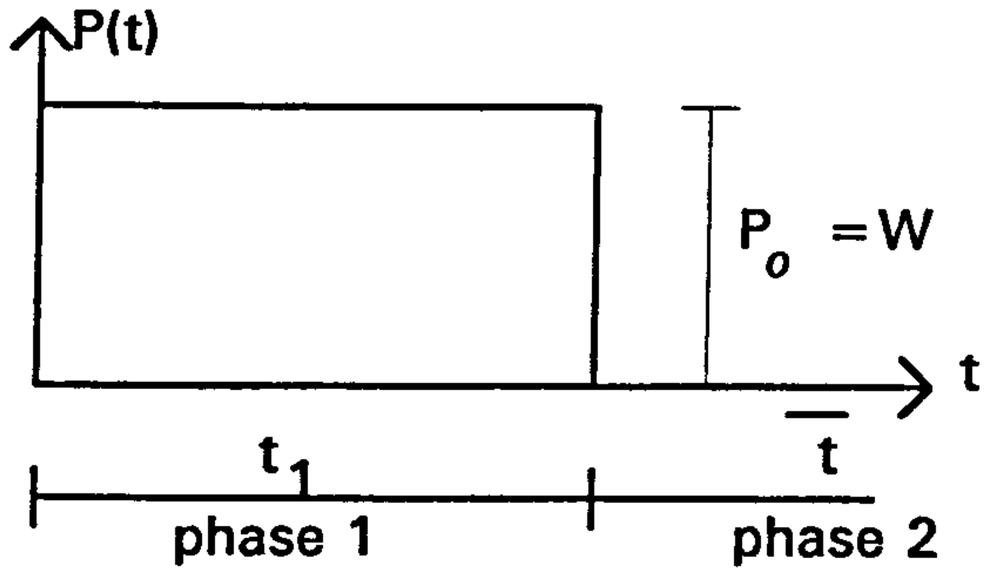

Figure 1 : Rectangular load-time distribution in an impact shock (the least case)

Where m = the mass of the system

$\ddot{v}$ = the acceleration of the mass

c = the damping constant of the system

$\dot{v}$ = the velocity of the system

k = the stiffness of the spring

v = the displacement

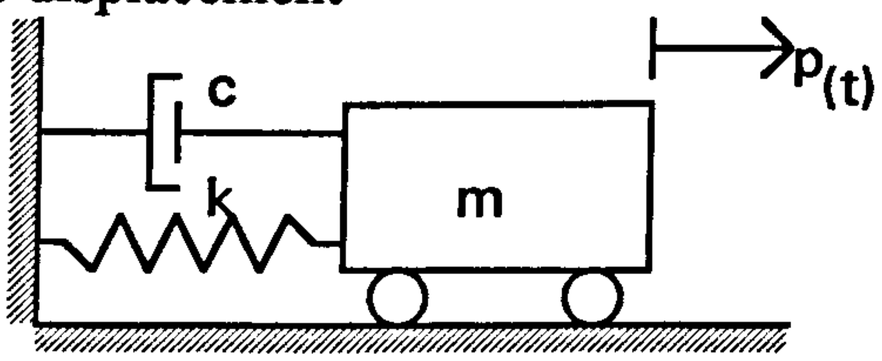

Figure 2 : A S-D-O-F system with damping

Ignoring the damping effect, we have: (fig 3)

$$m\ddot{v}+kv=p_{(t)} \qquad (2)$$

The response of the system can be divided into two phases, like that shown in figure 1.

Phase 1 : The loading phase $0 \le t \le t_1$

The particular solution for this kind of loading is simply the static deflection:

$$v_p = \frac{p_o}{k} \qquad (3)$$

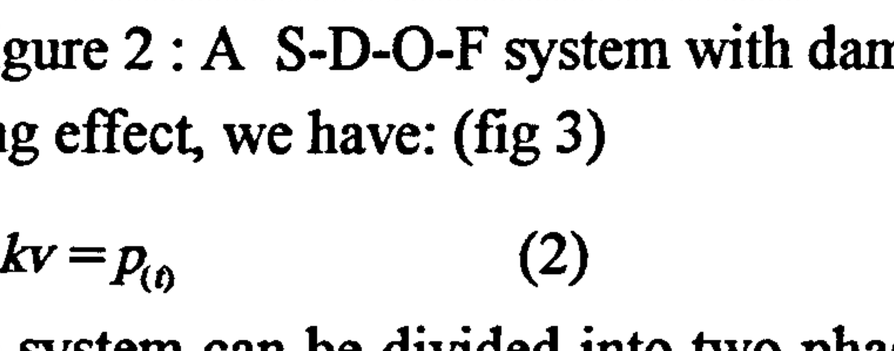

Figure 3 : A S-D-O-F system without damping

The total displacement v is expressed as the sum of the static displacement (particular solution), and the displacement due to a free vibration. In a free vibration without damping, we have:

$$m\ddot{v}_{(t)} + kv_{(t)} = 0 \qquad (4)$$

The solution of the above equation is of the form:

$$v_{(t)} = Ge^{st} \qquad (5)$$

Substituting this into equation (4) leads to:

$$(ms^2 + k)Ge^{st} = 0 \qquad (4)$$

After dividing equation (4) by mGe^{st} and introducing the notation:

$$\omega^2 = \frac{k}{m} \qquad (6)$$

We have:

$$s^2 + \omega^2 = 0 \qquad (7)$$

Or: $$s = \pm i\omega \qquad (8)$$

Hence the displacement due to a free vibration becomes:

$$v_{(t)} = G_1 e^{i\omega t} + G_2 e^{-i\omega t} \qquad (9)$$

Equation (9) can be put in a more convenient form, by using the Euler's equations:

$$e^{\pm i\omega t} = \cos\ \omega t \pm i \sin\ \omega t \qquad (10)$$

So, equation (9) may be written in a simpler form:

$$v_{(t)} = A \sin\ \omega t + B \cos\ \omega t \qquad (11)$$

Where A & B = coefficients which depend on the initial conditions

ω = the natural frequency of the system

The total displacement will be the sum of the values for the static and the free vibration solution:

$$v_{(t)} = A \sin\ \omega t + B \cos\ \omega t + \frac{p_o}{k} \qquad (12)$$

Assuming $v_{(0)} = 0$ and $\dot{v}_{(0)} = 0$, we have:

$$t = 0 \quad v_{(0)} = 0 \quad B + \frac{p_o}{k} = 0 \quad \Rightarrow \quad B = -\frac{p_o}{k}$$

$$t = 0 \quad \dot{v}_{(0)} = 0 \quad \Rightarrow \quad A = 0$$

So: $$v_{(t)} = \frac{p_o}{k}(1 - \cos\ \omega t) \qquad 0 \le t \le t_1 \qquad (13)$$

In which $\omega = \frac{2\pi}{T}$ and T is called the period.

It is seen that under the condition of $t_1 \ge \frac{T}{2}$, $v_{max} = \frac{2p_o}{k}$ and consequently the

dynamic magnification factor, D, will be equal to 2.

$$D = \frac{V_{max}}{P_o/k} \qquad t_1 \geq \frac{T}{2} \qquad (14)$$

Phase 2 : The free vibration phase $\bar{t} = t - t_1 \geq 0$

The response of the system in the free vibration phase can be again obtained from equation (11):

$$v_{(\bar{t})} = A \sin \omega \bar{t} + B \cos \omega \bar{t} \qquad (11)$$

Because of the initial conditions, $v_{(\bar{t}=0)} = v_{(t_1)}$ and $\dot{V}_{(\bar{t}=0)} = \dot{v}_{(t_1)}$, we have:

$$v_{(\bar{t}=0)} = v_{(t_1)} \qquad \Rightarrow \qquad B = v_{(t_1)}$$

$$\dot{V}_{(\bar{t}=0)} = \dot{v}_{(t_1)} \qquad \Rightarrow \qquad A = \frac{\dot{v}_{(t_1)}}{\omega}$$

Hence, equation (11) becomes:

$$v_{(\bar{t})} = \frac{\dot{V}_{(t_1)}}{\omega} \sin \omega \bar{t} + v_{(t_1)} \cos \omega \bar{t} \qquad \bar{t} = t - t_1 \geq 0 \quad (15)$$

The maximum response in this phase can be obtained from equation (15):

$$v_{max} = \sqrt{(\frac{\dot{V}_{(t_1)}}{\omega})^2 + (v_{(t_1)})^2} \qquad (16)$$

Substituting $\dot{v}_{(t_1)} = \frac{P_o \omega}{k} \sin \omega t_1$ and $v_{(t_1)} = \frac{P_o}{k}(1 - \cos \omega t_1)$, calculated from equation (13), into equation (16), we have:

$$v_{max} = \frac{P_o}{k}[\sin^2 \omega t_1 + (1 - 2 \cos \omega t_1 + \cos^2 \omega t_1)]^{1/2}$$

$$v_{max} = \frac{P_o}{k}[2(1 - \cos \omega t_1)]^{1/2}$$

Or:

$$v_{max} = \frac{P_o}{k}[2(1 - \cos \frac{2\pi}{T} t_1)]^{1/2}$$

$$v_{max} = \frac{P_o}{k}[2 \sin \frac{\pi}{T} t_1] \qquad (16)$$

So: $$D = \frac{V_{max}}{p_\circ / k} = 2 \sin \frac{\pi}{T} t_1 \qquad t_1 \leq \frac{T}{2} \qquad (17)$$

Hence, if $t_1 < T/2$, the maximum response will occur in phase 2, the free vibration phase. In this case the dynamic magnification factor D will be calculated from equation (17).

Considering the above procedure, one can draw the response spectra for each kind of impulsive loading, in which the maximum response of the system may be plotted against the impulsive length ratio, $\frac{t_1}{T}$. (fig 4) [C1]

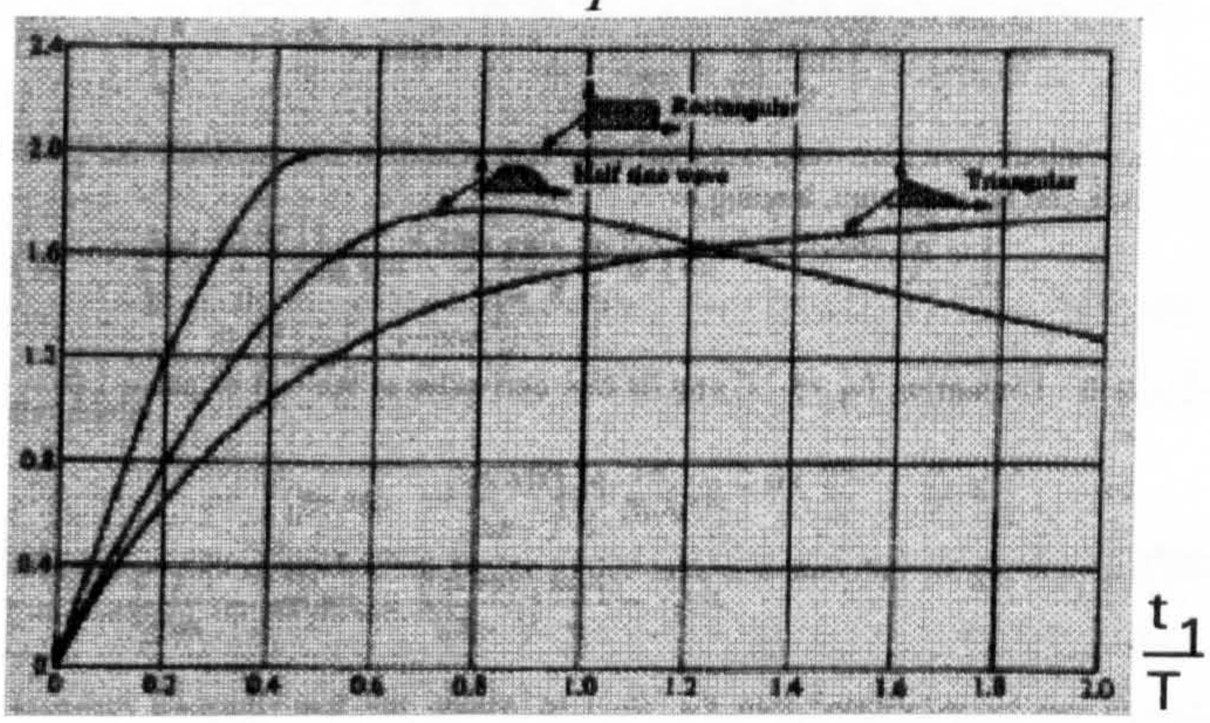

Figure 4 : Response spectra for three types of impulsive loads

Response to an impulsive load in a multi degree of freedom system

There are various methods for analysing a multi degree of freedom system. In this section it is intended to explain the Newmark method to represent the concept of dynamic solutions to a multi degree of freedom system. It should be added that the Newmark β method will be used for analysing the model in this investigation. First of all it should be noted that the analysing of a multi degree of freedom system is generally based on the discretization of the structure. Three methods of dicretization are generally used in the structural dynamics: [C1]

Lumped-mass procedure, the finite element concept and the generalized displacement method. The finite element method has been used in the current investigation.

In the finite element method, the displacements of any given structure are expressed in terms of a finite number of discrete displacement coordinates. In fact, this approach combines important features of both the lumped - mass and

the generalized coordinate procedures. The basis of this method is the finite element method of analysis of structural continua and provides a convenient and reliable idealization of the system. As in any normal finite element problem, the first step is to divide the structure into an appropriate number of elements. The displacements of the nodal points of these elements then will be the generalized coordinates of the structure. [C1] Now the stiffness matrix of the whole structure could be defined in the same way as that for any usual finite element problem.

The Newmark β method

The Newmark β method is a direct integration solution to the general equation of motion: (Here again for an undamped system)

$$m\ddot{v}+kv=p_{(t)} \qquad (2)$$

In this method the equations in (2) are integrated by using a numerical step-by-step procedure. This direct numerical integration method is based on two concepts:

The first is that instead of trying to satisfy equation (2) at any time t, it is intended to satisfy that at discrete time intervals Δt apart. The second concept is that a variation of displacements, velocities and accelerations within each time interval Δt is assumed. [C2, B1, B2]

In brief, the Newmark β method is based on the following assumptions:

$$\dot{v}_{t+\Delta t}=\dot{v}_t+[(1-\delta)\ddot{v}_t+\delta\ddot{v}_{t+\Delta t}]\Delta t \qquad (18)$$

$$v_{t+\Delta t}=v_t+\dot{v}_t\Delta t+[(\frac{1}{2}-\beta)\ddot{v}_t+\beta\ddot{v}_{t+\Delta t}]\Delta t^2 \qquad (19)$$

Where β and δ are parameters which are determined to obtain integration accuracy and stability. Newmark proposed $\delta=\frac{1}{2}$ and $\beta=\frac{1}{4}$, which are related to an unconditionally stable scheme based on the constant-average-acceleration method. (figure 5)

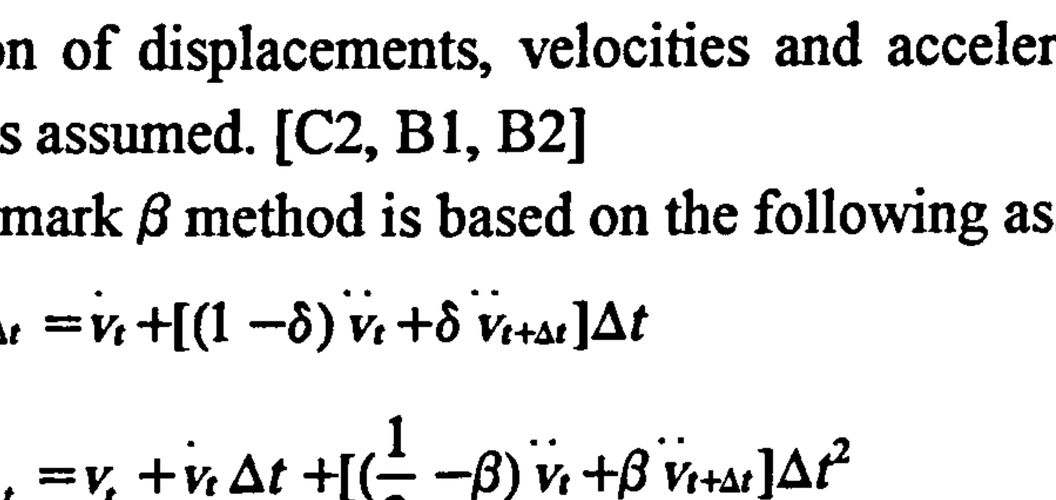

Figure 5 : Newmark's constant-average-acceleration proposal

In addition to the above assumptions, the equilibrium equations (2) at time $t+\Delta t$ are also considered:

$$m\ddot{v}_{t+\Delta t}+kv_{t+\Delta t}=p_{t+\Delta t} \qquad (20)$$

Solving equations (18) and (19), simultaneously, we can obtain equations for $\ddot{v}_{t+\Delta t}$ and $\dot{v}_{t+\Delta t}$, each in terms of the displacements $v_{t+\Delta t}$, which are unknown. Substituting these two equations for $\dot{v}_{t+\Delta t}$ and $\ddot{v}_{t+\Delta t}$ into equation (20), one can obtain $v_{t+\Delta t}$. Then from equations (18) and (19), $\ddot{v}_{t+\Delta t}$ and $\dot{v}_{t+\Delta t}$ can also be calculated. [B1, B2]

The complete algorithm using the Newmark scheme is shown as follows:

Step-by-step solution using the Newmark integration method

Section A : Initial calculations:

1- Forming stiffness matrix k and mass matrix m.

2- Calculating the initial values, v_0, $\dot{v}_0$, and $\ddot{v}_0$.

3- Selecting time step size Δt, parameters α and δ, and calculating integration constants as follows:

$\delta \geq 0.5$ and $\beta \geq 0.22(0.5+\delta)^2$

$$a_0=\frac{1}{\beta\,\Delta t^2},\quad a_2=\frac{1}{\beta\,\Delta t},\quad a_3=\frac{1}{2\beta}-1,\quad a_6=\Delta t(1-\delta)$$

$$a_7=\delta\,\Delta t$$

4- Forming effective stiffness matrix $\hat{k}$: $\hat{k}=k+a_0 m$

5- Triangularizing $\hat{k}$: $\hat{k}=LDL^T$

Section B : Calculating for each time step:

1- Calculating effective loads at time $t+\Delta t$:

$$\hat{p}_{t+\Delta t}=p_{t+\Delta t}+m(a_0 v_t+a_2\dot{v}_t+a_3\ddot{v}_t)$$

2- Solving for displacements at time $t+\Delta t$

$$LDL^T v_{t+\Delta t}=\hat{p}_{t+\Delta t}$$

3- Calculating accelerations and velocities at time $t+\Delta t$

$$\ddot{v}_{t+\Delta t}=a_0(v_{t+\Delta t}-v_t)-a_2\dot{v}_t-a_3\ddot{v}_t$$

$$\dot{v}_{t+\Delta t}=\dot{v}_t+a_6\ddot{v}_t+a_7\ddot{v}_{t+\Delta t}$$

A review of the two previous investigations into the impact shock

In this section, it is intended to review the two previous experimental works on the event of impact shock, which have been carried out by Mwape and Floros. [M1, F1]

First of all, it should be mentioned that the aim of this review is to define the appropriate theoretical models of these works and then, to evaluate the results on this basis. Hence, this review will not affect the validity of the above investigations as two scientific works.

Since both of the two investigators have used the BRE screed tester for their works, [R1] it is necessary to describe this instrument, briefly.

This tester consists of a tubular shaft along which, a 4 kg annular weight moves vertically. (fig 6) At the top of the instrument, there is a bull's-eye bubble, a handle, a trigger as well as a locking catch. At the bottom of the shaft, a case-hardened steel foot transmits the impact from its upper collar to a 500 mm^2 circular area of the surface of the specimen. [R1]

The recommended height of free-falling of the weight is 1m.

It must be added that, both Mwape and Floros, reported having used a 10 N weight from a height of 30 cm, in their tests, but it is thought that they may have actually used the 40 N weight. [M1, F1]

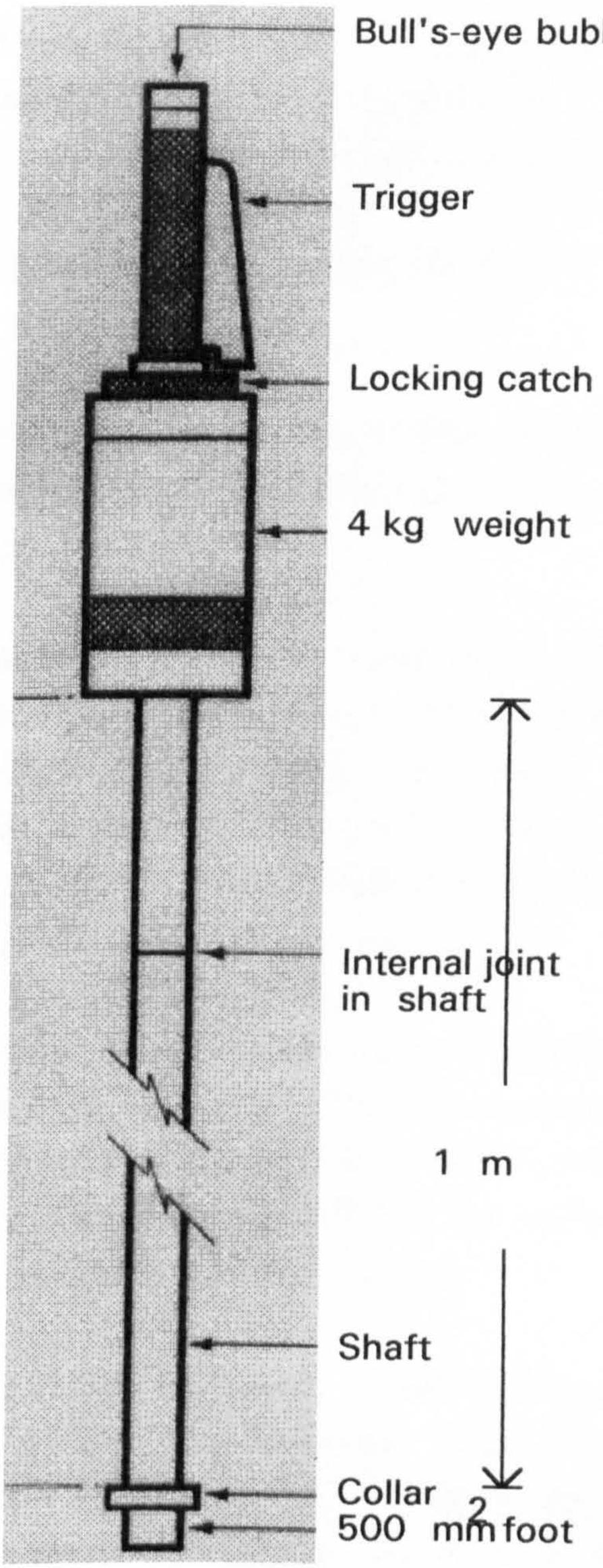

Figure 6 : The BRE screed tester

Mwape's work on the impact shock, in brief

Material tested:

The materials were polymer modified, cementitious concrete or epoxy resins.

All the materials tested were given code names. [M1]

Testing procedure:

The specimens consisted of a piece of concrete substrate on which the various materials mentioned above, were cast 5 mm thick in section. Each specimen was cast twice, one in the primed state and the other in the unprimed state.

The dimensions of some specimens were about 180 mm by 180 mm, and the rest were about 190 mm by 300 mm.

The samples were prepared properly and then were been curing for 12 days in accordance with BS. 1881. [M1]

Coring:

Before testing, all the specimens were cored by a radial arm drilling machine, using a water swivel and a 20 mm diamond tripped corer. The cores were cut for each specimens 5 mm in to the concrete substrate.

Impact experiment:

In this experiment the BRE tester was used to carry out the impact shock. The height of the travelling mass was reduced to 30 cm , because the specimens were cracking under the condition of an impact from the height of 1m. [M1]

To reduce the probability of breaking the specimens, a sand bed was used to put them in. At last the desired number of blows were imparted to the three cores prepared for the test, respectively. [M1]

Tensile pull-off test:

After the impact loading, the direct tensile strength of the 20 mm diameter cores was measured by using the elcometer pull-off tester. This test is carried out by measuring the force is to be applied to pull-off the dolly which is stuck on the surface of, for example, the cores. Before the pull-off test, the surface preparation and sticking the dollies to the cores were properly done.

Results:

In these tests, there was a relatively great scatter of results. Some specimens showed nil results, while some showed failures in the substrate. There were also some specimens which failed at the interface or in the upper layer. However the number of failures at the substrates were more than those in the mortars. [M1]

Floros' work on the impact shock, in brief

Materials tested:

The materials were small grading concrete (as the control mortar), P.C.C. and P.C. [F1]

Testing procedure:

Similar to the previous work, reinforced concrete blocks were used as the concrete substrate. The dimensions of these blocks were 230 mm long, 130 mm wide and 180 mm deep. The method of the tests were like those in the Mwape's work, except for the preparation of the places to where, the blows were to be imparted.

After forming a screed of 5 mm thick on top of the concrete blocks, plastic rings were sprayed with a debonding agent and then, pushed in the fresh mortar, at the located points. The internal diameter of each ring was 20 mm and the thickness was 0.5 mm. [F1]

Testing of samples:

When the curing process was completed, the samples were placed in a container with sand then subjected to the impact load. Like the Mwape's investigation, these tests were also carried out by using the BRE screed tester. "Each ring was subjected to different numbers of blows." [F1] After the impact loading, the direct tensile strength of the 20 mm diameter cores was measured by using the elcometer pull-off tester. The procedure was the same as that for the Mwape's work.

Results:

During the pull-off test, most of the samples failed at the mortar and few at the concrete substrate. [F1]

A theoretical discussion on the two previous investigations

At this stage, it will be tried to explain the behaviour of the systems used in the above experimental works.

In this investigation, the distribution of σ_{1max} stress along the interface of the two layered system, under the loading contact area will be plotted, at two critical times. Then the mechanism of the failures will be explained.

Assumptions and approximations

- Elastic behaviour is assumed for the materials used in this investigation. Because of the special conditions which have been considered in the Mwape's and Floros' works, it could be assumed that the behaviour of their structures have been elastic.

- Using three-dimensional elements in the finite element method. In this investigation eight node brick elements have been used.

-The finite element method assumes a solid connection between the two different layers through the nodes which are considered at the interface. [W1]

This assumption is consistent with the stress strain curve of the bond strength, which should be considered as having a relatively non ductile behaviour.

In this investigation the tensile stresses will be assumed positive, and the compression stresses will be represented in a negative form.

-Material properties:

Layer	Material	Thickness (mm)	Young's modulus (pa)	Poisson's ratio	Density (kg/m^3)
Lower layer	Concrete	35	30E9	0.2	2400
Upper layer	Pc or Pcc	5	20E9	0.2	2400

- It is also presumed that the critical lower limit of tensile stress for normal concrete is about 1E6 (pa) and for Pc or Pcc is about 4E6 (pa).

- For the purposes of convenience and some other considerations, instead of the real specimens, the idealised models showed in figures 10 and 11 have been analysed.

- Because of a large number of nodes, a large number of equations are to be solved simultaneously, however each node is mostly common between at least two elements, consequently we observe some differences among the results for each value of stress at the same node. Hence, in this investigation the average values for each layer (horizontally) have been used.

- Pafec software uses a limited number of dynamic degrees of freedom (masters) for calculating the natural frequencies. The program can automatically choose the best degrees of freedom for the purpose of this idealization. [H1] In this investigation, 78 dynamic degrees of freedom have been used, among which, 60 have been chosen by the program.

- In this investigation the effect of damping forces has been ignored. However, as mentioned before, this assumption is not far from reality.

- For the purpose of minimising the computing time, the dynamic response solution has been used only for the loading phase. However, this assumption

will not influence the conclusion of this investigation, mainly because of the fact that in all cases, the structures have been very stiff. Consequently the maximum responses have occurred during the loading phase.

- Determination of the behaviour regime in the impact situation:

There are many important factors which should be taken into account for a good prediction of the behaviour regime in an impact phenomenon. Some of these factors are: the relative speed of the impact, the physical properties of both the targets and the projectiles, Young's modulus, strain hardening or softening behaviour at different rates of strain, density and the degree of compressibility of the volumes of the materials, specific heat and conductivity and at last, the shape of the projectiles and other geometrical specifications. [J1]

"Many attempts have been made to categorise impact behaviour and non are wholly successful." [J1] However a simple method for predicting the behaviour regime of metals in impact events is to determine the non-dimensional factor, $\rho v^2 / \bar{Y}$. Where v is the relative speed at normal impact, ρ is the density and $\bar{Y}$ is the flow stress. This factor is to be calculated for both the projectile and target and then the maximum of these values will be considered. The following table shows the values of this factor for two kind of regimes. [J1]

Table 1 : The limit values of $\rho v^2 / \bar{Y}$, for two kind of regimes: (Both materials, target and projectile, have been assumed mild steel)

ft/sec	$\rho v^2 / \bar{Y}$	Regime
2.5	10^{-5}	quasi-static elastic
25	10^{-3}	plastic behaviour starts

In our case, we should firstly calculate the value of $\rho v^2 / \bar{Y}$ for P.C. or P.C.C. and then, compare with the limits. Although we have not a flow stress for the cementitious materials, we could assume the ultimate compression stress as a relatively good approximation for evaluating the behaviour regime of the impact experiments. Hence, we have:

$$\rho = 2400\ {}^{kg}/_{m^3} \quad , \quad \text{If} \quad g \approx 10\ {}^{m}/_{sec^2}$$

$$v^2 = 2gh \quad \Rightarrow \quad v^2 = 2 \times 10 \times .3 = 6\ {}^{m^2}/_{sec^2}$$

Assuming $\bar{Y} = 500\ {}^{kg}/_{cm^2} = 5 \times 10^7\ {}^{N}/_{m^2}$, we have:

$${}^{\rho v^2}/_{\bar{Y}} = 2.88 \times 10^{-4}$$

Hence, according to the limits of table 1, the above value indicates that the behaviour regime should be located between the elastic phase and plastic phase. However because of using a layer of sand bed during the tests, we could assume an elastic behaviour for our calculations.

- Since there is a big difference between the tensile and the compression strength of the materials, after occurring a tensile failure at each node, a new redistribution of the stresses will take place within the whole volume of the structure. So, the results of this investigation are based on an ideal behaviour of the materials. In other words, these results could predict the nodes at which, the first cracks may appear. The rest should be the task of the engineer to use his engineering judgement for explaining the behaviour of the structure, as it is.

- Dimensions:

1- Floros' work:

Model 1 : 260 mm by 260 mm by 40 mm like model 1, but a groove with a depth of 5 mm and a width of 10 mm, all around the contact area, is in existence. (fig 10)

2- Mwape' work:

Model 2 : 260 mm by 260 mm by 40 mm like model 1, but a groove with a depth of 10 mm and a width of 10 mm, all around the contact area, is in existence. (fig 11)

- Restraints:

1- Restrain conditions 1 : All nodes along the bottom of the model are restrained in the vertical direction. (Y direction)

- Load cases:

1- Floros' work:

For this case, it will be assumed that 30% of the vertical impact load acts directly on the surface of the lower layer, along the perimeter of the load contact area. This assumption is quite reasonable. Firstly, because of the fact that the circular area of the bottom of the BRE screed tester has been larger than the area surrounded by the plastic ring, and secondly because Floros has sprayed the rings with a debonding agent and then pushed in the fresh mortar.

(The external diameter of the bottom of the BRE screed tester is nearly 25.23 mm, whereas the external diameter of the plastic rings has been 20.5 mm.) [F1, R1]

2- Mwape's work:

Although the behaviour of the Mwape's model has been very complicated, mostly because of the action of coring the specimens, ideally it will be assumed that the whole of the impact load acts uniformly on the contact area. (like the vertical static load)

- Dynamic load - time distribution:

Considering an elastic behaviour for the impact test and using approximate equations for the energy loss, we may estimate the amount of strain energy due to the impact event. The energy loss due to dropping a sphere on a massive plane plate of the same material from a height of h can be obtained from the following equation: [G1]

$$\Delta T = mg(h - h^*) \qquad (21)$$

And:

$$e^2 = h^*/h \qquad (22)$$

Where ΔT is the energy loss, m is the mass of the weight, h is the initial height and h^* is the rebound height. Factor e is called the coefficient of restitution and is determined from the results of experimental tests, by dropping a particular mass on a massive plate from a height of h and observing the rebound height, h^*. [G1] Hence it could be presumed that the amount of energy which may cause the structure to deform, in the elastic phase, is $m_1 g h^*$. Using an appropriate experimental curve like that is shown in figure (7), one can estimate the coefficient of restitution for a particular situation. In this investigation an average value is assumed for e:

$$e \approx 0.2 \qquad (23)$$

So, the elastic strain energy becomes:

$$E_{strain} = e^2 mgh \qquad (24)$$

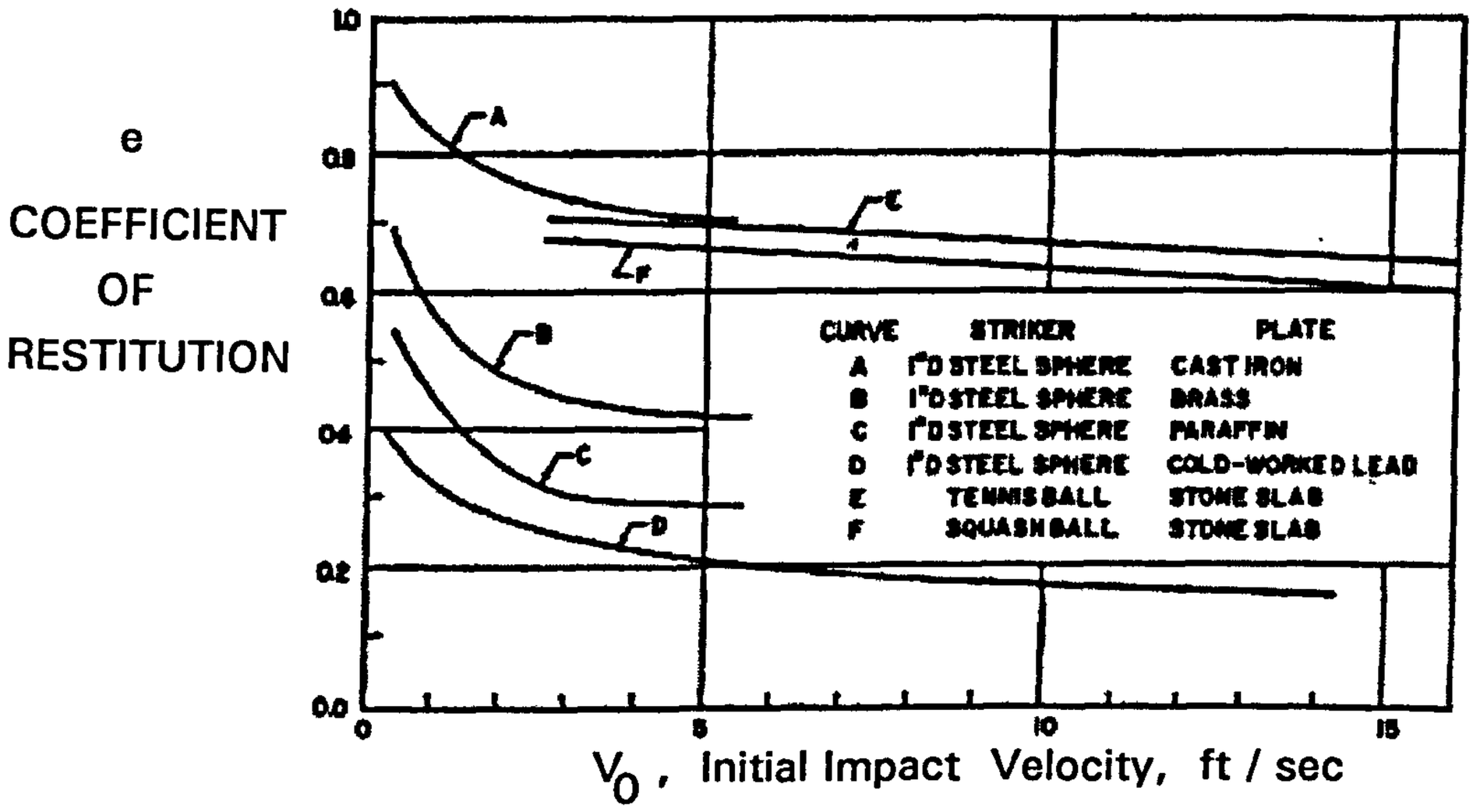

Figure 7 : Coefficient of Restitution for the Impact of spheres on Thick Plates [G1]

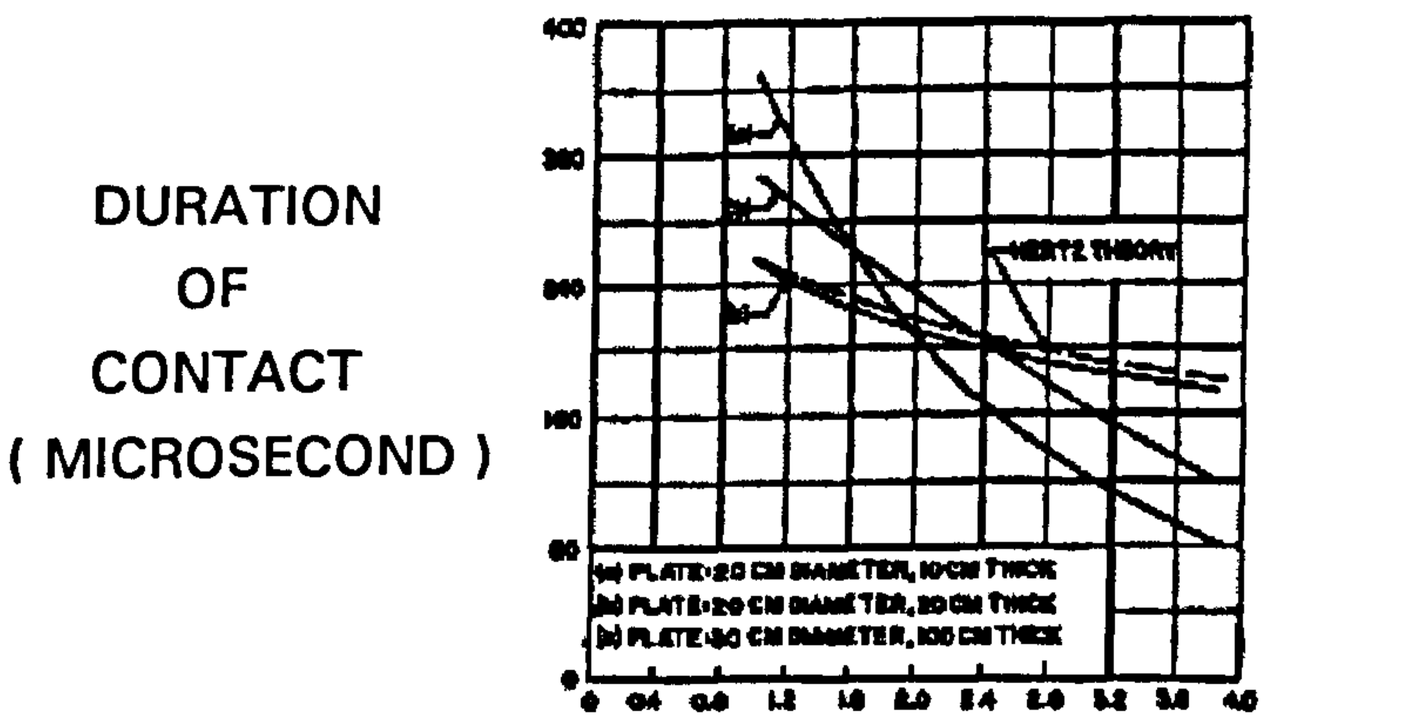

Figure 8 : Duration of contact for the Impact of steel spheres against Plates of various thickness [G1]

$$E_{strain} = 0.04 \times 4 \times 30 = 4.8 \text{ kg - cm}$$

If we assume a maximum elastic displacement of about 0.2E10-4 m, from an initial static solution, at the nodes which are along the contact area, we have:

$$\sigma_{bearing\ static} \times (5 \times 2) \times 0.2 \times 10^{-4} \times 10^{2} = 4.8\,(25)$$

$$\sigma_{bearing\ static} = 240\ {}^{kg}/_{cm^2} = 24 \times 10^{6}\ \text{pa}$$

Where $\sigma_{bearing\ static}$ is the maximum elastic bearing stress over the contact area during the impact shock, in a static solution. Considering an approximate value for the dynamic magnification factor equal to 2, and at the same time to make a quite conservative estimation, it is assumed that:

$$\sigma_{bearing\ dynamic} \approx 80\ {}^{kg}/_{cm^2} \qquad (26)$$

Where $\sigma_{bearing\ dynamic}$ is the bearing stress over the contact area during the impact shock, at time t=0.

So: $$P_0(t) = 80 \times (5 \times 2) \times 10 = 8000\ N \qquad (27)$$

Hence the dynamic load-time distribution becomes: (fig 9)

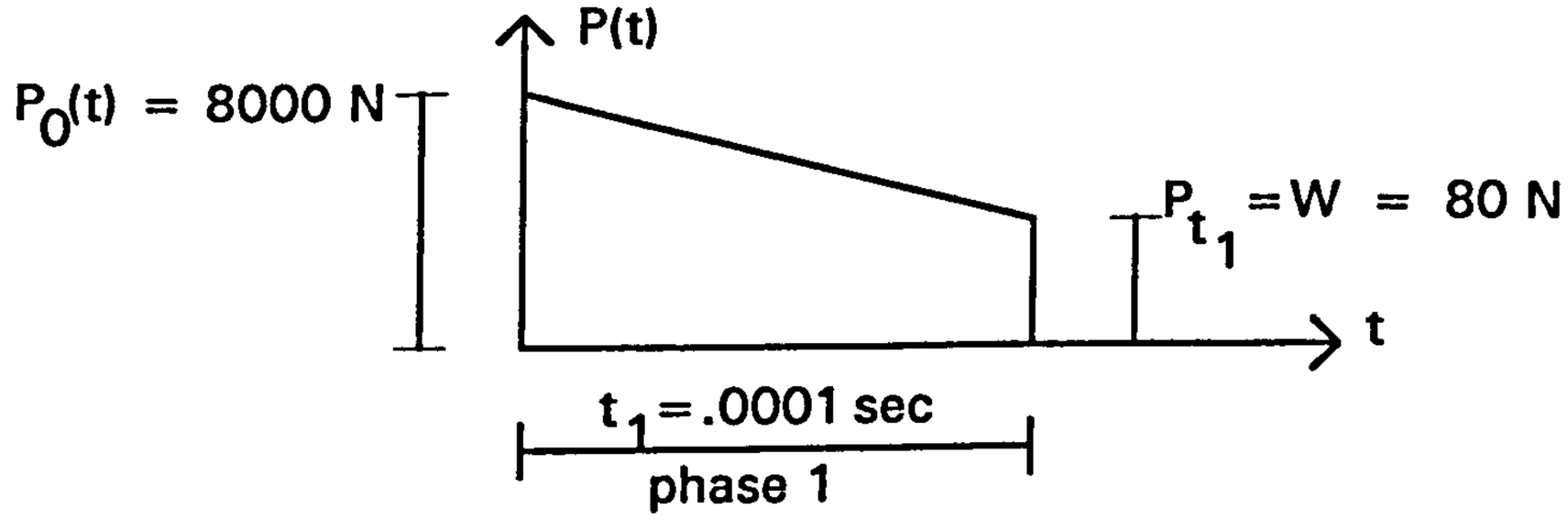

Figure 9 : The linear impulsive load proposed for the Mwape's and Floros' works

Where the value of t_1, the impact duration, has been taken from figure 8. [G1]

Dynamic response solution:

The Newmark beta method has been used for the response solution. [H1] As mentioned before, the effect of damping forces has been ignored. Other assumptions related to this solution are as follows:

Time step = 0.000001 second Beta (β) = 0.25

Finish time = 0.0001 second Output type = Displacement to be output

For the purpose of minimising the computing time, results have been only requested at the following degrees of freedom:

MODEL	Node Number	Direction	Co-ordinate		
			X (mm)	Y (mm)	Z (mm)
1	1158	Y	135	40	130
2	1620	Y	135	40	130

The importance of nodes 1158 and 1620 is that, they are located in the middle of the load contact area and consequently are directly subjected to the load. So, their displacements can be evaluated as the samples of largest displacements due to the dynamic load, at each time.
The results of the Newmark β solution for nodes 1158 and 1620, are shown in the next charts.

Explanation of the Floros' work

In the Floros' work, we saw that during the pull-off test, most of the samples failed at the mortar and few at the substrate. [F1]
Charts 1, 3, 4, model 1, could explain the failure mechanism of the Floros' specimens, clearly.
Using the plastic rings, Floros has imparted the blows to the surface of the lower layer, directly. As it is seen in chart 3, at time t=.000015 sec., the value of σ_{1max} for most of the nodes in the upper layer, at the interface, is more than 160 $^{kg}/_{cm^2}$, whereas the value of that for the same nodes in the lower layer is less than 21 $^{kg}/_{cm^2}$. Consequently, most of the specimens must fail at the mortar. On the other hand, chart 4, at time t=.000097 sec., shows that most of the nodes in the lower layer, at the interface, are in danger. However, because of the fact that most of the failures occurred before, at time t=.000015 sec., at the nodes in the upper layer, only few samples may fail at the substrate, during the pull-off test.

Explanation of the Mwape's work

In the Mwape's work, all the specimens were cored by a radial drilling machine, before testing. [M1]
In these test, there was a relatively great scatter of results. Some specimens showed nil results, while some showed failures in the substrate. There were also some specimens which failed at the interface or in the upper layer. However the number of failures occurred at the substrate were more than those

occurred at the mortar. [M1]

In Model 2 of this investigation, the effects of drilling action, on the two layered system, have not been taken into account. Hence it could explain the Mwape's work in an ideal situation, without the drilling effects.

As it is seen in chart 5, at time t=.000015 sec., there is not any problem with the system.

Considering the displacement history of node 1620, chart 2, we can find another critical time, t=.000086 sec., for this system. Chart 6 indicates that at this stage, most of the nodes in the lower layer, at the interface, should fail. This means that, in the condition of lacking the drilling effects, Mwape should have been faced with only few or no failures in the mortar. In other words, for the well primed and high strength mortars, the probability of failures occurring in the upper layer should be very low.

Hence, the main reason for the existence of such a great scatter of results, in the Mwape's work, should has been that he has cored the specimens with the drilling machine. What might have happened during the drilling process? It seems that while the drilling action is in progress, three kinds of forces may be produced; torsional forces, vertical compression forces and vibrational forces.

The torsional forces may induce tensile and compression stresses which would not affect the results, considerably. However the effect of the vertical forces due to the drilling may not be neglected. Since Mwape has cut the cores 5 mm in to the concrete substrate, he has subjected the surface of the substrate to the vertical forces, caused by the drilling action. At this stage the behaviour of the specimens might has been similar to the Floros' ones, chart 3, but with less intensity of stress, at each node. Perhaps, for this reason he has observed some failures in the upper layer.

The third factor is the effect of vibrations due to the drilling action which may, at least, weaken the cores.

Further discussion and conclusions

- According to the previous explanations, the results of the Mwape's and Floros' work represent the behaviour of a thin layered system under the condition of impact shock, in two particular ways.

- Isolating the cores, both of the two investigators have studied the effect of an impact load, right under the contact area. However the distribution of σ_{1max} along the interface of Model 2, the Mwape's work in an ideal situation, seems

to be more realistic than the Floros' work.

- Considering the results of the Floros' work or the distribution of σ_{1max} along the interface of Model 1, one could infer that the effect of subjecting the surface of the substrate to an impact force is very serious. Moreover the results of this investigation show that, in this condition the directions of σ_{1max} stresses, at the critical nodes, are very close to the vertical direction, which means that the directions of the subsequent probable cracks will be parallel to the interface. At last, the results of such a loading, may cause the screed to delaminate. For this reason, It may be concluded that in a real case of a thin layered system, any kind of defect occurring in the upper layer must be repaired, immediately.

- In an impact shock, both of the intensity and the sign of the stresses, within the structure, are changing during the loading and free vibration phases. In this investigation, the stress analysing has been done for two critical times, in accordance with the displacement history of an important node of the structure. The results of stress analysing at the second time, indicate that because of the σ_{1max} stress directions, the probable cracks at the interface will occur close to the horizontal direction, which again may result in a delamination at the interface.

- As the kinematic energy of a heavy object due to falling on the screed is generally very high, the screeds consist of materials with having more ductile behaviour and good tensile strength will show a better performance in absorbing the initial energy and protecting the system against the impact effects.

- In the places, on which some temporary rough operations are to be expected, the use of spreading or laying any appropriate kind of soft materials on the screed may be recommended. Such a temporary layer of soft materials can absorb a considerable amount of the initial kinematic energy and consequently protect the thin layered system against the subsequent impact effects.

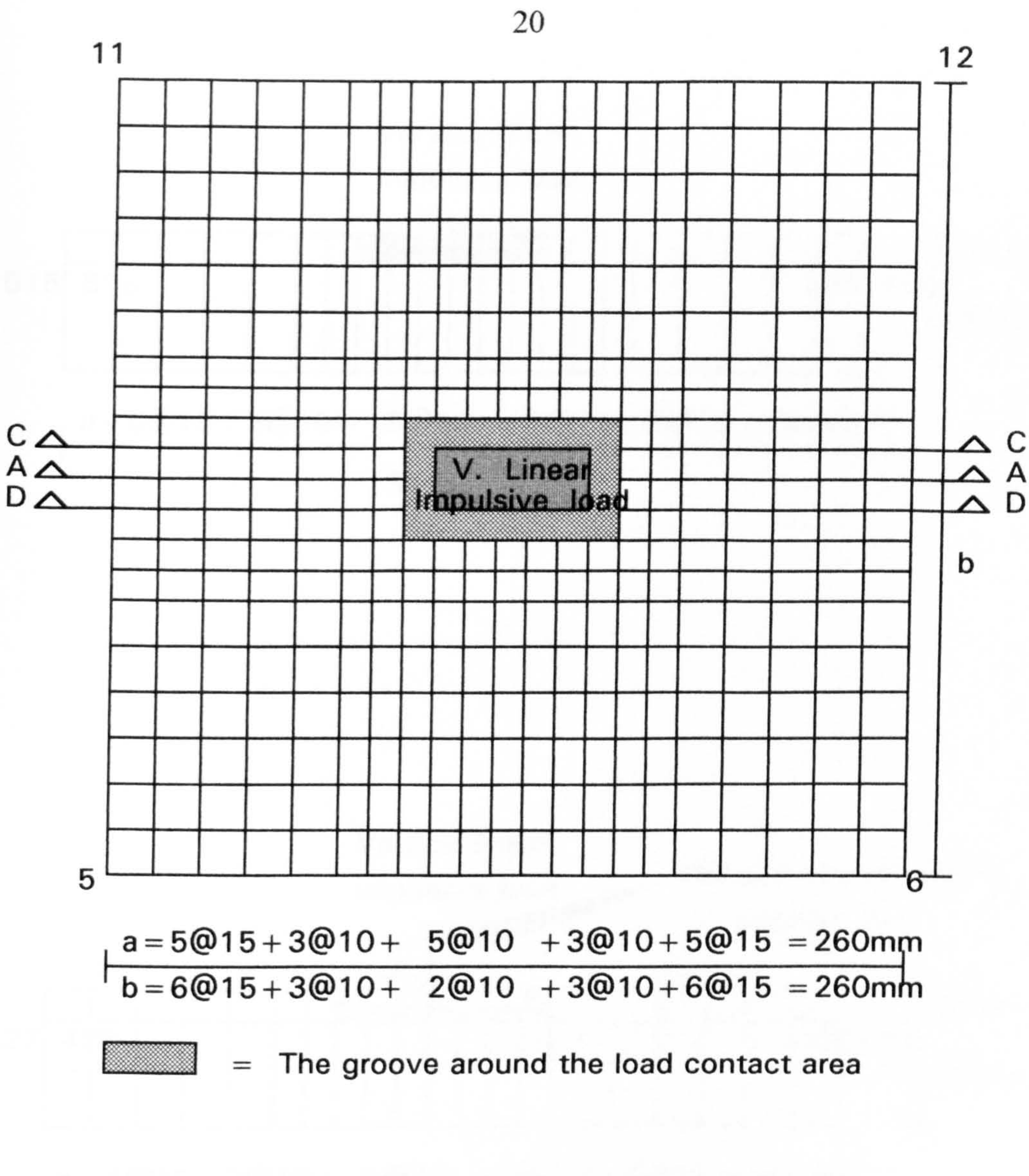

Figure 10 - a : The finite element mesh in Model 1
Vertical linear Impulsive load in Model 1
Section A-A

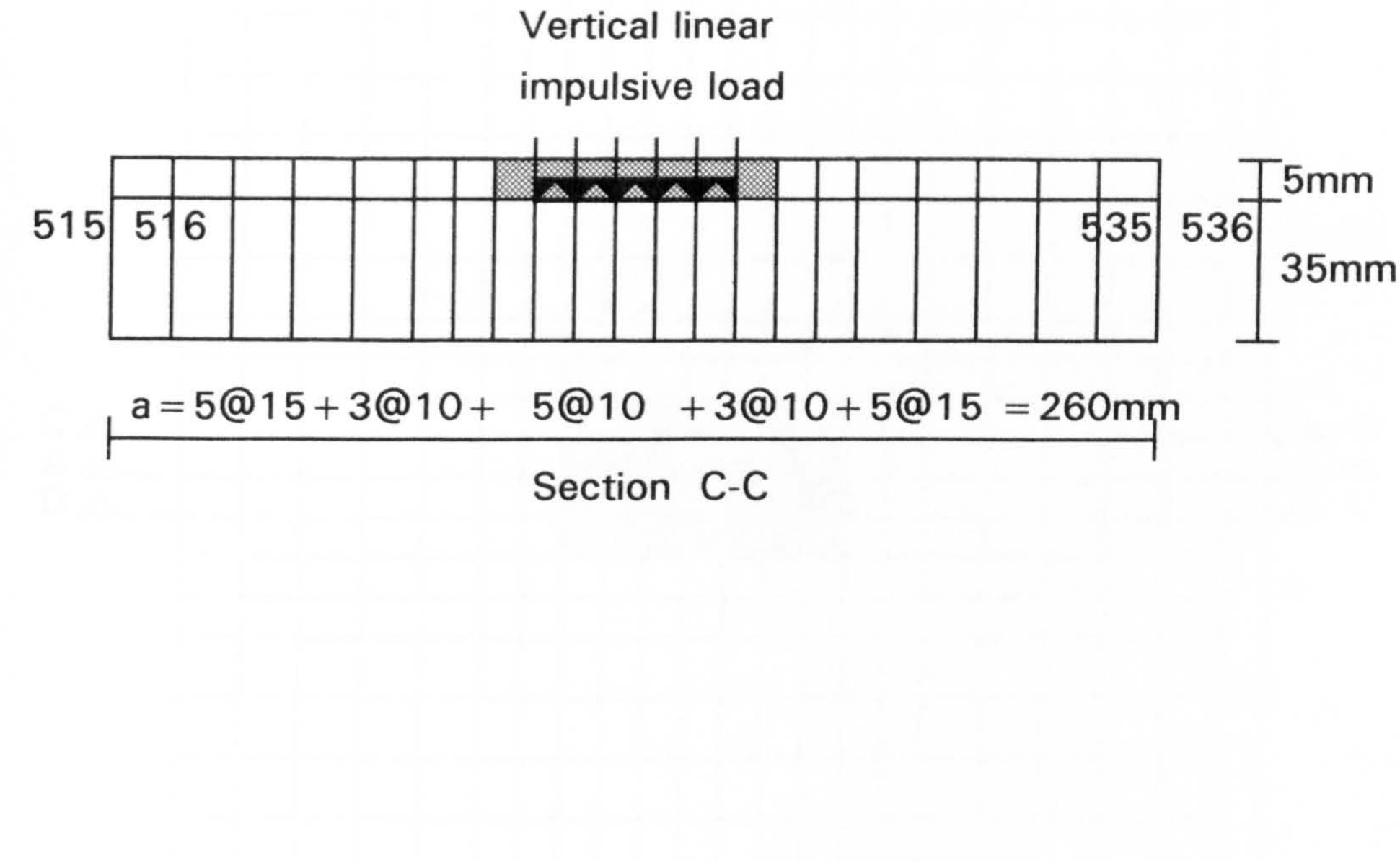

Figure 10 - b : Vertical linear Impulsive load in Model 1

Section C-C

Section D-D

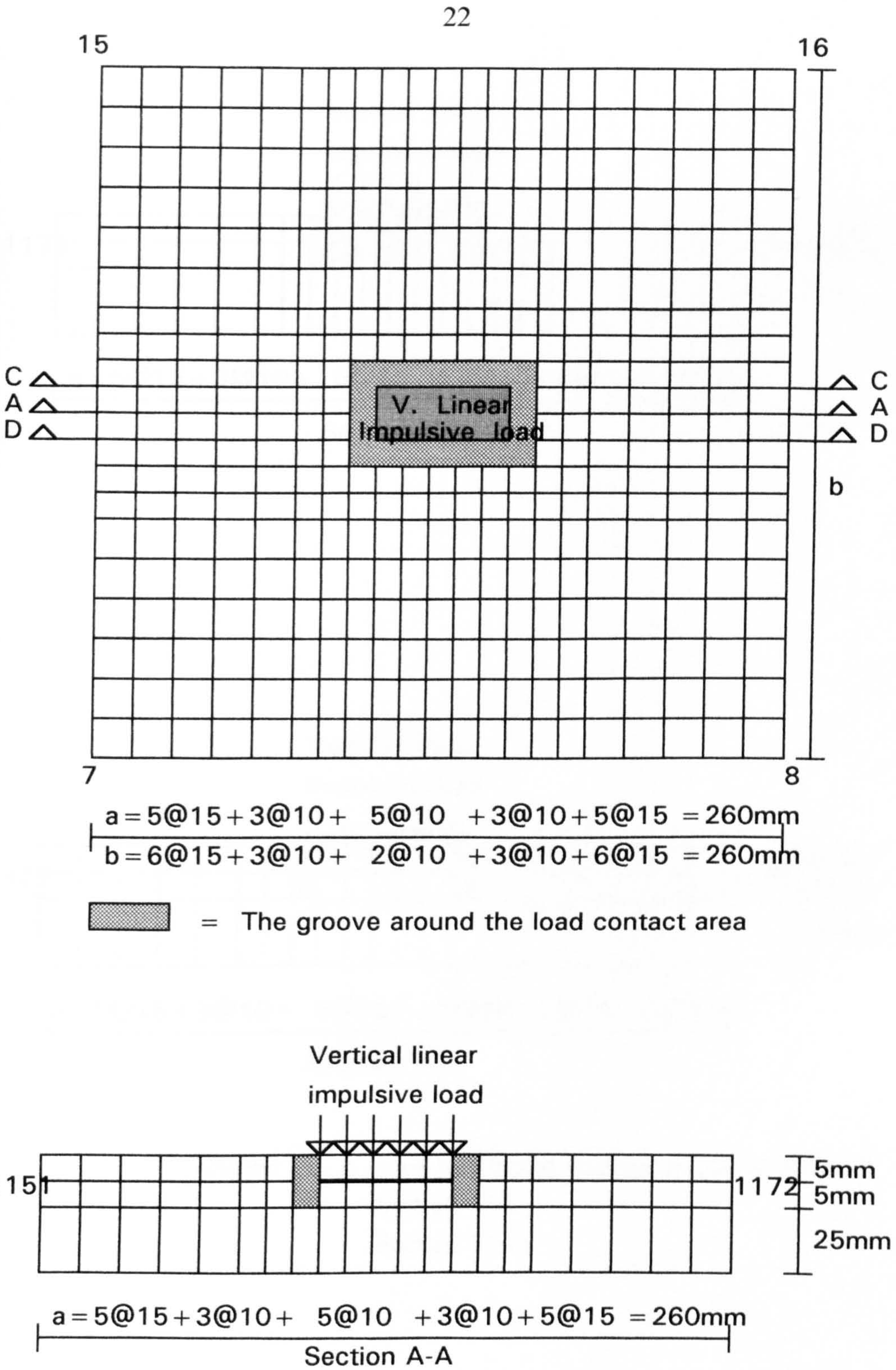

Figure 11 - a : The finite element mesh in Model 2
Vertical linear Impulsive load in Model 2
Section A-A

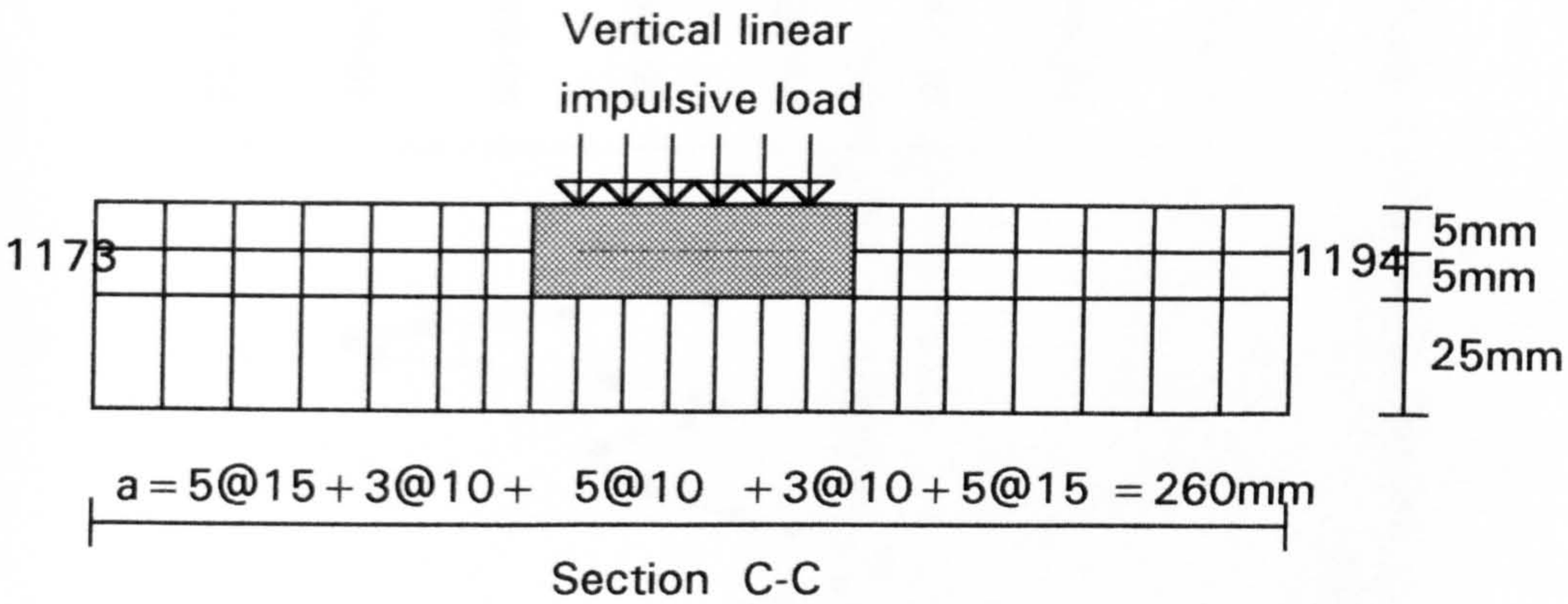

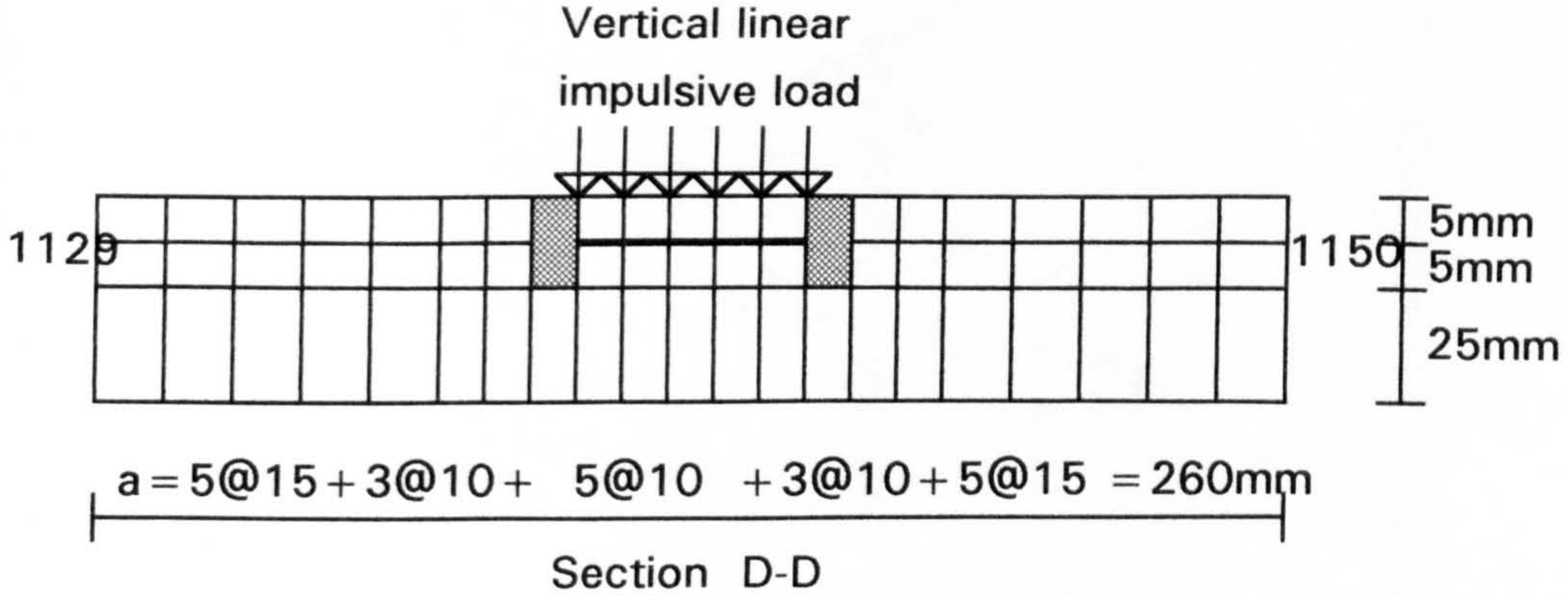

Figure 11 - b : Vertical linear Impulsive load in Model 2

Section C-C

Section D-D

THE DISPLACEMENT HISTORY AT NODE 1158 UNDER THE CONDITION OF A VERTICAL LINEAR IMPULSIVE LOAD

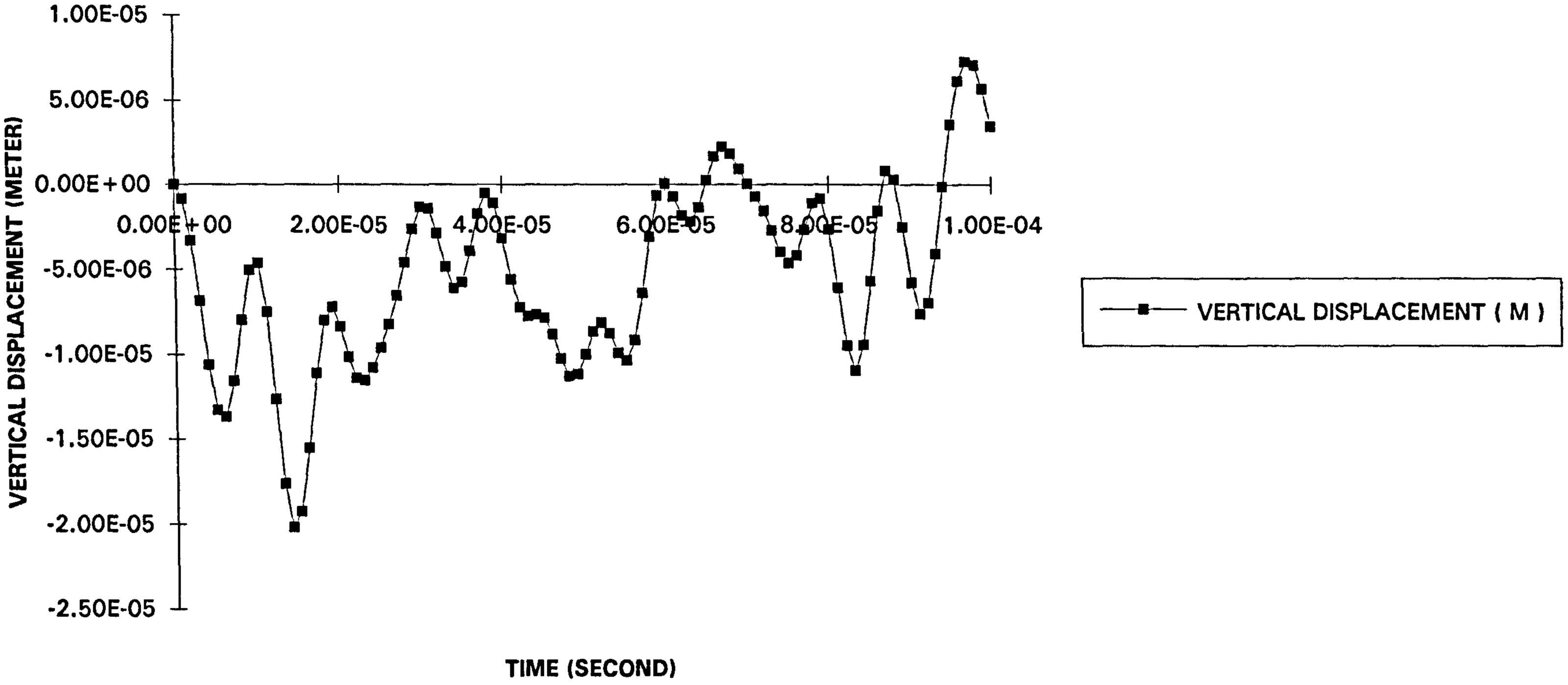

CHART 1

THE DISPLACEMENT HISTORY AT NODE 1620 UNDER THE CONDITION OF A VERTICAL LINEAR IMPULSIVE LOAD

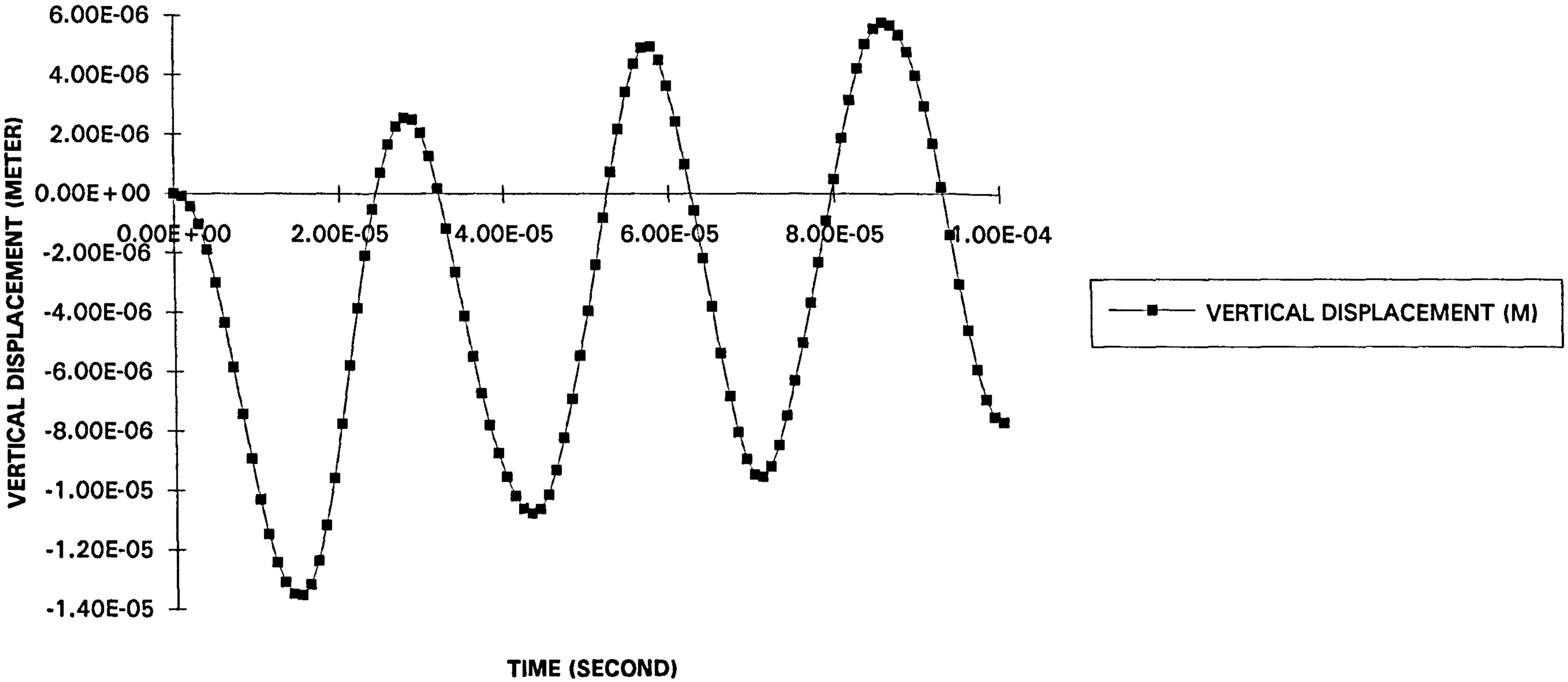

CHART 2

SIGMA-1 ALONG THE INTERFACE OF THE TWO LAYERED SYSTEM UNDER THE LOAD CONTACT AREA

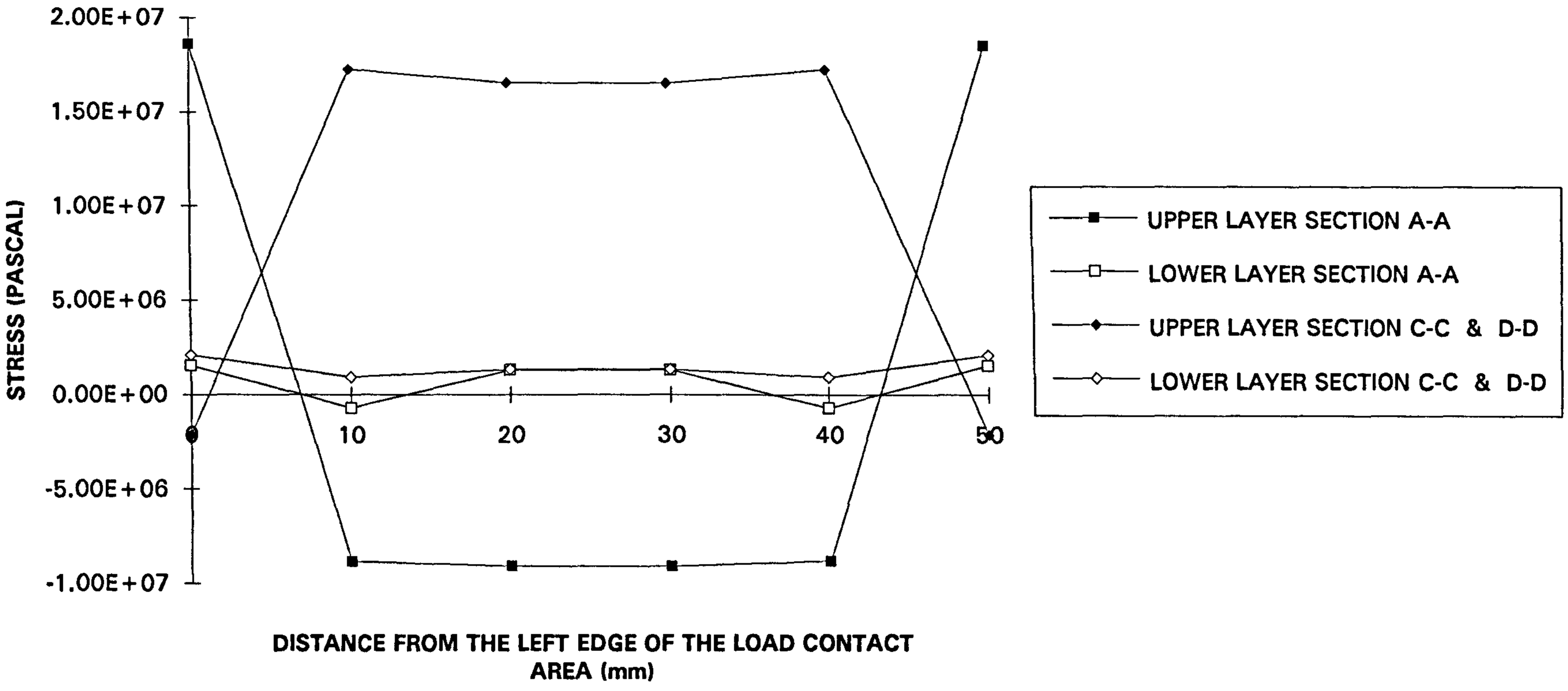

CHART 3

TIME = .000015 SECOND

SIGMA-1 ALONG THE INTERFACE OF THE TWO LAYERED SYSTEM UNDER THE LOAD CONTACT AREA

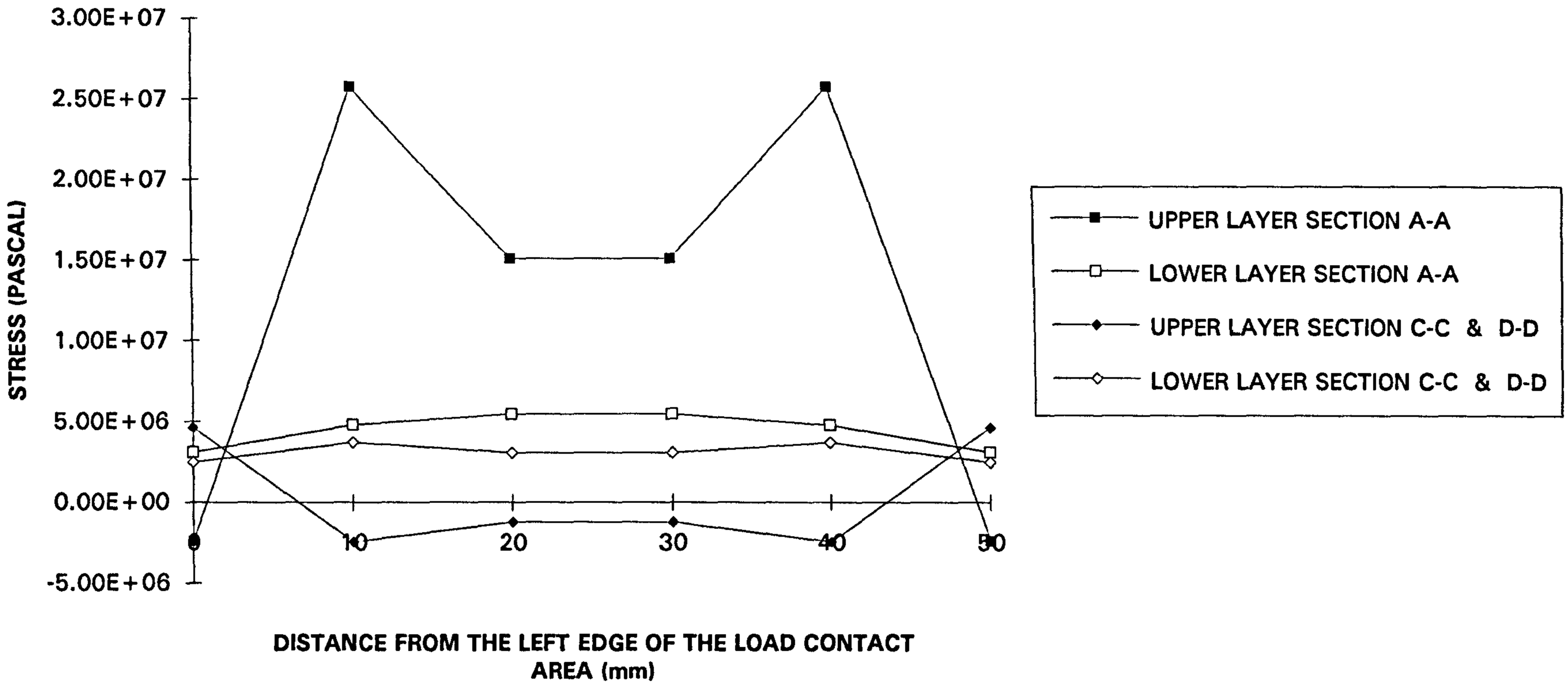

CHART 4

TIME = .000097 SECOND

SIGMA-1 ALONG THE INTERFACE OF THE TWO LAYERED SYSTEM UNDER THE LOAD CONTACT AREA

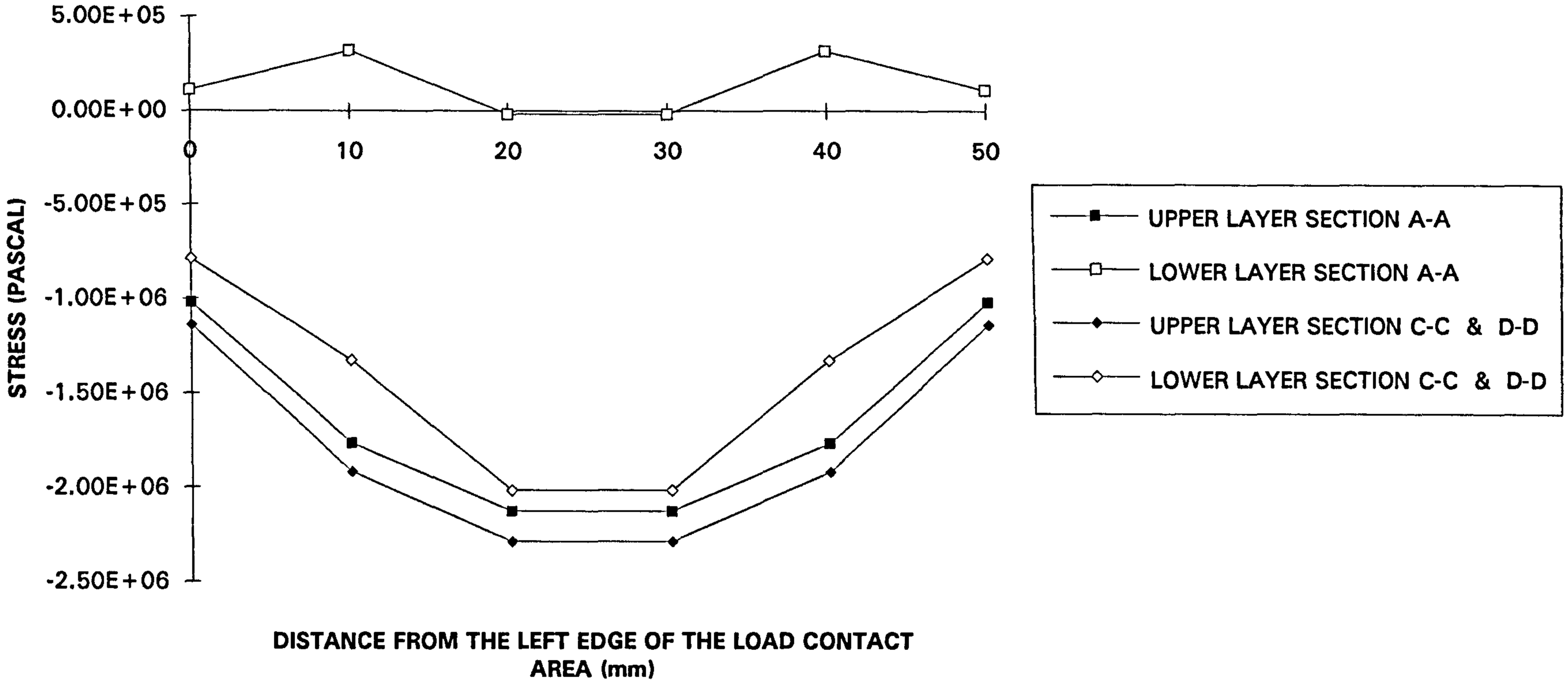

CHART 5

TIME = .000015 SECOND

SIGMA-1 ALONG THE INTERFACE OF THE TWO LAYERED SYSTEM UNDER THE LOAD CONTACT AREA

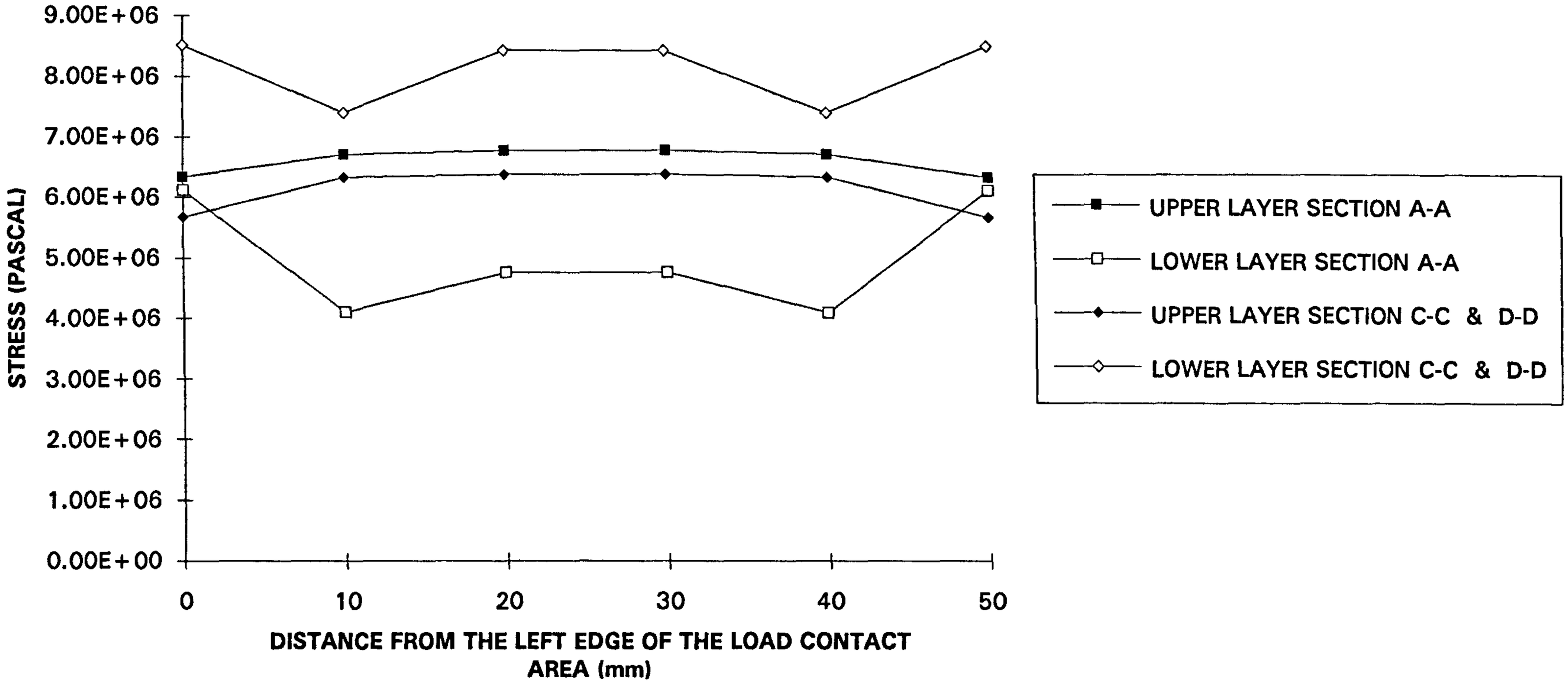

CHART 6

TIME = .000086 SECOND

REFERENCES

[B1] Bathe, K.J. FINITE ELEMENT PROCEDURES IN ENGINEERING ANALYSIS, 1982, Prentice-Hall, INC., Englewood Cliffs, New Jersey 07632

[B2] Bathe, K.J. Wilson, E.L. NUMERICAL METHODS IN FINITE ELEMENT ANALYSIS, 1976, Prentice-Hall, INC., Englewood Cliffs, New

[C1] Clough, R.W. Penzien, J. Dynamics of Structures, 1975, McGraw-Hill Kogakusha, Ltd

[C2] Clough, R.W. Penzien, J. Dynamics of Structures, second edition, 1993, McGraw-Hill Kogakusha, Ltd

[F1] Floros, T. Repair of compression zones in R.C. beams and the effect of interface bond strength, MPhil thesis, University of Newcastle Upon Tyne, Dec. , 1991

[G1] Goldsmith, W. IMPACT The theory and physical behaviour of colliding solids, 1960, Edward Arnold (Publishers) LTD., London

[H1] Henshell, R.D. PAFEC, Data preparation user manual 6.1, 1984,

[J1] Johnson, W. IMPACT STRENGTH OF MATERIALS, 1972, Edward Arnold (Publishers) Limited.

[K1] Prof. Knapton, J. DYNAMICS, lectures at the University of Newcastle Upon Tyne, Oct., 1993

[M1] Mwape, A.L. Durability of concrete and its protection. MSc

[P1] Plum, D.R. Materials-Why they fail. Construction Maintenance and Repair, vol. 5, no. 5, pp. 4-8, September/October 1991

[R1] Roberts, R.F. TESTING CEMENT-SAND SCREEDS USING THE BRE SCREED TESTER, 1986, cement and concrete association publication 48,057

[S1] Sohrabi, M. R. Investigation 2, Report on Thin layered cementitious systems, University of Newcastle Upon Tyne, Jan. , 1994.

[W1] Woodford C.H., Passaris E.K., Bull J.W. Engineering analysis using PAFEC finite element software, 1992, Blackie and Son Ltd